An Evaluation of Candidate Net Selectivity Models for 1990-2003 Yukon River Sonar Gill-net Catch Data

Alaska Fisheries Technical Report Number 75

by

Jeffrey F. Bromaghin
U. S. Fish and Wildlife Service
Division of Fisheries and Habitat Conservation
1011 E. Tudor Road
Anchorage, Alaska 99503

Key words: size selectivity, unequal probability sampling, maximum likelihood, SELECT

August 2004

Disclaimers

The mention of trade names or commercial products in this report does not constitute endorsement or recommendation for use by the Federal Government.

Nondiscrimination Clause

The U. S. Department of the Interior prohibits discrimination in programs on the basis of race, color, national origin, religion, sex, age, or disability. If you believe that you have been discriminated against in any program, activity, or facility operated by the U. S. Fish and Wildlife Service or if you desire further information please write to:

U. S. Department of the Interior
Office for Equal Opportunity
1849 C. Street, NW
Washington, D. C. 20240

The correct citation for this report is:

Bromaghin, J. F. 2004. An evaluation of candidate net selectivity models for 1990-2003 Yukon River Sonar gill-net catch data. U. S. Fish and Wildlife Service, Alaska Fisheries Technical Report Number 75, Anchorage, Alaska.

Abstract

Thirty eight net selectivity models were evaluated for their utility in representing catch data of a variety of fish species at the Yukon River sonar project on the mainstem Yukon River near Pilot Station, Alaska. Gill-net catch data collected from 1990 to 2003 were divided into 9 data sets representing species groups and each of the 38 models was fit to each of the 9 data sets. Model parameters were estimated using maximum likelihood techniques. Model utility was evaluated by comparing maximized values of the log-likelihood function, Akaike's Information Criterion statistics, scaled deviance statistics, and two types of diagnostic plots. One family of models almost universally provided the best representation of the catch data for all 9 species groups. One model from this family of models is recommended for use to apportion Yukon River sonar estimates of total fish abundance to species.

Table of Contents

Abstract iii

Table of Contents iv

List of Tables v

List of Figures vii

List of Appendices viii

Introduction 1

Methods 2
- Data Preparation 2
- Net Selectivity Models 3
- Parameter Estimation and Model Evaluation 4

Results 5
- Meshes and Catches 5
- Evaluating Model Fit 6
- Recommendations 6

Discussion 7

Acknowledgements 8

References 9

List of Tables

Table Page

1. Effort, in fathom-hours, of each mesh fished in each net suite at the Yukon River Sonar project site from 1990 to 2003 12

2. Number of fish with complete species and length data, by species category and mesh size, caught at the Yukon River Sonar project site from 1990 to 2003 13

3. Statistics summarizing the fit of net selectivity models to catch-per-unit-effort data of Chinook salmon caught at the Yukon River Sonar project site from 1990 to 2003 14

4. Statistics summarizing the fit of net selectivity models to catch-per-unit-effort data of summer chum salmon caught at the Yukon River Sonar project site from 1990 to 2003 15

5. Statistics summarizing the fit of net selectivity models to catch-per-unit-effort data of pink salmon caught at the Yukon River Sonar project site from 1990 to 2003 16

6. Statistics summarizing the fit of net selectivity models to catch-per-unit-effort data of fall chum salmon caught at the Yukon River Sonar project site from 1990 to 2003 17

7. Statistics summarizing the fit of net selectivity models to catch-per-unit-effort data of coho salmon caught at the Yukon River Sonar project site from 1990 to 2003 18

8. Statistics summarizing the fit of net selectivity models to catch-per-unit-effort data of broad whitefish caught at the Yukon River Sonar project site from 1990 to 2003 19

9. Statistics summarizing the fit of net selectivity models to catch-per-unit-effort data of humpback whitefish caught at the Yukon River Sonar project site from 1990 to 2003 20

10. Statistics summarizing the fit of net selectivity models to catch-per-unit-effort data of cisco caught at the Yukon River Sonar project site from 1990 to 2003 21

11. Statistics summarizing the fit of net selectivity models to pooled catch-per-unit-effort data from species included in the Other species group caught at the Yukon River Sonar project site from 1990 to 2003 22

List of Tables (continued)

Table Page

12. Maximum log-likelihood values ranked within species and the median model rank across species 23

13. Model SD scores ranked within species and the median model rank across species 24

14. Model AIC scores ranked within species and the median model rank across species 25

15. Estimated parameters of the Pearson T net selectivity model, by species 26

16. Initial, minimum, and maximum values used in the estimation of the parameters of the Pearson T net selectivity model, by species 27

List of Figures

Figure Page

1. An example of a net selectivity model with a tangling parameter.....28

List of Appendices

Appendix		Page
A.	Net selectivity models	29
B1.	Chinook salmon diagnostic plots; Figure B1.1 to Figure B1.38	42
B2.	Summer chum salmon diagnostic plots; Figure B2.1 to Figure B2.38	81
B3.	Pink salmon diagnostic plots; Figure B3.1 to Figure B3.38	120
B4.	Fall chum salmon diagnostic plots; Figure B4.1 to Figure B4.38	159
B5.	Coho salmon diagnostic plots; Figure B5.1 to Figure B5.38	198
B6.	Broad whitefish diagnostic plots; Figure B6.1 to Figure B6.38	237
B7.	Humpback whitefish diagnostic plots; Figure B7.1 to Figure B7.38	276
B8.	Cisco diagnostic plots; Figure B8.1 to Figure B8.34	315
B9.	Other species group diagnostic plots; Figure B9.1 to Figure B9.36	350

Introduction

The Yukon River sonar project, operated by the Alaska Department of Fish and Game (ADFG), has provided annual estimates of the abundance of migrating salmon (*Oncorhynchus* spp) in most years since 1986 (Pfisterer 2002). The project is located on the Yukon River main stem nearly 200 km from the river mouth near Pilot Station, Alaska. Abundance estimates from the project are extremely important for managing commercial and subsistence salmon fisheries throughout the drainage (Vania et al. 2002). Numerous species in addition to salmon also are present and captured at the site.

Estimates of total fish abundance derived from hydroacoustic data are apportioned to species using gill-net catch-per-unit-effort (CPUE) data. A brief summary of the method follows; additional detail is provided by Pfisterer (2002). Gill-nets of a single mesh size are drifted in 3 zones of the river thought to potentially contain different mixtures of species. A variety of mesh sizes have been used through the history of the project, though meshes with perimeters of 139.7 and 431.8 mm have generally been the smallest and largest used, respectively. Catches are enumerated by mesh, species, and length and adjusted for the time each net is fished. The resultant CPUE data for each species and length are then adjusted for the selectivity of the mesh fished. In effect, adjustments for effort and net selectivity are intended to account for the unequal probability with which fish are captured. The selectivity-adjusted CPUE data are summed across length within a species, and the relative magnitudes of the species sums are taken as estimates of the species composition.

The methods used to estimate net selectivity have evolved since the inception of the project. However, indirect estimation methods (e.g., Reiger and Robson 1966; Hamley 1975), based on the relative efficiency of different mesh sizes for fish of a common size, have been used throughout the project's history. The methods of McCombie and Fry (1960) and Holt (1963), or slight modifications, were used for different species prior to either 1992 or 1993 (e.g., Fleischman et al. 1992). The parametric method of Holt (1963) was then abandoned in favor of a nonparametric method modified from McCombie and Fry (1960) and Ishida (1969) (Fleischman et al. 1995). A least-squares method similar to that of Helser et al. (1994) was subsequently adopted in the mid 1990s, but its development was largely un-documented. Maxwell (2000) provides a graphical display of the net selectivity models used in 1998, but no information about the estimation of model parameters is provided. Very little work to evaluate the suitability of potential selectivity models has been done to date.

Net selectivity models for gill-nets represent the relative probability that a fish that comes into contact with the gear is captured (Millar and Fryer 1999). While fish can become entangled in a gill-net by several body parts, most are caught as their heads pass into the mesh and the gear catches behind the operculum. Therefore, gill-nets are most efficient, with relative selectivity 1.0, for fish with a girth behind the head somewhat less than the perimeter of the mesh size. As fish size decreases or increases from this optimum size, selectivity decreases.

Conceptually, the relationship between size and selectivity could take nearly any conceivable form. Although catch data don't contain specific information about the shape of the underlying relationship (Millar 1995), gross features such as the mode and skewness are usually observable in the data. Most estimates of selectivity are either approximately symmetric (e.g., Kirkwood and Walker 1986; Millar and Holst 1997) or somewhat right-skewed (e.g., Pierce et al. 1994; Helser et al. 1998). As one would not usually wish the model used to overly determine the form of the estimates, net selectivity models should be both numerically stable and sufficiently flexible to assume a variety of shapes.

This report summarizes an evaluation of the fit of 38 candidate net selectivity models to Yukon River sonar CPUE data. The goal of the work was to recommend a net selectivity model for each species group to be used to apportion Yukon River sonar estimates of fish abundance. CPUE data for 9 species groups collected from 1990 to 2003 were assembled and each of the 38 models were fit to the data. Model parameters were estimated using a maximum likelihood method very similar to the SELECT method (e.g., Millar and Fryer 1999). Note that while Millar (2000) offers a convincing argument that maximum likelihood methods are superior to least-squares methods, it is clear that he didn't fully understand the scaling method incorporated into the least squares method of Helser et al. (1994; 1998). Model fit was evaluated using the maximized values of the log-likelihood functions obtained, Akaike's Information Criterion (AIC; e.g., Akaike 1983; Burnham and Anderson 2002), scaled deviance (SD; Agresti 2002), and two types of diagnostic plots.

Methods

Data Preparation

Gill-net catch data from 1990 to 2003 were assembled. As indirect net selectivity estimation usually requires a large quantity of data, a minimum catch of 1,500 fish was initially and arbitrarily selected as the minimum number of individuals necessary for fitting net selectivity models to data from an individual species. Data from species not meeting this criterion were pooled and the data were treated as having come from an individual species.

Fish missing length information were excluded from the analysis. All fish with length information were categorized into discrete length groups. Chinook salmon (*O. tshawytscha*) were placed into 20 mm length bins, while all other species were placed into 10 mm bins. For each species, mean length was computed within each bin and used to represent the length of all fish in each bin.

All mesh sizes fished during a single day are, collectively, termed a net suite. The suite fished each day was determined and unique suites were identified. Let N_{snlmd} denote the number of fish of species s in length bin l caught in mesh m of net suite n on day d, and

let E_{nmd} denote the effort, in fathom-hours, that mesh m of net suite n was fished on day d; see Pfisterer (2002) for details on calculation of E_{nmd}. CPUE (C_{snlmd}) was computed as

$$C_{snlmd} = \frac{N_{snlmd}}{E_{nmd}}, \tag{1}$$

and summed over all days in the database, i.e.,

$$C_{snlm} = \sum_{d} C_{snlmd} . \tag{2}$$

The data C_{snlm} were used to estimate the parameters of the candidate net selectivity models.

Net Selectivity Models

Thirteen models, termed base models, were identified as candidate models based on either their past use as selectivity models (e.g., Millar and Fryer 1999) or a subjective assessment of their potential suitability as a model. Several additional models were formed by using a different parameterization for each limb descending from the mode of the model. For example, a two-tailed model based on the normal probability density function (Johnson et al. 1994) would have one parameter describing the location of the mode, μ, and two scale parameters σ_1 and σ_2, one for each limb descending from the mode. Such models are termed two-tailed models and denoted with a '2T' preceding the name of the base model.

For most of the base and two-tailed models, selectivity decreases from 1.0 at the mode of the model to 0.0 on the left and right limbs as fish size becomes relatively small or large, respectively. That is a realistic model for the left limb of the model because small fish are rarely captured in large mesh nets. However, it is common for small nets to capture relatively large fish, most of which are caught by body parts other than the operculum. For that reason, additional models were created from those mentioned above by adding a parameter to describe fish tangling in gill-nets. The probability of a fish being retained by tangling is probably much less dependent on size than is the probability of being gilled, and tangled fish tend to be larger than the optimum size for being gilled in a net. The tangling parameter implemented here assumes that at some measure of size greater than optimum, relative selectivity is a constant value for all fish greater than or equal to that size. An example of this type of model is provided in Figure 1. Models with a tangling parameter are denoted by the addition of a 'T' after the name of the base model.

A total of 38 models, 13 base models and 25 additional models constructed as described, were evaluated for their capability of providing a good representation of the CPUE data. The ratio of fish length mm to the perimeter of the mesh mm (LPR) was used as the measure of size in all models. Equations and parameter constraints for all models are presented in Appendix A.

Parameter Estimation and Model Evaluation

Model parameters were estimated using maximum likelihood techniques very similar to the SELECT method (e.g., Millar and Fryer 1999). The log-likelihood function for a given species s is

$$\log L = \sum_n \sum_l \sum_m C_{snlm} \log_e \left(\frac{S_{slm}}{\sum_m S_{slm}} \right), \tag{3}$$

where S_{slm} denotes the relative selectivity for an individual of species s and length l in mesh m. The log-likelihood function was maximized using a computer program written in the FORTRAN programming language (e.g., Metcalf and Reid 1996), as implemented in version 6.6.B of the Compaq Visual FORTRAN Professional compiler (Compaq 1999). Components of the Visual Numerics subroutine and function library bundled with the compiler were used to maximize the log-likelihood function and obtain variance estimates through numerical approximation.

Two summary statistics, AIC (e.g., Akaike 1983; Burnham and Anderson 2002) and SD (e.g., Agresti 2002), were used to evaluate model fit. AIC is computed as

$$AIC = 2(K_1 - \log L), \tag{4}$$

where K_1 is the sum of the number of parameters in a net selectivity model and the number of net suite and length combinations having at least one mesh with nonzero CPUE. AIC favors models that obtain large values of the log-likelihood function, but penalizes them for over-parameterization; small values of AIC reflect models that fit the data well without using too many parameters. Deviance is computed as twice the difference between the log-likelihood of a model and that of the saturated model (Agresti 2002), i.e.,

$$D = 2\left\{ \sum_n \sum_l \sum_m C_{snlm} \log_e \left(\frac{C_{snlm}}{\sum_m C_{snlm}} \right) - \log L \right\}. \tag{5}$$

SD is the ratio of D and its associated degrees of freedom. For deviance, the number of degrees of freedom is the number of meshes having nonzero values of CPUE among those combinations of net suite and length bin having at least 2 meshes with nonzero CPUE.

Two types of diagnostic plots were used to evaluate model fit. CPUE residuals were computed as

$$R_{snlm} = \left(\frac{S_{slm}}{\sum_m S_{slm}} \right) \sum_m C_{snlm} - C_{snlm} \tag{6}$$

(Millar 2000), which transforms net selectivity estimates to the CPUE scale. Positive and negative residuals were plotted separately, by mesh size and length. The area of a circle symbol used in residual plots is proportional to the magnitude of the absolute value of the residual. The maximum circle size is the same for each species, with the largest circle being associated with the largest residual, in absolute value, for each species. For this reason, one should only compare residual plots between models within a species. While large circles indicate large discrepancies between the data and the model, no information regarding the importance of the data points is provided. For example, large residuals may be associated with data points having low information content, such as a rarely fished suite that caught few fish. Large residuals can be a sign of noisy data, rather than a poorly fitting model.

The second type of diagnostic plot transforms CPUE data to the net selectivity scale. Scaled CPUE was computed as

$$V_{snlm} = \left(\frac{C_{snlm}}{\sum_m C_{snlm}} \right) \sum_m S_{slm} \ . \tag{7}$$

Values of V_{snlm} were plotted with the corresponding estimated net selectivity model. The size of circle symbols in these plots is proportional to the sum of the CPUE across meshes for a particular combination of species, net suite, and length bin (C_{snl}). The maximum circle size is the same for each species, with the largest circles being associated with the suite and length bin having the largest summed CPUE for each species. For that reason, as with the CPUE residual plots, comparisons of figures should only be made within a given species. In these plots, large circles indicate concentrations of data.

Results

Meshes and Catches

Nine different mesh sizes, with perimeters of 139.7, 203.2, 254.0, 266.7, 279.4, 292.1, 330.2, 381.0, and 431.8 mm, were fished from 1990 to 2003. Sixty-six unique net suites were identified in the data set. Unique net suites and the effort, in fathom-hours, each mesh was fished are presented in Table 1.

The number of fish with complete species and length data is presented in Table 2, by species and mesh. Fourteen species and a combination of other species, labeled 'Other', were present in the data, though the group 'Cisco' likely consists of multiple *Coregonus*

species. Eight species were judged sufficiently abundant to attempt estimation of net selectivity; all other species were combined into a ninth species group collectively referred to as 'Other' (Table 2).

Evaluating Model Fit

Maximum likelihood estimates of the parameters of each of the 38 net selectivity models were obtained for each of the 9 species groups. The maximization algorithm failed in 5 of the 342 combinations of model and species group (< 2%). Variance estimates were also obtained, but were unrealistically small and are not presented in the interests of space.

Values of the maximized log-likelihood function, AIC, SD, and associated quantities for the 9 species groups are presented in Table 3 through Table 11, ordered by model. Tables 12 through 14 contain ranked log-likelihood values, AIC statistics, and SD statistics, respectively, with median ranks computed across species for each model. A low median rank indicated a model that tends to fit data from many species groups well.

The Pearson family of models, models 19, 20, 37, and 38, provide the best fit to the data from nearly all the species. Based on log-likelihood and SD measures, these 4 models as a group provide the best fit to the data from nearly every species group, with very few exceptions (Table 12; Table 13). The relatively large number of parameters of the two-tailed models, models 37 and 38, tends to inflate their AIC scores and make them appear undesirable (Table 14), but the models still fit the data very well. One of these 4 models is the best model no matter which of the statistics is used to rank models, with the single exception of pink salmon using AIC as the ranking criterion (Table 14). A few of the other models, particularly the bi-normal, Schnute, and logistic models, fit the data from some species well, but provide quite poor fit in other cases.

Diagnostic plots are presented in appendices B1 through B9 for the 9 species groups. The diagnostic plots confirm the conclusions reached from an examination of the summary statistics. The Pearson family of models fit the data from all species groups quite well. The plots on the selectivity scale tend to pass through or near the larger circles, which represent the greatest concentrations of CPUE data. The residual plots for these models do not appear to contain any patterns, which indicates that these models provide a good overall representation of the primary structure in the data. The presence of patterns in the residual plots could, for example, indicate a structural departure from the rather constraining model assumption that selectivity is a function of LPR alone. However, there is no indication that a more complicated relationship between mesh size, fish size, and selectivity exists.

Recommendation

In general, the two-tailed Pearson model with a tangling parameter, model 38, provides the best fit to the CPUE data. However, the shape of the model around the mode is somewhat unrealistic for several species, particularly pink salmon and broad whitefish

(appendix figures B3.38 and B6.38). The unrealistic shape is caused by the discontinuity of the model at the mode combined with an extremely flexible model perhaps over-fitting data in the two tails. For that reason, use of the Pearson model with a tangling parameter, model 20, is recommended. This model fits the data for all species groups nearly as well as the two-tailed version of the model, without discontinuity at the mode. Parameter estimates of this model are presented in Table 15, while starting values and permissible ranges used in maximization of the likelihood function are listed in Table 16.

Discussion

Separate net selectivity models for broad and humpback whitefish were obtained for the first time in this analysis. These two species had previously been pooled into a single whitefish species group (e.g., Rich 2001). The models for these species appear fairly similar (appendix figures B6.20 and B7.20), and they could probably be combined into a single species group without substantially changing estimates of species composition. However, it is probably preferable to separate them. The humpback whitefish model fits the data quite well, so separating the two species could be expected to lead to some improvement in the estimation of the relative abundance of this species. The broad whitefish data appear to contain more noise than the humpback whitefish data, but the model appears to pass through the central portion of the data so estimation should be approximately unbiased, though perhaps variable. Even though the estimated models appear relatively similar, the collection of additional catch data for these species may lead to increased differentiation between the species over time.

Variance estimation remains problematic. Millar and Fryer (1999) recommend the use of estimates based on the second partial derivative matrix, or information matrix (Rao 1973). However, the applications they considered did not require adjustment for variable fishing effort, and how best to incorporate variable effort into variance estimation isn't clear. The method attempted in this analysis was based on a numerical approximation of the variance matrix, and unrealistically small variance estimates were obtained. Whether this disappointing result was caused by a poor approximation is unknown. Unfortunately, the complexity of the data and the models precludes analytic computation of the information matrix, so no comparison between an exact computation and an approximation can be made. The most promising method of obtaining realistic variance estimates may be bootstrapping (Chernick 1999) the CPUE data. However, the data could be bootstrapped at several levels ranging from the catch from an individual drift to the total CPUE of a suite and length bin, and some weighting scheme will undoubtedly be necessary.. The level that will produce the best estimates is not certain, though the later seems most likely to prove fruitful. In any case, additional investigation is required.

Acknowledgements

The author would like to thank Toshihide Hamazaki and Carl Pfisterer of the Alaska Department of Fish and Game, Commercial Fisheries Division, for providing the data used in this modeling effort. Rod Simmons, Nick Hetrick, and Chrissy Apodaca of the U. S. Fish and Wildlife Service, Bonnie Borba and Toshihide Hamazaki of the Alaska Department of Fish and Game, and Sandy Johnston of the Department of Fisheries and Oceans Canada provided review comments which substantially improved the report.

References

Agresti, A. 2002. Categorical Data Analysis, 2nd edition. John Wiley & Sons, Hoboken, New Jersey.

Akaike, H. 1983. Information measures and model selection. Proceedings of the 44th session of the International Statistical Institute 1: 277-291.

Burnham, K. P. and D. R. Anderson. 2002. Model Selection and Multimodel Inference: A Practical Information-Theoretic Approach, 2nd edition. Springer-Verlag, New York.

Chernick, M. R. 1999. Bootstrap Methods: A Practitioner's Guide. John Wiley and Sons, New York.

Compaq Computer Corporation. 1999. Compaq Fortran Language Reference Manual. Compaq Computer Corporation, Houston, Texas.

Fleischman, S. J., D. C. Mesiar, and P. A. Skvorc. 1995. Lower Yukon River Sonar project report 1993. Alaska Department of Fish and Game, Commercial Fisheries Management and Development Division, Regional Information Report No. 3A95-33, Anchorage, Alaska.

Fleischman, S., D. C. Mesiar, and P. A. Skvorc. 1992. Yukon River Sonar escapement estimate 1991. Alaska Department of Fish and Game, Division of Commercial Fisheries, Regional Information Report No. 3A92-08, Anchorage, Alaska.

Hamley, J. M. 1975. Review of gillnet selectivity. Journal of the Fisheries Research Board of Canada 32: 1943-1969.

Helser, T. E., J. P. Geaghan, and R. E. Condrey. 1998. Estimating gillnet selectivity using nonlinear response surface regression. Canadian Journal of Fisheries and Aquatic Sciences 55: 1328-1337.

Helser, T. E., J. P. Geaghan, and R. E. Condrey. 1994. Estimating size composition and associated variances of a fish population from gillnet selectivity, with an example for spotted seatrout (*Cynoscion nebulosus*). Fisheries Research 19: 65-86.

Holt, S. J. 1963. A method for determining gear selectivity and its application. ICNAF Special Publication 5: 106-115.

Ishida, T. 1969. The salmon gillnet mesh selectivity curve. International North Pacific Fisheries Commission Bulletin 26: 1-11.

Johnson, N. L., S. Kotz, and N. Balakrishnan. 1994. Continuous Univariate Distributions, Volume 1, 2nd edition. John Wiley & Sons, New York.

Kirkwood, G. P. and T. I. Walker. 1986. Gill net mesh selectivities for Gummy Shark, *Mustelus antarcticus* Günther, taken in south-eastern Australian waters. Australian Journal of Marine and Freshwater Research 37: 689-697.

Maxwell, S. L. 2000. Yukon River Sonar project report. Alaska Department of Fish and Game, Commercial Fisheries Division, Regional Information Report No. 3A00-04, Anchorage, Alaska.

McCombie, A. M. and F. E. J. Fry. 1960. Selectivity of gill nets for Lake Whitefish, *Coregonus clupeaformis*. Transactions of the American Fisheries Society 89: 176-184.

Metcalf, M. and J. Reid. 1996. FORTRAN 90/95 Explained. Oxford University Press, New York.

Millar, R. B. 2000. Untangling the confusion surrounding the estimation of gillnet selectivity. Canadian Journal of Fisheries and Aquatic Sciences 57: 507-511.

Millar, R. B. 1995. The functional form of hook and gillnet selection curves cannot be determined from comparative catch data alone. Canadian Journal of Fisheries and Aquatic Sciences 52: 883-891.

Millar, R. B. and R. J. Fryer. 1999. Estimating the size-selection curves of towed gears, traps, nets and hooks. Reviews in Fish Biology and Fisheries 9: 89-116.

Millar, R. B. and R. Holst. 1997. Estimation of gillnet and hook selectivity using log-linear models. ICES Journal of Marine Science 54: 471-477.

Pierce, R. B., C. M. Tomcko, and T. D. Kolander. 1994. Indirect and direct estimates of gill-net size selectivity for Northern Pike. North American Journal of Fisheries Management 14: 170-177.

Pfisterer, C. T. 2002. Estimation of Yukon River salmon passage in 2001 using hydroacoustic methodologies. Alaska Department of Fish and Game, Commercial Fisheries Division, Regional Information Report No. 3A02-24, Anchorage, Alaska.

Rao, C. R. 1973. Linear Statistical Inference and Its Applications, 2nd edition. John Wiley and Sons, New York.

Reiger, H. A. and D. S. Robson. 1966. Selectivity of gill nets, especially to Lake Whitefish. Journal of the Fisheries Research Board of Canada 23: 423-454.

Rich, C. F. 2001. Yukon River sonar project report 2000. Alaska Department of Fish and Game, Commercial Fisheries Division, Regional Information Report No. 3A01-13, Anchorage, Alaska.

Vania, T., V. Golembeski, B. M. Borba, T. L. Lingnau, J. S. Hayes, K. R. Boeck, and W. H. Busher. 2002. Annual management report Yukon and Northern areas 2000. Alaska Department of Fish and Game, Division of Commercial Fisheries, Regional Information Report No. 3A02-29, Anchorage, Alaska.

Table 1. Effort, in fathom-hours, of each mesh fished in each net suite at the Yukon River Sonar project site from 1990 to 2003.

	Mesh Perimeter (mm)									
Suite	139.7	203.2	254.0	266.7	279.4	292.1	330.2	381.0	431.8	Total
1								10.4	11.1	21.5
2							9.8			9.8
3					7.4					7.4
4					64.4		60.8	263.0	258.7	647.0
5				12.5			10.2	9.4	7.5	39.6
6			21.6				22.7			44.3
7			17.3				15.4	24.2	33.2	89.9
8			52.0		82.6		69.3			203.9
9			4.1		5.5		17.3	47.5	44.9	119.3
10		41.4			39.8			39.2		120.4
11		11.4			18.3			32.5	35.9	98.1
12		16.5			19.6		16.8			52.9
13		10.7			9.3		8.7	9.7		38.4
14		8.5			17.0		12.1	45.2	47.9	130.8
15		11.4		9.5					10.0	30.9
16		8.8		21.7			18.4			48.9
17		22.8		23.5			21.5		22.3	90.1
18		9.4		14.3			13.6	7.3		44.6
19		20.2		18.9			18.2	10.7	8.7	76.6
20		21.4	13.5				13.9		13.8	62.5
21		6.3	17.6				16.2	16.7		56.9
22		6.2	14.3				6.4	16.2	16.0	59.1
23		17.4	18.6			17.7	18.2			71.8
24		11.6	9.8		11.3			12.1		44.7
25		404.7	394.4		951.7		947.1			2697.8
26		380.4	366.5		366.7		400.2	1181.3	1181.9	3877.1
27		8.5	9.2	9.1		9.2	27.0	8.6		71.6
28	2.3				8.1					10.4
29	26.2			14.9			15.3		24.7	81.1
30	28.8			21.9			21.5	30.6		102.8
31	6.7		9.6							16.3
32	14.2		15.1					12.2		41.4
33	52.3		52.6				59.8			164.7
34	27.9		25.9				27.1		36.6	117.5
35	18.4		18.5				21.2	19.9		77.9
36	27.0		24.4				24.1	13.1	15.9	104.4
37	17.9		19.3			18.4	16.8			72.3
38	18.9		22.2		20.6				16.7	78.3
39	6.2		6.3		6.2			6.0	5.7	30.4
40	117.1		110.1		104.9		120.3			452.4
41	20.0		21.0		30.8		22.1	23.5		117.4
42	50.1		25.0		28.1		22.1	30.3	27.3	182.8
43	9.0	9.5				8.8	8.5			35.8
44	8.1	9.2			7.5					24.8
45	48.0	48.1			47.9			46.8		190.9
46	102.4	58.2			105.4		94.6			360.6
47	5.8	4.8			6.8		5.0		7.2	29.6
48	9.1	10.4			10.0		5.2	14.3		49.0
49	414.9	402.4		1314.0			797.4			2928.6
50	55.2	61.6		104.2			100.4		77.9	399.3
51	9.4	9.8		11.1			11.4	18.3		60.0
52	2216.1	2165.2		3745.9			3776.7	2087.9	2128.2	16120.0
53	8.6	9.0		9.8		18.8	17.1	8.9		72.3
54	9.7	9.5	6.9					8.2	7.5	41.8
55	139.4	136.8	138.4				132.1			546.6
56	25.2	33.7	44.3				47.9	37.2		188.3
57	690.5	654.3	1060.1				1026.0	638.5	656.3	4725.7
58	25.9	25.9	25.8			46.2	50.1			173.9
59	2142.5	2129.5	2532.8			3630.9	3967.0	2061.4		16464.1
60	10.8	4.2	3.2		2.7			9.1		30.2
61	77.9	32.5	38.8		72.0			35.0	38.7	295.0
62	2894.1	1867.5	2433.9		3135.1		3140.4			13471.0
63	20.0	18.4	13.3		12.8		14.3		16.0	94.9
64	60.3	61.8	67.7		56.7		57.1	66.0		369.5
65	709.5	371.5	320.4		362.4		410.7	539.1	536.6	3250.0
66	8.5	9.9	9.9	8.4		44.3	19.5	9.5		109.9
Total	10134.6	9160.9	7984.1	5339.8	5611.8	3794.3	15775.4	7449.9	5287.1	70537.8

Table 2. Number of fish with complete species and length data, by species category and mesh size, caught at the Yukon River Sonar project site from 1990 to 2003.

Original Species Group	New Species Group	Mesh Perimeter (mm)									Total
		139.7	203.2	254.0	266.7	279.4	292.1	330.2	381.0	431.8	
Chinook	Chinook	118	410	372	692	290	18	1,674	2,016	1,671	7,261
Summer Chum	Summer Chum	871	1,906	6,623	8,814	4,690	62	10,212	3,956	2,388	39,522
Pink	Pink	240	1,048	464	582	262	50	417	122	90	3,275
Fall Chum	Fall Chum	200	486	2,287	1,113	3,412	3,025	7,144	1,023	56	18,746
Coho	Coho	244	933	2,240	797	1,771	2,147	2,628	261	0	11,021
Broad	Broad	272	416	323	110	206	89	118	16	1	1,551
Humpback	Humpback	353	1,261	651	361	25	174	102	14	3	2,944
Cisco	Cisco	5,083	525	13	17	7	1	11	5	2	5,664
Sheefish	Other	35	89	96	163	50	35	340	168	59	1,035
Sucker	Other	216	28	3	2	0	1	0	1	3	254
Burbot	Other	48	51	26	43	6	16	16	2	1	209
Sockeye	Other	6	19	19	31	3	19	46	7	5	155
Char	Other	41	52	5	3	2	3	1	0	0	107
Pike	Other	10	11	3	5	0	0	2	1	1	33
Other	Other	150	53	14	0	20	0	10	4	1	252
Total		7,887	7,288	13,139	12,733	10,744	5,640	22,721	7,596	4,281	92,029

Table 3. Statistics summarizing the fit of net selectivity models to catch-per-unit-effort data of chinook salmon caught at the Yukon River Sonar project site from 1990 to 2003.

Model Number	Model Name	Log Likelihood	No.Parameters Model	No.Parameters Total	AIC	Deviance	Degrees Of Freedom	Scaled Deviance
1	Normal	-1349.89	2	278	3255.77	403.006	715	0.564
2	Normal T	-1319.62	3	279	3197.24	342.472	714	0.480
3	Logistic	-1338.93	2	278	3233.87	381.101	715	0.533
4	Logistic T	-1317.79	3	279	3193.58	338.819	714	0.475
5	Logistic DR	-1320.25	2	278	3196.50	343.734	715	0.481
6	Logistic DR T	-1313.16	3	279	3184.32	329.556	714	0.462
7	Exponential Power	-1309.01	2	278	3174.02	321.250	715	0.449
8	Exponential Power T	-1308.24	3	279	3174.48	319.718	714	0.448
9	Gaussian-Lorentzian	-1310.80	3	279	3179.61	324.843	714	0.455
10	Gaussian-Lorentzian T	-1310.05	4	280	3180.10	323.337	713	0.453
11	Lognormal	-1314.97	3	279	3187.95	333.183	714	0.467
12	Lognormal T	-1311.99	4	280	3183.97	327.207	713	0.459
13	Logistic Power	-1331.26	3	279	3220.51	365.746	714	0.512
14	Logistic Power T	-1300.99	4	280	3161.99	305.221	713	0.428
15	Weibull	-1337.32	3	279	3232.63	377.869	714	0.529
16	Weibull T	-1320.44	4	280	3200.87	344.105	713	0.483
17	Schnute	-1320.71	3	279	3199.41	344.648	714	0.483
18	Schnute T	-1312.83	4	280	3185.67	328.901	713	0.461
19	Pearson	-1290.09	4	280	3140.19	283.421	713	0.398
20	Pearson T	-1290.09	5	281	3142.19	283.421	712	0.398
21	Inverse Gaussian	-1316.36	4	280	3192.72	335.957	713	0.471
22	Inverse Gaussian T	-1314.35	5	281	3190.71	331.942	712	0.466
23	Sigmoid	-1302.72	4	280	3165.44	308.679	713	0.433
24	Sigmoid T	-1300.20	5	281	3162.41	303.640	712	0.426
25	Bi-normal	-1293.77	5	281	3149.55	290.781	712	0.408
26	Bi-normal T	-1290.33	6	282	3144.65	283.886	711	0.399
27	2T Normal	-1349.89	3	279	3257.77	403.006	714	0.564
28	2T Normal T	-1314.63	4	280	3189.27	332.500	713	0.466
29	2T Exponential Power	-1308.85	3	279	3175.70	320.937	714	0.449
30	2T Exponential Power T	-1308.85	4	280	3177.70	320.937	713	0.450
31	2T Logistic DR	-1307.79	3	279	3173.58	318.813	714	0.447
32	2T Logistic DR T	-1307.79	4	280	3175.58	318.813	713	0.447
33	2T Logistic Power	-1297.40	5	281	3156.81	298.041	712	0.419
34	2T Logistic Power T	-1299.37	6	282	3162.74	301.970	711	0.425
35	2T Schnute	-1296.78	5	281	3155.56	296.798	712	0.417
36	2T Schnute T	-1294.85	6	282	3153.70	292.938	711	0.412
37	2T Pearson	-1289.03	7	283	3144.06	281.296	710	0.396
38	2T Pearson T	-1289.03	8	284	3146.06	281.296	709	0.397

Table 4. Statistics summarizing the fit of net selectivity models to catch-per-unit-effort data of summer chum salmon caught at the Yukon River Sonar project site from 1990 to 2003.

Model Number	Model Name	Log Likelihood	No.Parameters Model	No.Parameters Total	AIC	Deviance	Degrees Of Freedom	Scaled Deviance
1	Normal	-8389.49	2	382	17542.97	3151.913	1033	3.051
2	Normal T	-7305.03	3	383	15376.05	982.992	1032	0.953
3	Logistic	-7867.39	2	382	16498.79	2107.727	1033	2.040
4	Logistic T	-7209.46	3	383	15184.92	791.860	1032	0.767
5	Logistic DR	-7574.72	2	382	15913.43	1522.371	1033	1.474
6	Logistic DR T	-7252.96	3	383	15271.92	878.858	1032	0.852
7	Exponential Power	-7831.82	2	382	16427.63	2036.572	1033	1.972
8	Exponential Power T	-7821.42	3	383	16408.84	2015.774	1032	1.953
9	Gaussian-Lorentzian	-7242.98	3	383	15251.96	858.897	1032	0.832
10	Gaussian-Lorentzian T	-7152.31	4	384	15072.62	677.560	1031	0.657
11	Lognormal	-7775.07	3	383	16316.14	1923.076	1032	1.863
12	Lognormal T	-7277.85	4	384	15323.70	928.635	1031	0.901
13	Logistic Power	-7660.13	3	383	16086.25	1693.193	1032	1.641
14	Logistic Power T	-7208.94	4	384	15185.88	790.816	1031	0.767
15	Weibull	-8649.50	3	383	18065.00	3671.939	1032	3.558
16	Weibull T	-7247.37	4	384	15262.75	867.686	1031	0.842
17	Schnute	-7660.13	3	383	16086.25	1693.193	1032	1.641
18	Schnute T	-7197.17	4	384	15162.35	767.289	1031	0.744
19	Pearson	-7139.07	4	384	15046.14	651.083	1031	0.632
20	Pearson T	-7120.23	5	385	15010.47	613.409	1030	0.596
21	Inverse Gaussian	-7805.14	4	384	16378.28	1983.219	1031	1.924
22	Inverse Gaussian T	-7431.97	5	385	15633.93	1236.870	1030	1.201
23	Sigmoid	-7444.26	4	384	15656.52	1261.462	1031	1.224
24	Sigmoid T	-7177.98	5	385	15125.97	728.909	1030	0.708
25	Bi-normal	-7119.06	5	385	15008.12	611.060	1030	0.593
26	Bi-normal T	-7110.19	6	386	14992.38	593.315	1029	0.577
27	2T Normal	-7890.26	3	383	16546.53	2153.466	1032	2.087
28	2T Normal T	-7284.21	4	384	15336.41	941.349	1031	0.913
29	2T Exponential Power	-7674.30	3	383	16114.60	1721.536	1032	1.668
30	2T Exponential Power T	-7436.43	4	384	15640.87	1245.806	1031	1.208
31	2T Logistic DR	-7496.49	3	383	15758.99	1365.929	1032	1.324
32	2T Logistic DR T	-7237.34	4	384	15242.67	847.613	1031	0.822
33	2T Logistic Power	-7380.47	5	385	15530.94	1133.882	1030	1.101
34	2T Logistic Power T	-7186.97	6	386	15145.93	746.870	1029	0.726
35	2T Schnute	-7322.39	5	385	15414.79	1017.729	1030	0.988
36	2T Schnute T	-7188.19	6	386	15148.37	749.312	1029	0.728
37	2T Pearson	-7105.13	7	387	14984.27	583.206	1028	0.567
38	2T Pearson T	-7105.13	8	388	14986.27	583.206	1027	0.568

Table 5. Statistics summarizing the fit of net selectivity models to catch-per-unit-effort data of pink salmon caught at the Yukon River Sonar project site from 1990 to 2003.

Model Number	Model Name	Log Likelihood	No. Parameters Model	No. Parameters Total	AIC	Deviance	Degrees Of Freedom	Scaled Deviance
1	Normal	-508.96	2	164	1345.93	188.155	397	0.474
2	Normal T	-496.15	3	165	1322.31	162.538	396	0.410
3	Logistic	-506.65	2	164	1341.29	183.521	397	0.462
4	Logistic T	-493.20	3	165	1316.41	156.638	396	0.396
5	Logistic DR	-499.06	2	164	1326.13	168.358	397	0.424
6	Logistic DR T	-495.80	3	165	1321.59	161.821	396	0.409
7	Exponential Power	-520.07	2	164	1368.14	210.422	397	0.530
8	Exponential Power T	-520.10	3	165	1370.19	210.422	396	0.531
9	Gaussian-Lorentzian	-501.37	3	165	1332.73	172.963	369	0.469
10	Gaussian-Lorentzian T	-492.74	4	166	1317.48	155.705	395	0.394
11	Lognormal	-503.00	3	165	1335.99	176.222	396	0.445
12	Lognormal T	-494.37	4	166	1320.75	158.976	395	0.402
13	Logistic Power	-499.73	3	165	1329.47	169.696	396	0.429
14	Logistic Power T	-492.77	4	166	1317.53	155.760	395	0.394
15	Weibull	-510.30	3	165	1350.61	190.838	396	0.482
16	Weibull T	-493.31	4	166	1318.62	156.851	395	0.397
17	Schnute	-499.73	3	165	1329.47	169.696	396	0.429
18	Schnute T	-492.77	4	166	1317.53	155.760	395	0.394
19	Pearson	-493.34	4	166	1318.68	156.909	395	0.397
20	Pearson T	-492.55	5	167	1319.10	155.327	394	0.394
21	Inverse Gaussian	-505.09	4	166	1342.18	180.406	395	0.457
22	Inverse Gaussian T	-503.78	5	167	1341.57	177.796	394	0.451
23	Sigmoid	-495.56	4	166	1323.12	161.345	395	0.408
24	Sigmoid T	-492.69	5	167	1319.39	155.616	394	0.395
25	Bi-normal	-492.34	5	167	1318.68	154.909	394	0.393
26	Bi-normal T	-492.33	6	168	1320.66	154.885	393	0.394
27	2T Normal	-502.04	3	165	1334.08	174.305	396	0.440
28	2T Normal T	-494.39	4	166	1320.78	159.011	395	0.403
29	2T Exponential Power	-507.22	3	165	1344.44	184.664	396	0.466
30	2T Exponential Power T	-502.92	4	166	1337.83	176.061	395	0.446
31	2T Logistic DR	-498.21	3	165	1326.43	166.657	396	0.421
32	2T Logistic DR T	-493.93	4	166	1319.86	158.092	395	0.400
33	2T Logistic Power	-495.28	5	167	1324.56	160.786	394	0.408
34	2T Logistic Power T	-492.61	6	168	1321.22	155.450	393	0.396
35	2T Schnute	-494.33	5	167	1322.66	158.890	394	0.403
36	2T Schnute T	-492.81	6	168	1321.62	155.853	393	0.397
37	2T Pearson	-491.47	7	169	1320.94	153.172	392	0.391
38	2T Pearson T	-491.47	8	170	1322.94	153.168	391	0.392

Table 6. Statistics summarizing the fit of net selectivity models to catch-per-unit-effort data of fall chum salmon caught at the Yukon River Sonar project site from 1990 to 2003.

Model Number	Model Name	Log Likelihood	No.Parameters Model	No.Parameters Total	AIC	Deviance	Degrees Of Freedom	Scaled Deviance
1	Normal	-1909.65	2	280	4379.30	704.433	590	1.194
2	Normal T	-1678.77	3	281	3919.53	242.665	589	0.412
3	Logistic	-1819.58	2	280	4199.16	524.289	590	0.889
4	Logistic T	-1673.76	3	281	3909.53	232.662	589	0.395
5	Logistic DR	-1755.91	2	280	4071.81	396.946	590	0.673
6	Logistic DR T	-1668.29	3	281	3898.59	221.718	589	0.376
7	Exponential Power	-1730.11	2	280	4020.21	345.344	590	0.585
8	Exponential Power T	-1712.89	3	281	3987.78	310.912	589	0.528
9	Gaussian-Lorentzian	-1678.55	3	281	3919.10	242.233	589	0.411
10	Gaussian-Lorentzian T	-1678.55	4	282	3921.10	242.233	588	0.412
11	Lognormal	-1770.64	3	281	4103.28	426.409	589	0.724
12	Lognormal T	-1675.16	4	282	3914.32	235.456	588	0.400
13	Logistic Power	-1756.17	3	281	4074.33	397.464	589	0.675
14	Logistic Power T	-1661.01	4	282	3886.03	207.159	588	0.352
15	Weibull	-1883.85	3	281	4329.70	652.834	589	1.108
16	Weibull T	-1691.29	4	282	3946.58	267.714	588	0.455
17	Schnute	-1756.11	3	281	4074.22	397.353	589	0.675
18	Schnute T	-1666.00	4	282	3896.00	218.700	588	0.372
19	Pearson	-1658.77	4	282	3881.53	202.665	588	0.345
20	Pearson T	-1655.79	5	283	3877.59	196.719	587	0.335
21	Inverse Gaussian	-1781.12	4	282	4126.23	447.363	588	0.761
22	Inverse Gaussian T	-1675.60	5	283	3917.21	236.337	587	0.403
23	Sigmoid	-1701.73	4	282	3967.46	288.593	588	0.491
24	Sigmoid T	-1659.72	5	283	3885.44	204.577	587	0.349
25	Bi-normal	-1660.91	5	283	3887.82	206.951	587	0.353
26	Bi-normal T	-1656.95	6	284	3881.90	199.034	586	0.340
27	2T Normal	-1821.62	3	281	4205.24	528.374	589	0.897
28	2T Normal T	-1672.67	4	282	3909.34	230.477	588	0.392
29	2T Exponential Power	-1726.38	3	281	4014.77	337.897	589	0.574
30	2T Exponential Power T	-1683.92	4	282	3931.84	252.969	588	0.430
31	2T Logistic DR	-1707.55	3	281	3977.09	300.223	589	0.510
32	2T Logistic DR T	-1663.66	4	282	3891.31	212.446	588	0.361
33	2T Logistic Power	-1719.84	5	283	4005.68	324.811	587	0.553
34	2T Logistic Power T	-1659.28	6	284	3886.55	203.686	586	0.348
35	2T Schnute	-1732.21	5	283	4030.42	349.556	587	0.595
36	2T Schnute T	-1659.37	6	284	3886.74	203.868	586	0.348
37	2T Pearson	-1652.69	7	285	3875.37	190.503	585	0.326
38	2T Pearson T	-1652.69	8	286	3877.37	190.503	584	0.326

Table 7. Statistics summarizing the fit of net selectivity models to catch-per-unit-effort data of coho salmon caught at the Yukon River Sonar project site from 1990 to 2003.

Model Number	Model Name	Log Likelihood	No.Parameters Model	No.Parameters Total	AIC	Deviance	Degrees Of Freedom	Scaled Deviance
1	Normal	-1188.96	2	184	2745.92	233.293	439	0.531
2	Normal T	-1145.07	3	185	2660.14	145.516	438	0.332
3	Logistic	-1171.99	2	184	2711.99	199.364	439	0.454
4	Logistic T	-1145.13	3	185	2660.26	145.635	438	0.333
5	Logistic DR	-1149.58	2	184	2667.16	154.533	439	0.352
6	Logistic DR T	-1135.01	3	185	2640.03	125.404	438	0.286
7	Exponential Power	-1131.73	2	184	2631.46	118.841	439	0.271
8	Exponential Power T	-1129.94	3	185	2629.87	115.250	438	0.263
9	Gaussian-Lorentzian	-1145.69	3	185	2661.38	146.759	438	0.335
10	Gaussian-Lorentzian T	-1142.04	4	186	2656.08	139.452	437	0.319
11	Lognormal	-1139.12	3	185	2648.25	133.622	438	0.305
12	Lognormal T	-1129.72	4	186	2631.44	114.818	437	0.263
13	Logistic Power	-1141.78	3	185	2653.56	138.933	438	0.317
14	Logistic Power T	-1121.71	4	186	2615.41	98.790	437	0.226
15	Weibull	-1238.06	3	185	2846.13	331.505	438	0.757
16	Weibull T	-1146.25	4	186	2664.51	147.883	437	0.338
17	Schnute	-1139.84	3	185	2649.69	135.065	438	0.308
18	Schnute T	-1128.07	4	186	2628.14	111.518	437	0.255
19	Pearson	-1121.15	4	186	2614.30	97.674	437	0.224
20	Pearson T	-1120.97	5	187	2615.94	97.313	436	0.223
21	Inverse Gaussian	-1140.44	4	186	2652.89	136.264	437	0.312
22	Inverse Gaussian T	-1129.41	5	187	2632.81	114.189	436	0.262
23	Sigmoid	-1123.31	4	186	2618.61	101.988	437	0.233
24	Sigmoid T	-1121.46	5	187	2616.93	98.306	436	0.225
25	Bi-normal	-1125.78	5	187	2625.57	106.945	436	0.245
26	Bi-normal T	-1121.72	6	188	2619.44	98.817	435	0.227
27	2T Normal	-1140.86	3	185	2651.73	137.102	438	0.313
28	2T Normal T	-1126.38	4	186	2624.76	108.139	437	0.247
29	2T Exponential Power	-1131.71	3	185	2633.41	118.787	438	0.271
30	2T Exponential Power T	-1128.99	4	186	2629.99	113.363	437	0.259
31	2T Logistic DR	-1125.93	3	185	2621.85	107.230	438	0.245
32	2T Logistic DR T	-1122.85	4	186	2617.70	101.079	437	0.231
33	2T Logistic Power	-1123.83	5	187	2621.66	103.038	436	0.236
34	2T Logistic Power T	-1122.60	6	188	2621.20	100.575	435	0.231
35	2T Schnute	-1122.91	5	187	2619.82	101.199	436	0.232
36	2T Schnute T	-1121.42	6	188	2618.83	98.208	435	0.226
37	2T Pearson	-1120.52	7	189	2619.04	96.413	434	0.222
38	2T Pearson T	-1120.52	8	190	2621.04	96.413	433	0.223

Table 8. Statistics summarizing the fit of net selectivity models to catch-per-unit-effort data of broad whitefish caught at the Yukon River Sonar project site from 1990 to 2003.

Model Number	Model Name	Log Likelihood	No. Parameters Model	No. Parameters Total	AIC	Deviance	Degrees Of Freedom	Scaled Deviance
1	Normal	-165.79	2	129	589.59	143.406	216	0.664
2	Normal T	-148.65	3	130	557.29	109.111	215	0.507
3	Logistic	-164.83	2	129	587.65	141.474	216	0.655
4	Logistic T	-148.64	3	130	557.27	109.093	215	0.507
5	Logistic DR	-155.64	2	129	569.29	123.105	216	0.570
6	Logistic DR T	-148.10	3	130	556.20	108.017	215	0.502
7	Exponential Power	-154.30	2	129	566.60	120.421	216	0.558
8	Exponential Power T	-154.30	3	130	568.60	120.421	215	0.560
9	Gaussian-Lorentzian	-165.56	3	130	591.12	142.939	215	0.665
10	Gaussian-Lorentzian T	-148.33	4	131	558.65	108.470	214	0.507
11	Lognormal	-153.08	3	130	566.15	117.971	215	0.549
12	Lognormal T	-148.63	4	131	559.25	109.073	214	0.510
13	Logistic Power	-151.06	3	130	562.12	113.939	215	0.530
14	Logistic Power T	-145.36	4	131	552.72	102.540	214	0.479
15	Weibull	-169.60	3	130	599.21	151.028	215	0.702
16	Weibull T	-165.62	4	131	593.24	143.055	214	0.668
17	Schnute	-151.06	3	130	562.12	113.939	215	0.530
18	Schnute T	-147.48	4	131	556.96	106.777	214	0.499
19	Pearson	-144.52	4	131	551.03	100.852	214	0.471
20	Pearson T	-144.46	5	132	552.92	100.737	213	0.473
21	Inverse Gaussian	-153.45	4	131	568.91	118.727	214	0.555
22	Inverse Gaussian T	-149.60	5	132	563.20	111.019	213	0.521
23	Sigmoid	-145.51	4	131	553.01	102.833	214	0.481
24	Sigmoid T	-145.18	5	132	554.36	102.180	213	0.480
25	Bi-normal	-145.63	5	132	555.25	103.070	213	0.484
26	Bi-normal T	-144.34	6	133	554.68	100.503	212	0.474
27	2T Normal	-149.64	3	130	559.28	111.099	215	0.517
28	2T Normal T	-147.98	4	131	557.97	107.789	214	0.504
29	2T Exponential Power	-153.26	3	130	566.52	118.341	215	0.550
30	2T Exponential Power T	-152.76	4	131	567.52	117.334	214	0.548
31	2T Logistic DR	-146.52	3	130	553.03	104.853	215	0.488
32	2T Logistic DR T	-146.07	4	131	554.15	103.968	214	0.486
33	2T Logistic Power	-145.17	5	132	554.33	102.151	213	0.480
34	2T Logistic Power T	-145.08	6	133	556.17	101.985	212	0.481
35	2T Schnute	-144.97	5	132	553.94	101.756	213	0.478
36	2T Schnute T	-144.74	6	133	555.47	101.290	212	0.478
37	2T Pearson	-144.30	7	134	556.60	100.421	211	0.476
38	2T Pearson T	-144.24	8	135	558.47	100.293	210	0.478

Table 9. Statistics summarizing the fit of net selectivity models to catch-per-unit-effort data of humpback whitefish caught at the Yukon River Sonar project site from 1990 to 2003.

Model Number	Model Name	Log Likelihood	No. Parameters Model	No. Parameters Total	AIC	Deviance	Degrees Of Freedom	Scaled Deviance
1	Normal	-289.39	2	131	840.79	147.639	239	0.618
2	Normal T	-259.17	3	132	782.34	87.198	238	0.366
3	Logistic	-286.39	2	131	834.78	141.630	239	0.593
4	Logistic T	-258.31	3	132	780.63	85.480	238	0.359
5	Logistic DR	-270.57	2	131	803.13	109.987	239	0.460
6	Logistic DR T	-257.40	3	132	778.80	83.652	238	0.351
7	Exponential Power	-296.49	2	131	854.98	161.831	239	0.677
8	Exponential Power T	-296.49	3	132	856.98	161.831	238	0.680
9	Gaussian-Lorentzian	-288.19	3	132	840.38	145.235	238	0.610
10	Gaussian-Lorentzian T	-258.00	4	133	782.00	84.854	237	0.358
11	Lognormal	-272.43	3	132	808.86	113.717	238	0.478
12	Lognormal T	-259.09	4	133	784.17	87.028	237	0.367
13	Logistic Power	-263.85	3	132	791.70	96.552	238	0.406
14	Logistic Power T	-253.22	4	133	772.44	75.290	237	0.318
15	Weibull	-375.66	3	132	1015.32	320.173	238	1.345
16	Weibull T	-261.29	4	133	788.59	91.441	237	0.386
17	Schnute	-263.85	3	132	791.70	96.552	238	0.406
18	Schnute T	-256.00	4	133	778.00	80.850	237	0.341
19	Pearson	-251.36	4	133	768.71	71.566	237	0.302
20	Pearson T	-251.25	5	134	770.49	71.346	236	0.302
21	Inverse Gaussian	-273.20	4	133	812.40	115.251	237	0.486
22	Inverse Gaussian T	-264.60	5	134	797.20	98.053	236	0.415
23	Sigmoid	-253.97	4	133	773.94	76.798	237	0.324
24	Sigmoid T	-252.84	5	134	773.67	74.525	236	0.316
25	Bi-normal	-253.52	5	134	775.04	75.889	236	0.322
26	Bi-normal T	-251.88	6	135	773.75	72.604	235	0.309
27	2T Normal	-264.71	3	132	793.42	98.275	238	0.413
28	2T Normal T	-258.41	4	133	782.83	85.679	237	0.362
29	2T Exponential Power	-282.83	3	132	829.66	134.518	238	0.565
30	2T Exponential Power T	-277.69	4	133	821.37	124.228	237	0.524
31	2T Logistic DR	-256.86	3	132	777.73	82.582	238	0.347
32	2T Logistic DR T	-255.05	4	133	776.10	78.956	237	0.333
33	2T Logistic Power	-252.97	5	134	773.93	74.787	236	0.317
34	2T Logistic Power T	-252.57	6	135	775.13	73.988	235	0.315
35	2T Schnute	-252.99	5	134	773.98	74.833	236	0.317
36	2T Schnute T	-252.24	6	135	774.48	73.331	235	0.312
37	2T Pearson	-251.18	7	136	774.37	71.221	234	0.304
38	2T Pearson T	-251.18	8	137	776.37	71.221	233	0.306

Table 10. Statistics summarizing the fit of net selectivity models to catch-per-unit-effort data of cisco caught at the Yukon River Sonar project site from 1990 to 2003.

Model Number	Model Name	Log Likelihood	No. Parameters Model	No. Parameters Total	AIC	Deviance	Degrees Of Freedom	Scaled Deviance
1	Normal	-131.15	2	97	456.30	82.990	112	0.741
2	Normal T	-126.34	3	98	448.67	73.367	111	0.661
3	Logistic	-126.80	2	97	447.60	74.298	112	0.663
4	Logistic T	-120.38	3	98	436.75	61.447	111	0.554
5	Logistic DR	-125.94	2	97	445.87	72.569	112	0.648
6	Logistic DR T	-123.64	3	98	443.28	67.976	111	0.612
7	Exponential Power	-165.57	2	97	525.14	151.839	112	1.356
8	Exponential Power T	-165.57	3	98	527.14	151.839	111	1.368
9	Gaussian-Lorentzian	-127.84	3	98	451.68	76.373	111	0.688
10	Gaussian-Lorentzian T	-120.23	4	99	438.45	61.146	110	0.556
11	Lognormal	-131.14	3	98	458.29	82.980	111	0.748
12	Lognormal T	-123.38	4	99	444.75	67.449	110	0.613
13	Logistic Power	-123.57	3	98	443.14	67.830	111	0.611
14	Logistic Power T	-120.21	4	99	438.43	61.124	110	0.556
15	Weibull	-148.25	3	98	492.49	117.187	111	1.056
16	Weibull T	-120.28	4	99	438.56	61.255	110	0.557
17	Schnute	-123.57	3	98	443.14	67.830	111	0.611
18	Schnute T	-119.94	4	99	437.88	60.571	110	0.551
19	Pearson	-117.87	4	99	433.75	56.443	110	0.513
20	Pearson T	-116.53	5	100	433.05	53.745	109	0.493
21	Inverse Gaussian	-144.59	4	99	487.18	109.875	110	0.999
22	Inverse Gaussian T	-143.52	5	100	487.04	107.734	109	0.988
23	Sigmoid	-120.89	4	99	439.78	62.472	110	0.568
24	Sigmoid T	-120.32	5	100	440.63	61.325	109	0.563
25	Bi-normal	-131.15	5	100	462.30	82.990	109	0.761
26	Bi-normal T	-131.15	6	101	464.30	92.990	108	0.861
27	2T Normal	-130.40	3	98	456.79	81.489	111	0.734
28	2T Normal T	-127.55	4	99	453.09	75.786	110	0.689
29	2T Exponential Power	-126.88	3	98	449.76	74.454	111	0.671
30	2T Exponential Power T	-123.56	4	99	445.12	67.811	110	0.616
31	2T Logistic DR	-125.34	3	98	446.67	71.370	111	0.643
32	2T Logistic DR T	-123.60	4	99	445.21	67.901	110	0.617
33	2T Logistic Power			Model failed to converge.				
34	2T Logistic Power T			Model failed to converge.				
35	2T Schnute			Model failed to converge.				
36	2T Schnute T			Model failed to converge.				
37	2T Pearson	-116.51	7	102	437.02	53.712	107	0.502
38	2T Pearson T	-116.42	8	103	438.84	53.533	106	0.505

Table 11. Statistics summarizing the fit of net selectivity models to pooled catch-per-unit-effort data from species included in the Other species group caught at the Yukon River Sonar project site from 1990 to 2003.

Model Number	Model Name	Log Likelihood	No. Parameters Model	No. Parameters Total	AIC	Deviance	Degrees Of Freedom	Scaled Deviance
1	Normal	-255.07	2	205	920.15	239.464	401	0.597
2	Normal T	-226.61	3	206	865.23	182.542	400	0.456
3	Logistic	-251.72	2	205	913.45	232.761	401	0.580
4	Logistic T	-228.03	3	206	868.06	185.372	400	0.463
5	Logistic DR	-236.29	2	205	882.57	201.887	401	0.503
6	Logistic DR T	-226.28	3	206	864.56	181.879	400	0.455
7	Exponential Power	-247.96	2	205	905.92	225.233	401	0.562
8	Exponential Power T	-247.96	3	206	907.92	225.233	400	0.563
9	Gaussian-Lorentzian	-248.91	3	206	909.82	227.139	400	0.568
10	Gaussian-Lorentzian T	-225.40	4	207	864.81	180.121	399	0.451
11	Lognormal	-236.28	3	206	884.57	201.881	400	0.505
12	Lognormal T	-226.54	4	207	867.07	182.390	399	0.457
13	Logistic Power	-232.13	3	206	876.26	193.573	400	0.484
14	Logistic Power T	-224.81	4	207	863.62	178.936	399	0.448
15	Weibull	-444.55	3	206	1301.10	618.420	400	1.546
16	Weibull T	-230.07	4	207	874.13	189.447	399	0.475
17	Schnute	-232.13	3	206	876.26	193.573	400	0.484
18	Schnute T	-224.81	4	207	863.62	178.936	399	0.448
19	Pearson	-220.98	4	207	855.97	171.281	399	0.429
20	Pearson T	-220.94	5	208	857.89	171.201	398	0.430
21	Inverse Gaussian	-237.40	4	207	888.81	204.126	399	0.512
22	Inverse Gaussian T	-232.64	5	208	881.27	194.589	398	0.489
23	Sigmoid	-222.65	4	207	859.30	174.620	399	0.438
24	Sigmoid T	-222.38	5	208	860.77	174.083	398	0.437
25	Bi-normal	-224.00	5	208	864.00	177.313	398	0.446
26	Bi-normal T	-223.05	6	209	864.09	175.409	397	0.442
27	2T Normal	-228.71	3	206	869.42	186.739	400	0.467
28	2T Normal T	-225.41	4	207	864.81	180.130	399	0.451
29	2T Exponential Power	-243.34	3	206	898.67	215.990	400	0.540
30	2T Exponential Power T	-239.85	4	207	893.69	209.006	399	0.524
31	2T Logistic DR	-224.81	3	206	861.61	178.930	400	0.447
32	2T Logistic DR T	-224.22	4	207	862.43	177.750	399	0.445
33	2T Logistic Power	Model failed to converge.						
34	2T Logistic Power T	-221.82	6	209	861.64	172.957	397	0.436
35	2T Schnute	-221.81	5	208	859.63	172.945	398	0.435
36	2T Schnute T	-221.69	6	209	861.37	172.686	397	0.435
37	2T Pearson	-220.93	7	210	861.87	171.184	396	0.432
38	2T Pearson T	-220.91	8	211	863.82	171.140	395	0.433

Table 12. Maximum log-likelihood values ranked within species and the median model rank across species.

Model Number	Model Name	Chinook	Summer Chum	Pink	Fall Chum	Coho	Broad Whitefish	Humpback Whitefish	Cisco	Other	Median
37	2T Pearson	1.5	1.5	2	1.5	1.5	2	1.5	2	2	1.5
38	2T Pearson T	1.5	1.5	1	1.5	1.5	1	1.5	1	1	1.5
20	Pearson T	3.5	5	5	3	3	4	3	3	3	3
19	Pearson	3.5	6	14	5	4	5	4	4	4	4
26	Bi-normal T	5	3	3	4	8	3	5	28	10	5
36	2T Schnute T	7	10	11	7	5	6	6	36.5	5	7
24	Sigmoid T	11	8	7	8	6	10	8	9	8	8
34	2T Logistic Power T	10	9	6	6	9	8	7	36.5	7	8
14	Logistic Power T	12	12	9.5	10	7	11	11	6	14	11
25	Bi-normal	6	4	4	9	14	13	12	28	11	11
35	2T Schnute	8	21	16	29	11	7	10	36.5	6	11
23	Sigmoid	13	25	20	23	12	12	13	11	9	13
18	Schnute T	23	11	9.5	12	17	16	15	5	14	14
32	2T Logistic DR T	14.5	14	15	11	10	14	14	16	12	14
31	2T Logistic DR	14.5	26	23	24	15	15	16	18	14	16
6	Logistic DR T	24	17	21	13	24	18	17	17	18	18
10	Gaussian-Lorentzian T	20	7	8	18.5	30	19	18	7	16	18
28	2T Normal T	26	19	18	14	16	17	20	23	17	18
4	Logistic T	29	13	12	15	32	21	19	10	21	19
12	Lognormal T	22	18	17	16	20	20	21	12	19	19
33	2T Logistic Power	9	22	19	26	13	9	9	36.5	38	19
2	Normal T	30	20	22	20	31	22	22	20	20	22
16	Weibull T	32	16	13	22	34	36	23	8	23	23
30	2T Exponential Power T	17.5	24	29	21	18	27	31	13	30	24
22	Inverse Gaussian T	25	23	31	17	19	23	26	30	26	25
13	Logistic Power	34	28.5	25.5	32	29	25.5	24.5	14.5	24.5	26
17	Schnute	33	28.5	25.5	31	26	25.5	24.5	14.5	24.5	26
9	Gaussian-Lorentzian	21	15	27	18.5	33	35	34	24	34	27
5	Logistic DR	31	27	24	30	35	33	28	19	28	28
11	Lognormal	27	31	30	33	25	28	29	26	27	28
27	2T Normal	37.5	36	28	36	28	24	27	25	22	28
29	2T Exponential Power	17.5	30	34	27	22	29	32	22	31	29
21	Inverse Gaussian	28	32	32	34	27	30	30	31	29	30
7	Exponential Power	19	34	37	28	23	31.5	36.5	33.5	32.5	33
8	Exponential Power T	16	33	38	25	21	31.5	36.5	33.5	32.5	33
3	Logistic	36	35	33	35	36	34	33	21	35	35
1	Normal	37.5	37	35	38	37	37	35	28	36	37
15	Weibull	35	38	36	37	38	38	38	32	37	37

Table 13. Model SD scores ranked within species and the median model rank across species.

Model Number	Model Name	Chinook	Summer Chum	Pink	Fall Chum	Coho	Broad Whitefish	Humpback Whitefish	Cisco	Other	Median
37	2T Pearson	1	1	1	1	1	4	3	2	36	1
38	2T Pearson T	2	2	2	2	2	5	4	3	19	2
20	Pearson T	4	5	6	3	3	2	2	1	35	3
19	Pearson	3	6	14	5	4	1	1	4	21	4
26	Bi-normal T	5	3	4	4	8	3	5	29	27	5
36	2T Schnute T	7	10	12	7	6	7	6	36.5	18	7
14	Logistic Power T	12	12	7.5	9	7	8	11	7	33	9
24	Sigmoid T	11	8	9	8	5	10	8	10	32	9
34	2T Logistic Power T	10	9	10	6	9	12	7	36.5	16.5	10
25	Bi-normal	6	4	3	10	15	13	12	28	34	12
23	Sigmoid	13	25	20	23	12	11	13	11	20	13
32	2T Logistic DR T	15	14	15	11	10	14	14	17	14.5	14
4	Logistic T	29	13	11	15	32	20	19	6	1	15
18	Schnute T	23	11	7.5	12	17	16	15	5	24.5	15
6	Logistic DR T	24	17	21	13	24	17	17	14	23	17
12	Lognormal T	22	18	16	16	20	22	22	15	2	18
28	2T Normal T	26	19	17	14	16	18	20	24	14.5	18
31	2T Logistic DR	14	26	23	24	14	15	16	18	37	18
35	2T Schnute	8	21	18	29	11	6	10	36.5	28	18
10	Gaussian-Lorentzian T	20	7	5	19	30	19	18	8	24.5	19
33	2T Logistic Power	9	22	19	26	13	9	9	36.5	29	19
2	Normal T	30	20	22	20	31	21	21	20	26	21
30	2T Exponential Power T	19	24	29	21	18	27	31	16	8	21
16	Weibull T	32	16	13	22	34	37	23	9	9	22
9	Gaussian-Lorentzian	21	15	34	18	33	36	34	23	5.5	23
22	Inverse Gaussian T	25	23	30	17	19	24	27	30	12	24
13	Logistic Power	34	28	25.5	32	29	25.5	24.5	12.5	10	25.5
17	Schnute	33	28	25.5	31	26	25.5	24.5	12.5	22	25.5
27	2T Normal	38	36	27	36	28	23	26	25	16.5	27
29	2T Exponential Power	18	30	33	27	23	29	32	22	13	27
11	Lognormal	27	31	28	33	25	28	29	27	30	28
5	Logistic DR	31	27	24	30	35	33	28	19	31	30
21	Inverse Gaussian	28	32	31	34	27	30	30	31	11	30
8	Exponential Power T	16	33	38	25	21	32	37	34	7	32
7	Exponential Power	17	34	37	28	22	31	36	33	38	33
3	Logistic	36	35	32	35	36	34	33	21	5.5	34
1	Normal	37	37	35	38	37	35	35	26	3	35
15	Weibull	35	38	36	37	38	38	38	32	4	37

Table 14. Model AIC scores ranked within species and the median model rank across species.

Model Number	Model Name	Chinook	Summer Chum	Pink	Fall Chum	Coho	Broad Whitefish	Humpback Whitefish	Cisco	Other	Median
19	Pearson	1	6	7	4	1	1	1	2	36	2
20	Pearson T	2	5	8	3	3	3	2	1	19	3
14	Logistic Power T	10	13	3.5	7	2	2	3	6	35	6
37	2T Pearson	3	1	14	1	8	15	9	4	21	8
24	Sigmoid T	11	8	9	6	4	9	4	11	27	9
26	Bi-normal T	4	3	11	5	9	10	5	29	16	9
36	2T Schnute T	7	10	17	9	7	12	10	36.5	33	10
25	Bi-normal	6	4	6	10	16	11	11	28	28	11
38	2T Pearson T	5	2	20	2	11	20	14	9	17.5	11
34	2T Logistic Power T	12	9	15	8	12	13	12	36.5	11.5	12
23	Sigmoid	13	25	21	23	6	4	7	10	32	13
32	2T Logistic DR T	17	14	10	11	5	7	13	17	20	13
18	Schnute T	24	11	3.5	12	17	16	16	5	24.5	16
4	Logistic T	29	12	1	15	32	17	18	3	24.5	17
6	Logistic DR T	23	17	16	13	24	14	17	14	23	17
12	Lognormal T	22	18	12	16	20	22	22	15	1	18
10	Gaussian-Lorentzian T	21	7	2	20	30	21	19	7	11.5	19
28	2T Normal T	26	19	13	14	15	19	21	24	2	19
31	2T Logistic DR	14	26	24	24	14	5	15	19	37	19
35	2T Schnute	8	21	19	29	10	6	8	36.5	34	19
2	Normal T	31	20	18	19	31	18	20	21	29	20
30	2T Exponential Power T	19	24	30	21	19	30	31	16	5	21
16	Weibull T	33	16	5	22	34	37	23	8	3	22
33	2T Logistic Power	9	22	22	26	13	8	6	36.5	26	22
9	Gaussian-Lorentzian	20	15	27	18	33	36	34	23	17.5	23
13	Logistic Power	34	28.5	25.5	32	29	24.5	24.5	12.5	15	25.5
17	Schnute	32	28.5	25.5	31	26	24.5	24.5	12.5	14	25.5
22	Inverse Gaussian T	27	23	32	17	22	26	27	30	22	26
29	2T Exponential Power	18	30	34	27	23	28	32	22	7	27
5	Logistic DR	30	27	23	30	35	33	28	18	10	28
27	2T Normal	38	36	28	36	27	23	26	26	30	28
11	Lognormal	25	31	29	33	25	27	29	27	31	29
8	Exponential Power T	16	33	38	25	18	31	37	34	4	31
21	Inverse Gaussian	28	32	33	34	28	32	30	31	8	31
7	Exponential Power	15	34	37	28	21	29	36	33	38	33
3	Logistic	36	35	31	35	36	34	33	20	6	34
1	Normal	37	37	35	38	37	35	35	25	9	35
15	Weibull	35	38	36	37	38	38	38	32	13	37

Table 15. Estimated parameters of the Pearson T net selectivity model, by species.

Species Group	Parameter				
	τ	σ	θ	λ	ω
Chinook Salmon	1.920358	0.236804	0.621645	-0.547099	0.031161
Summer Chum	1.958998	0.184460	0.962853	-0.398320	0.038810
Pink	1.880302	0.505761	2.076237	-0.018621	0.141585
Fall Chum	1.882127	0.218895	1.188834	-0.934505	0.027642
Coho	1.975873	0.333240	1.091830	-1.690772	0.084270
Broad	1.839759	0.204851	0.914451	-1.919453	0.118968
Humpback	1.910523	0.244936	1.172361	-1.949714	0.105534
Cisco	2.063146	0.202726	1.866034	-1.252703	0.170574
Other	2.211003	0.301054	0.833062	-2.058630	0.102486

Table 16. Initial, minimum, and maximum values used in the estimation of the parameters of the Pearson T net selectivity model, by species.

		Species								
Parameter	Value	Chinook	Summer Chum	Pink	Fall Chum	Coho	Broad	Humpback	Cisco	Other
	Initial	2.0E+00	2.0E+00	2.0E+00	2.0E+00	2.0E+00	2.0E+00	2.0E+00	2.1E+00	2.0E+00
τ	Minimum	5.0E-01	-5.0E-01	5.0E-01	5.0E-01	5.0E-01	5.0E-01	5.0E-01	5.0E-01	5.0E-01
	Maximum	5.0E+00	5.0E+00	5.0E+00	5.0E+00	5.0E+00	5.0E+00	5.0E+00	5.0E+00	5.0E+00
	Initial	2.0E+00	1.0E+00	1.0E+00	1.0E+00	1.0E+00	1.0E+00	1.0E+00	2.5E-01	5.0E-01
σ	Minimum	1.0E-02	1.0E-02	1.0E-02	1.0E-02	1.0E-02	1.0E-02	1.0E-02	1.0E-02	1.0E-02
	Maximum	1.0E+99	1.0E+99	1.0E+99	1.0E+99	1.0E+99	1.0E+99	1.0E+99	1.0E+99	1.0E+99
	Initial	3.0E+00	4.0E+00	4.0E+00	4.0E+00	4.0E+00	4.0E+00	4.0E+00	1.2E+00	1.0E+00
θ	Minimum	1.0E-02	1.0E-02	1.0E-02	1.0E-02	1.0E-02	1.0E-02	1.0E-02	1.0E-02	1.0E-02
	Maximum	1.0E+99	1.0E+99	1.0E+99	1.0E+99	1.0E+99	1.0E+99	1.0E+99	1.0E+99	1.0E+99
	Initial	0.0E+00	0.0E+00	0.0E+00	0.0E+00	0.0E+00	0.0E+00	0.0E+00	0.0E+00	-2.0E+00
λ	Minimum	-1.0E+99	-1.0E+99	-1.0E+99	-1.0E+99	-1.0E+99	-1.0E+99	-1.0E+99	-1.0E+99	-1.0E+99
	Maximum	1.0E+99	1.0E+99	1.0E+99	1.0E+99	1.0E+99	1.0E+99	1.0E+99	1.0E+99	1.0E+99
	Initial	2.0E-01	1.5E-01	1.5E-01	1.5E-01	1.5E-01	1.5E-01	1.5E-01	1.5E-01	1.5E-01
ω	Minimum	0.0E+00	0.0E+00	0.0E+00	0.0E+00	0.0E+00	0.0E+00	0.0E+00	0.0E+00	0.0E+00
	Maximum	5.0E-01	5.0E-01	5.0E-01	5.0E-01	5.0E-01	5.0E-01	5.0E-01	5.0E-01	5.0E-01

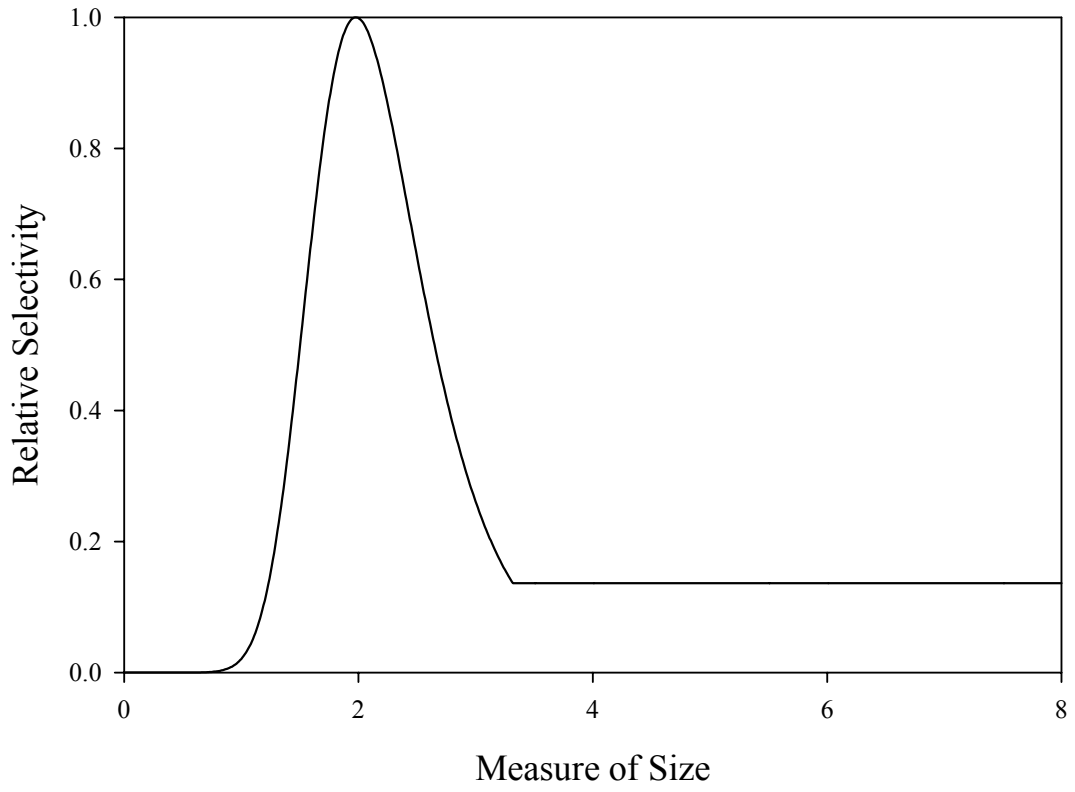

Figure 1. An example of a net selectivity model with a tangling parameter.

Appendix A
Net Selectivity Models

Notation:

x	=	ratio of length (mm) to mesh perimeter (mm)
s(x)	=	relative selectivity of x
X_g	=	that value of x that maximizes the function g(x)
G	=	the maximum value of the function g(x), i.e., $G \equiv g(X_g)$

1. Normal

$$s(x) = \exp\left[-\frac{1}{2}\left(\frac{x-\tau}{\sigma}\right)^2\right]$$

Constraints: $\sigma > 0$

2. Normal T

$$g(x) = \exp\left[-\frac{1}{2}\left(\frac{x-\tau}{\sigma}\right)^2\right]$$

$$s(x) = \begin{cases} \omega, & x > \tau \text{ and } g(x) \le \omega \\ g(x), & \text{otherwise} \end{cases}$$

Constraints: $\sigma > 0;\ 0 \le \omega \le 1$

3. Logistic

$$s(x) = \frac{4\exp\left[-\left(\frac{x-\tau}{\sigma}\right)\right]}{\left\{1+\exp\left[-\left(\frac{x-\tau}{\sigma}\right)\right]\right\}^2}$$

Constraints: $\sigma > 0$

4. Logistic T

$$g(x) = \frac{4\exp\left[-\left(\frac{x-\tau}{\sigma}\right)\right]}{\left\{1+\exp\left[-\left(\frac{x-\tau}{\sigma}\right)\right]\right\}^2}$$

$$s(x) = \begin{cases} \omega, & x > \tau \text{ and } g(x) \le \omega \\ g(x), & \text{otherwise} \end{cases}$$

Constraints: $\sigma > 0$; $0 \le \omega \le 1$

5. Logistic DR

$$s(x) = \frac{4x^{-\sigma-1}\tau^{\sigma+1}\sigma^2}{\left(\sigma - 1 + \sigma x^{-\sigma}\tau^{\sigma} + x^{-\sigma}\tau^{\sigma}\right)^2}$$

Constraints: $\tau > 0$; $\sigma > 1$

6. Logistic DR T

$$g(x) = \frac{4x^{-\sigma-1}\tau^{\sigma+1}\sigma^2}{\left(\sigma - 1 + \sigma x^{-\sigma}\tau^{\sigma} + x^{-\sigma}\tau^{\sigma}\right)^2}$$

$$s(x) = \begin{cases} \omega, & x > \tau \text{ and } g(x) \le \omega \\ g(x), & \text{otherwise} \end{cases}$$

Constraints: $\tau > 0$; $\sigma > 1$; $0 \le \omega \le 1$

7. Exponential Power

$$s(x) = x^{-\sigma-1}\tau^{\sigma+1}\exp\left[\frac{\left(\tau^{\sigma}x^{-\sigma} - 1\right)\left(-\sigma - 1\right)}{\sigma}\right]$$

Constraints: $\tau > 0$; $\sigma < -1$ or $\sigma > 0$

8. Exponential Power T

$$g(x) = x^{-\sigma-1}\tau^{\sigma+1}\exp\left[\frac{\left(\tau^{\sigma}x^{-\sigma} - 1\right)\left(-\sigma - 1\right)}{\sigma}\right]$$

$$s(x) = \begin{cases} \omega, & x > \tau \text{ and } g(x) \le \omega \\ g(x), & \text{otherwise} \end{cases}$$

Constraints: $\tau > 0$; $\sigma < -1$ or $\sigma > 0$; $0 \le \omega \le 1$

9. Gaussian-Lorentzian

$$s(x) = \left\{1 + \theta\left(\frac{x - \tau}{\sigma}\right)^2 \exp\left[\frac{1 - \theta}{2}\left(\frac{x - \tau}{\sigma}\right)^2\right]^{-1}\right.$$

Constraints: $\sigma > 0$; $0 \le \theta \le 1$

10. Gaussian-Lorentzian T

$$g(x) = \left\{1 + \theta\left(\frac{x - \tau}{\sigma}\right)^2 \exp\left[\frac{1 - \theta}{2}\left(\frac{x - \tau}{\sigma}\right)^2\right]^{-1}\right.$$

$$s(x) = \begin{cases} \omega, & x > \tau \text{ and } g(x) \le \omega \\ g(x), & \text{otherwise} \end{cases}$$

Constraints: $\sigma > 0$; $0 \le \theta \le 1$; $0 \le \omega \le 1$

11. Log Normal

$$g(x) = \exp\left[-\frac{\ln(2)}{\ln(\theta n^2}\ln\left(\frac{(x-\tau)(\theta^2-1)}{\sigma\theta}+1\right)^2\right]$$

$$k = \tau - \frac{\sigma\theta}{\theta^2-1}$$

$$s(x) = \begin{cases} 0, & x > k \text{ and } \theta > 1; \quad x < k \text{ and } \theta < 1 \\ g(x), & \text{otherwise} \end{cases}$$

Constraints: $\sigma > 0;\ \theta > 0, \theta \neq 1$

12. Log Normal T

$$g(x) = \exp\left[-\frac{\ln(2)}{\ln(\theta n^2}\ln\left(\frac{(x-\tau)(\theta^2-1)}{\sigma\theta}+1\right)^2\right]$$

$$k = \tau - \frac{\sigma\theta}{\theta^2-1}$$

$$h(x) = \begin{cases} 0, & x > k \text{ and } \theta > 1; \quad x < k \text{ and } \theta < 1 \\ g(x), & \text{otherwise} \end{cases}$$

$$s(x) = \begin{cases} \omega, & x > \tau \text{ and } g(x) \leq \omega \\ g(x), & \text{otherwise} \end{cases}$$

Constraints: $\sigma > 0;\ \theta > 0, \theta \neq 1;\ 0 \leq \omega \leq 1$

13. Logistic Power

$$s(x) = \frac{1}{\theta}\left[1+\exp\left(\frac{x+\sigma\ln(\theta)-\tau}{\sigma}\right)\right]^{\frac{-\theta-1}{\theta}}\exp\left(\frac{x+\sigma\ln(\theta)-\tau}{\sigma}\right)(\theta+1)^{\frac{\theta+1}{\theta}}$$

Constraints: $\sigma \neq 0;\ \theta > 0$

14. Logistic Power T

$$g(x) = \frac{1}{\theta}\left[1 + \exp\left(\frac{x + \sigma\ln(\theta) - \tau}{\sigma}\right)\right]^{\frac{-\theta-1}{\theta}} \exp\left(\frac{x + \sigma\ln(\theta) - \tau}{\sigma}\right)(\theta + 1)^{\frac{\theta+1}{\theta}}$$

$$s(x) = \begin{cases} \omega, & x > \tau \text{ and } g(x) \le \omega \\ g(x), & \text{otherwise} \end{cases}$$

Constraints: $\sigma \neq 0;\ \theta > 0;\ 0 \le \omega \le 1$

15. Weibull

$$g(x) = \left(\frac{\theta - 1}{\theta}\right)^{\frac{1-\theta}{\theta}} \left[\frac{x - \tau}{\sigma} + \left(\frac{\theta - 1}{\theta}\right)^{\frac{1}{\theta}}\right]^{\theta-1} \exp\left[-\left(\frac{x - \tau}{\sigma} + \left(\frac{\theta - 1}{\theta}\right)^{\frac{1}{\theta}}\right)^{\theta} + \frac{\theta - 1}{\theta}\right]$$

$$k = \tau - \sigma\left(\frac{\theta - 1}{\theta}\right)^{\frac{1}{\theta}}$$

$$s(x) = \begin{cases} 0, & x < k \\ g(x), & \text{otherwise} \end{cases}$$

Constraints: $\sigma > 0;\ \theta > 1$

16. Weibull T

$$g(x) = \left(\frac{\theta - 1}{\theta}\right)^{\frac{1-\theta}{\theta}} \left[\frac{x - \tau}{\sigma} + \left(\frac{\theta - 1}{\theta}\right)^{\frac{1}{\theta}}\right]^{\theta - 1} \exp\left[-\left(\frac{x - \tau}{\sigma} + \left(\frac{\theta - 1}{\theta}\right)^{\frac{1}{\theta}}\right)^{\theta} + \frac{\theta - 1}{\theta}\right]$$

$$k = \tau - \sigma\left(\frac{\theta - 1}{\theta}\right)^{\frac{1}{\theta}}$$

$$s(x) = \begin{cases} 0, & x \le k \\ \omega, & x > \tau; \quad g(x) < \omega \\ g(x), & \text{otherwise} \end{cases}$$

Constraints: $\sigma > 0$; $\theta > 1$; $0 \le \omega \le 1$

17. Schnute

$$g(x) = \exp[-\alpha(x - \tau)](1 - \beta)^{1 - \frac{1}{\beta}} \{1 - \mathrm{MIN}(1, \beta\exp[-\alpha(x - \tau)])\}^{\frac{1}{\beta} - 1}$$

$$s(x) = \begin{cases} g(x), & \beta \ne 0 \\ \exp[-\alpha(x - \tau)], & \beta = 0, \quad x \ge \tau \\ 0, & \beta = 0, \quad x < \tau \end{cases}$$

Constraints: $\alpha > 0$; $\beta < 1$

18. Schnute T

$$g(x) = \exp[-\alpha(x-\tau)](1-\beta)^{1-\frac{1}{\beta}}\{1 - \mathrm{MIN}(1, \beta\exp[-\alpha(x-\tau)])\}^{\frac{1}{\beta}-1}$$

$$h(x) = \begin{cases} g(x), & \beta \neq 0 \\ \exp[-\alpha(x-\tau)], & \beta = 0, \quad x \geq \tau \\ 0, & \beta = 0, \quad x < \tau \end{cases}$$

$$s(x) = \begin{cases} \omega, & x > \tau, \quad h(x) < \omega \\ h(x), & \text{otherwise} \end{cases}$$

Constraints: $\alpha > 0$; $\beta < 1$; $0 \leq \omega \leq 1$

19. Pearson

$$s(x) = \left(1 + \frac{\lambda^2}{4\theta^2}\right)^{\theta} \left[1 + \frac{\left(x - \frac{\sigma\lambda}{2\theta} - \tau\right)^2}{\sigma^2}\right]^{-\theta} \exp\left\{-\lambda\left[\tan^{-1}\left(\frac{x - \frac{\sigma\lambda}{2\theta} - \tau}{\sigma}\right) + \tan^{-1}\left(\frac{\lambda}{2\theta}\right)\right]\right\}$$

Constraints: $\sigma > 0$; $\theta > 0$

20. Pearson T

$$g(x) = \left(1 + \frac{\lambda^2}{4\theta^2}\right)^{\theta} \left[1 + \frac{\left(x - \frac{\sigma\lambda}{2\theta} - \tau\right)^2}{\sigma^2}\right]^{-\theta} \exp\left\{-\lambda\left[\tan^{-1}\left(\frac{x - \frac{\sigma\lambda}{2\theta} - \tau}{\sigma}\right) + \tan^{-1}\left(\frac{\lambda}{2\theta}\right)\right]\right\}$$

$$s(x) = \begin{cases} \omega, & x > \tau \text{ and } g(x) \leq \omega \\ g(x), & \text{otherwise} \end{cases}$$

Constraints: $\sigma > 0$; $\theta > 0$; $0 \leq \omega \leq 1$

21. Inverse Gaussian

$$\theta = \left(1 + \frac{9\mu^2}{4\lambda^2}\right)^{\frac{1}{2}} + \frac{3\mu}{2\lambda}$$

$$s(x) = \left(\frac{\sigma\mu\theta}{x - \tau}\right)^{\frac{3}{2}} \exp\left[\frac{\lambda}{2\mu}\left(\frac{(\theta - 1)^2}{\theta} - \frac{(x - \tau - \sigma\mu)^2}{\sigma\mu(x - \tau)}\right)\right]$$

Constraints: $\mu > 0;\ \lambda > 0;\ \sigma > 0$

22. Inverse Gaussian T

$$\theta = \left(1 + \frac{9\mu^2}{4\lambda^2}\right)^{\frac{1}{2}} + \frac{3\mu}{2\lambda}$$

$$g(x) = \left(\frac{\sigma\mu\theta}{x - \tau}\right)^{\frac{3}{2}} \exp\left[\frac{\lambda}{2\mu}\left(\frac{(\theta - 1)^2}{\theta} - \frac{(x - \tau - \sigma\mu)^2}{\sigma\mu(x - \tau)}\right)\right]$$

$$k = \sigma\mu\theta + \tau$$

$$s(x) = \begin{cases} \omega, & x > k \text{ and } g(x) \le \omega \\ g(x), & \text{otherwise} \end{cases}$$

Constraints: $\mu > 0;\ \lambda > 0;\ \sigma > 0;\ 0 \le \omega \le 1$

23. Sigmoid

$$g(x) = \left[1 + \exp\left(-\frac{x - \tau + \frac{\sigma}{2}}{\theta}\right)\right]^{-1}\left[1 - \left\{1 + \exp\left(-\frac{x - \tau - \frac{\sigma}{2}}{\lambda}\right)\right\}^{-1}\right]$$

$$s(x) = g(x)/G$$

Constraints: $\sigma > 0;\ \theta > 0;\ \lambda > 0$

24. Sigmoid T

$$g(x) = \left[1 + \exp\left(-\frac{x - \tau + \frac{\sigma}{2}}{\theta}\right)\right]^{-1}\left[1 - \left\{1 + \exp\left(-\frac{x - \tau - \frac{\sigma}{2}}{\lambda}\right)\right\}^{-1}\right]$$

$$h(x) = g(x)/G$$

$$s(x) = \begin{cases} \omega, & x > X_g \text{ and } h(x) \le \omega \\ h(x), & \text{otherwise} \end{cases}$$

Constraints: $\sigma > 0;\ \theta > 0;\ \lambda > 0$

25. Bi-normal

$$g(x) = \exp\left[-\frac{1}{2}\left(\frac{x - \tau_1}{\sigma_1}\right)^2\right] + \alpha\exp\left[-\frac{1}{2}\left(\frac{x - \tau_2}{\sigma_2}\right)^2\right]$$

$$s(x) = g(x)/G$$

Constraints: $\sigma_1 > 0;\ \sigma_2 > 0;\ \alpha > 0$

26. Bi-normal T

$$g(x) = \exp\left[-\frac{1}{2}\left(\frac{x-\tau_1}{\sigma_1}\right)^2\right] + \alpha\exp\left[-\frac{1}{2}\left(\frac{x-\tau_2}{\sigma_2}\right)^2\right]$$

$$h(x) = g(x)/G$$

$$s(x) = \begin{cases} \omega, & x > X_g \text{ and } h(x) \le \omega \\ h(x), & \text{otherwise} \end{cases}$$

Constraints: $\sigma_1 > 0$; $\sigma_2 > 0$; $\alpha > 0$

27. 2T Normal

This model is composed of two 'tails' of the form given in Model 1, which intersect at $x = \tau$.

$$g_1(x) = \exp\left[-\frac{1}{2}\left(\frac{x-\tau}{\sigma_1}\right)^2\right]$$

$$g_2(x) = \exp\left[-\frac{1}{2}\left(\frac{x-\tau}{\sigma_2}\right)^2\right]$$

$$s(x) = \begin{cases} g_1(x), & x < \tau \\ g_2(x), & x \ge \tau \end{cases}$$

Constraints: $\sigma_1 > 0$; $\sigma_2 > 0$

All the following two-tailed (2T) models are formed similarly, from other models, so the equations of subsequent models will be omitted.

28. 2T Normal T

This model is composed of two 'tails' of the form given in Model 2, which intersect at $x = \tau$. Also see the example given within the description of Model 27.

29. 2T Exponential Power

This model is composed of two 'tails' of the form given in Model 7, which intersect at $x = \tau$. Also see the example given within the description of Model 27.

30. 2T Exponential Power T

This model is composed of two 'tails' of the form given in Model 8, which intersect at $x = \tau$. Also see the example given within the description of Model 27.

31. 2T Logistic DR

This model is composed of two 'tails' of the form given in Model 5, which intersect at $x = \tau$. Also see the example given within the description of Model 27.

32. 2T Logistic DR T

This model is composed of two 'tails' of the form given in Model 6, which intersect at $x = \tau$. Also see the example given within the description of Model 27.

33. 2T Logistic Power

This model is composed of two 'tails' of the form given in Model 13, which intersect at $x = \tau$. Also see the example given within the description of Model 27.

34. 2T Logistic Power T

This model is composed of two 'tails' of the form given in Model 14, which intersect at $x = \tau$. Also see the example given within the description of Model 27.

35. 2T Schnute

This model is composed of two 'tails' of the form given in Model 17, which intersect at $x = \tau$. Also see the example given within the description of Model 27.

36. 2T Schnute T

This model is composed of two 'tails' of the form given in Model 18, which intersect at $x = \tau$. Also see the example given within the description of Model 27.

37. 2T Pearson

This model is composed of two 'tails' of the form given in Model 19, which intersect at $x = \tau$. Also see the example given within the description of Model 27.

38. 2T Pearson T

This model is composed of two 'tails' of the form given in Model 20, which intersect at $x = \tau$. Also see the example given within the description of Model 27.

Appendix B1
Chinook Salmon Diagnostic Plots
Figure B1.1 to Figure B1.38

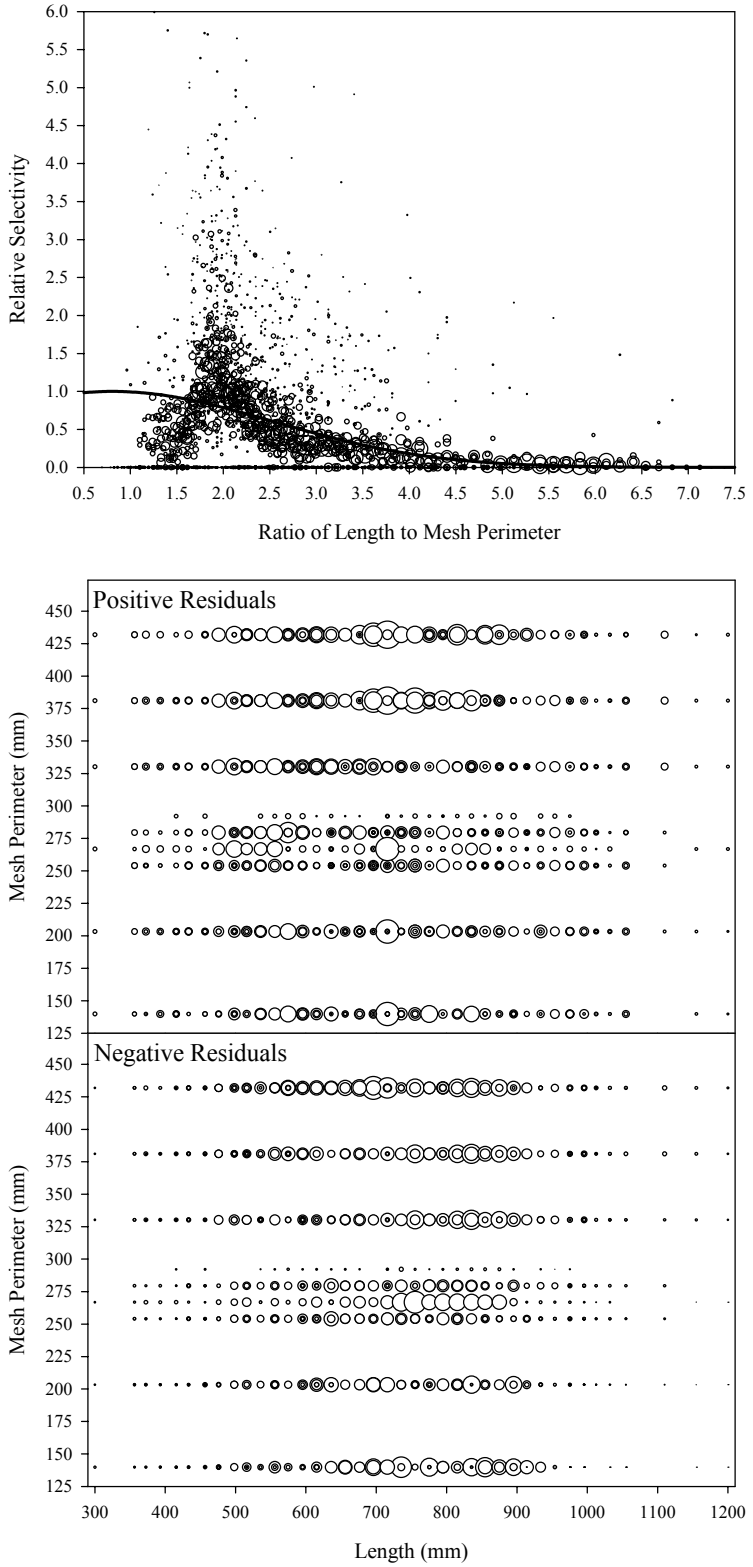

Figure B1.1. Plots of CPUE data scaled to a net selectivity model (top) and CPUE residuals (bottom); Chinook salmon data and Model 1.

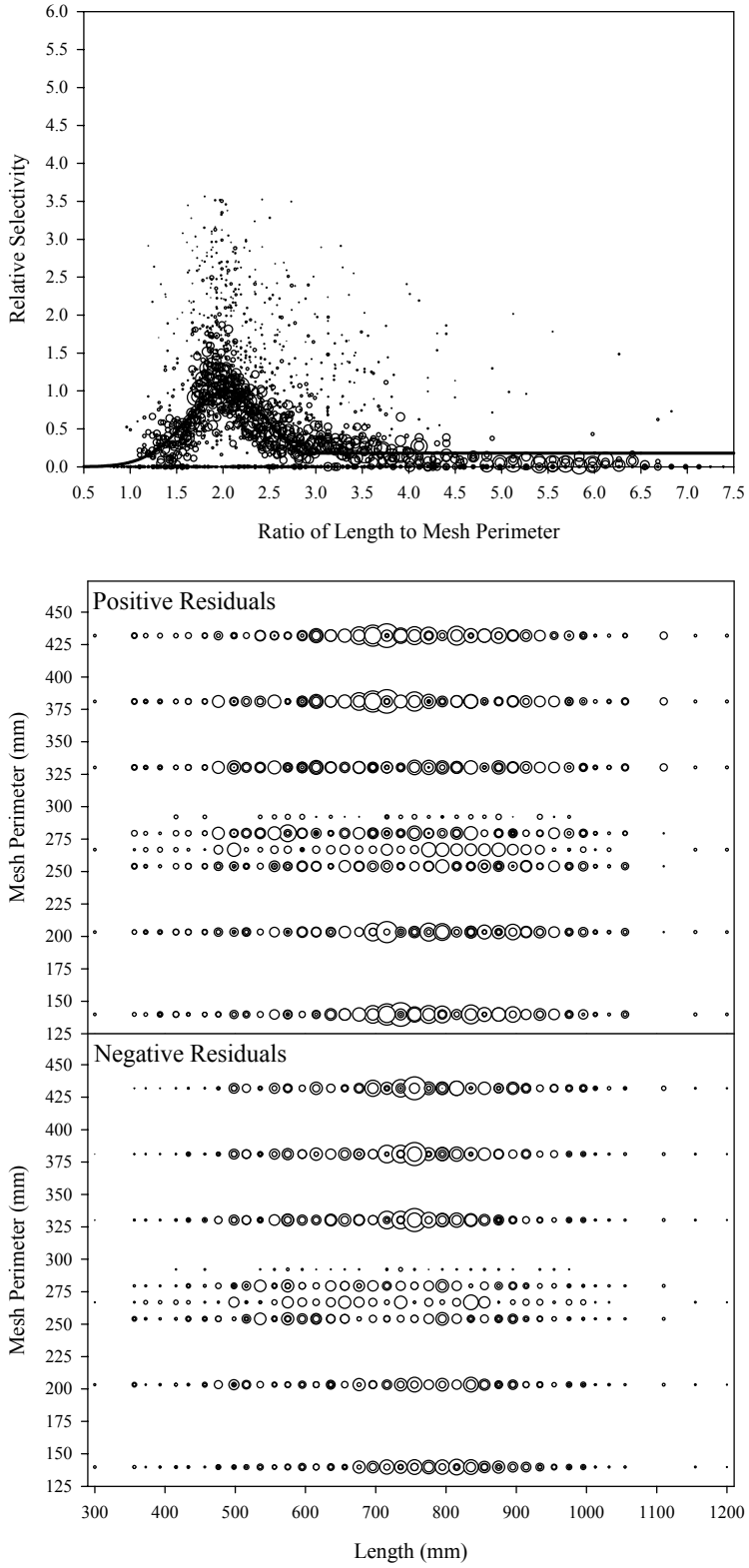

Figure B1.2. Plots of CPUE data scaled to a net selectivity model (top) and CPUE residuals (bottom); Chinook salmon data and Model 2.

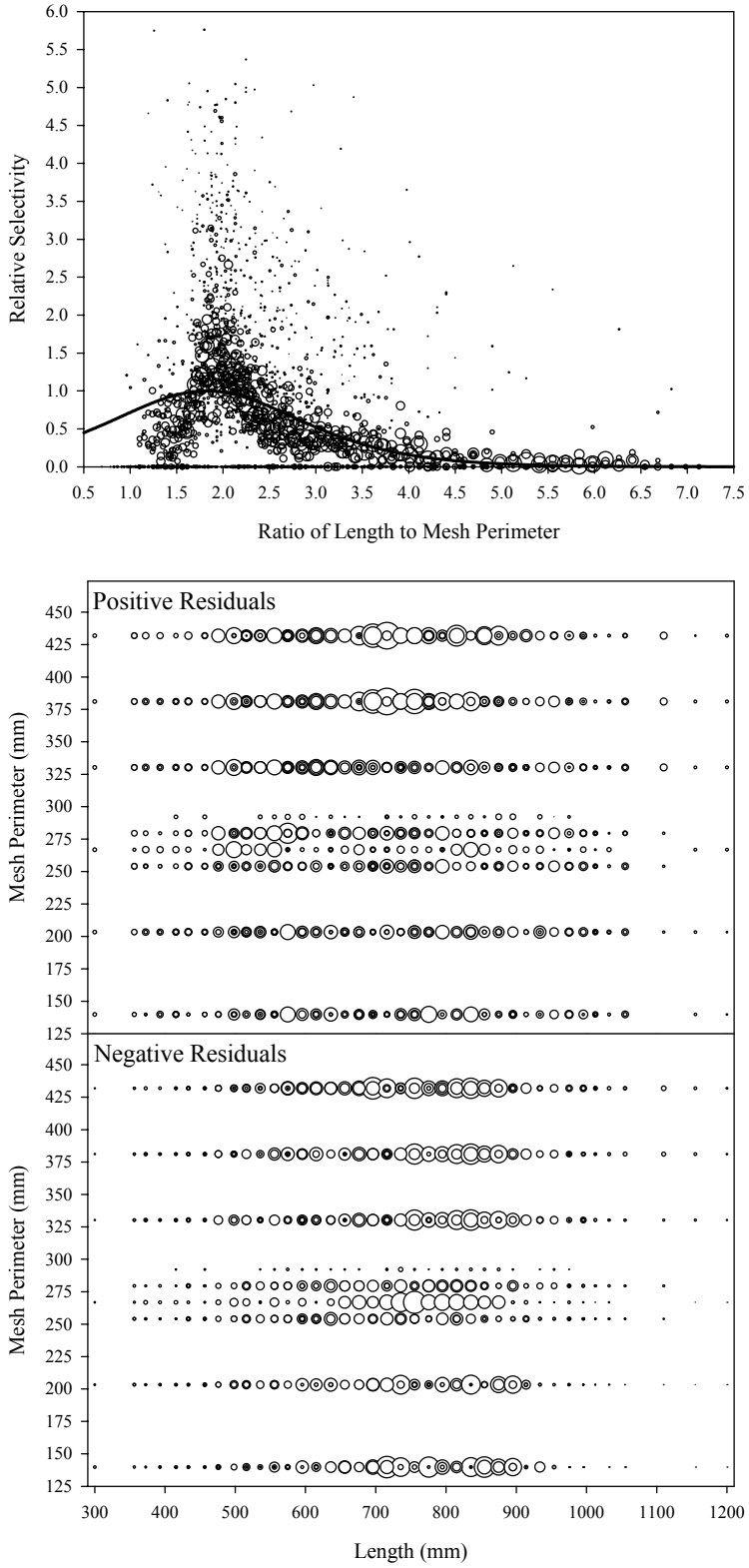

Figure B1.3. Plots of CPUE data scaled to a net selectivity model (top) and CPUE residuals (bottom); Chinook salmon data and Model 3.

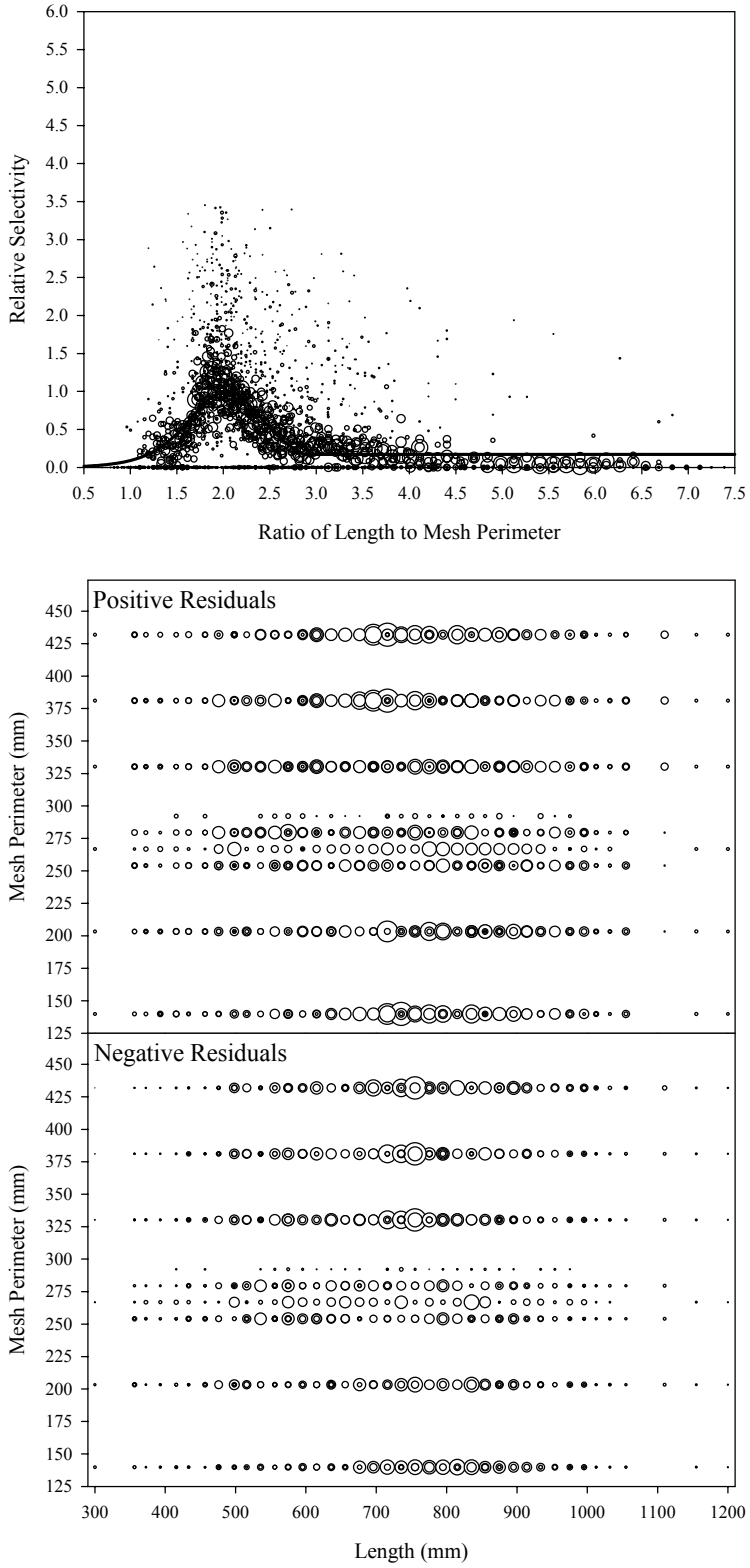

Figure B1.4. Plots of CPUE data scaled to a net selectivity model (top) and CPUE residuals (bottom); Chinook salmon data and Model 4.

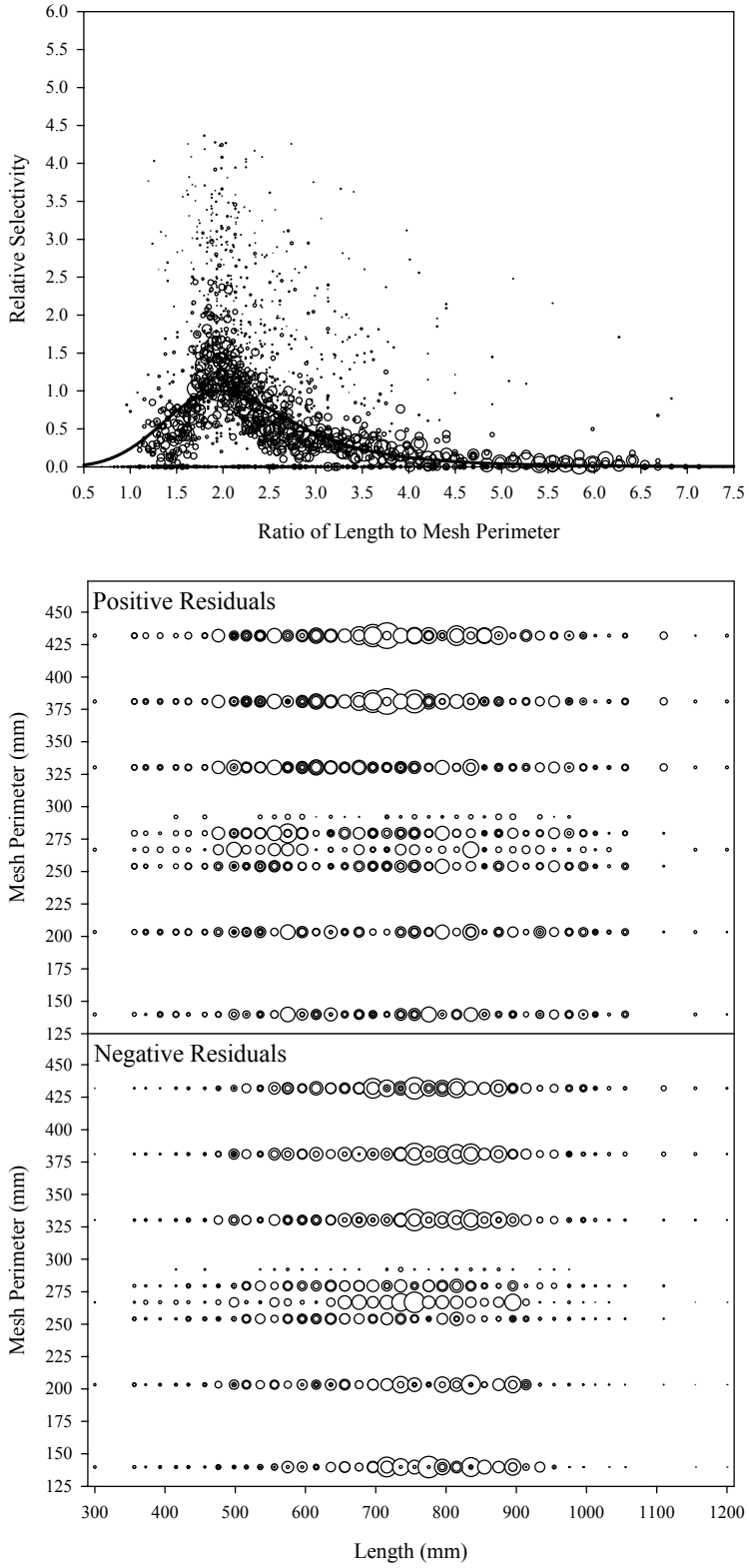

Figure B1.5. Plots of CPUE data scaled to a net selectivity model (top) and CPUE residuals (bottom); Chinook salmon data and Model 5.

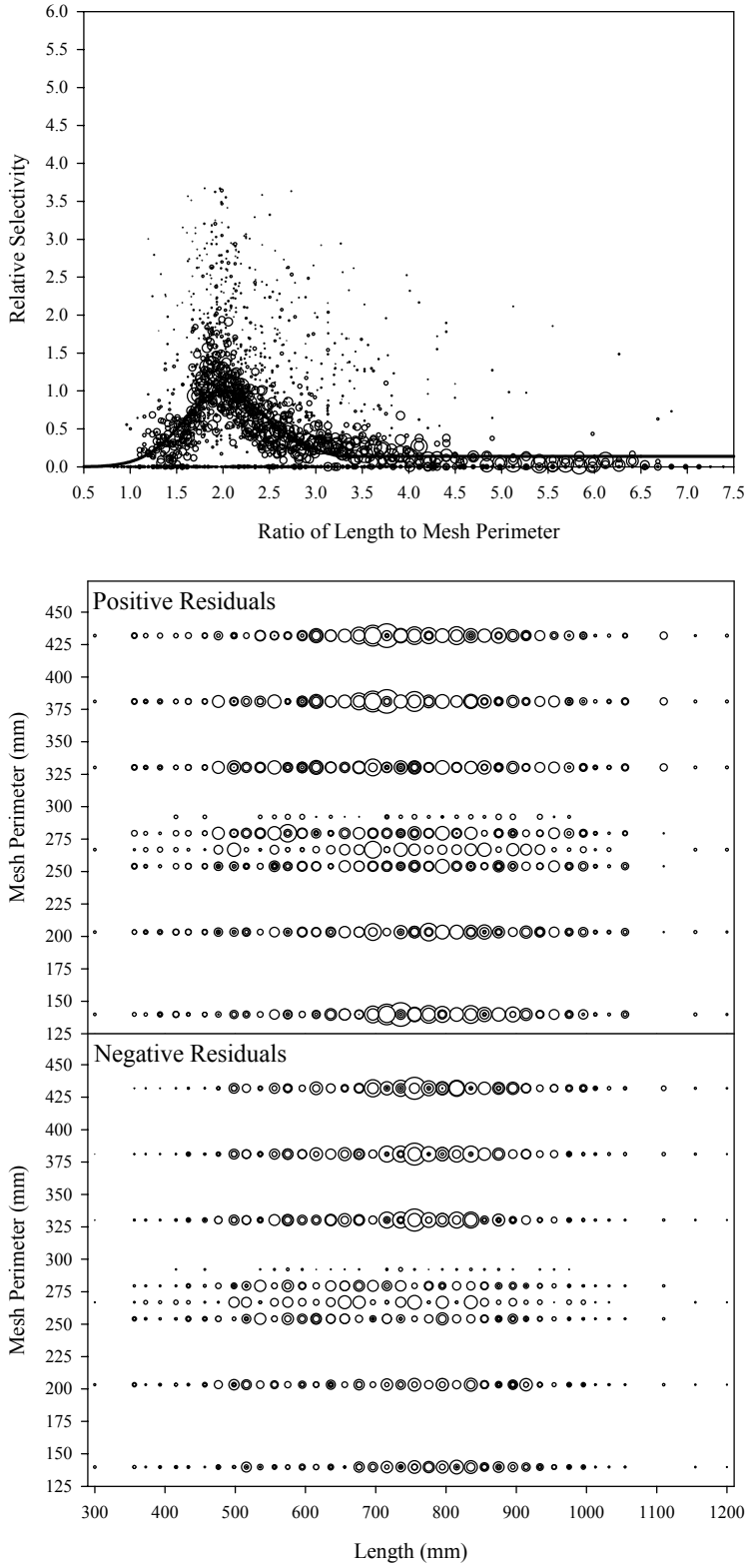

Figure B1.6. Plots of CPUE data scaled to a net selectivity model (top) and CPUE residuals (bottom); Chinook salmon data and Model 6.

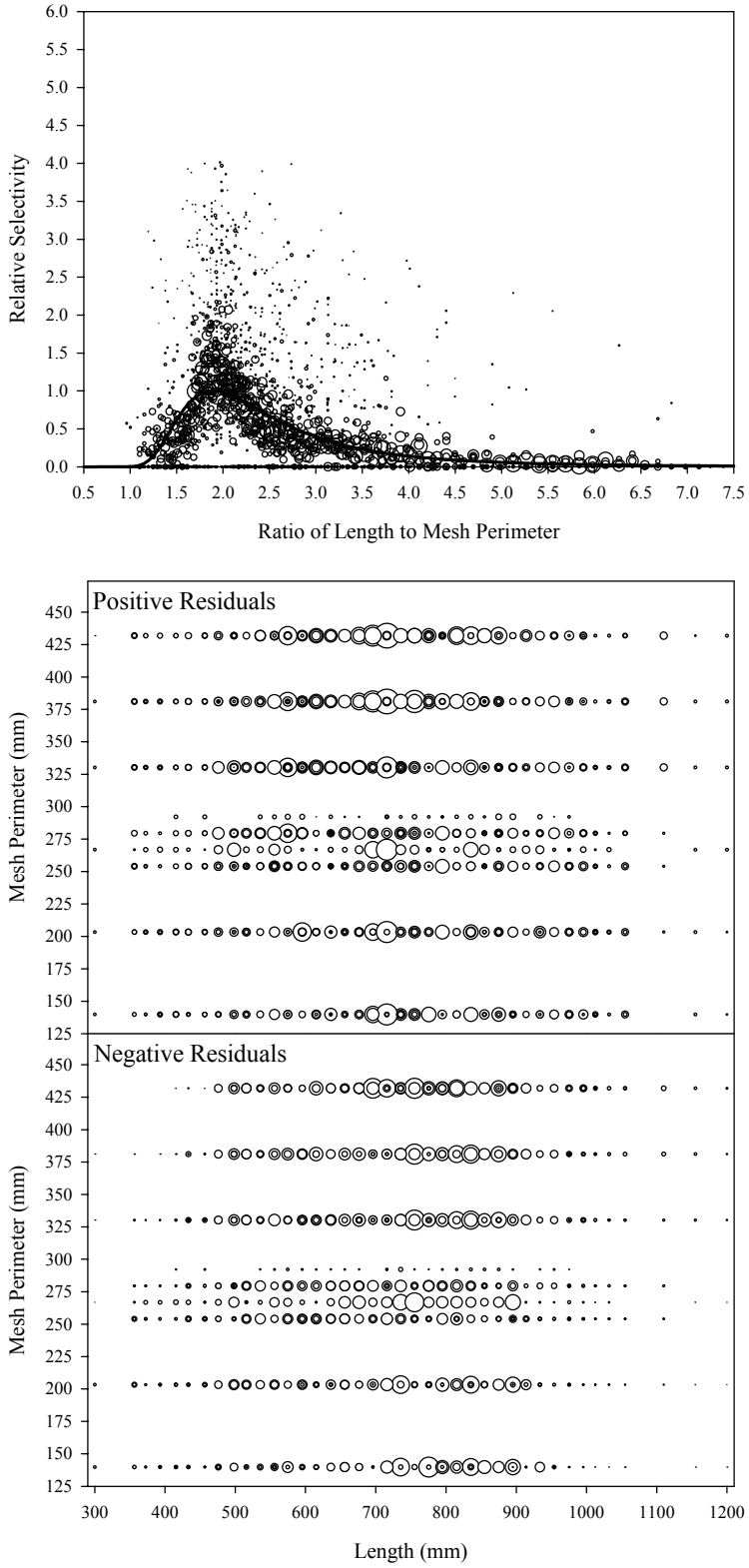

Figure B1.7. Plots of CPUE data scaled to a net selectivity model (top) and CPUE residuals (bottom); Chinook salmon data and Model 7.

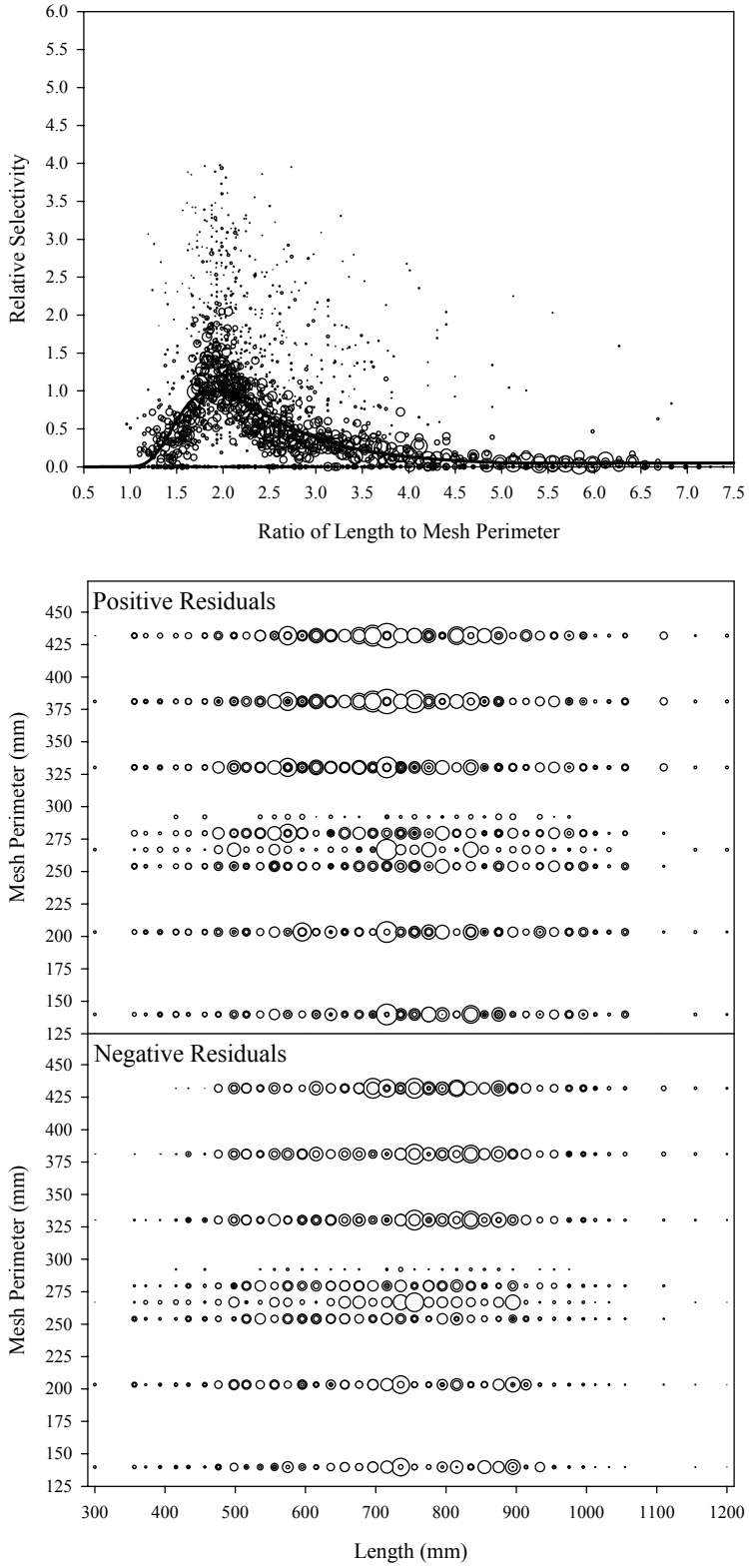

Figure B1.8. Plots of CPUE data scaled to a net selectivity model (top) and CPUE residuals (bottom); Chinook salmon data and Model 8.

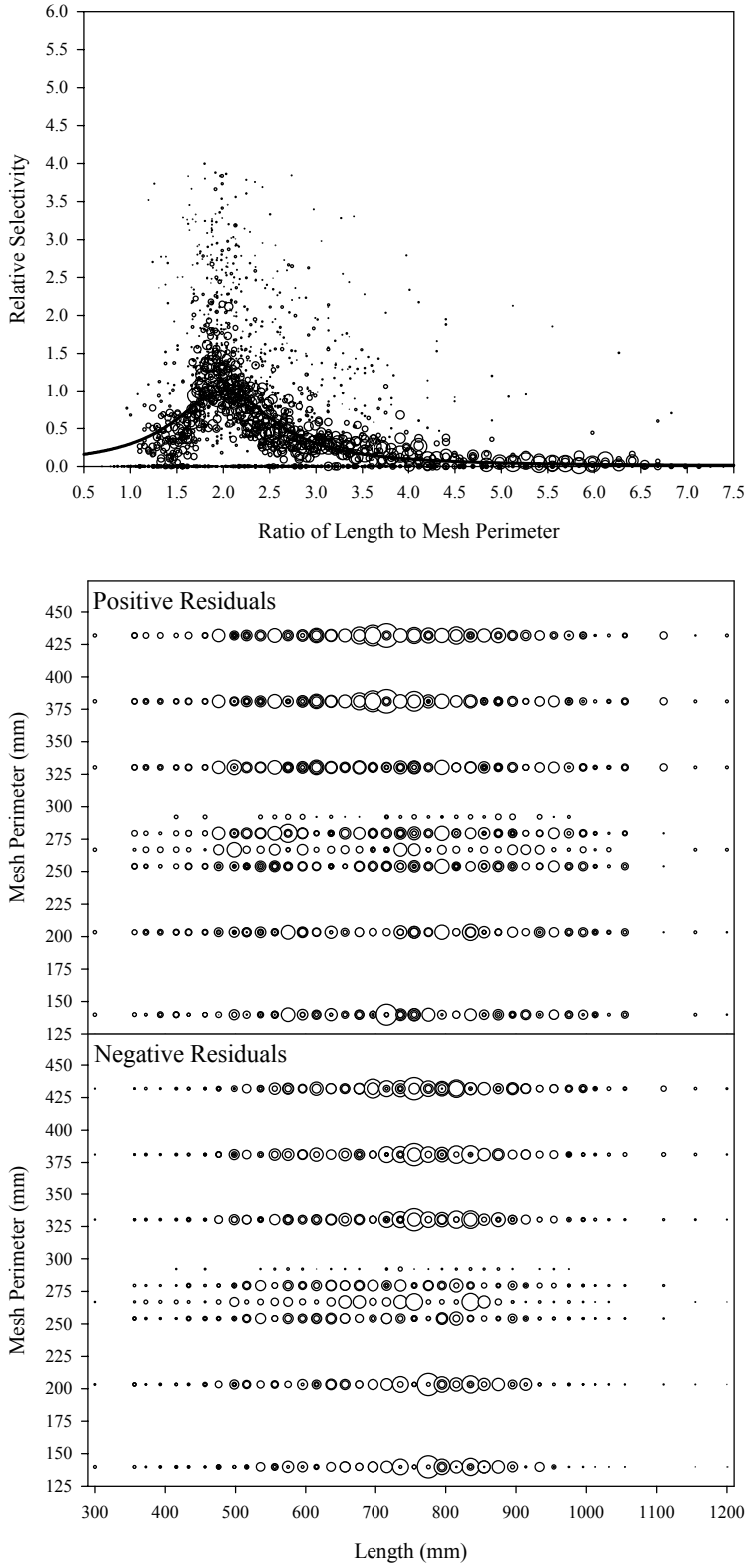

Figure B1.9. Plots of CPUE data scaled to a net selectivity model (top) and CPUE residuals (bottom); Chinook salmon data and Model 9.

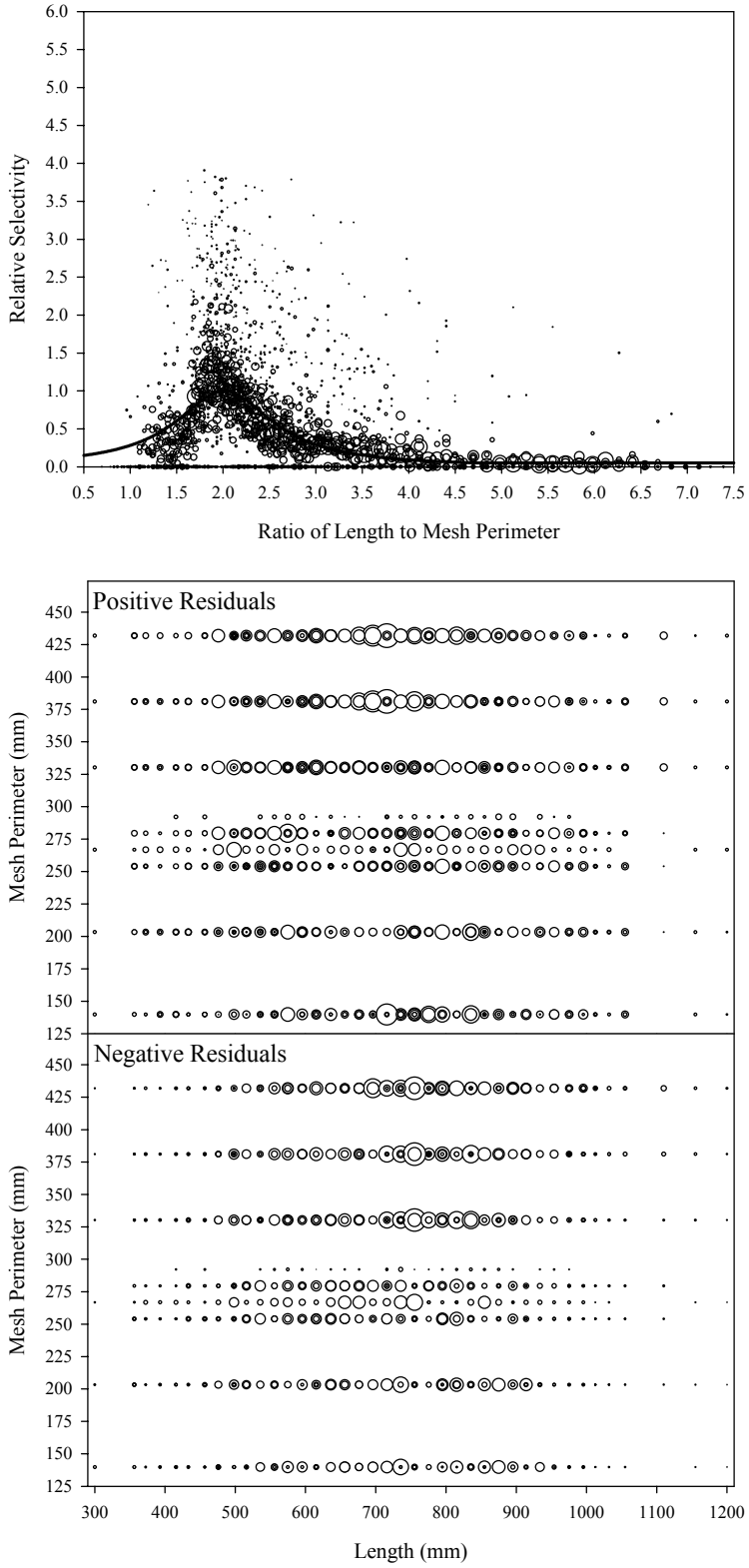

Figure B1.10. Plots of CPUE data scaled to a net selectivity model (top) and CPUE residuals (bottom); Chinook salmon data and Model 10.

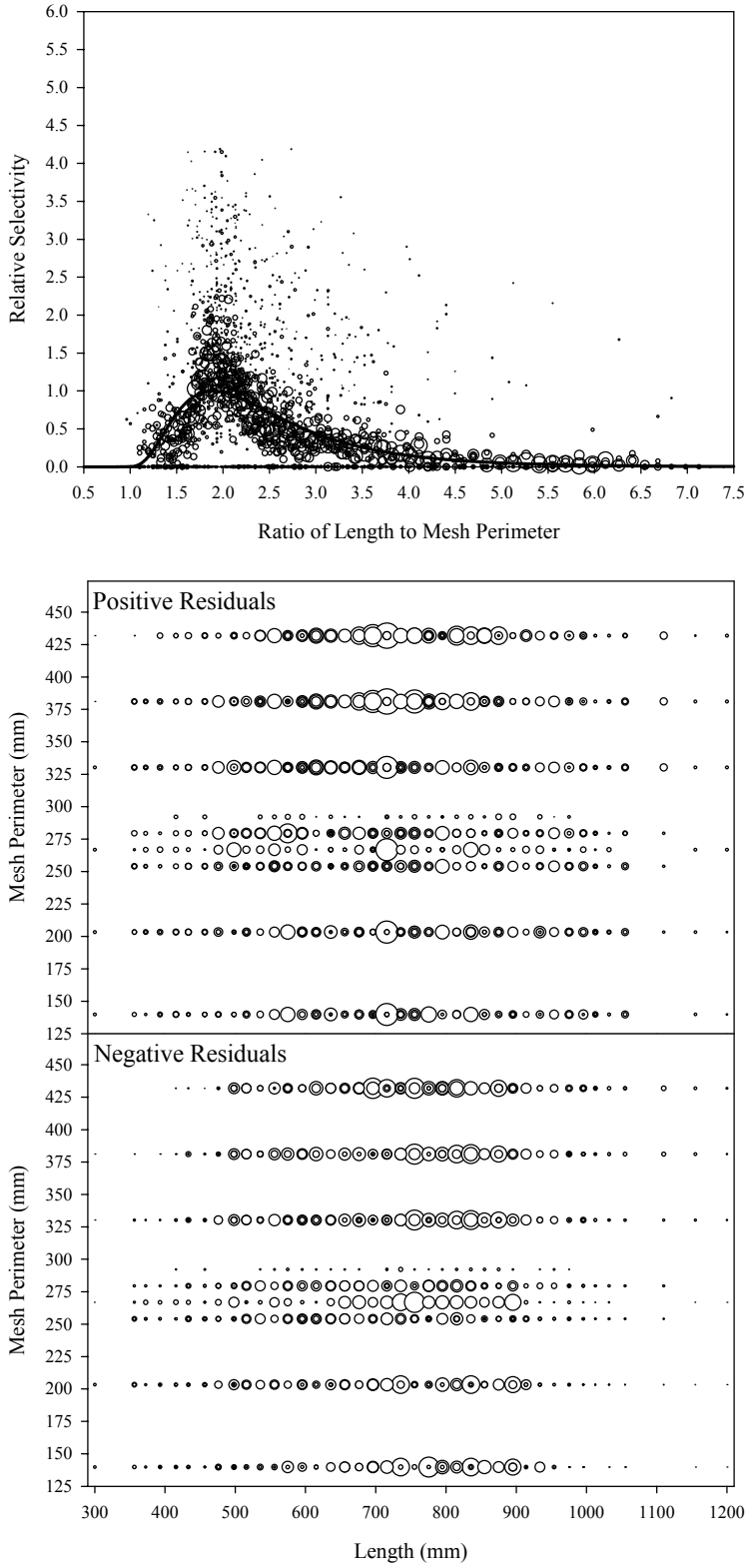

Figure B1.11. Plots of CPUE data scaled to a net selectivity model (top) and CPUE residuals (bottom); Chinook salmon data and Model 11.

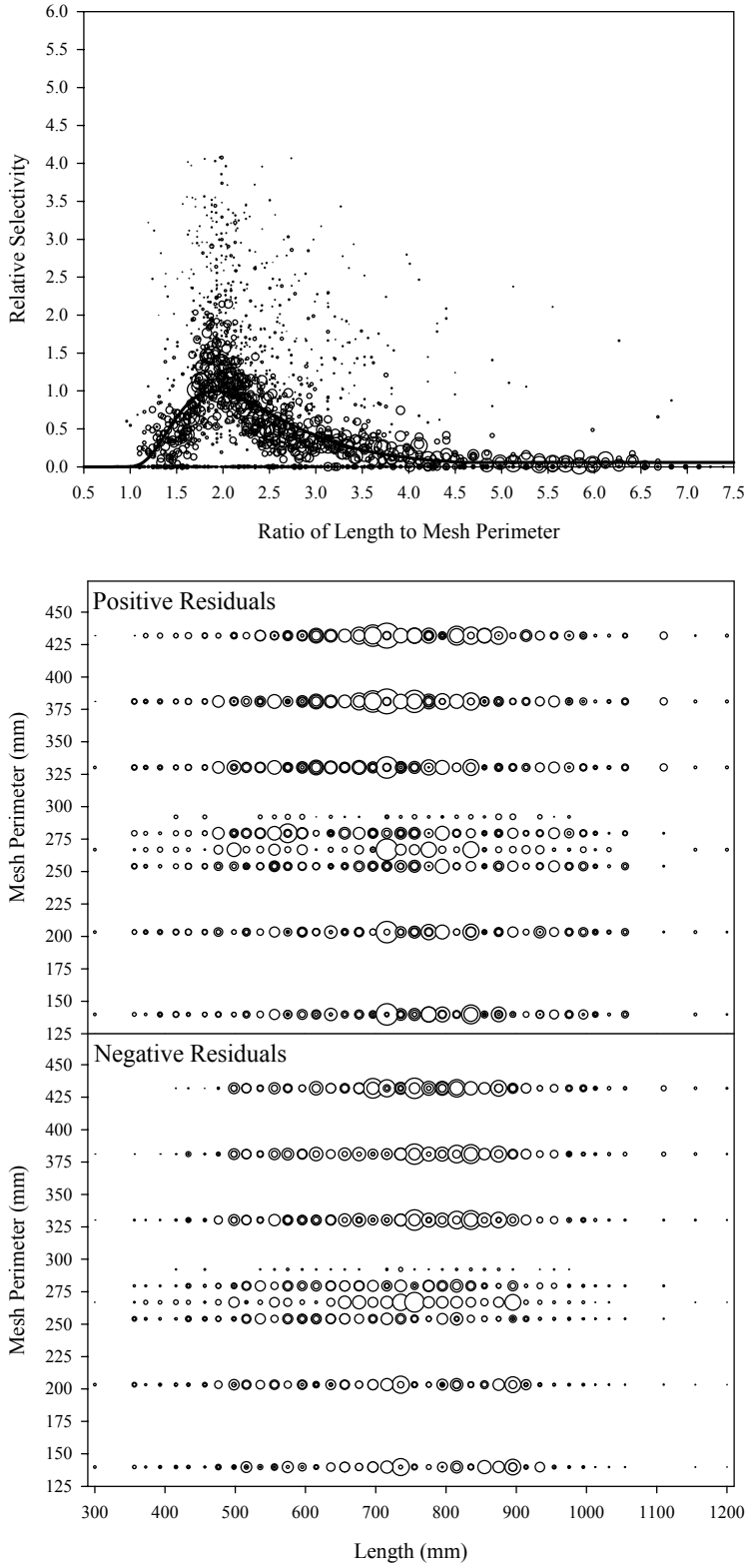

Figure B1.12. Plots of CPUE data scaled to a net selectivity model (top) and CPUE residuals (bottom); Chinook salmon data and Model 12.

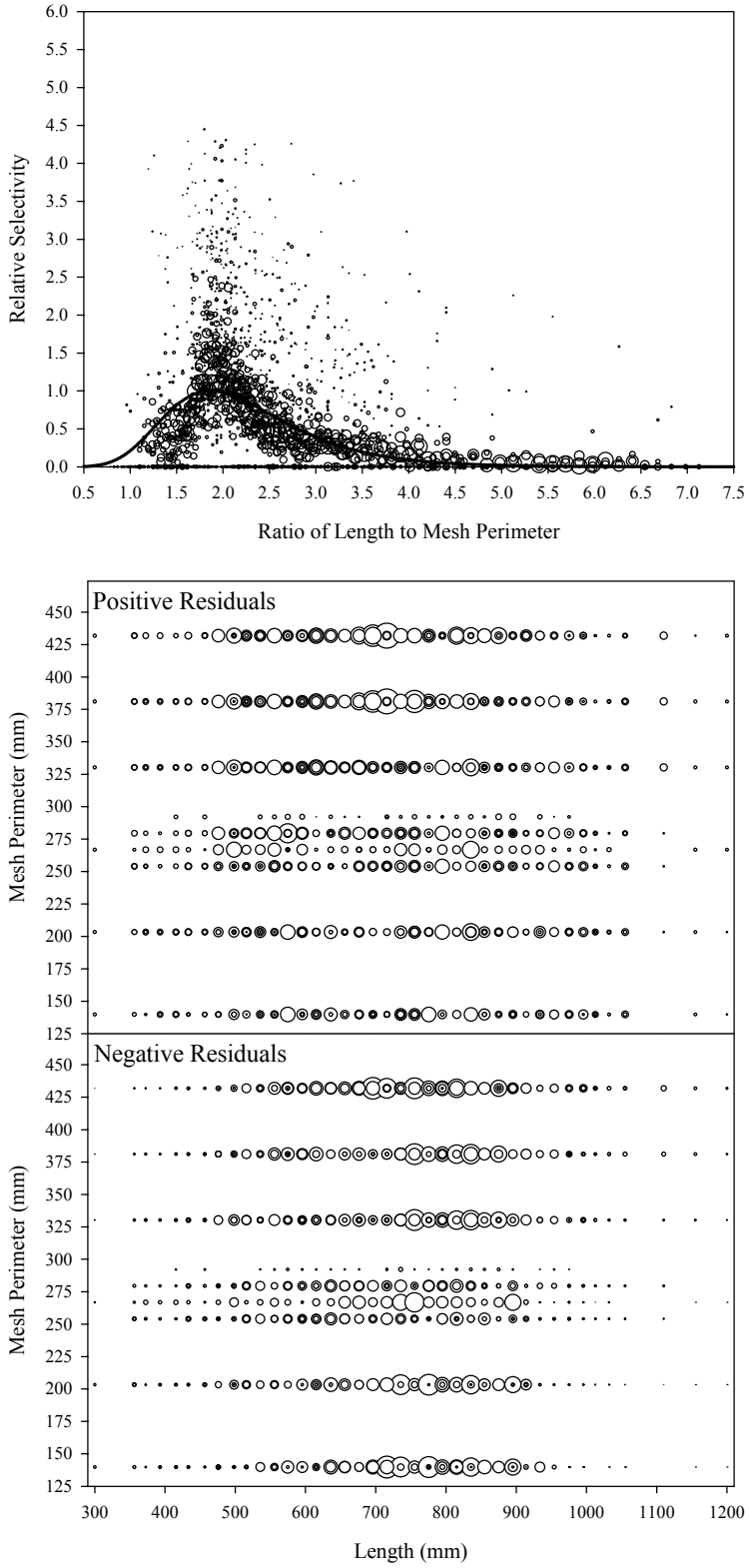

Figure B1.13. Plots of CPUE data scaled to a net selectivity model (top) and CPUE residuals (bottom); Chinook salmon data and Model 13.

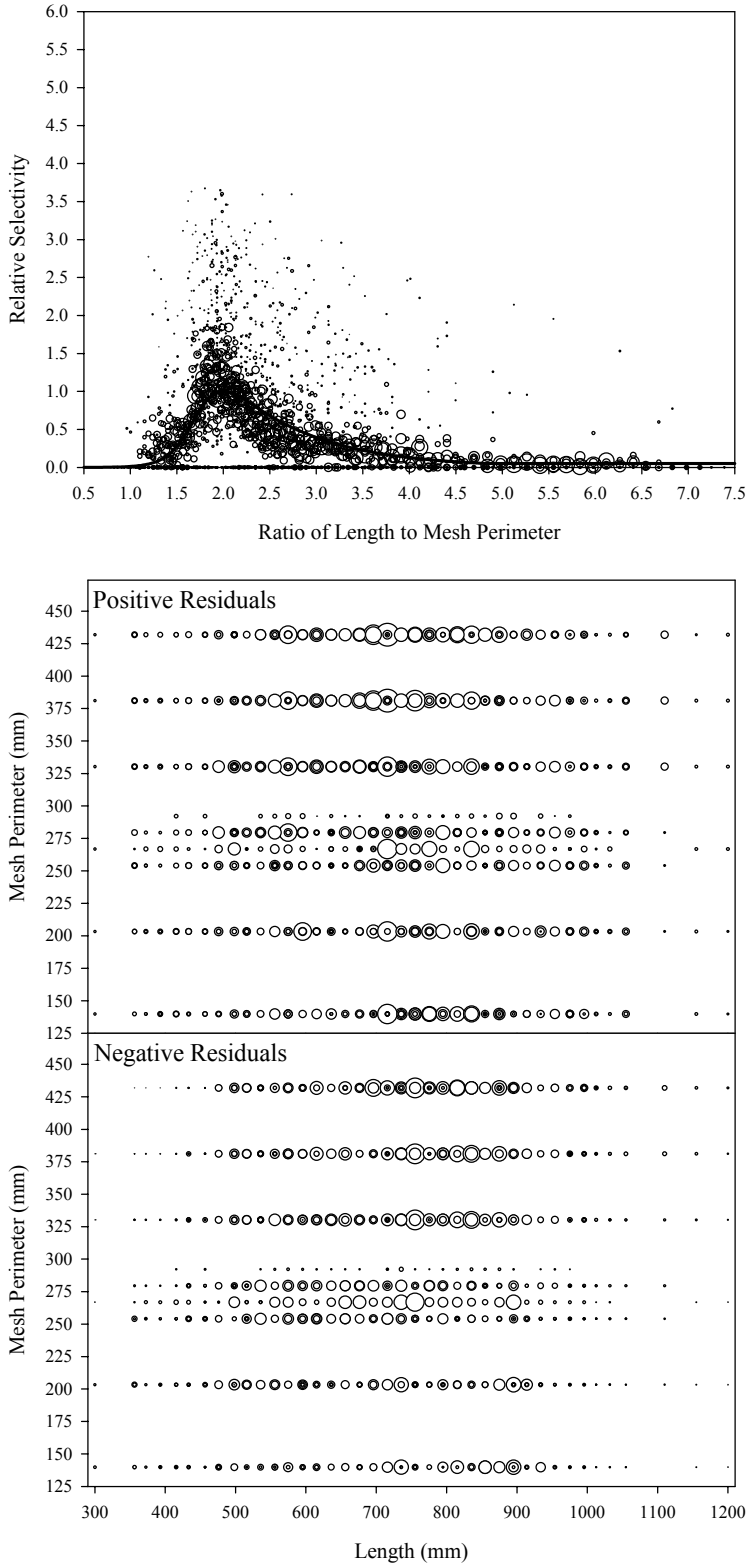

Figure B1.14. Plots of CPUE data scaled to a net selectivity model (top) and CPUE residuals (bottom); Chinook salmon data and Model 14.

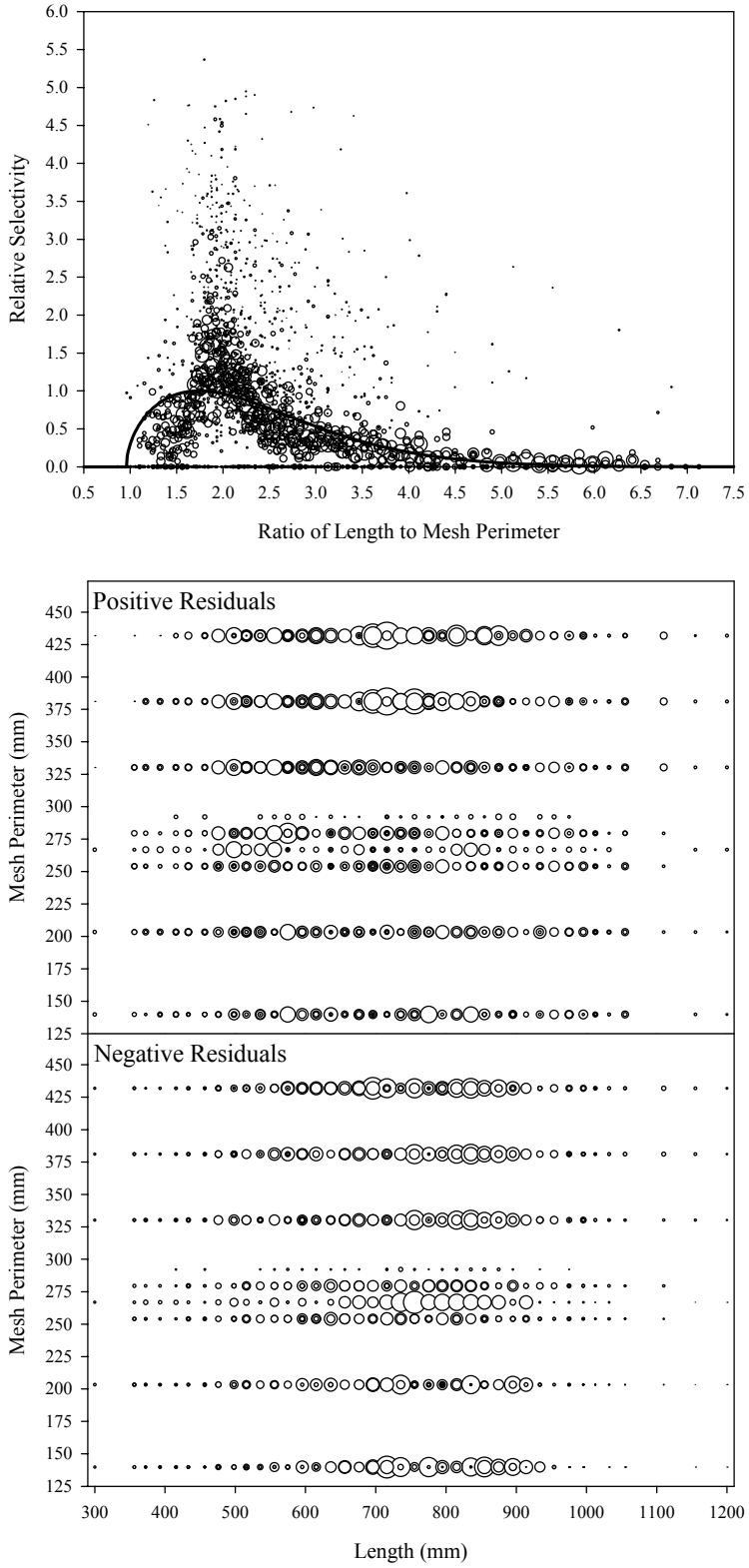

Figure B1.15. Plots of CPUE data scaled to a net selectivity model (top) and CPUE residuals (bottom); Chinook salmon data and Model 15.

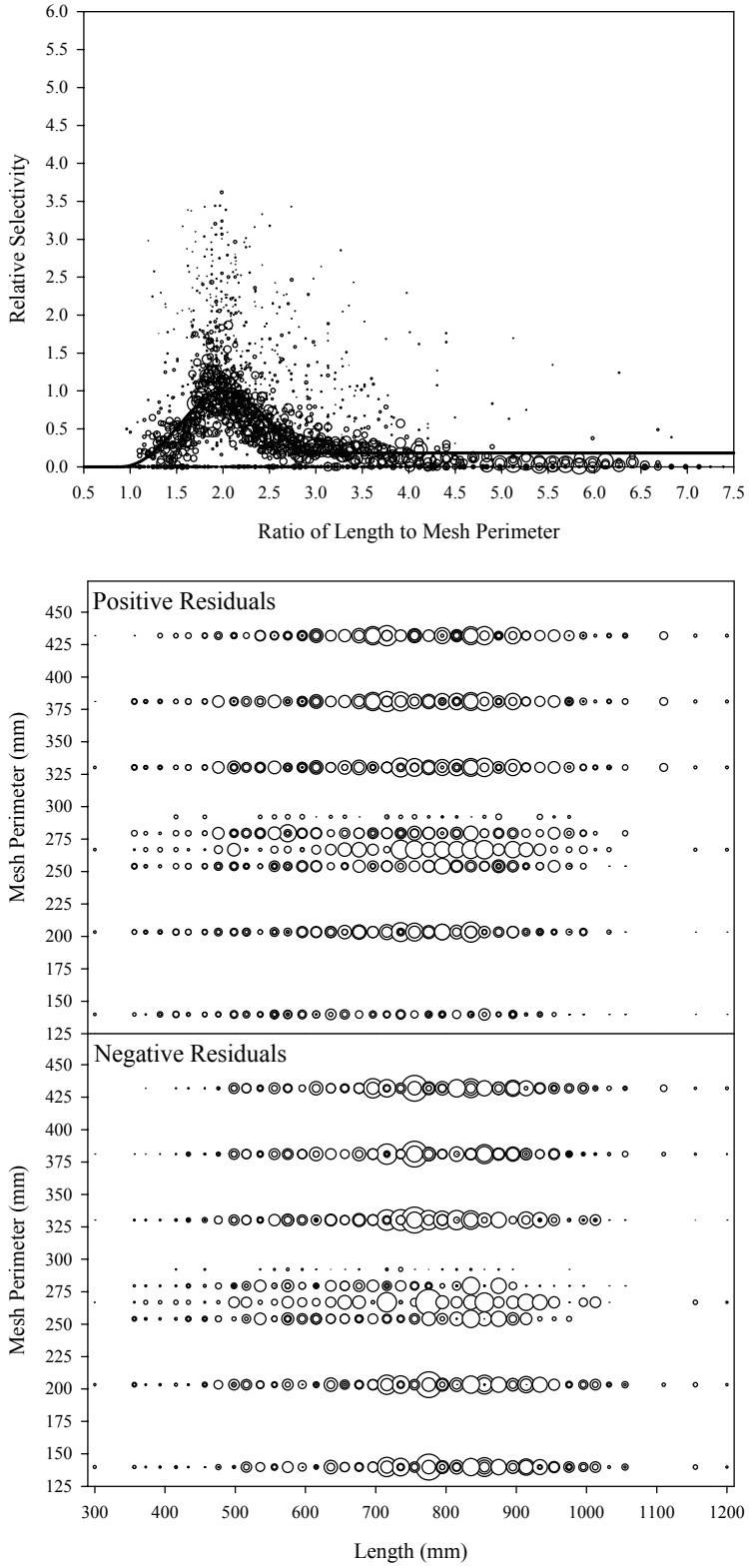

Figure B1.16. Plots of CPUE data scaled to a net selectivity model (top) and CPUE residuals (bottom); Chinook salmon data and Model 16.

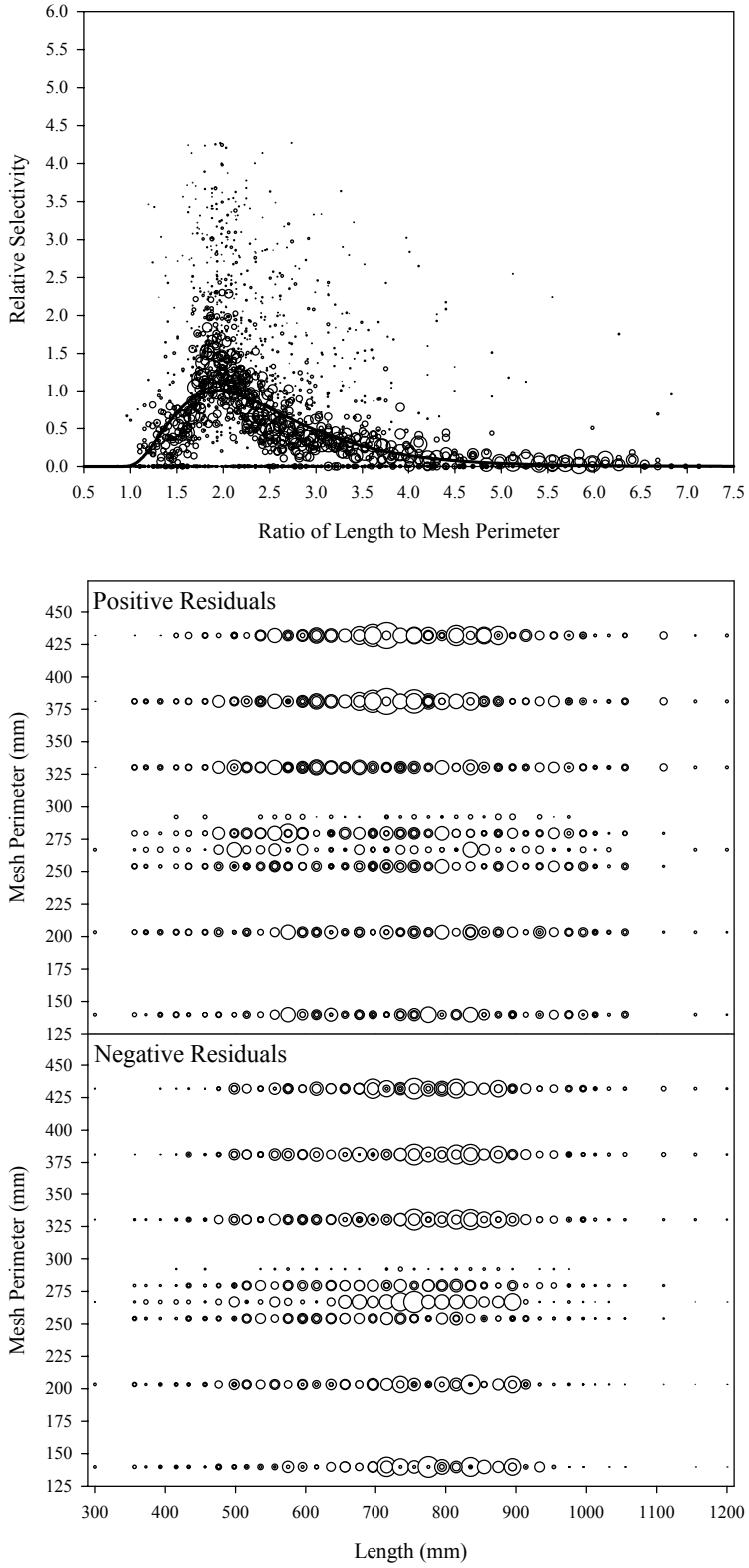

Figure B1.17. Plots of CPUE data scaled to a net selectivity model (top) and CPUE residuals (bottom); Chinook salmon data and Model 17.

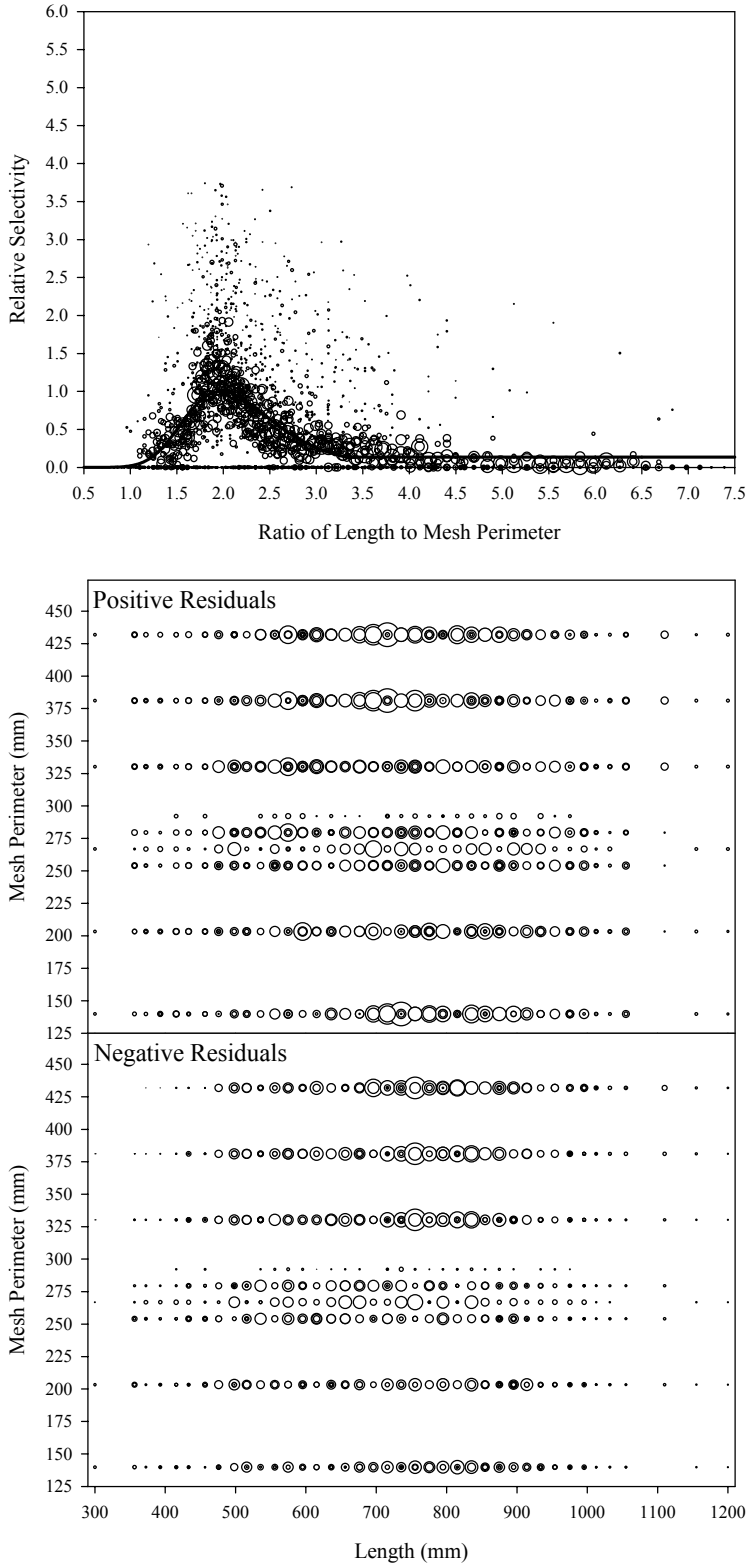

Figure B1.18. Plots of CPUE data scaled to a net selectivity model (top) and CPUE residuals (bottom); Chinook salmon data and Model 18.

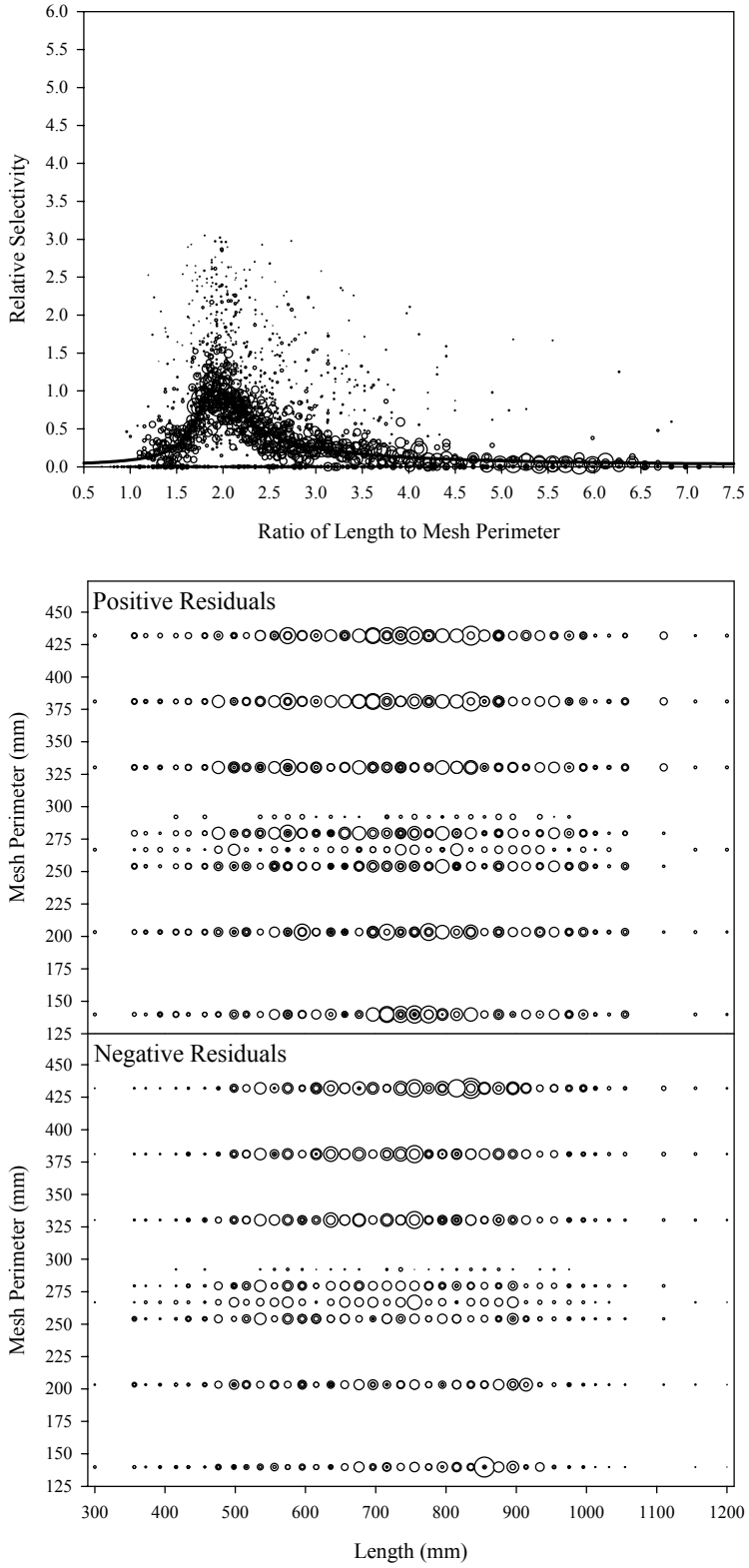

Figure B1.19. Plots of CPUE data scaled to a net selectivity model (top) and CPUE residuals (bottom); Chinook salmon data and Model 19.

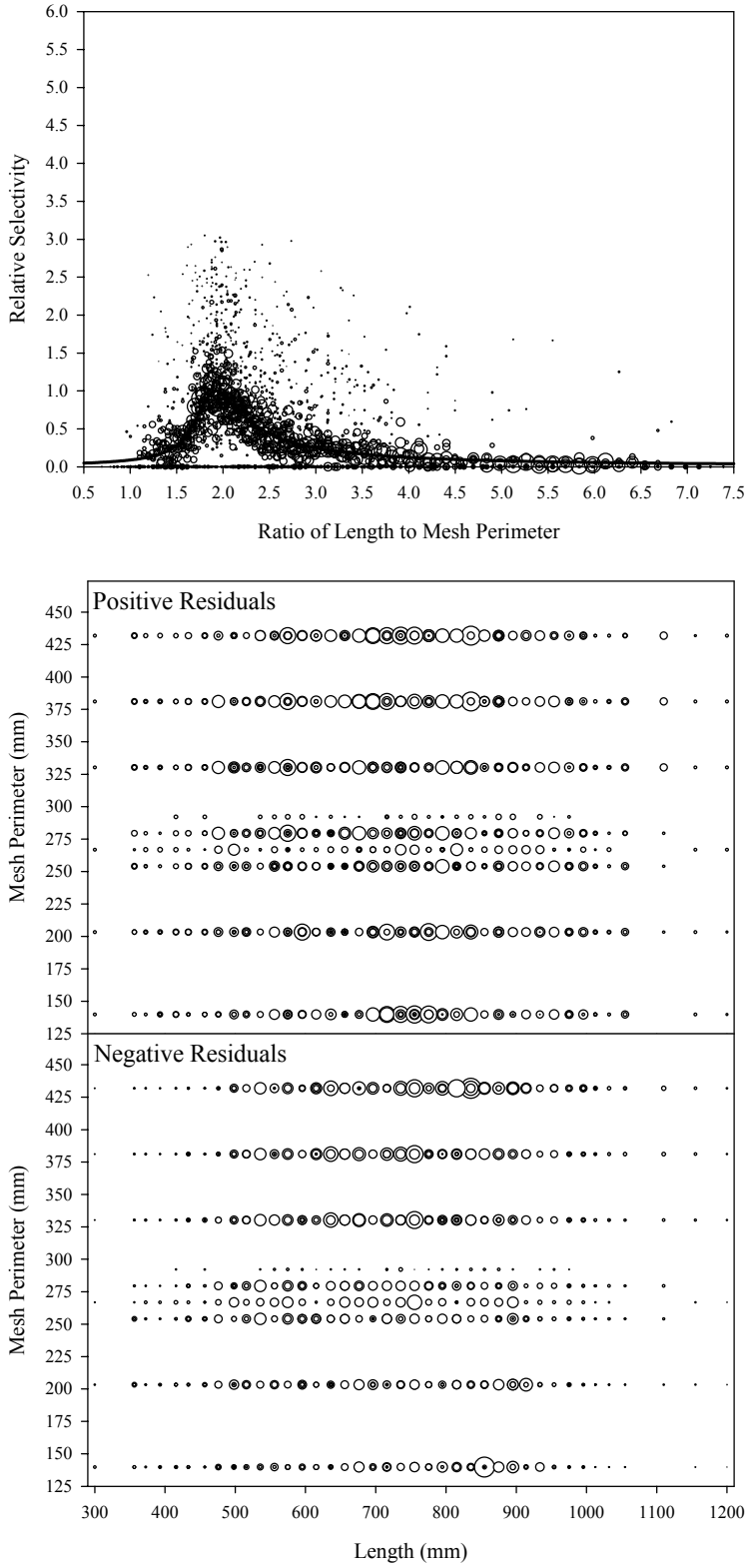

Figure B1.20. Plots of CPUE data scaled to a net selectivity model (top) and CPUE residuals (bottom); Chinook salmon data and Model 20.

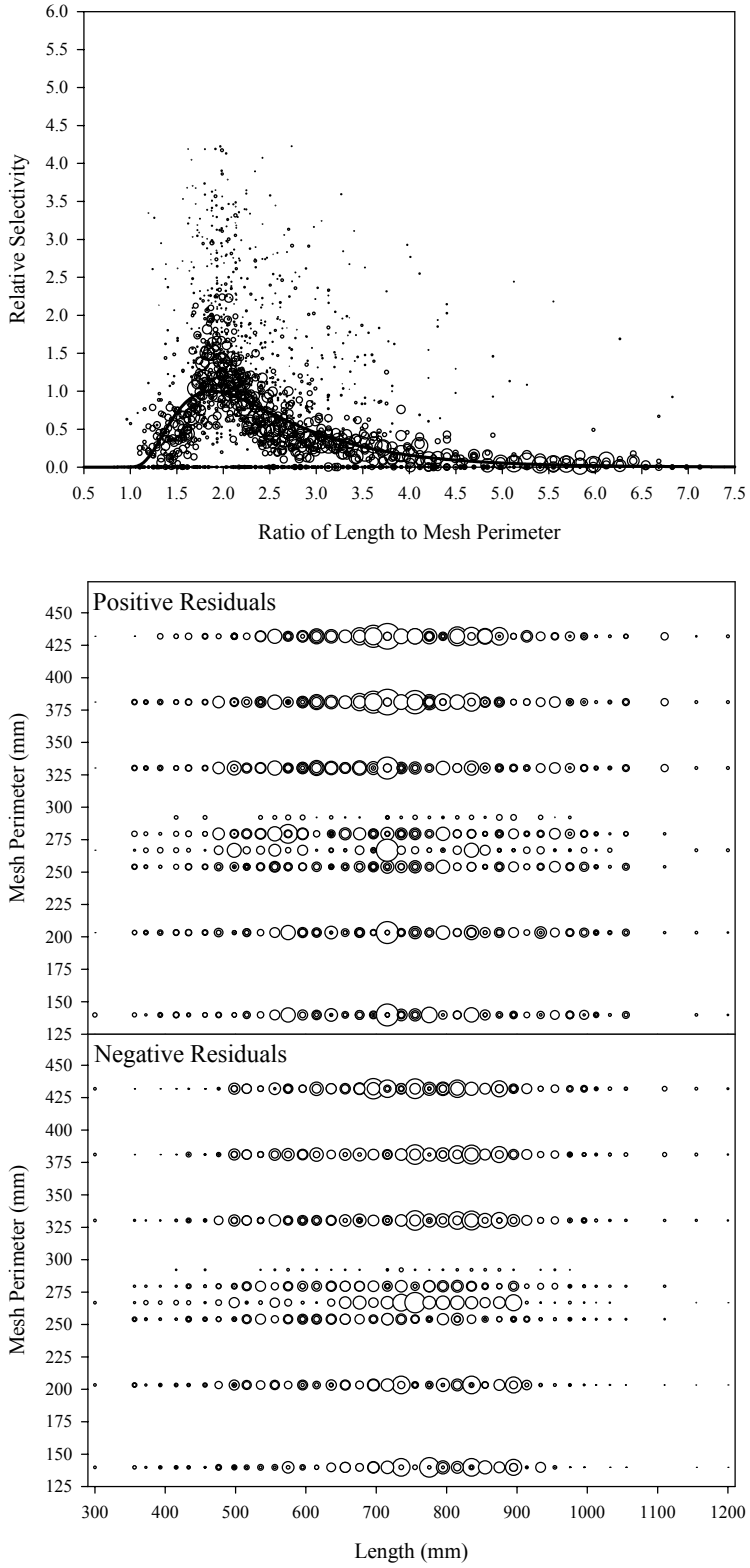

Figure B1.21. Plots of CPUE data scaled to a net selectivity model (top) and CPUE residuals (bottom); Chinook salmon data and Model 21.

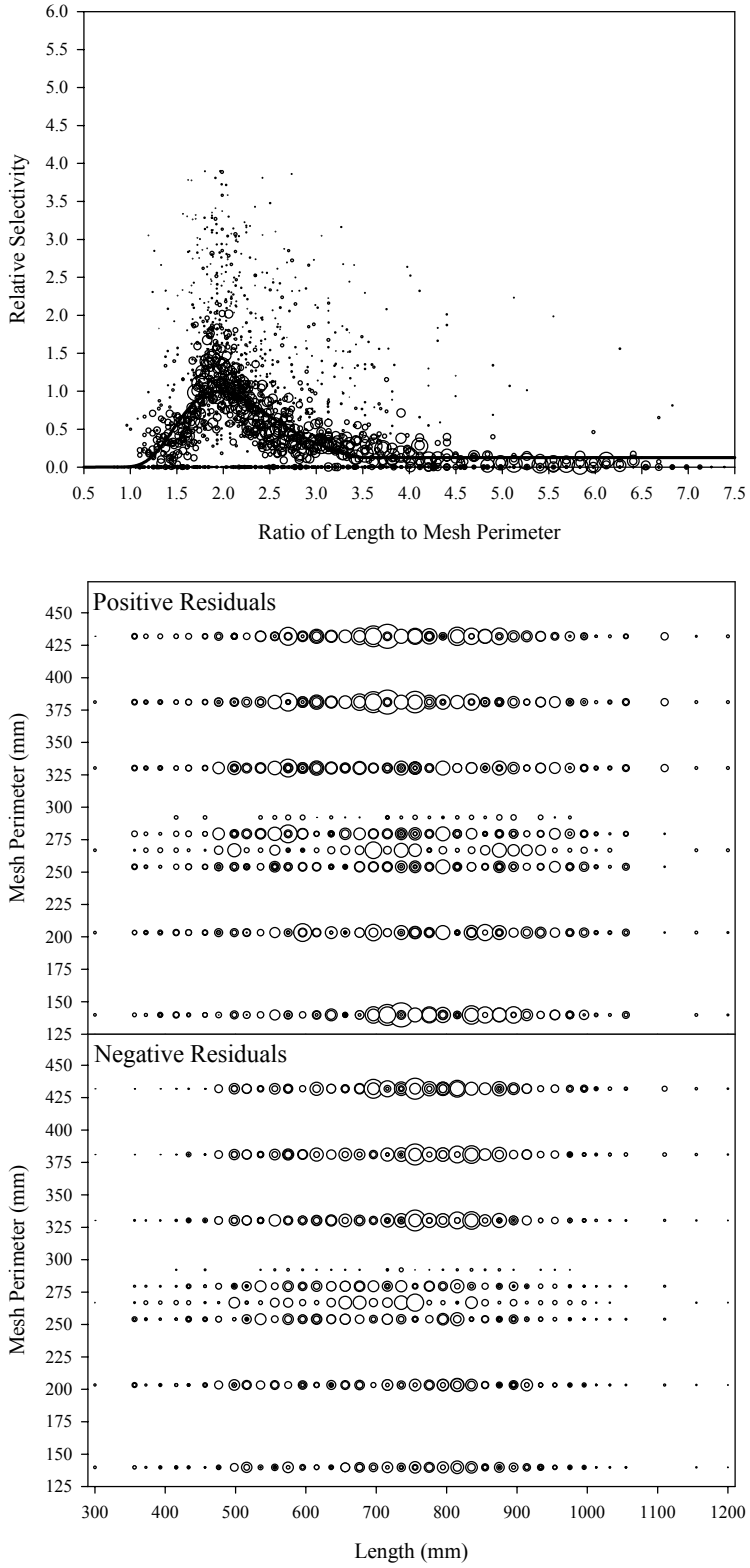

Figure B1.22. Plots of CPUE data scaled to a net selectivity model (top) and CPUE residuals (bottom); Chinook salmon data and Model 22.

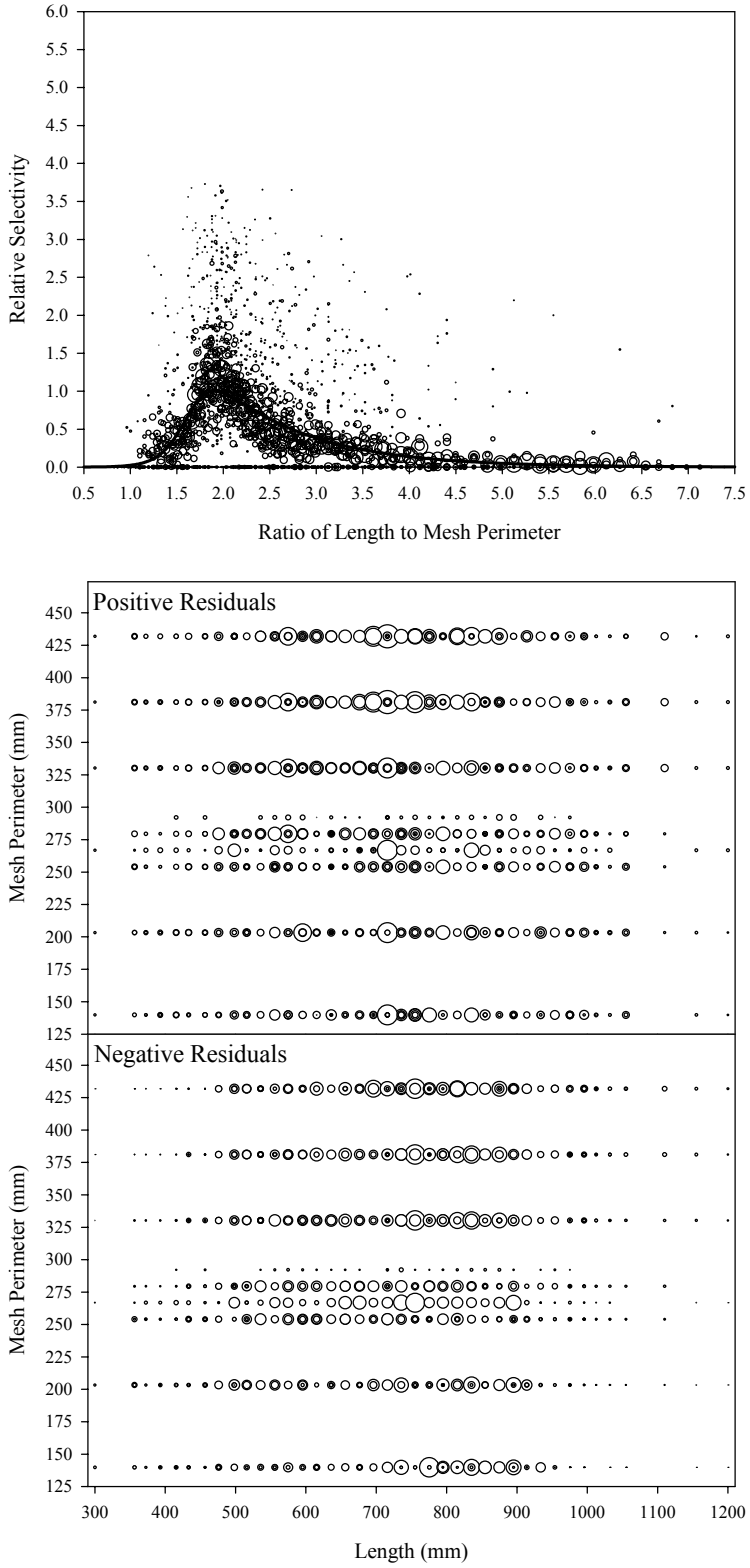

Figure B1.23. Plots of CPUE data scaled to a net selectivity model (top) and CPUE residuals (bottom); Chinook salmon data and Model 23.

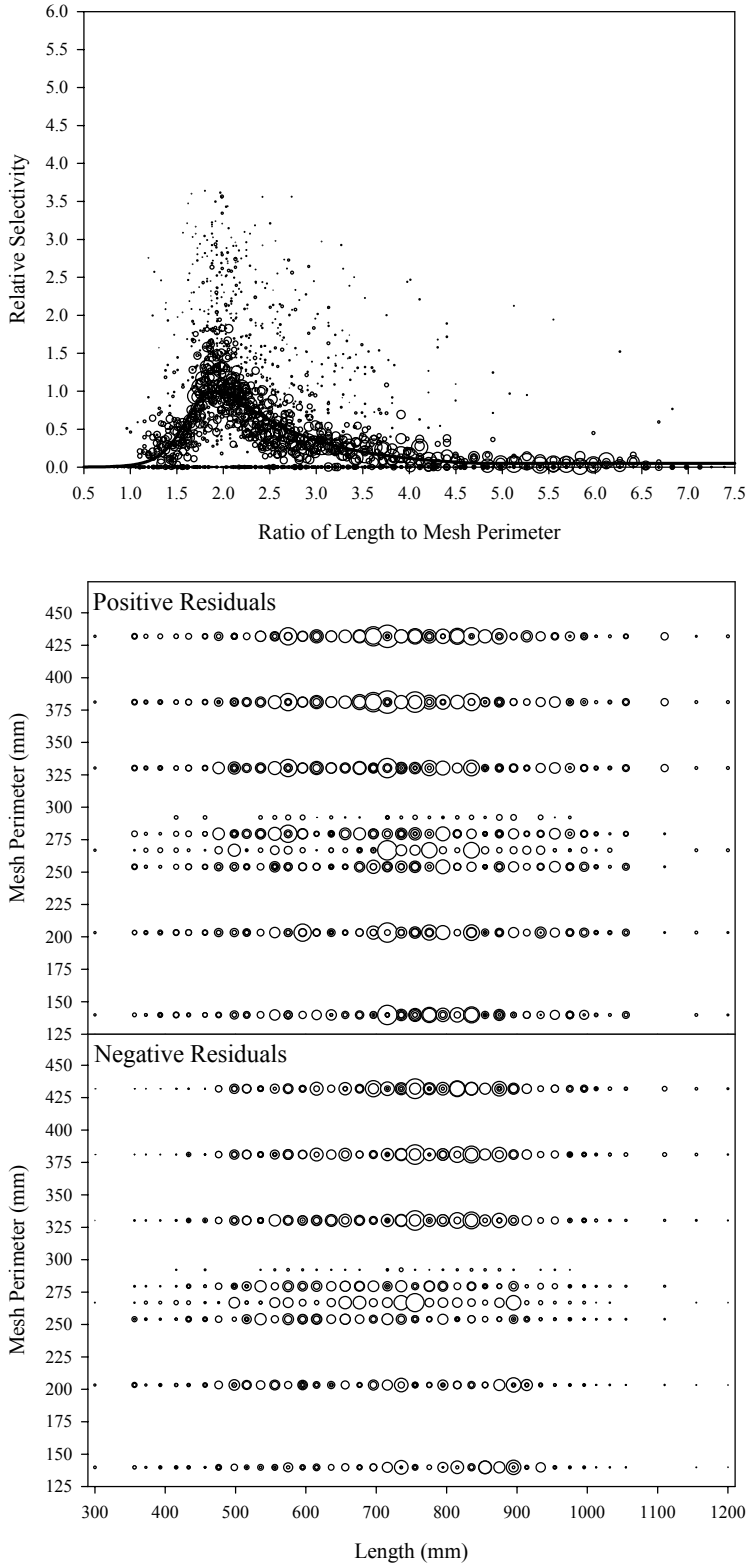

Figure B1.24. Plots of CPUE data scaled to a net selectivity model (top) and CPUE residuals (bottom); Chinook salmon data and Model 24.

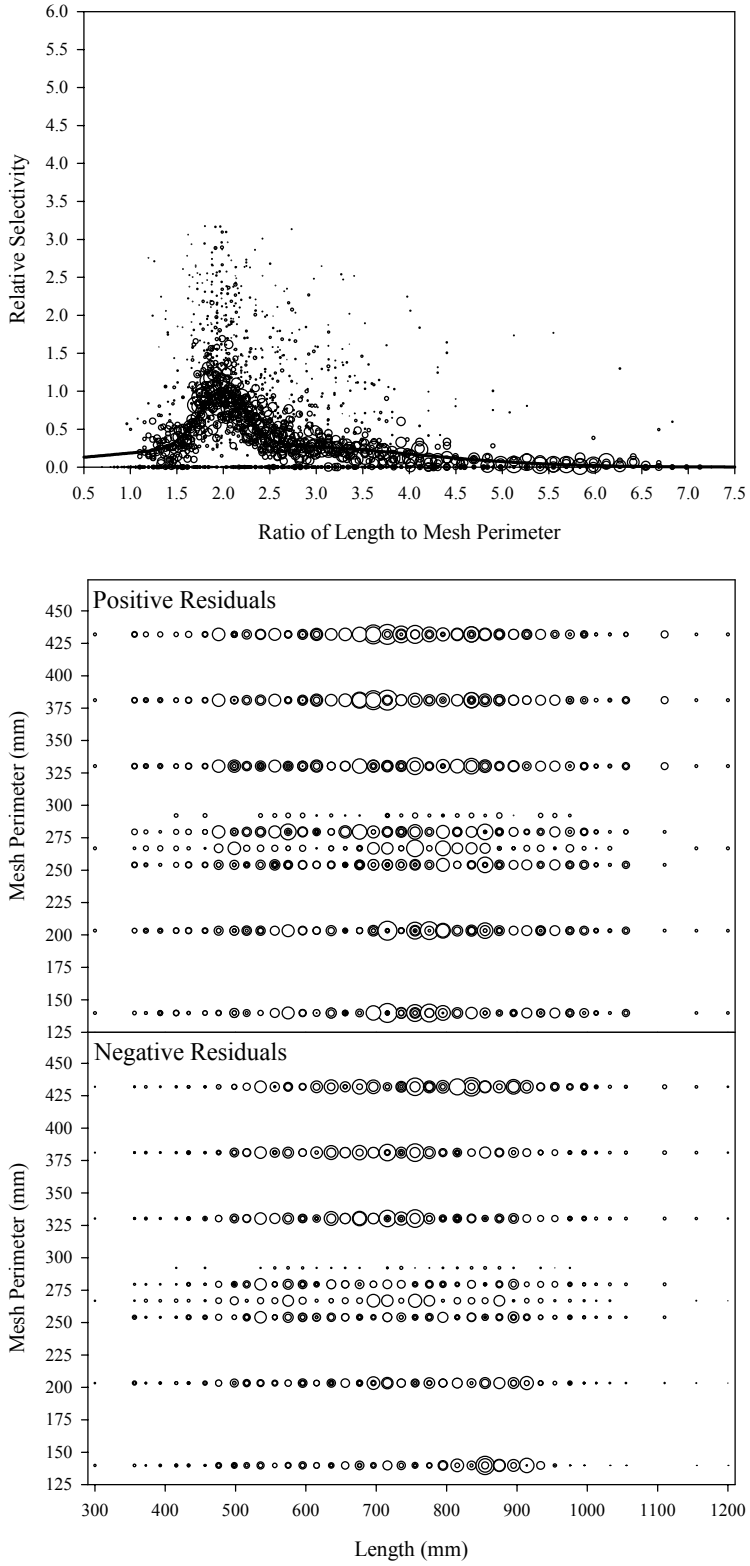

Figure B1.25. Plots of CPUE data scaled to a net selectivity model (top) and CPUE residuals (bottom); Chinook salmon data and Model 25.

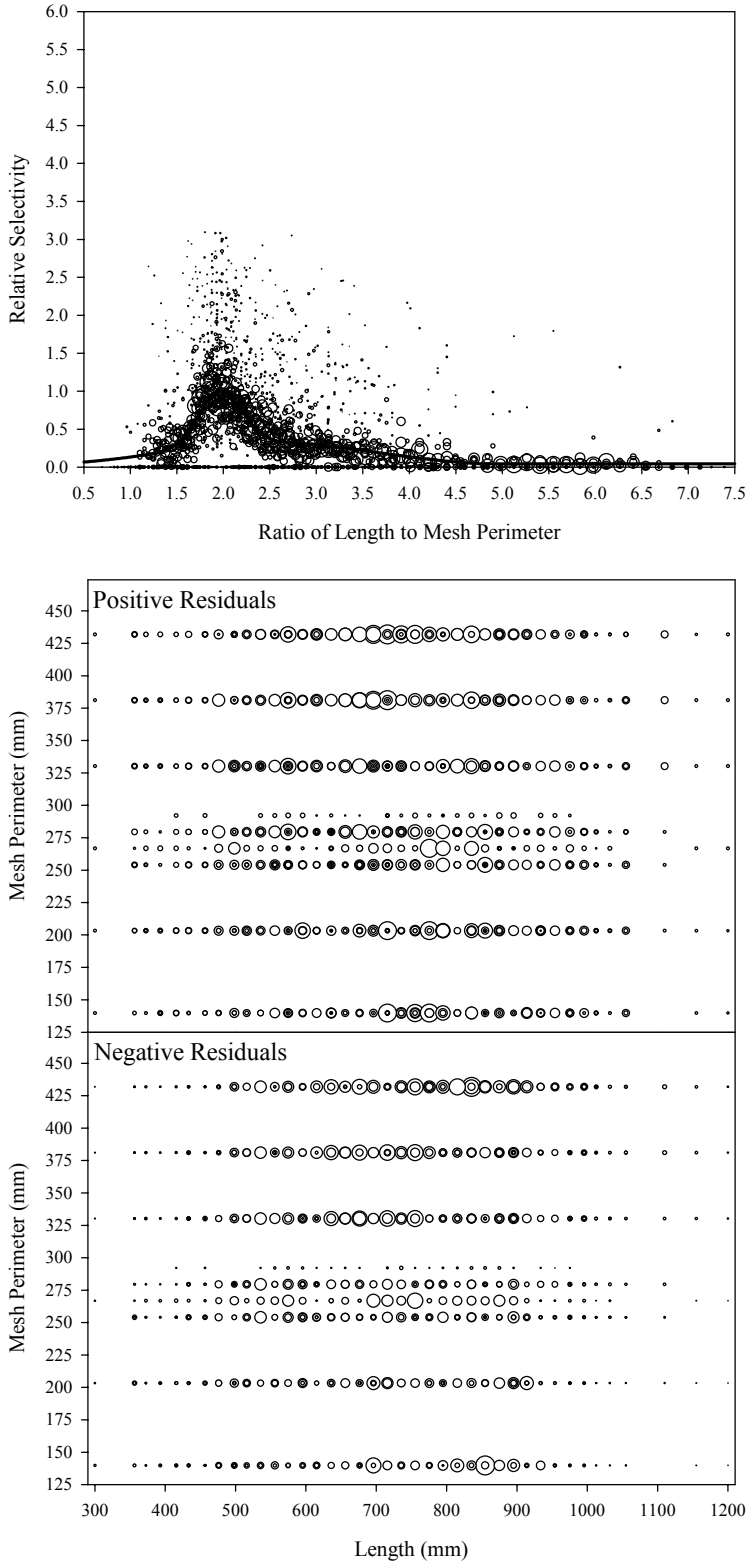

Figure B1.26. Plots of CPUE data scaled to a net selectivity model (top) and CPUE residuals (bottom); Chinook salmon data and Model 26.

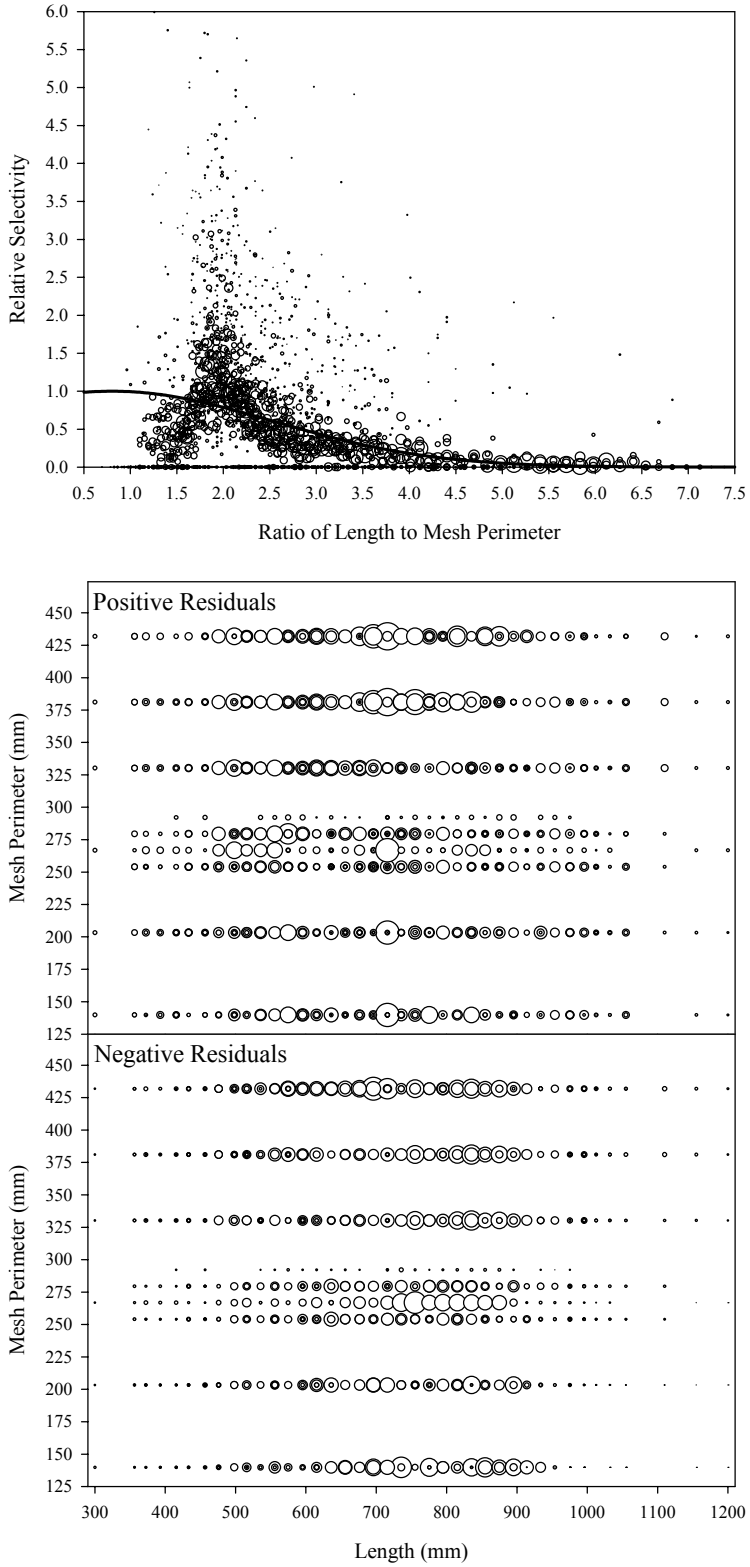

Figure B1.27. Plots of CPUE data scaled to a net selectivity model (top) and CPUE residuals (bottom); Chinook salmon data and Model 27.

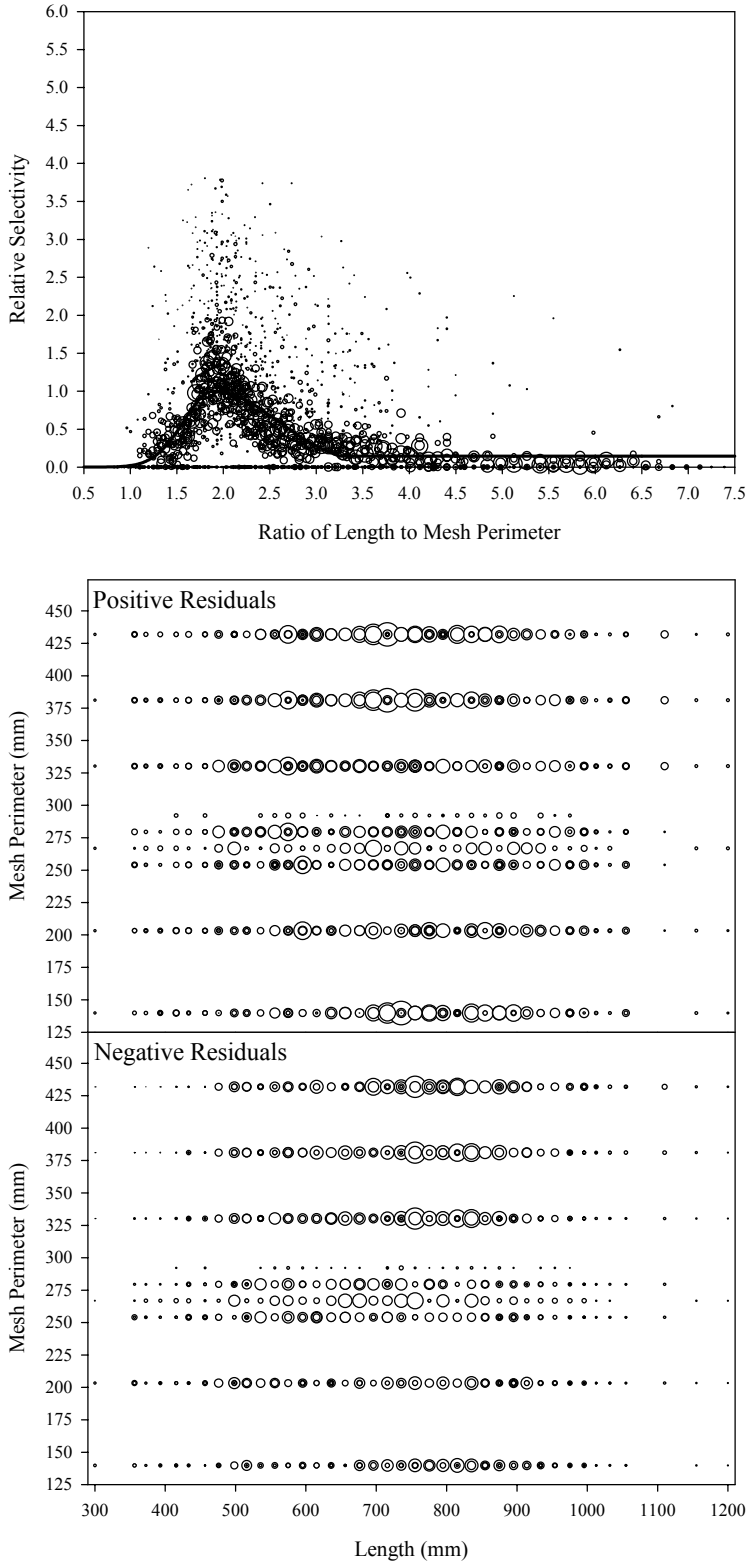

Figure B1.28. Plots of CPUE data scaled to a net selectivity model (top) and CPUE residuals (bottom); Chinook salmon data and Model 28.

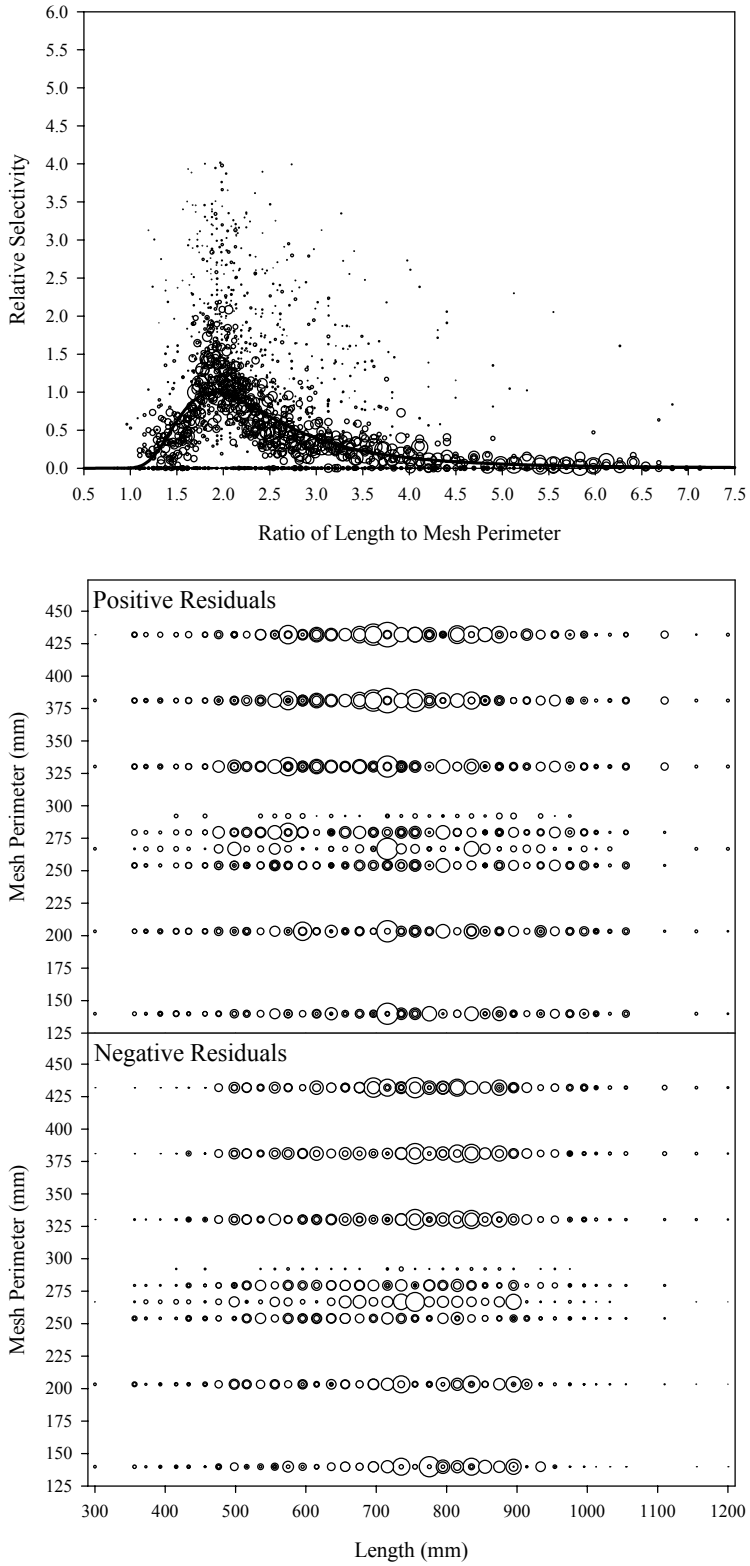

Figure B1.29. Plots of CPUE data scaled to a net selectivity model (top) and CPUE residuals (bottom); Chinook salmon data and Model 29.

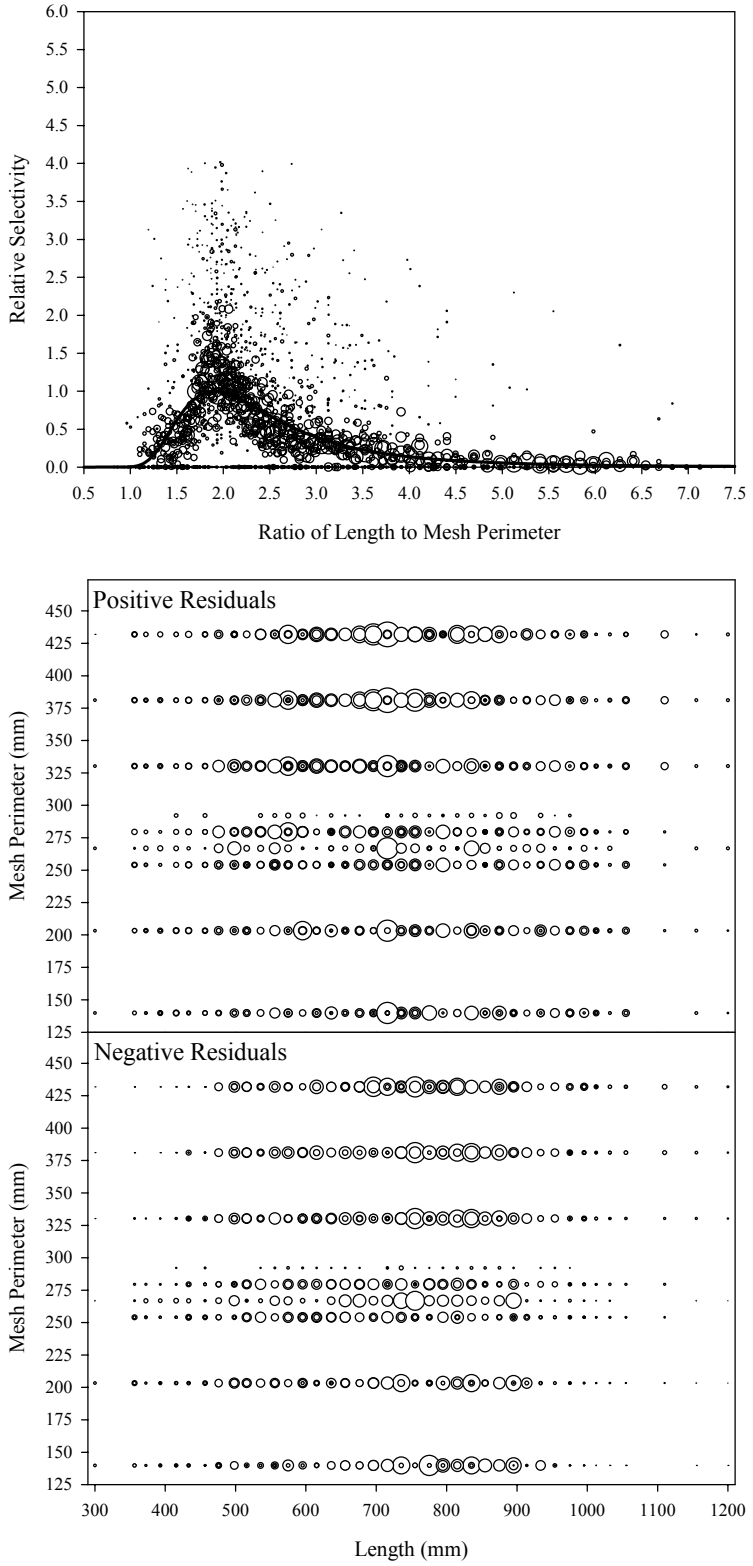

Figure B1.30. Plots of CPUE data scaled to a net selectivity model (top) and CPUE residuals (bottom); Chinook salmon data and Model 30.

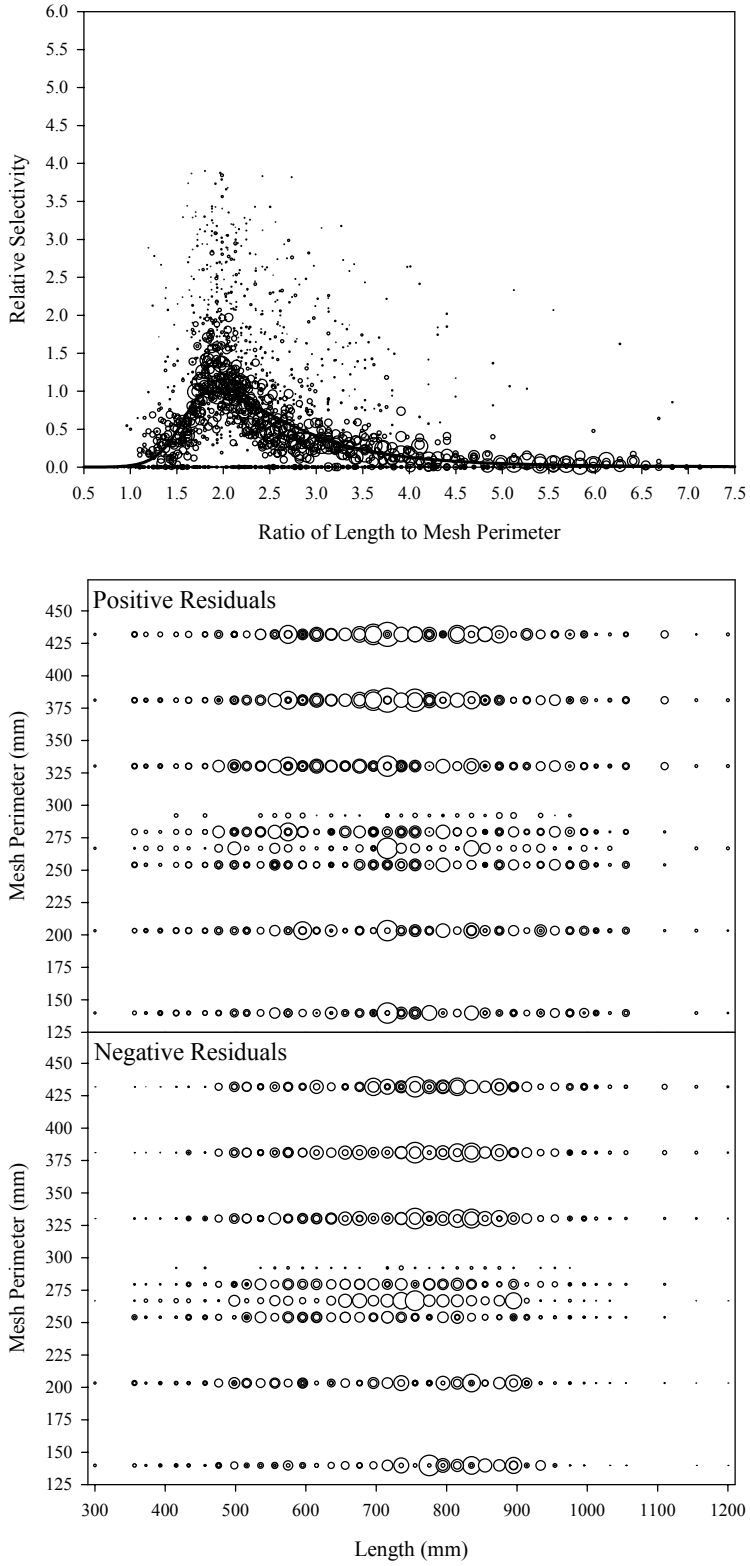

Figure B1.31. Plots of CPUE data scaled to a net selectivity model (top) and CPUE residuals (bottom); Chinook salmon data and Model 31.

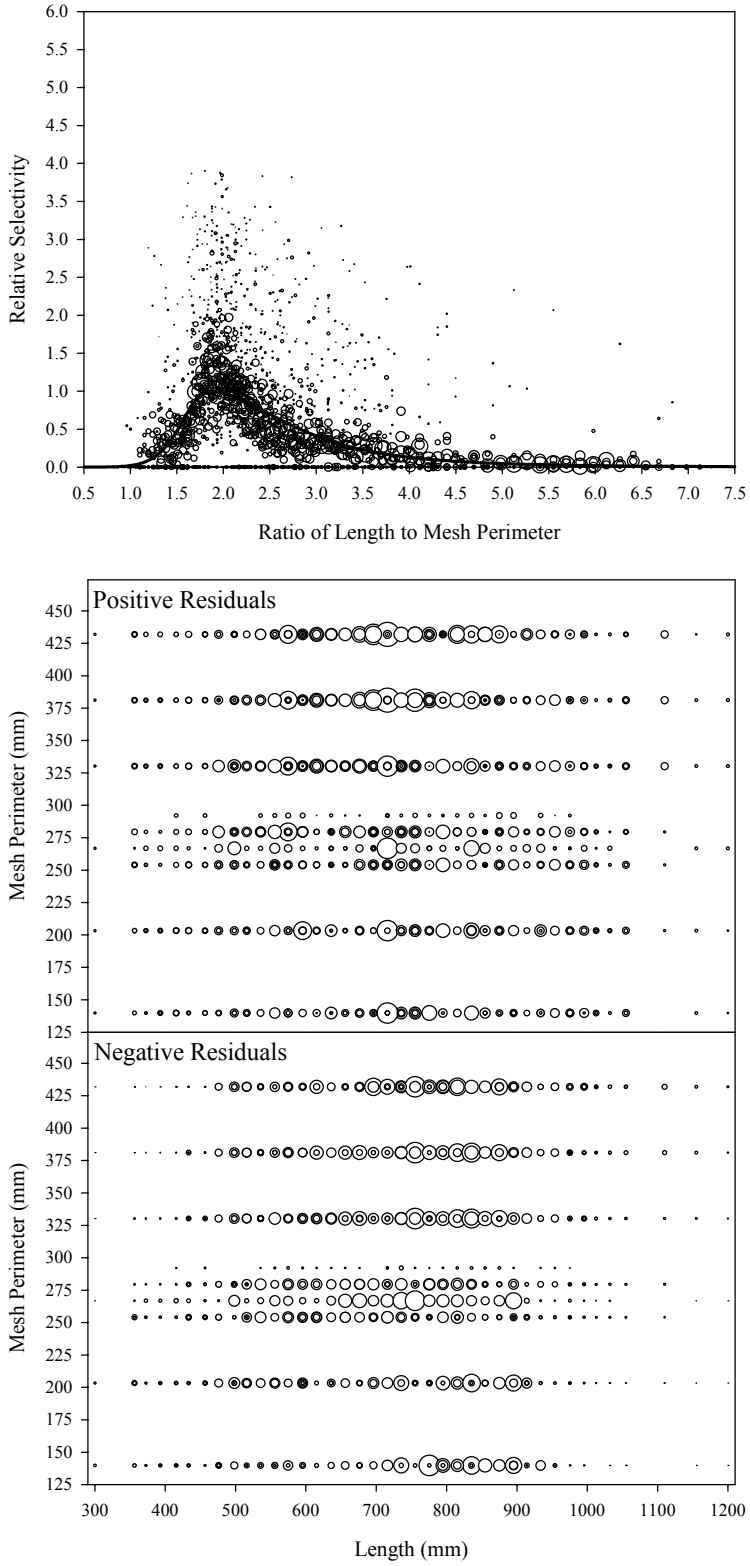

Figure B1.32. Plots of CPUE data scaled to a net selectivity model (top) and CPUE residuals (bottom); Chinook salmon data and Model 32.

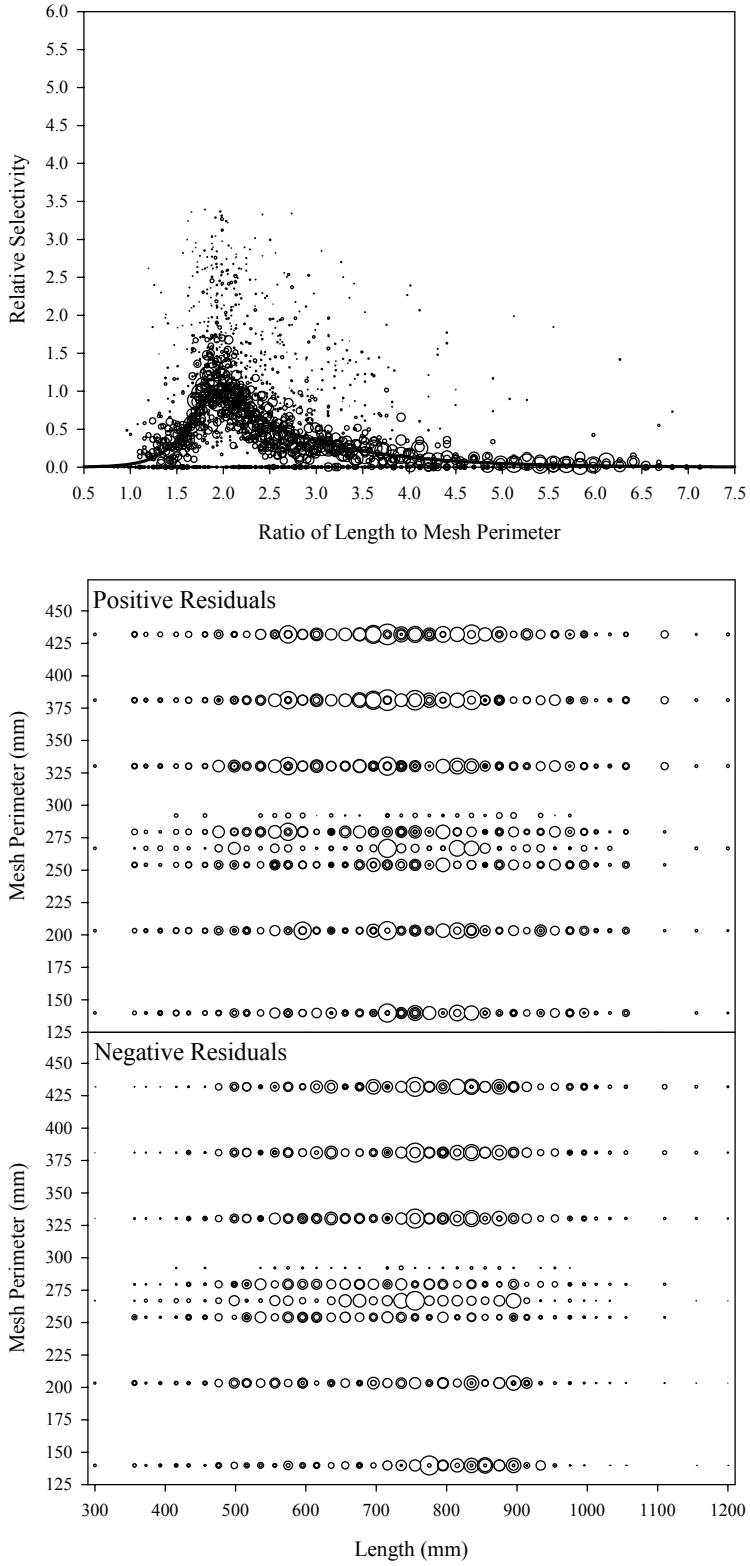

Figure B1.33. Plots of CPUE data scaled to a net selectivity model (top) and CPUE residuals (bottom); Chinook salmon data and Model 33.

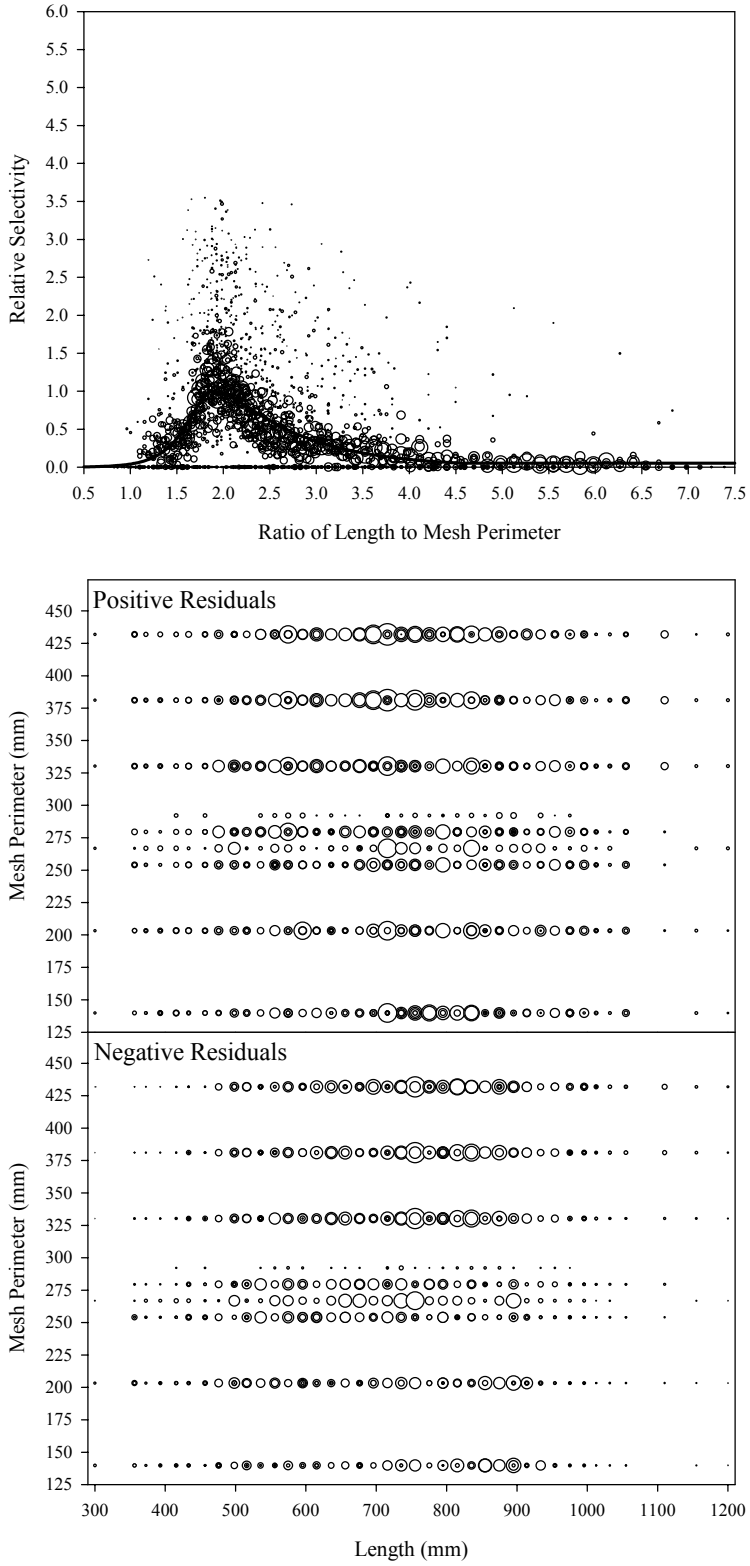

Figure B1.34. Plots of CPUE data scaled to a net selectivity model (top) and CPUE residuals (bottom); Chinook salmon data and Model 34.

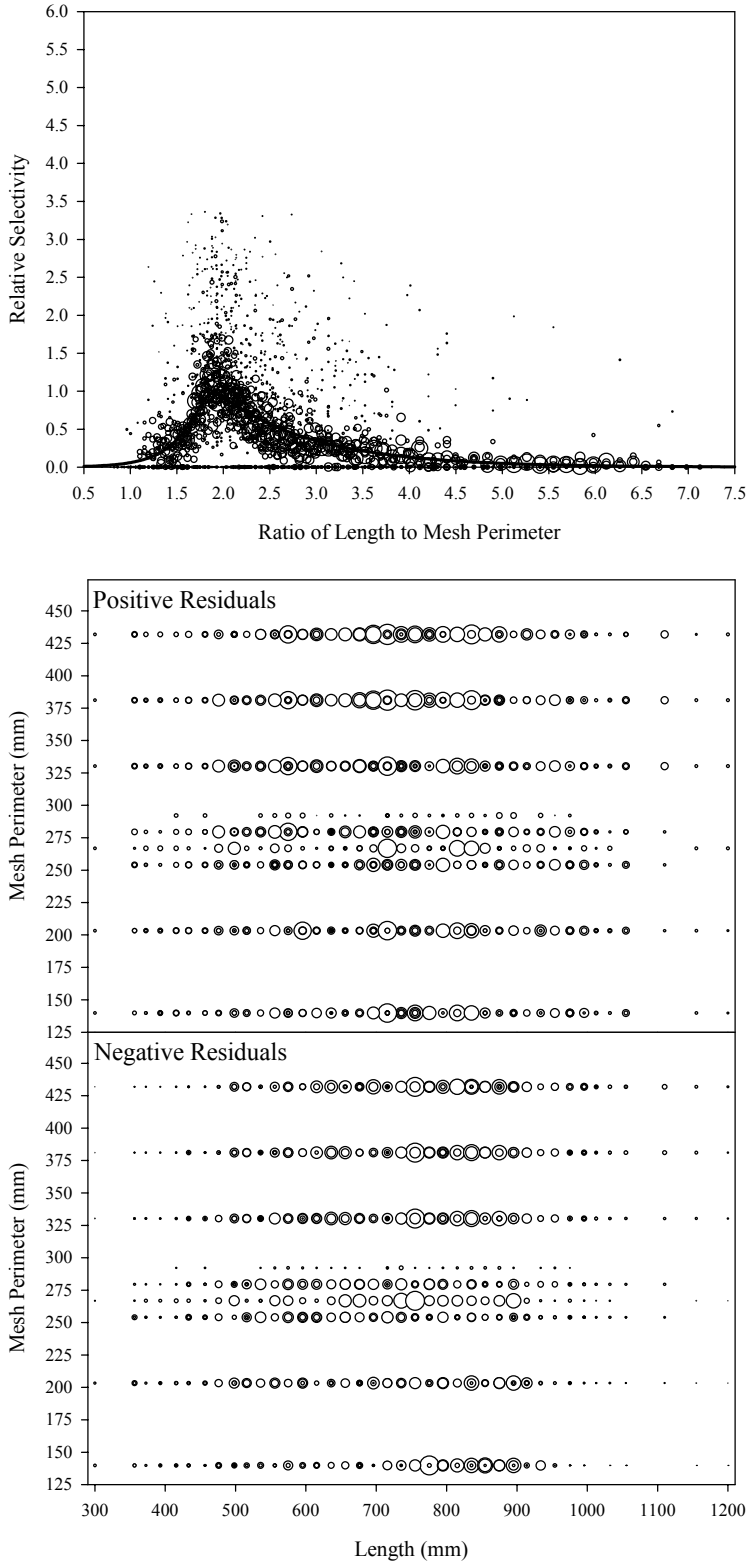

Figure B1.35. Plots of CPUE data scaled to a net selectivity model (top) and CPUE residuals (bottom); Chinook salmon data and Model 35.

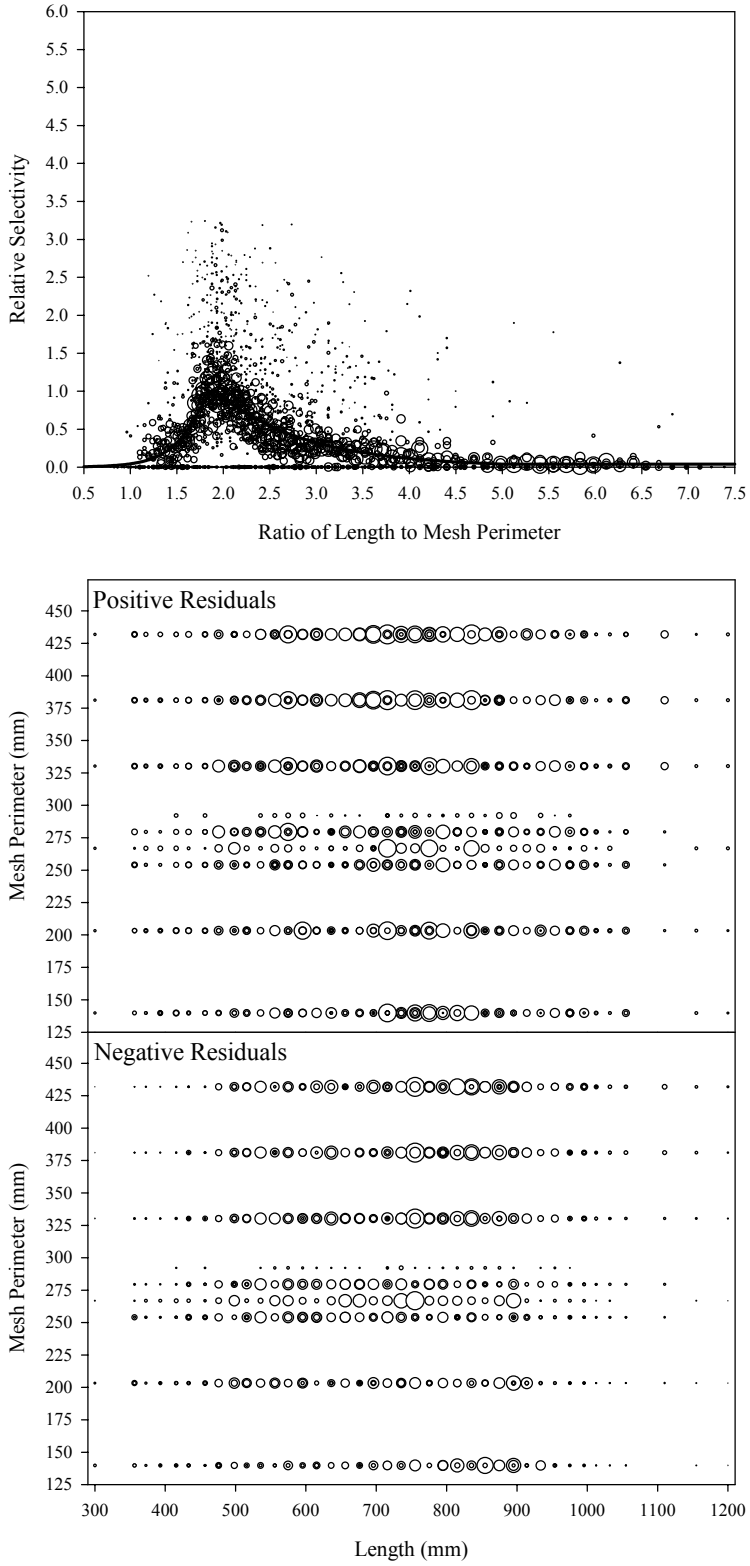

Figure B1.36. Plots of CPUE data scaled to a net selectivity model (top) and CPUE residuals (bottom); Chinook salmon data and Model 36.

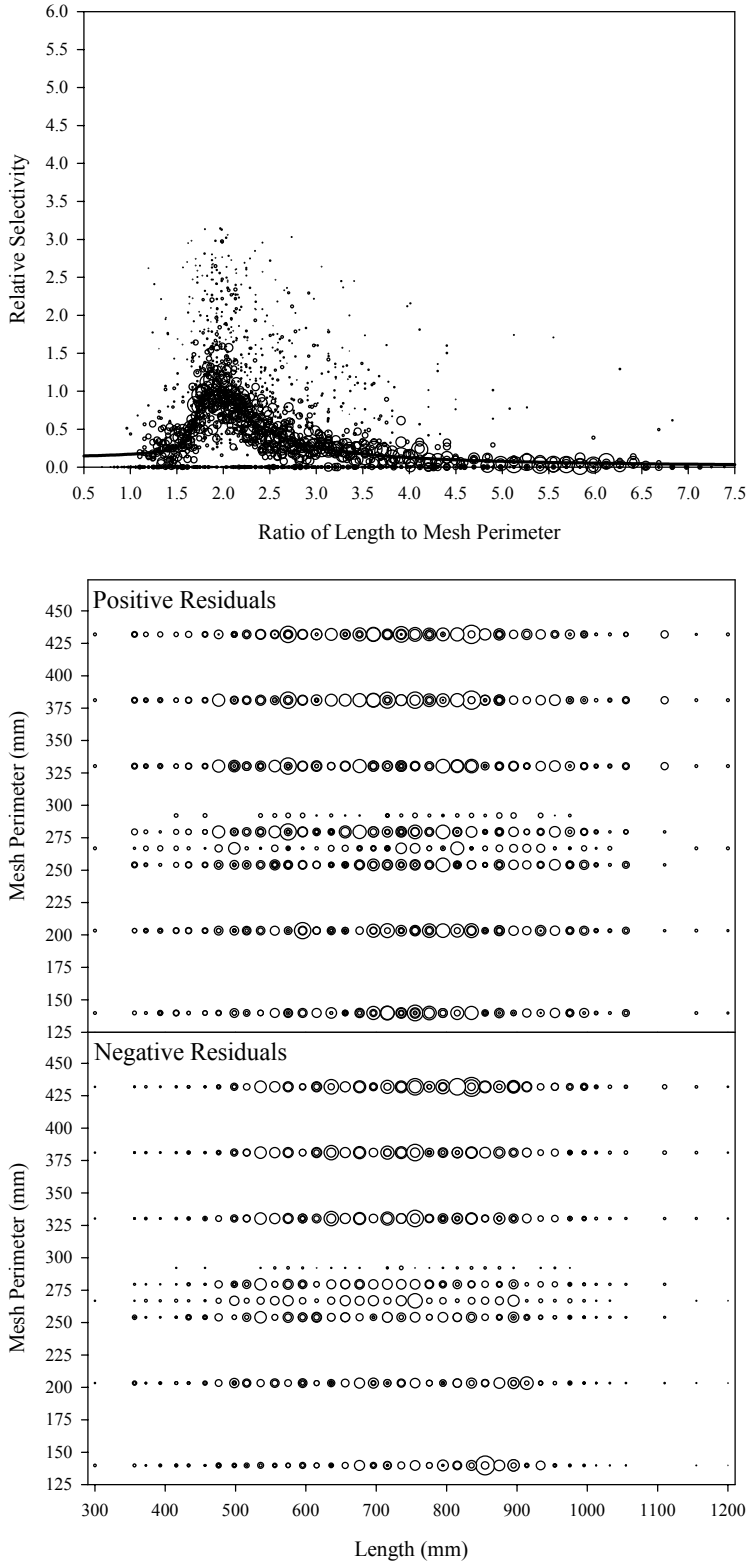

Figure B1.37. Plots of CPUE data scaled to a net selectivity model (top) and CPUE residuals (bottom); Chinook salmon data and Model 37.

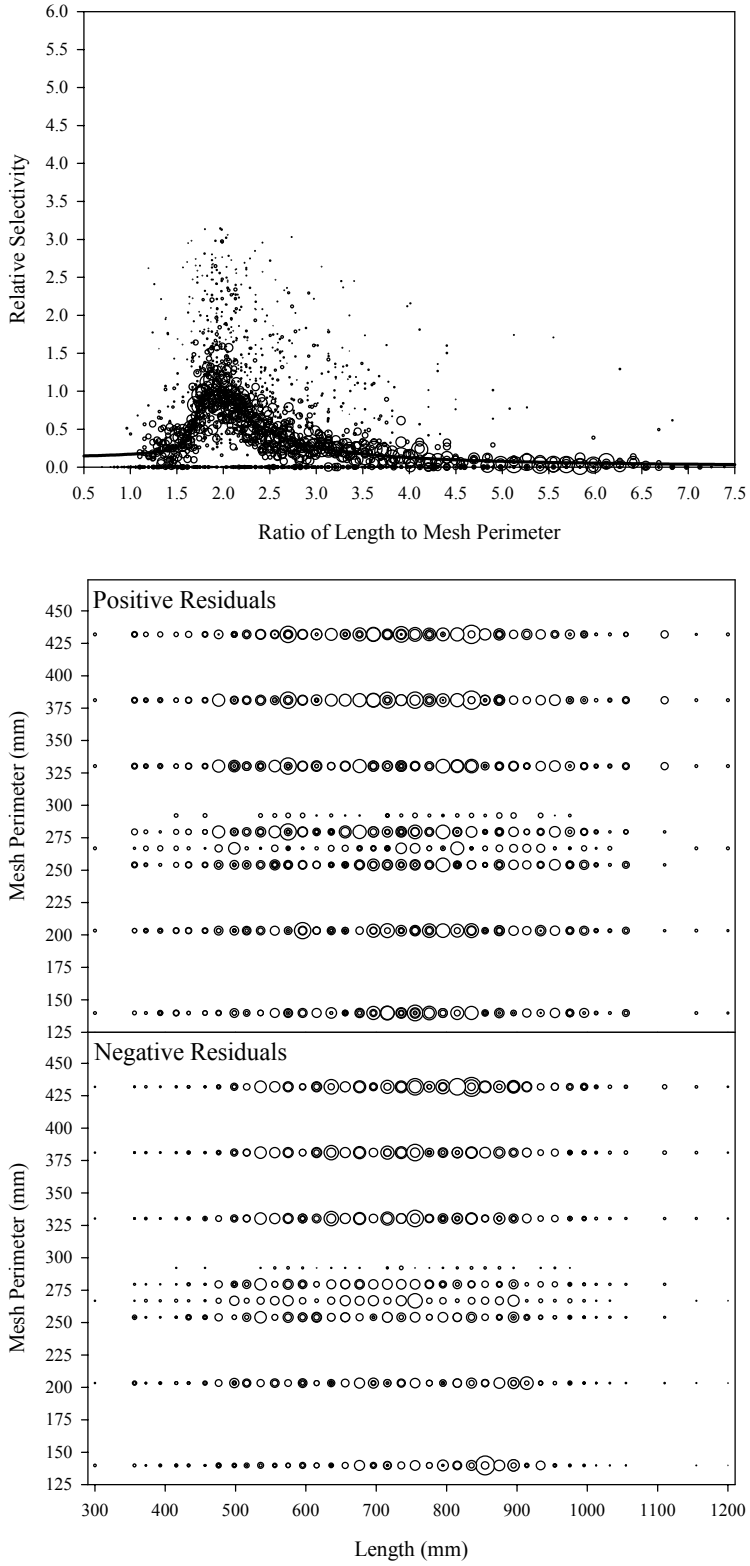

Figure B1.38. Plots of CPUE data scaled to a net selectivity model (top) and CPUE residuals (bottom); Chinook salmon data and Model 38.

Appendix B2
Summer Chum Salmon Diagnostic Plots
Figure B2.1 to Figure B2.38

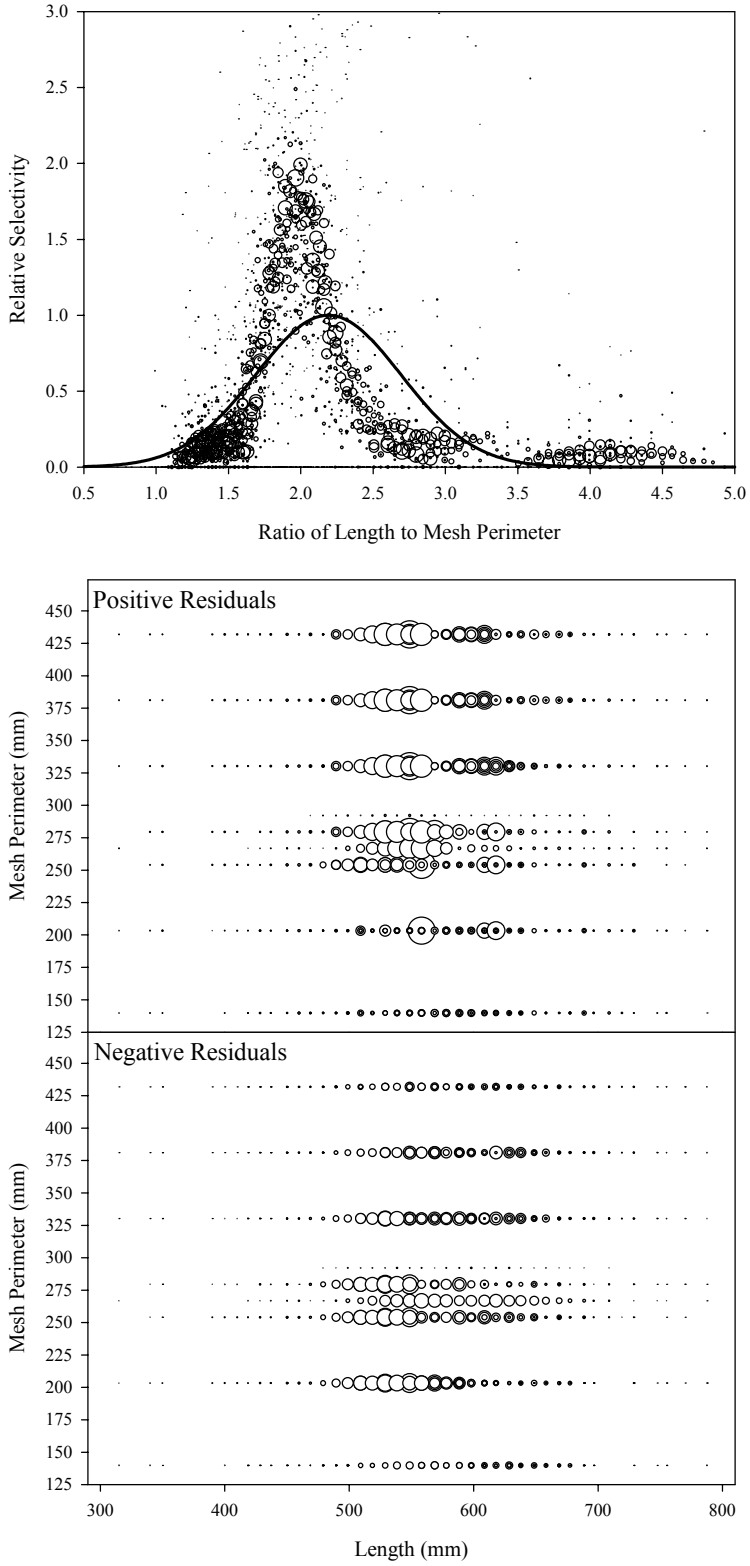

Figure B2.1. Plots of CPUE data scaled to a net selectivity model (top) and CPUE residuals (bottom); summer chum salmon data and Model 1.

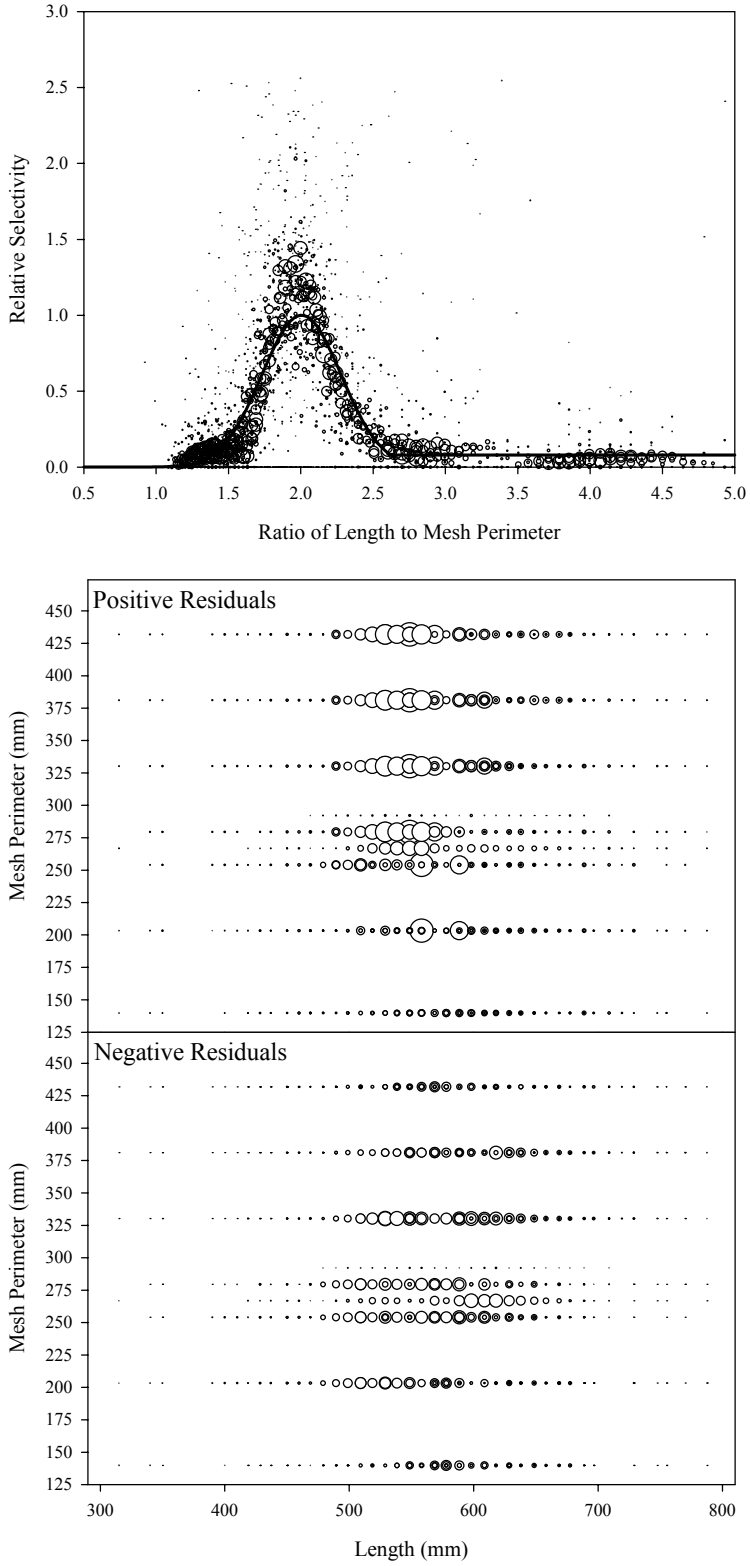

Figure B2.2. Plots of CPUE data scaled to a net selectivity model (top) and CPUE residuals (bottom); summer chum salmon data and Model 2.

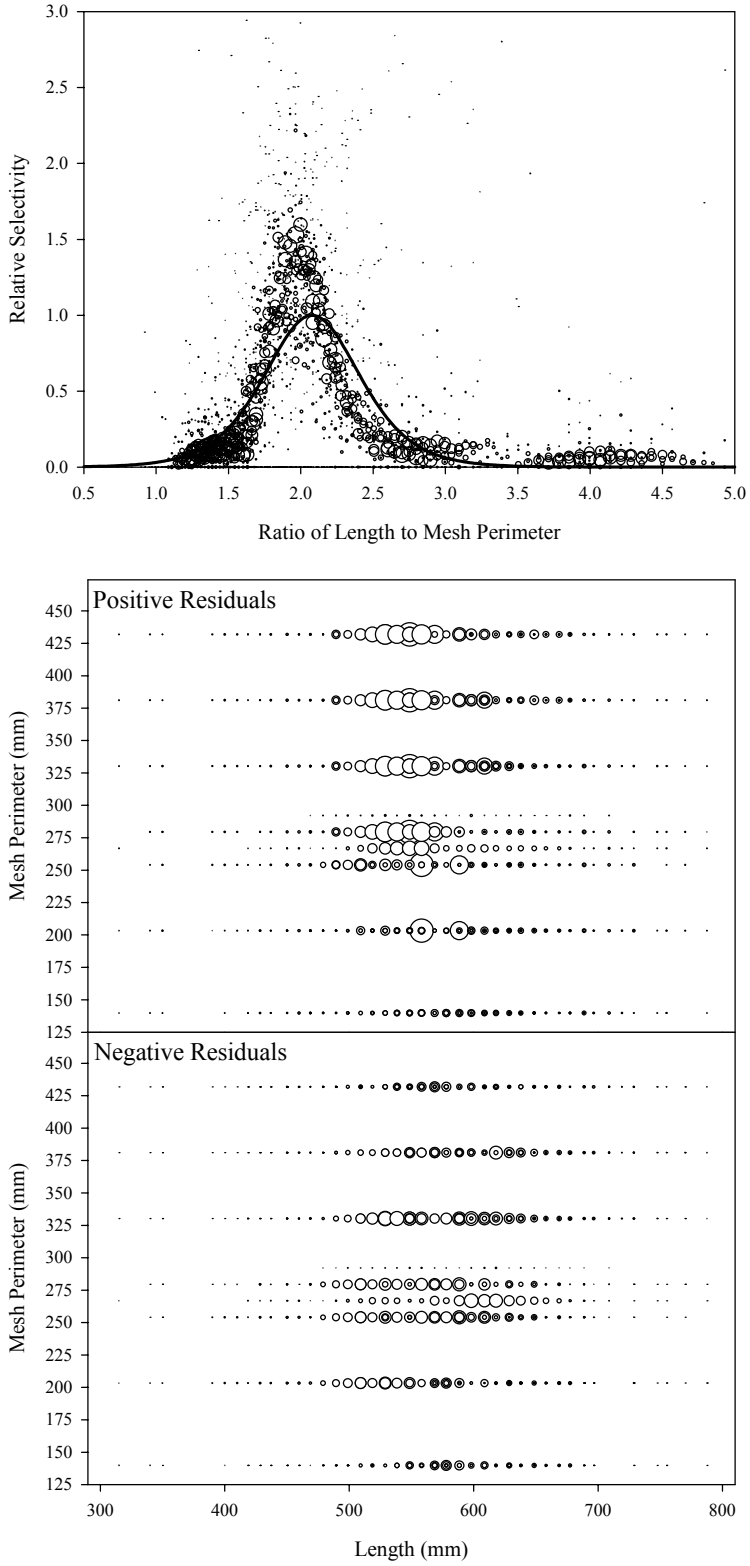

Figure B2.3. Plots of CPUE data scaled to a net selectivity model (top) and CPUE residuals (bottom); summer chum salmon data and Model 3.

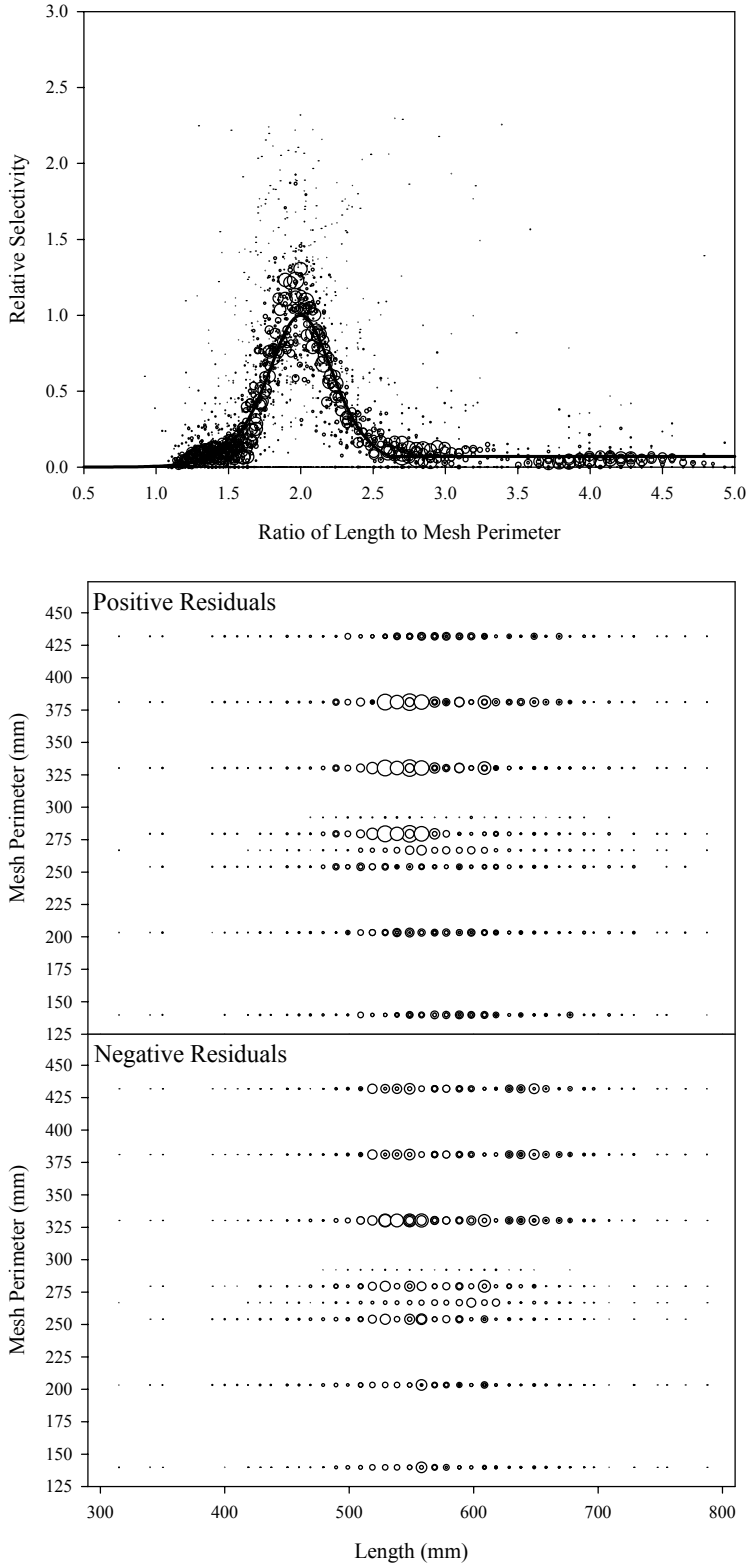

Figure B2.4. Plots of CPUE data scaled to a net selectivity model (top) and CPUE residuals (bottom); summer chum salmon data and Model 4.

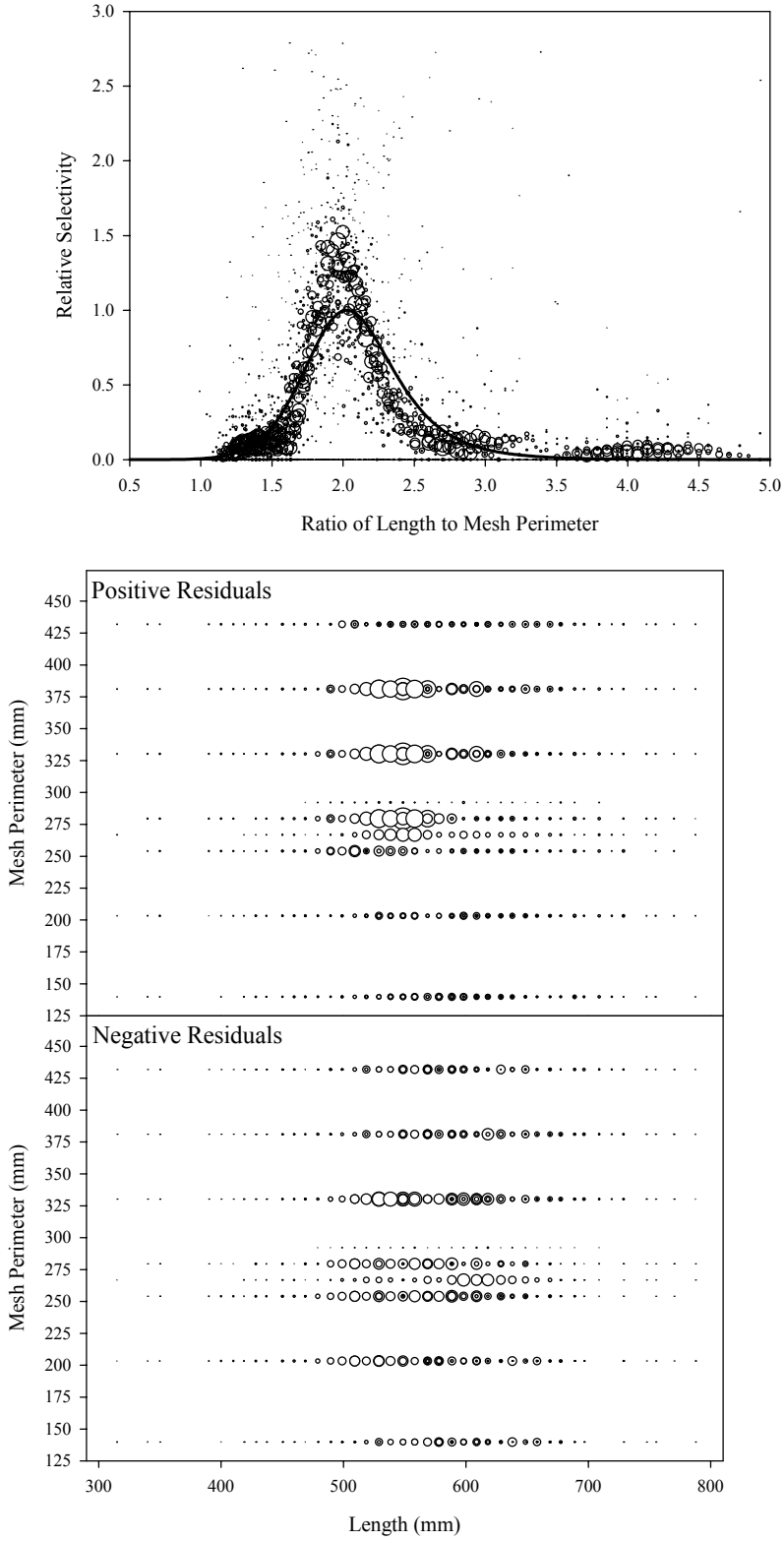

Figure B2.5. Plots of CPUE data scaled to a net selectivity model (top) and CPUE residuals (bottom); summer chum salmon data and Model 5.

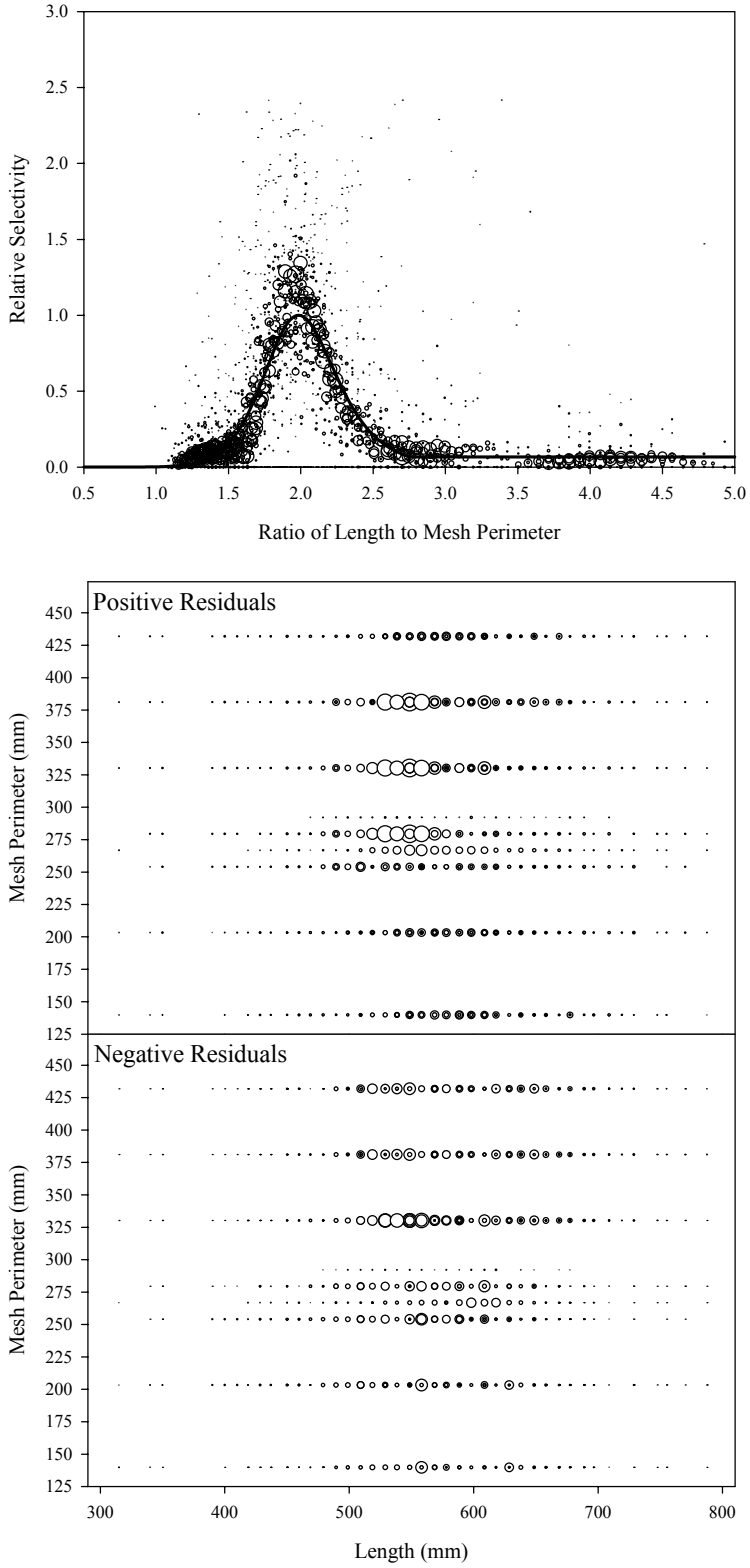

Figure B2.6. Plots of CPUE data scaled to a net selectivity model (top) and CPUE residuals (bottom); summer chum salmon data and Model 6.

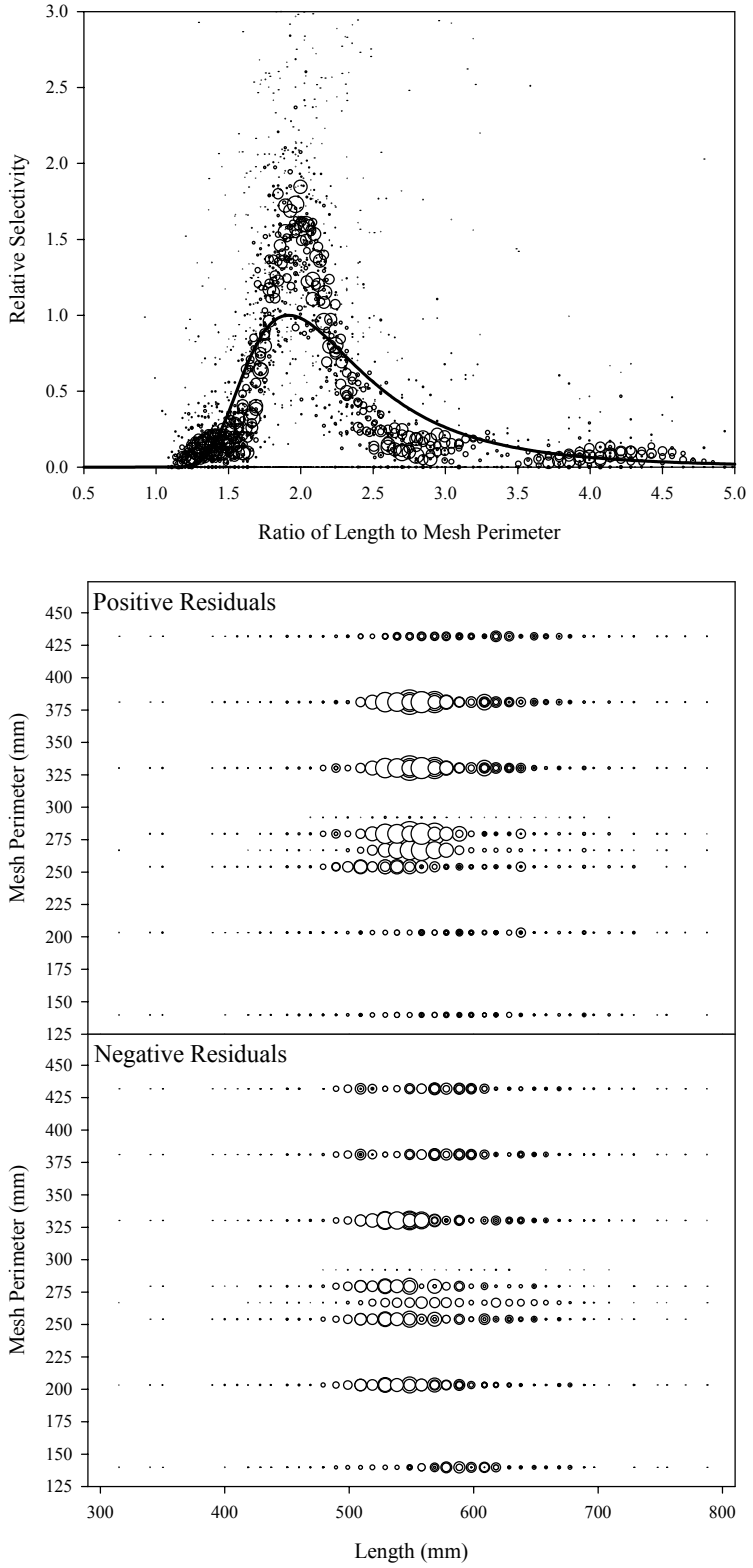

Figure B2.7. Plots of CPUE data scaled to a net selectivity model (top) and CPUE residuals (bottom); summer chum salmon data and Model 7.

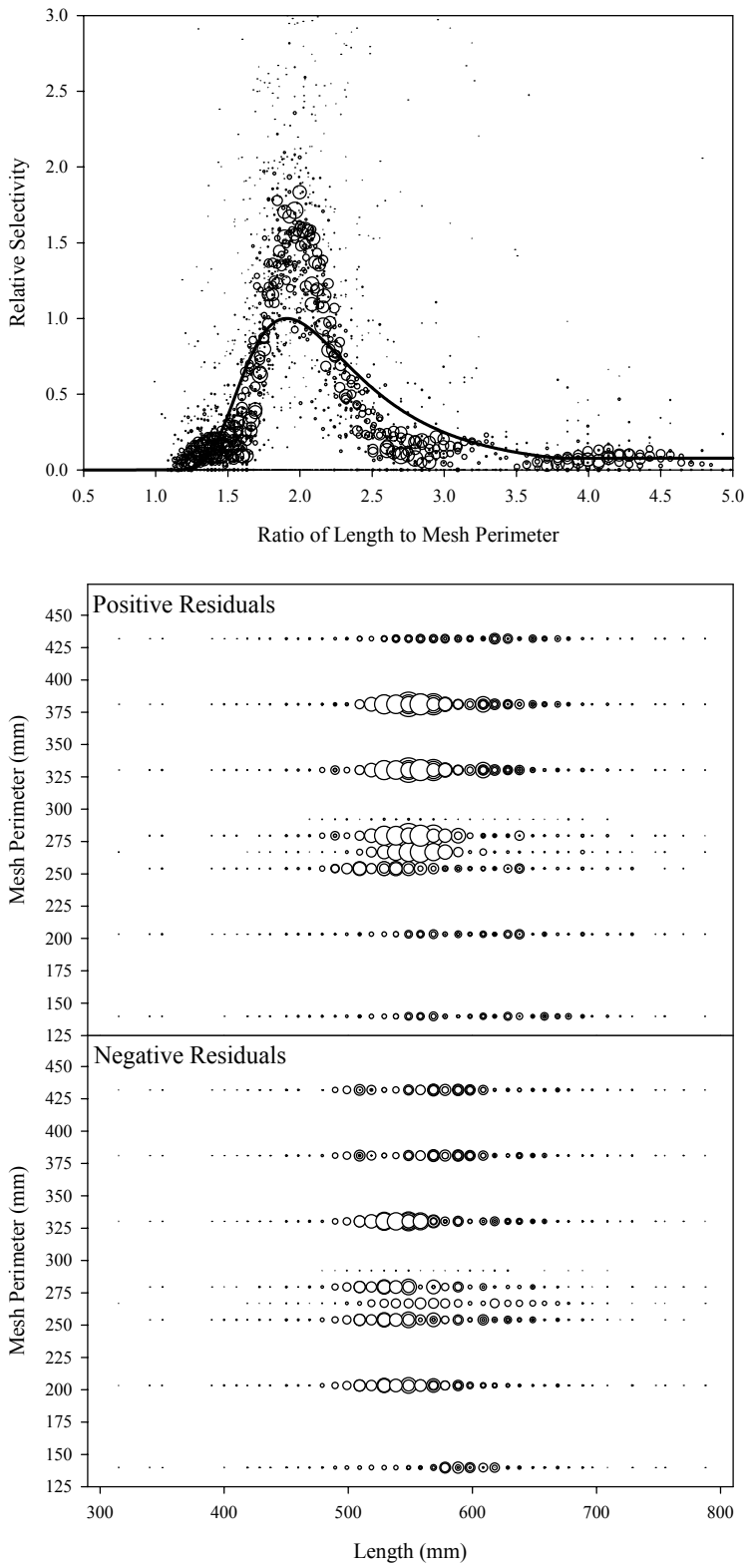

Figure B2.8. Plots of CPUE data scaled to a net selectivity model (top) and CPUE residuals (bottom); summer chum salmon data and Model 8.

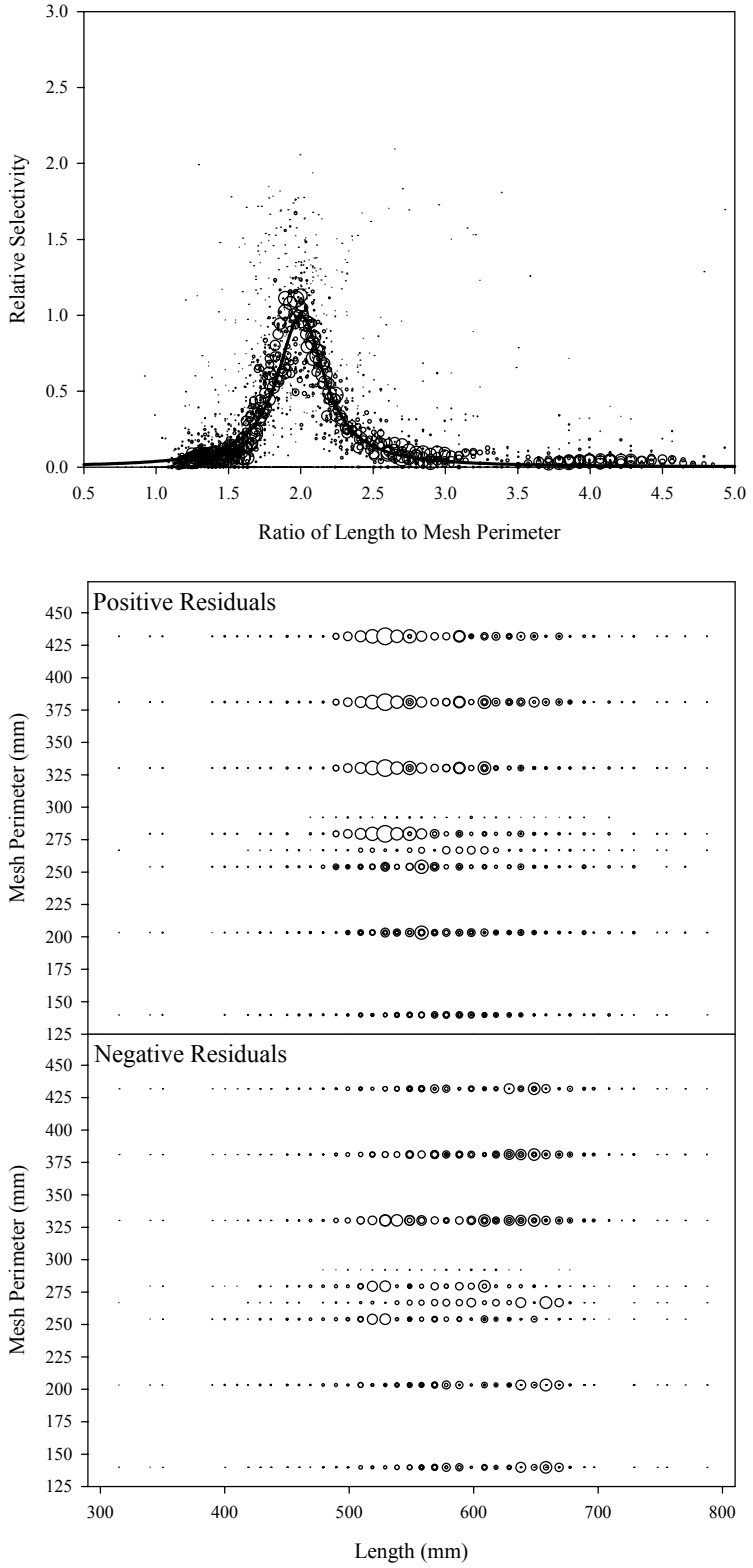

Figure B2.9. Plots of CPUE data scaled to a net selectivity model (top) and CPUE residuals (bottom); summer chum salmon data and Model 9.

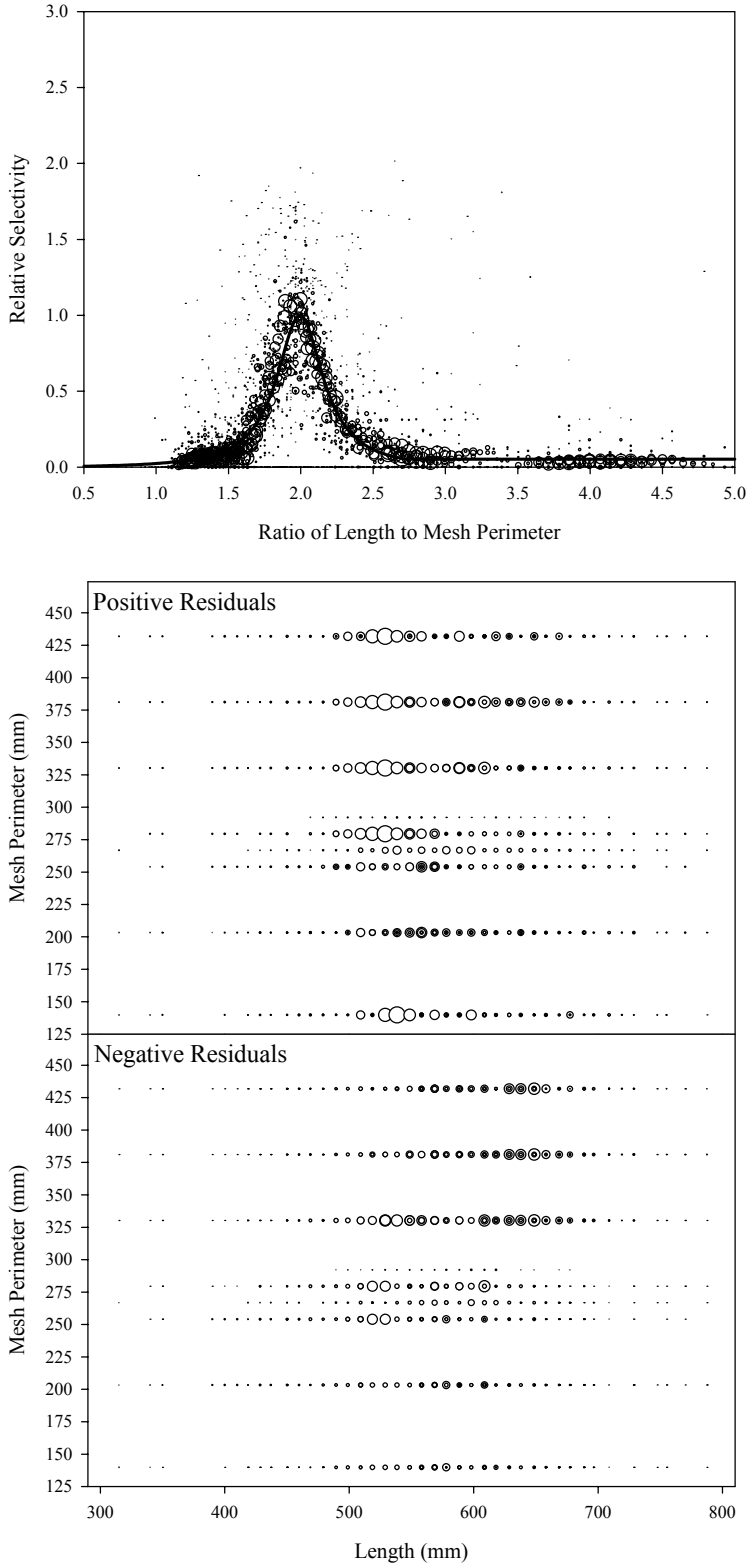

Figure B2.10. Plots of CPUE data scaled to a net selectivity model (top) and CPUE residuals (bottom); summer chum salmon data and Model 10.

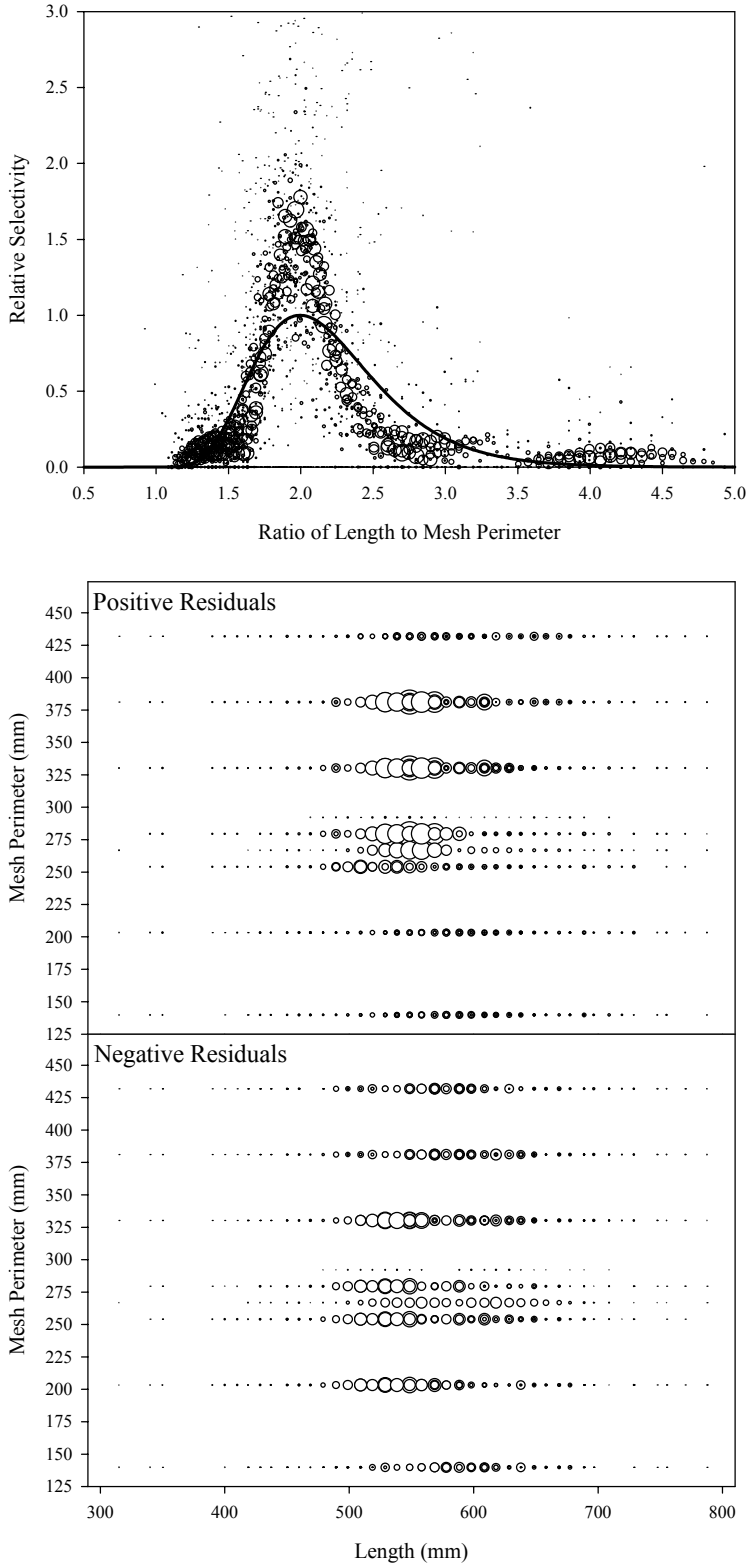

Figure B2.11. Plots of CPUE data scaled to a net selectivity model (top) and CPUE residuals (bottom); summer chum salmon data and Model 11.

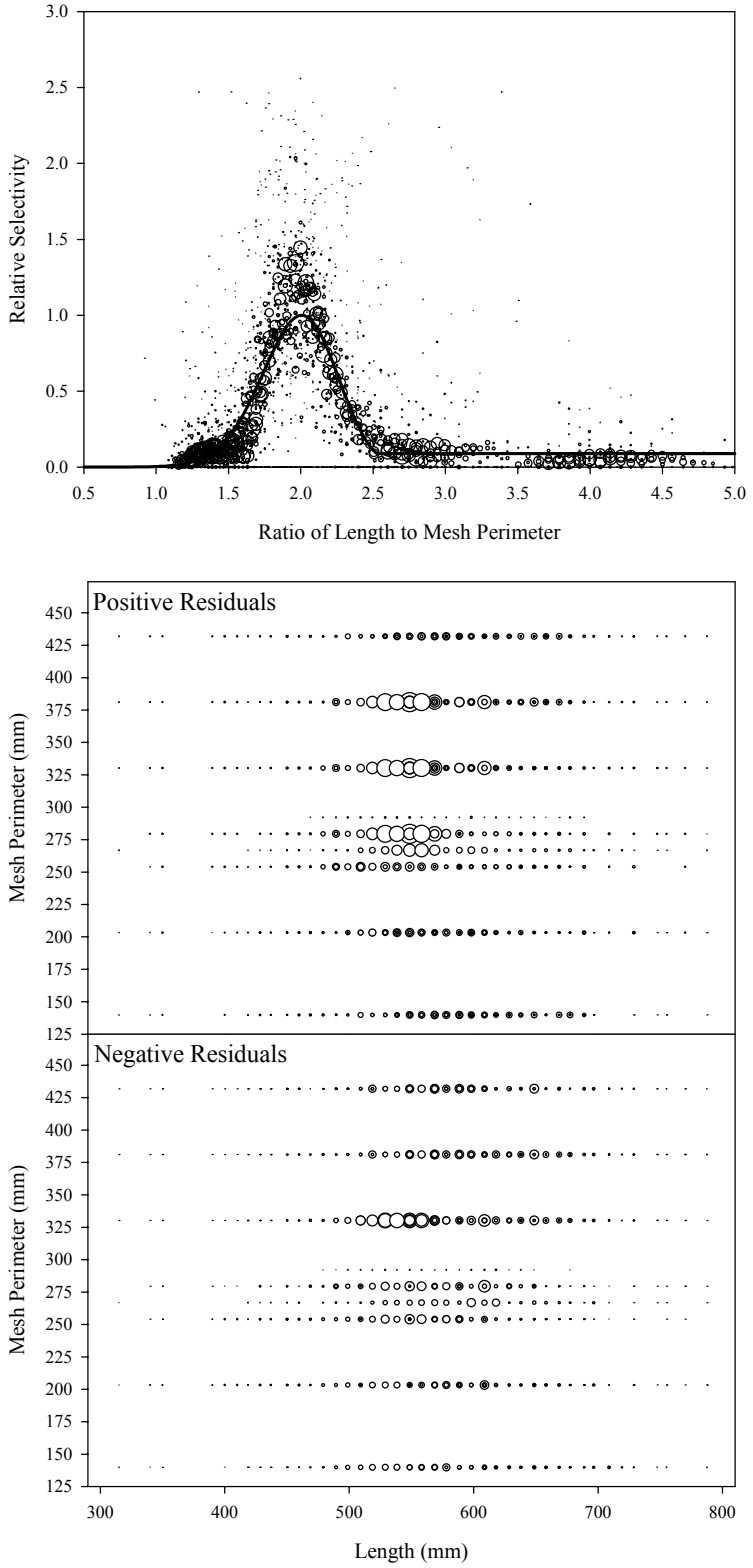

Figure B2.12. Plots of CPUE data scaled to a net selectivity model (top) and CPUE residuals (bottom); summer chum salmon data and Model 12.

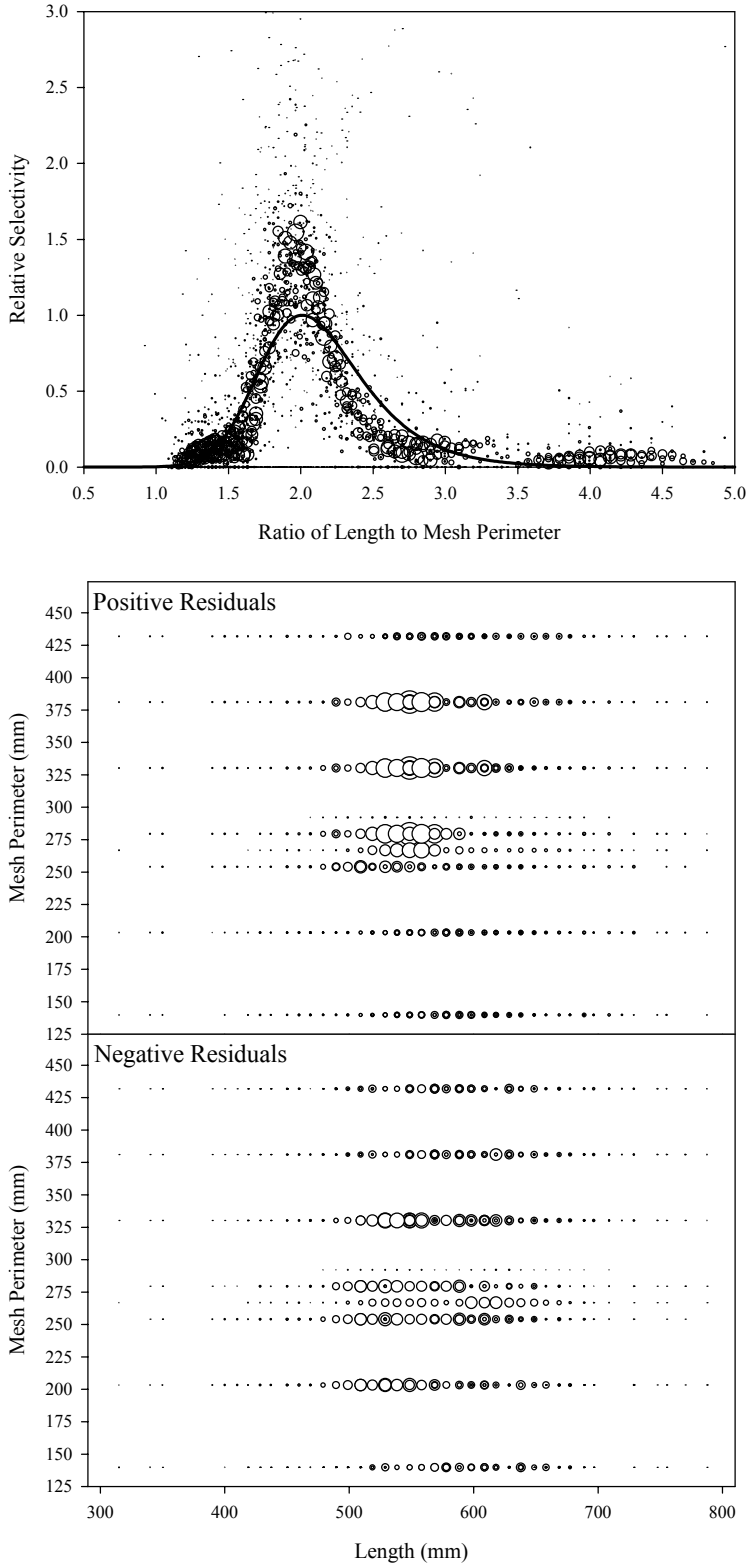

Figure B2.13. Plots of CPUE data scaled to a net selectivity model (top) and CPUE residuals (bottom); summer chum salmon data and Model 13.

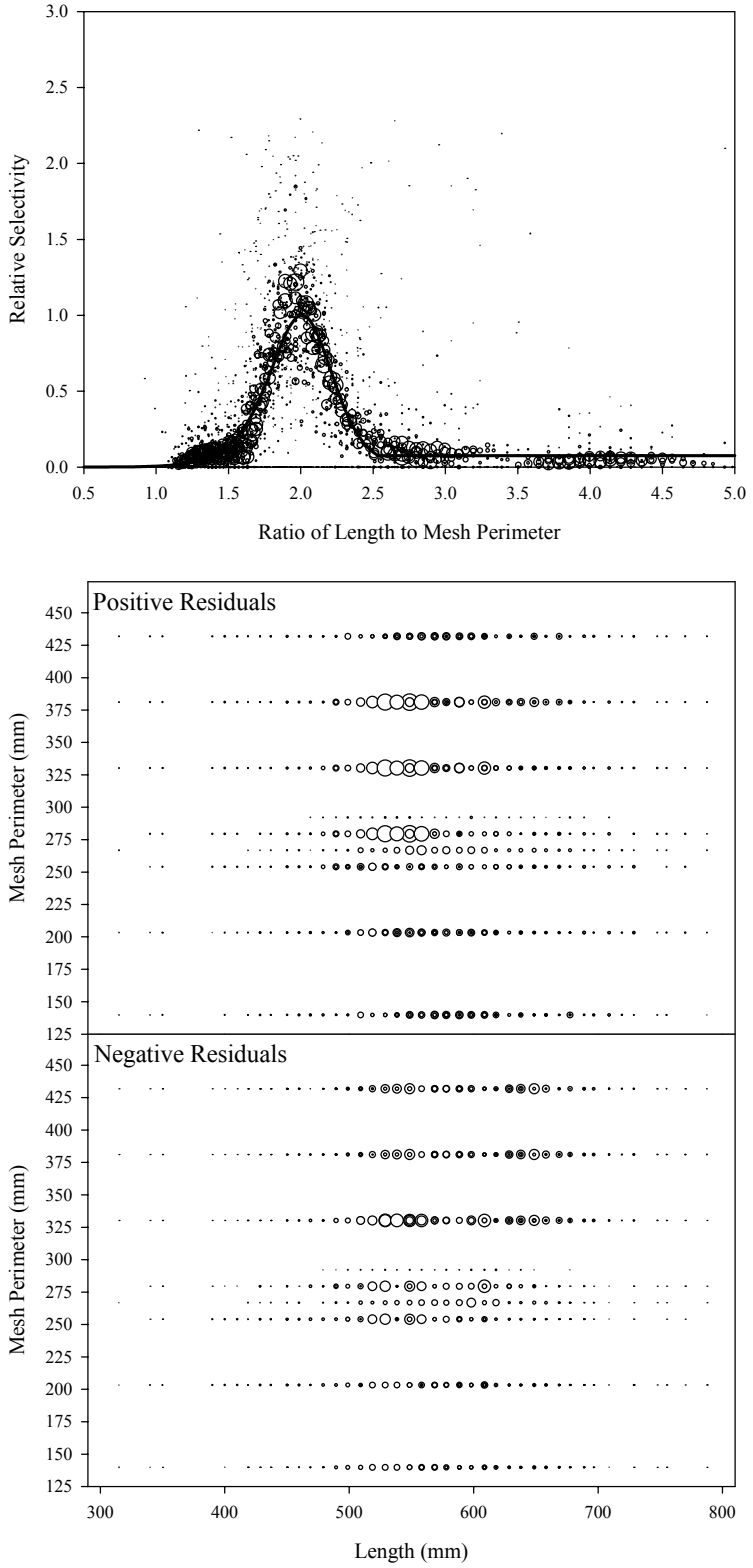

Figure B2.14. Plots of CPUE data scaled to a net selectivity model (top) and CPUE residuals (bottom); summer chum salmon data and Model 14.

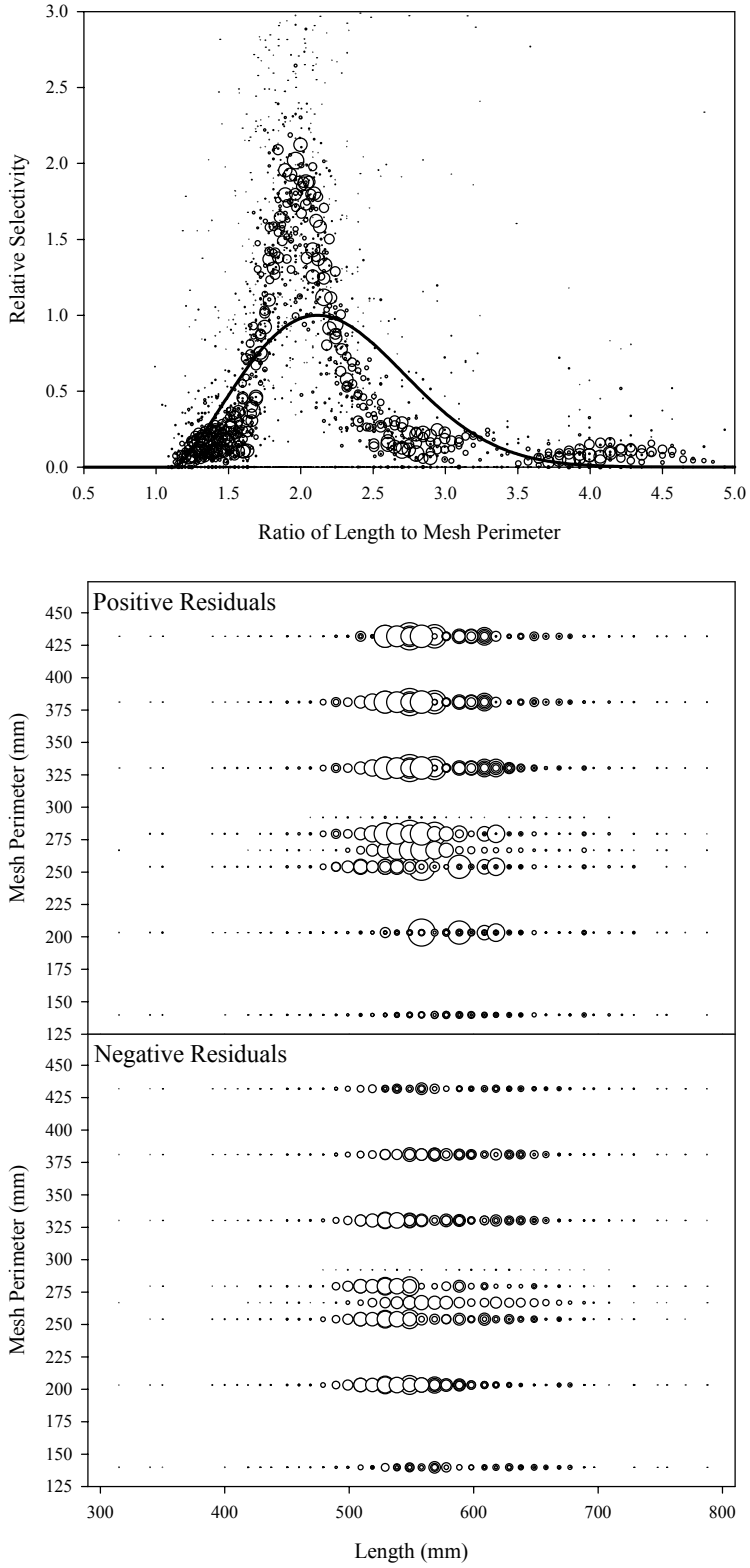

Figure B2.15. Plots of CPUE data scaled to a net selectivity model (top) and CPUE residuals (bottom); summer chum salmon data and Model 15.

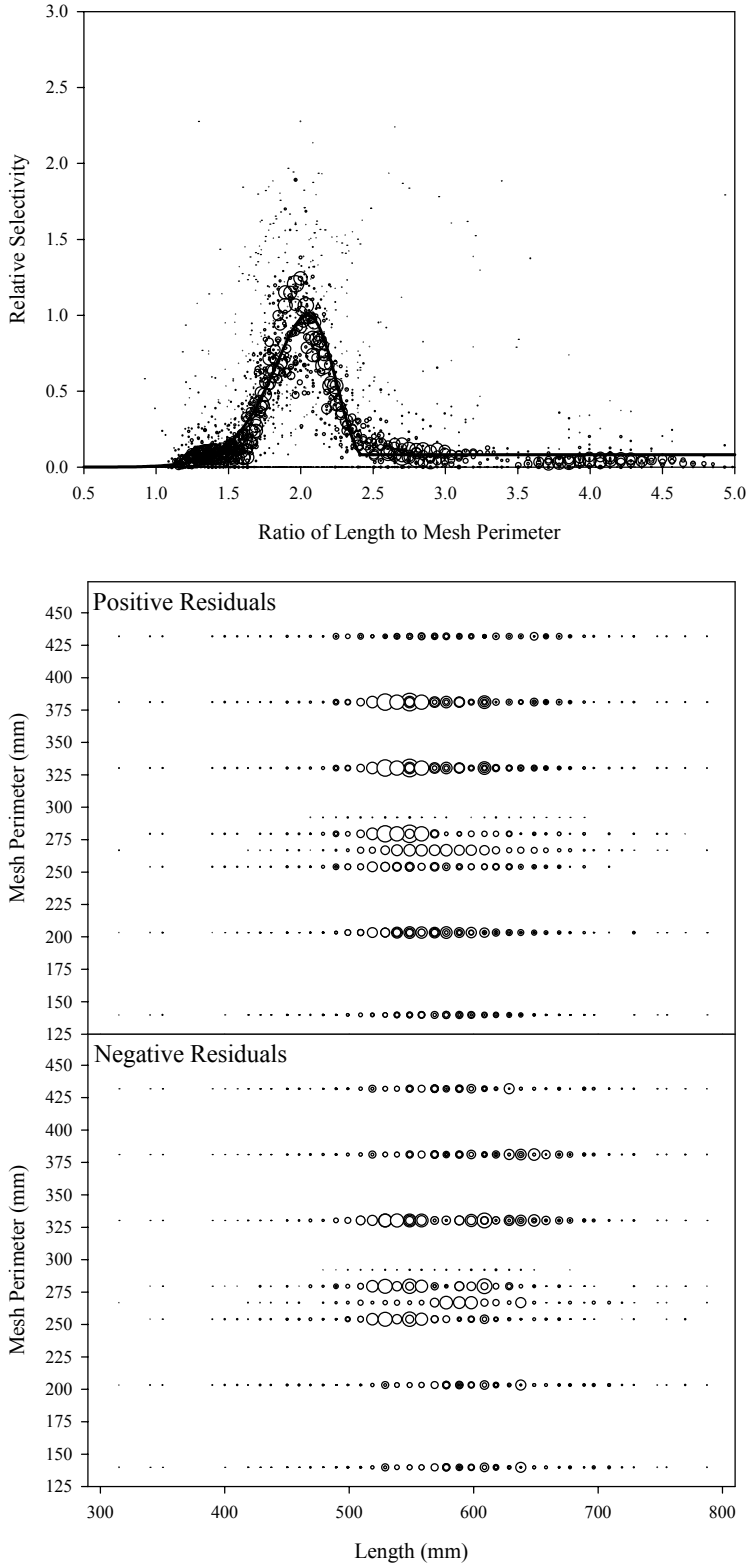

Figure B2.16. Plots of CPUE data scaled to a net selectivity model (top) and CPUE residuals (bottom); summer chum salmon data and Model 16.

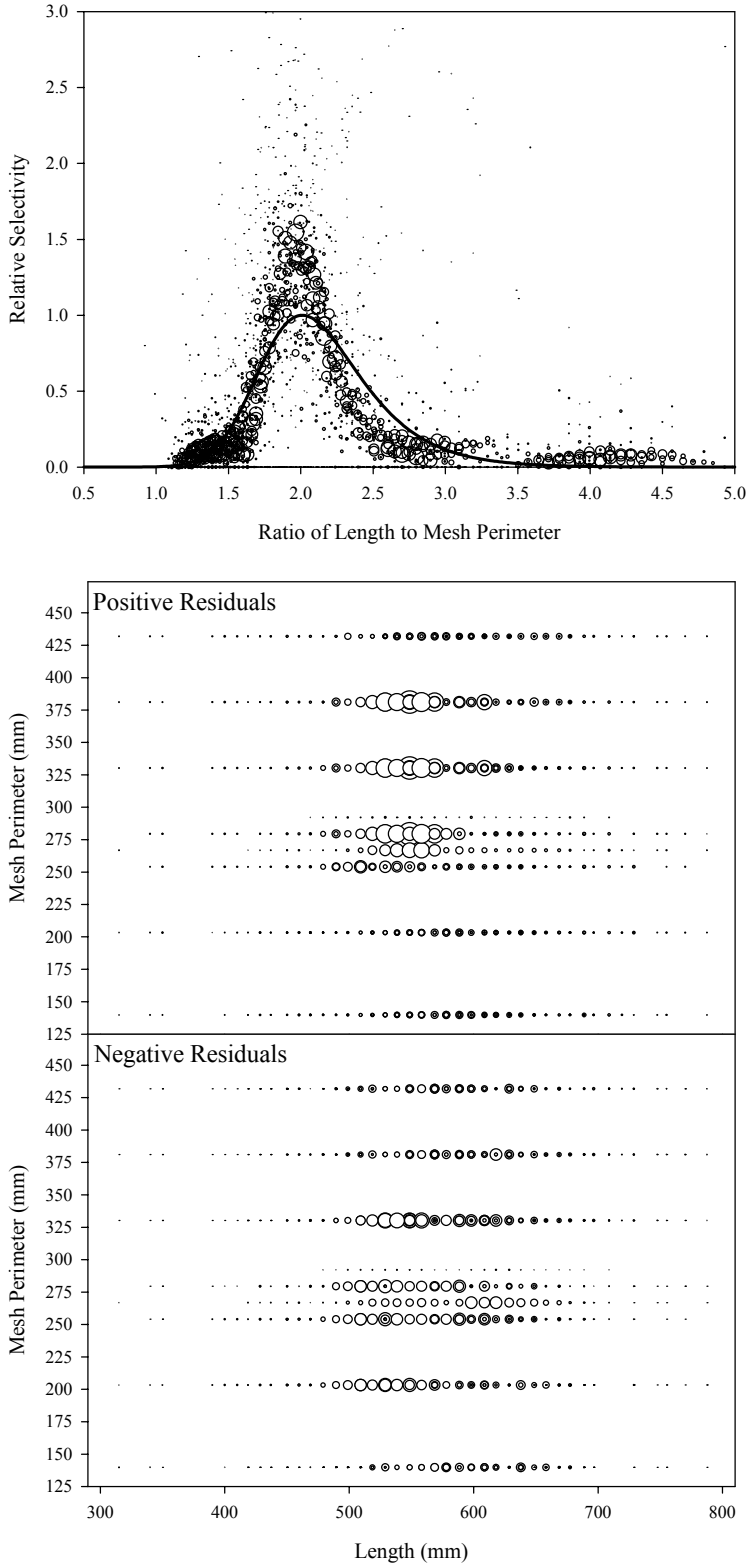

Figure B2.17. Plots of CPUE data scaled to a net selectivity model (top) and CPUE residuals (bottom); summer chum salmon data and Model 17.

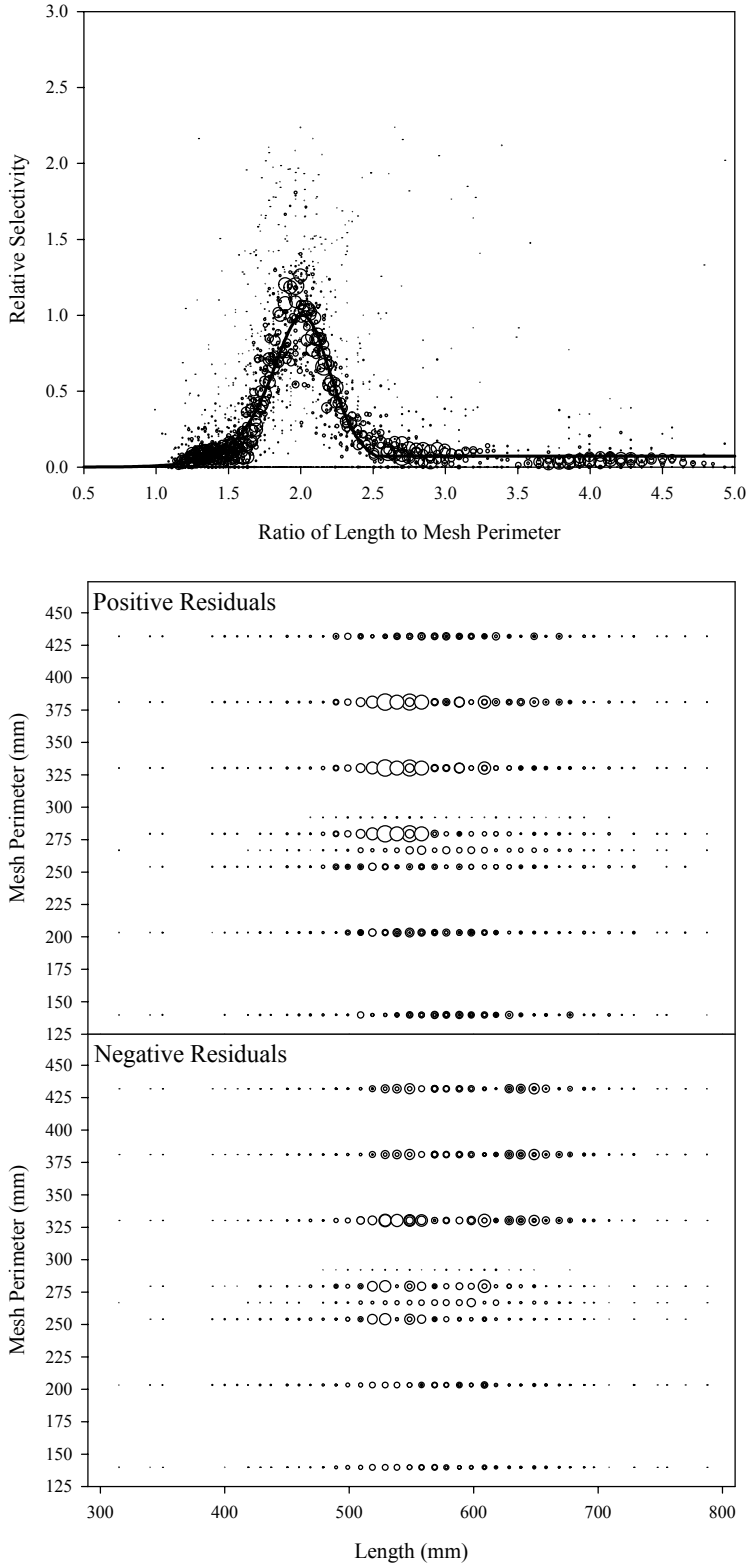

Figure B2.18. Plots of CPUE data scaled to a net selectivity model (top) and CPUE residuals (bottom); summer chum salmon data and Model 18.

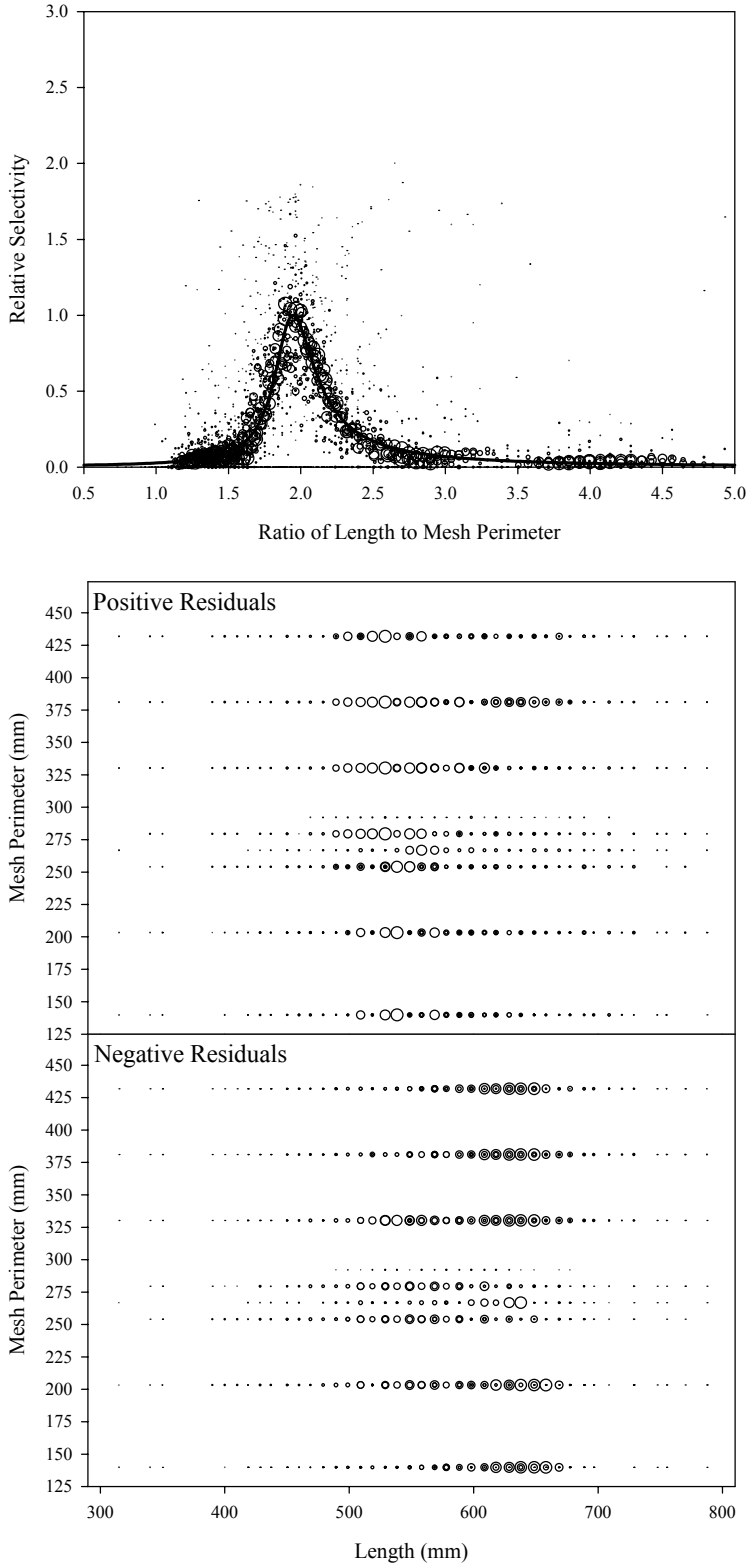

Figure B2.19. Plots of CPUE data scaled to a net selectivity model (top) and CPUE residuals (bottom); summer chum salmon data and Model 19.

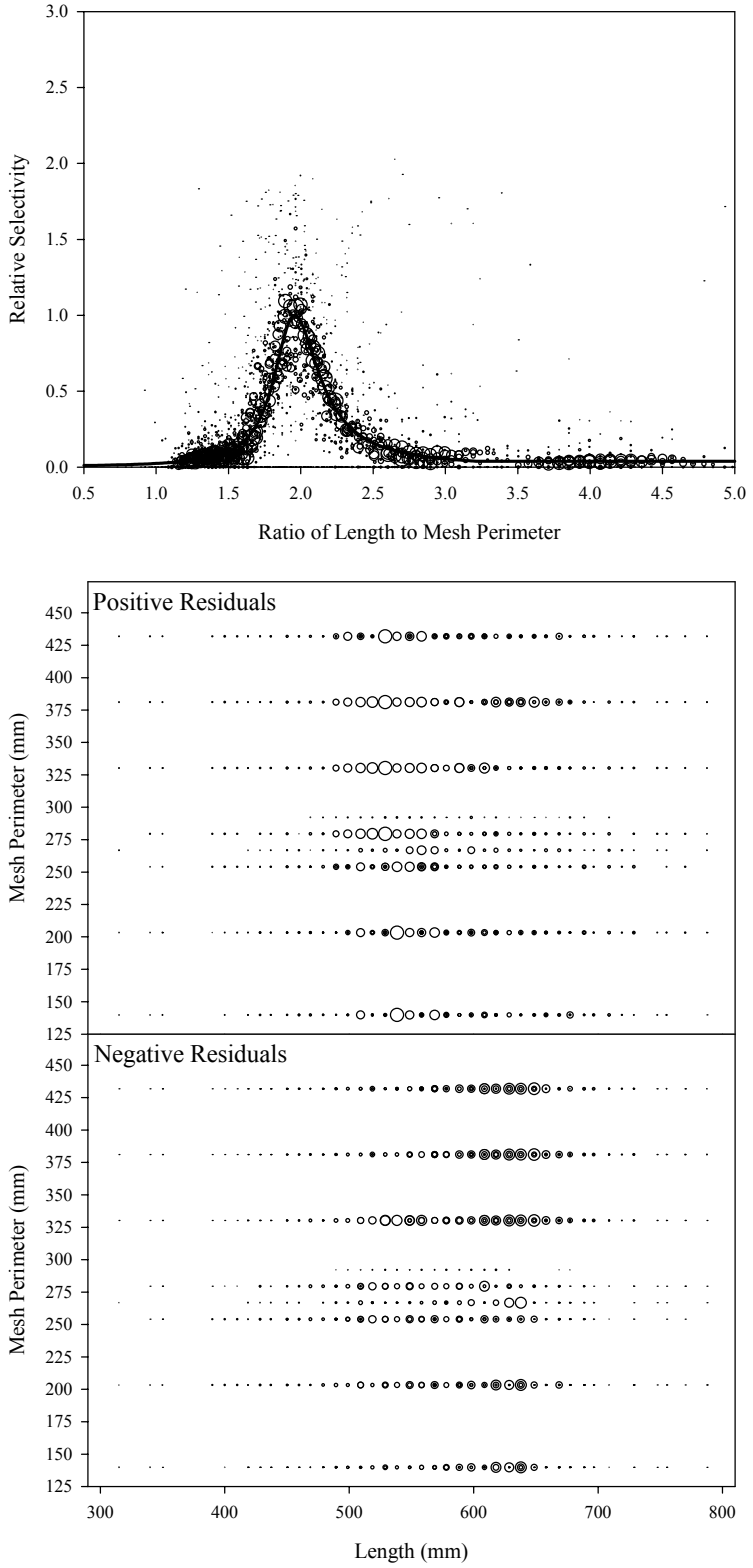

Figure B2.20. Plots of CPUE data scaled to a net selectivity model (top) and CPUE residuals (bottom); summer chum salmon data and Model 20.

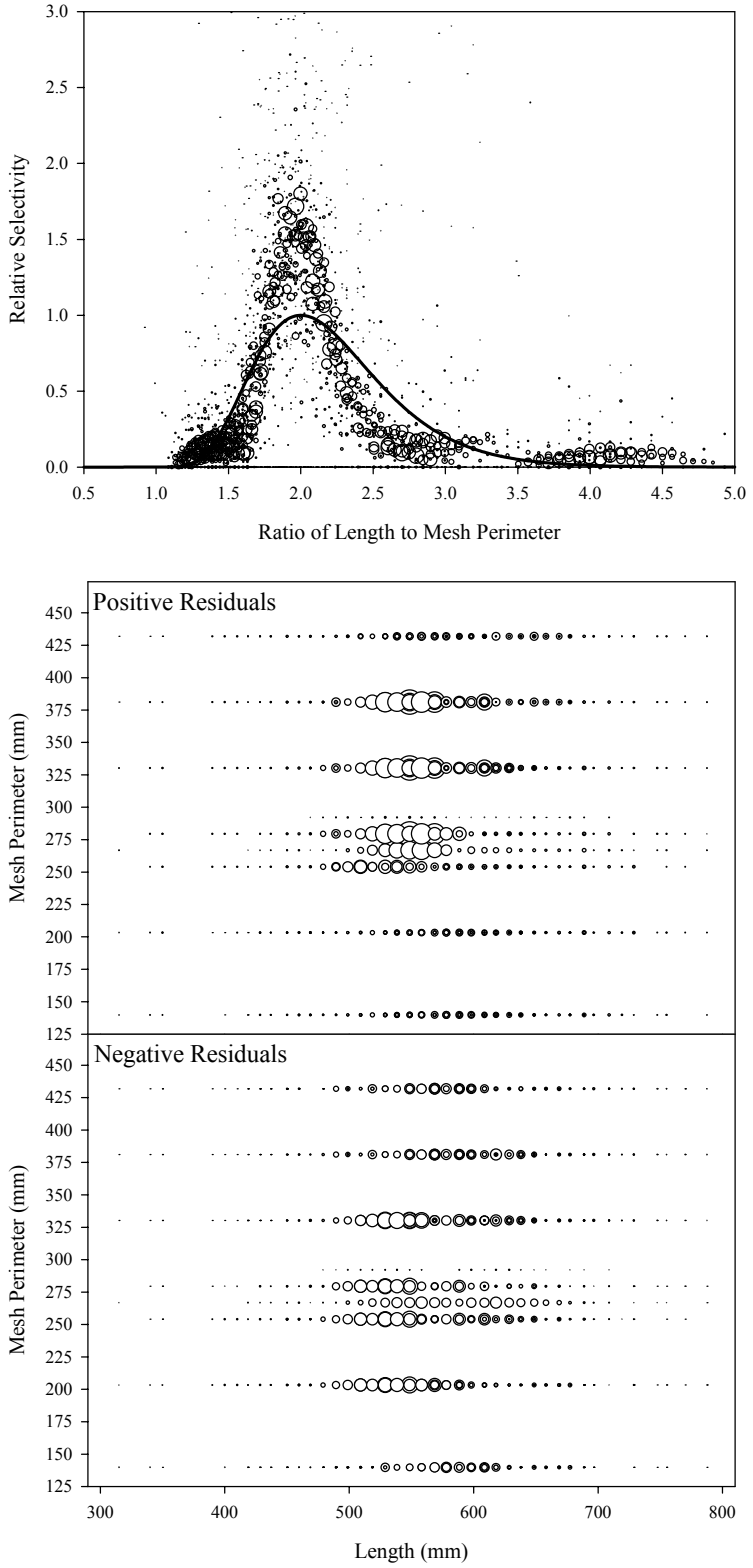

Figure B2.21. Plots of CPUE data scaled to a net selectivity model (top) and CPUE residuals (bottom); summer chum salmon data and Model 21.

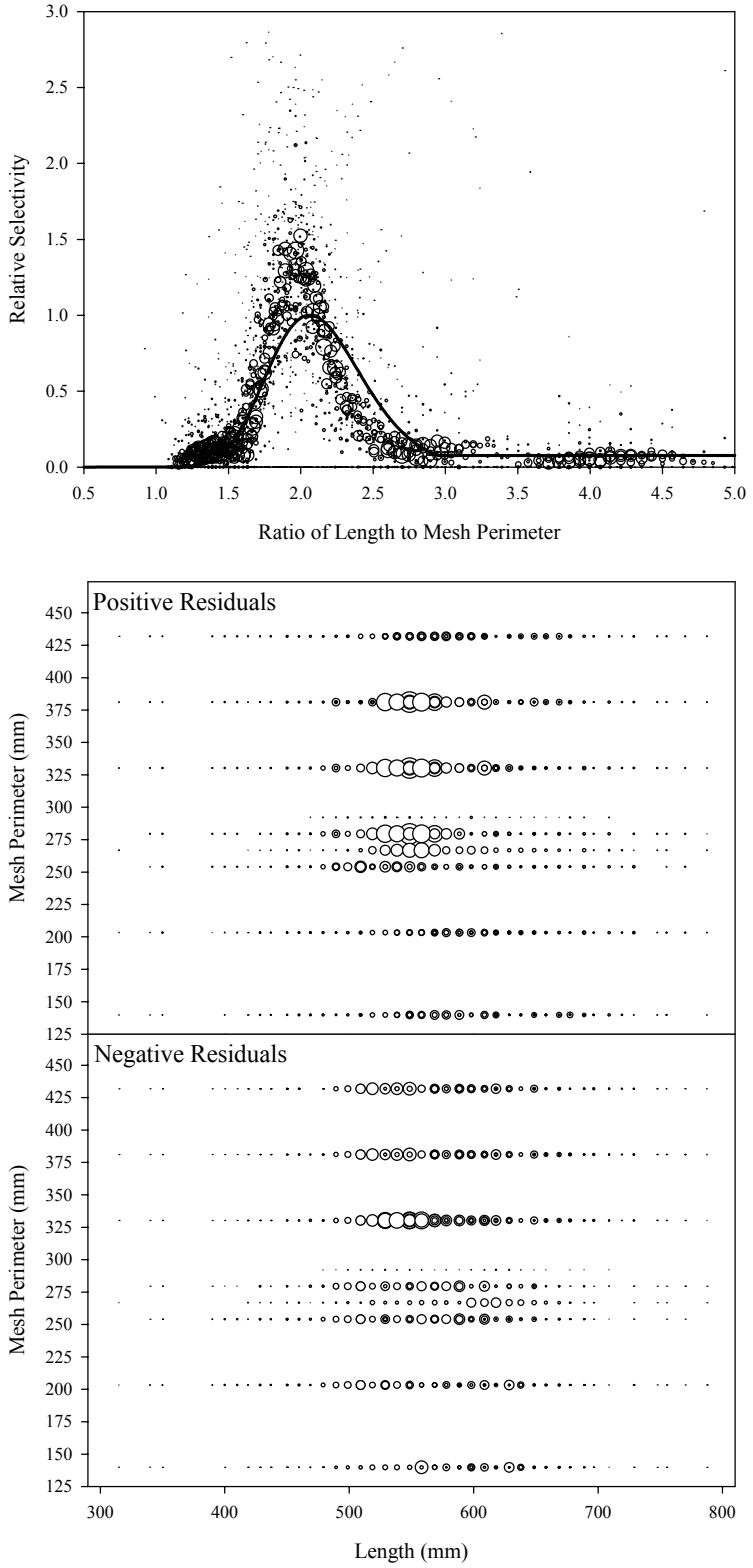

Figure B2.22. Plots of CPUE data scaled to a net selectivity model (top) and CPUE residuals (bottom); summer chum salmon data and Model 22.

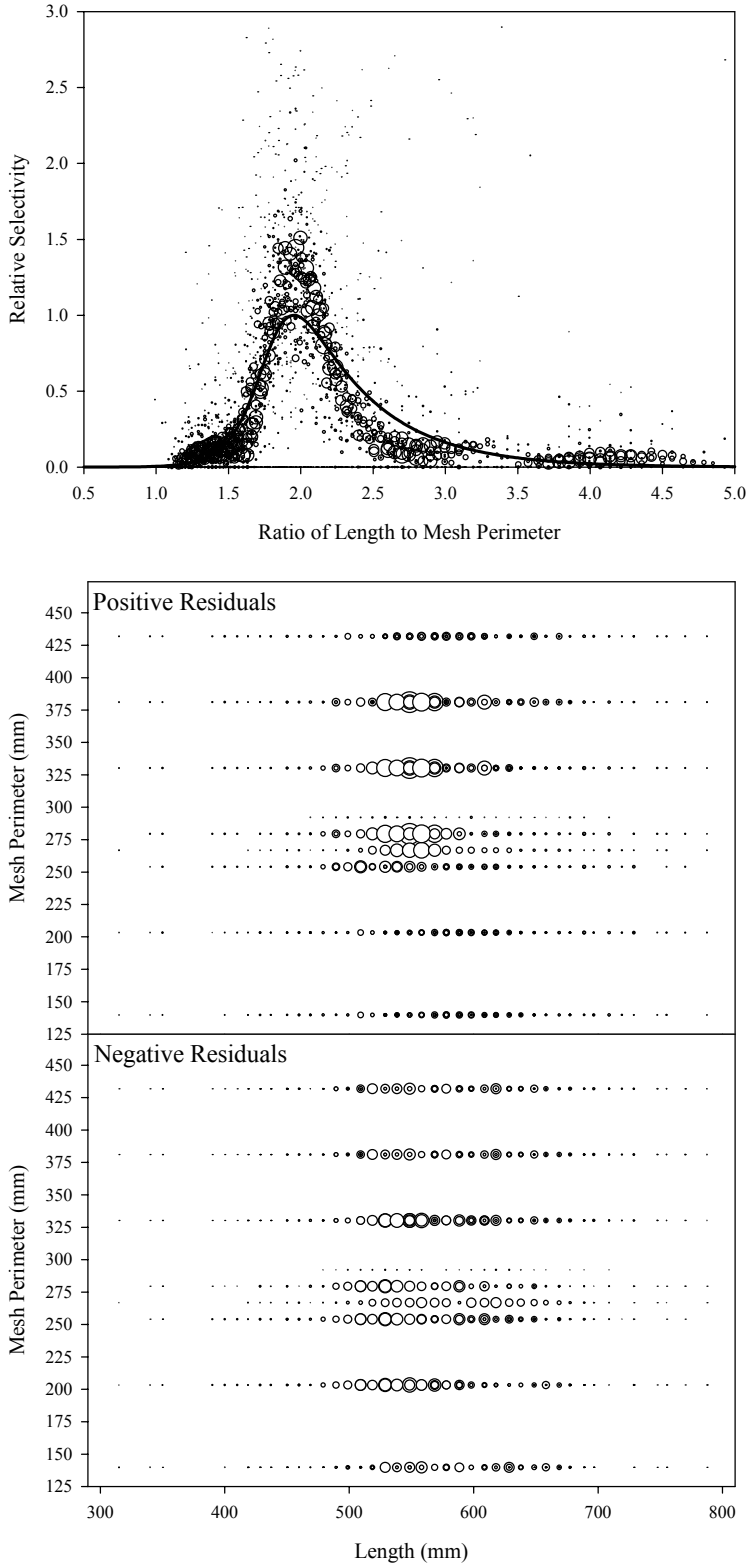

Figure B2.23. Plots of CPUE data scaled to a net selectivity model (top) and CPUE residuals (bottom); summer chum salmon data and Model 23.

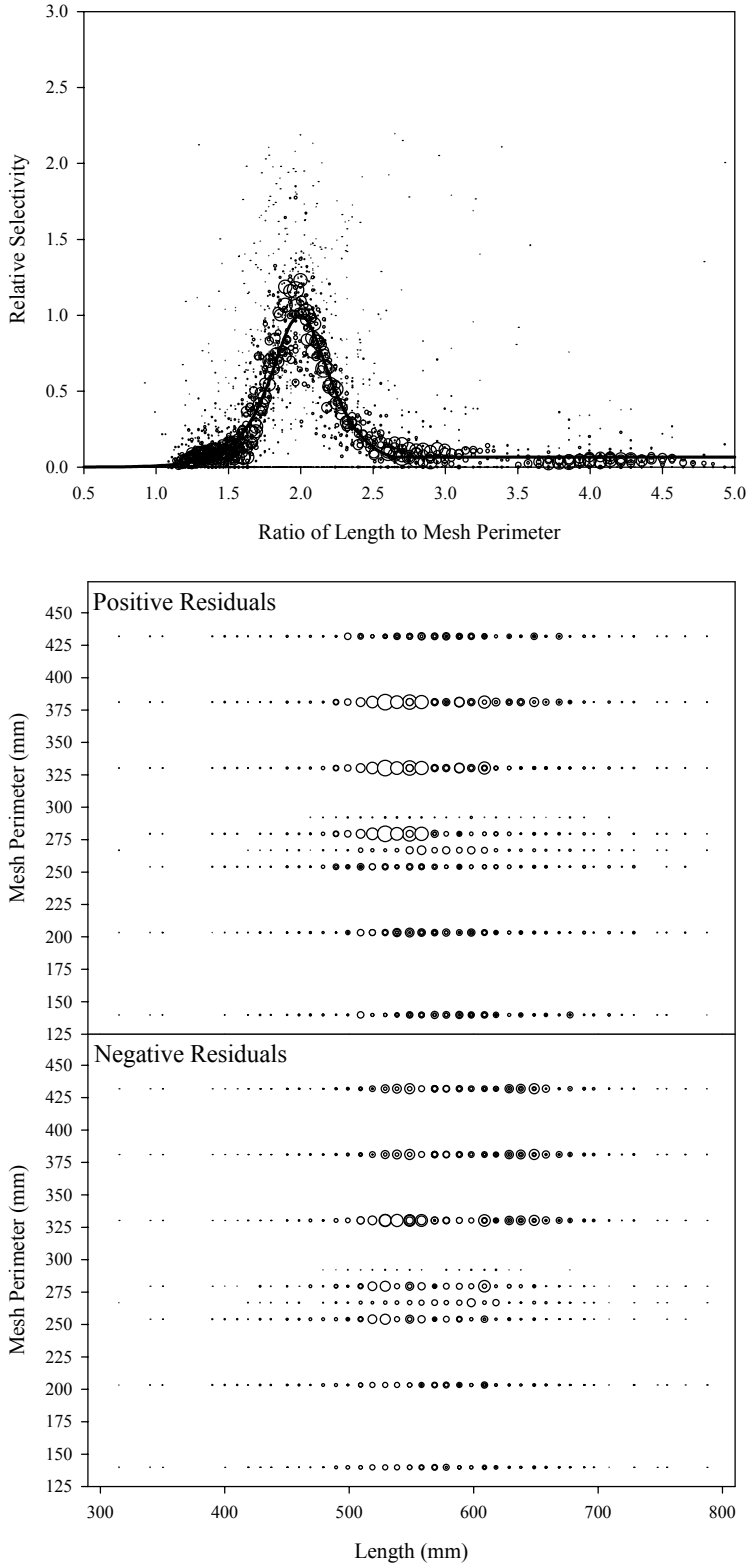

Figure B2.24. Plots of CPUE data scaled to a net selectivity model (top) and CPUE residuals (bottom); summer chum salmon data and Model 24.

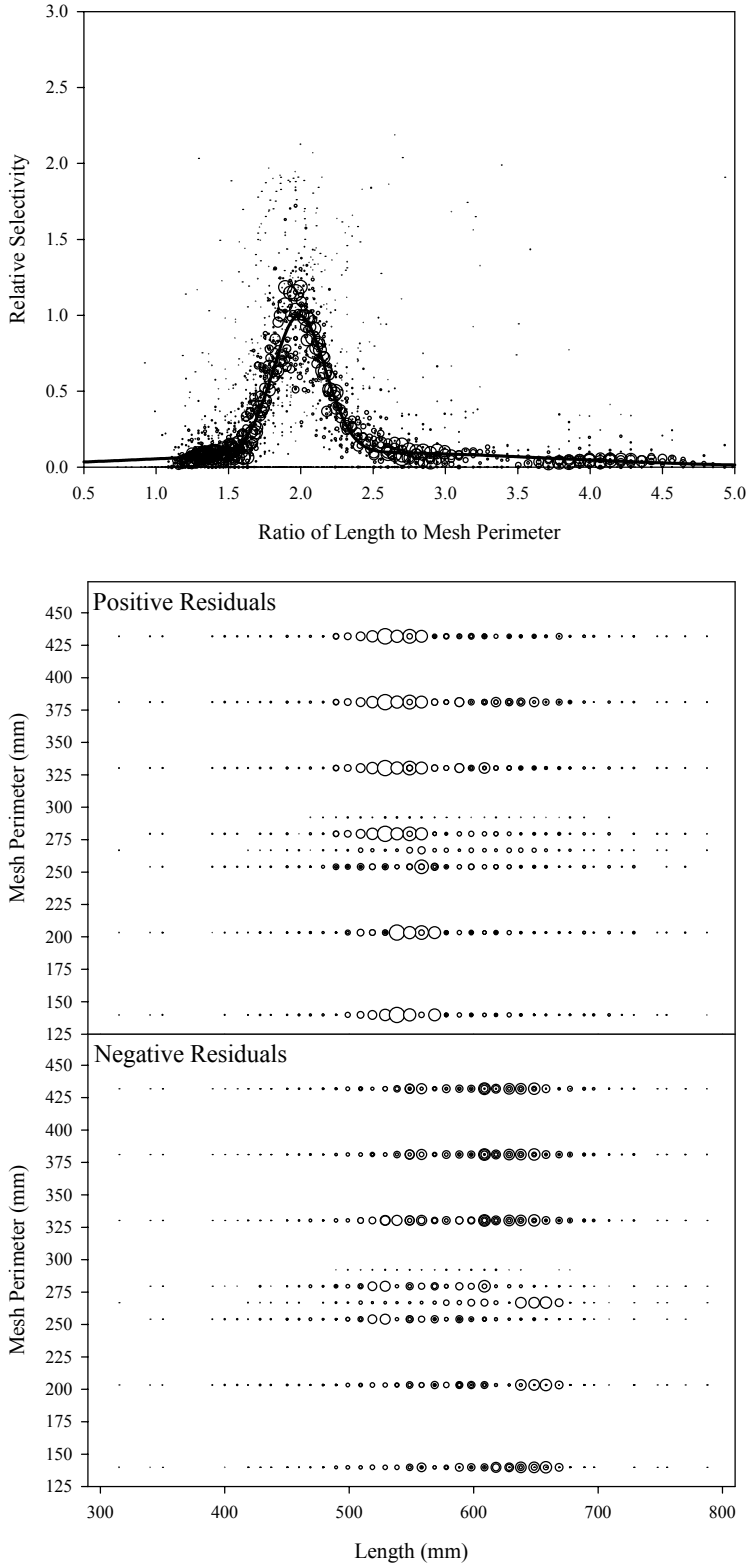

Figure B2.25. Plots of CPUE data scaled to a net selectivity model (top) and CPUE residuals (bottom); summer chum salmon data and Model 25.

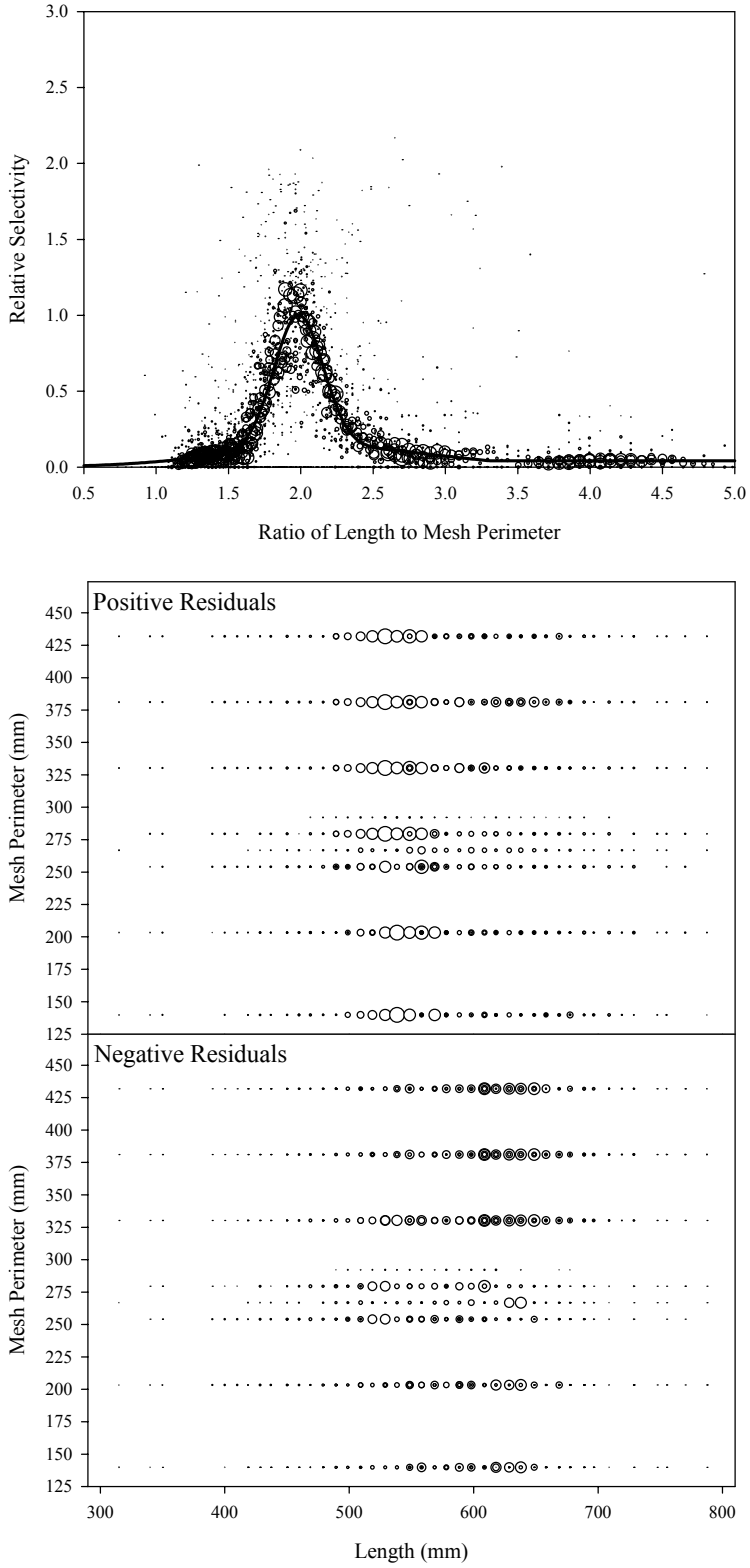

Figure B2.26. Plots of CPUE data scaled to a net selectivity model (top) and CPUE residuals (bottom); summer chum salmon data and Model 26.

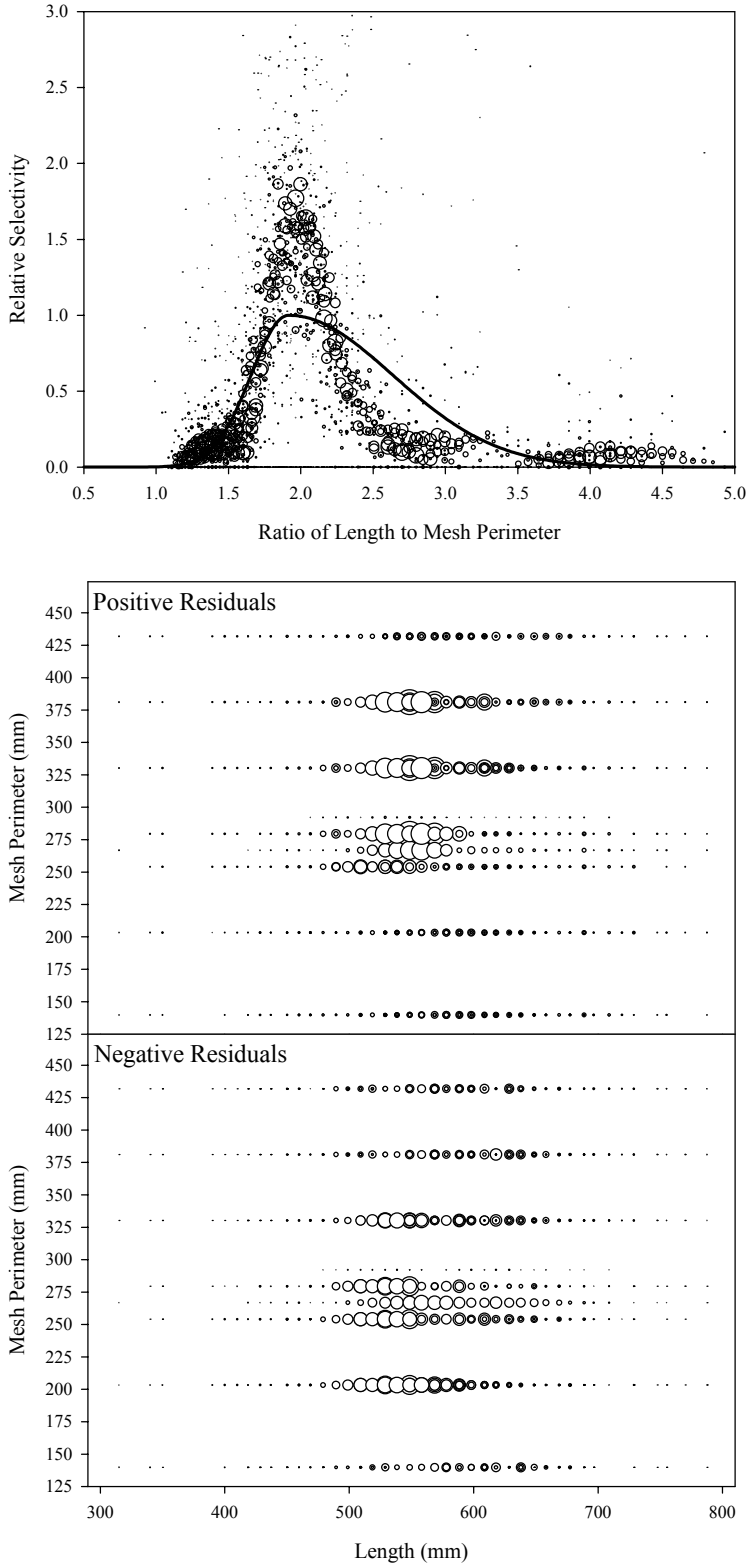

Figure B2.27. Plots of CPUE data scaled to a net selectivity model (top) and CPUE residuals (bottom); summer chum salmon data and Model 27.

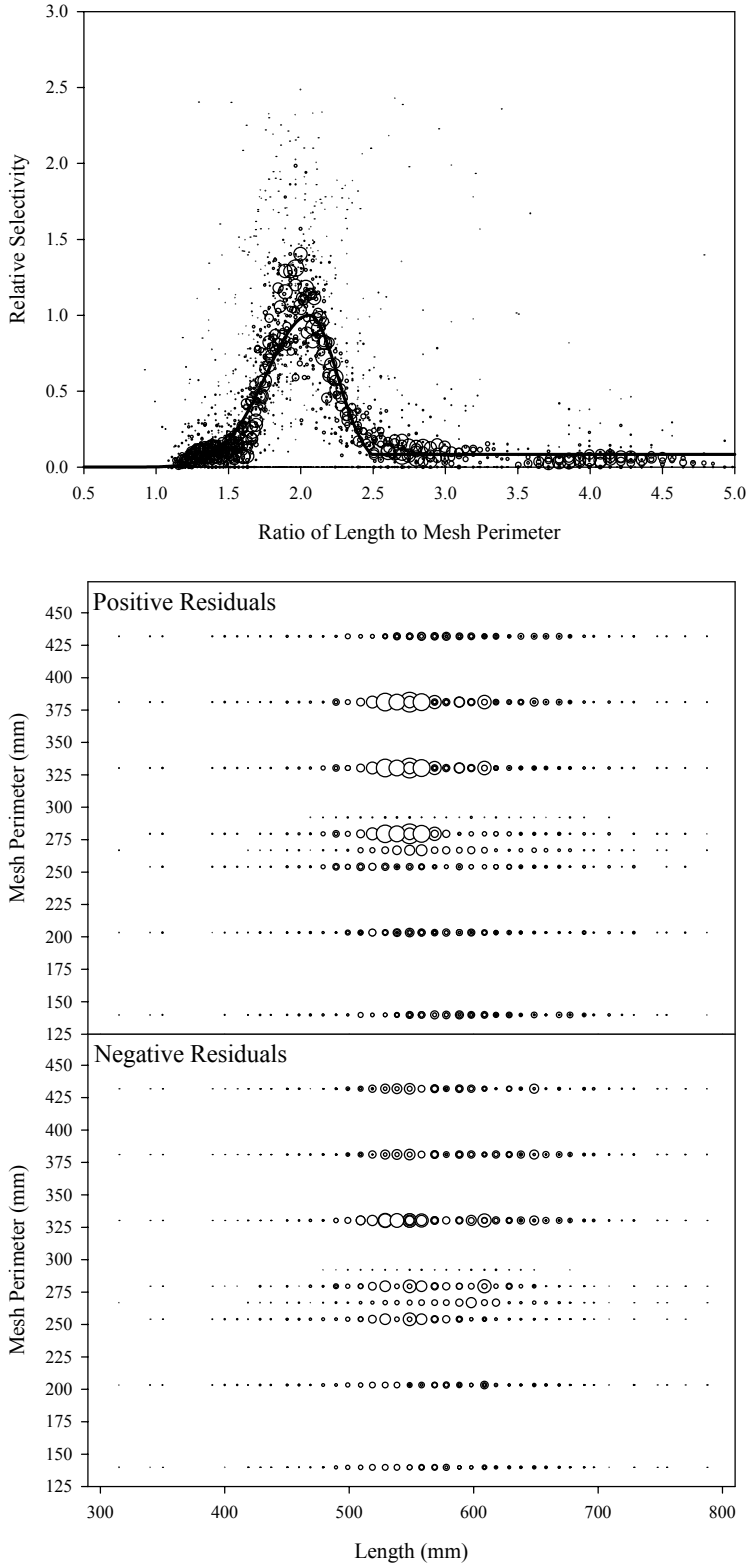

Figure B2.28. Plots of CPUE data scaled to a net selectivity model (top) and CPUE residuals (bottom); summer chum salmon data and Model 28.

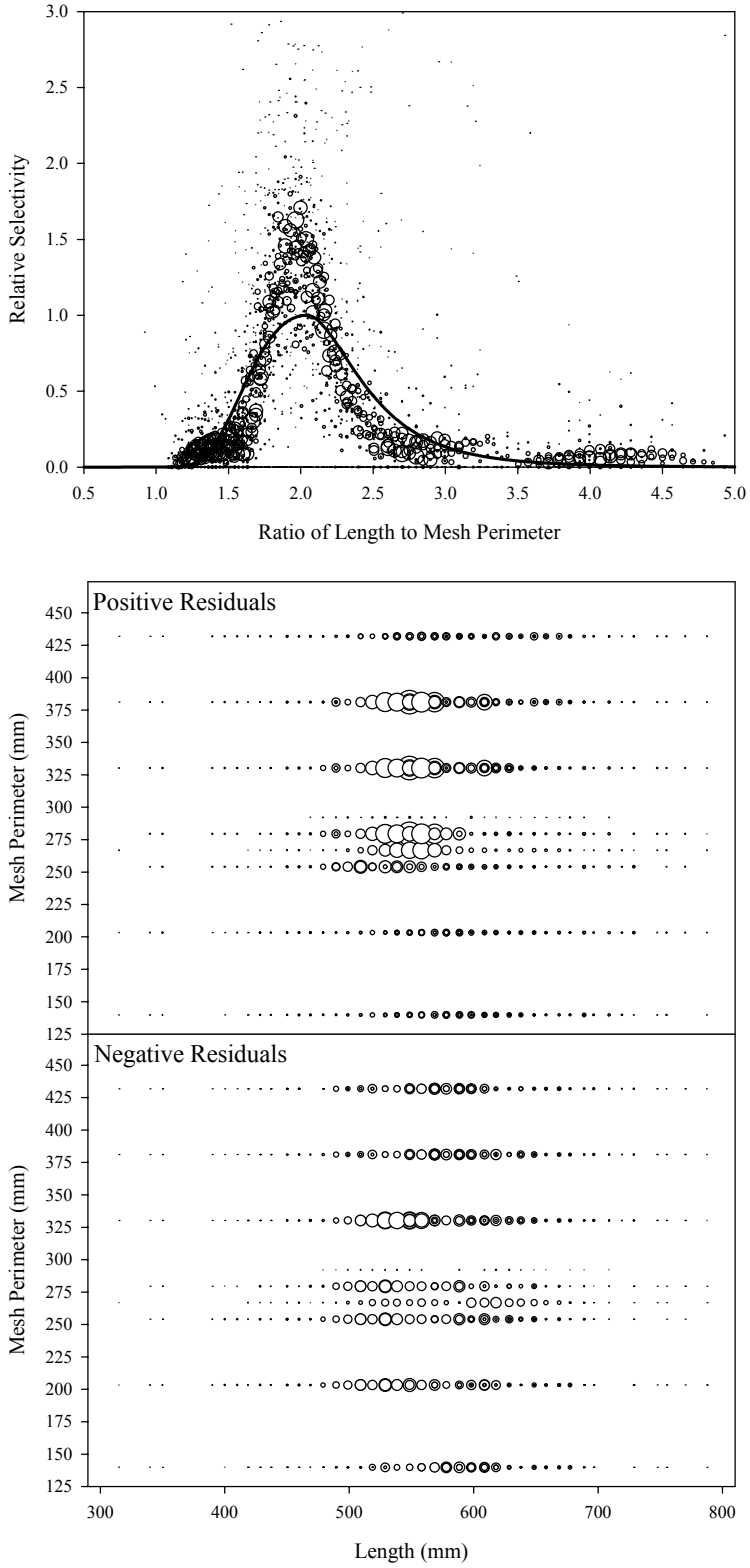

Figure B2.29. Plots of CPUE data scaled to a net selectivity model (top) and CPUE residuals (bottom); summer chum salmon data and Model 29.

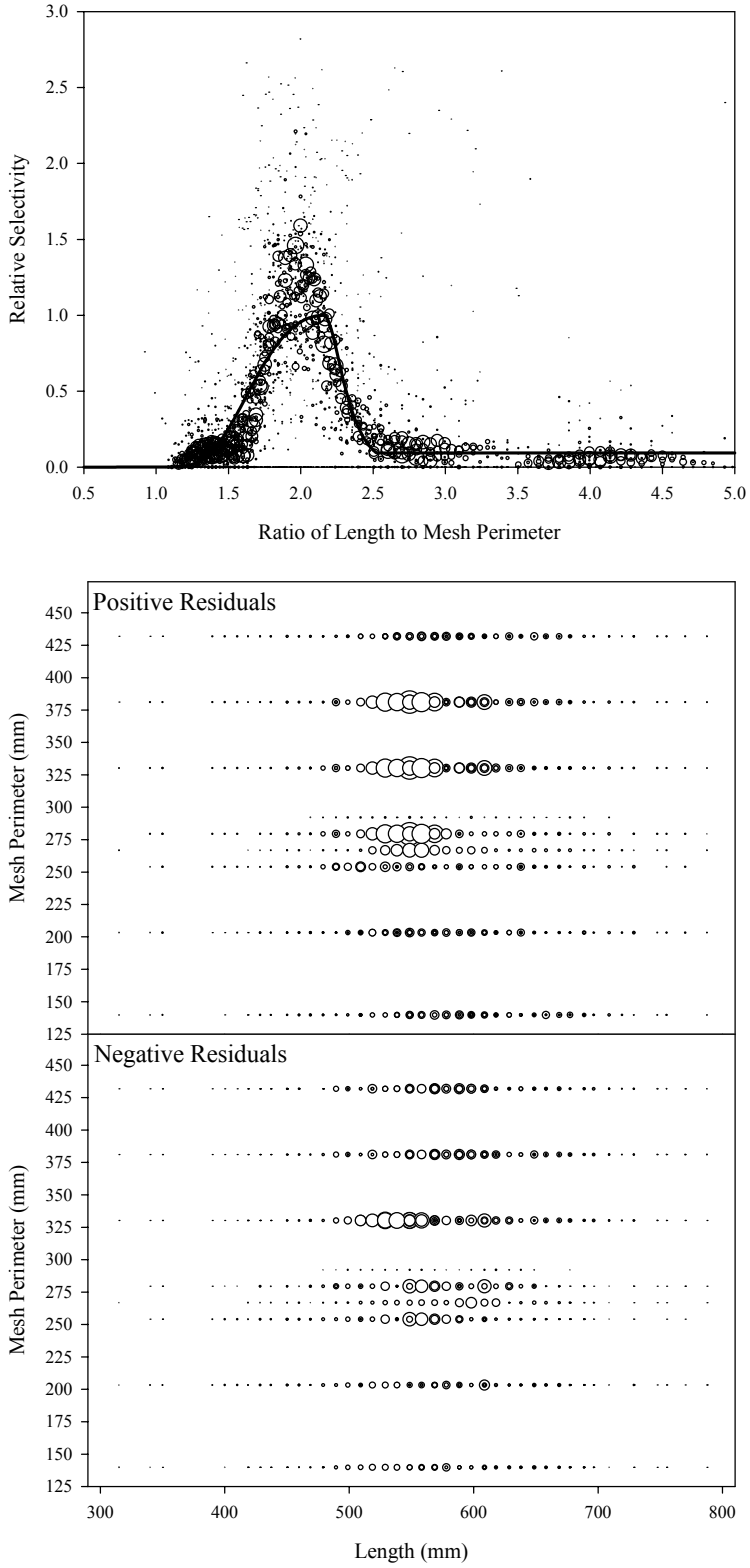

Figure B2.30. Plots of CPUE data scaled to a net selectivity model (top) and CPUE residuals (bottom); summer chum salmon data and Model 30.

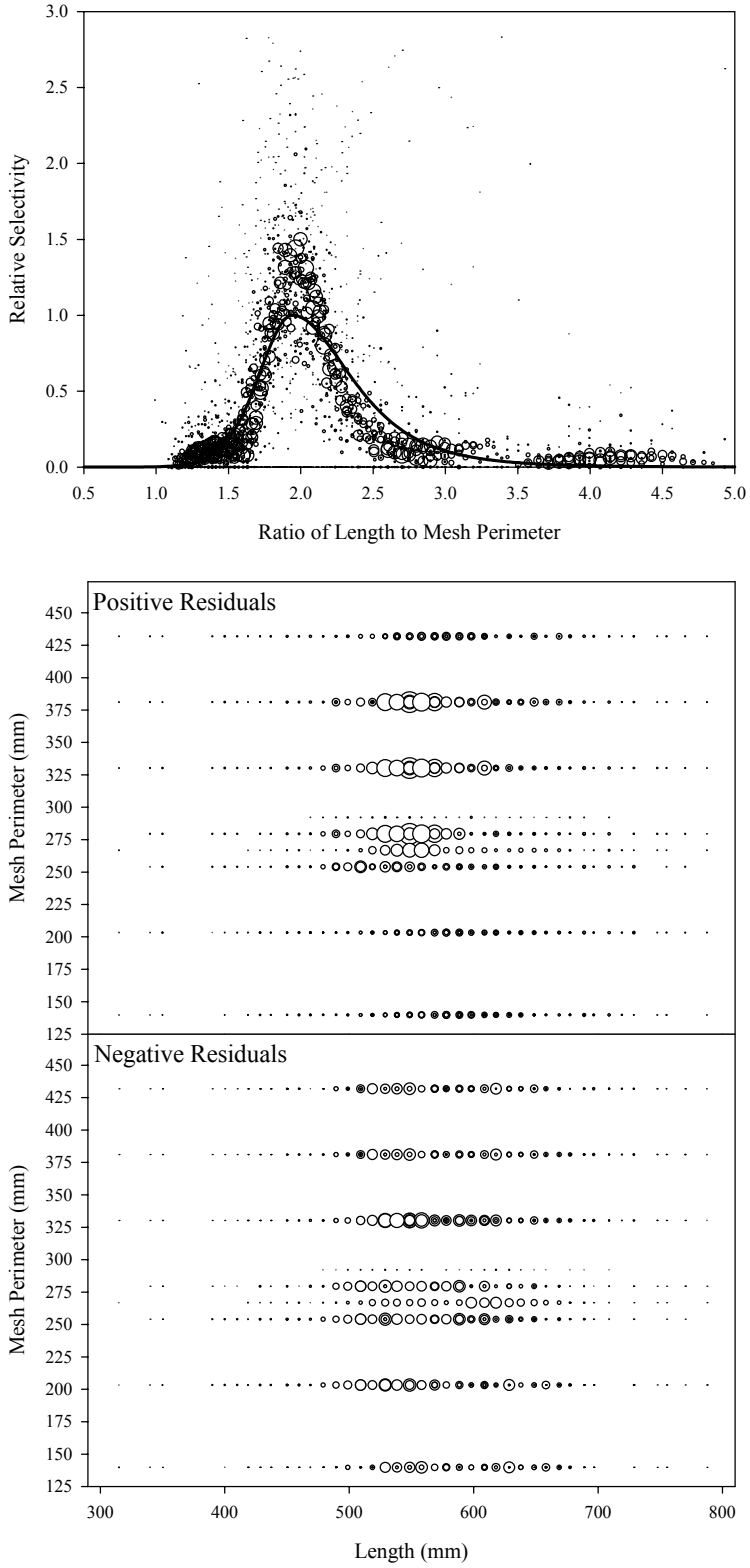

Figure B2.31. Plots of CPUE data scaled to a net selectivity model (top) and CPUE residuals (bottom); summer chum salmon data and Model 31.

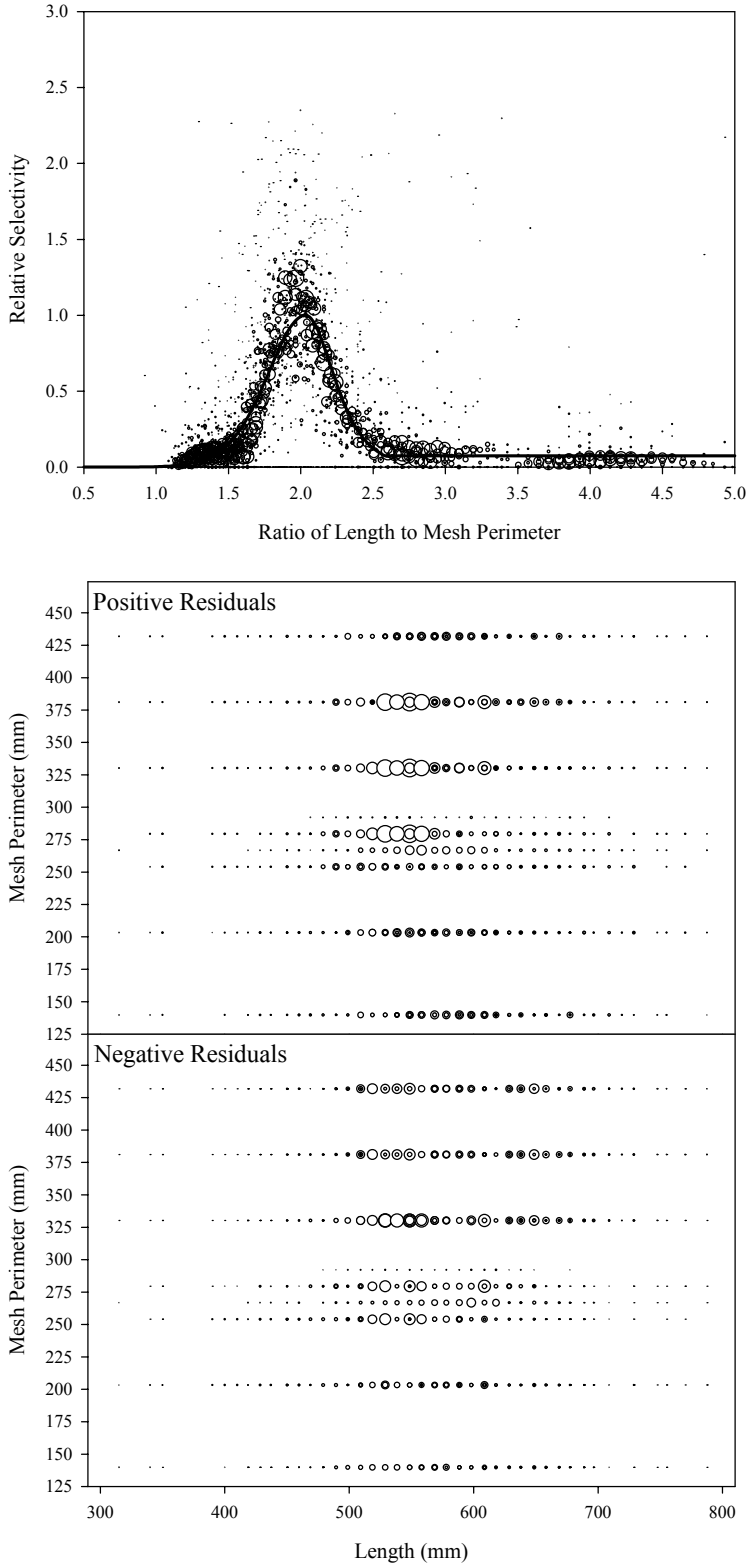

Figure B2.32. Plots of CPUE data scaled to a net selectivity model (top) and CPUE residuals (bottom); summer chum salmon data and Model 32.

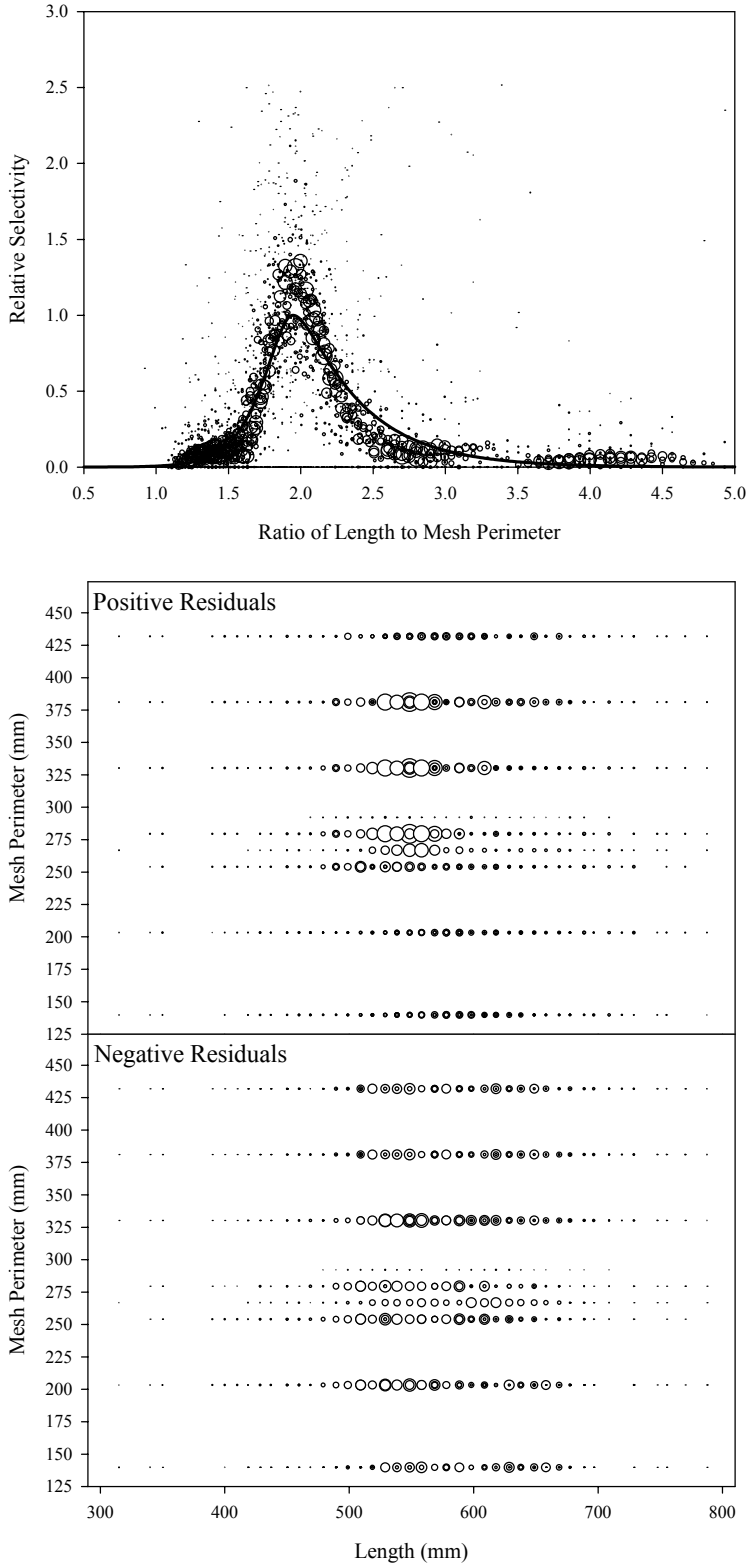

Figure B2.33. Plots of CPUE data scaled to a net selectivity model (top) and CPUE residuals (bottom); summer chum salmon data and Model 33.

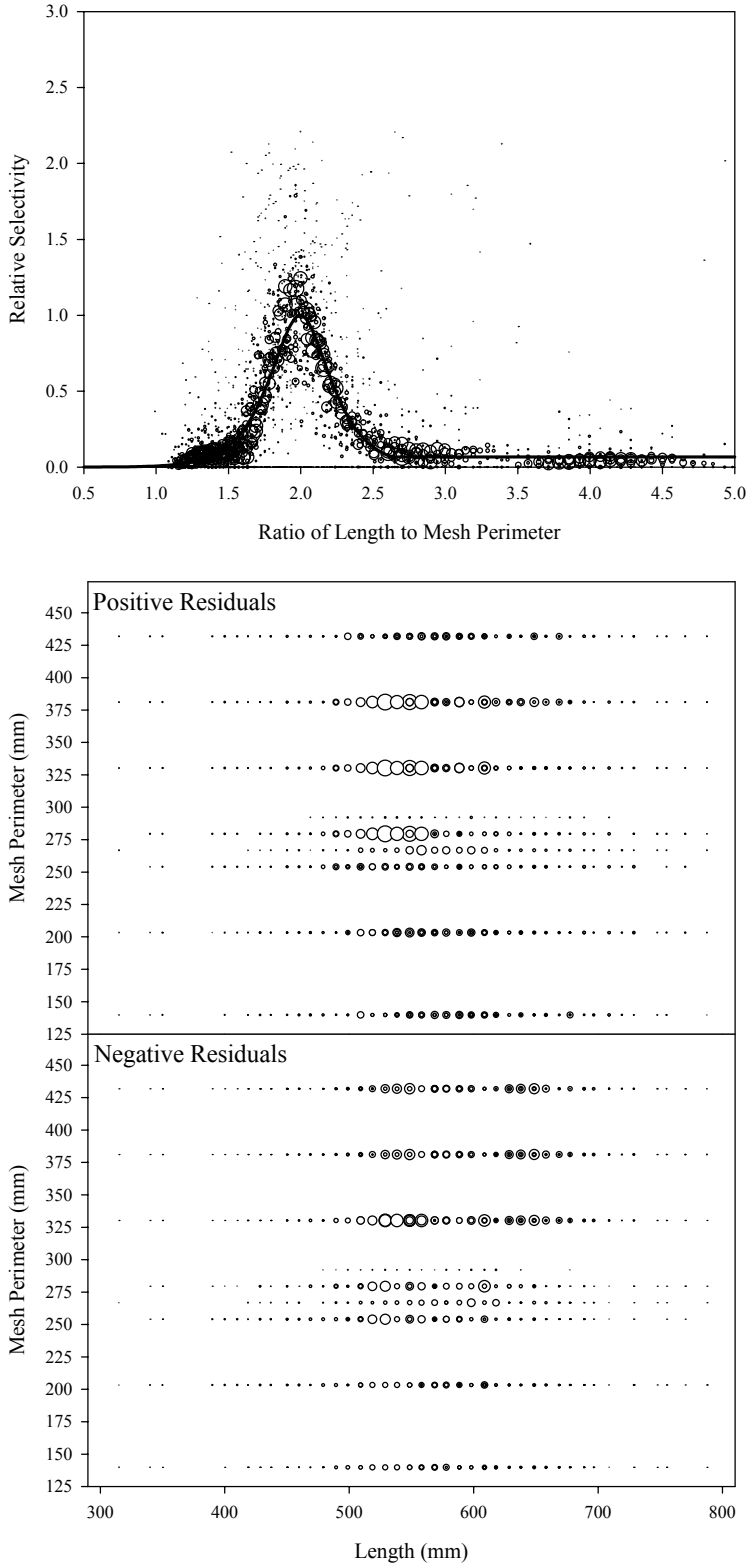

Figure B2.34. Plots of CPUE data scaled to a net selectivity model (top) and CPUE residuals (bottom); summer chum salmon data and Model 34.

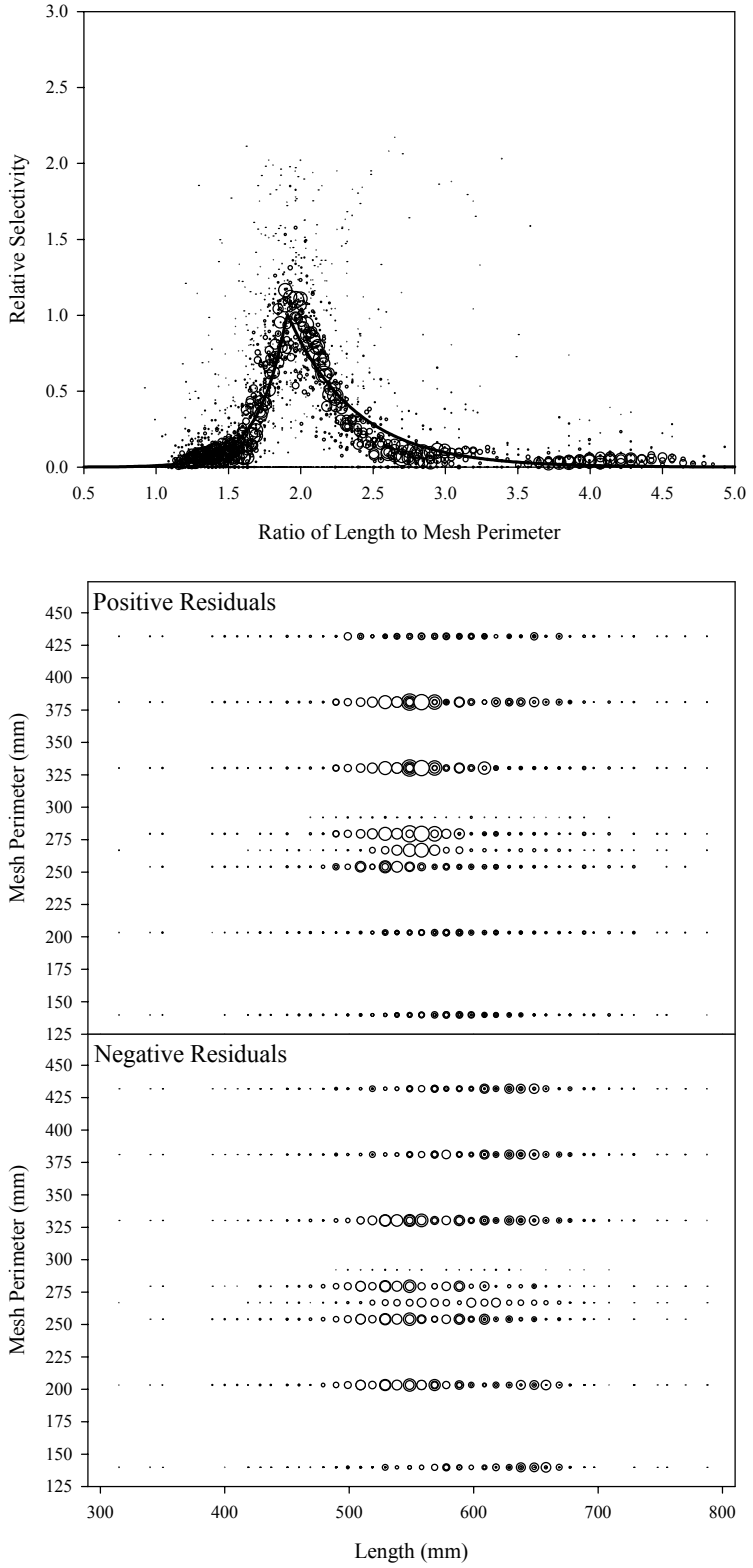

Figure B2.35. Plots of CPUE data scaled to a net selectivity model (top) and CPUE residuals (bottom); summer chum salmon data and Model 35.

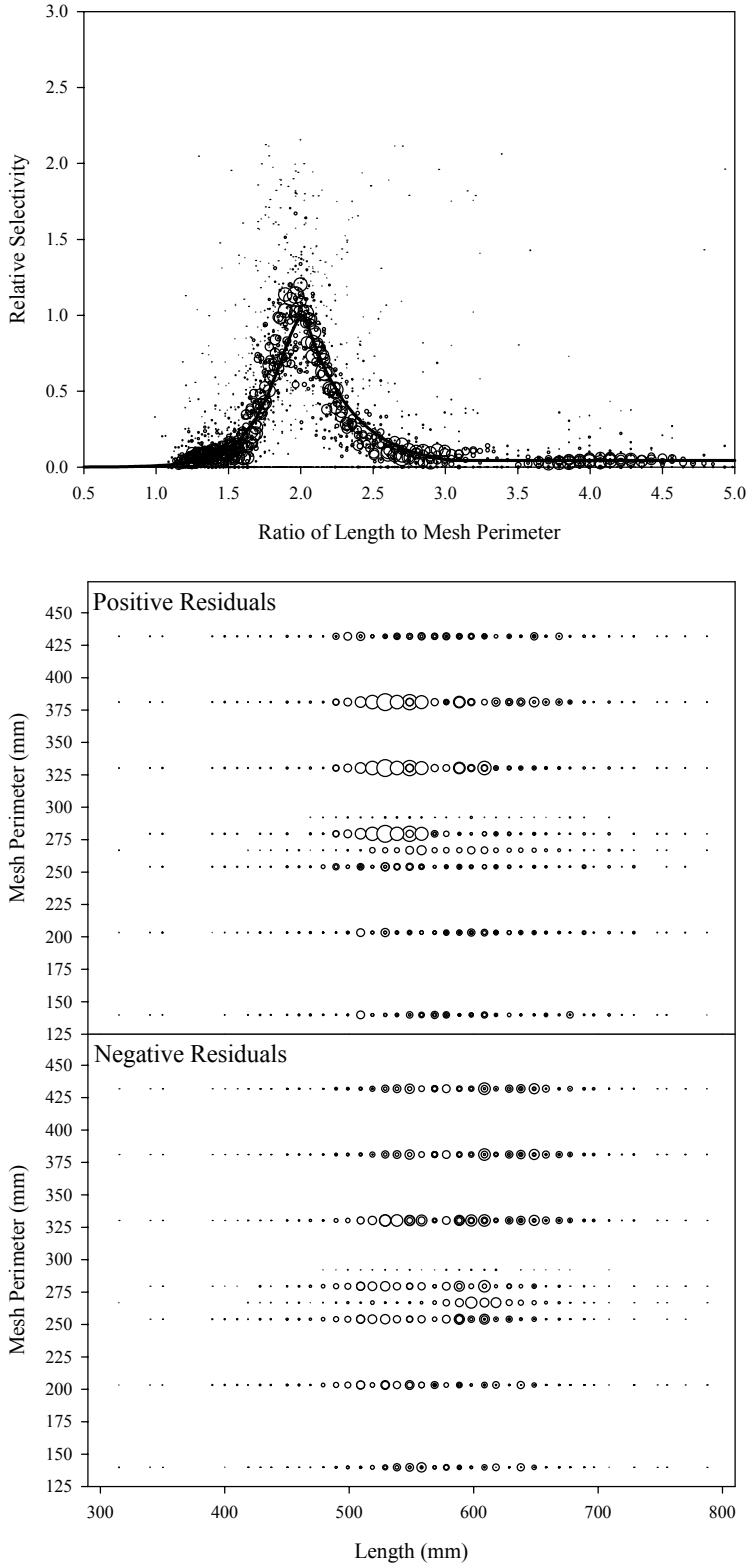

Figure B2.36. Plots of CPUE data scaled to a net selectivity model (top) and CPUE residuals (bottom); summer chum salmon data and Model 36.

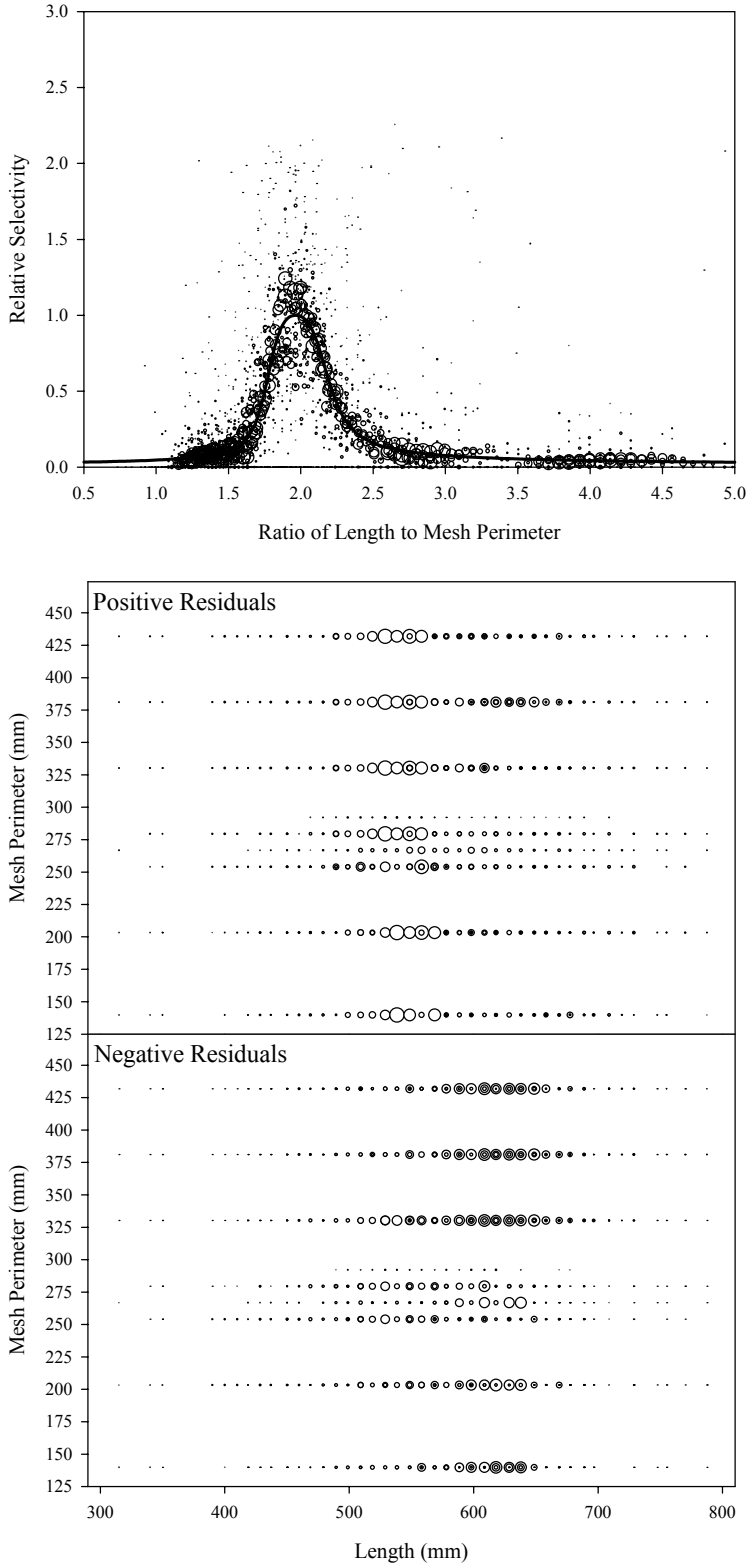

Figure B2.37. Plots of CPUE data scaled to a net selectivity model (top) and CPUE residuals (bottom); summer chum salmon data and Model 37.

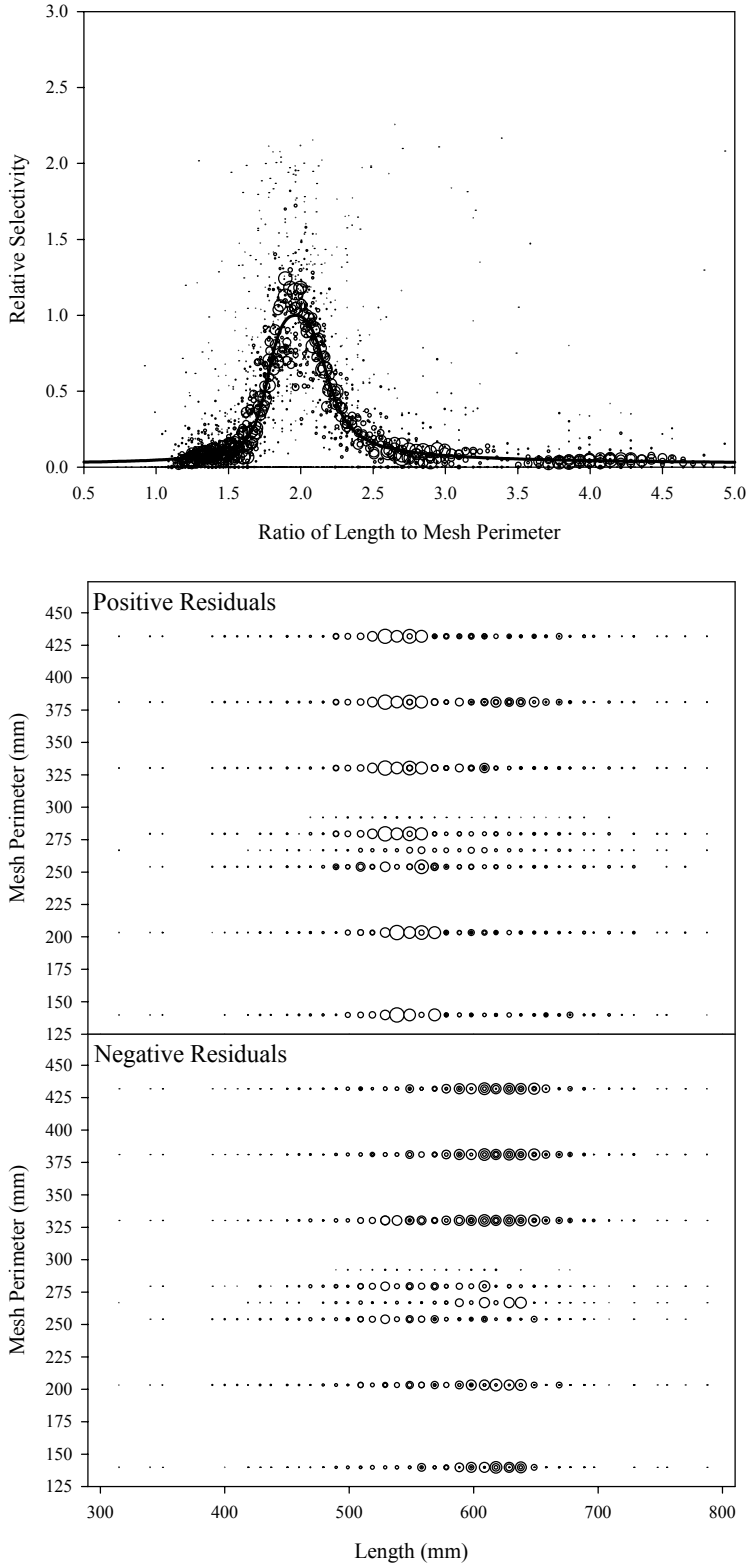

Figure B2.38. Plots of CPUE data scaled to a net selectivity model (top) and CPUE residuals (bottom); summer chum salmon data and Model 38.

Appendix B3
Pink Salmon Diagnostic Plots
Figure B3.1 to Figure B3.38

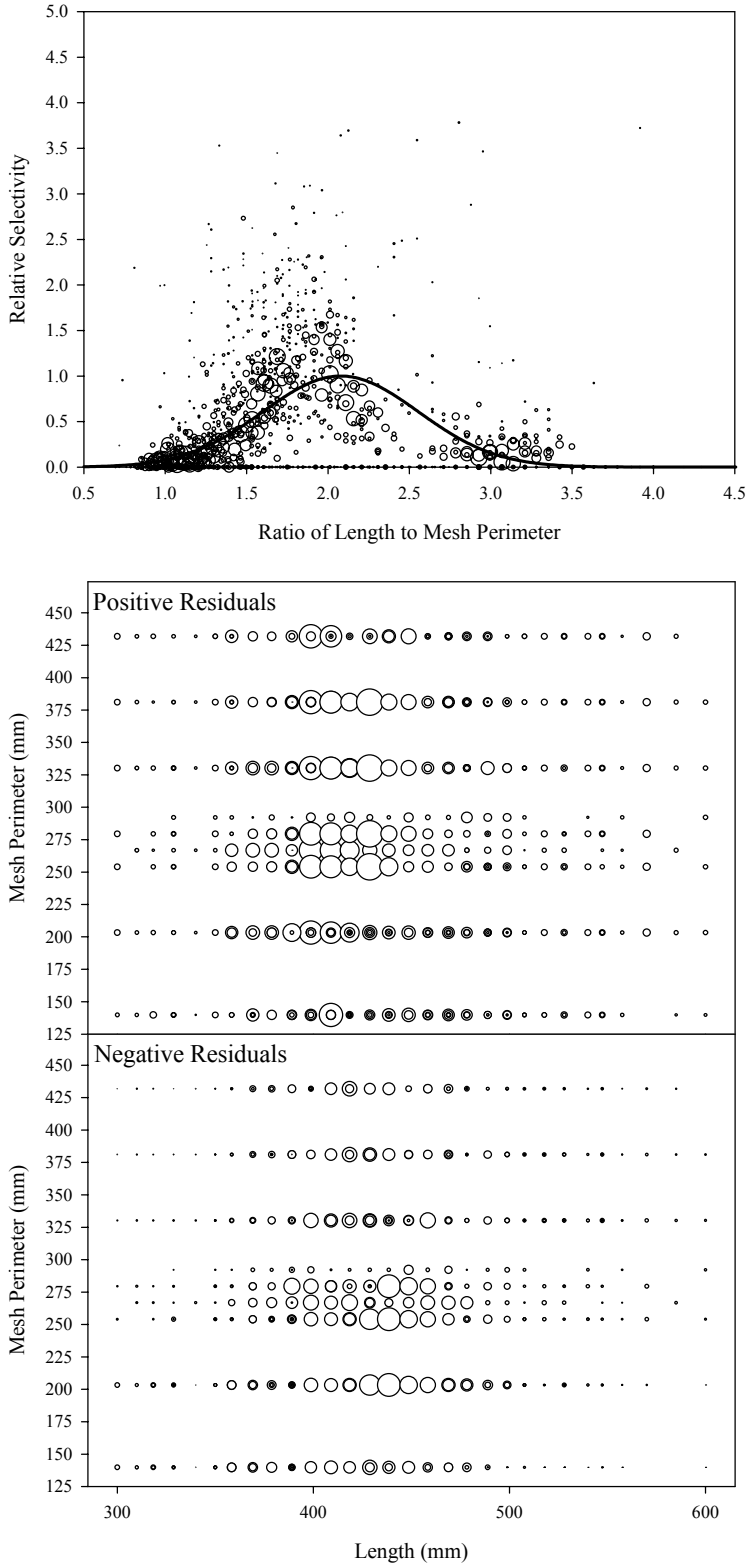

Figure B3.1. Plots of CPUE data scaled to a net selectivity model (top) and CPUE residuals (bottom); pink salmon data and Model 1.

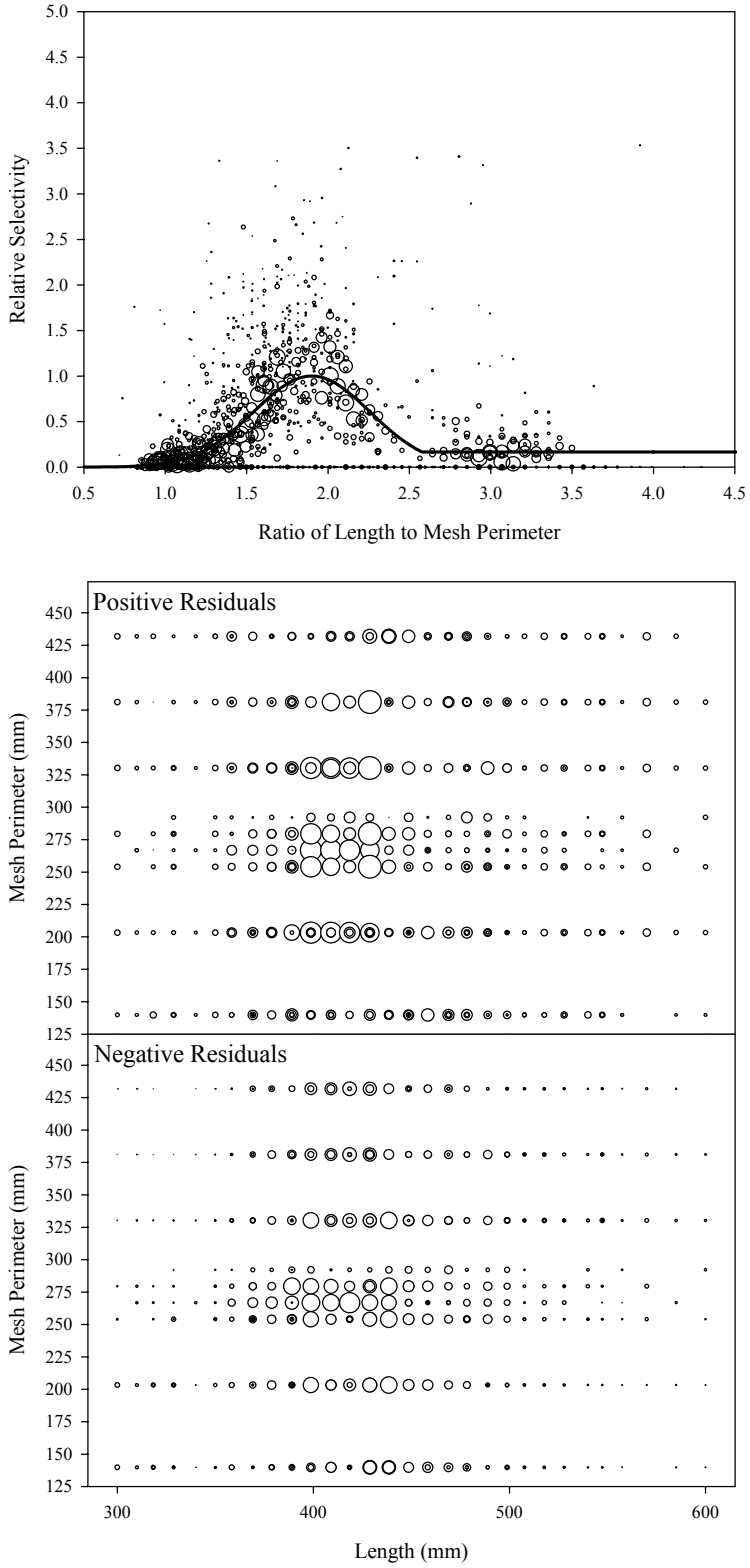

Figure B3.2. Plots of CPUE data scaled to a net selectivity model (top) and CPUE residuals (bottom); pink salmon data and Model 2.

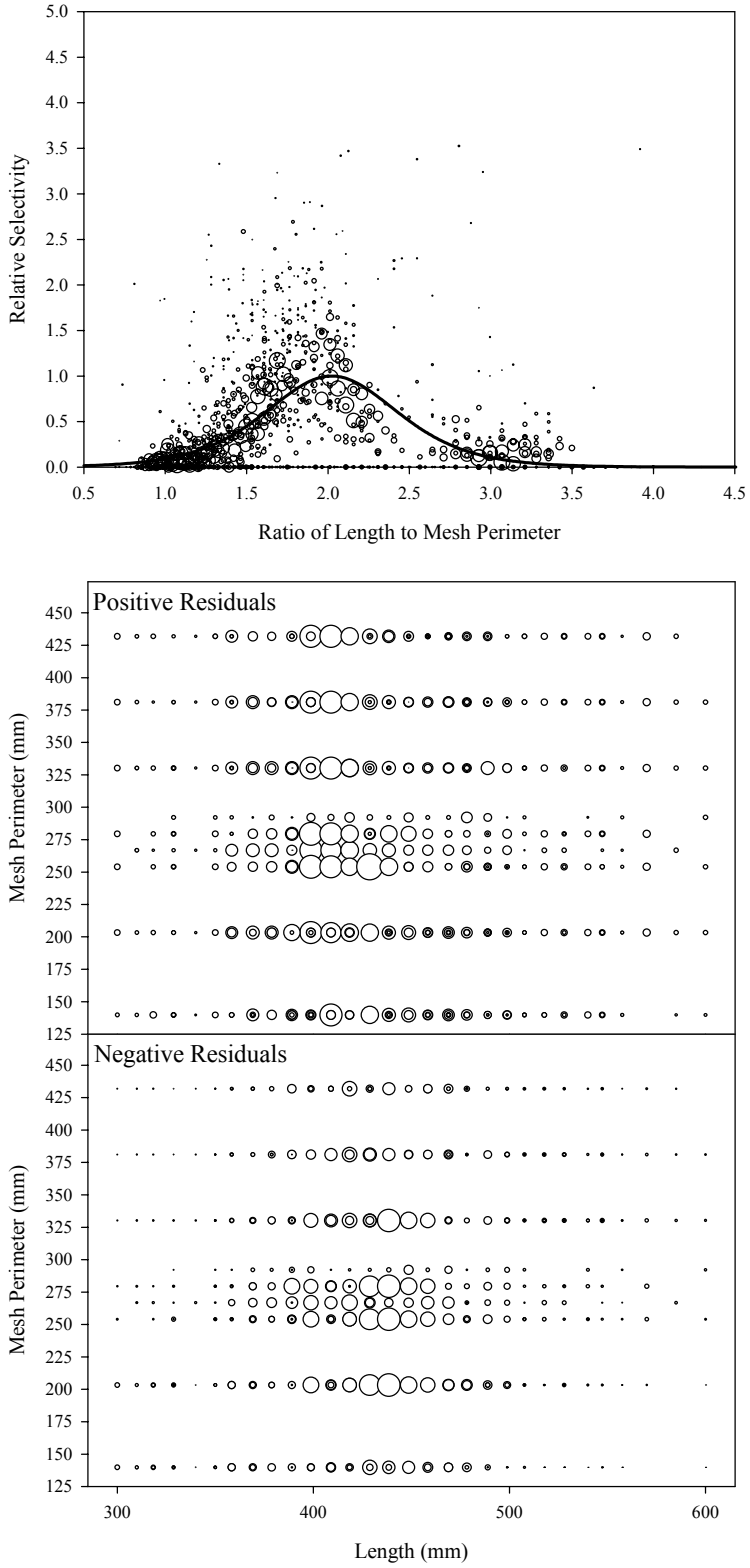

Figure B3.3. Plots of CPUE data scaled to a net selectivity model (top) and CPUE residuals (bottom); pink salmon data and Model 3.

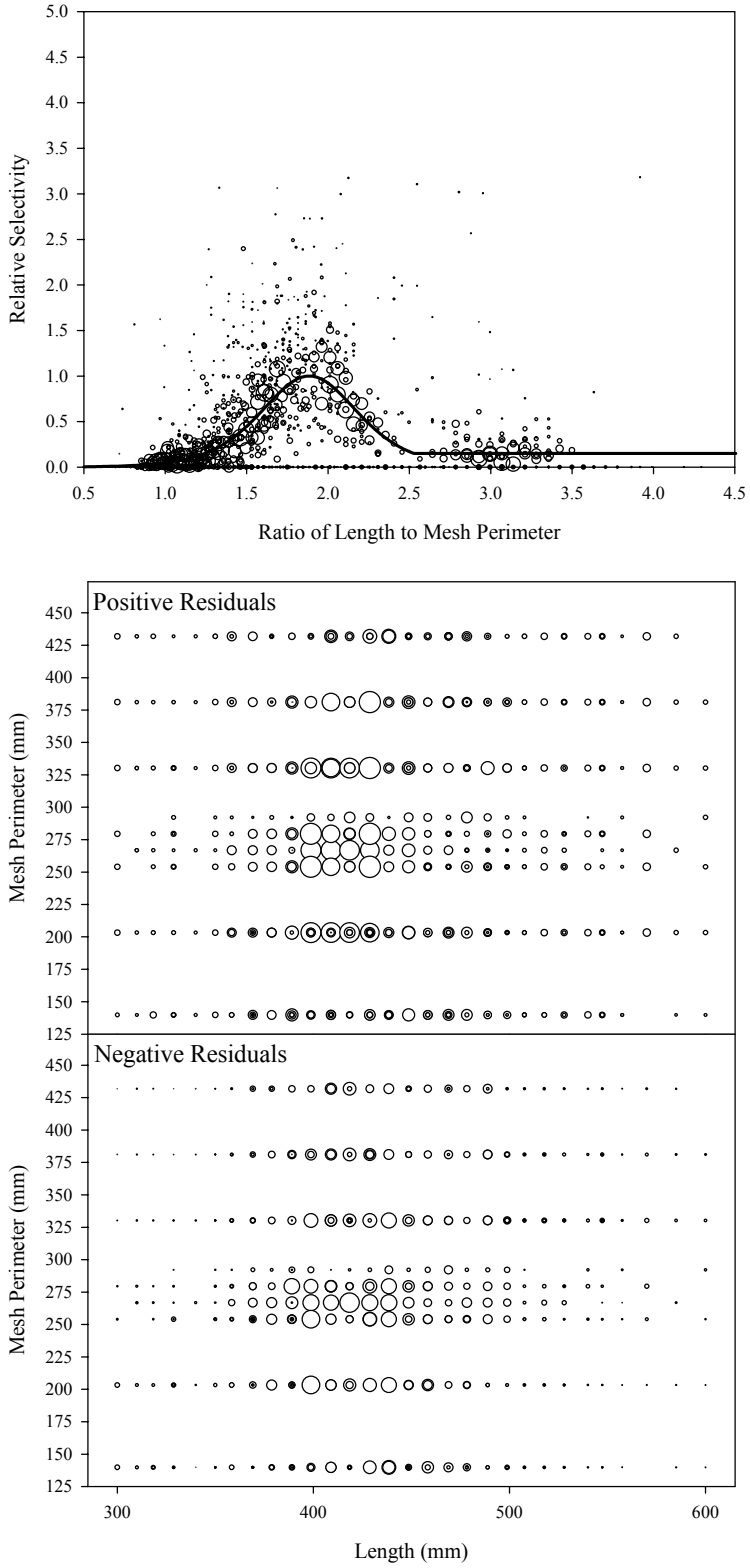

Figure B3.4. Plots of CPUE data scaled to a net selectivity model (top) and CPUE residuals (bottom); pink salmon data and Model 4.

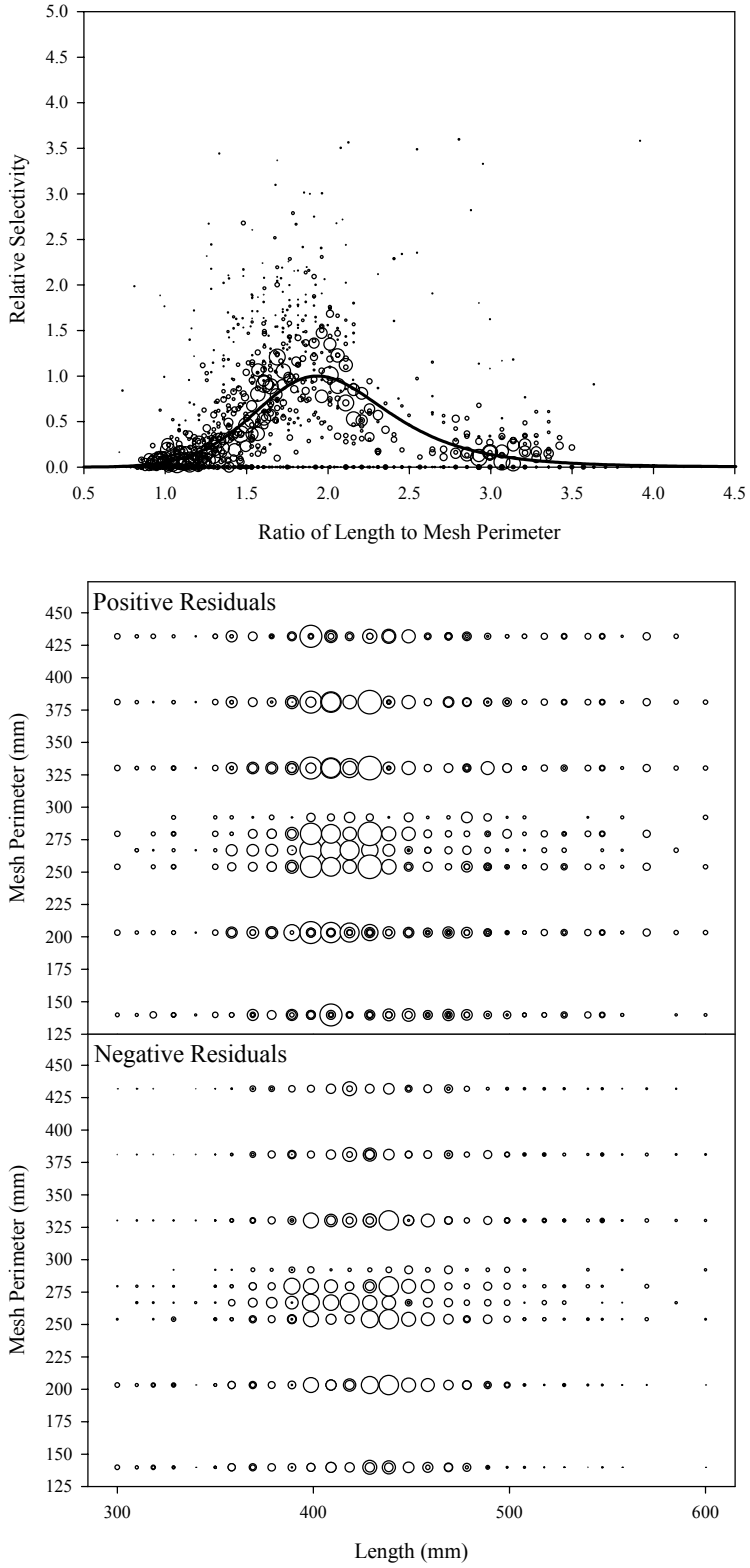

Figure B3.5. Plots of CPUE data scaled to a net selectivity model (top) and CPUE residuals (bottom); pink salmon data and Model 5.

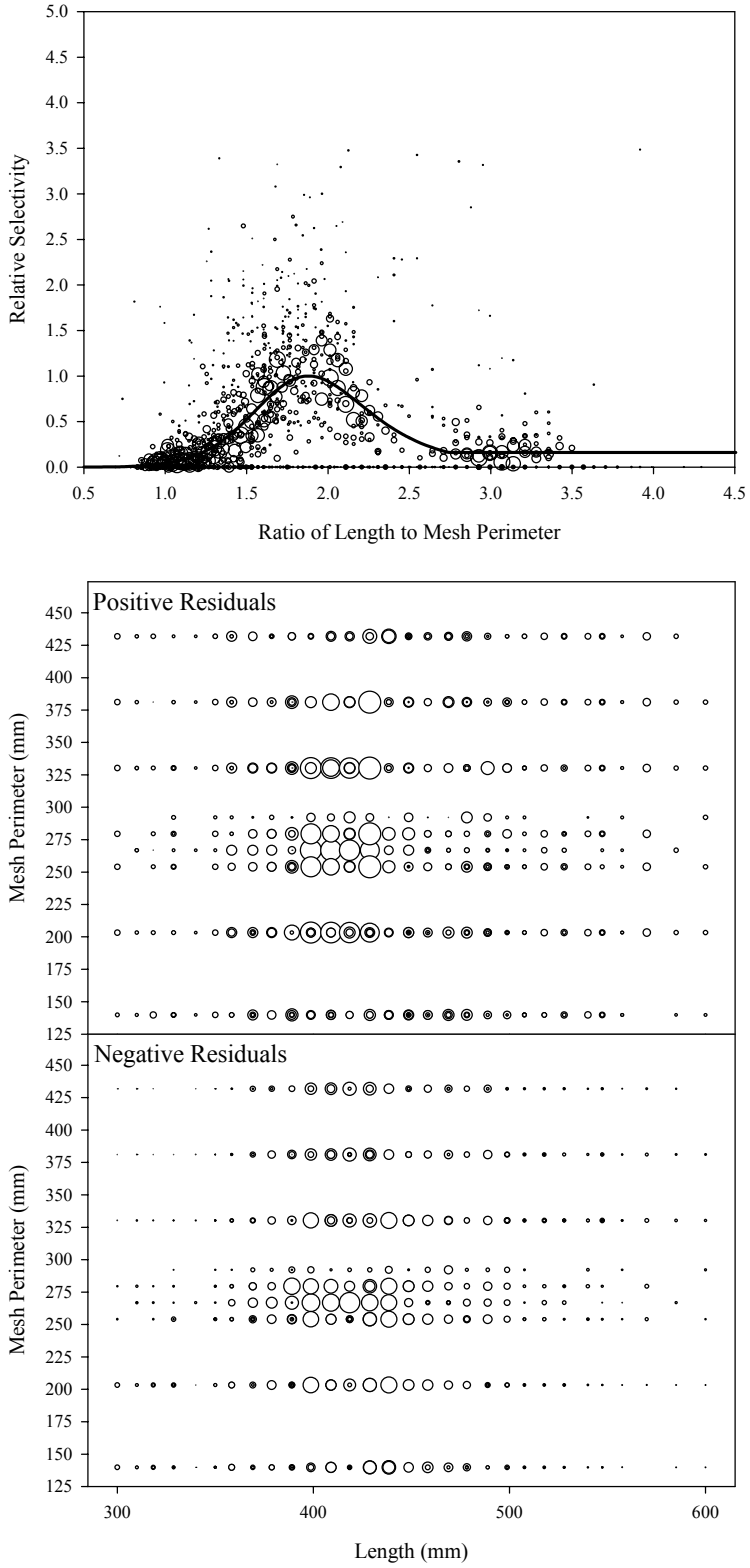

Figure B3.6. Plots of CPUE data scaled to a net selectivity model (top) and CPUE residuals (bottom); pink salmon data and Model 6.

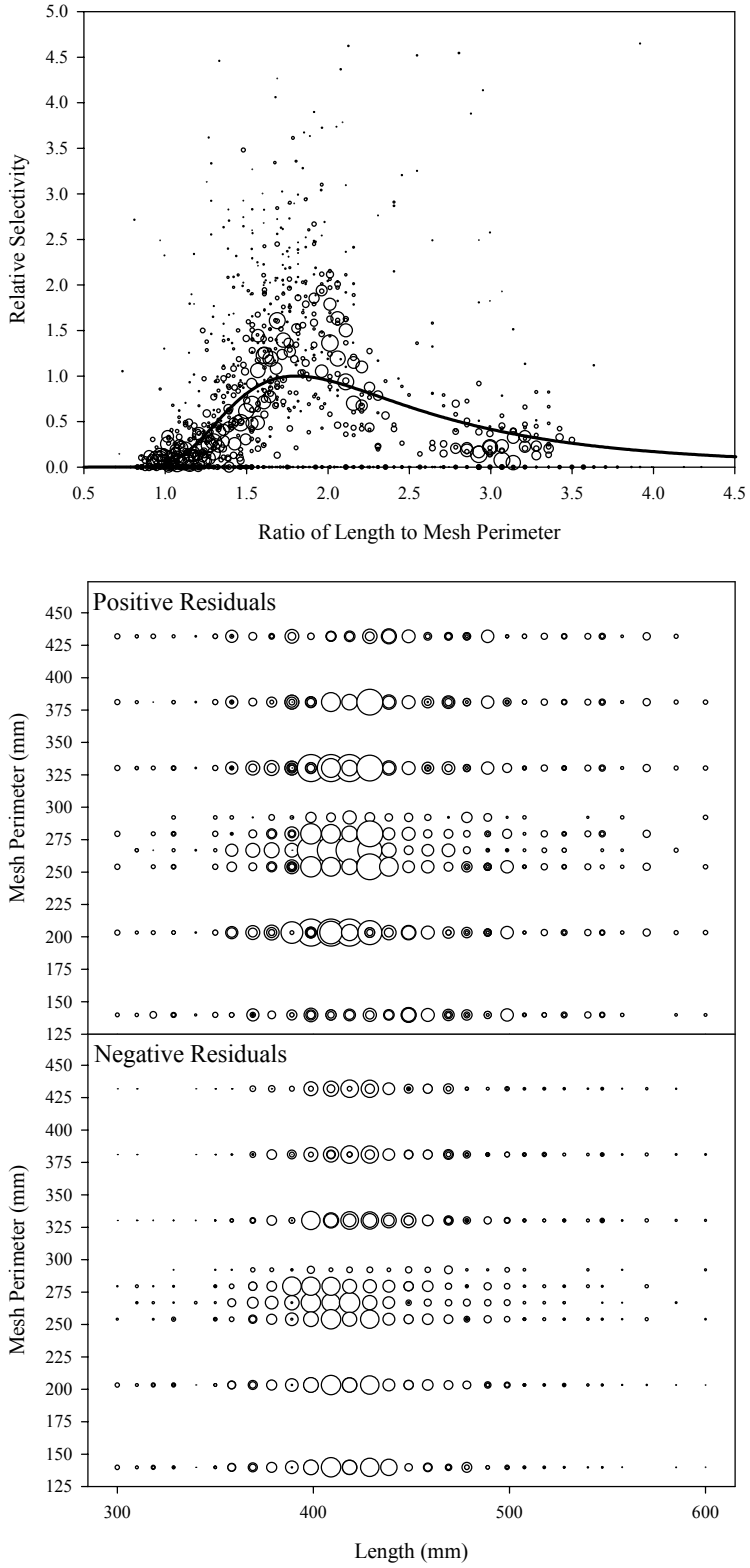

Figure B3.7. Plots of CPUE data scaled to a net selectivity model (top) and CPUE residuals (bottom); pink salmon data and Model 7.

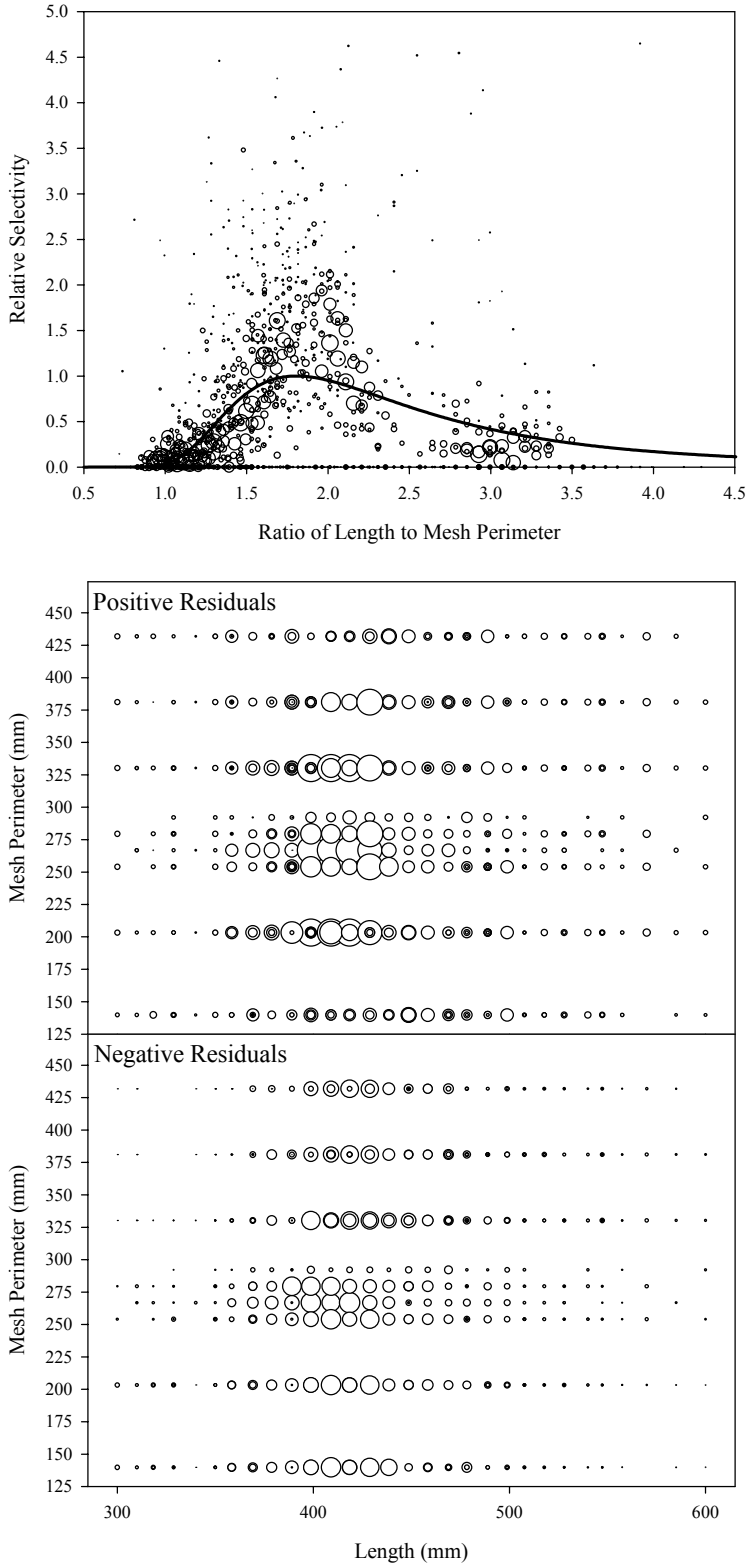

Figure B3.8. Plots of CPUE data scaled to a net selectivity model (top) and CPUE residuals (bottom); pink salmon data and Model 8.

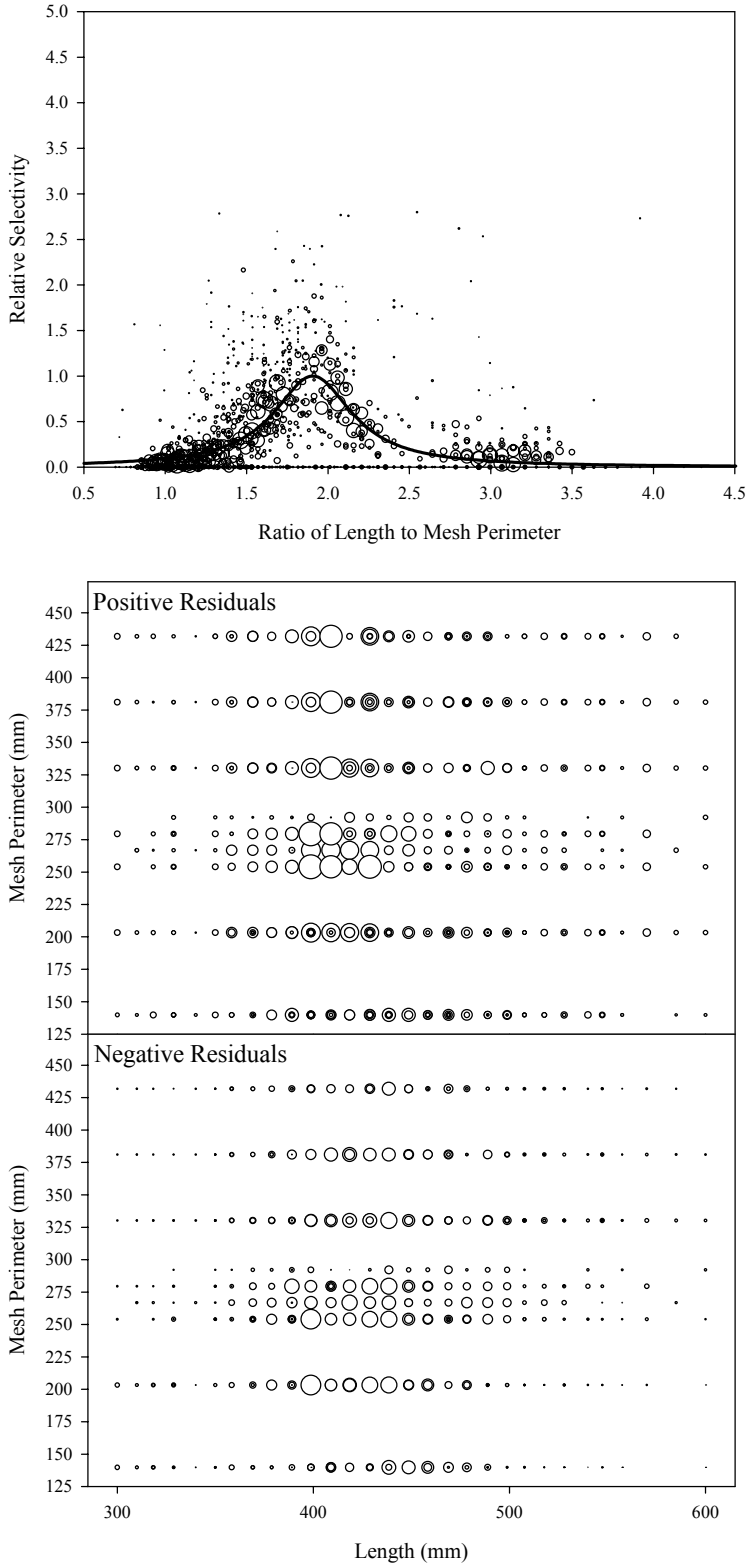

Figure B3.9. Plots of CPUE data scaled to a net selectivity model (top) and CPUE residuals (bottom); pink salmon data and Model 9.

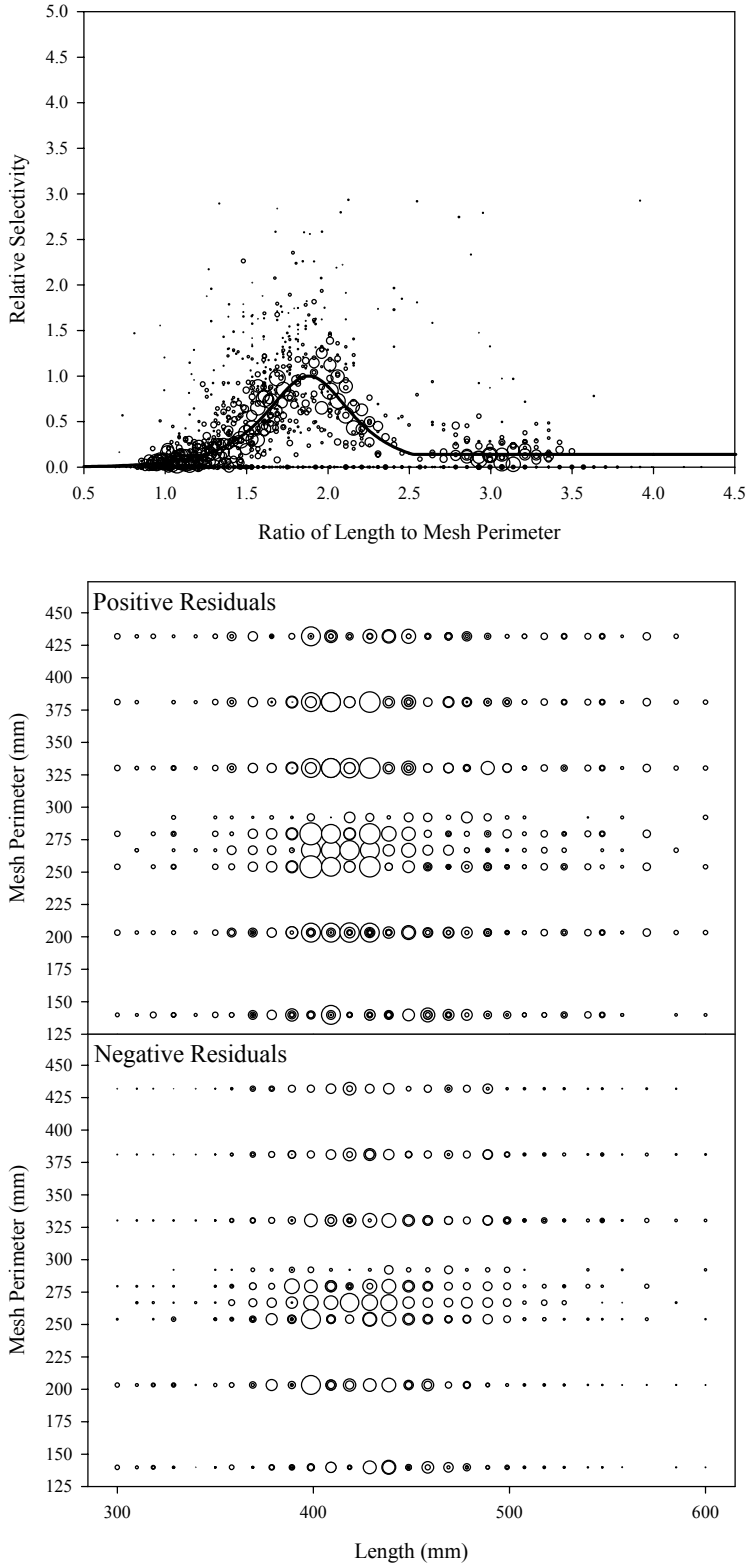

Figure B3.10. Plots of CPUE data scaled to a net selectivity model (top) and CPUE residuals (bottom); pink salmon data and Model 10.

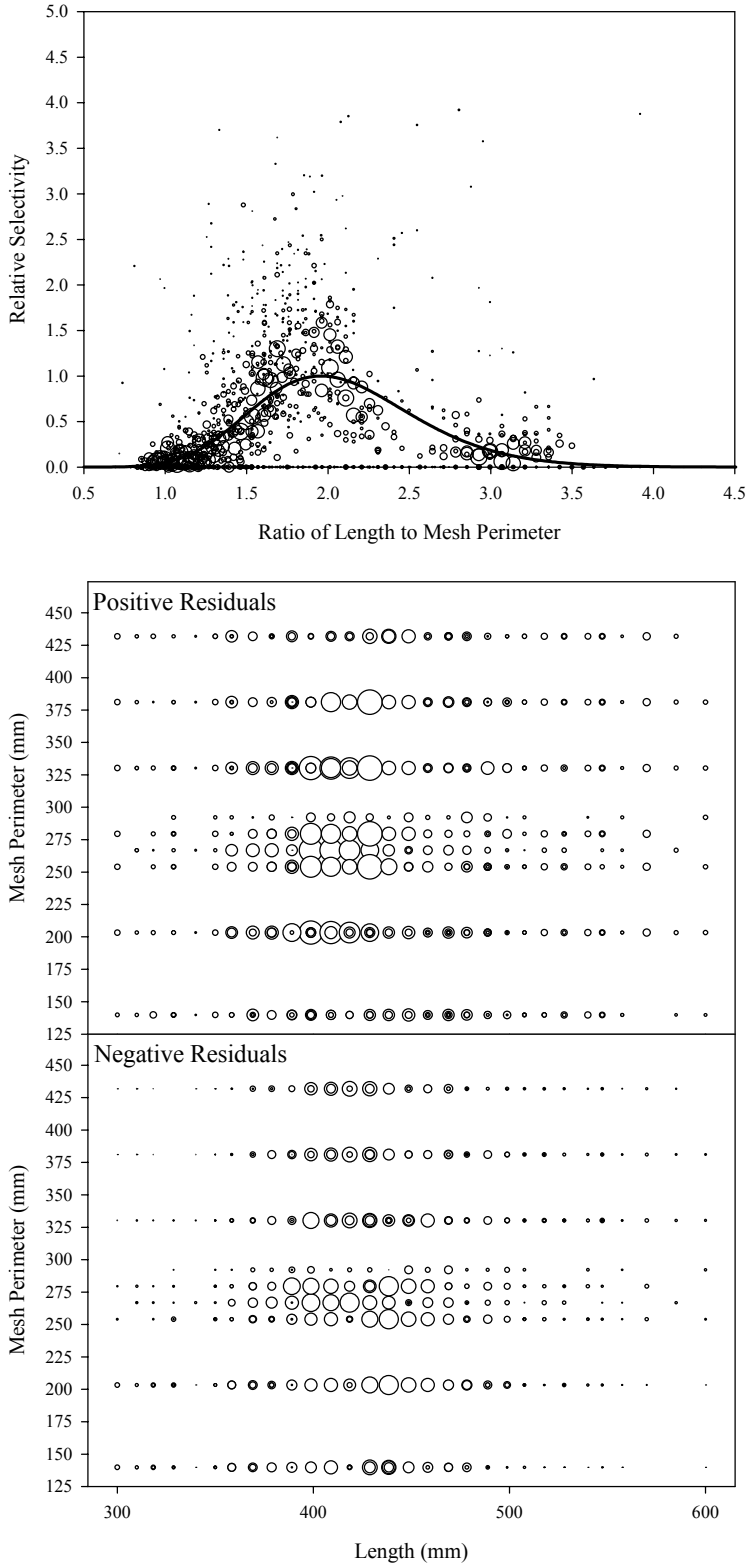

Figure B3.11. Plots of CPUE data scaled to a net selectivity model (top) and CPUE residuals (bottom); pink salmon data and Model 11.

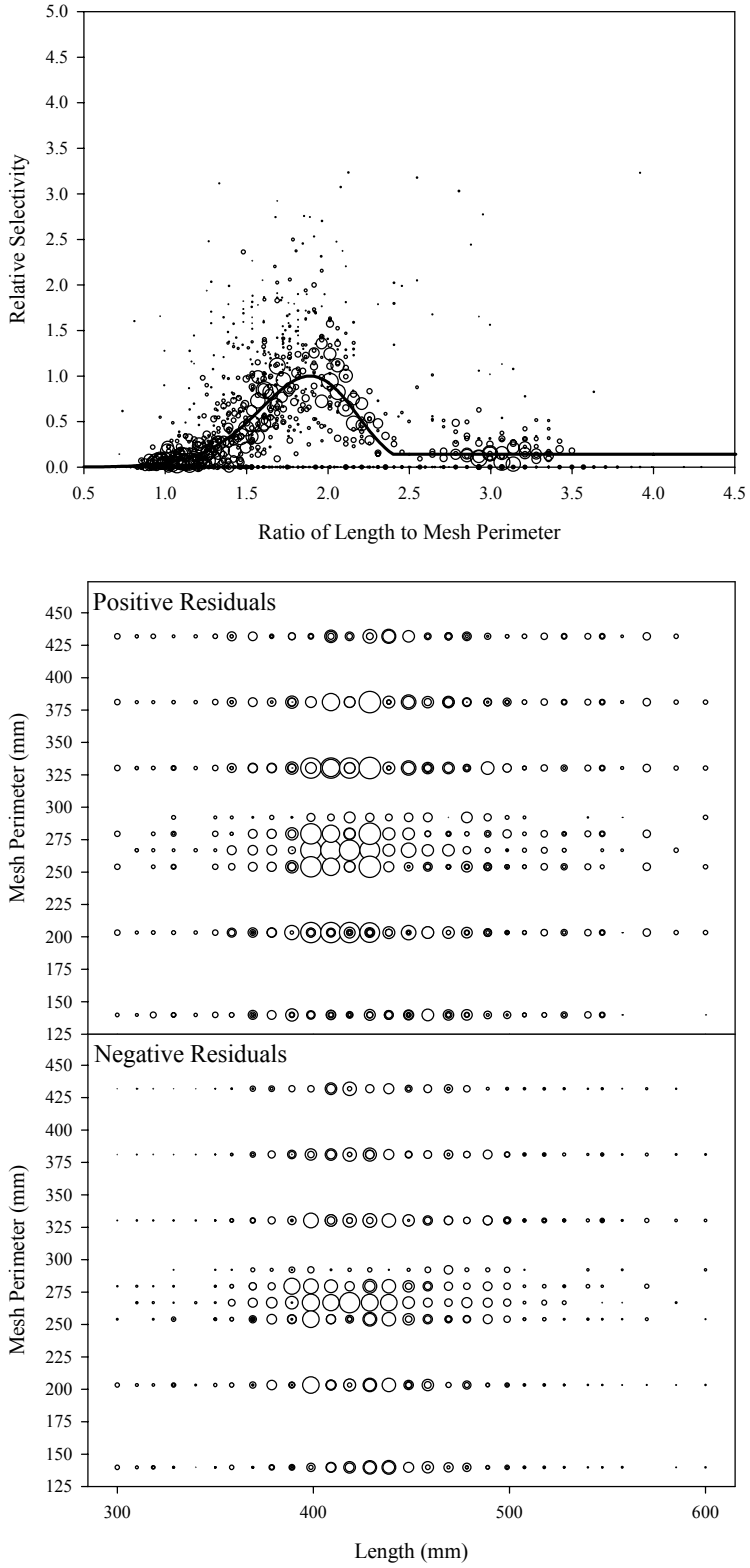

Figure B3.12. Plots of CPUE data scaled to a net selectivity model (top) and CPUE residuals (bottom); pink salmon data and Model 12.

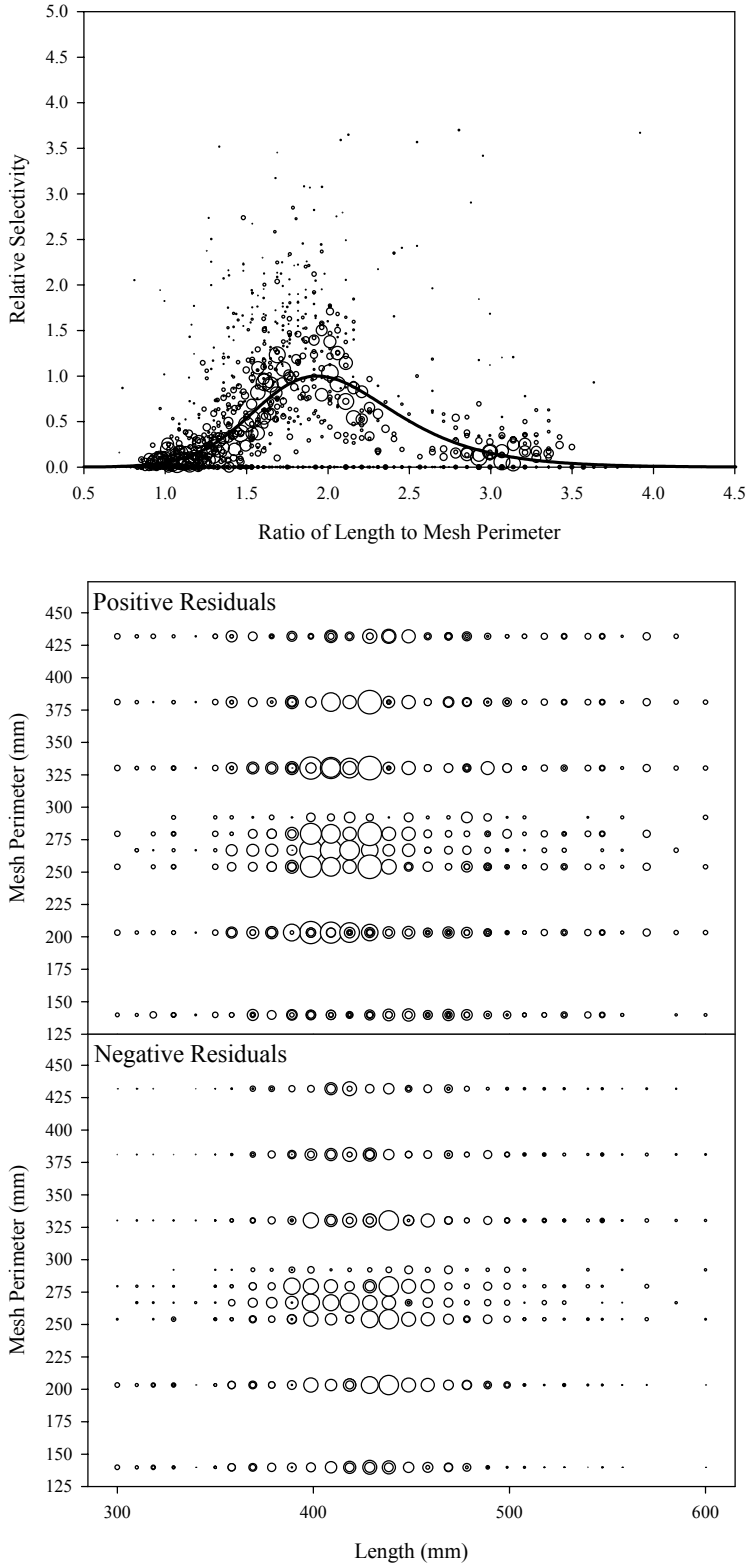

Figure B3.13. Plots of CPUE data scaled to a net selectivity model (top) and CPUE residuals (bottom); pink salmon data and Model 13.

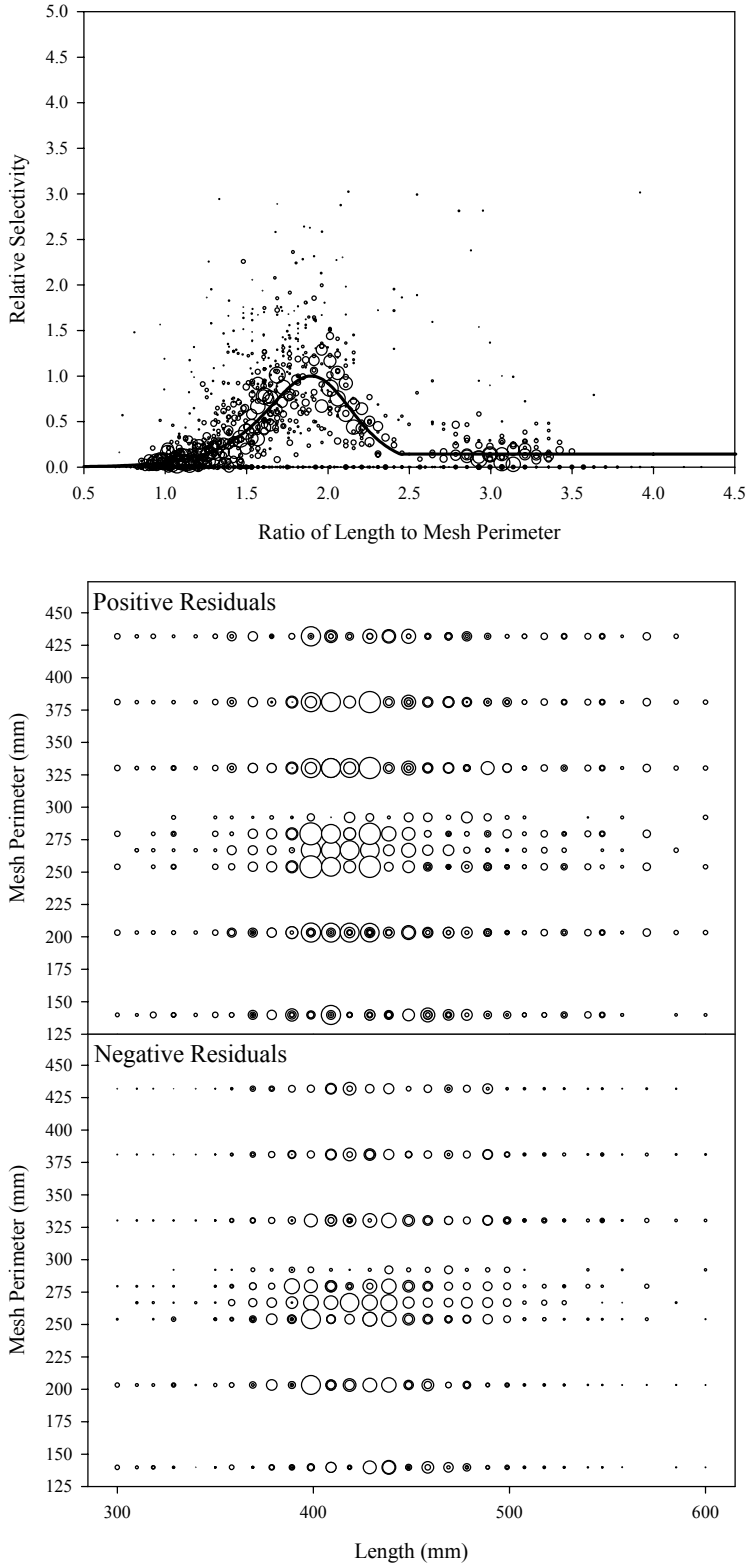

Figure B3.14. Plots of CPUE data scaled to a net selectivity model (top) and CPUE residuals (bottom); pink salmon data and Model 14.

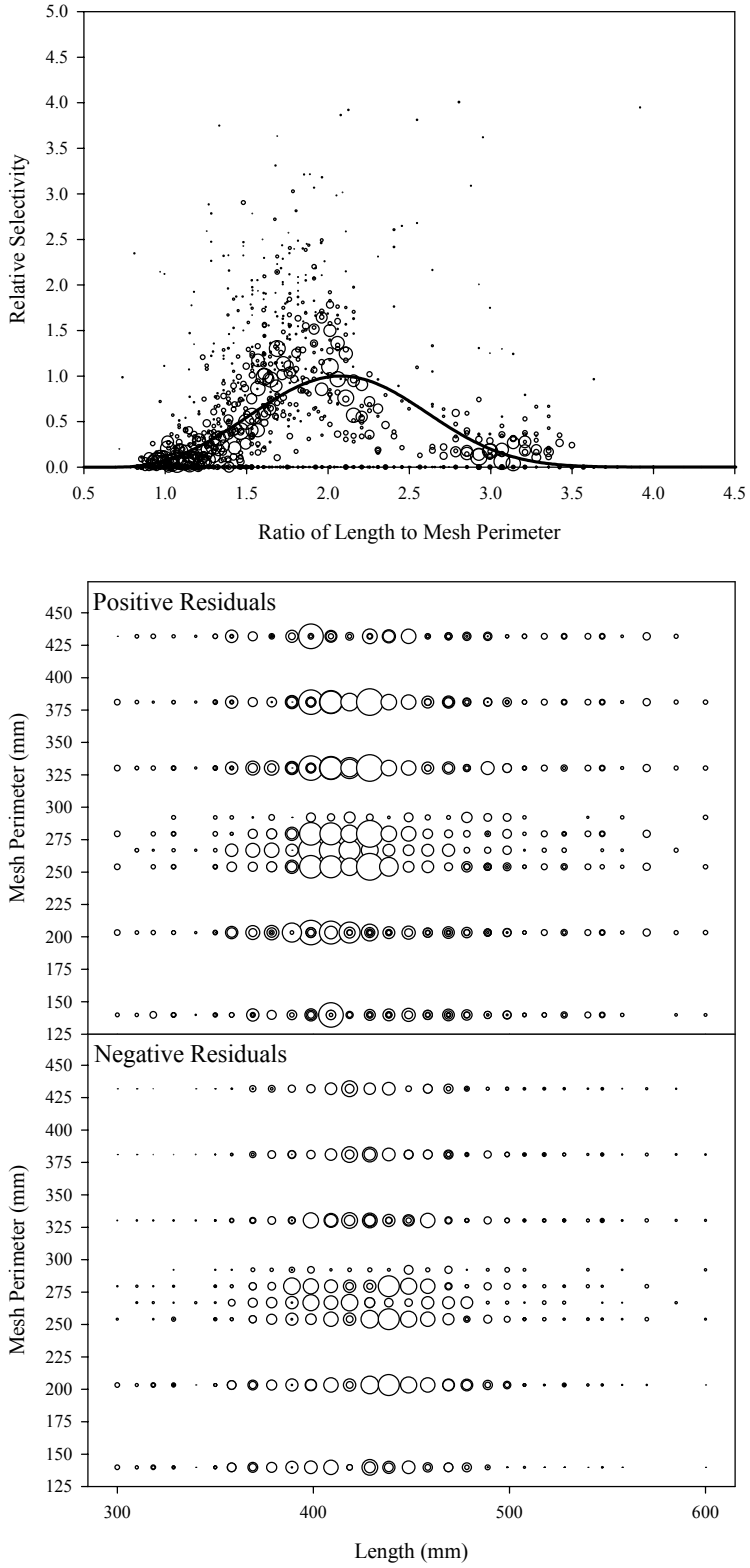

Figure B3.15. Plots of CPUE data scaled to a net selectivity model (top) and CPUE residuals (bottom); pink salmon data and Model 15.

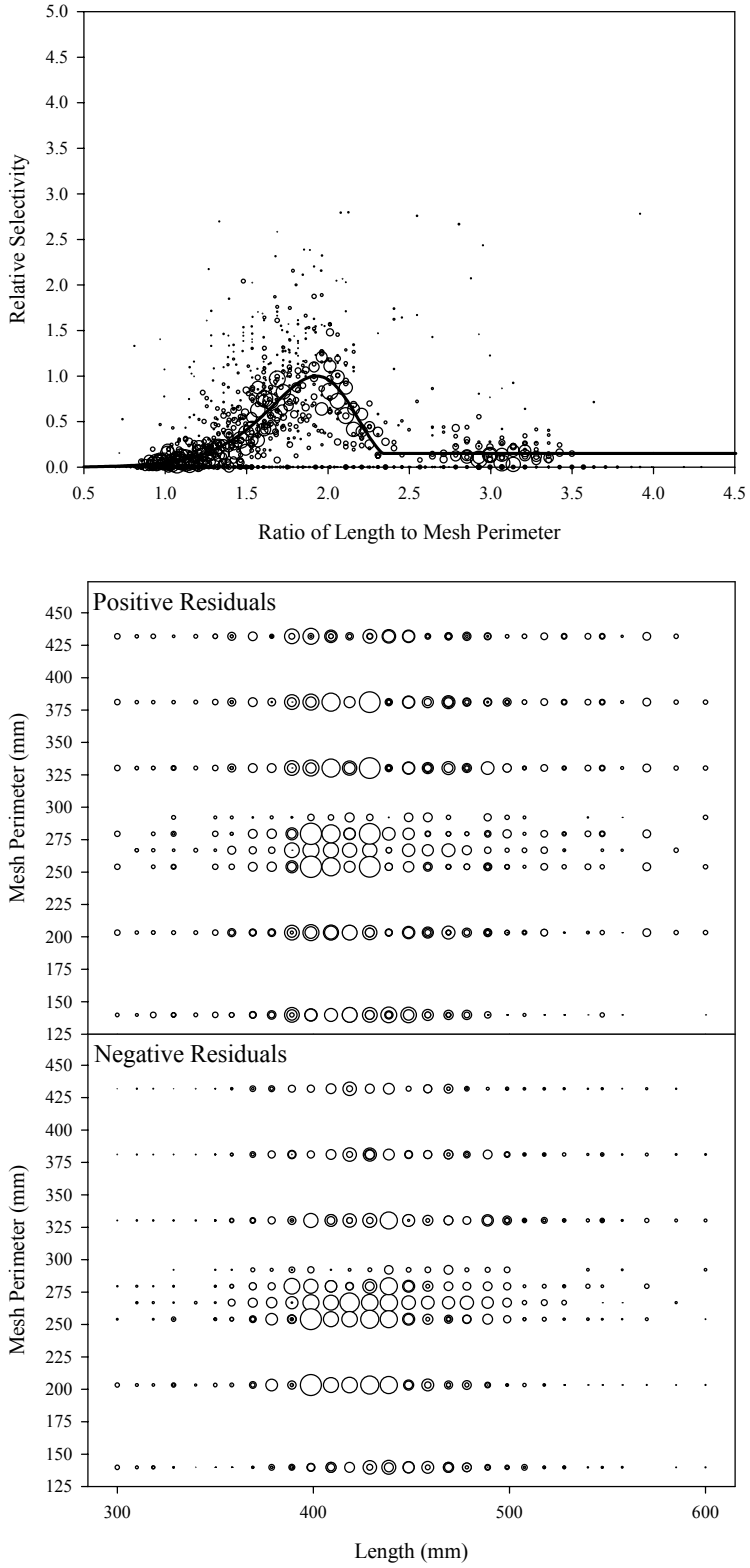

Figure B3.16. Plots of CPUE data scaled to a net selectivity model (top) and CPUE residuals (bottom); pink salmon data and Model 16.

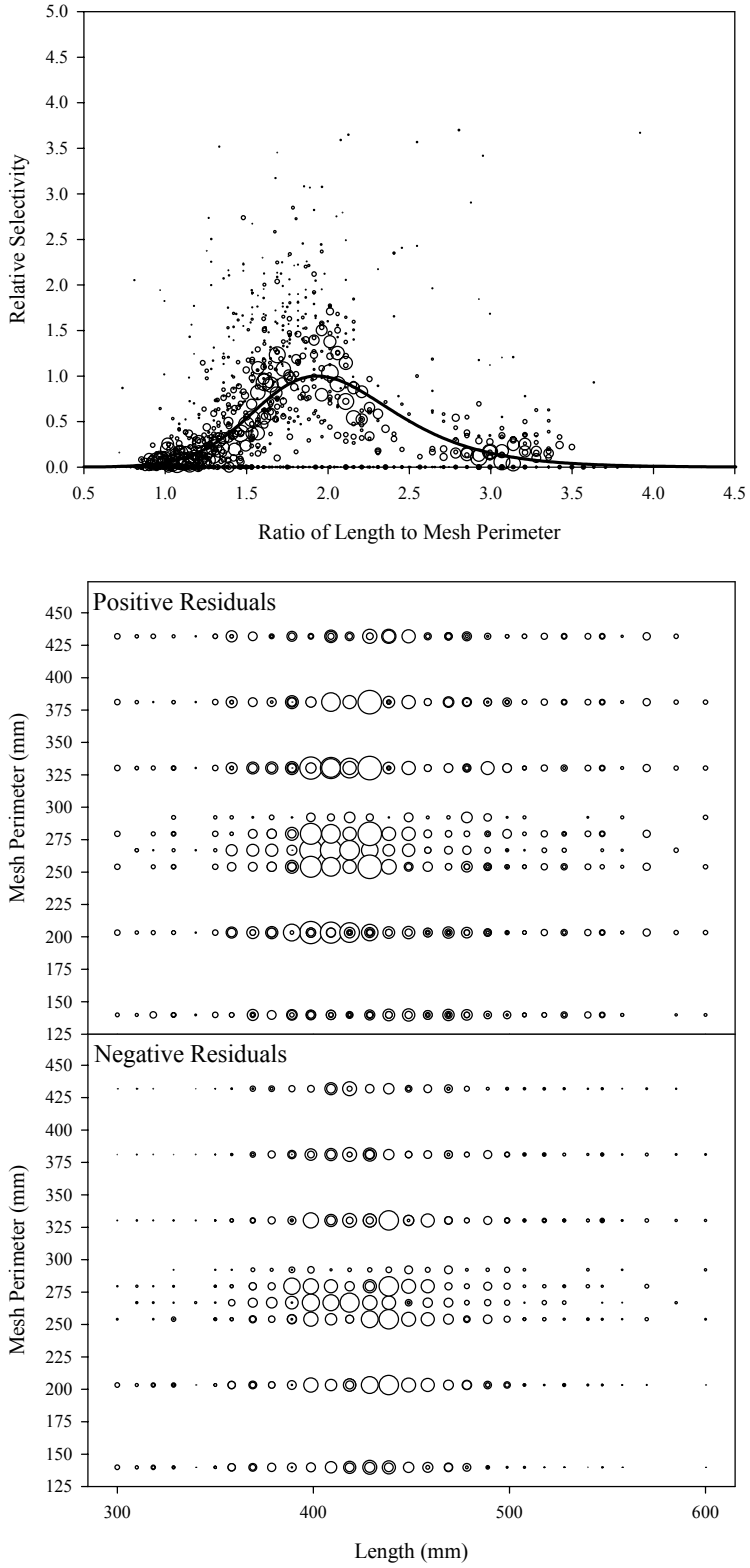

Figure B3.17. Plots of CPUE data scaled to a net selectivity model (top) and CPUE residuals (bottom); pink salmon data and Model 17.

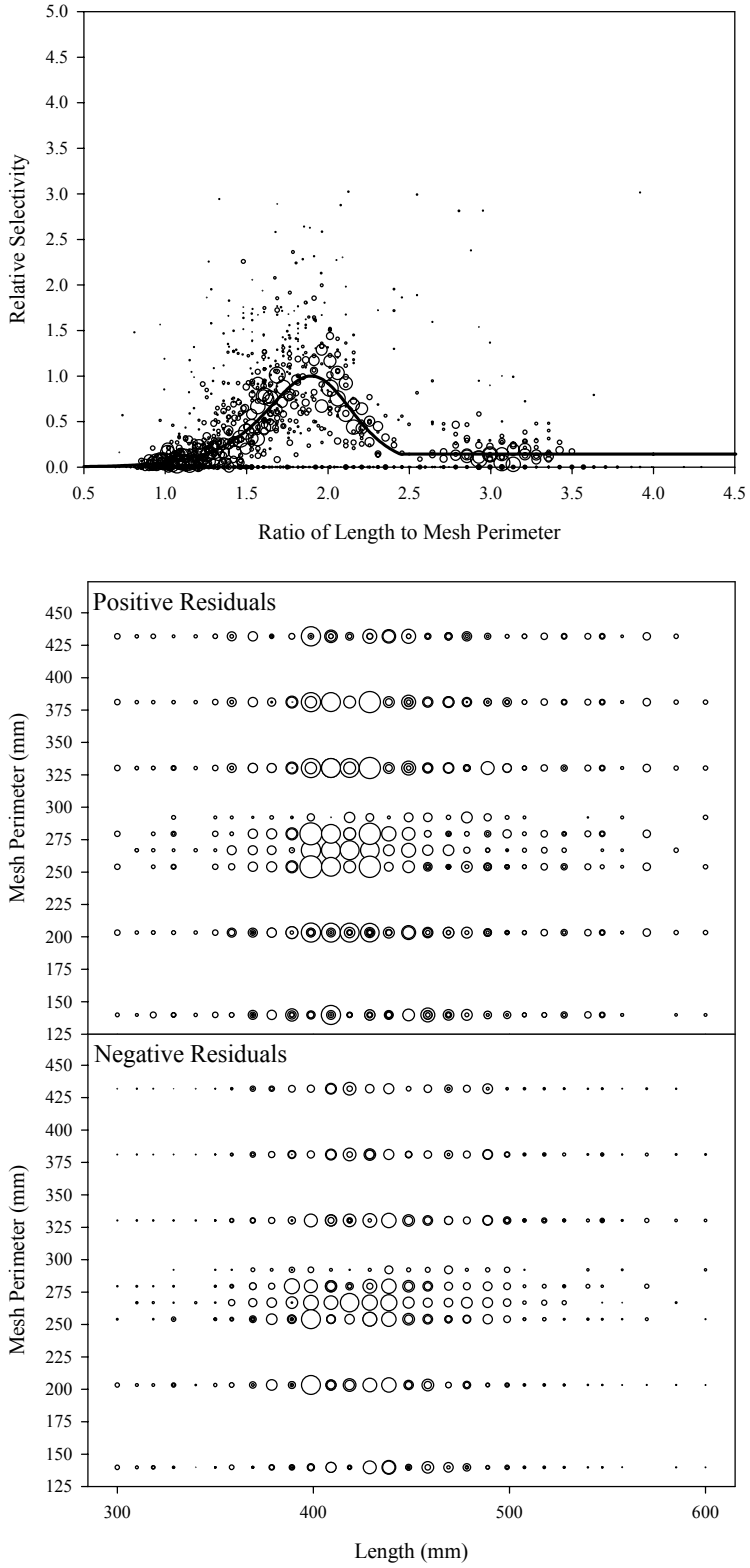

Figure B3.18. Plots of CPUE data scaled to a net selectivity model (top) and CPUE residuals (bottom); pink salmon data and Model 18.

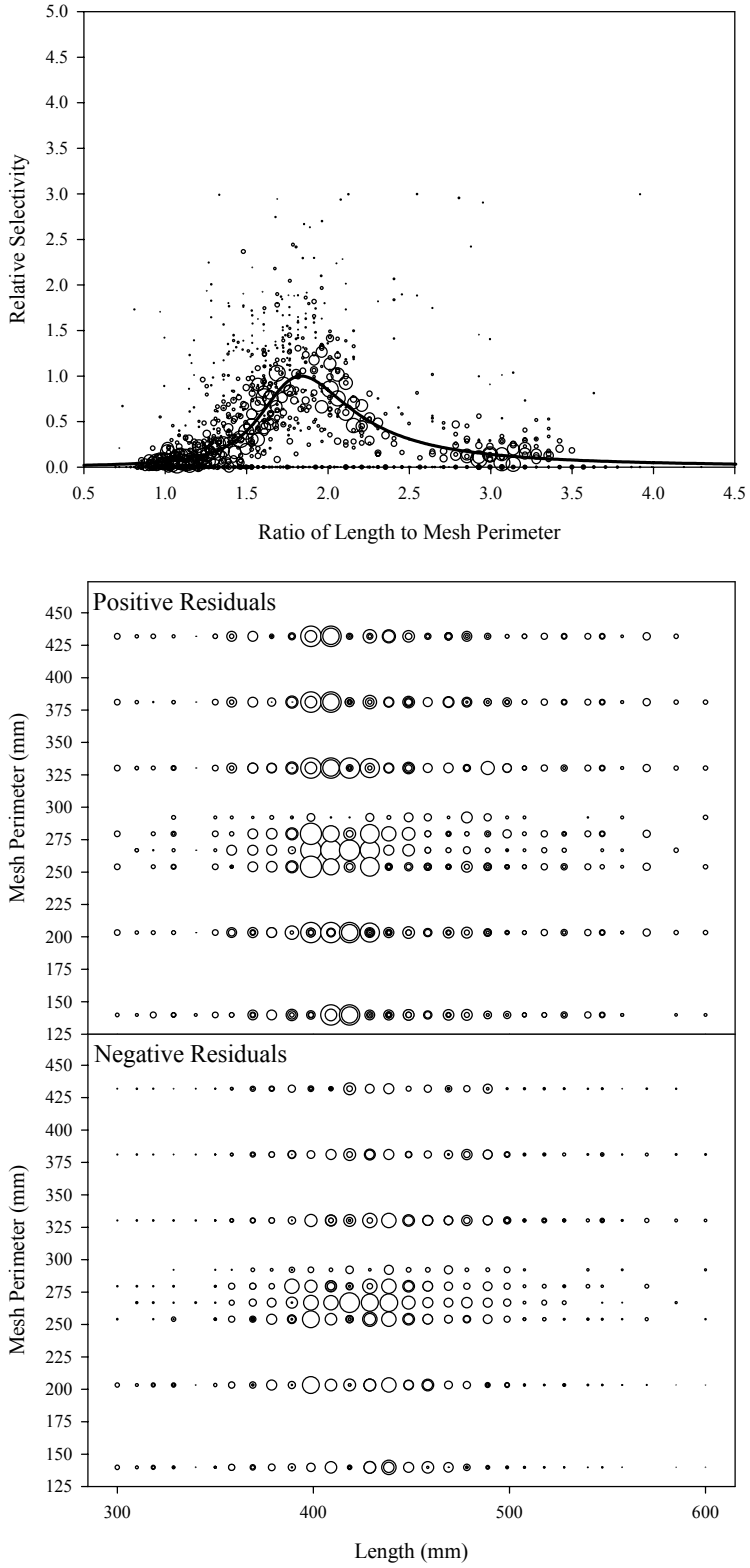

Figure B3.19. Plots of CPUE data scaled to a net selectivity model (top) and CPUE residuals (bottom); pink salmon data and Model 19.

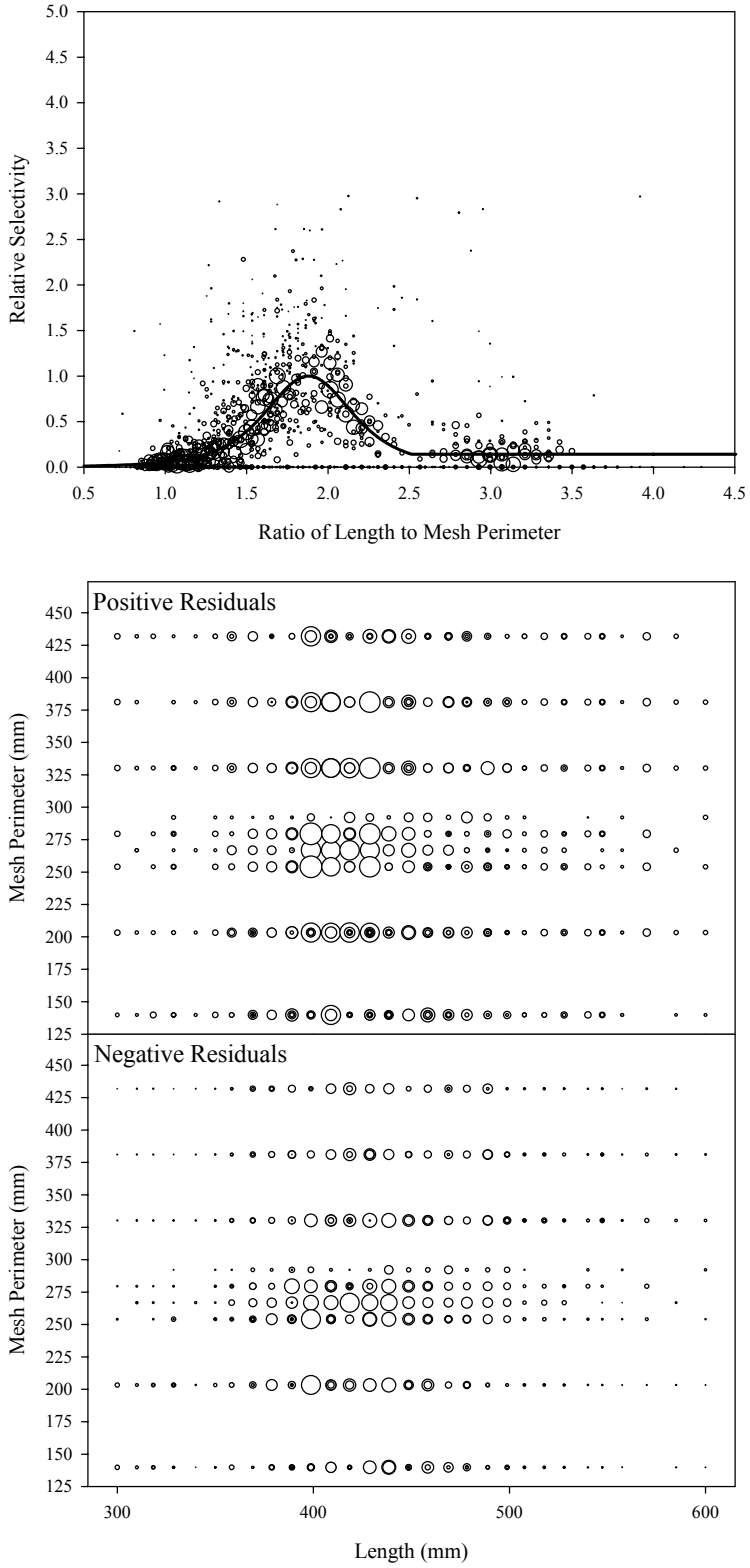

Figure B3.20. Plots of CPUE data scaled to a net selectivity model (top) and CPUE residuals (bottom); pink salmon data and Model 20.

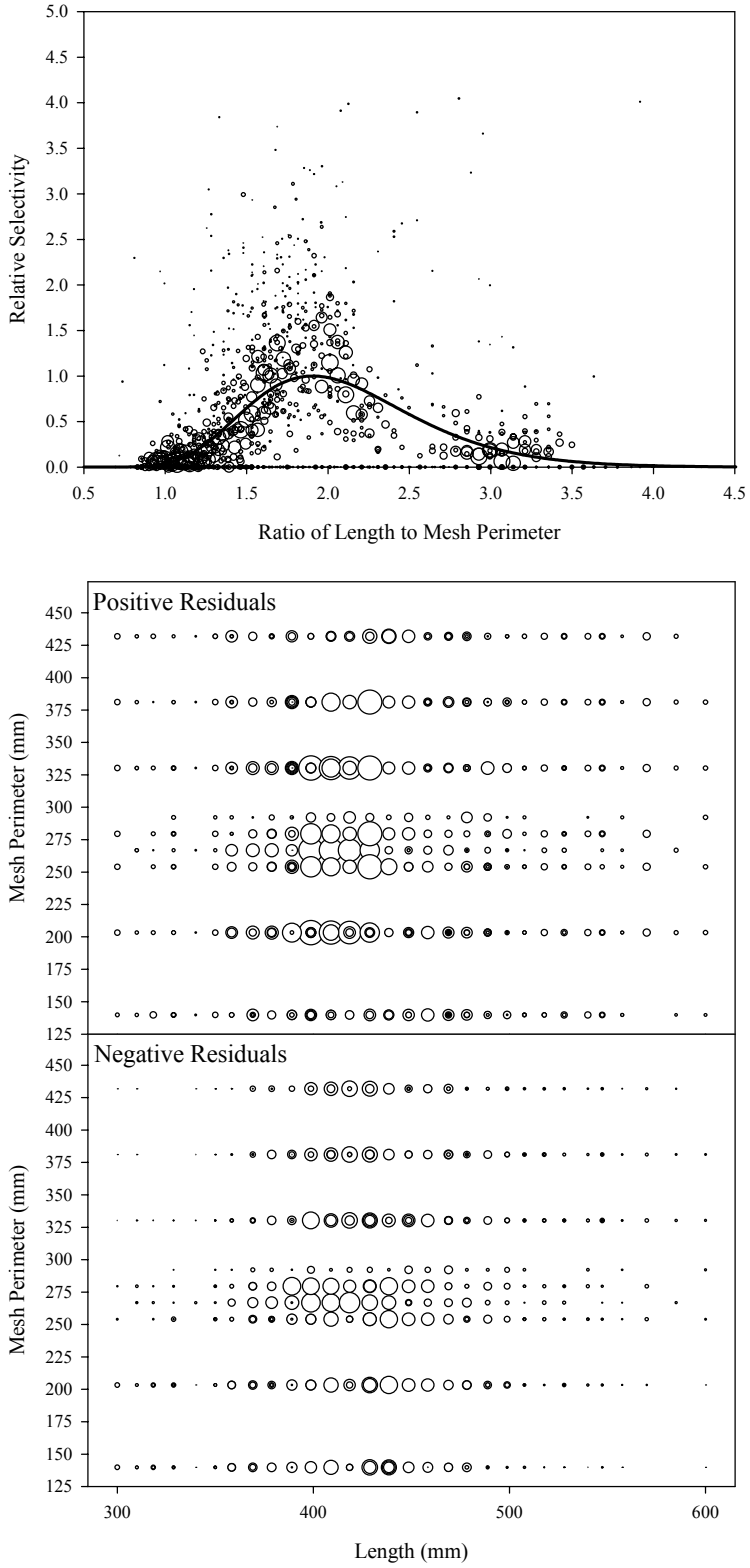

Figure B3.21. Plots of CPUE data scaled to a net selectivity model (top) and CPUE residuals (bottom); pink salmon data and Model 21.

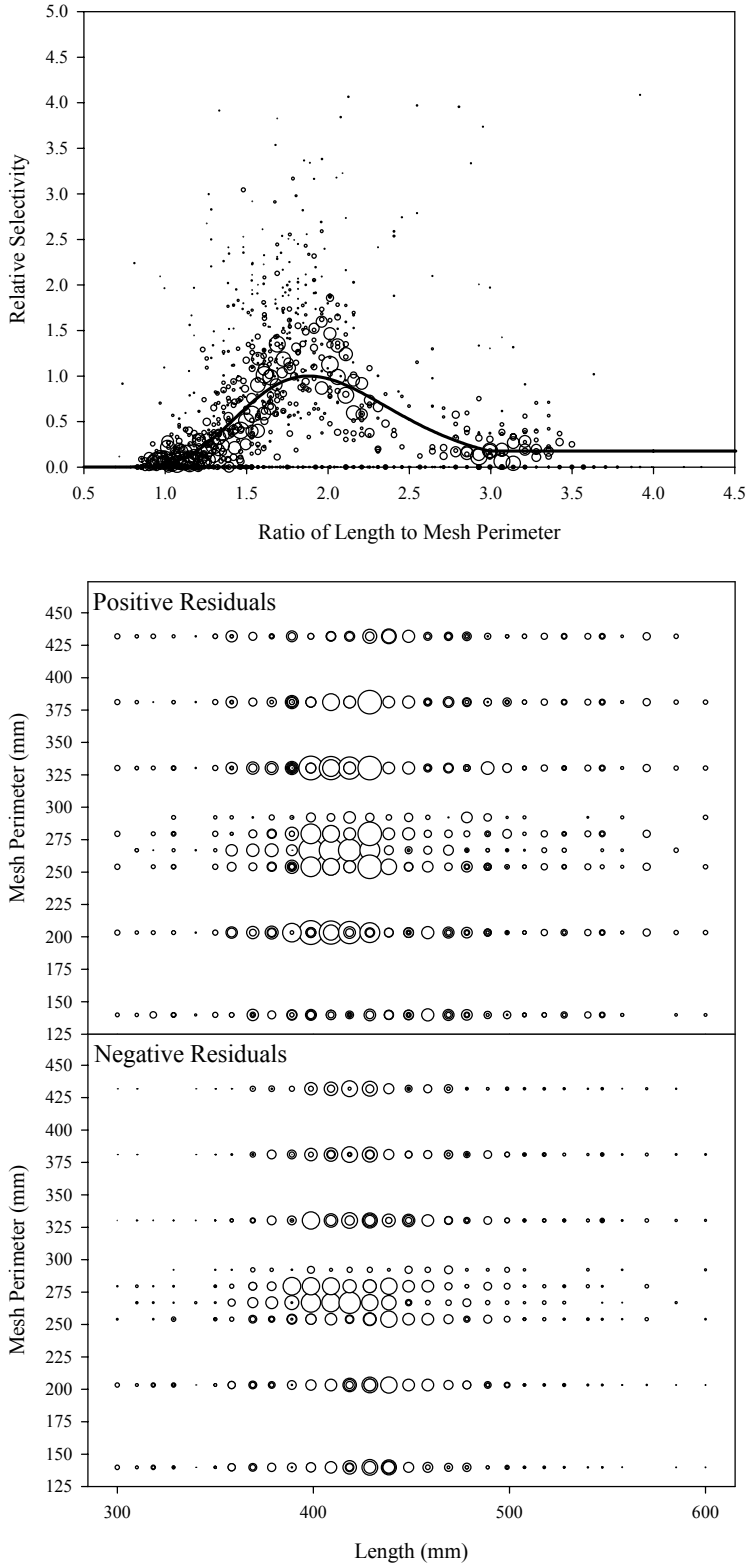

Figure B3.22. Plots of CPUE data scaled to a net selectivity model (top) and CPUE residuals (bottom); pink salmon data and Model 22.

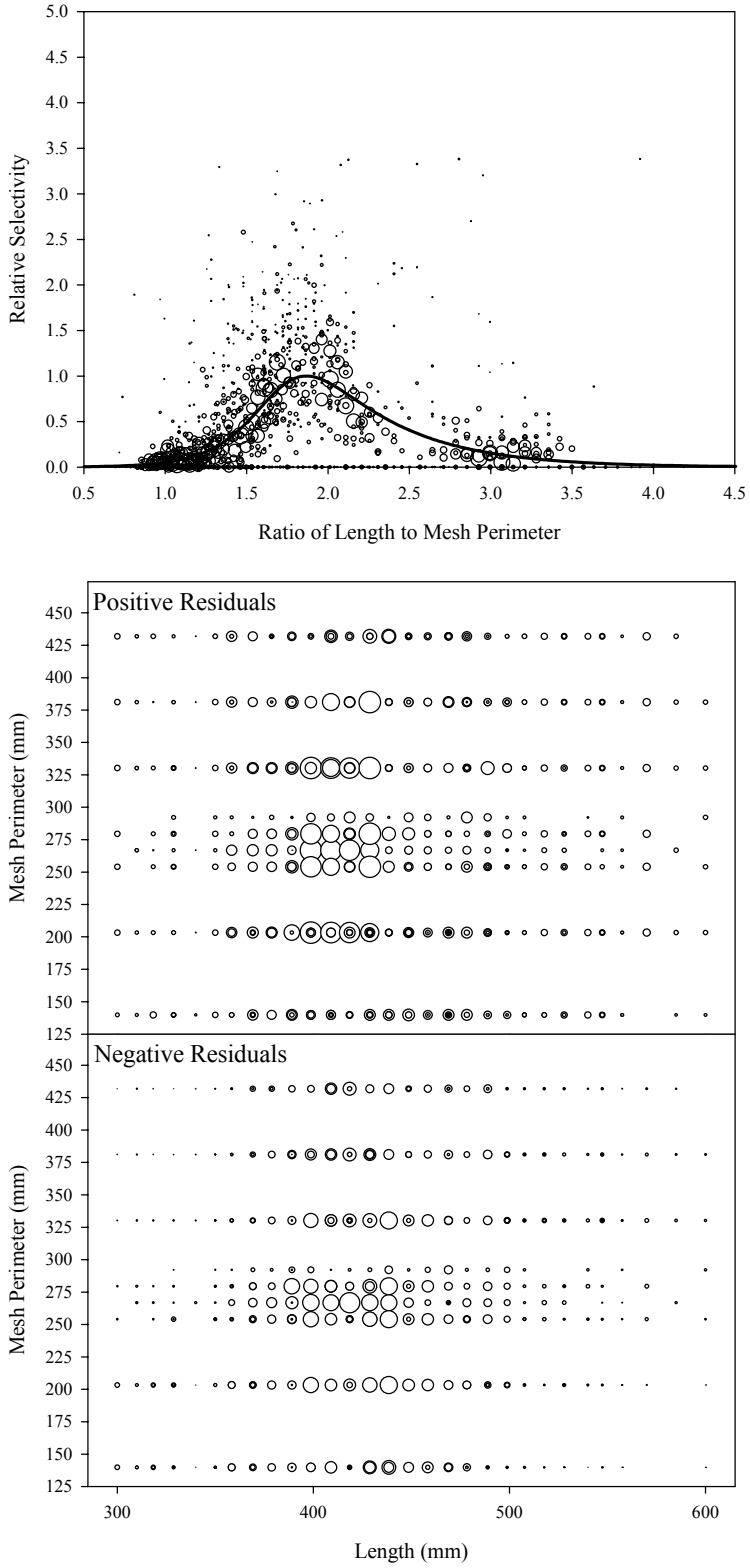

Figure B3.23. Plots of CPUE data scaled to a net selectivity model (top) and CPUE residuals (bottom); pink salmon data and Model 23.

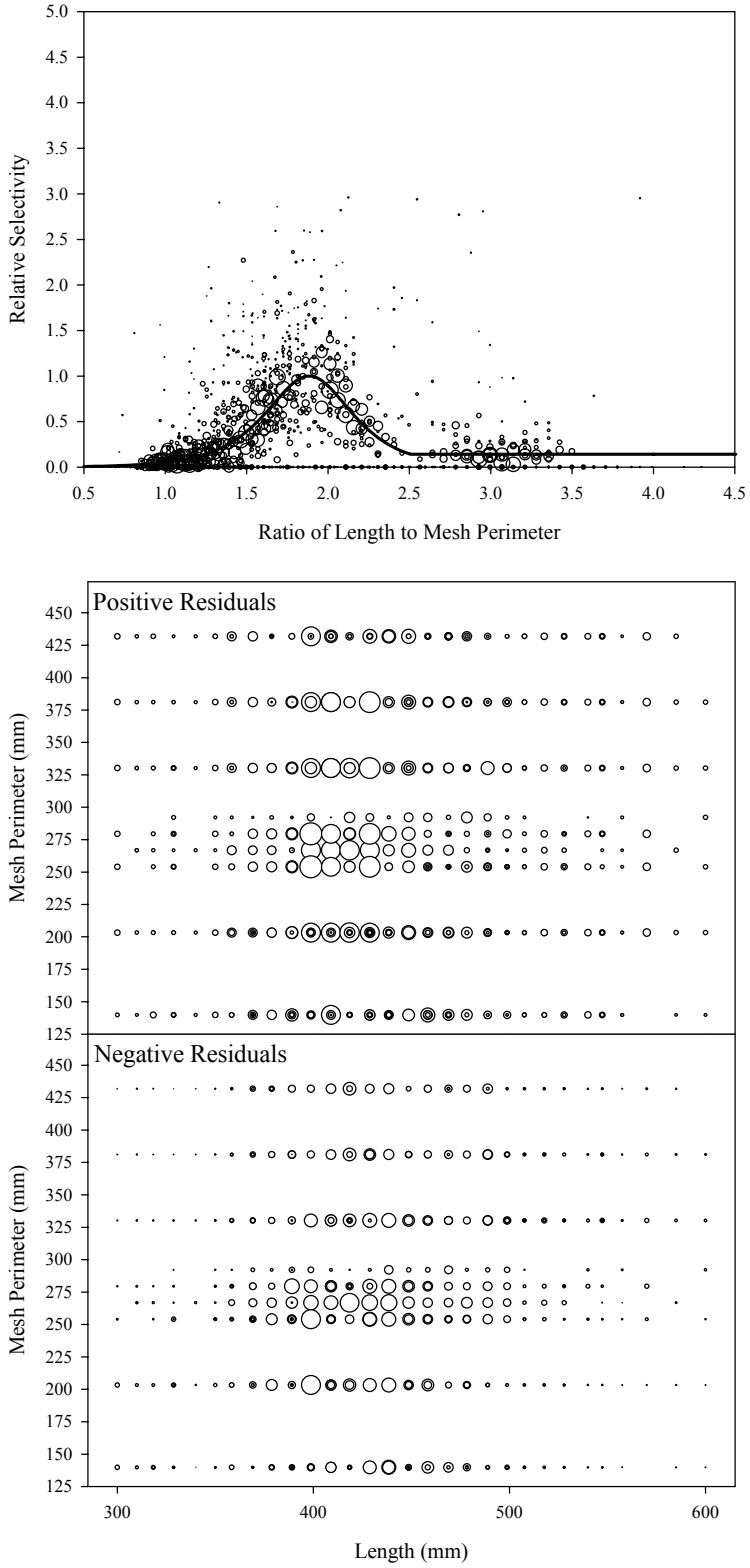

Figure B3.24. Plots of CPUE data scaled to a net selectivity model (top) and CPUE residuals (bottom); pink salmon data and Model 24.

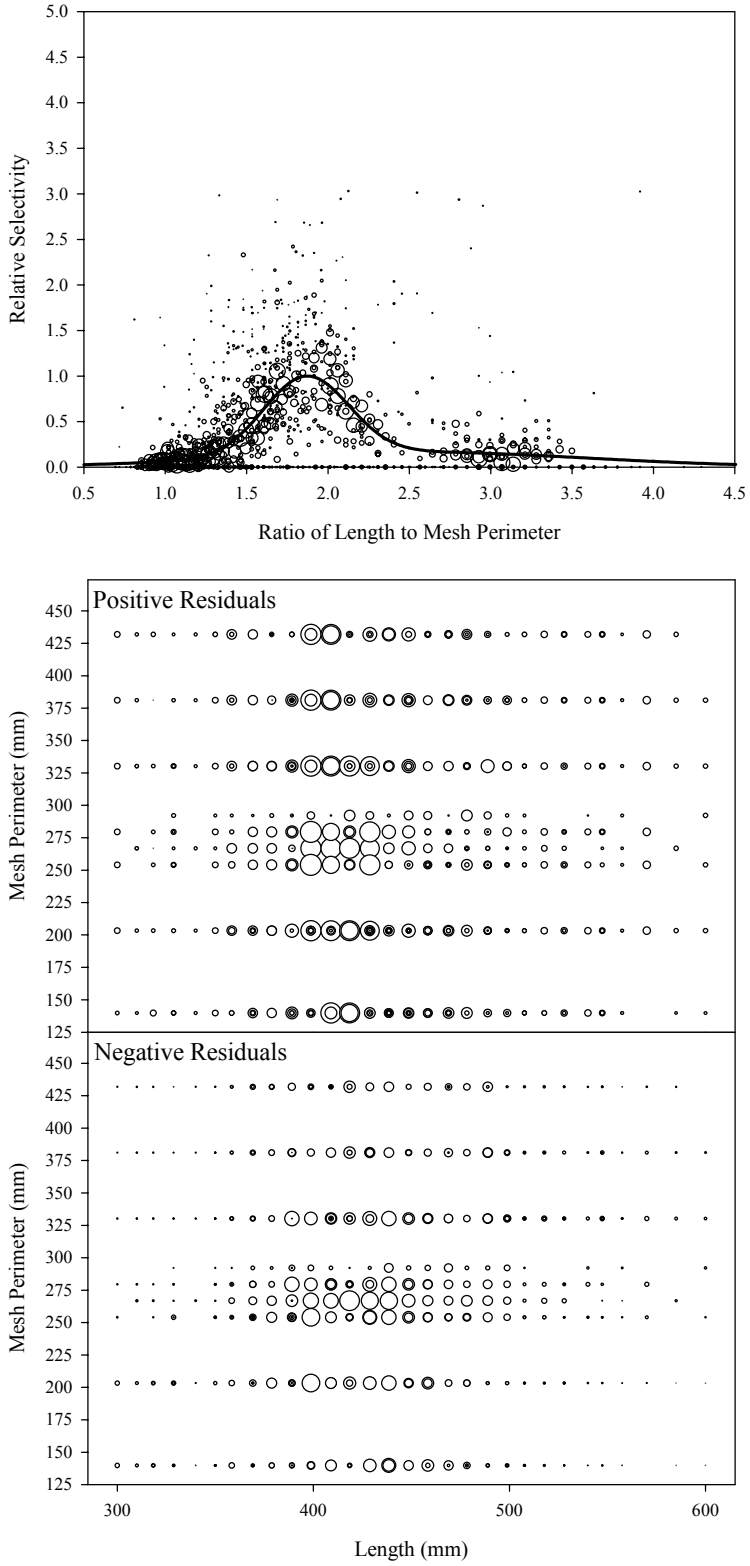

Figure B3.25. Plots of CPUE data scaled to a net selectivity model (top) and CPUE residuals (bottom); pink salmon data and Model 25.

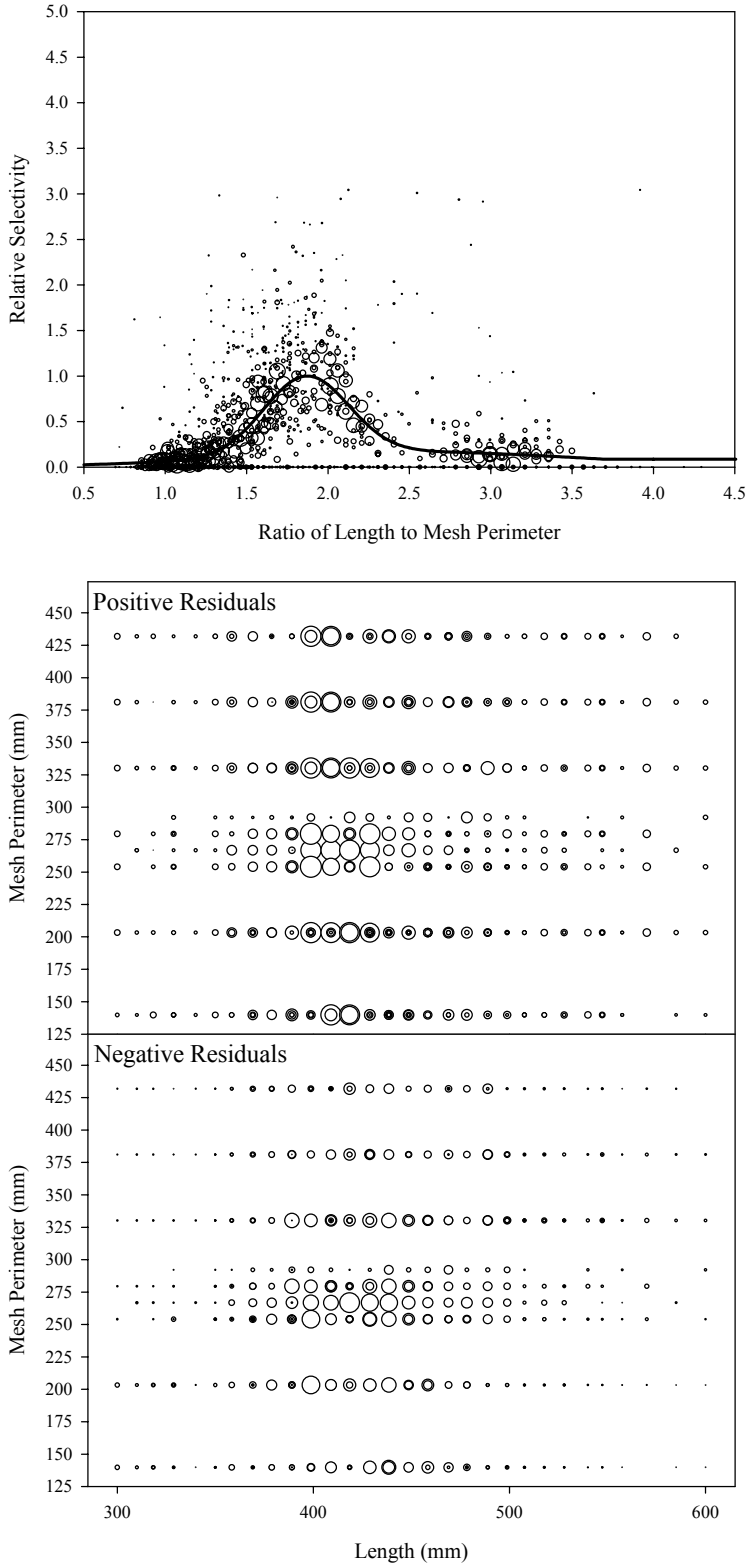

Figure B3.26. Plots of CPUE data scaled to a net selectivity model (top) and CPUE residuals (bottom); pink salmon data and Model 26.

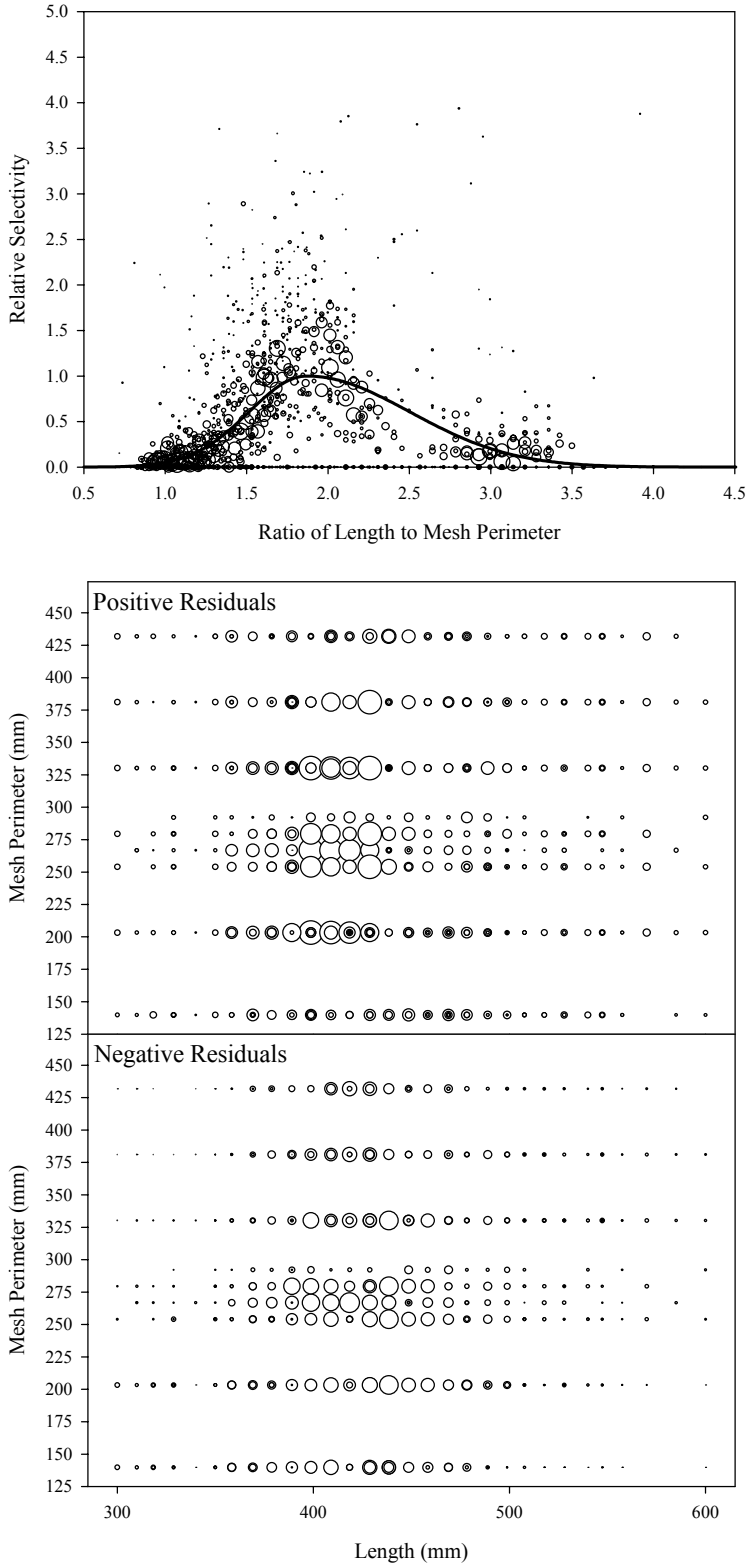

Figure B3.27. Plots of CPUE data scaled to a net selectivity model (top) and CPUE residuals (bottom); pink salmon data and Model 27.

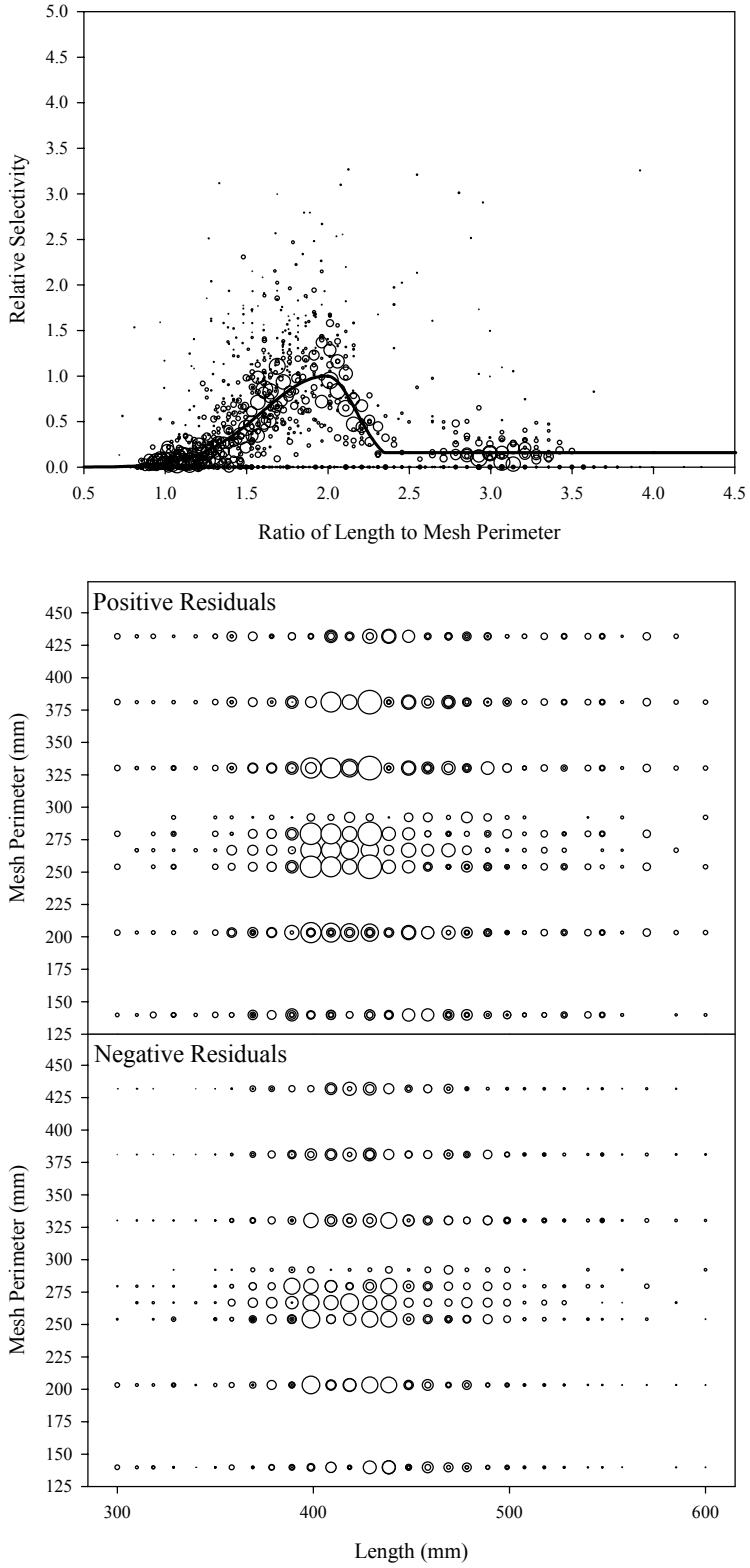

Figure B3.28. Plots of CPUE data scaled to a net selectivity model (top) and CPUE residuals (bottom); pink salmon data and Model 28.

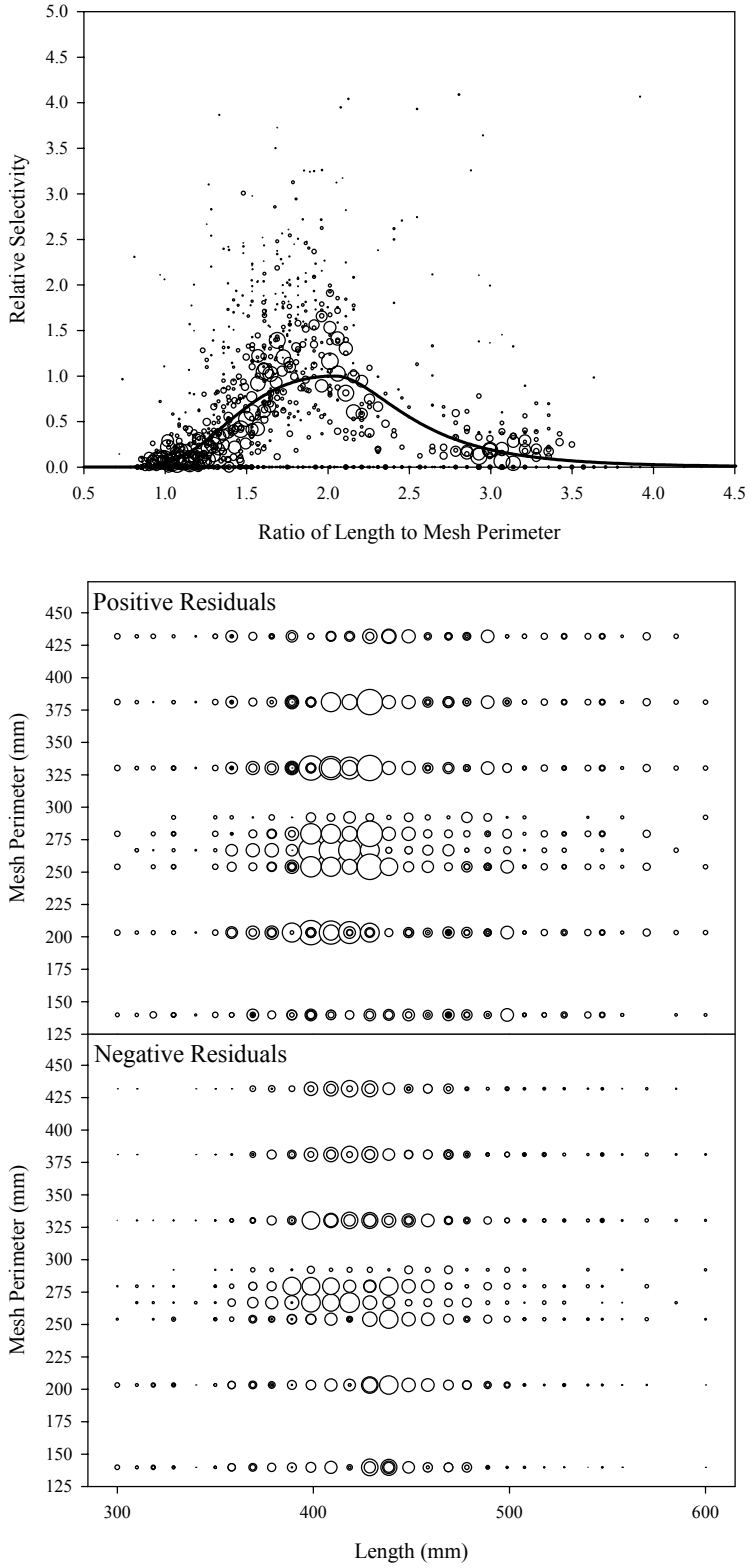

Figure B3.29. Plots of CPUE data scaled to a net selectivity model (top) and CPUE residuals (bottom); pink salmon data and Model 29.

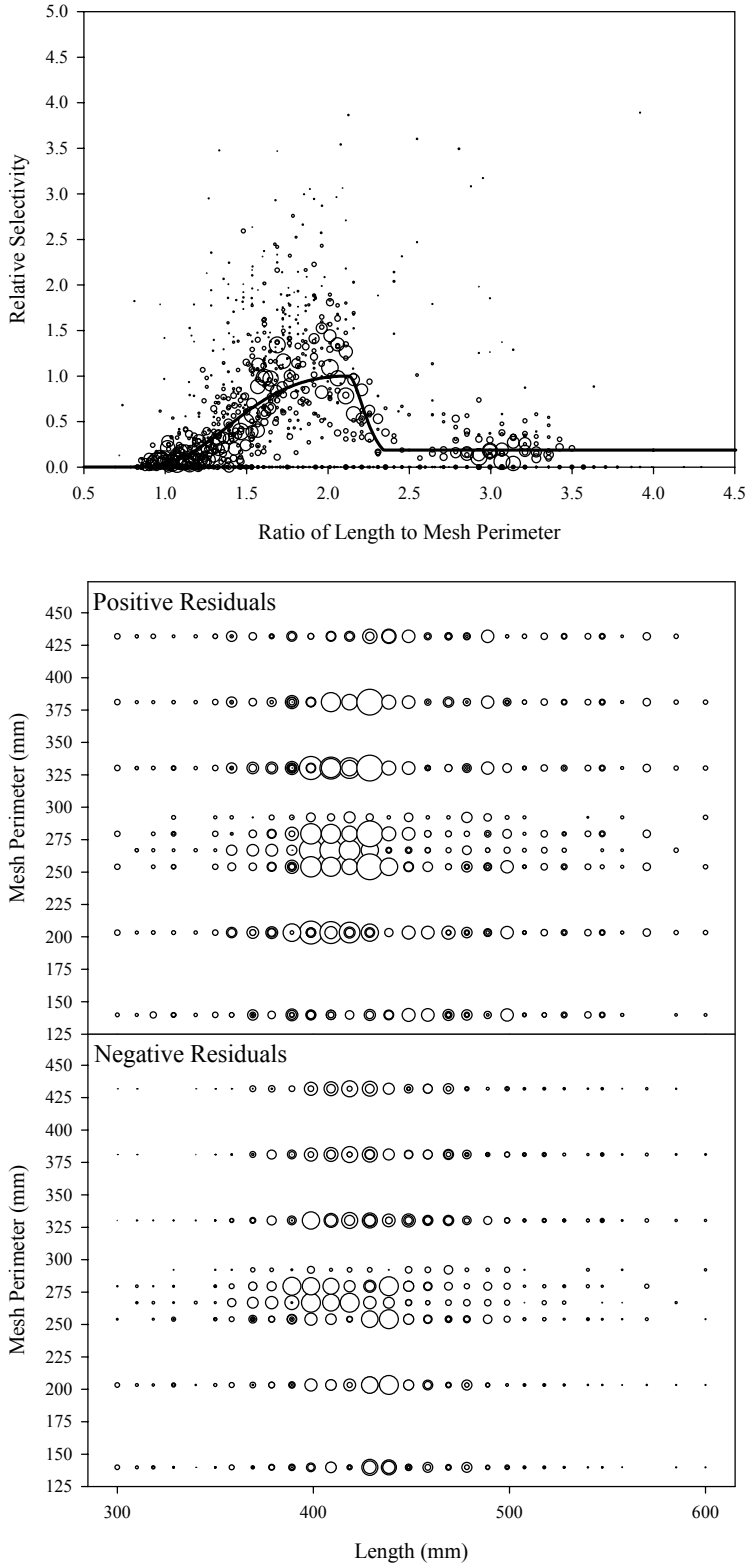

Figure B3.30. Plots of CPUE data scaled to a net selectivity model (top) and CPUE residuals (bottom); pink salmon data and Model 30.

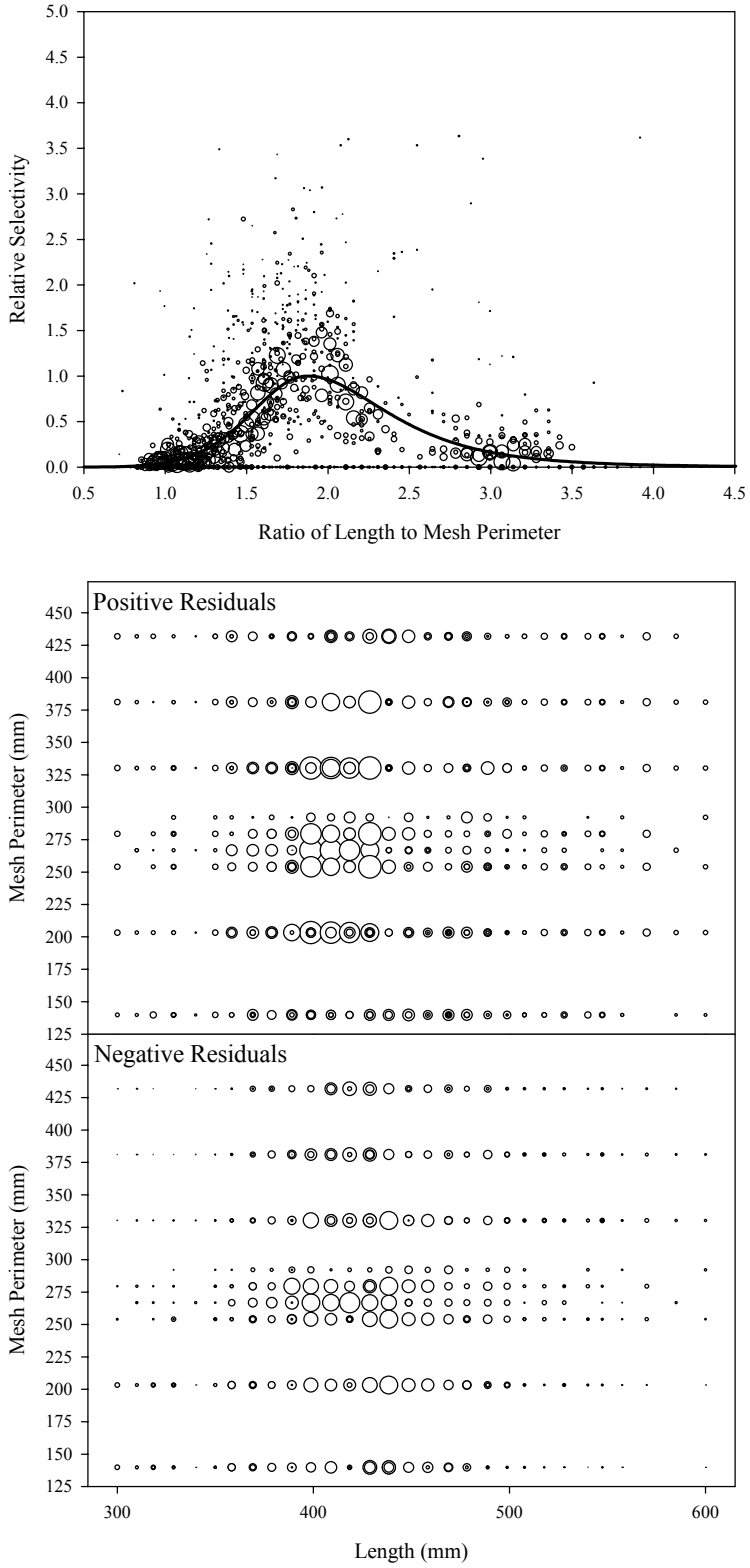

Figure B3.31. Plots of CPUE data scaled to a net selectivity model (top) and CPUE residuals (bottom); pink salmon data and Model 31.

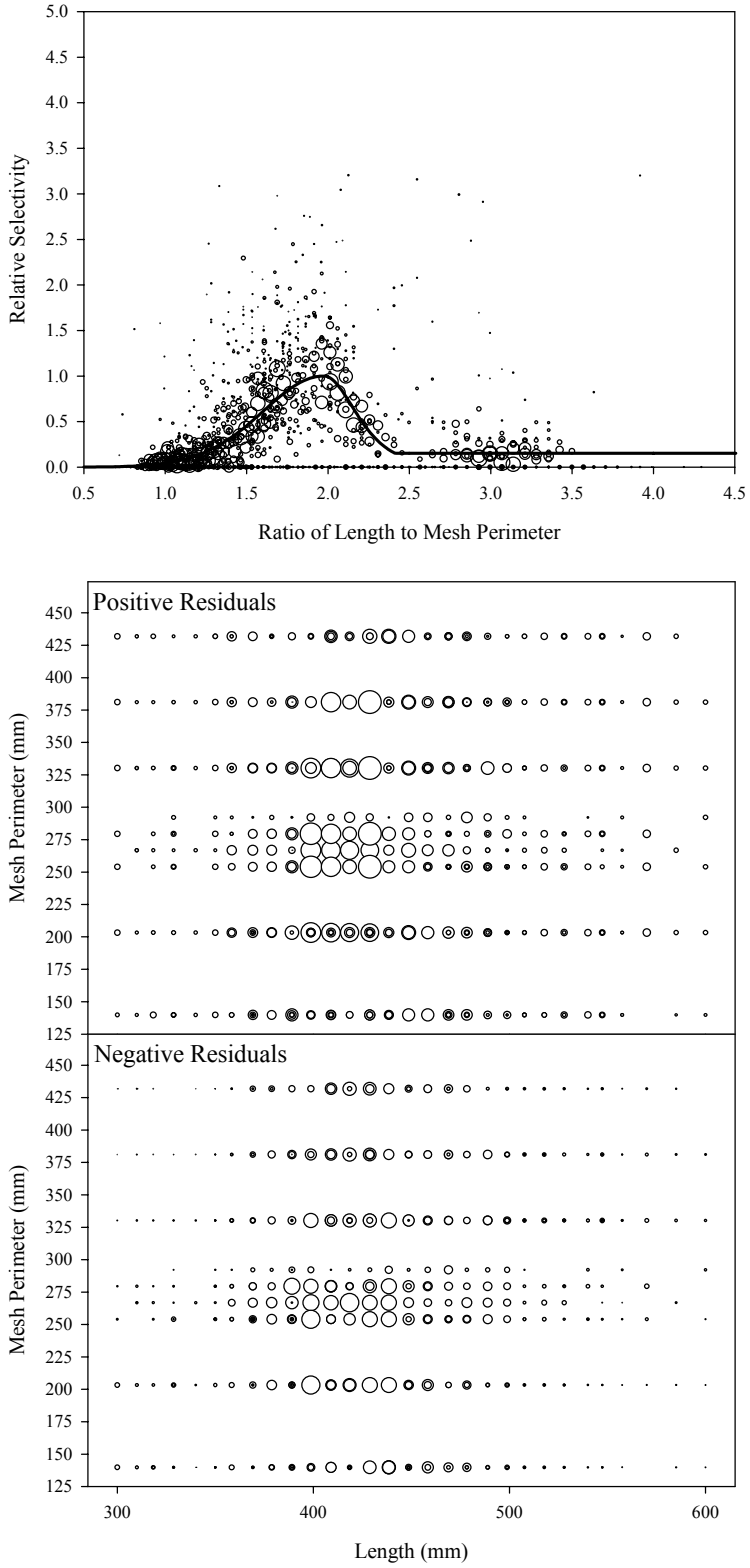

Figure B3.32. Plots of CPUE data scaled to a net selectivity model (top) and CPUE residuals (bottom); pink salmon data and Model 32.

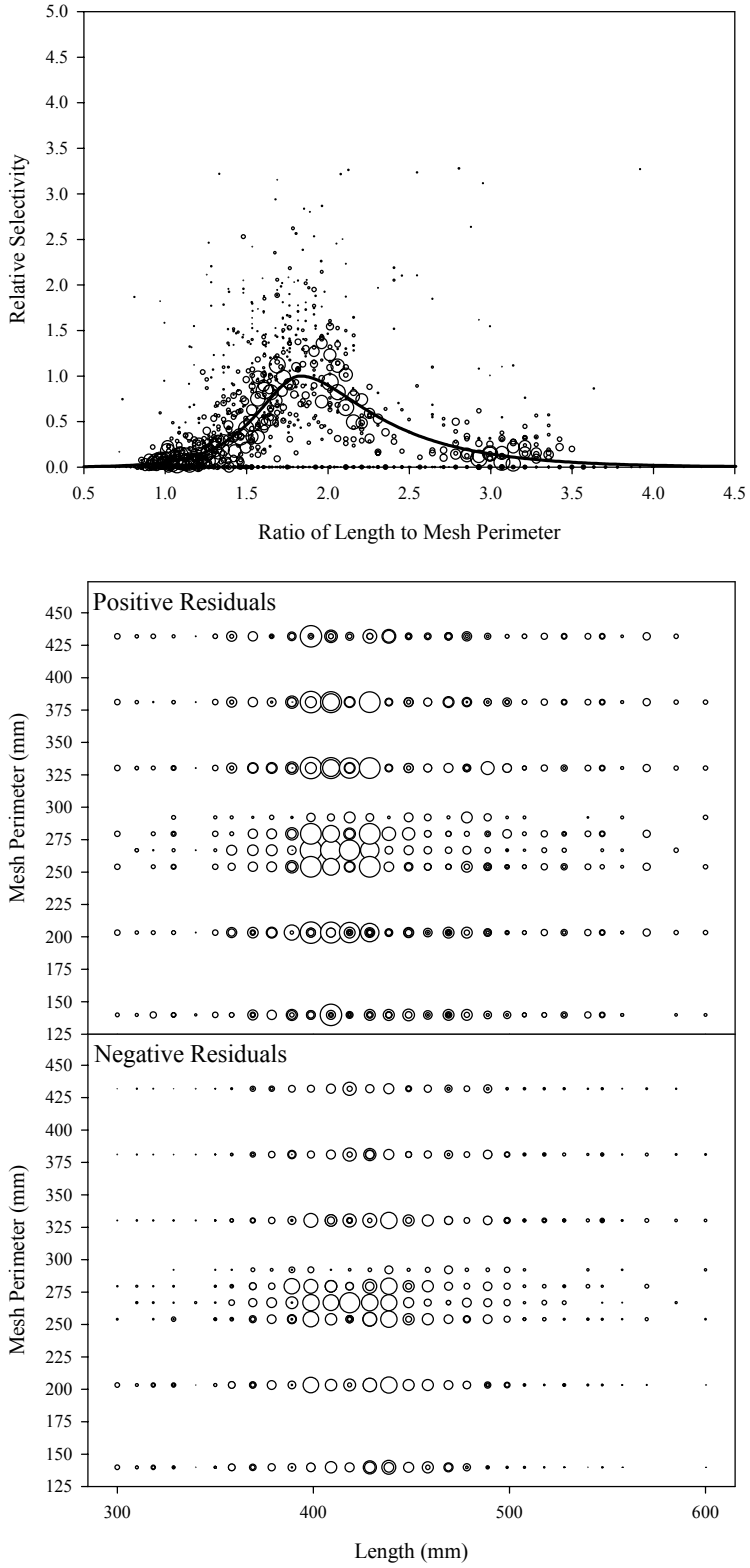

Figure B3.33. Plots of CPUE data scaled to a net selectivity model (top) and CPUE residuals (bottom); pink salmon data and Model 33.

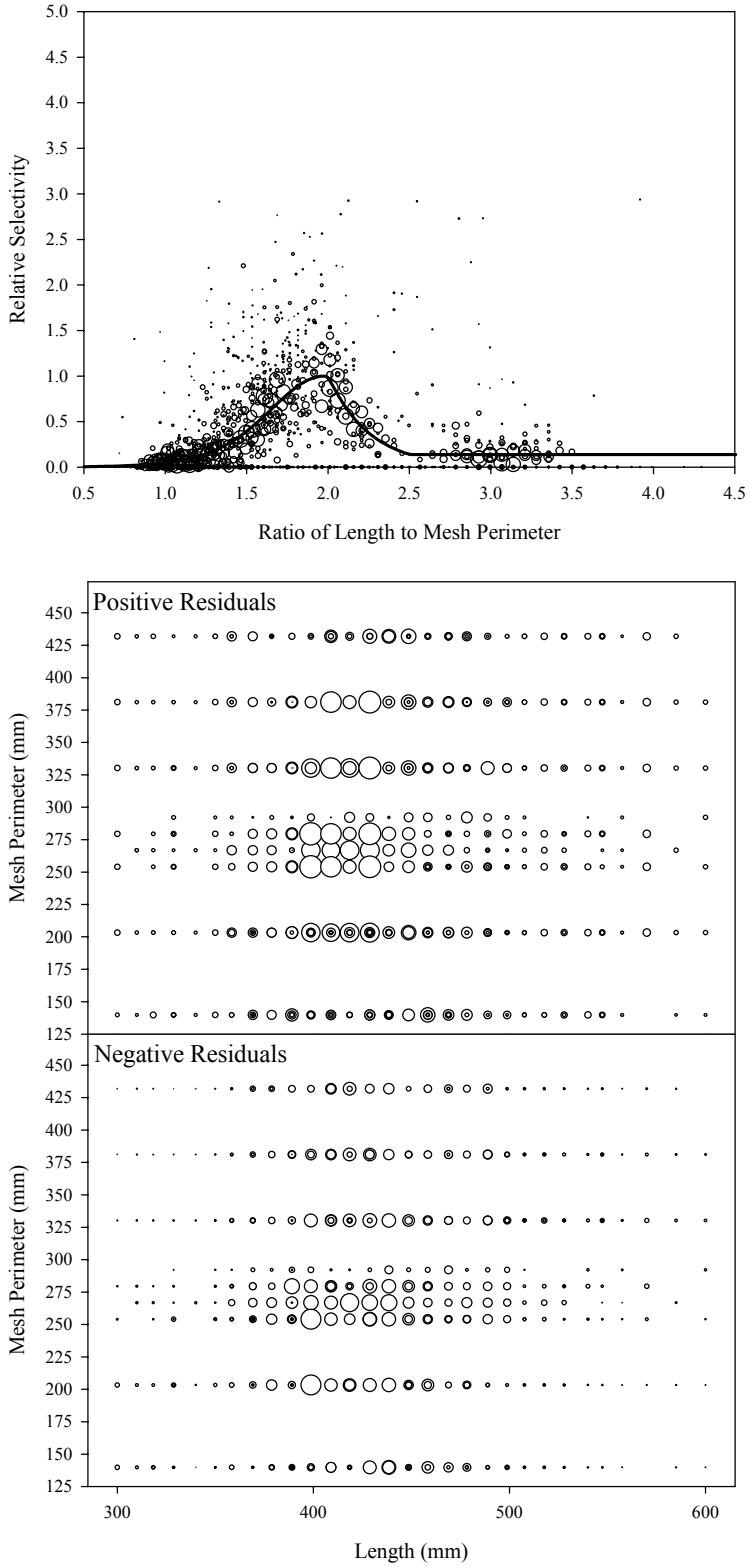

Figure B3.34. Plots of CPUE data scaled to a net selectivity model (top) and CPUE residuals (bottom); pink salmon data and Model 34.

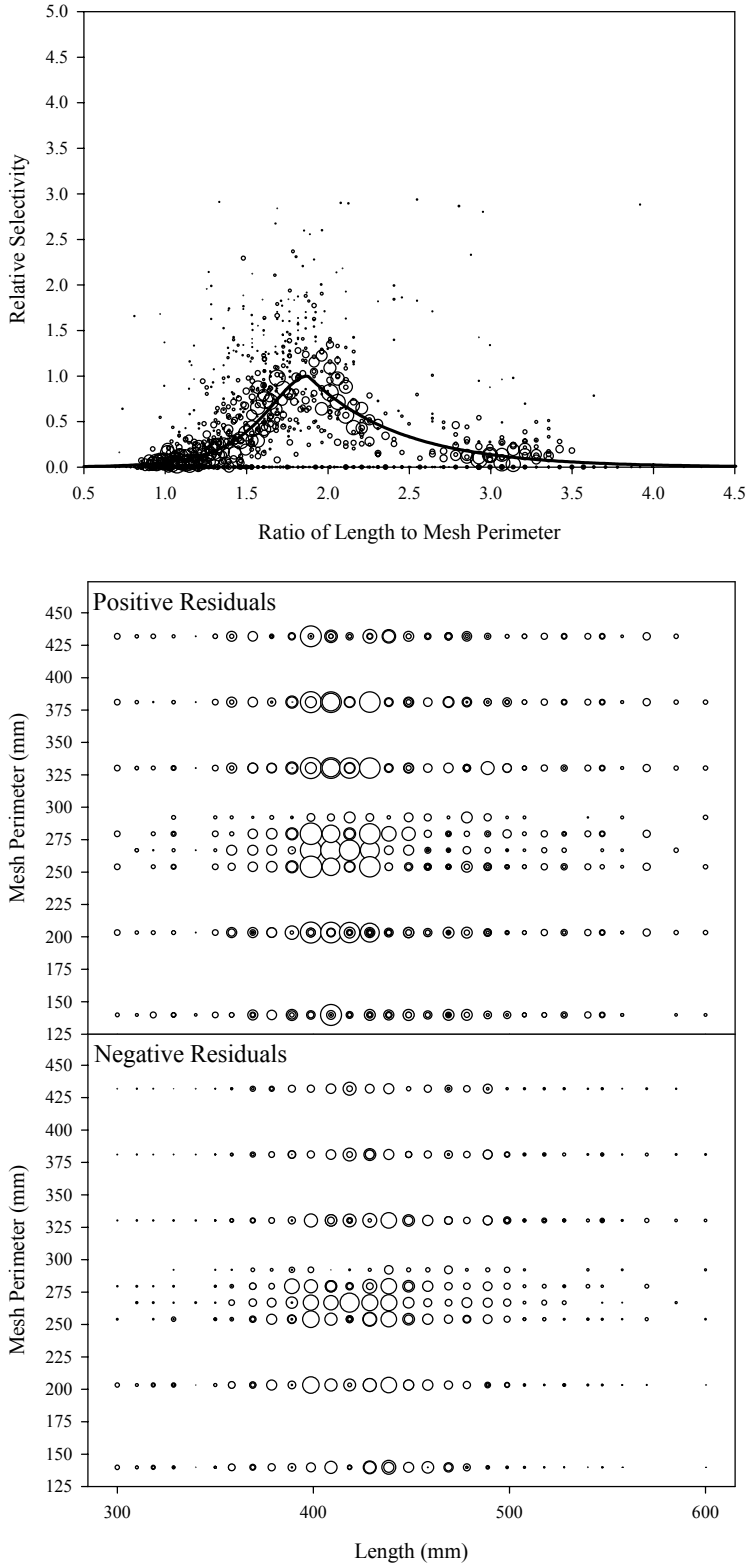

Figure B3.35. Plots of CPUE data scaled to a net selectivity model (top) and CPUE residuals (bottom); pink salmon data and Model 35.

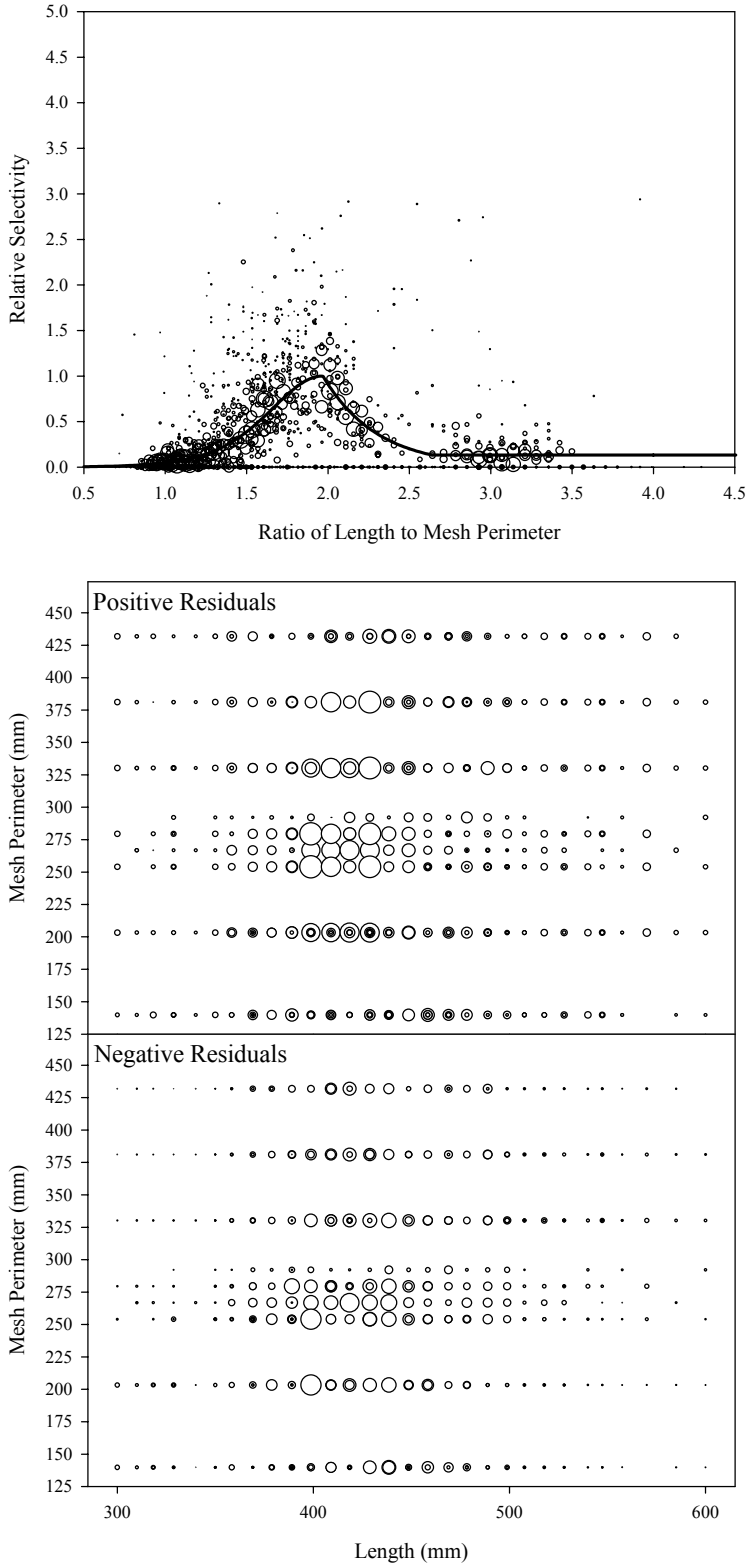

Figure B3.36. Plots of CPUE data scaled to a net selectivity model (top) and CPUE residuals (bottom); pink salmon data and Model 36.

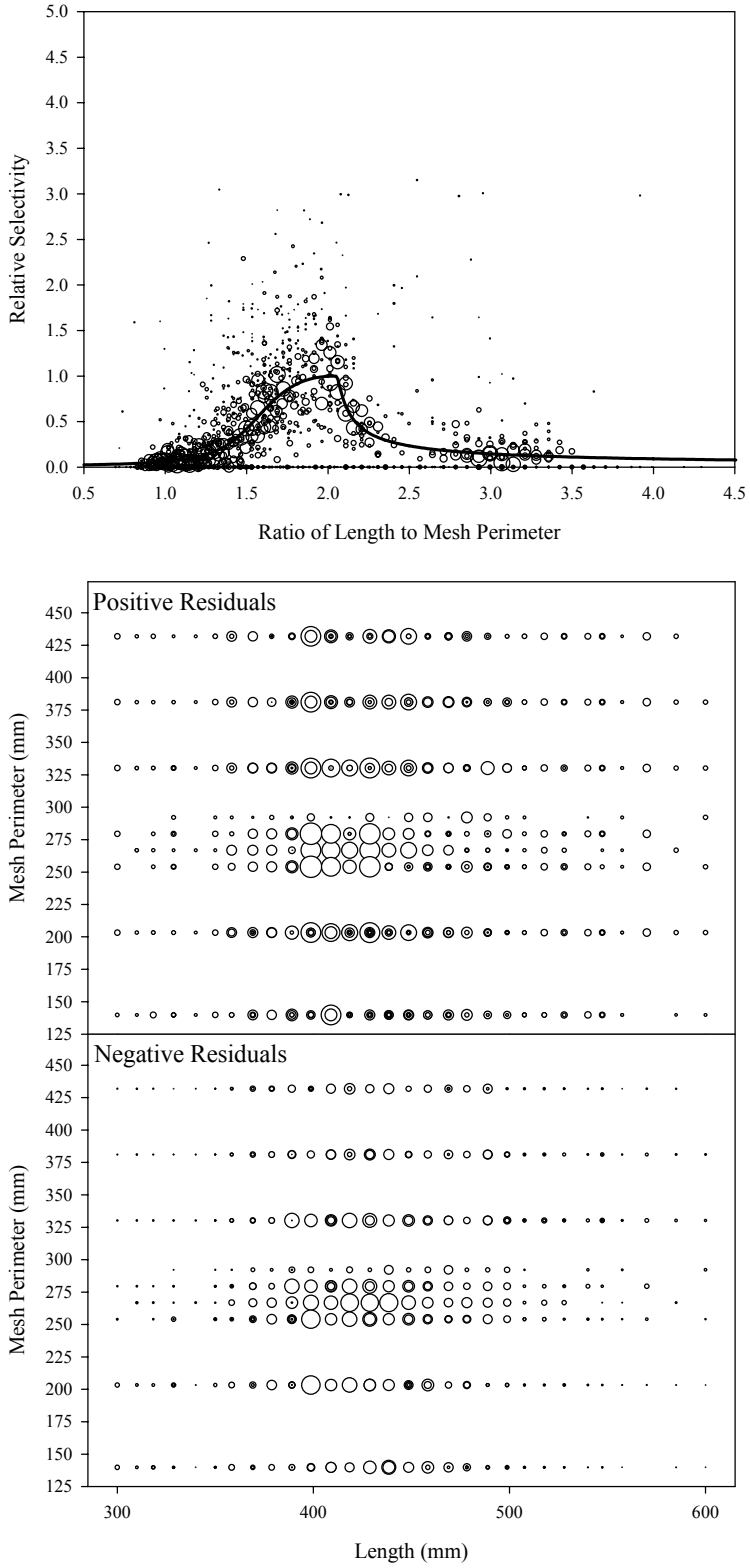

Figure B3.37. Plots of CPUE data scaled to a net selectivity model (top) and CPUE residuals (bottom); pink salmon data and Model 37.

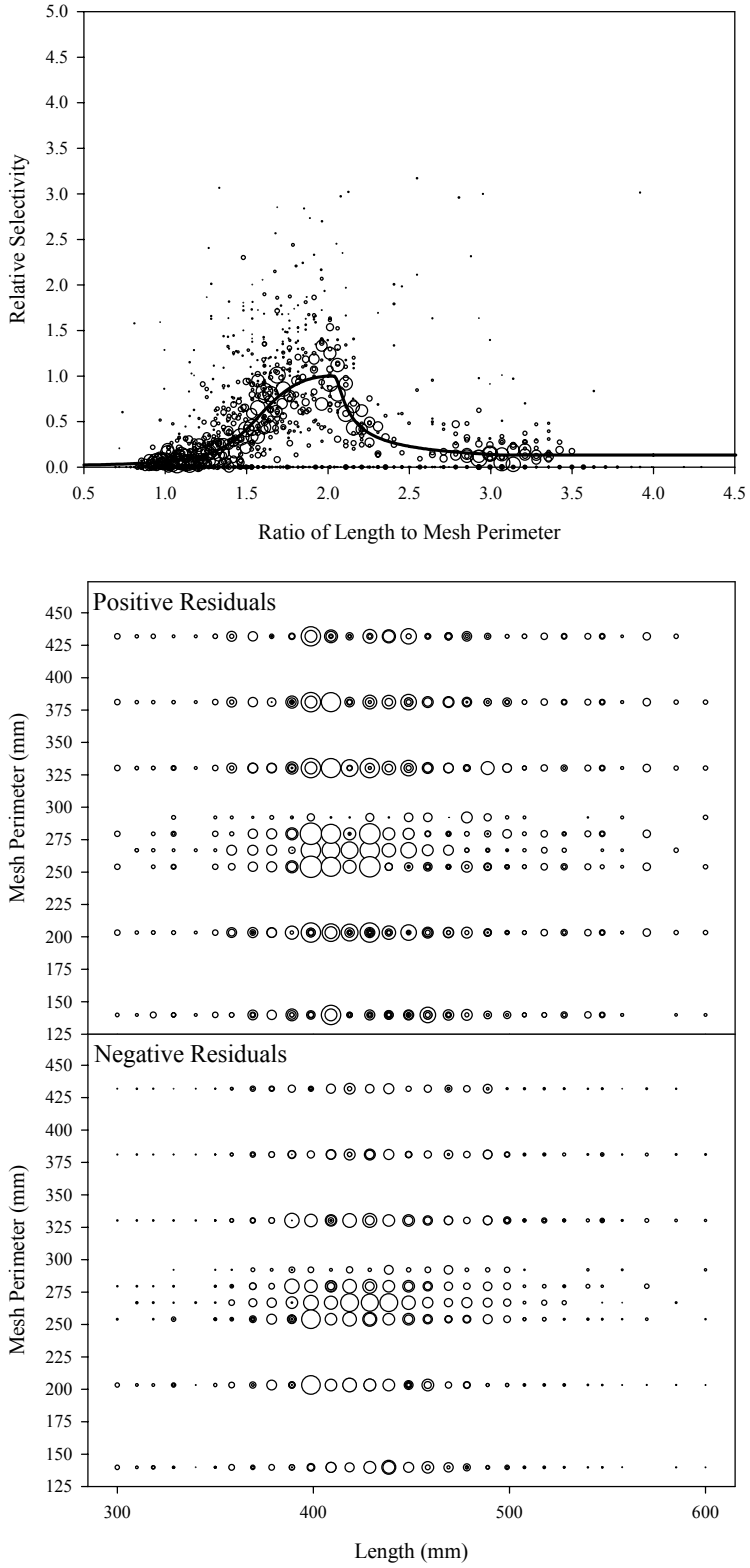

Figure B3.38. Plots of CPUE data scaled to a net selectivity model (top) and CPUE residuals (bottom); pink salmon data and Model 38.

Appendix B4
Fall Chum Salmon Diagnostic Plots
Figure B4.1 to Figure B4.38

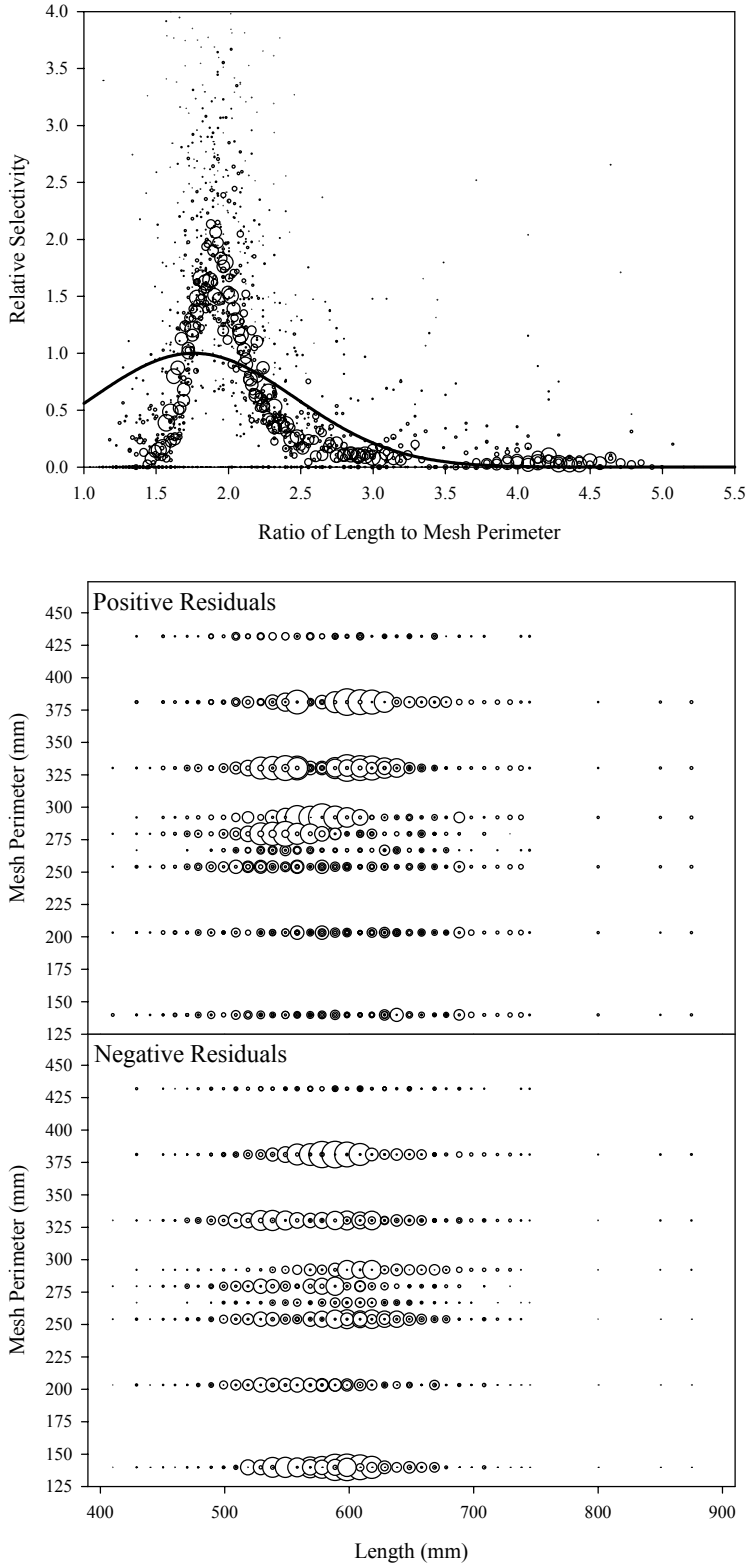

Figure B4.1. Plots of CPUE data scaled to a net selectivity model (top) and CPUE residuals (bottom); fall chum salmon data and Model 1.

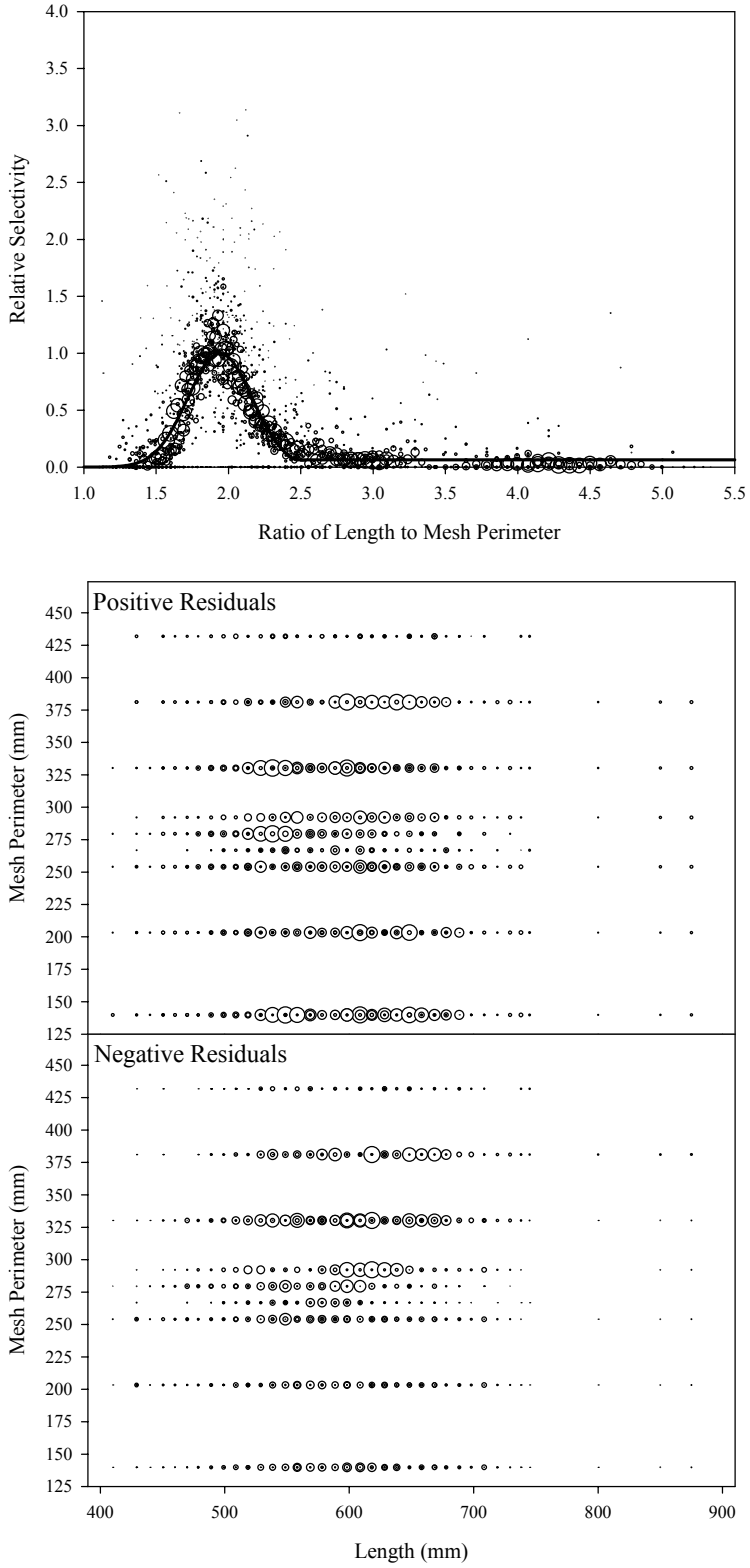

Figure B4.2. Plots of CPUE data scaled to a net selectivity model (top) and CPUE residuals (bottom); fall chum salmon data and Model 2.

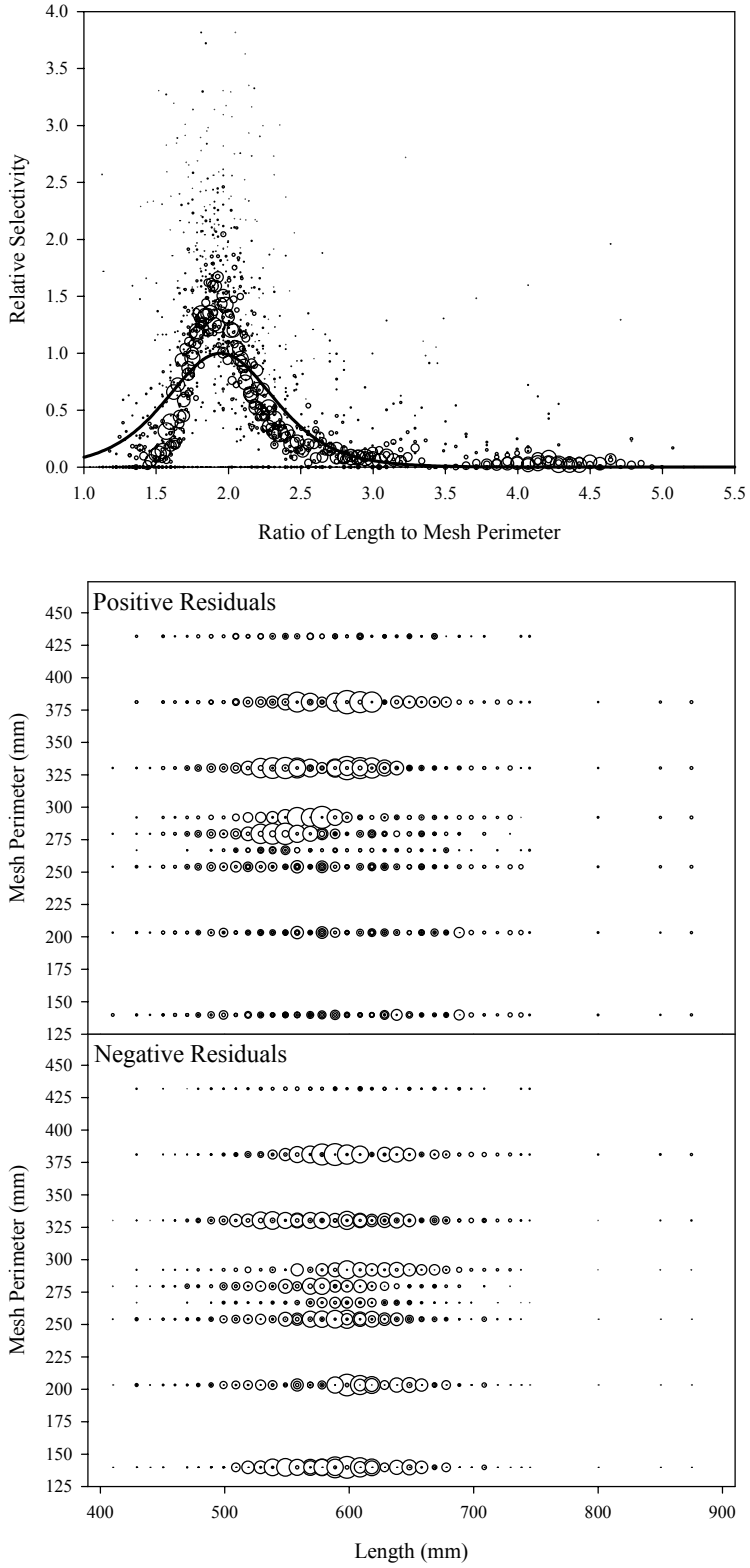

Figure B4.3. Plots of CPUE data scaled to a net selectivity model (top) and CPUE residuals (bottom); fall chum salmon data and Model 3.

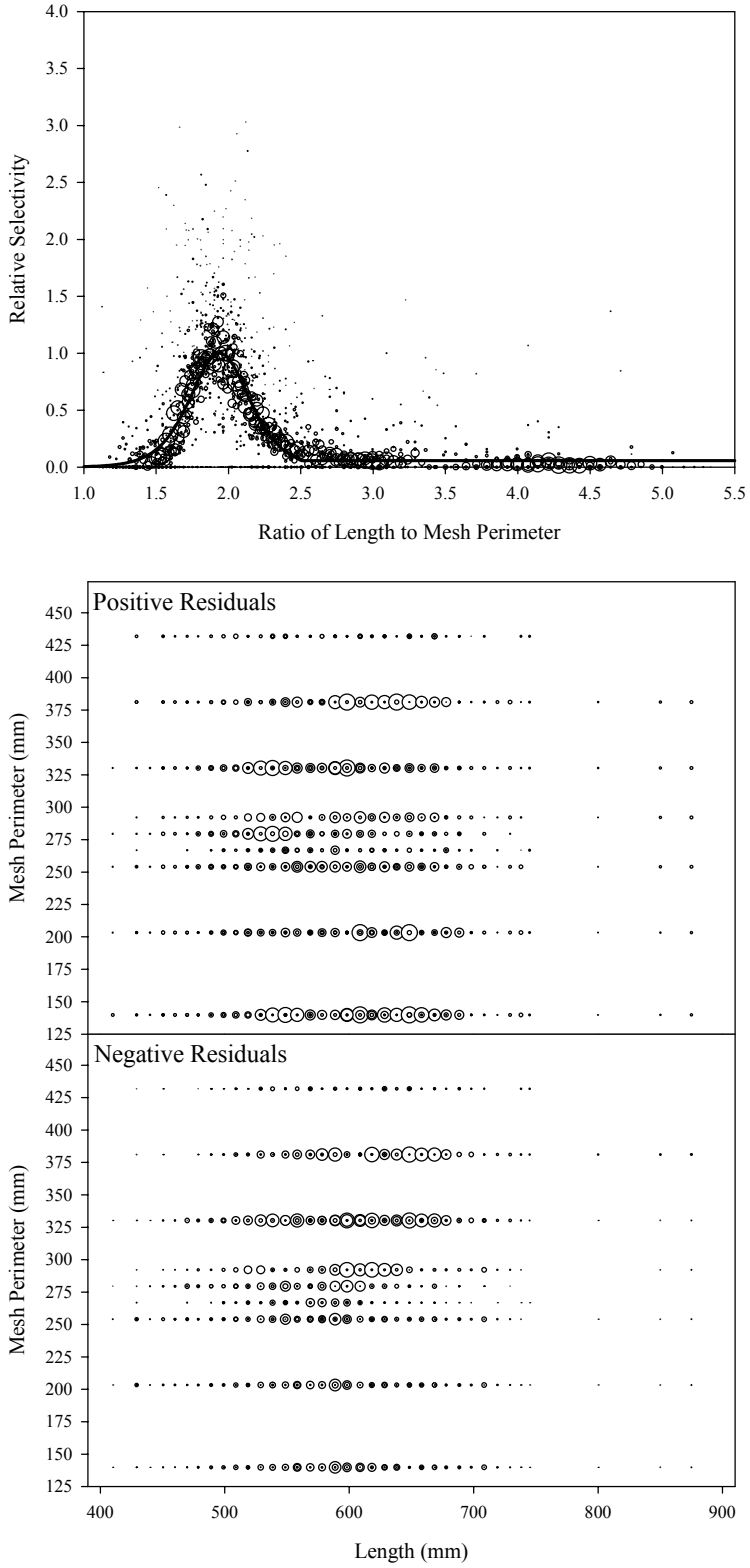

Figure B4.4. Plots of CPUE data scaled to a net selectivity model (top) and CPUE residuals (bottom); fall chum salmon data and Model 4.

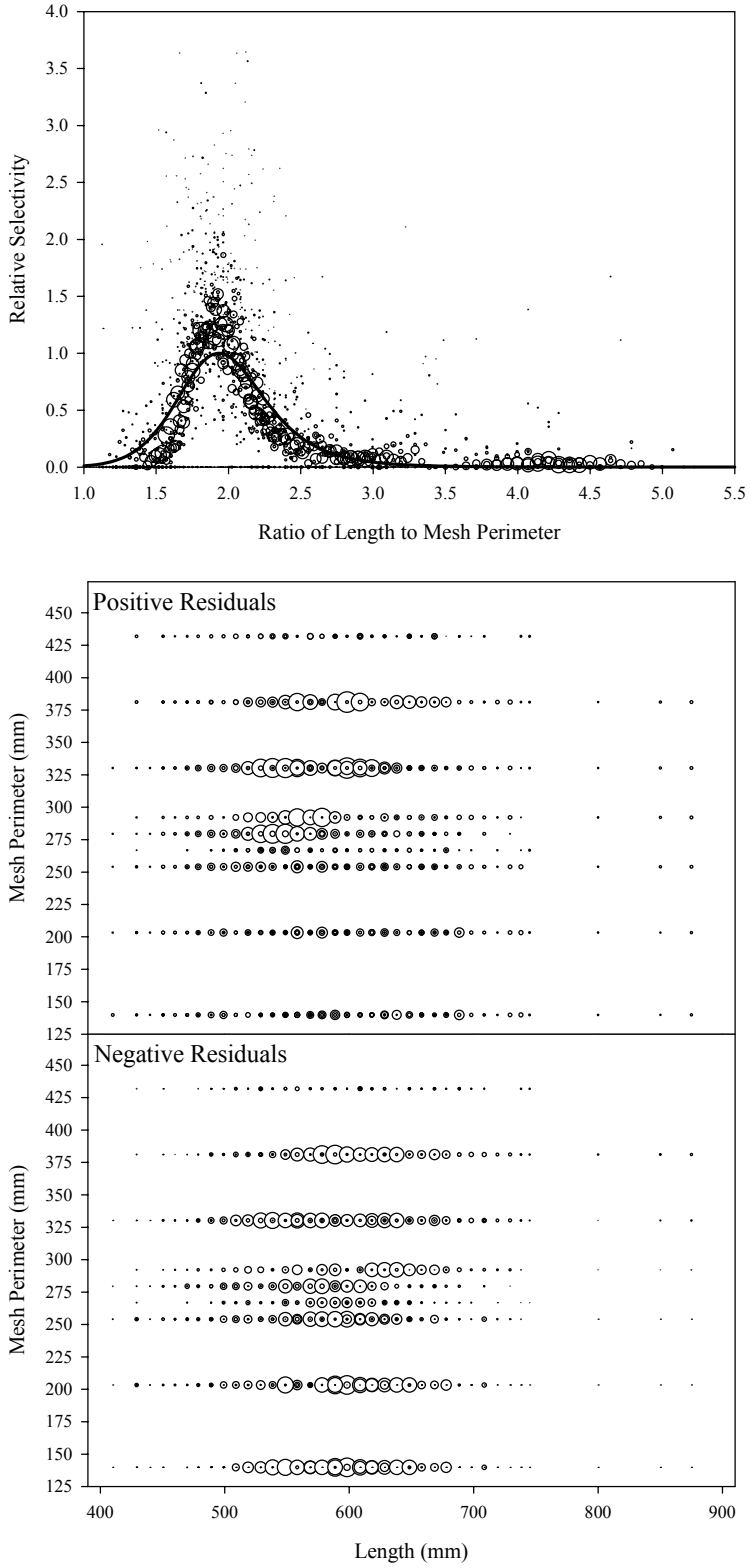

Figure B4.5. Plots of CPUE data scaled to a net selectivity model (top) and CPUE residuals (bottom); fall chum salmon data and Model 5.

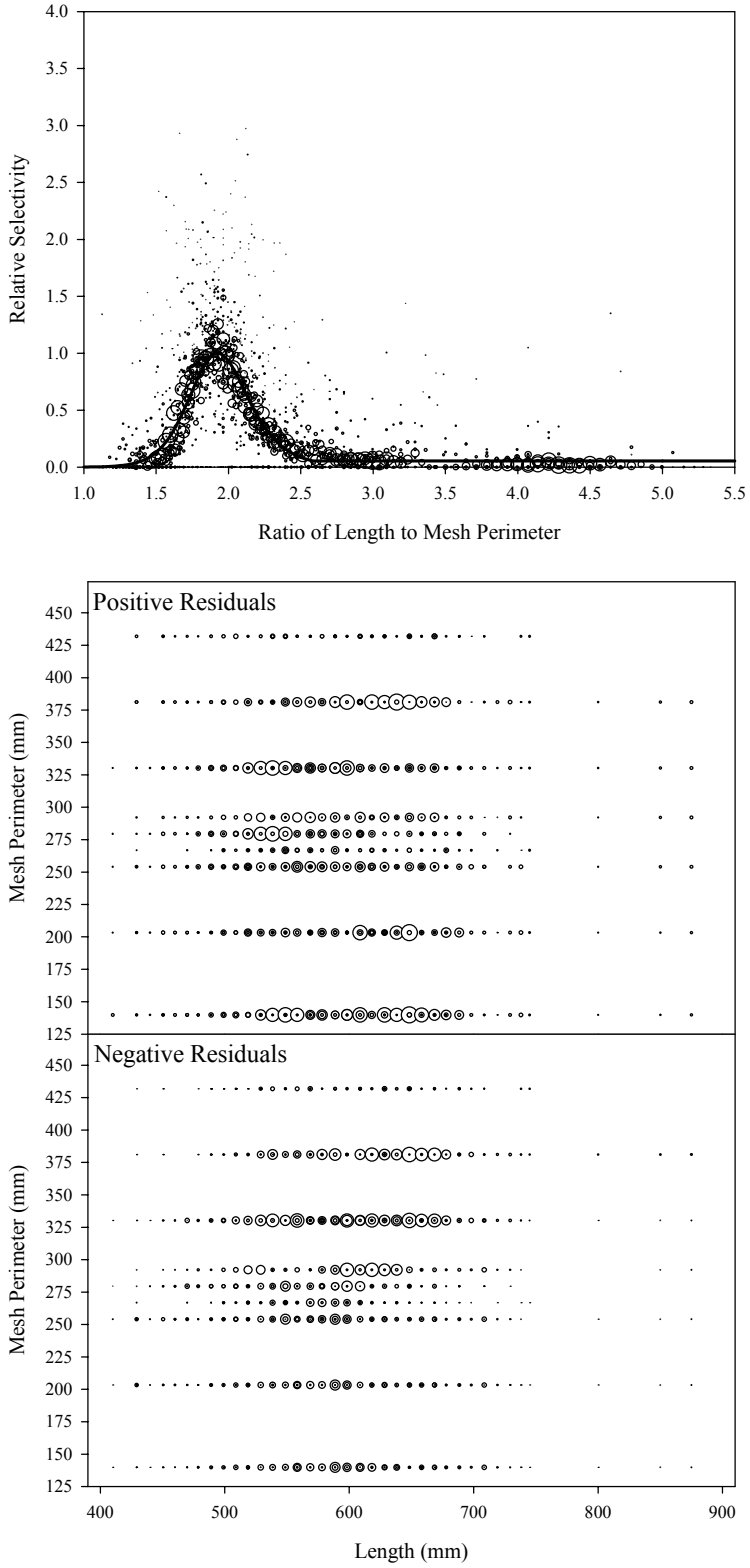

Figure B4.6. Plots of CPUE data scaled to a net selectivity model (top) and CPUE residuals (bottom); fall chum salmon data and Model 6.

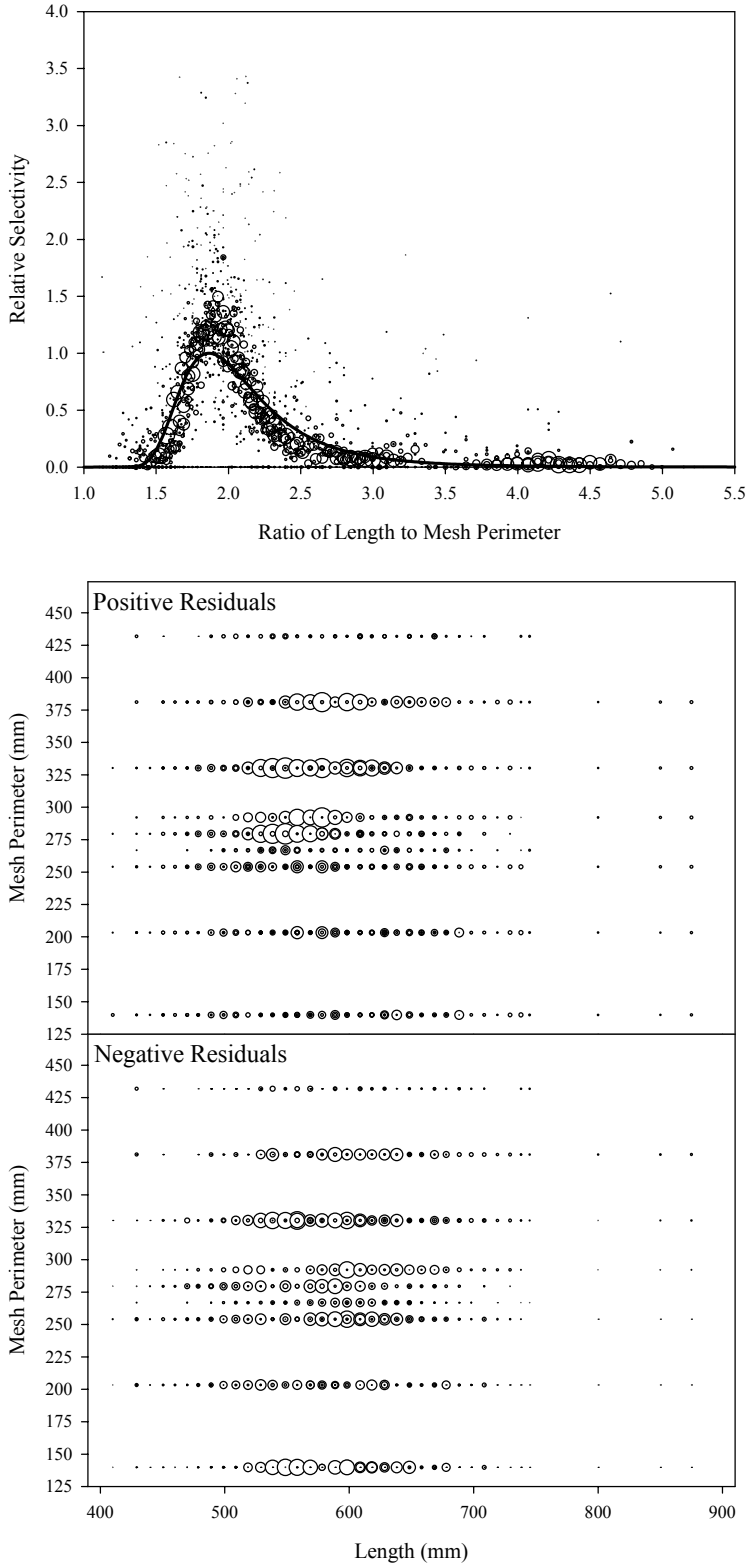

Figure B4.7. Plots of CPUE data scaled to a net selectivity model (top) and CPUE residuals (bottom); fall chum salmon data and Model 7.

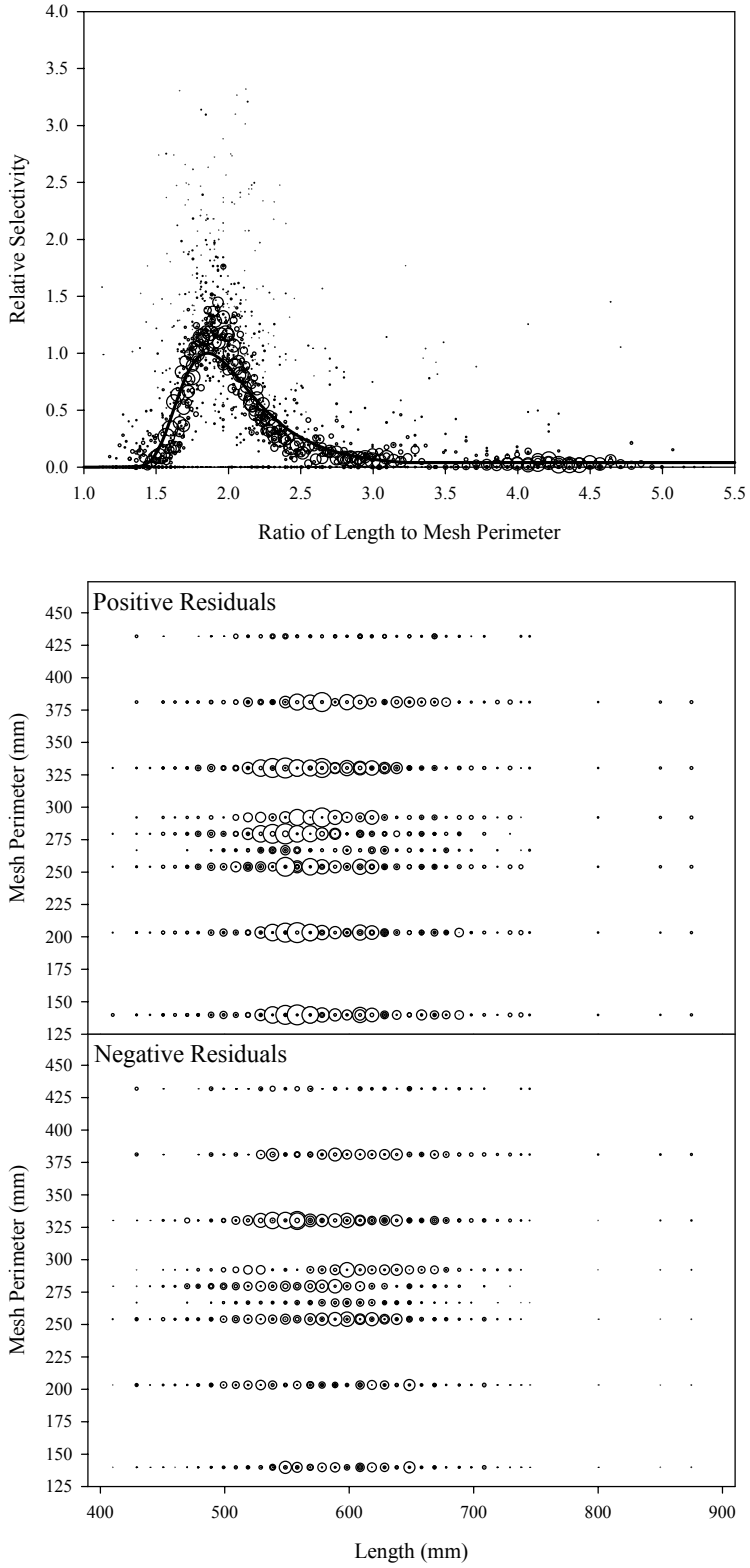

Figure B4.8. Plots of CPUE data scaled to a net selectivity model (top) and CPUE residuals (bottom); fall chum salmon data and Model 8.

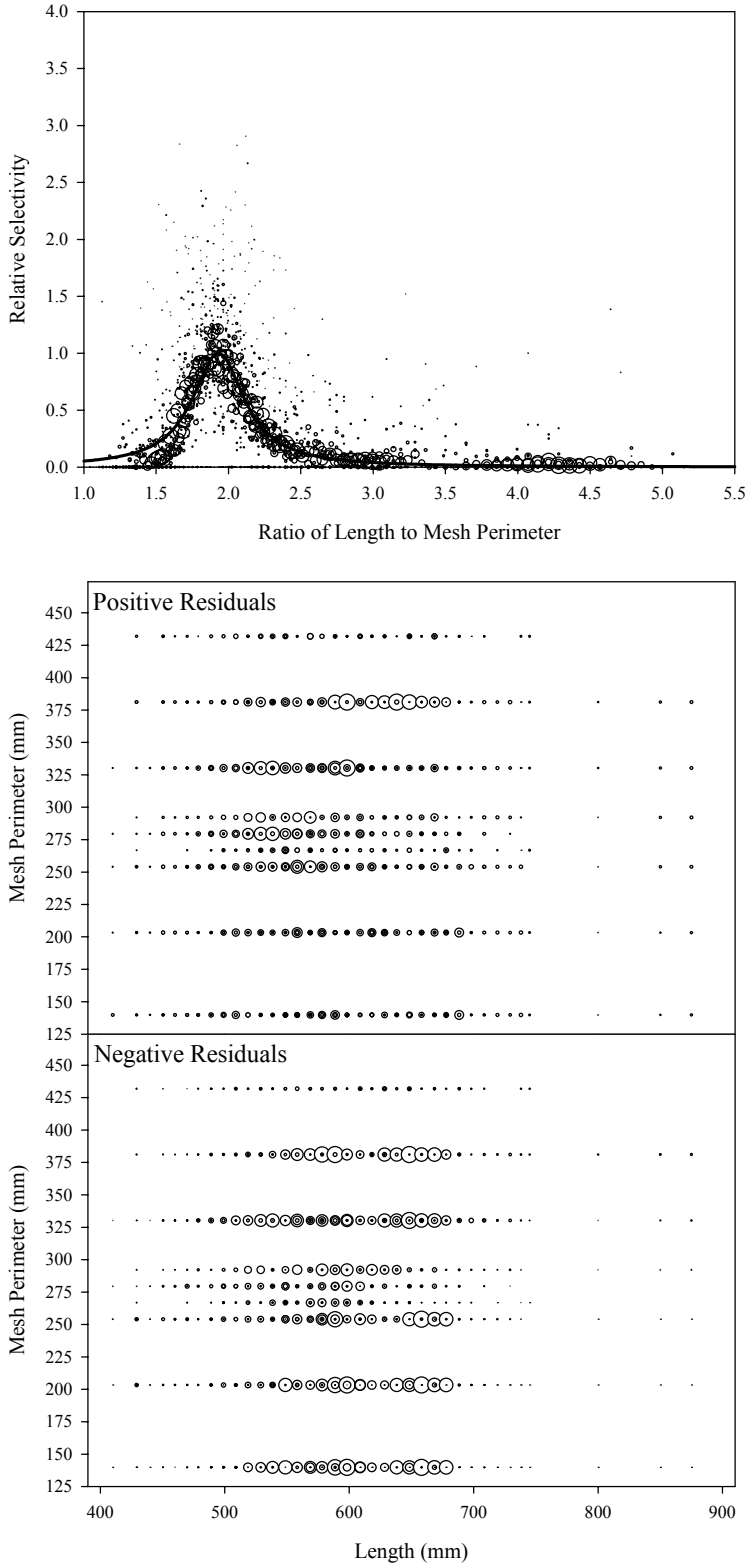

Figure B4.9. Plots of CPUE data scaled to a net selectivity model (top) and CPUE residuals (bottom); fall chum salmon data and Model 9.

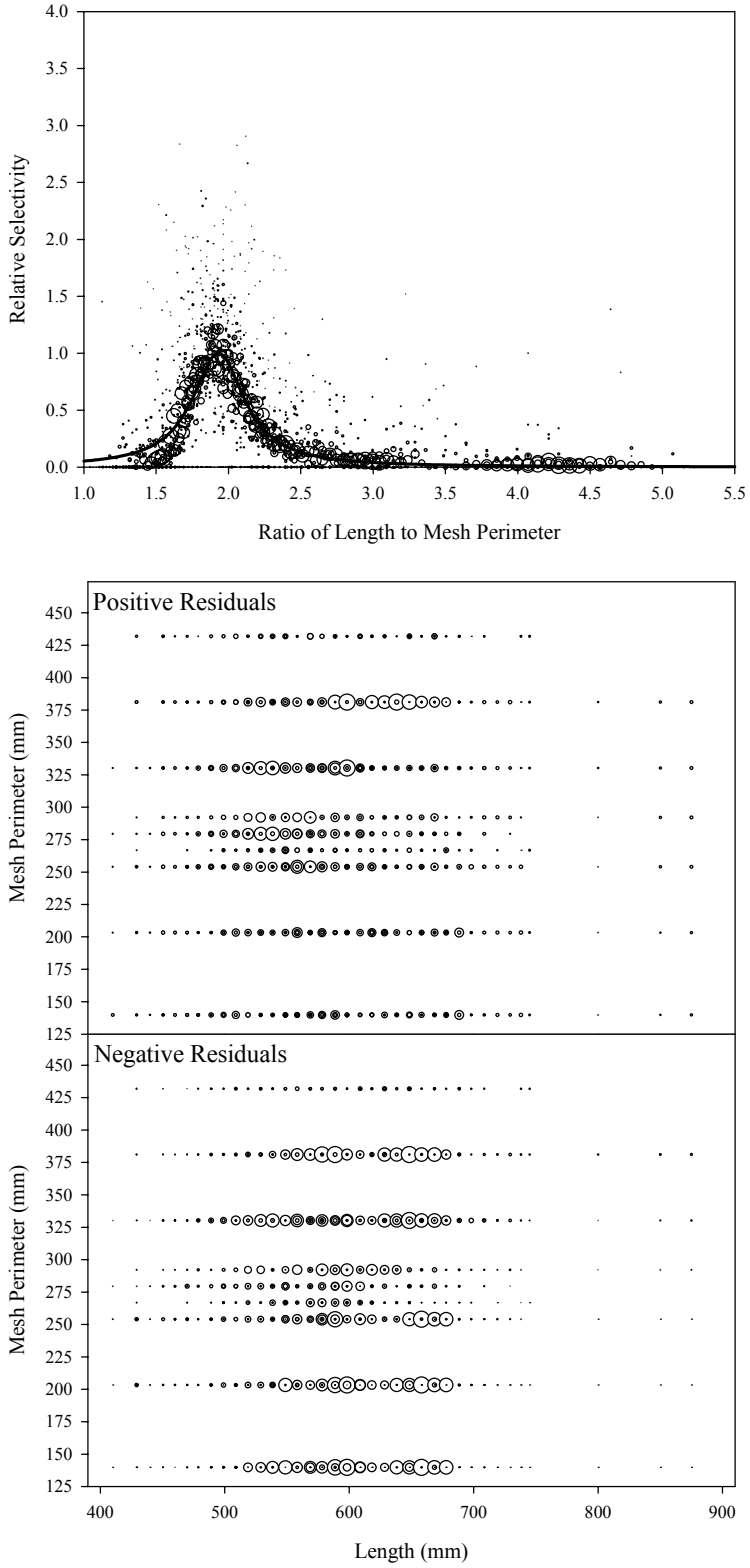

Figure B4.10. Plots of CPUE data scaled to a net selectivity model (top) and CPUE residuals (bottom); fall chum salmon data and Model 10.

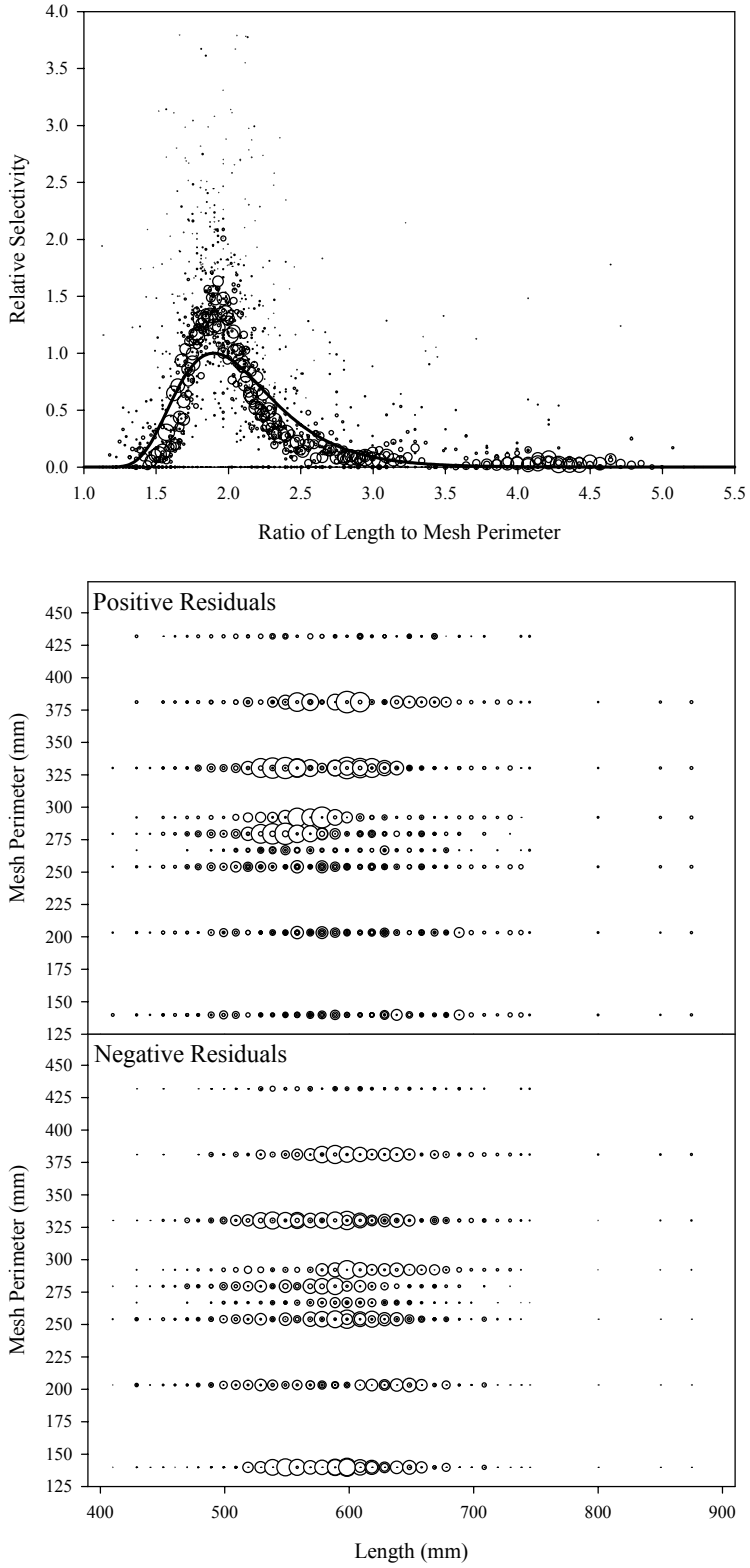

Figure B4.11. Plots of CPUE data scaled to a net selectivity model (top) and CPUE residuals (bottom); fall chum salmon data and Model 11.

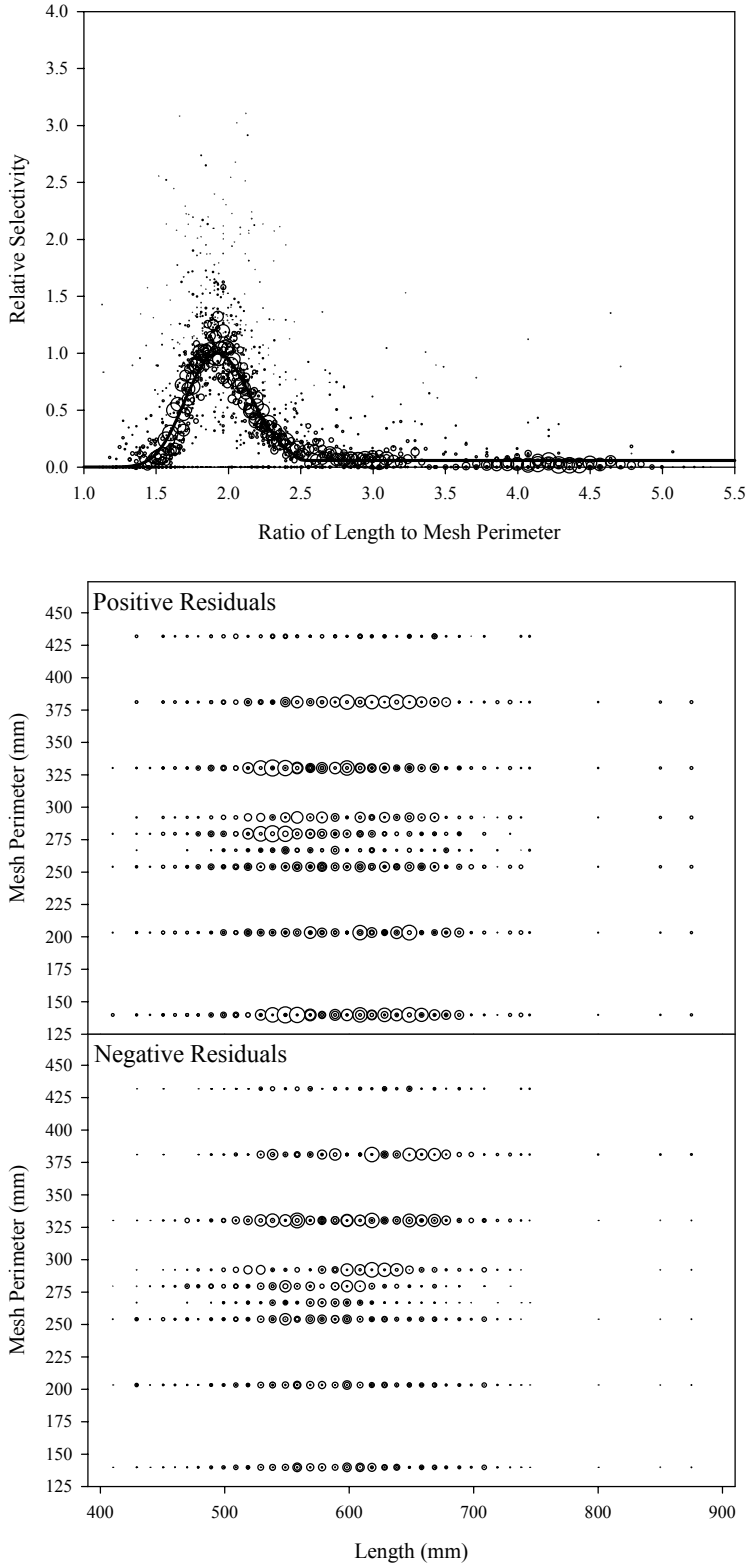

Figure B4.12. Plots of CPUE data scaled to a net selectivity model (top) and CPUE residuals (bottom); fall chum salmon data and Model 12.

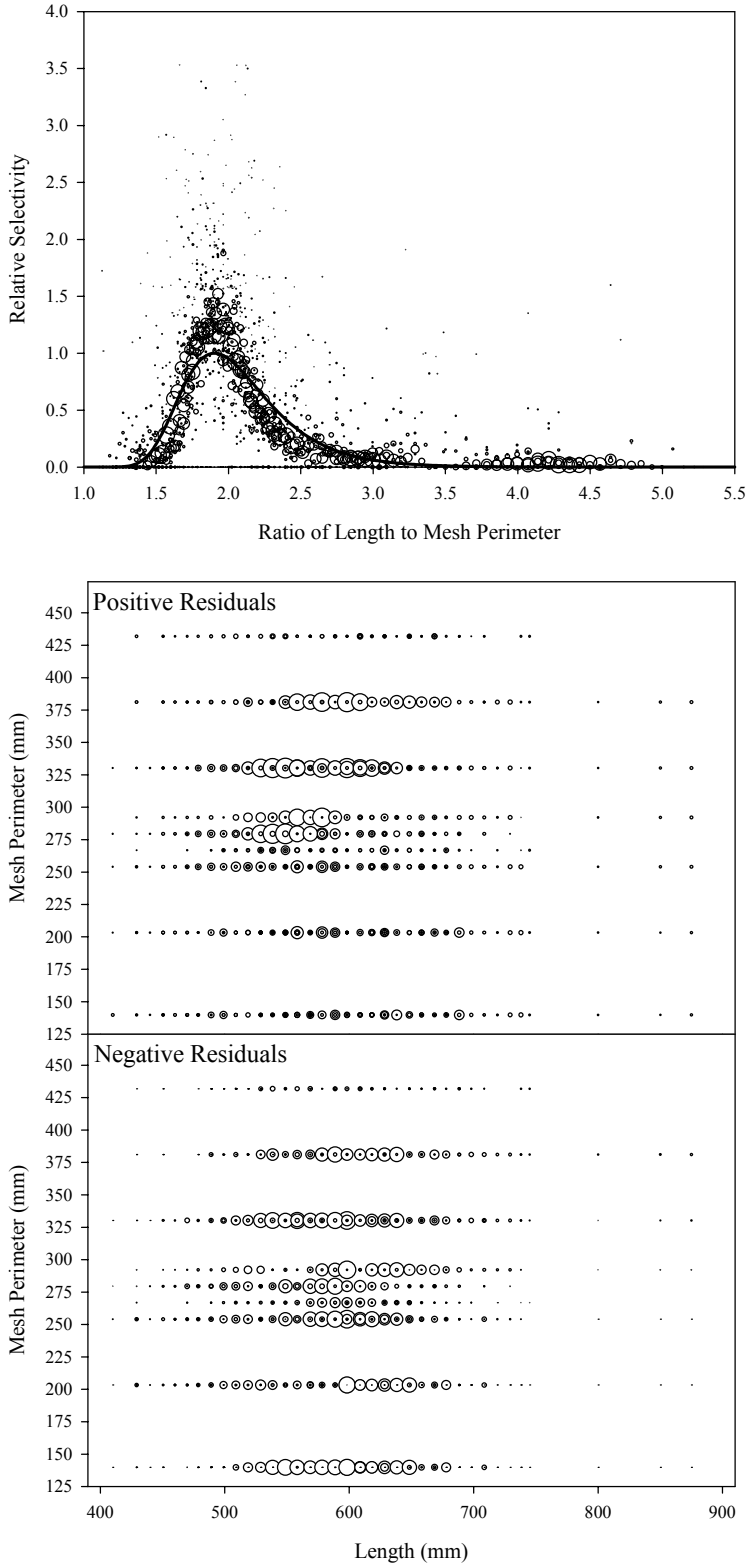

Figure B4.13. Plots of CPUE data scaled to a net selectivity model (top) and CPUE residuals (bottom); fall chum salmon data and Model 13.

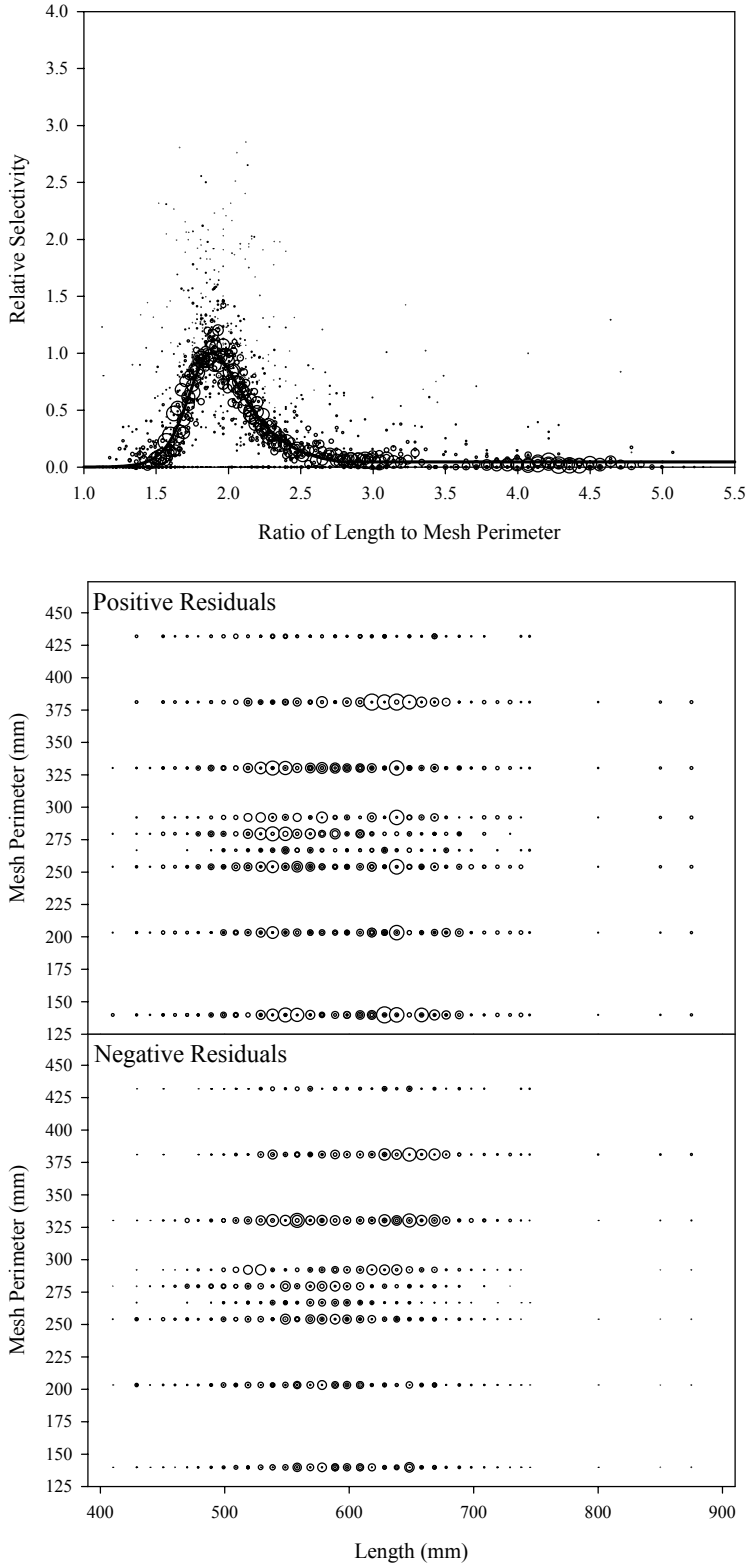

Figure B4.14. Plots of CPUE data scaled to a net selectivity model (top) and CPUE residuals (bottom); fall chum salmon data and Model 14.

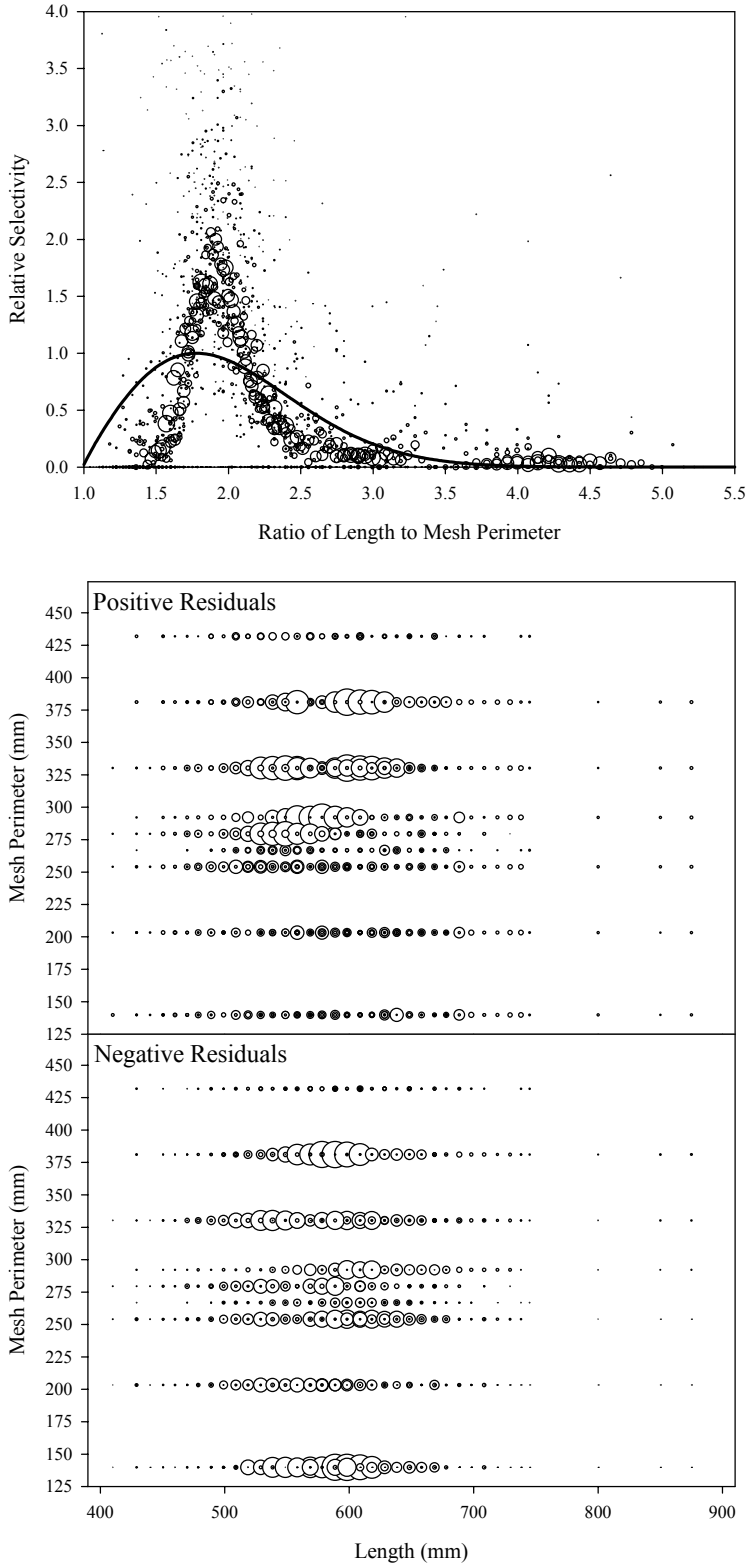

Figure B4.15. Plots of CPUE data scaled to a net selectivity model (top) and CPUE residuals (bottom); fall chum salmon data and Model 15.

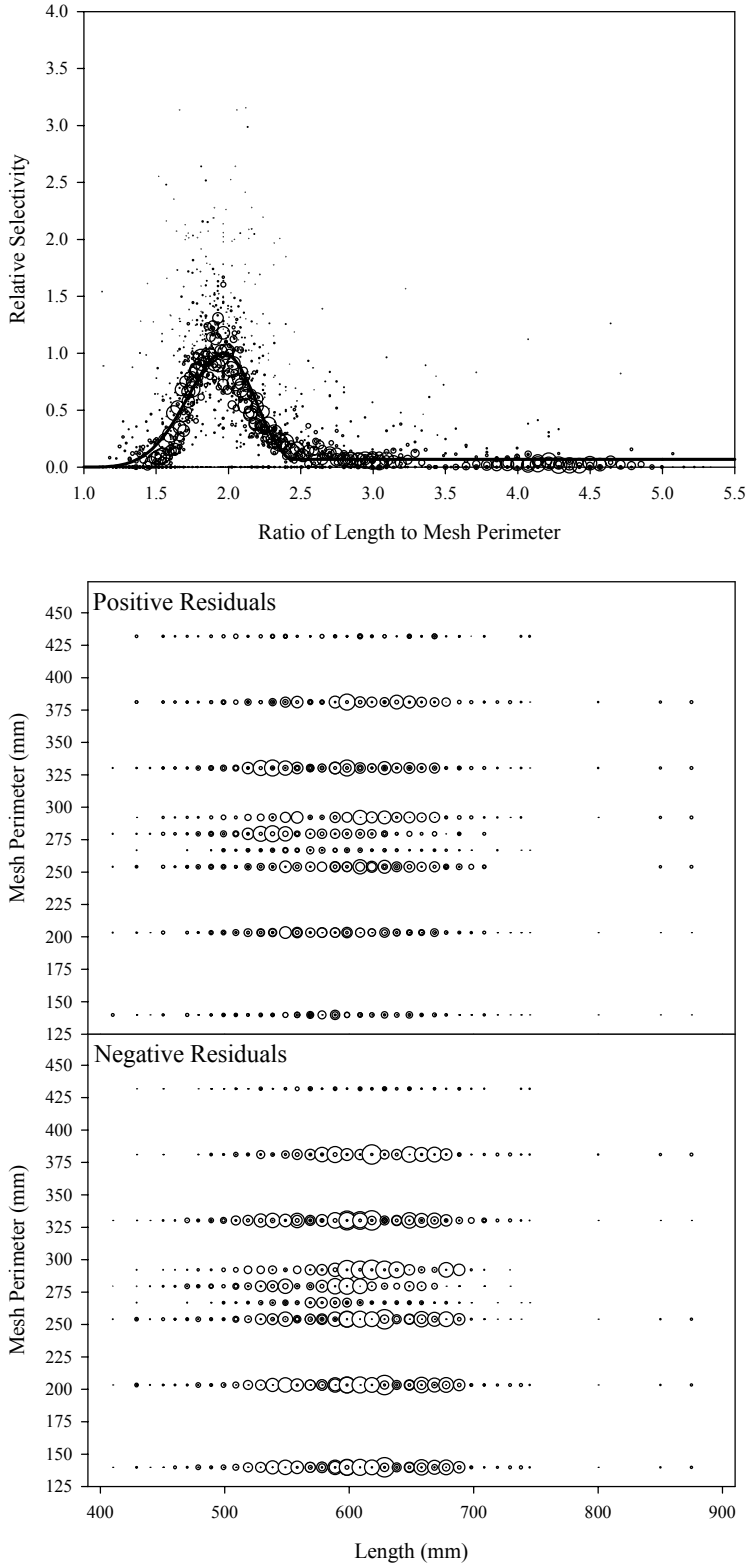

Figure B4.16. Plots of CPUE data scaled to a net selectivity model (top) and CPUE residuals (bottom); fall chum salmon data and Model 16.

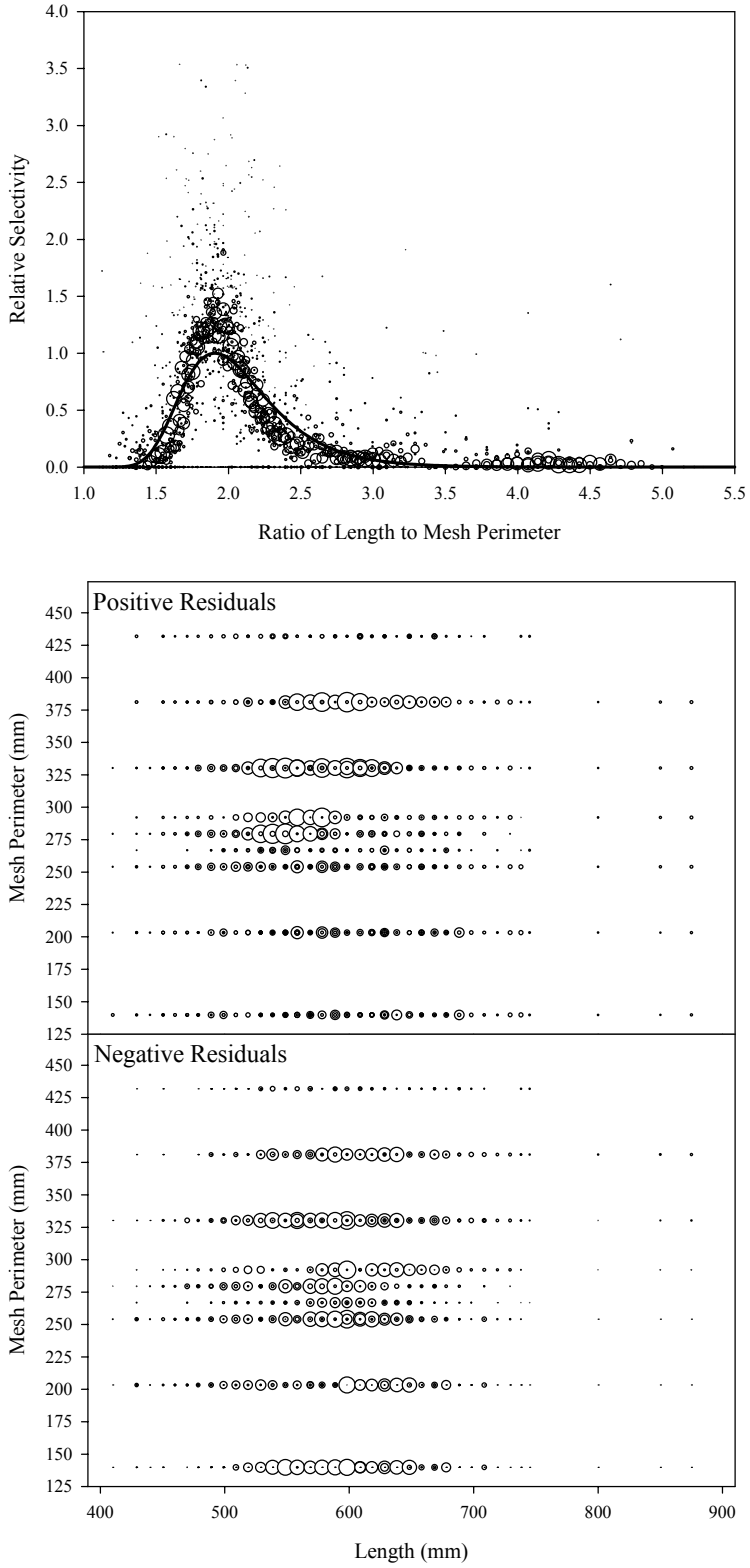

Figure B4.17. Plots of CPUE data scaled to a net selectivity model (top) and CPUE residuals (bottom); fall chum salmon data and Model 17.

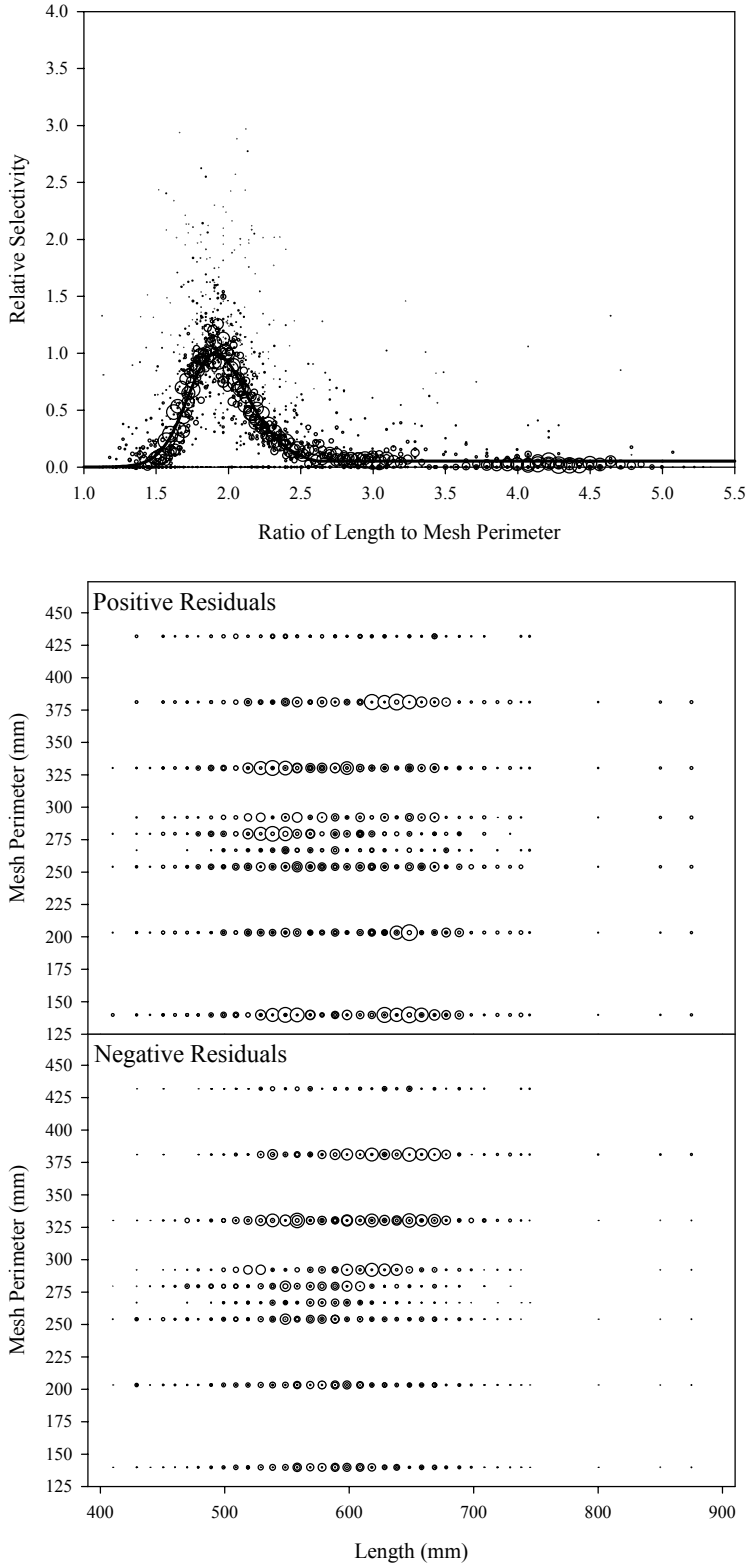

Figure B4.18. Plots of CPUE data scaled to a net selectivity model (top) and CPUE residuals (bottom); fall chum salmon data and Model 18.

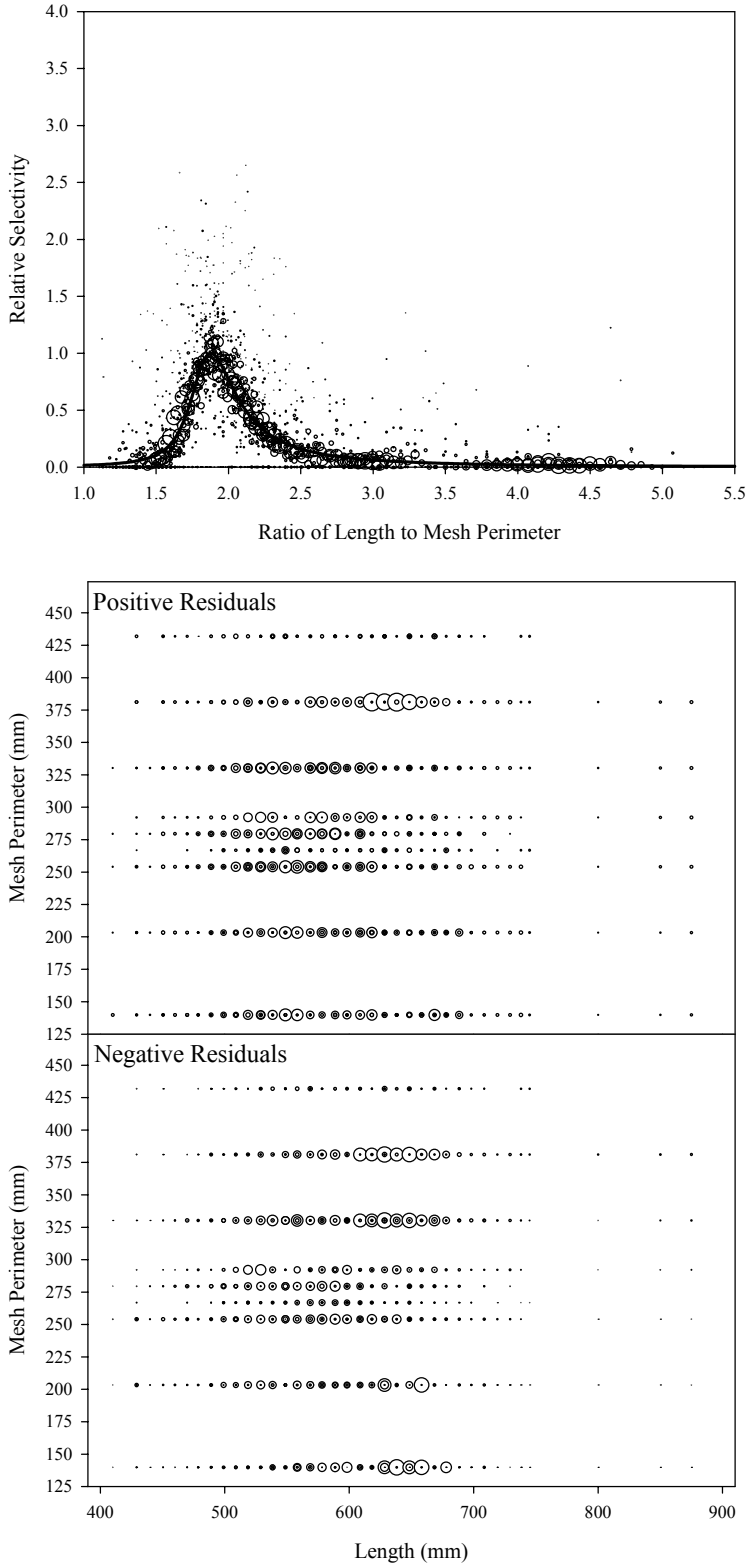

Figure B4.19. Plots of CPUE data scaled to a net selectivity model (top) and CPUE residuals (bottom); fall chum salmon data and Model 19.

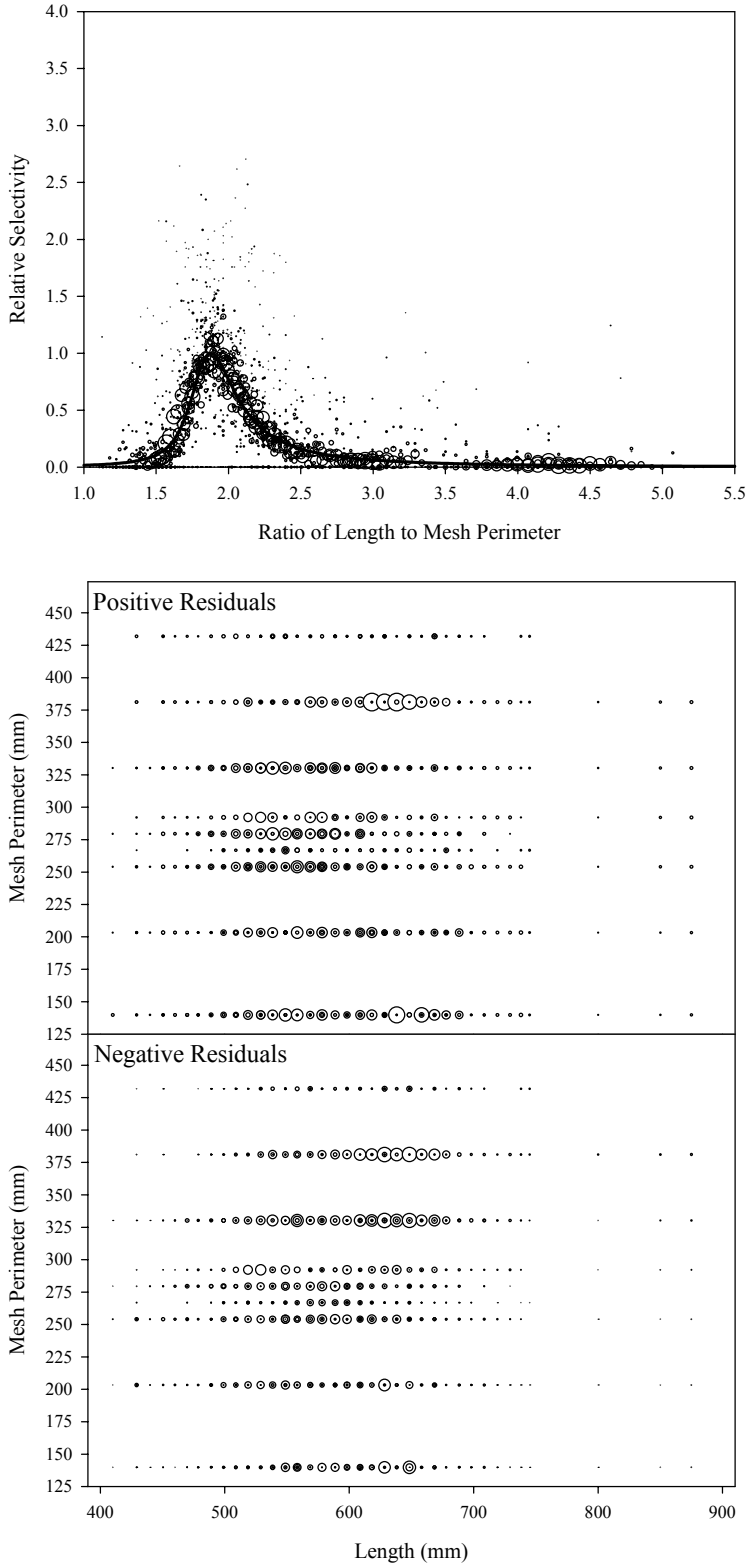

Figure B4.20. Plots of CPUE data scaled to a net selectivity model (top) and CPUE residuals (bottom); fall chum salmon data and Model 20.

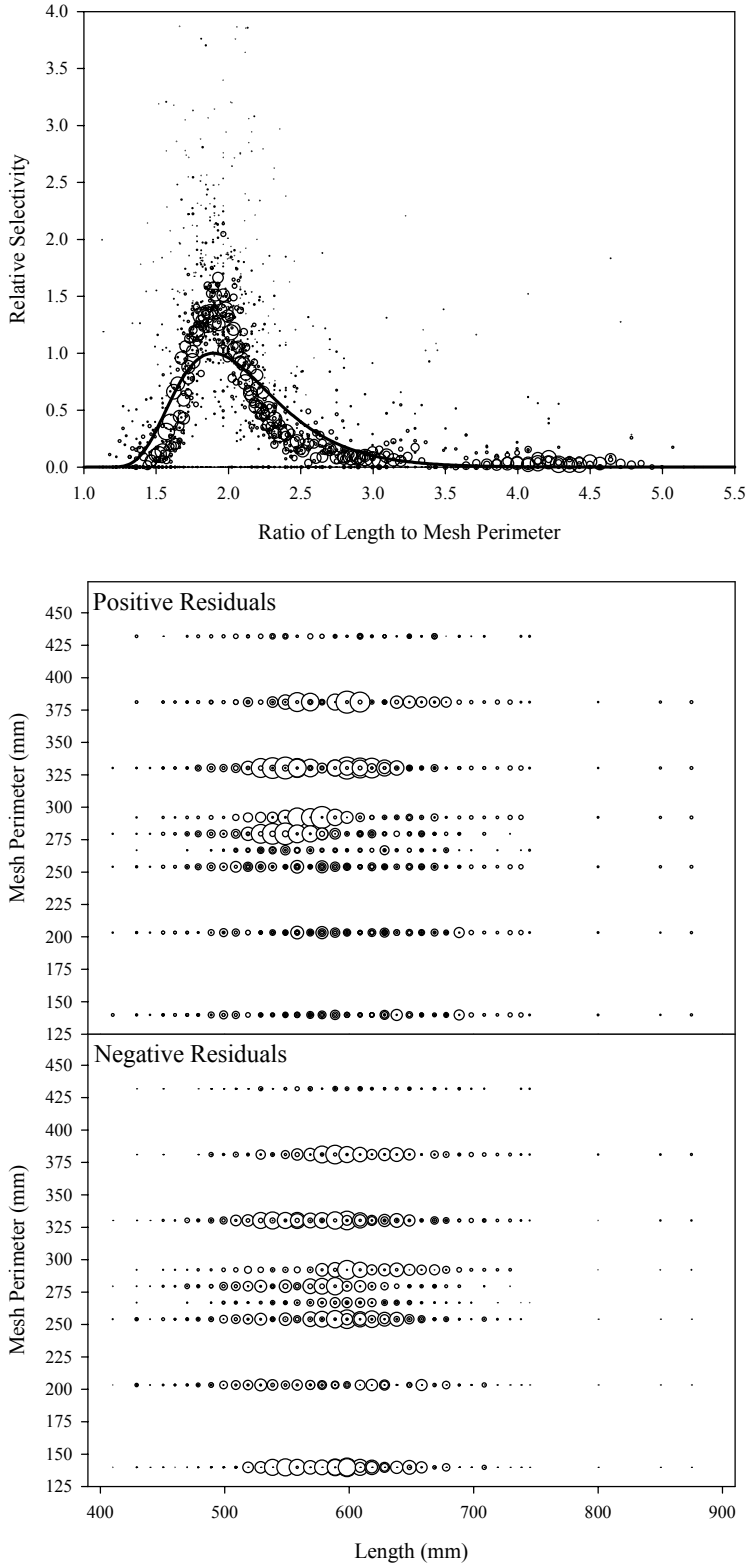

Figure B4.21. Plots of CPUE data scaled to a net selectivity model (top) and CPUE residuals (bottom); fall chum salmon data and Model 21.

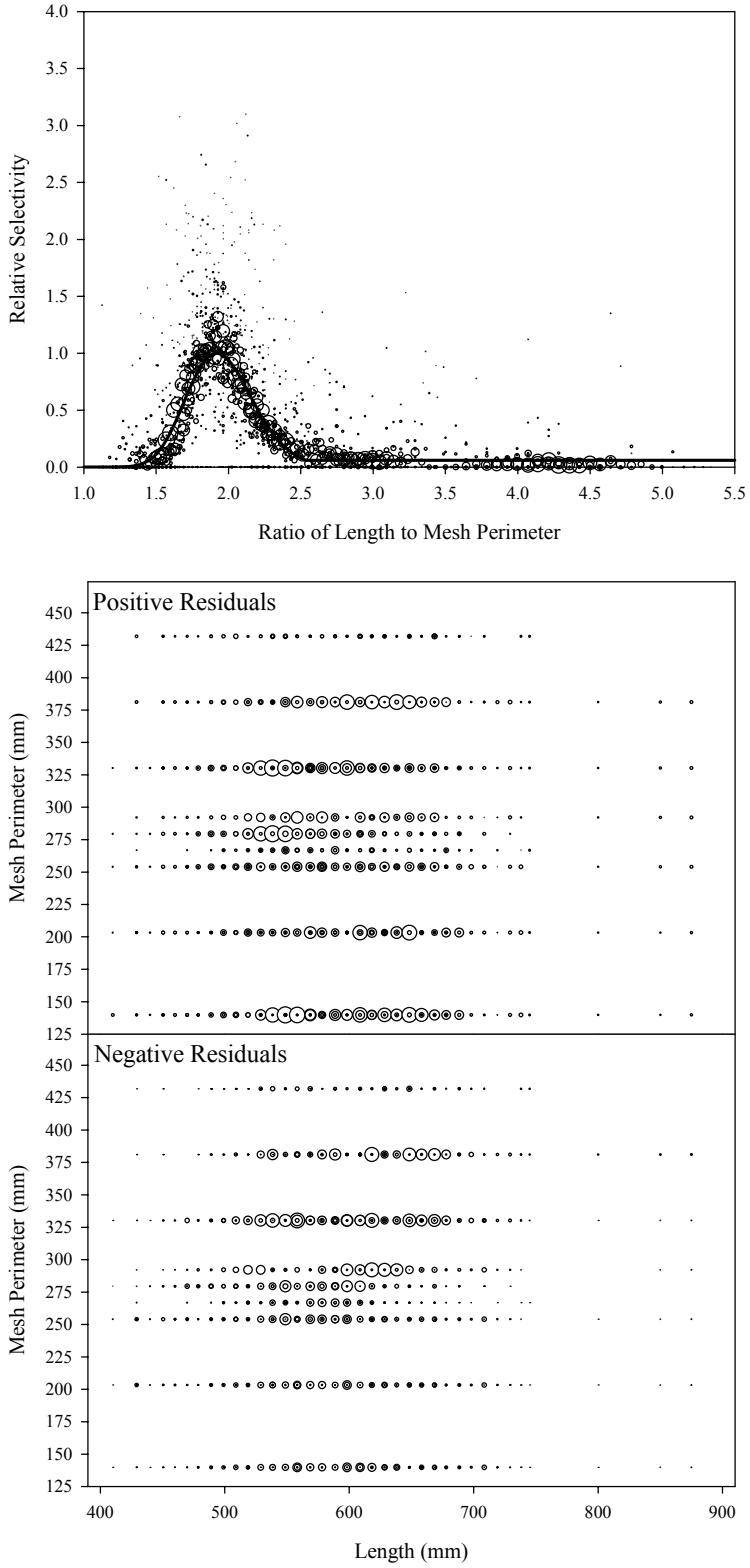

Figure B4.22. Plots of CPUE data scaled to a net selectivity model (top) and CPUE residuals (bottom); fall chum salmon data and Model 22.

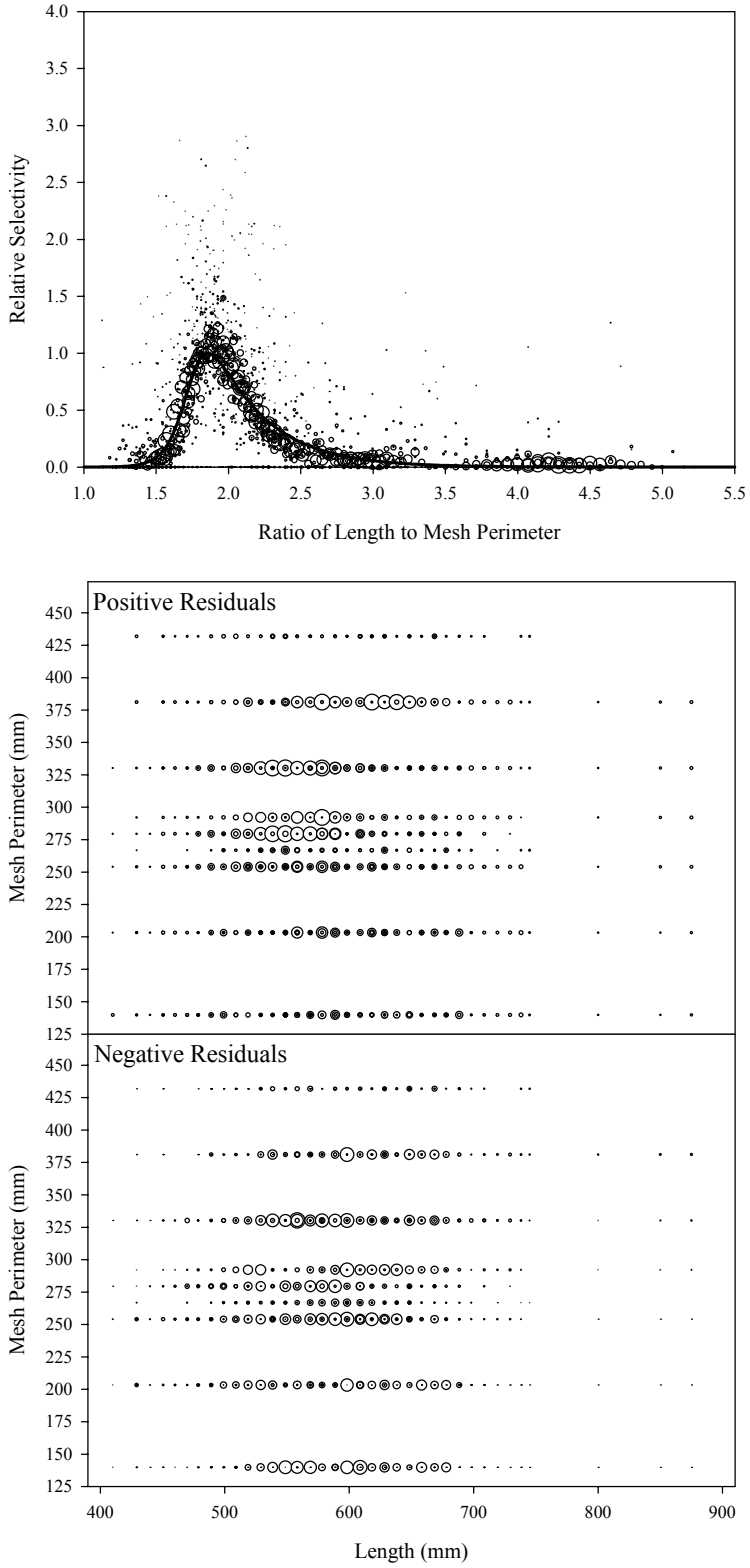

Figure B4.23. Plots of CPUE data scaled to a net selectivity model (top) and CPUE residuals (bottom); fall chum salmon data and Model 23.

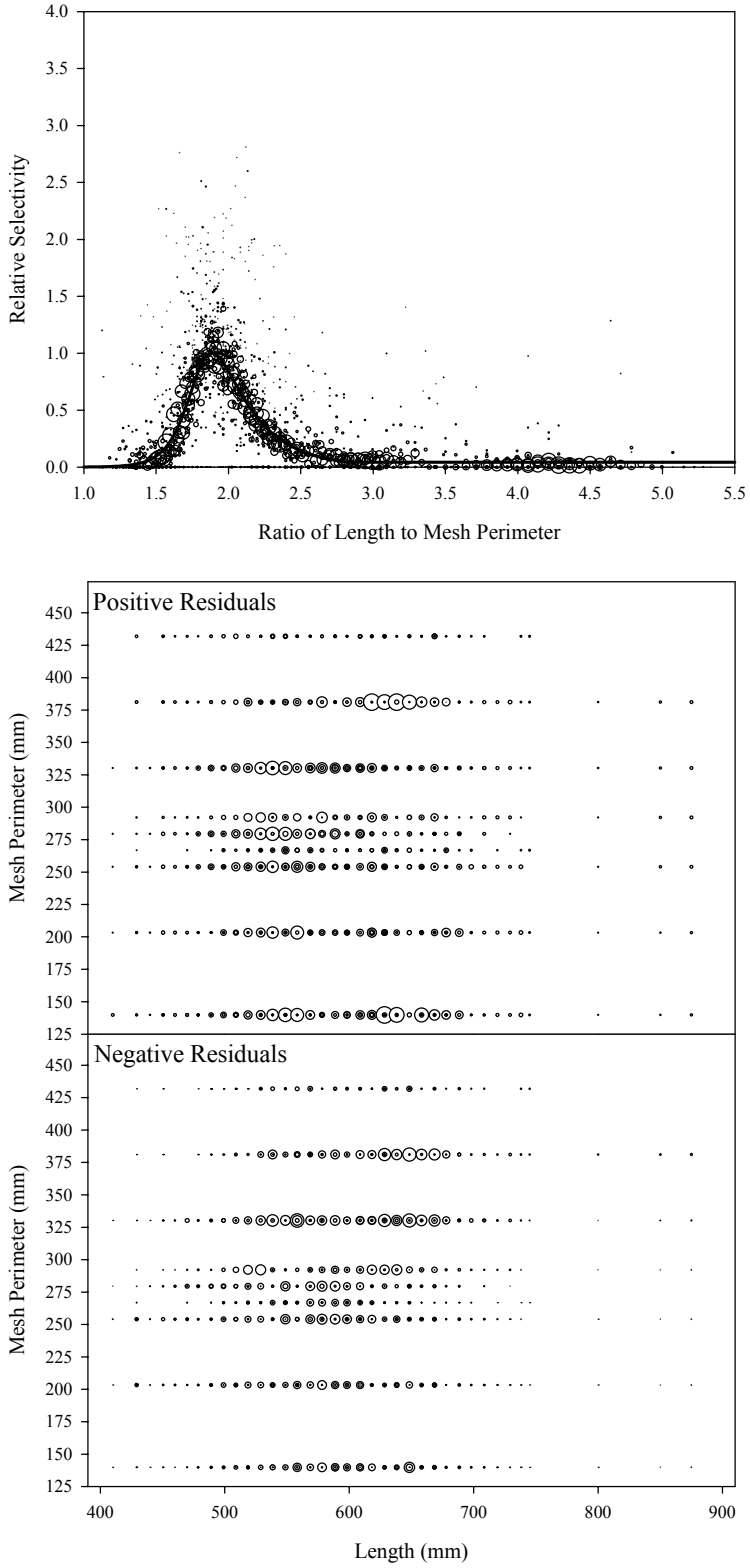

Figure B4.24. Plots of CPUE data scaled to a net selectivity model (top) and CPUE residuals (bottom); fall chum salmon data and Model 24.

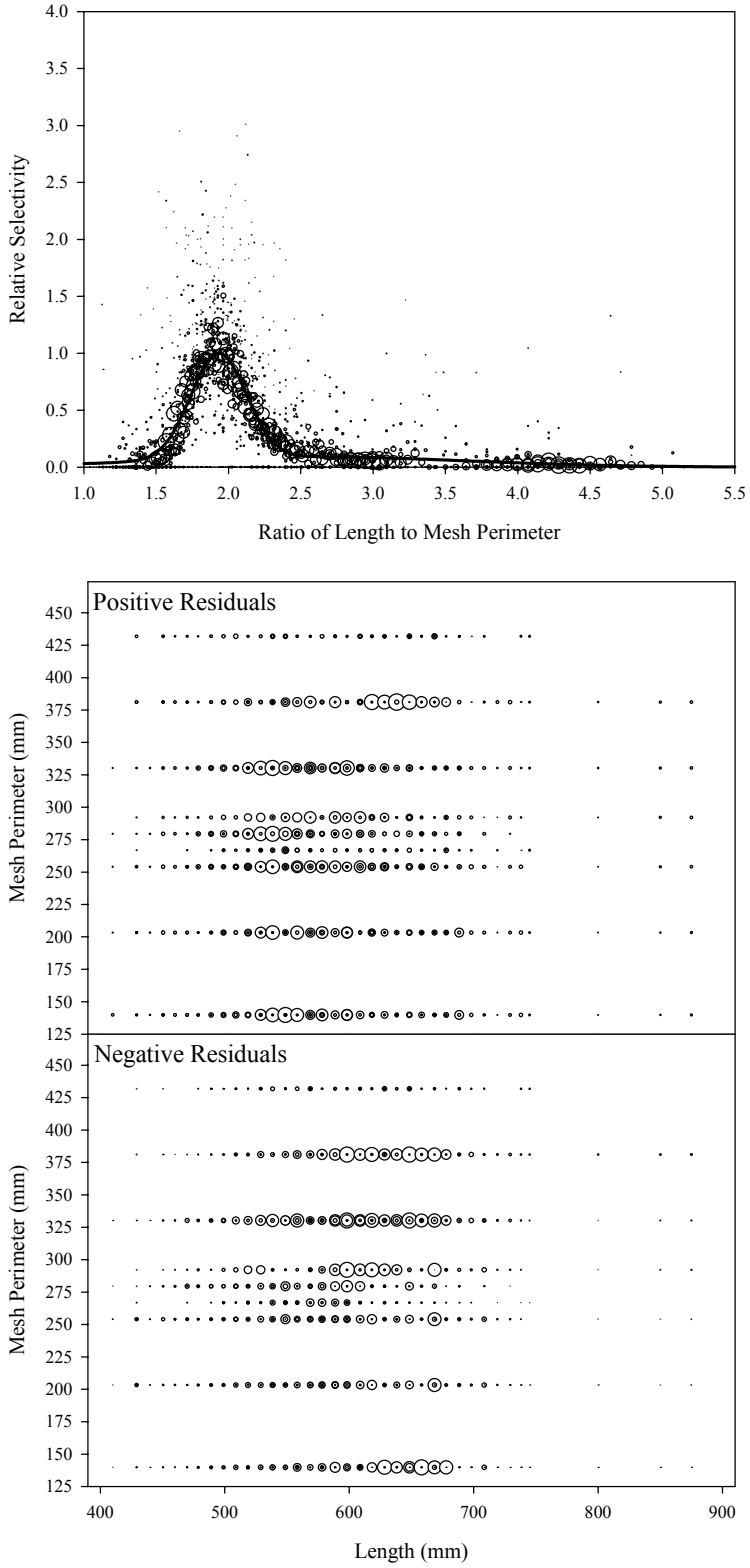

Figure B4.25. Plots of CPUE data scaled to a net selectivity model (top) and CPUE residuals (bottom); fall chum salmon data and Model 25.

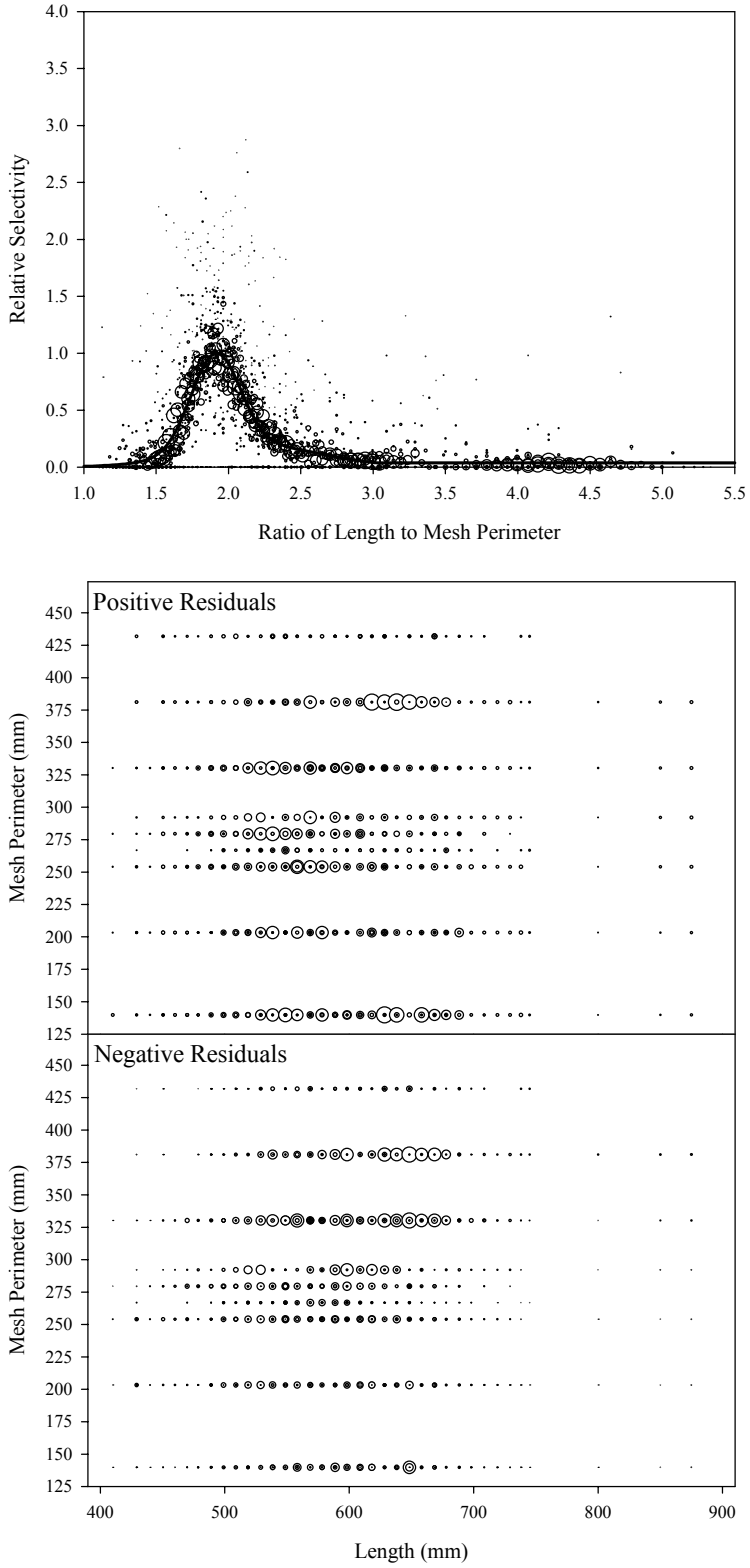

Figure B4.26. Plots of CPUE data scaled to a net selectivity model (top) and CPUE residuals (bottom); fall chum salmon data and Model 26.

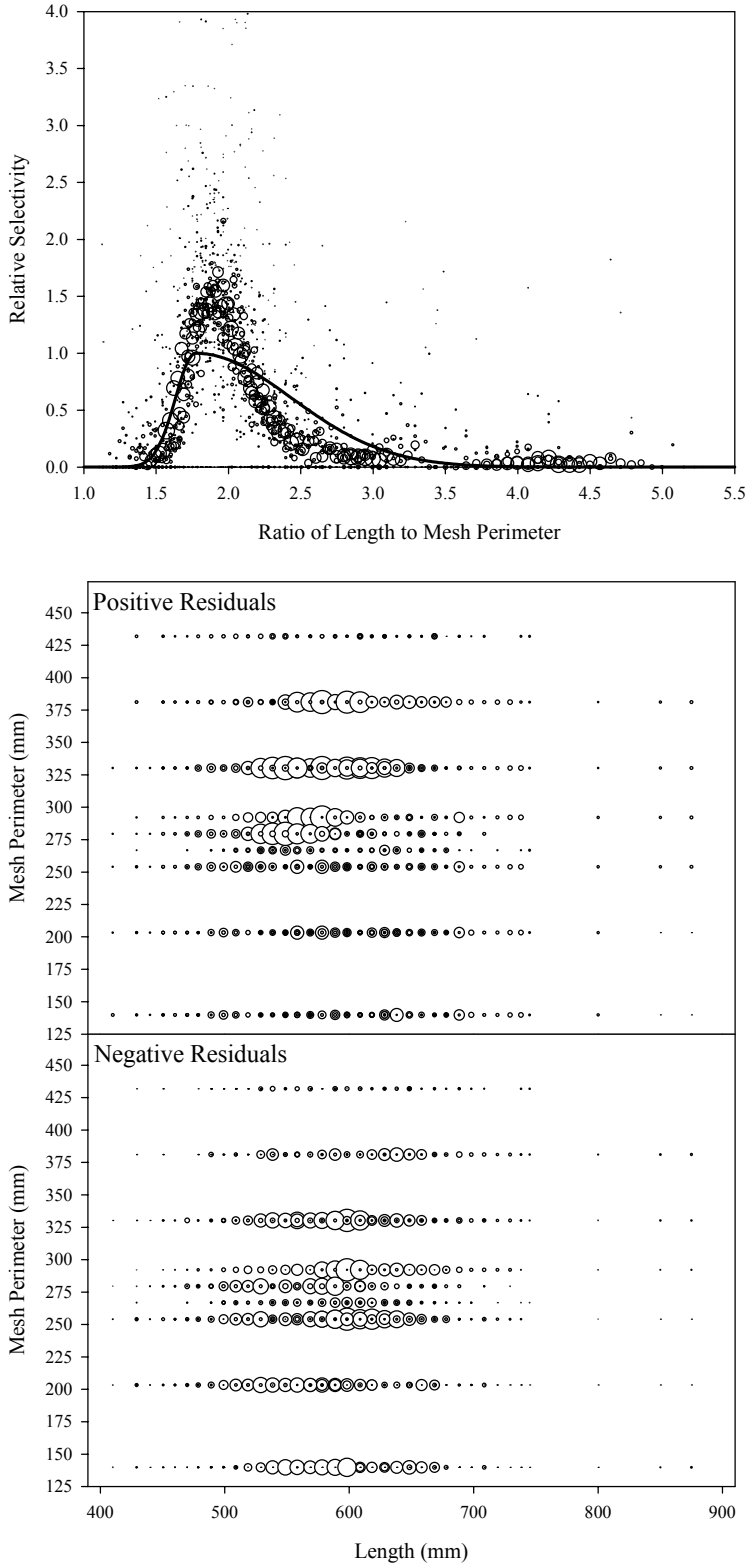

Figure B4.27. Plots of CPUE data scaled to a net selectivity model (top) and CPUE residuals (bottom); fall chum salmon data and Model 27.

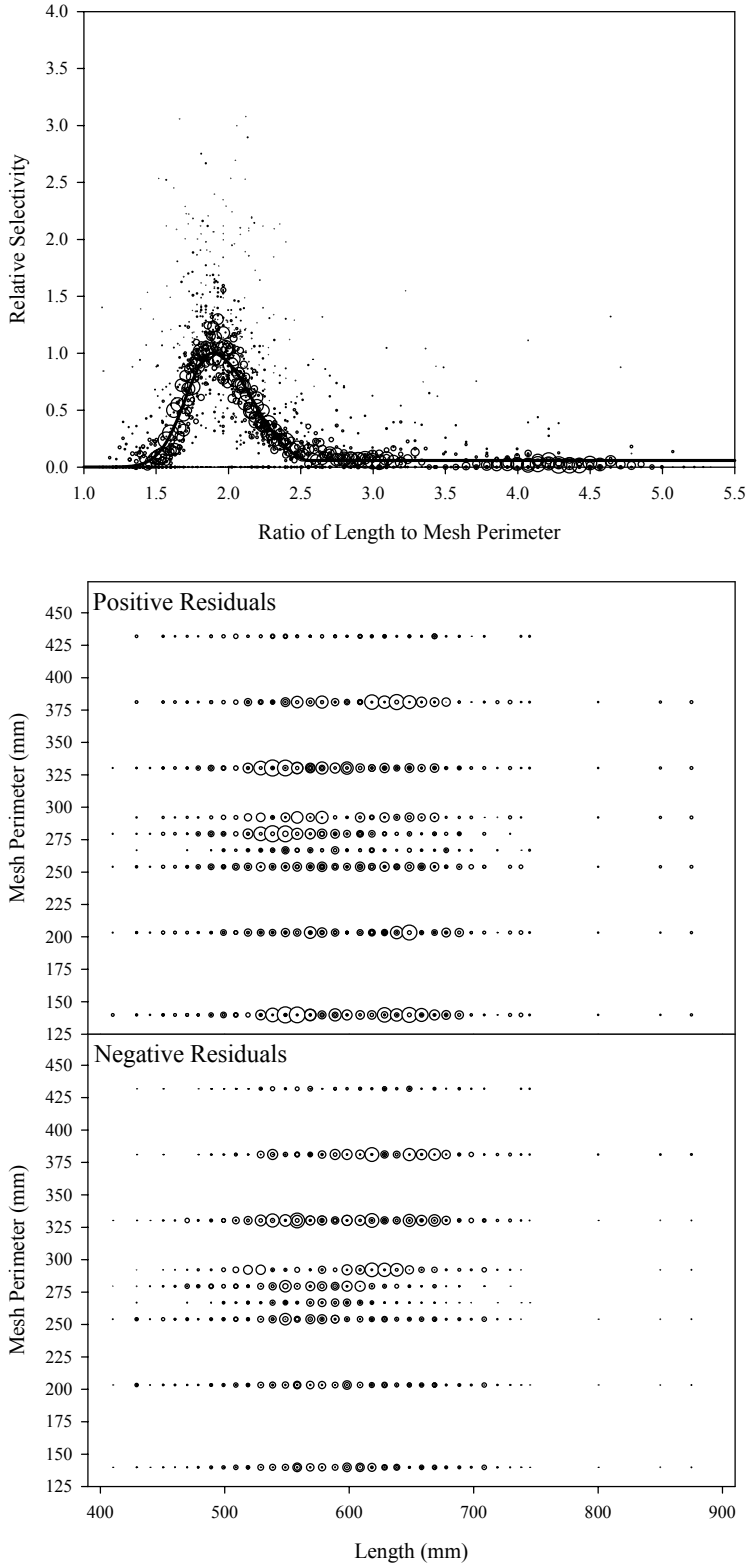

Figure B4.28. Plots of CPUE data scaled to a net selectivity model (top) and CPUE residuals (bottom); fall chum salmon data and Model 28.

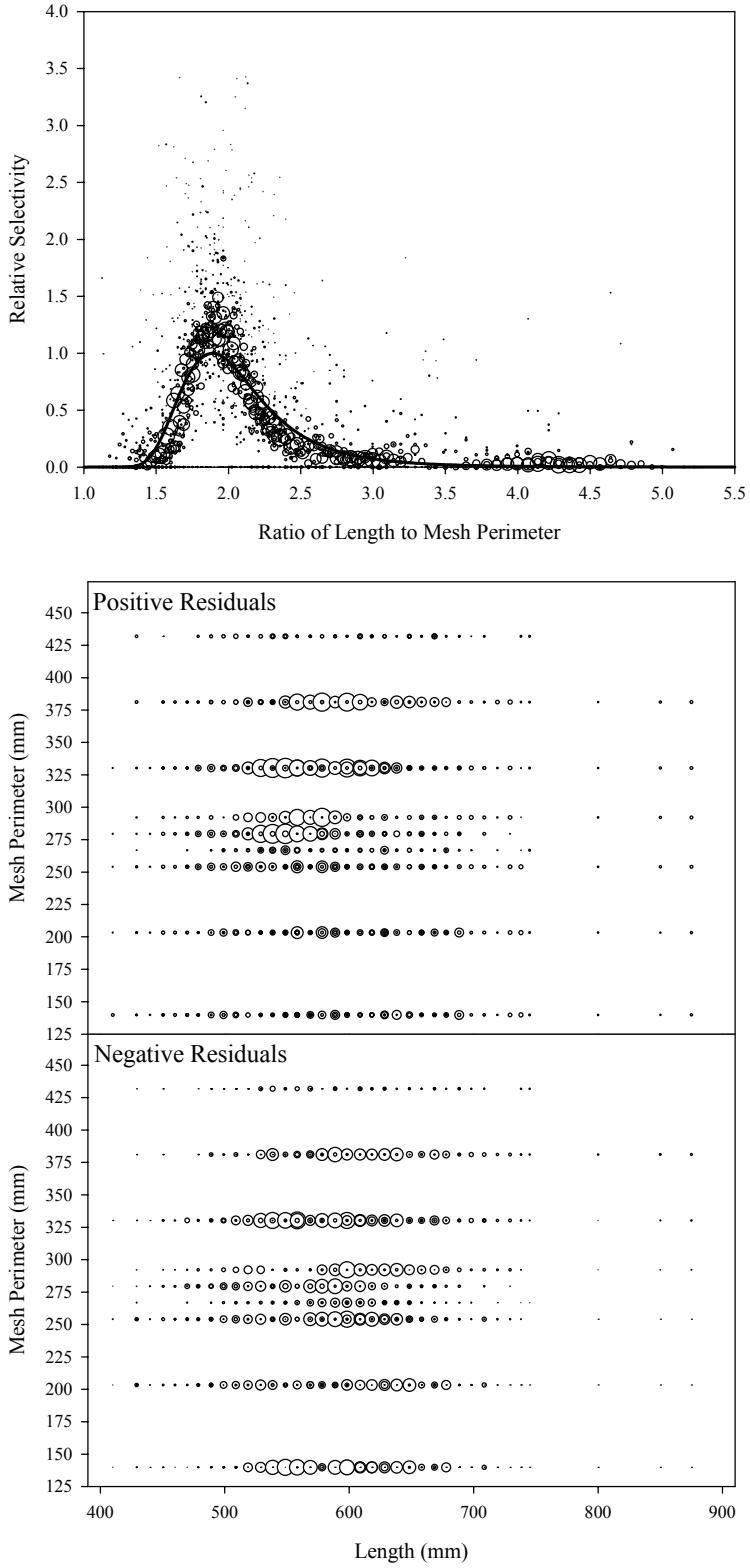

Figure B4.29. Plots of CPUE data scaled to a net selectivity model (top) and CPUE residuals (bottom); fall chum salmon data and Model 29.

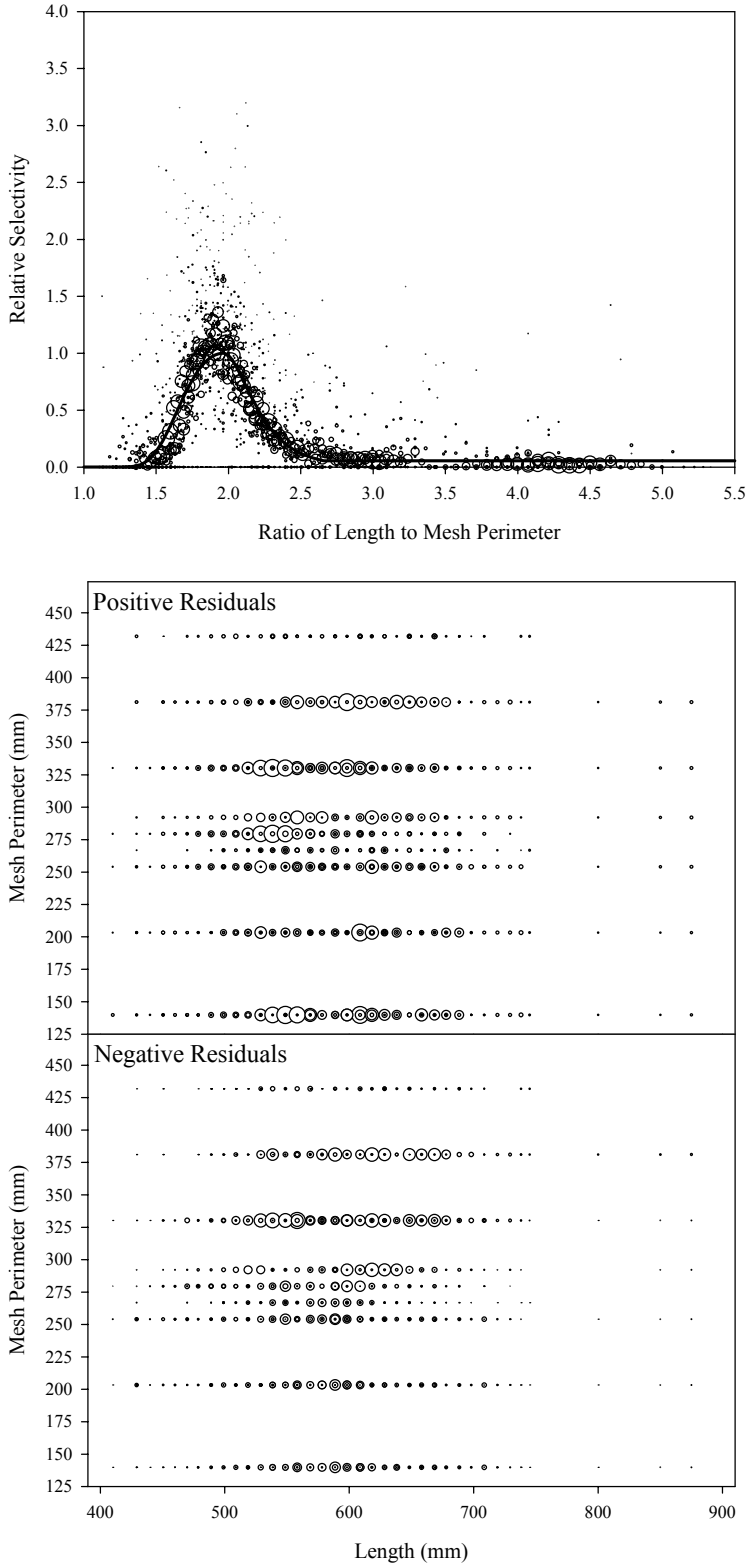

Figure B4.30. Plots of CPUE data scaled to a net selectivity model (top) and CPUE residuals (bottom); fall chum salmon data and Model 30.

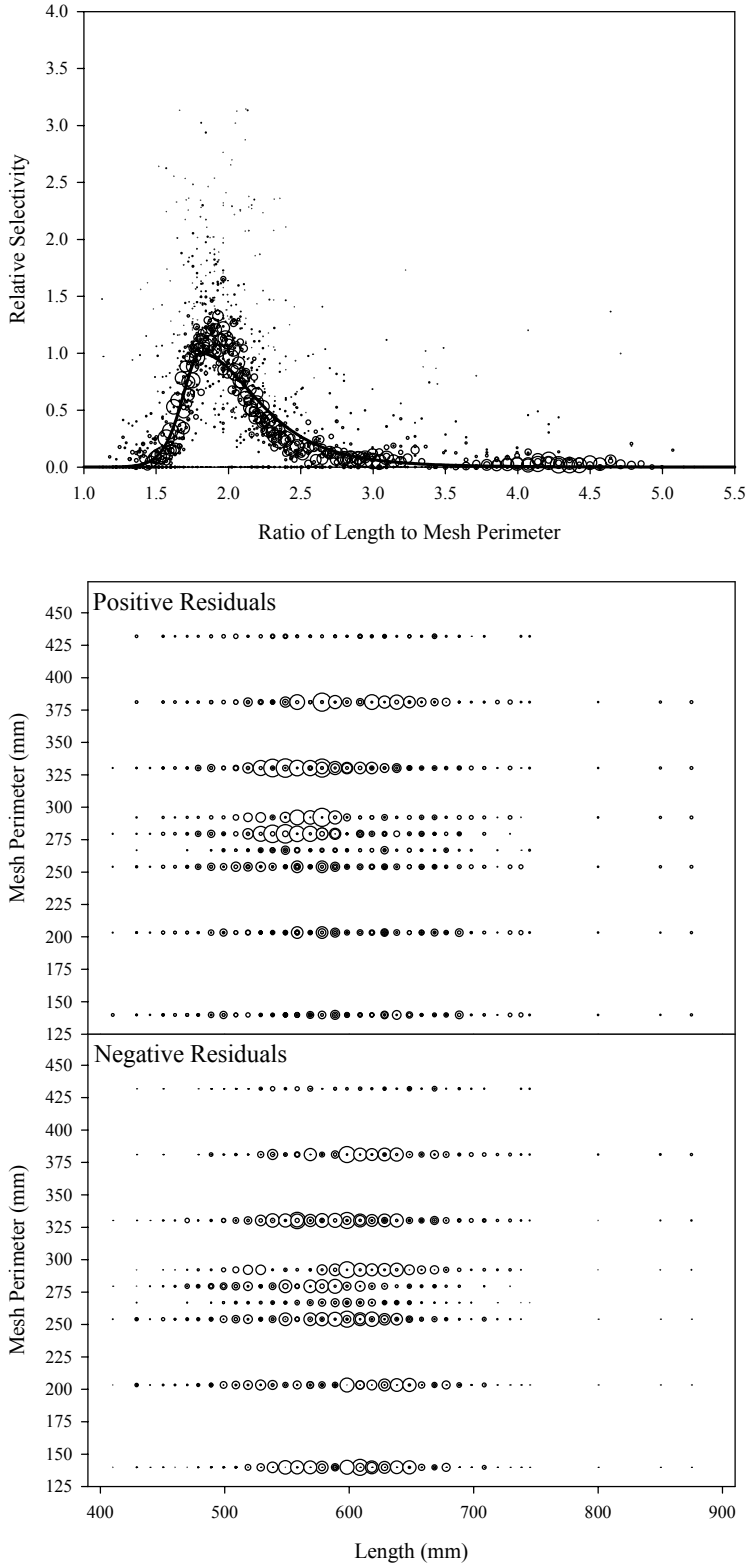

Figure B4.31. Plots of CPUE data scaled to a net selectivity model (top) and CPUE residuals (bottom); fall chum salmon data and Model 31.

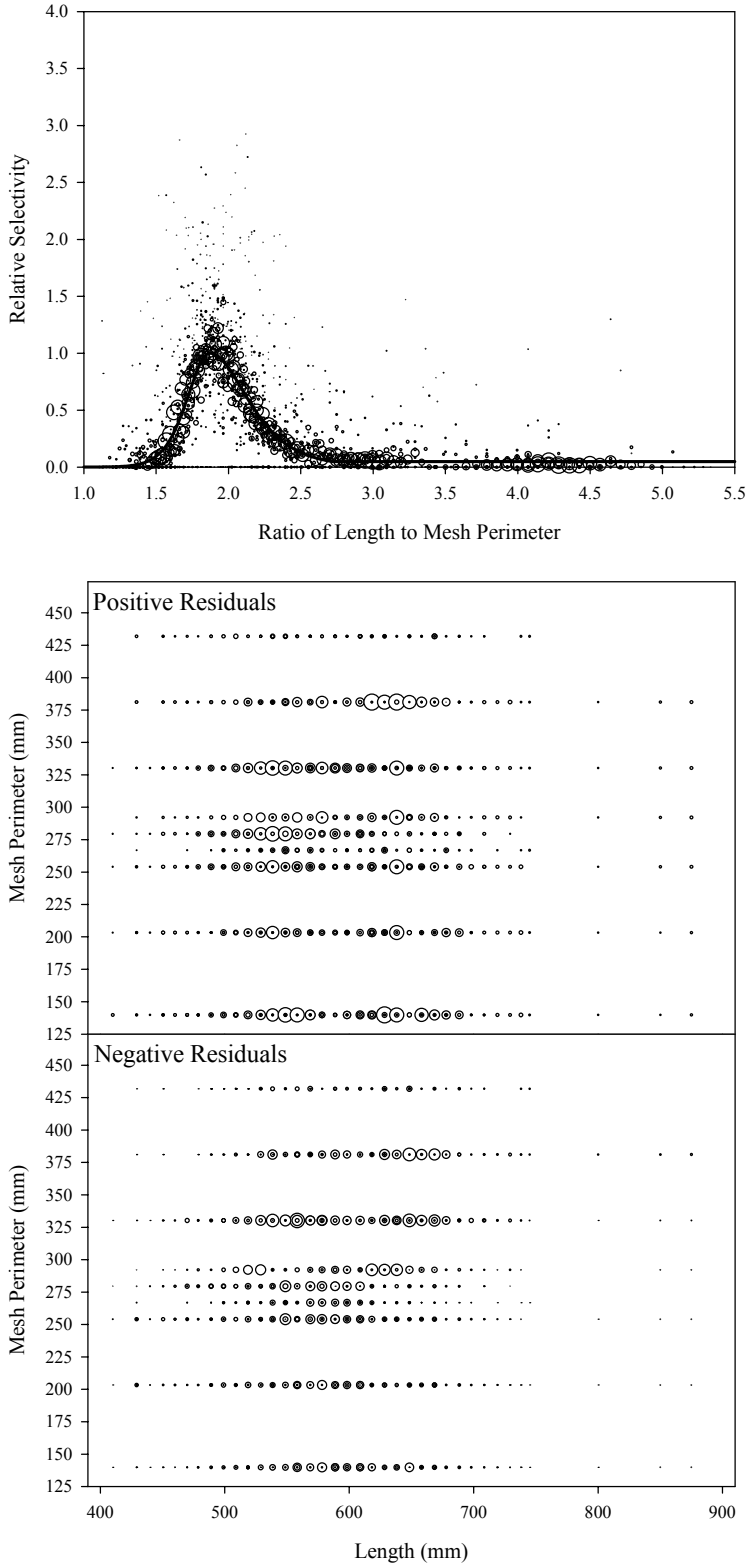

Figure B4.32. Plots of CPUE data scaled to a net selectivity model (top) and CPUE residuals (bottom); fall chum salmon data and Model 32.

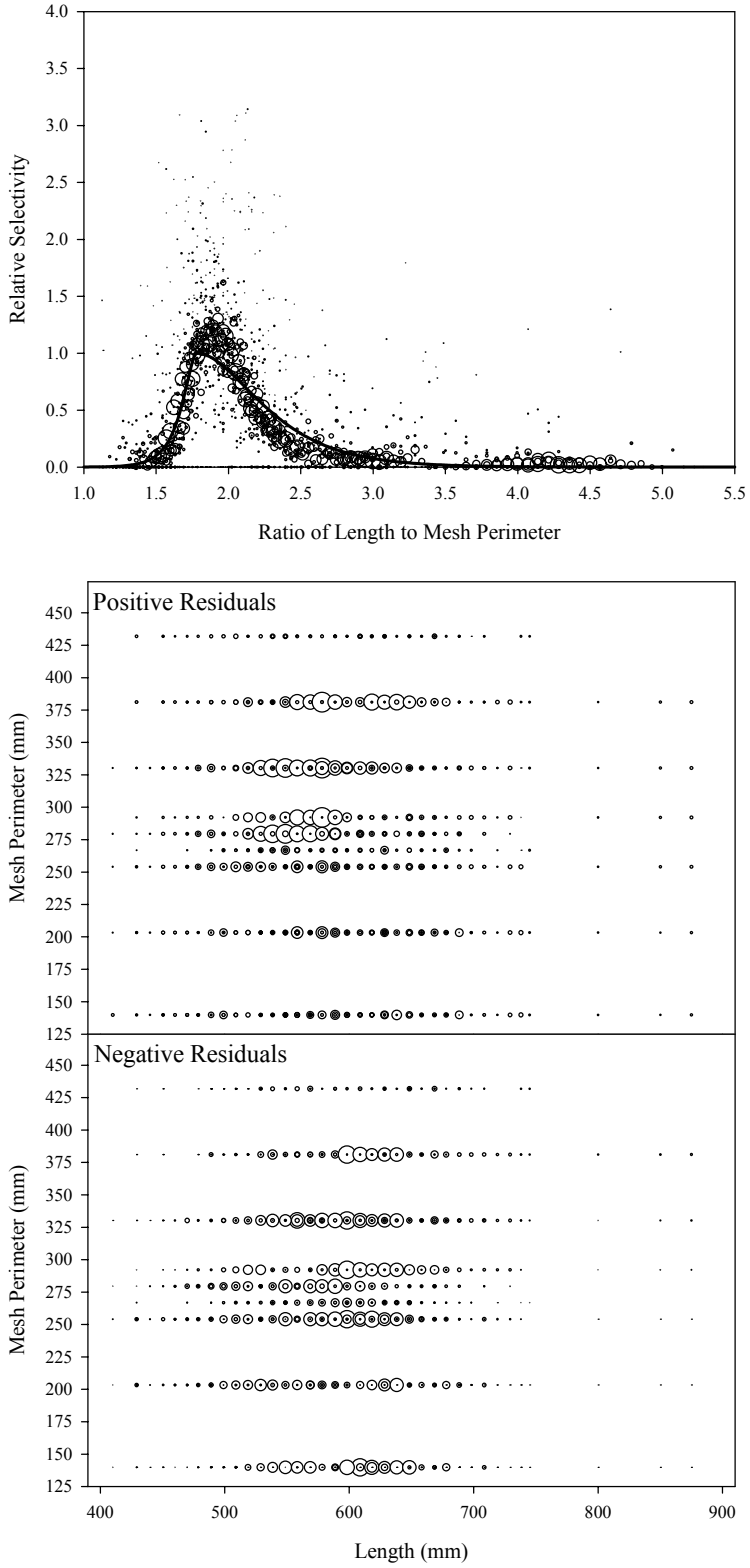

Figure B4.33. Plots of CPUE data scaled to a net selectivity model (top) and CPUE residuals (bottom); fall chum salmon data and Model 33.

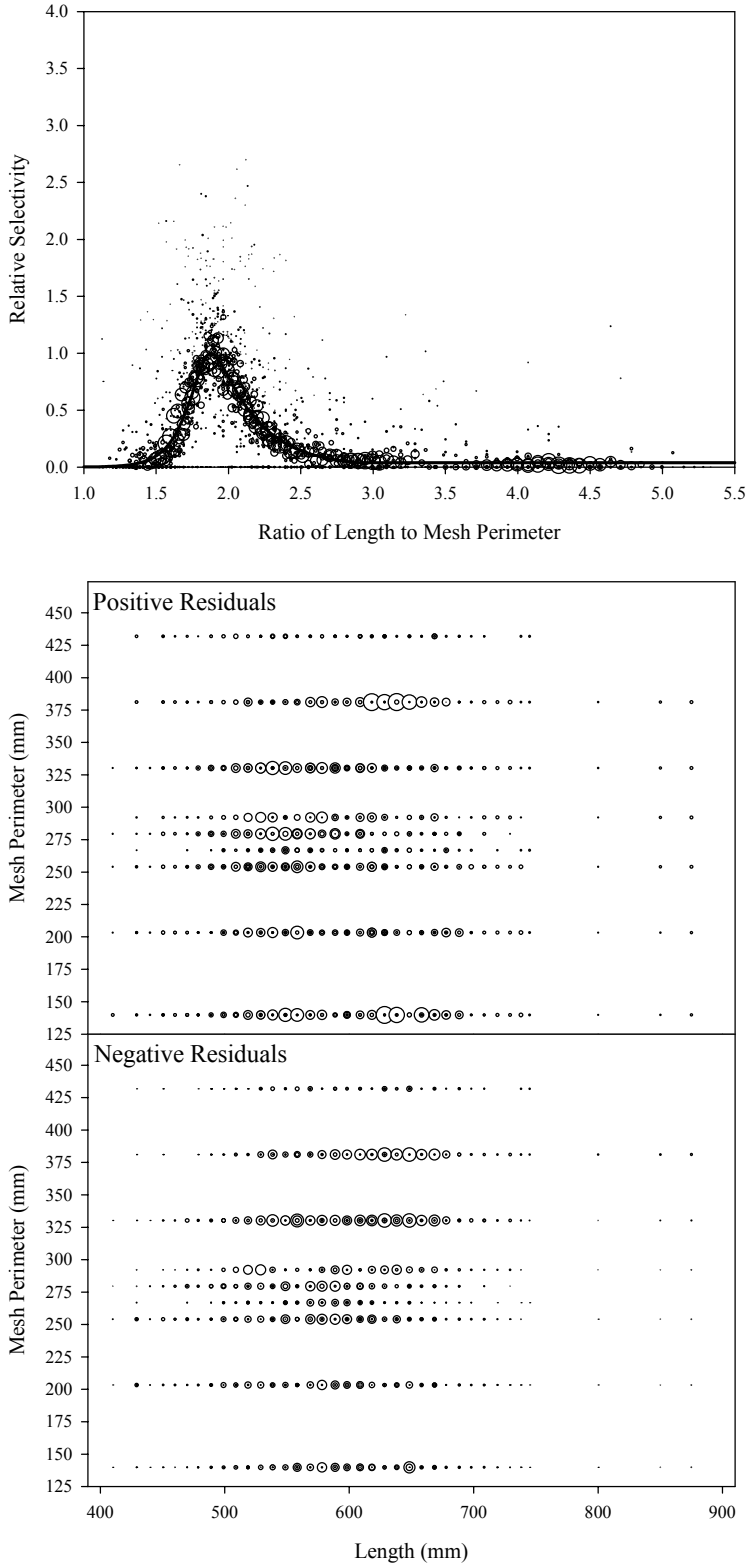

Figure B4.34. Plots of CPUE data scaled to a net selectivity model (top) and CPUE residuals (bottom); fall chum salmon data and Model 34.

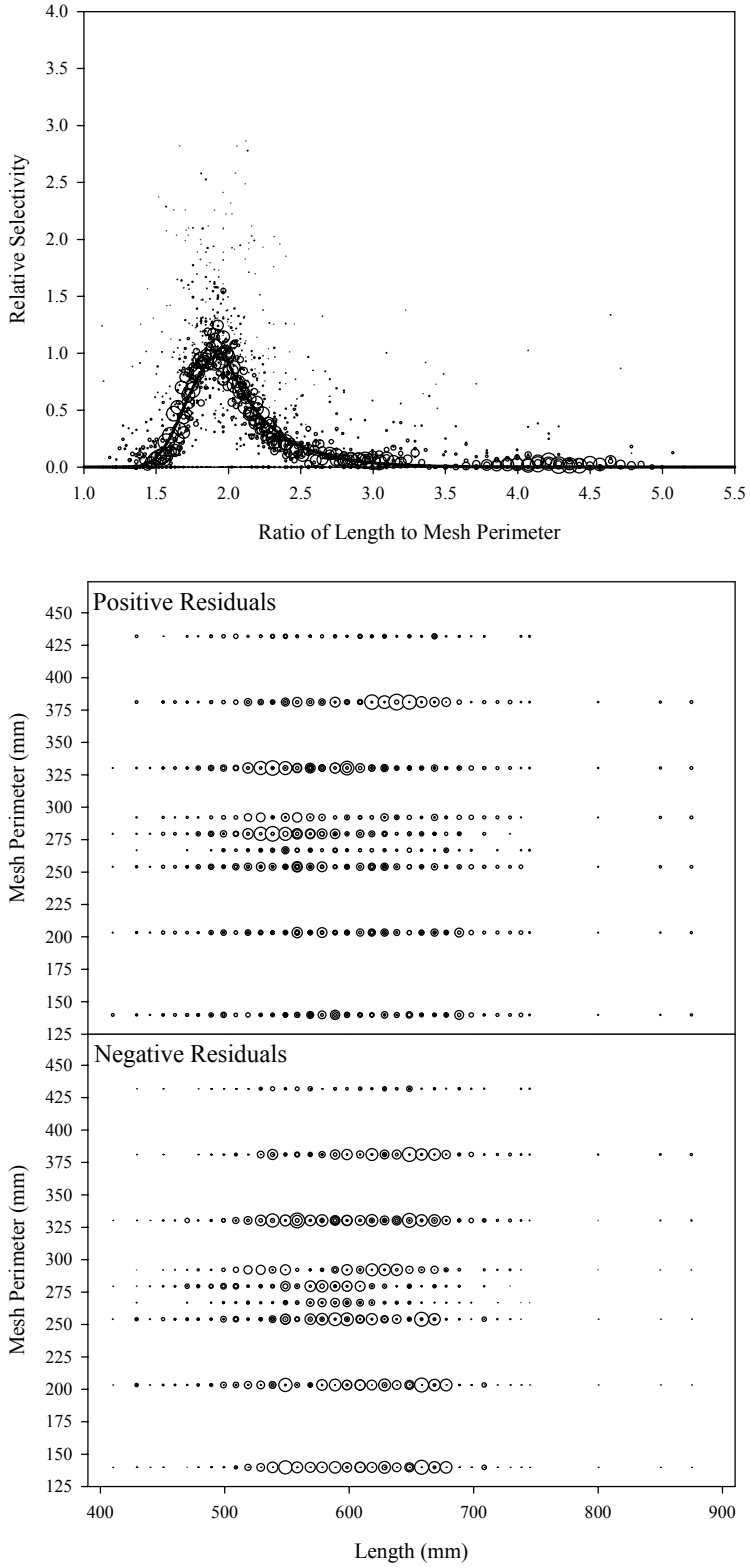

Figure B4.35. Plots of CPUE data scaled to a net selectivity model (top) and CPUE residuals (bottom); fall chum salmon data and Model 35.

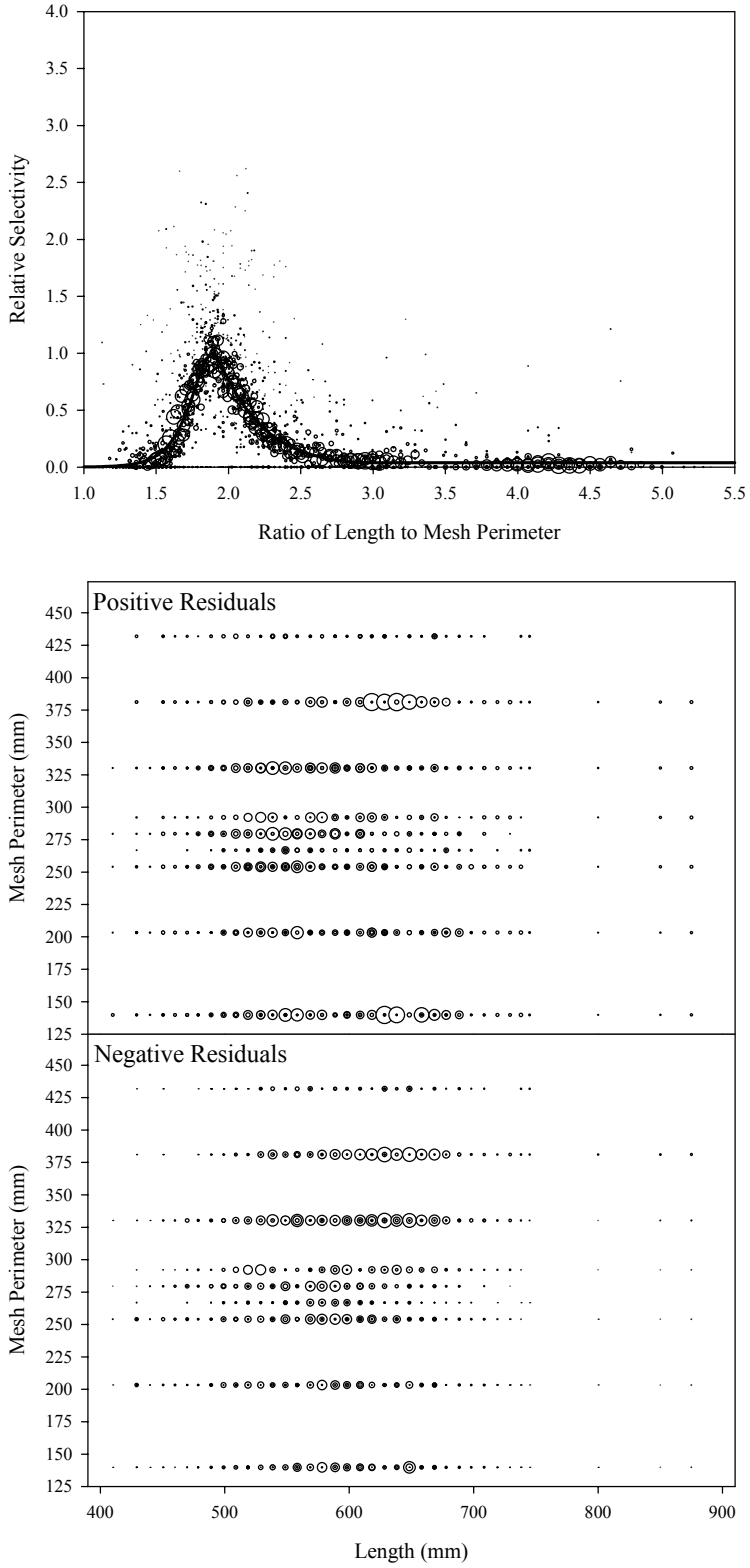

Figure B4.36. Plots of CPUE data scaled to a net selectivity model (top) and CPUE residuals (bottom); fall chum salmon data and Model 36.

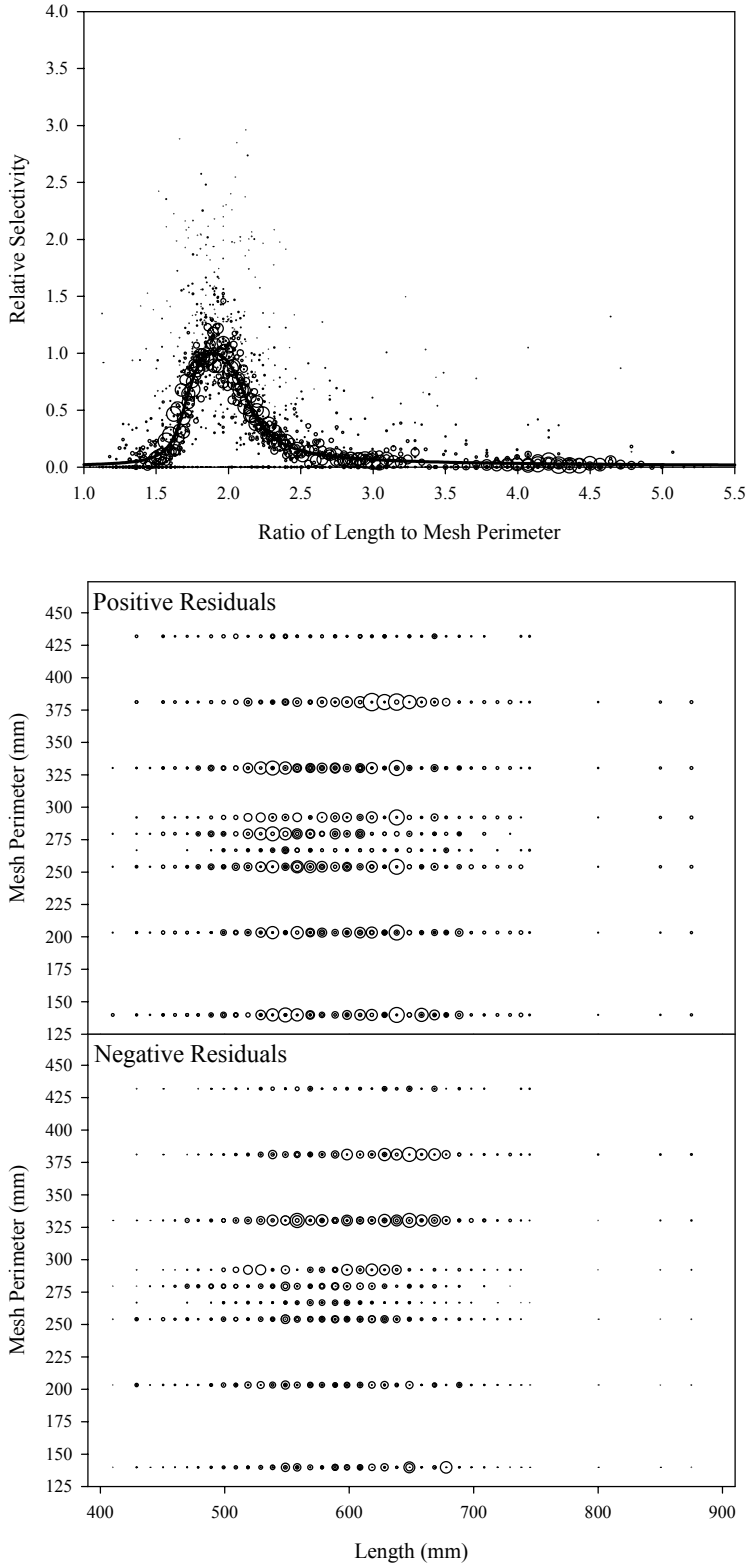

Figure B4.37. Plots of CPUE data scaled to a net selectivity model (top) and CPUE residuals (bottom); fall chum salmon data and Model 37.

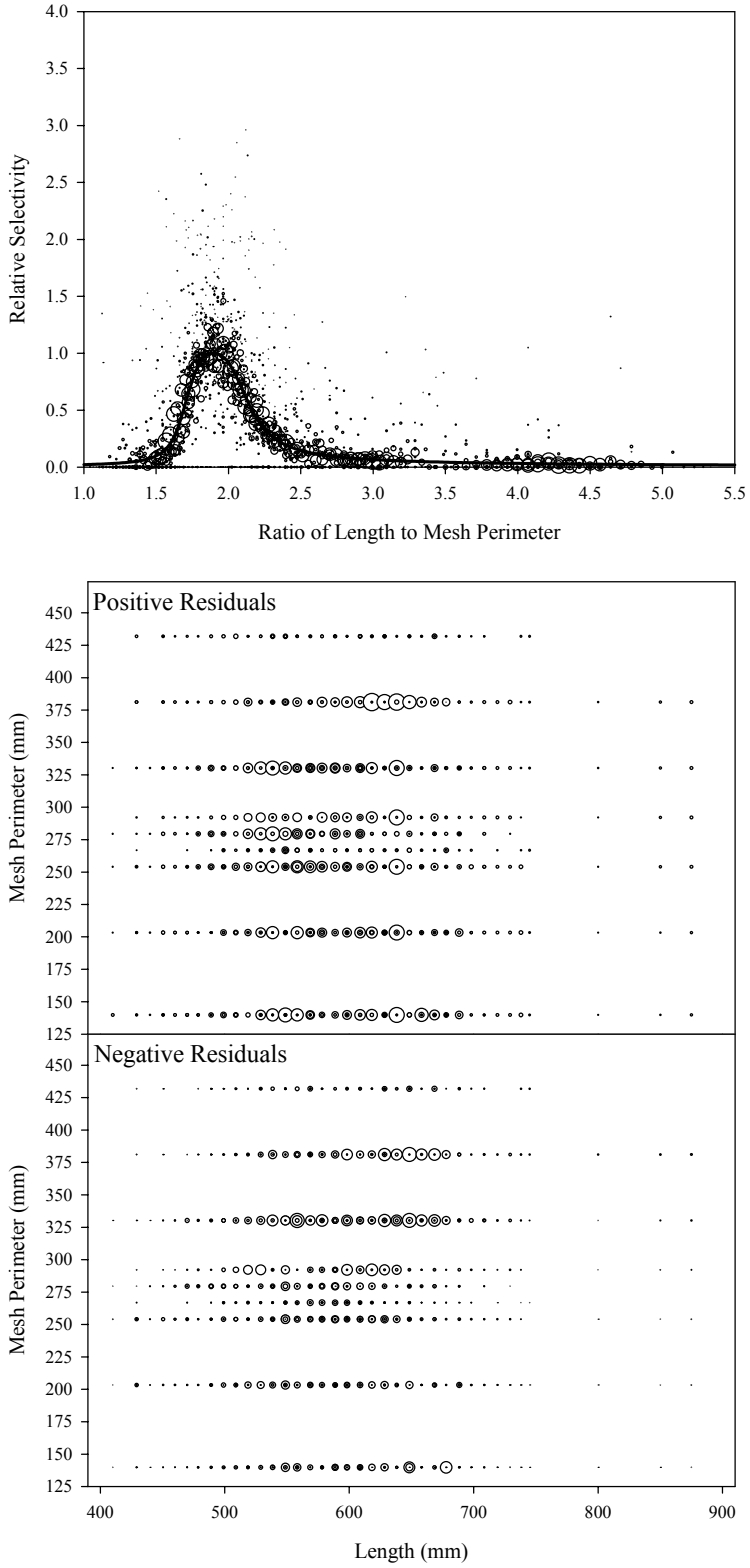

Figure B4.38. Plots of CPUE data scaled to a net selectivity model (top) and CPUE residuals (bottom); fall chum salmon data and Model 38.

Appendix B5
Coho Salmon Diagnostic Plots
Figure B5.1 to Figure B5.38

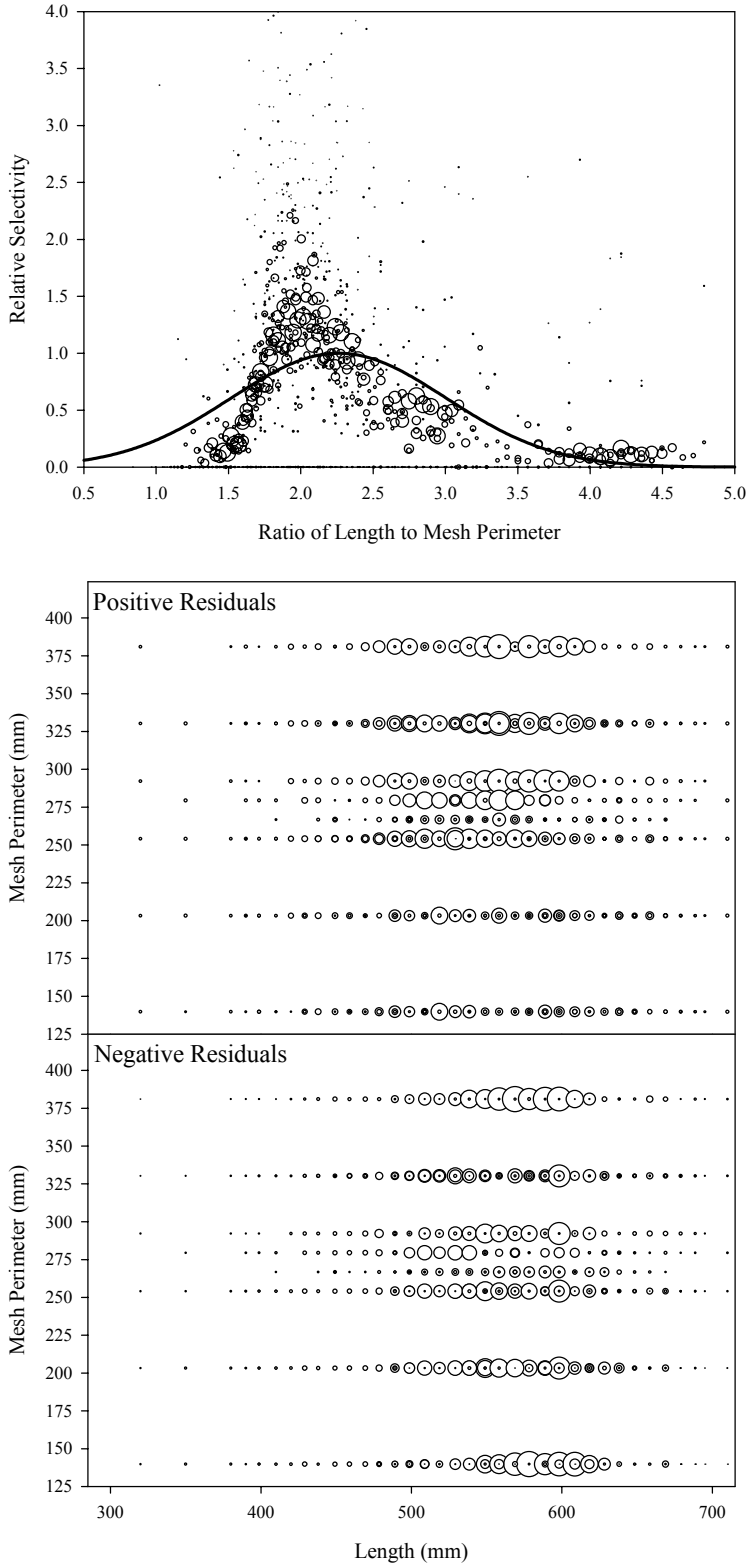

Figure B5.1. Plots of CPUE data scaled to a net selectivity model (top) and CPUE residuals (bottom); coho salmon data and Model 1.

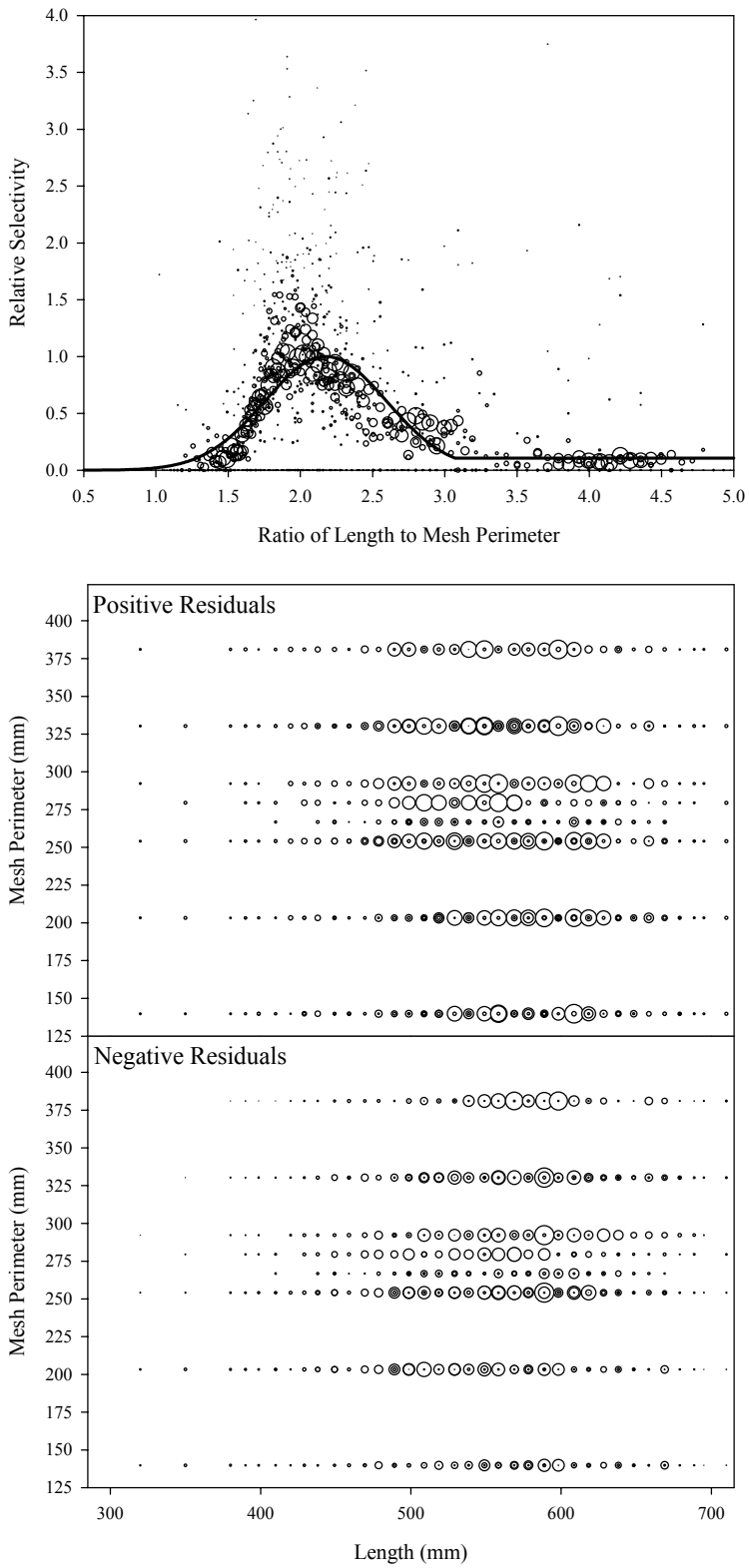

Figure B5.2. Plots of CPUE data scaled to a net selectivity model (top) and CPUE residuals (bottom); coho salmon data and Model 2.

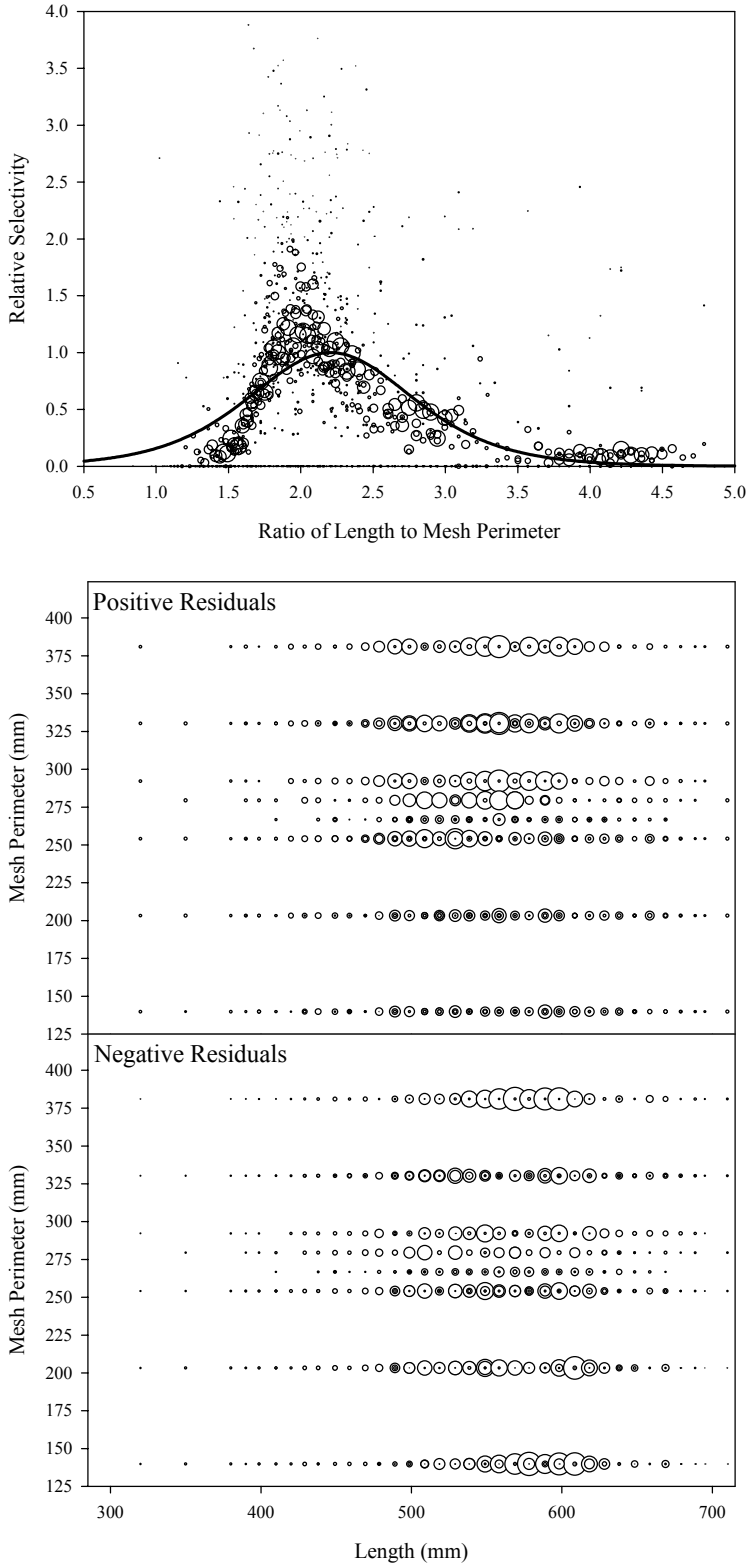

Figure B5.3. Plots of CPUE data scaled to a net selectivity model (top) and CPUE residuals (bottom); coho salmon data and Model 3.

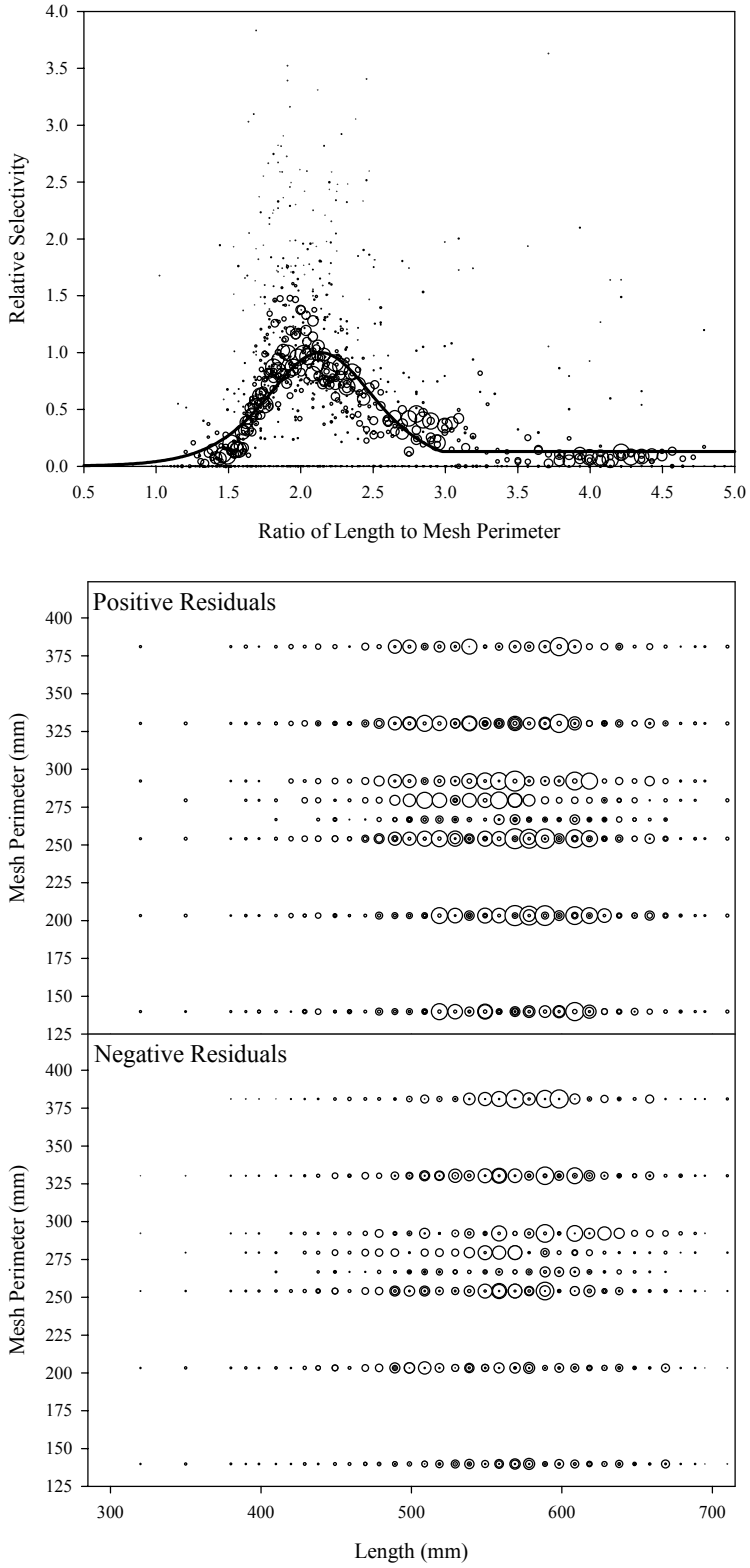

Figure B5.4. Plots of CPUE data scaled to a net selectivity model (top) and CPUE residuals (bottom); coho salmon data and Model 4.

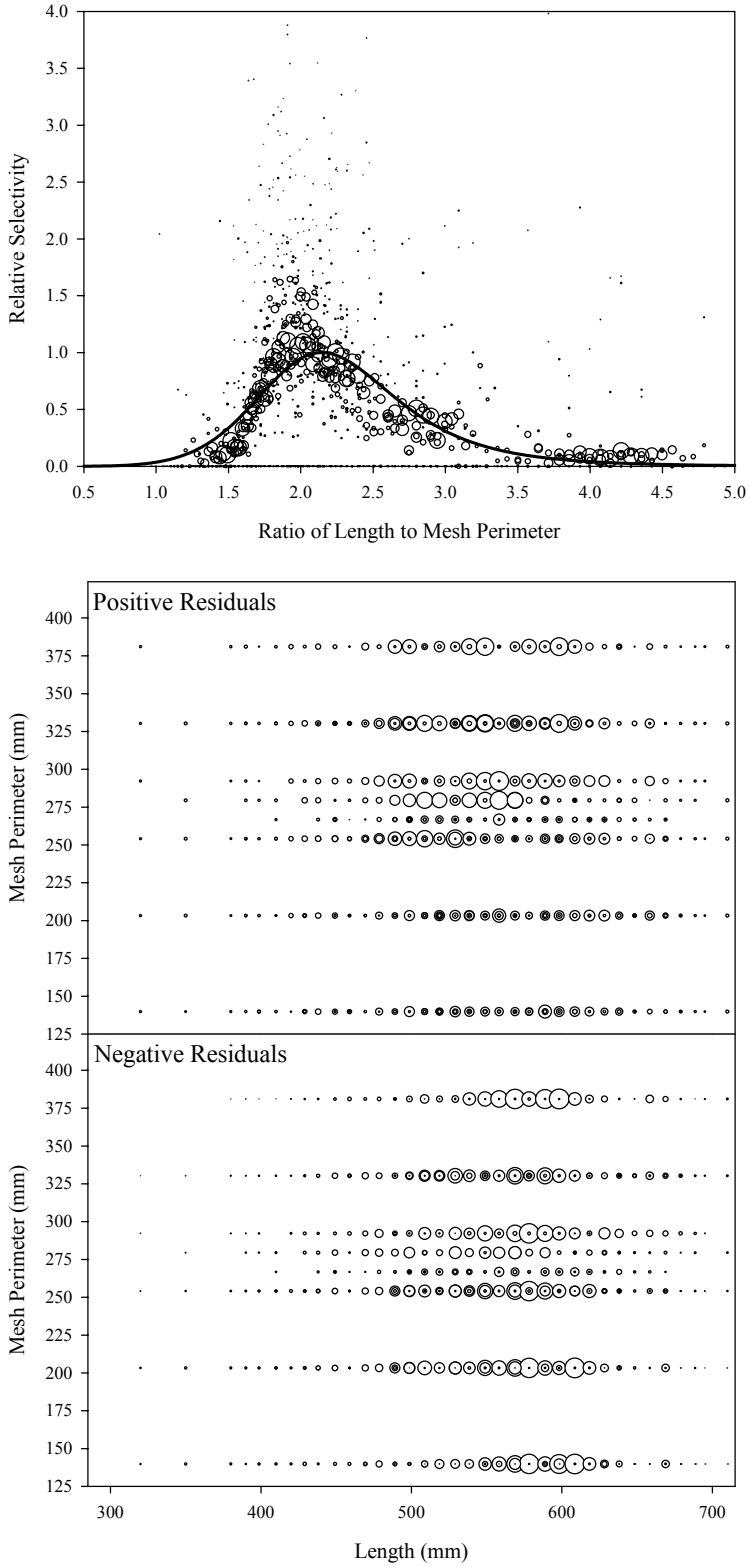

Figure B5.5. Plots of CPUE data scaled to a net selectivity model (top) and CPUE residuals (bottom); coho salmon data and Model 5.

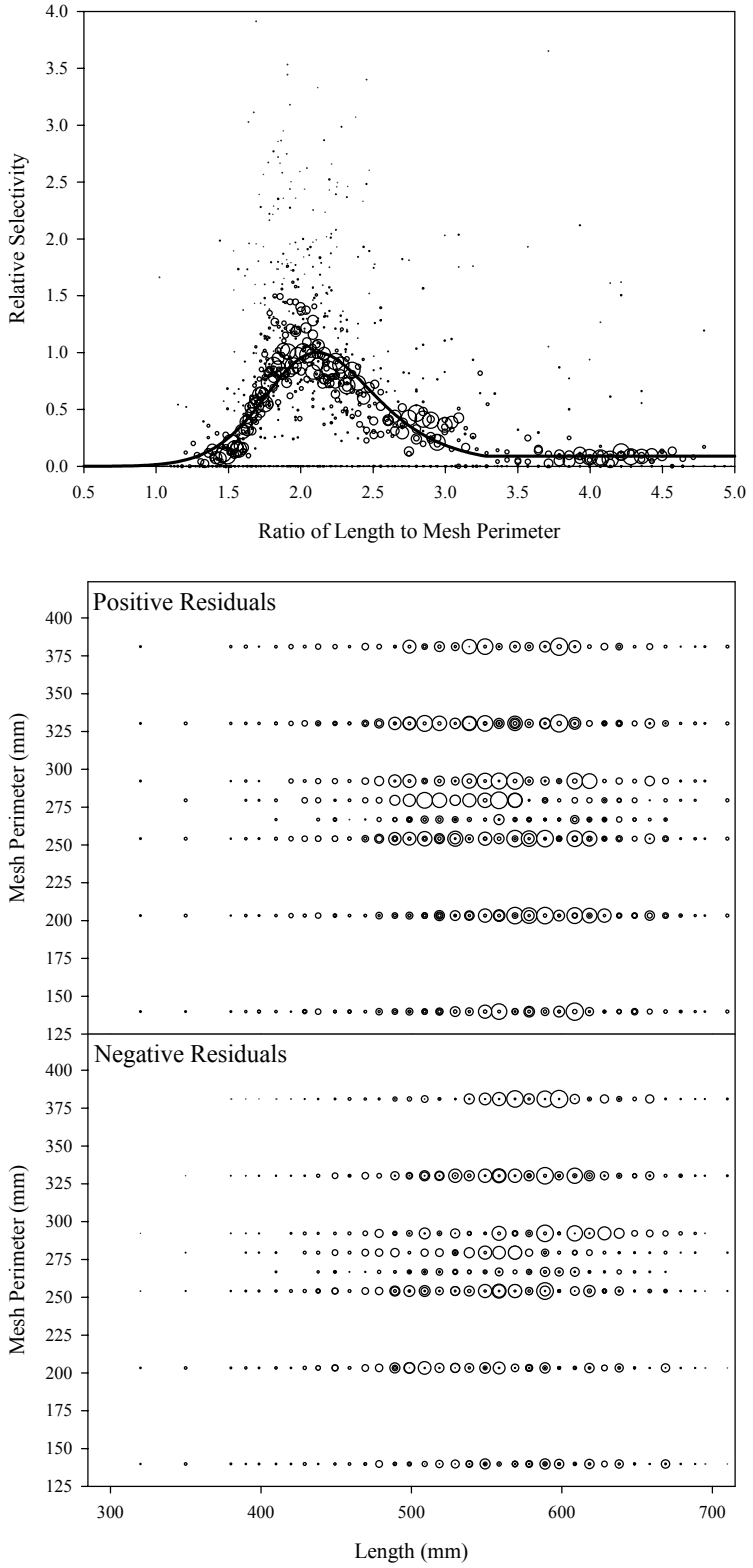

Figure B5.6. Plots of CPUE data scaled to a net selectivity model (top) and CPUE residuals (bottom); coho salmon data and Model 6.

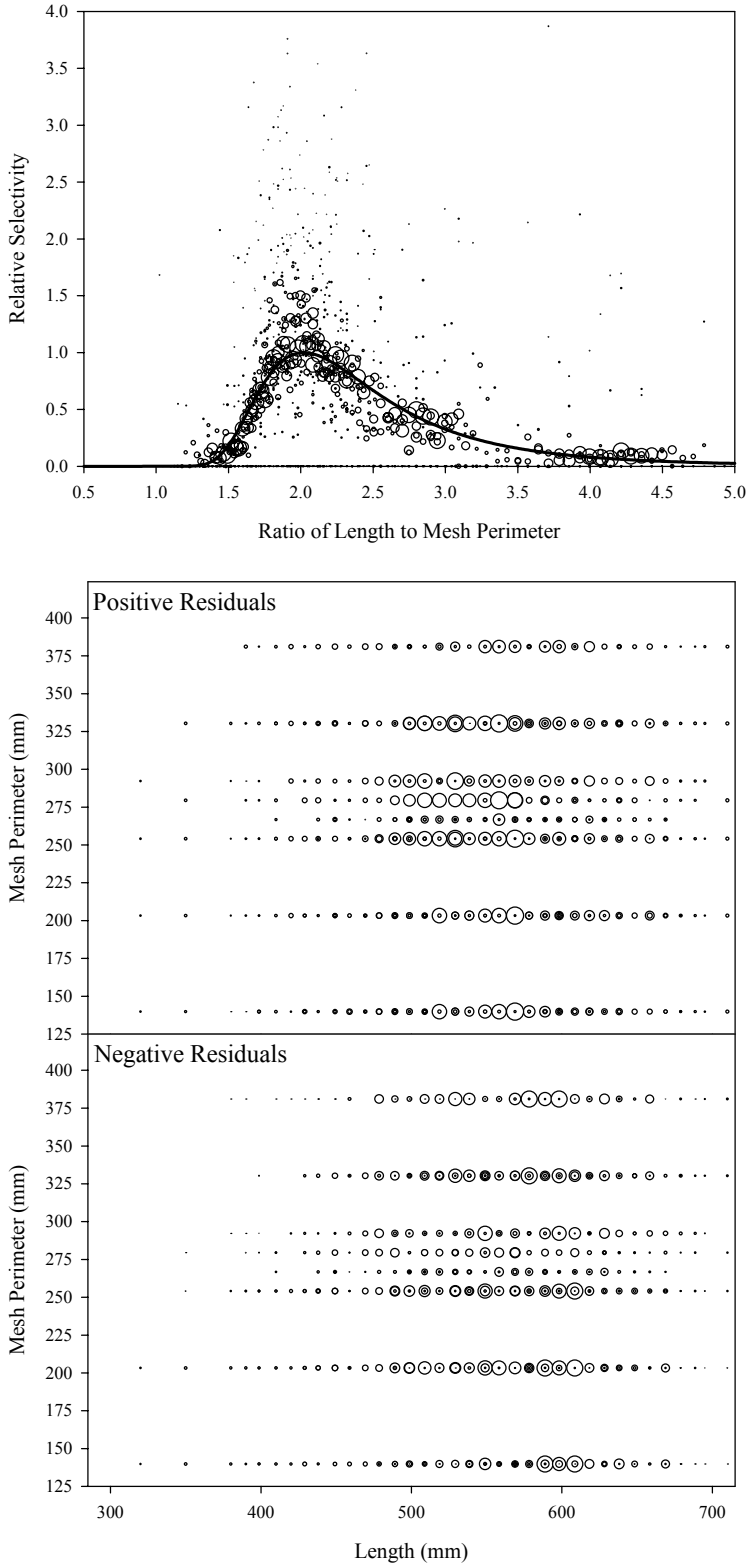

Figure B5.7. Plots of CPUE data scaled to a net selectivity model (top) and CPUE residuals (bottom); coho salmon data and Model 7.

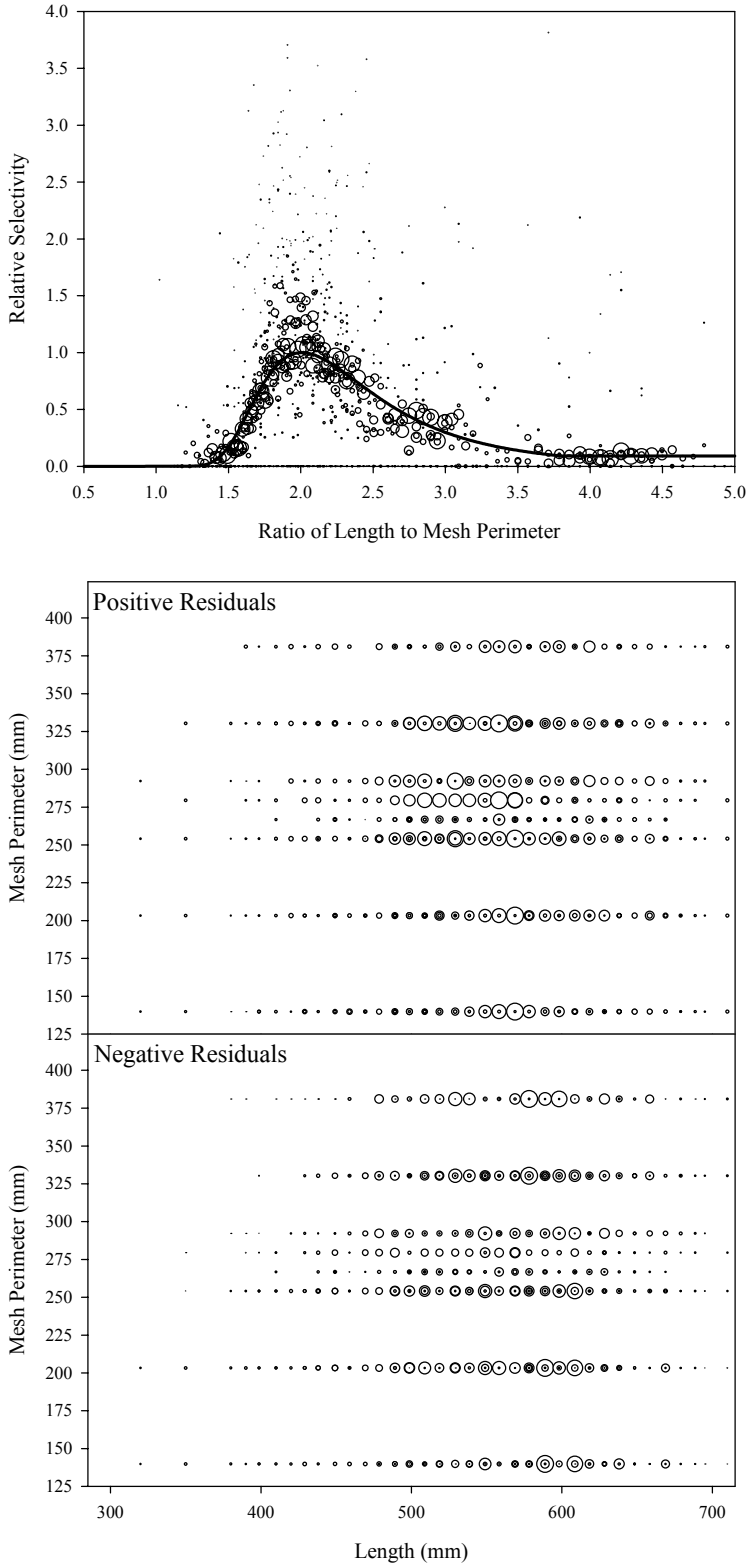

Figure B5.8. Plots of CPUE data scaled to a net selectivity model (top) and CPUE residuals (bottom); coho salmon data and Model 8.

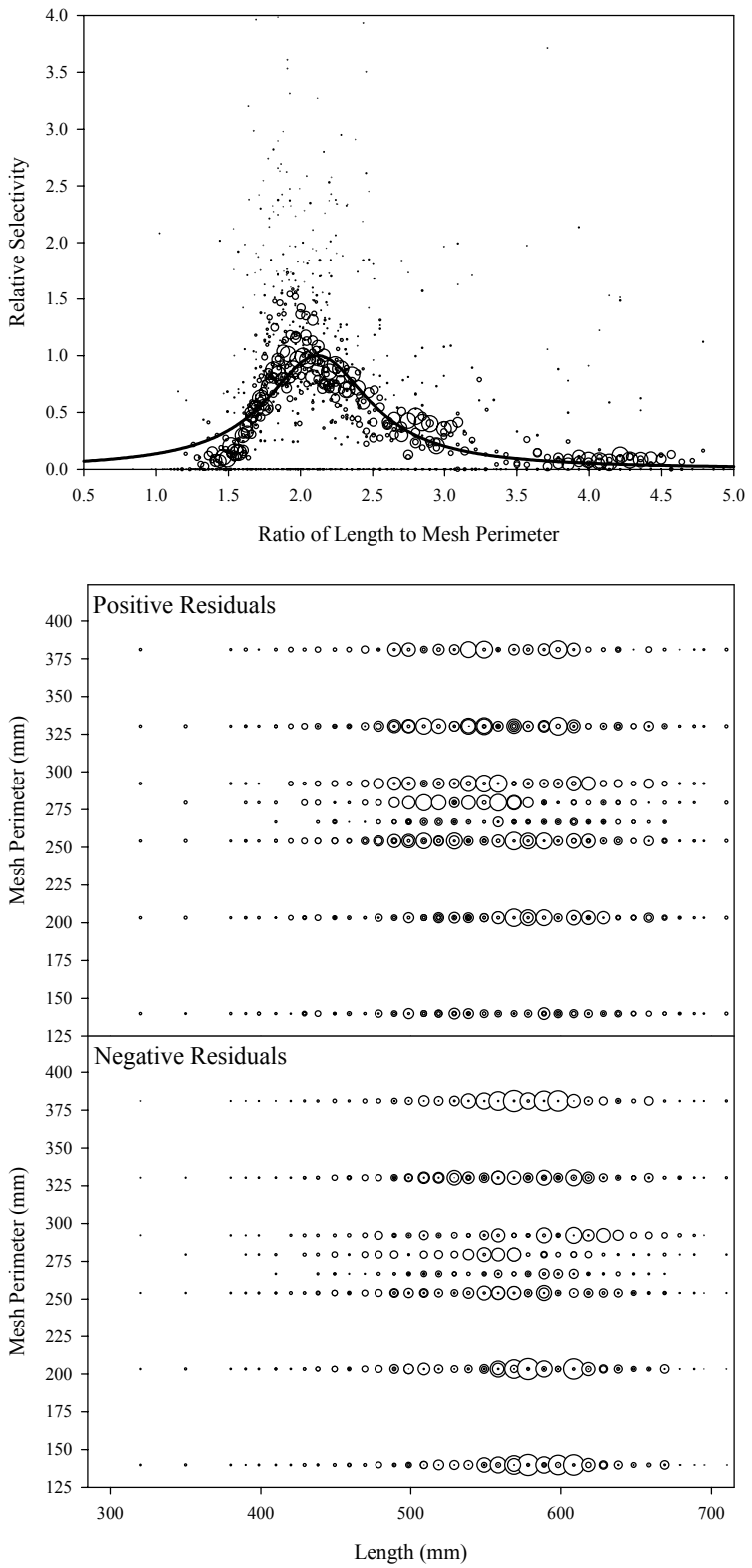

Figure B5.9. Plots of CPUE data scaled to a net selectivity model (top) and CPUE residuals (bottom); coho salmon data and Model 9.

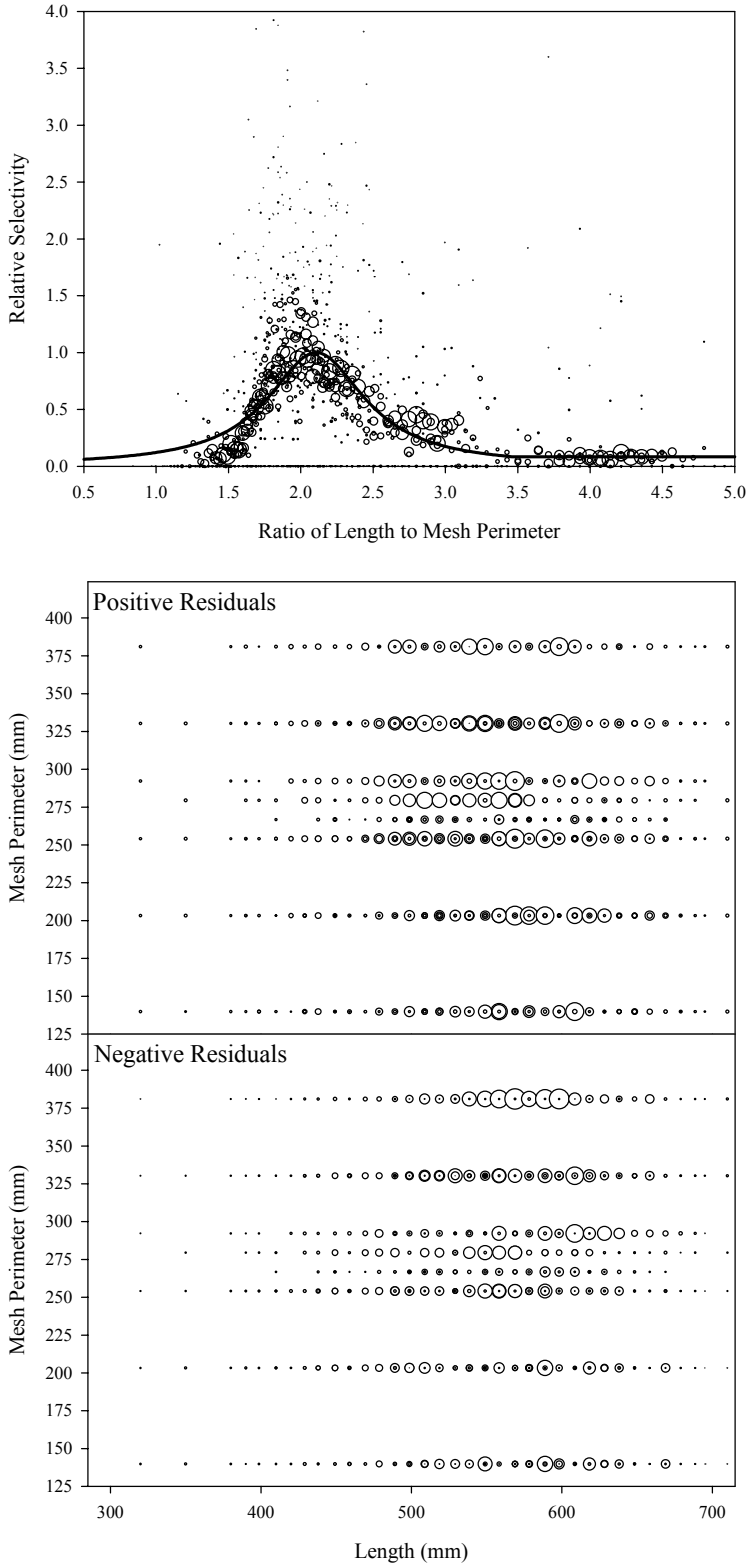

Figure B5.10. Plots of CPUE data scaled to a net selectivity model (top) and CPUE residuals (bottom); coho salmon data and Model 10.

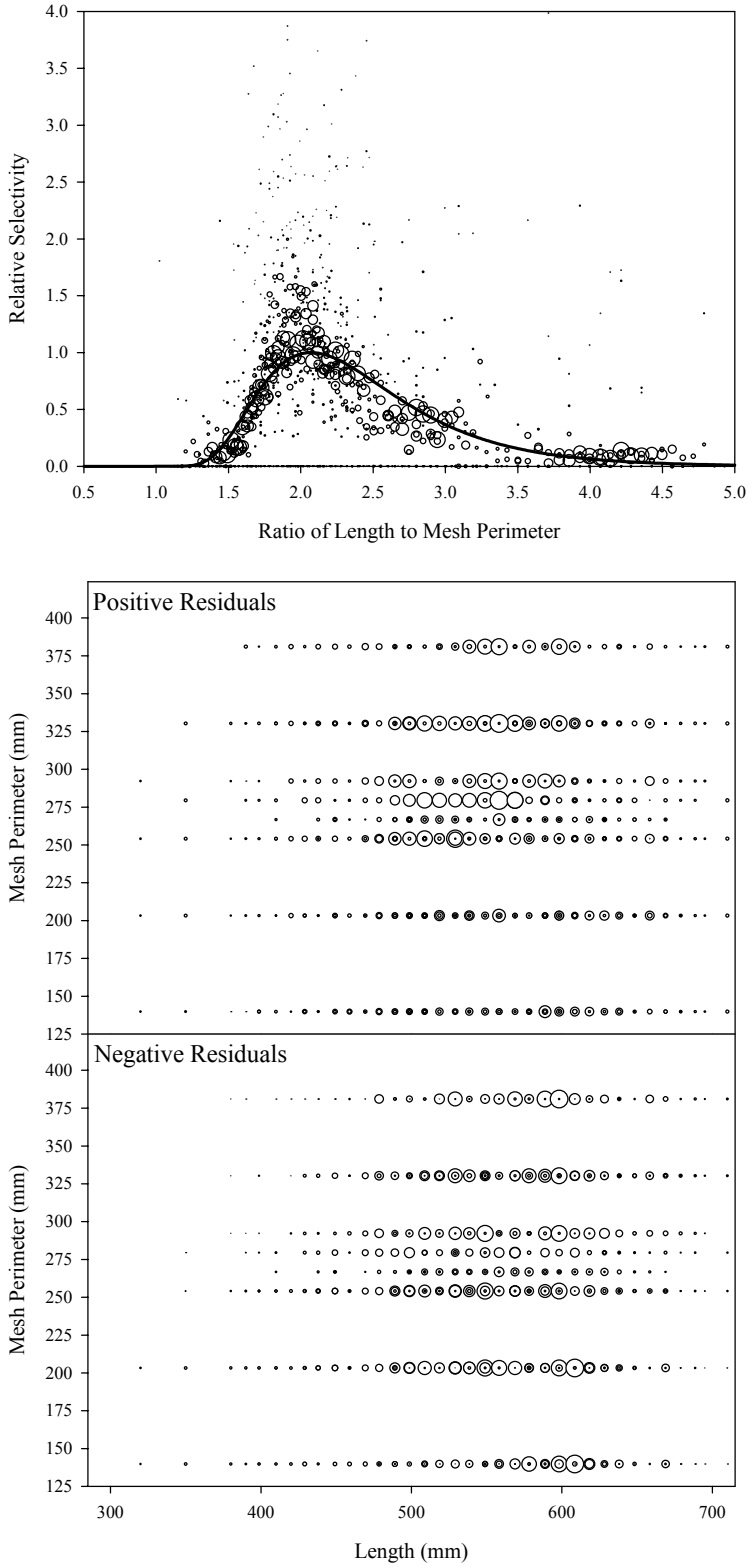

Figure B5.11. Plots of CPUE data scaled to a net selectivity model (top) and CPUE residuals (bottom); coho salmon data and Model 11.

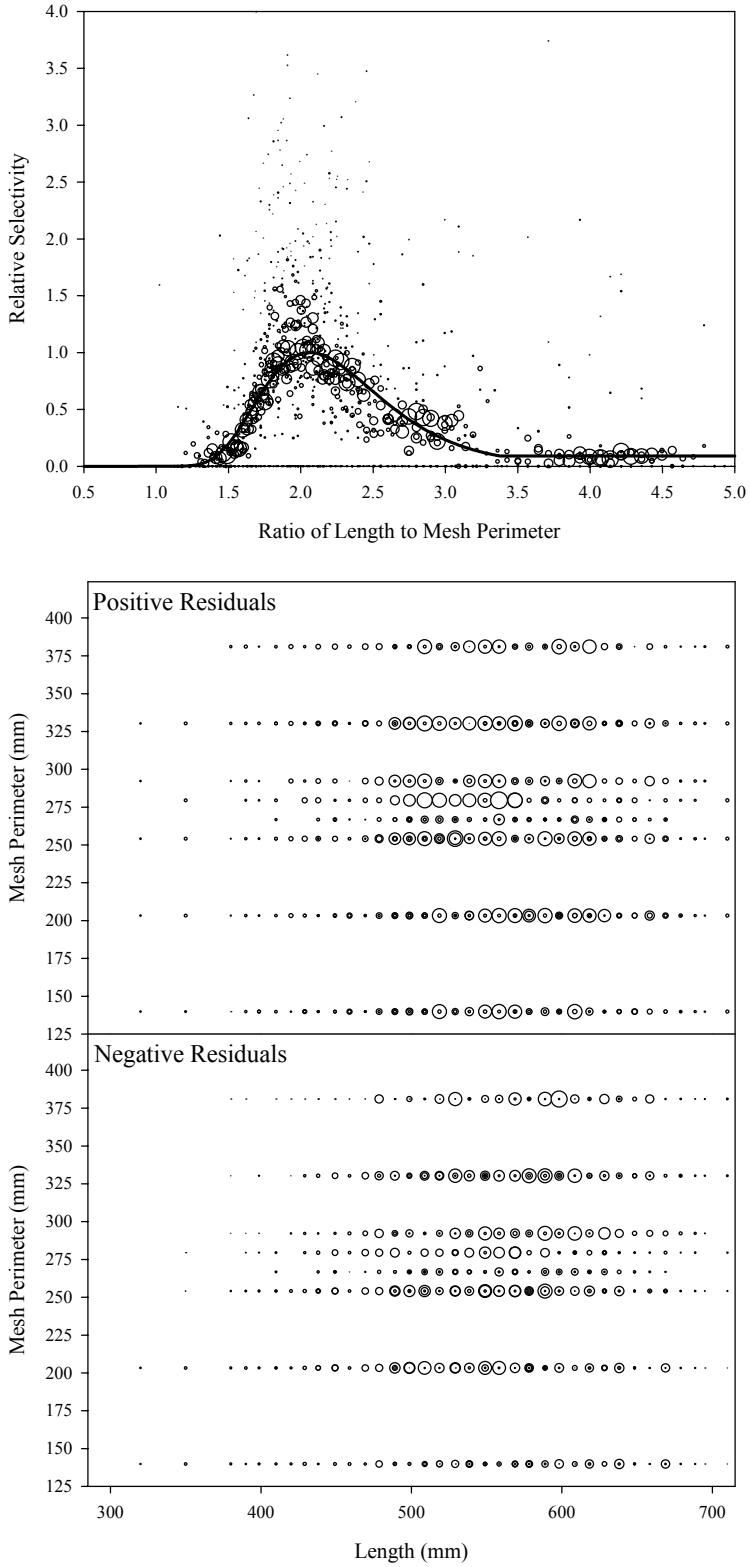

Figure B5.12. Plots of CPUE data scaled to a net selectivity model (top) and CPUE residuals (bottom); coho salmon data and Model 12.

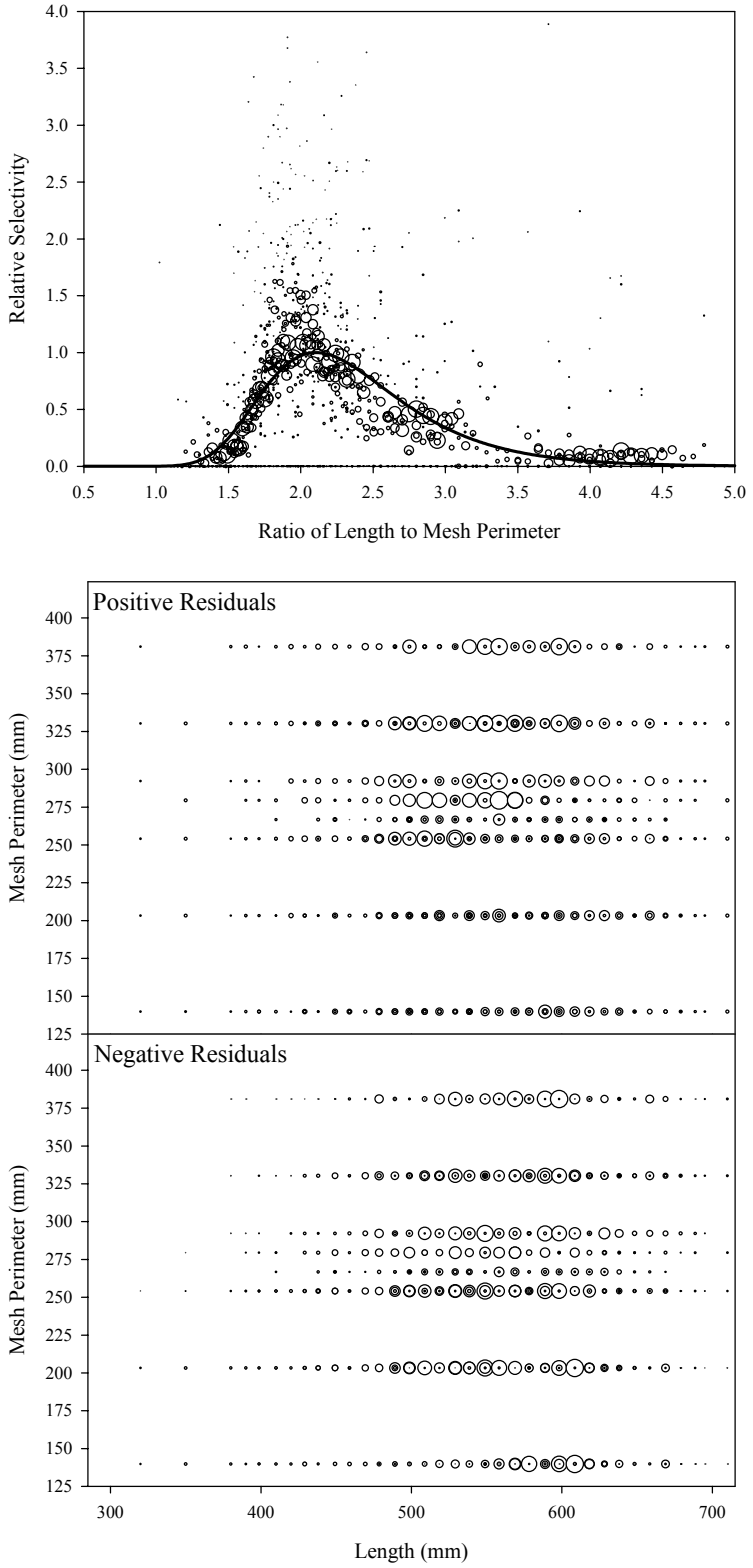

Figure B5.13. Plots of CPUE data scaled to a net selectivity model (top) and CPUE residuals (bottom); coho salmon data and Model 13.

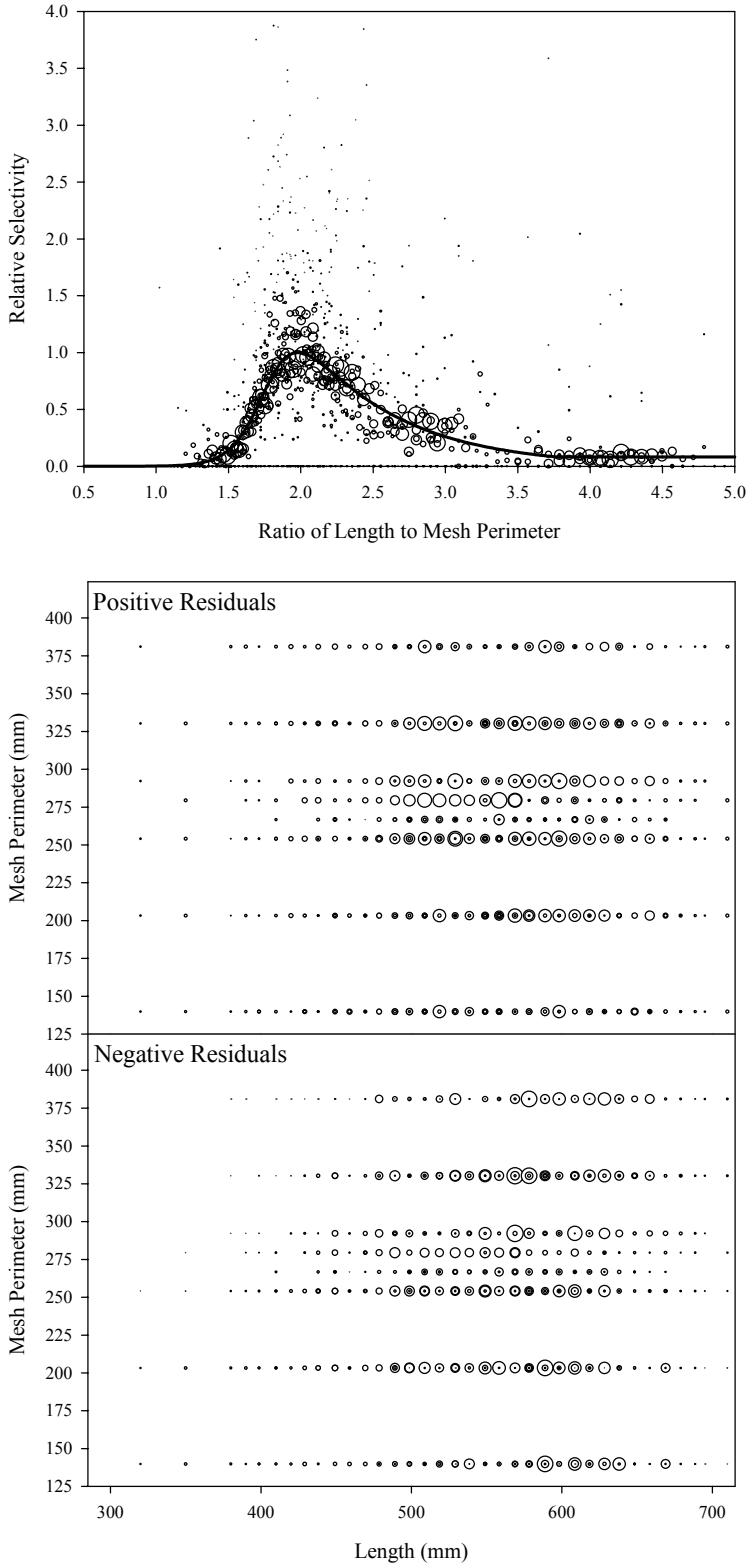

Figure B5.14. Plots of CPUE data scaled to a net selectivity model (top) and CPUE residuals (bottom); coho salmon data and Model 14.

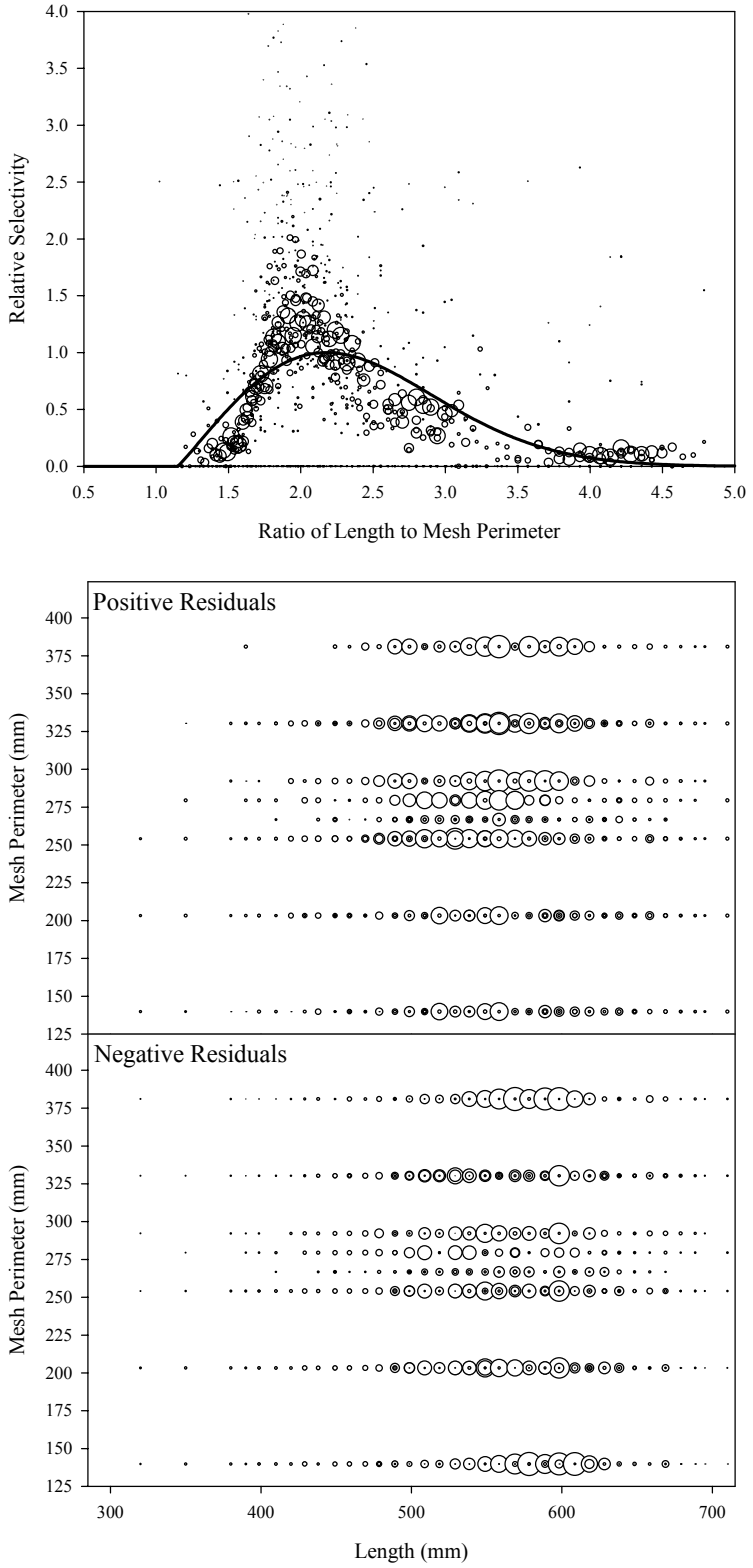

Figure B5.15. Plots of CPUE data scaled to a net selectivity model (top) and CPUE residuals (bottom); coho salmon data and Model 15.

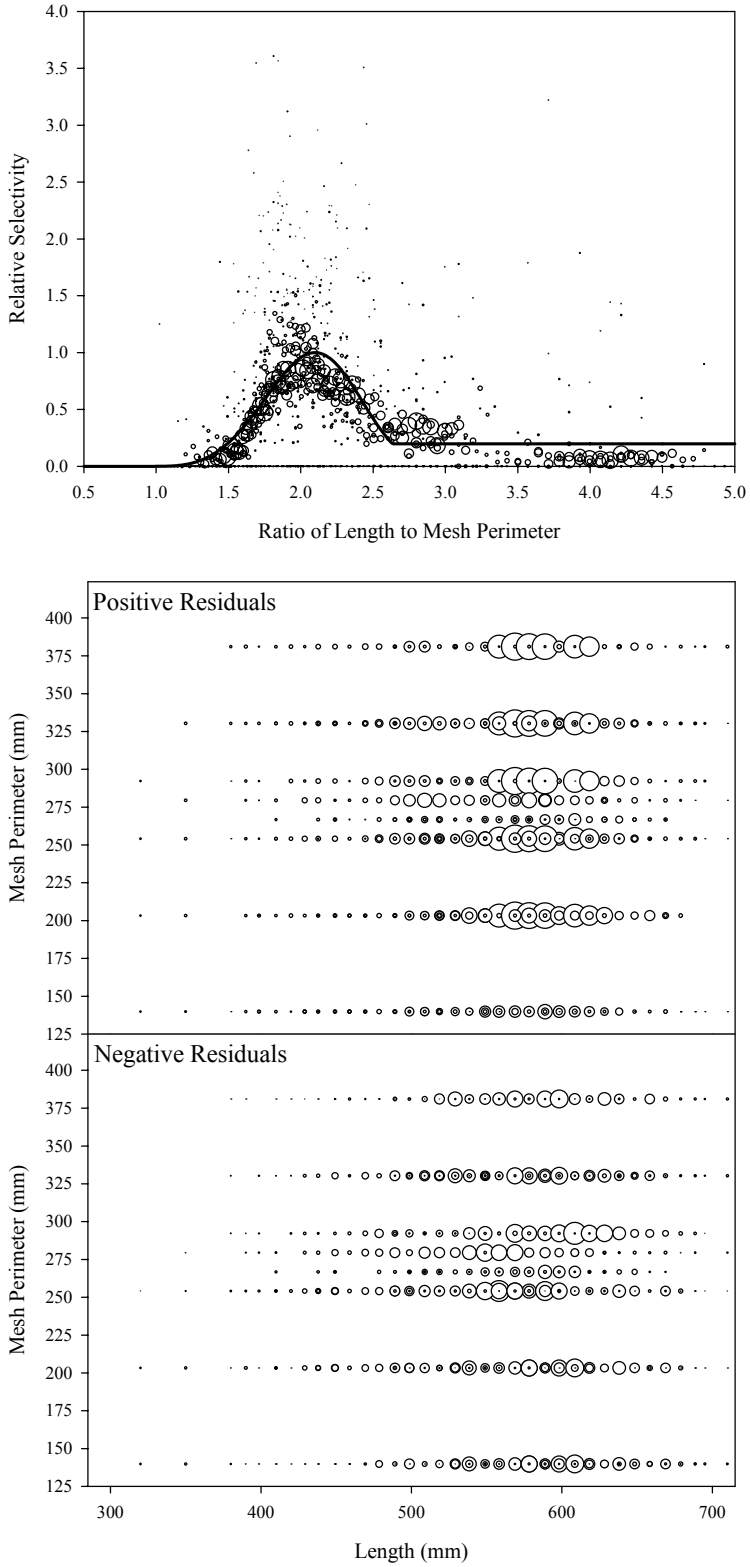

Figure B5.16. Plots of CPUE data scaled to a net selectivity model (top) and CPUE residuals (bottom); coho salmon data and Model 16.

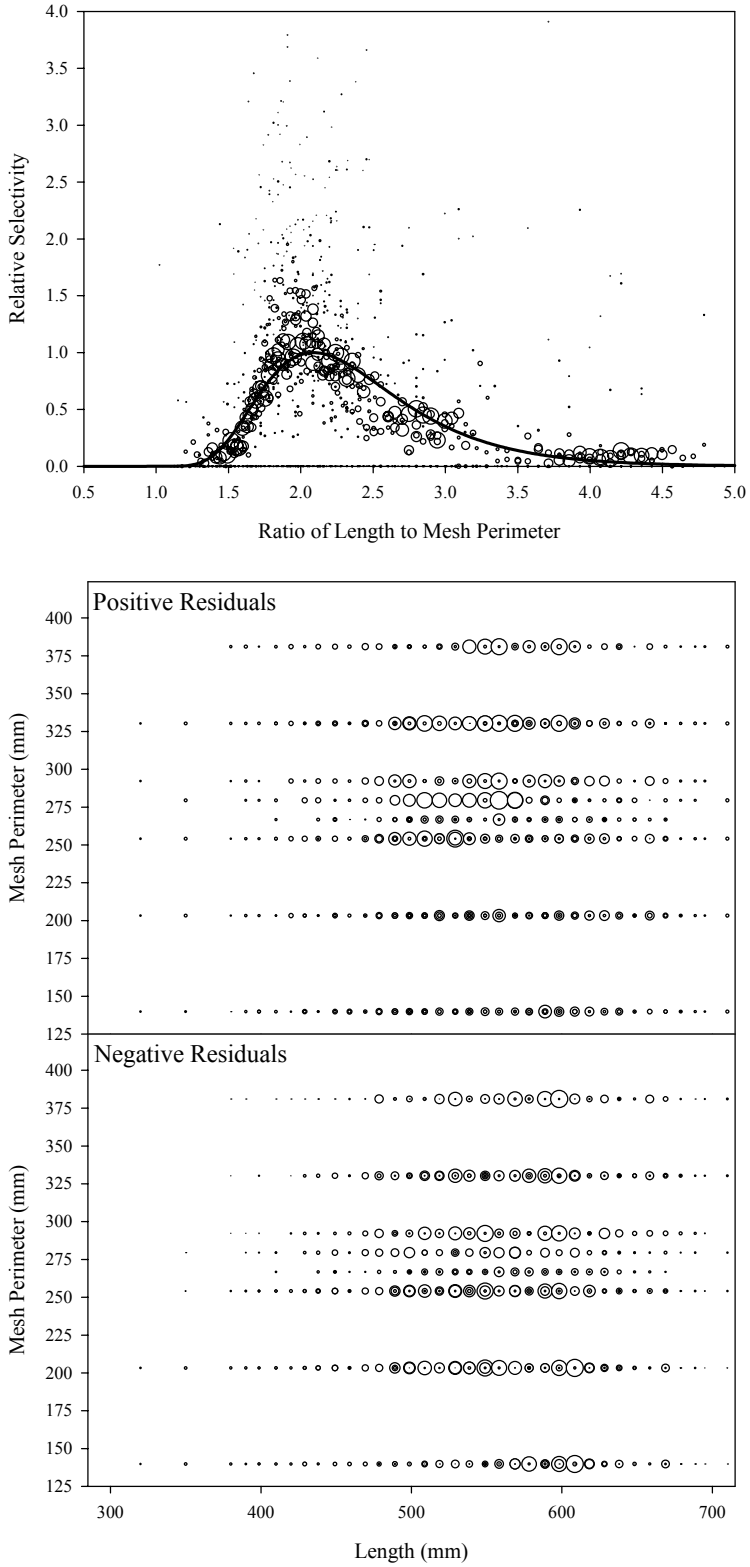

Figure B5.17. Plots of CPUE data scaled to a net selectivity model (top) and CPUE residuals (bottom); coho salmon data and Model 17.

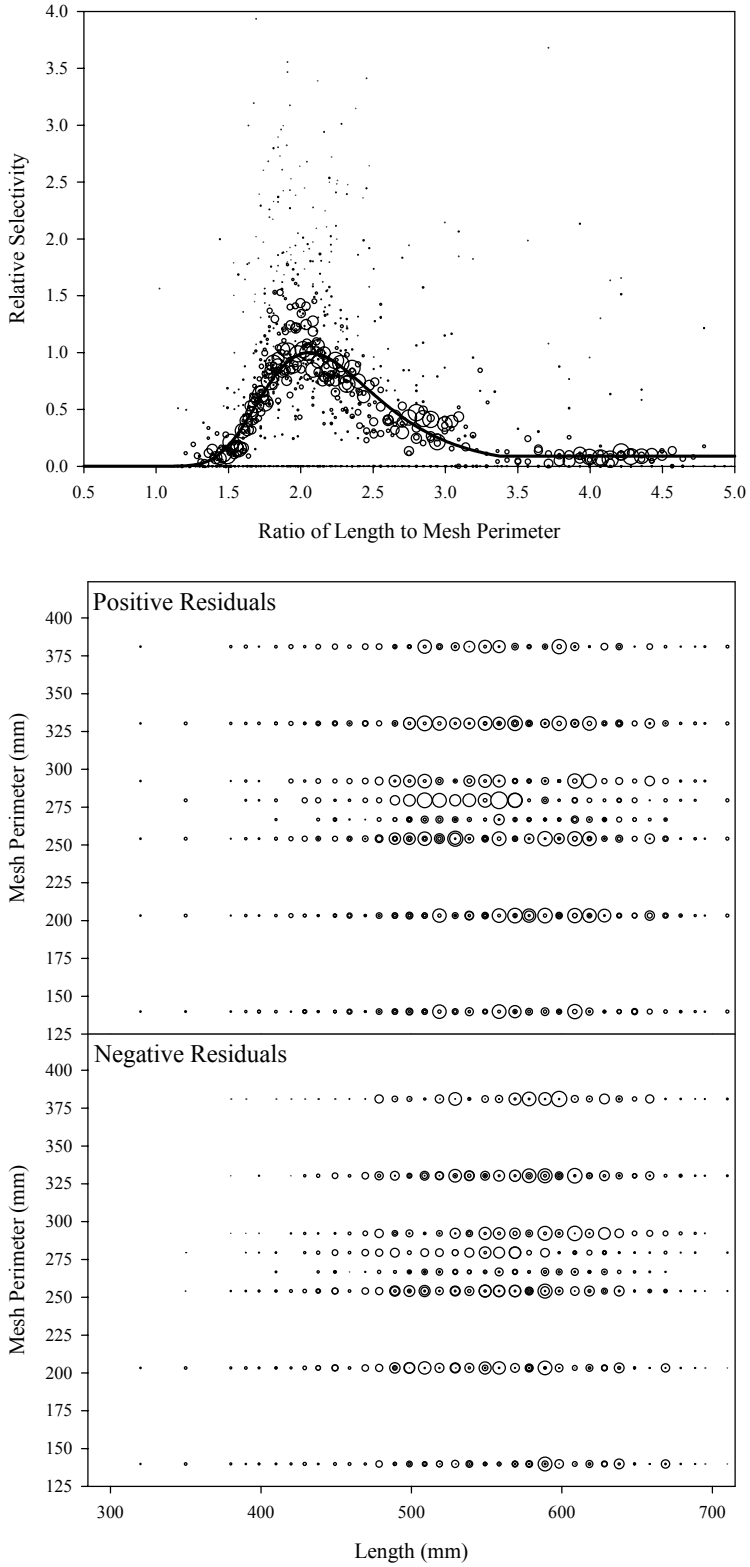

Figure B5.18. Plots of CPUE data scaled to a net selectivity model (top) and CPUE residuals (bottom); coho salmon data and Model 18.

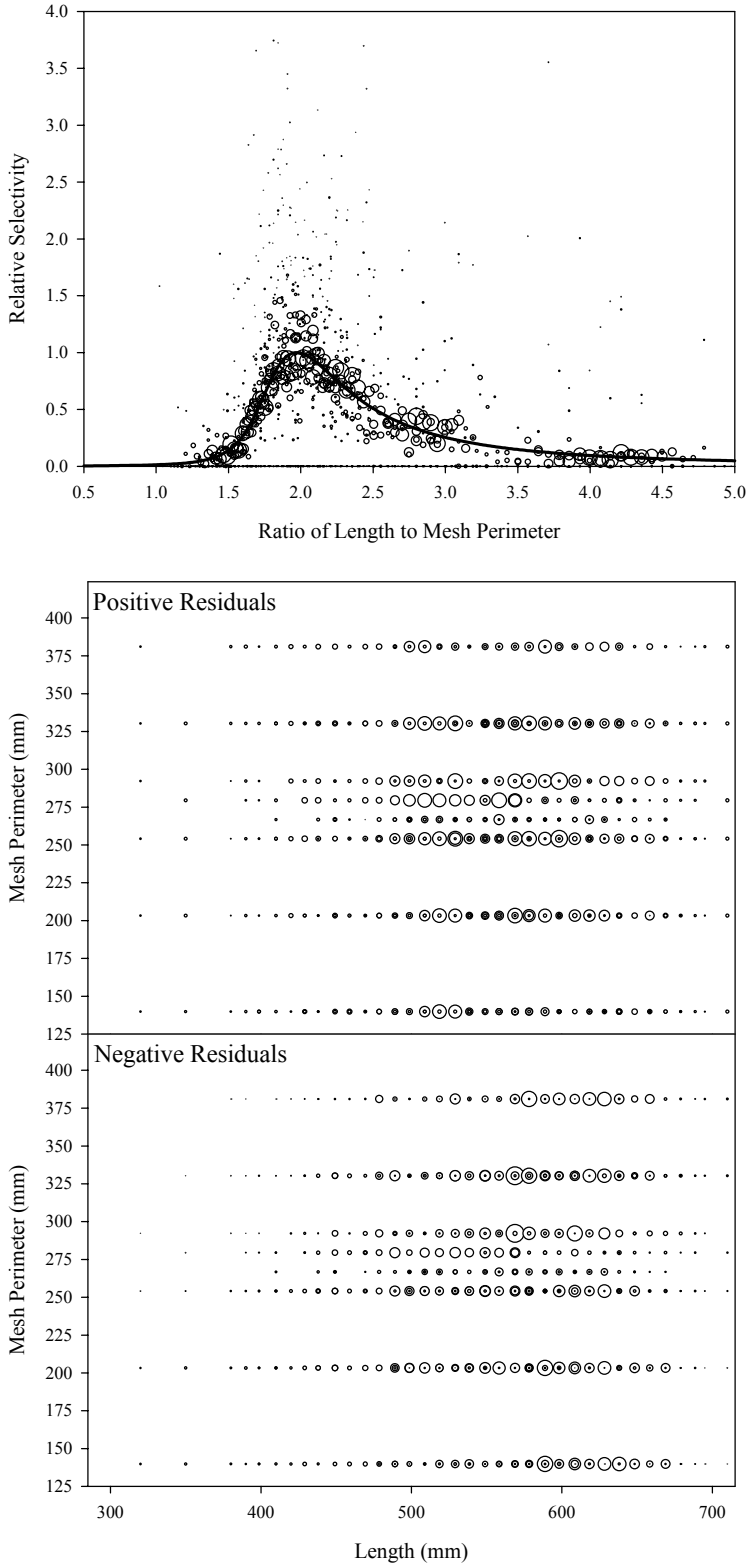

Figure B5.19. Plots of CPUE data scaled to a net selectivity model (top) and CPUE residuals (bottom); coho salmon data and Model 19.

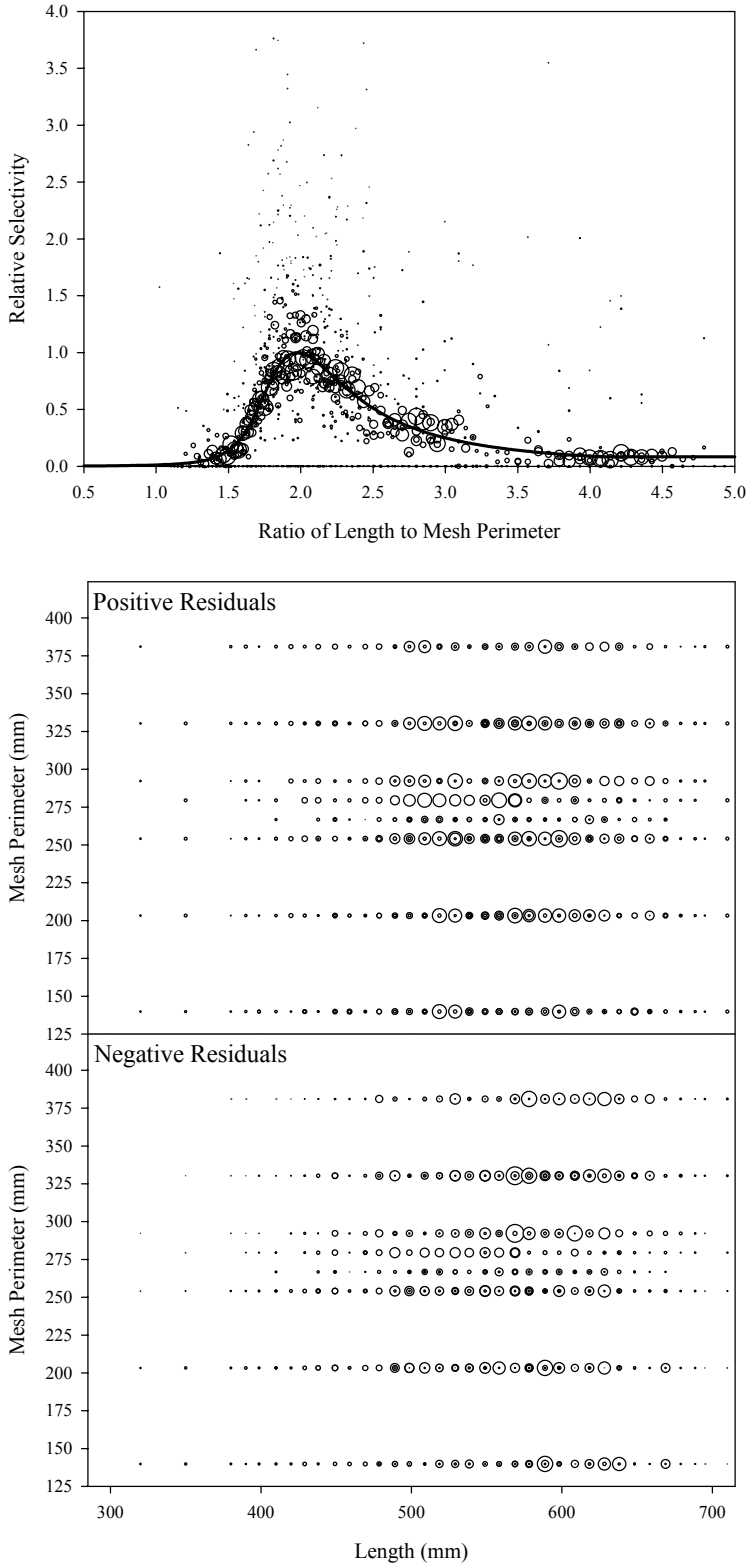

Figure B5.20. Plots of CPUE data scaled to a net selectivity model (top) and CPUE residuals (bottom); coho salmon data and Model 20.

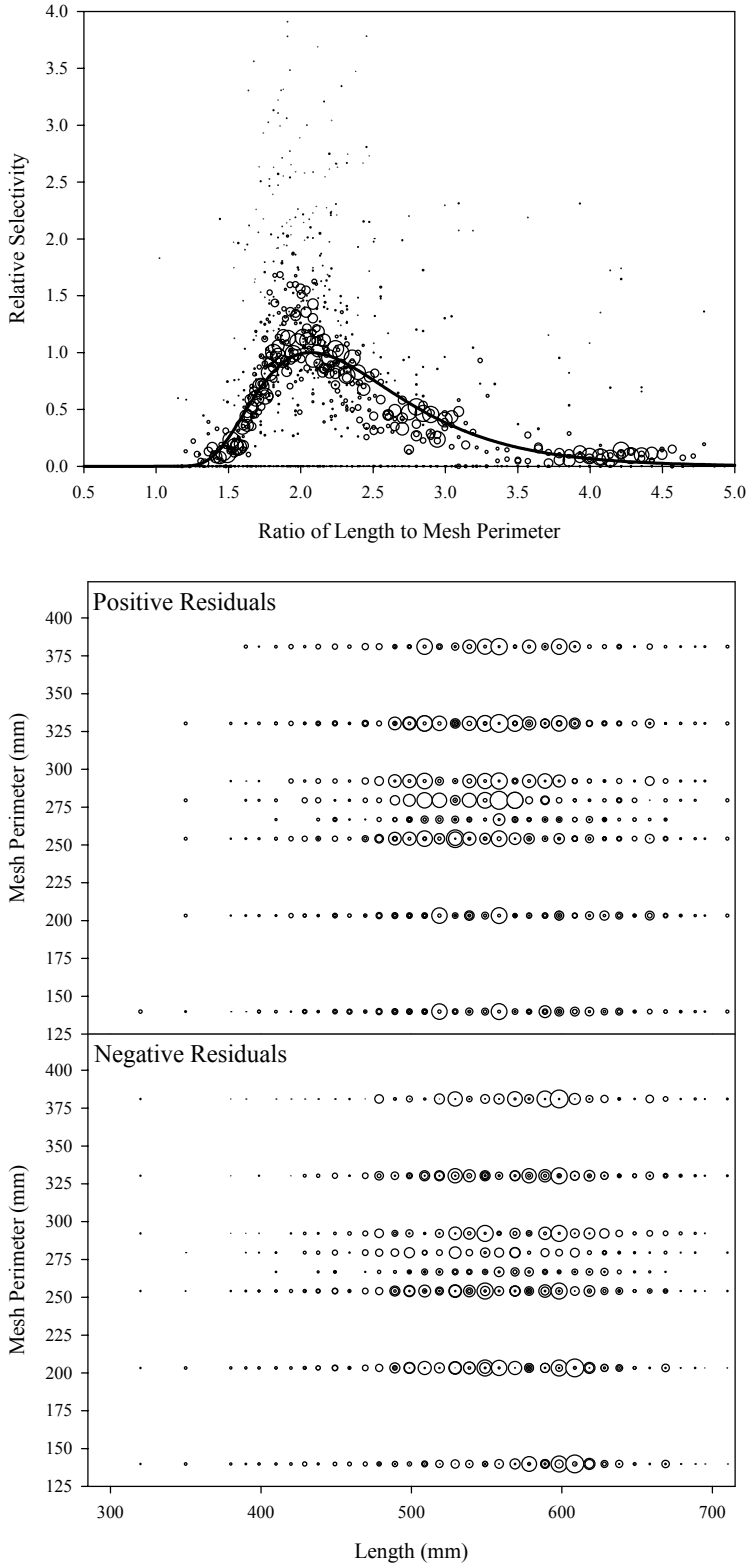

Figure B5.21. Plots of CPUE data scaled to a net selectivity model (top) and CPUE residuals (bottom); coho salmon data and Model 21.

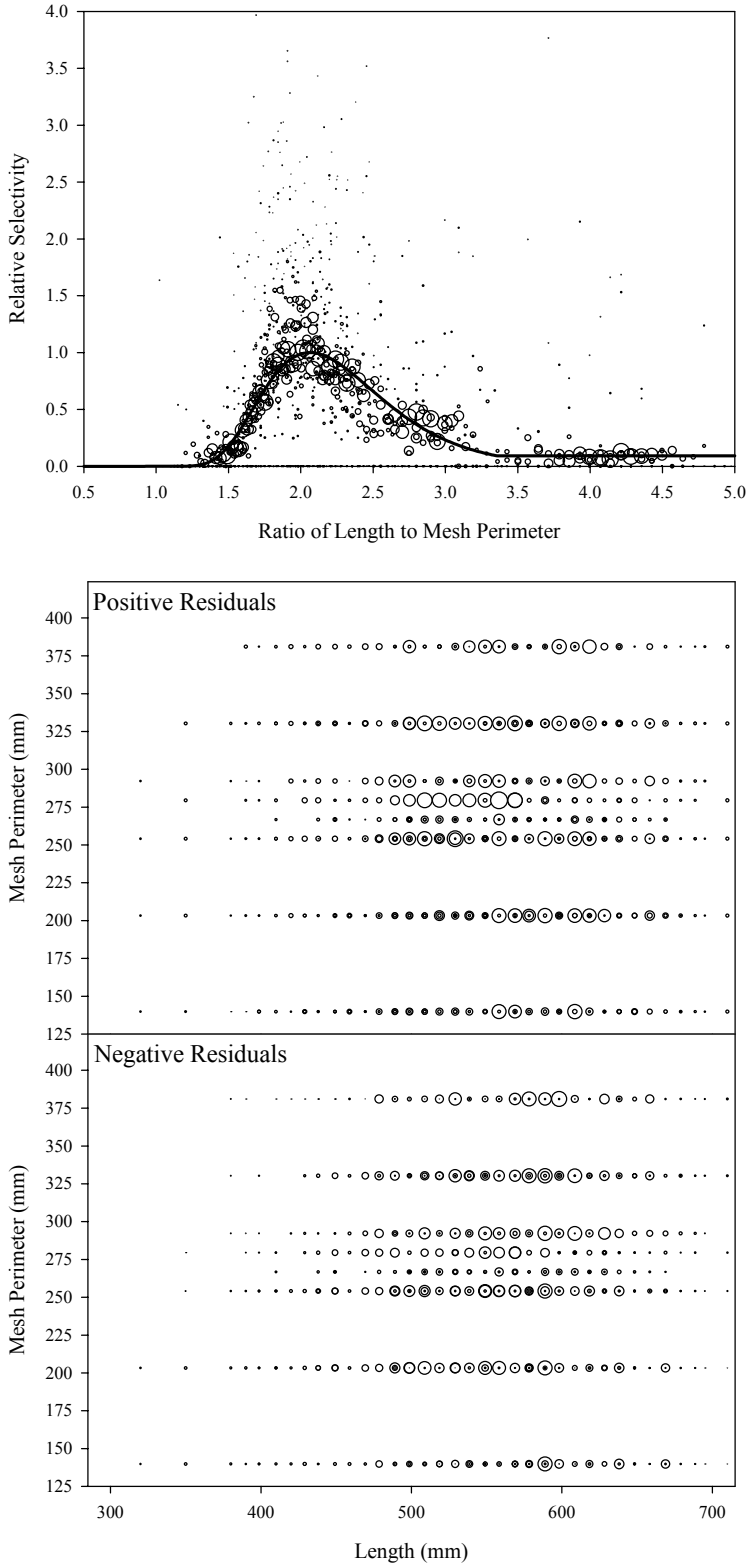

Figure B5.22. Plots of CPUE data scaled to a net selectivity model (top) and CPUE residuals (bottom); coho salmon data and Model 22.

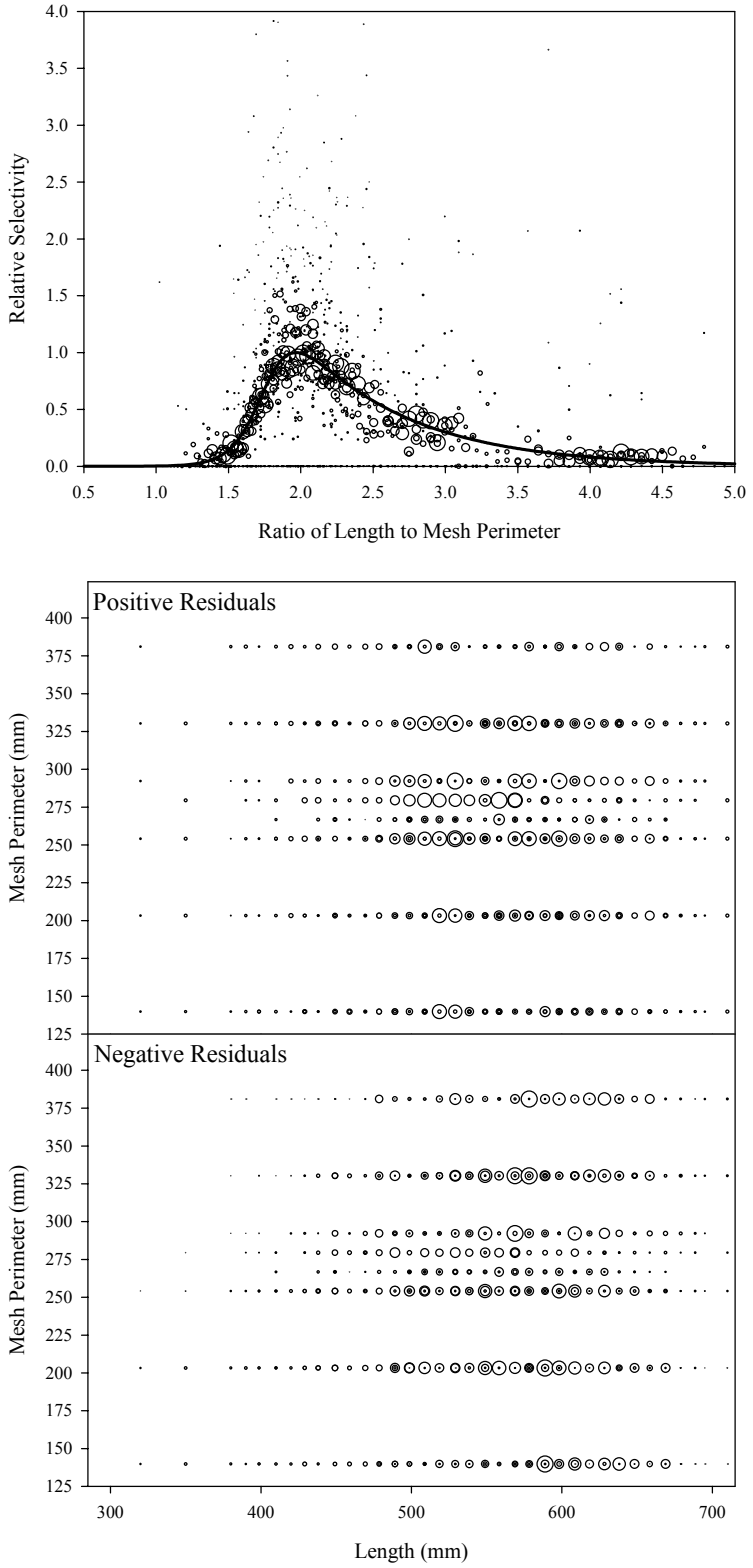

Figure B5.23. Plots of CPUE data scaled to a net selectivity model (top) and CPUE residuals (bottom); coho salmon data and Model 23.

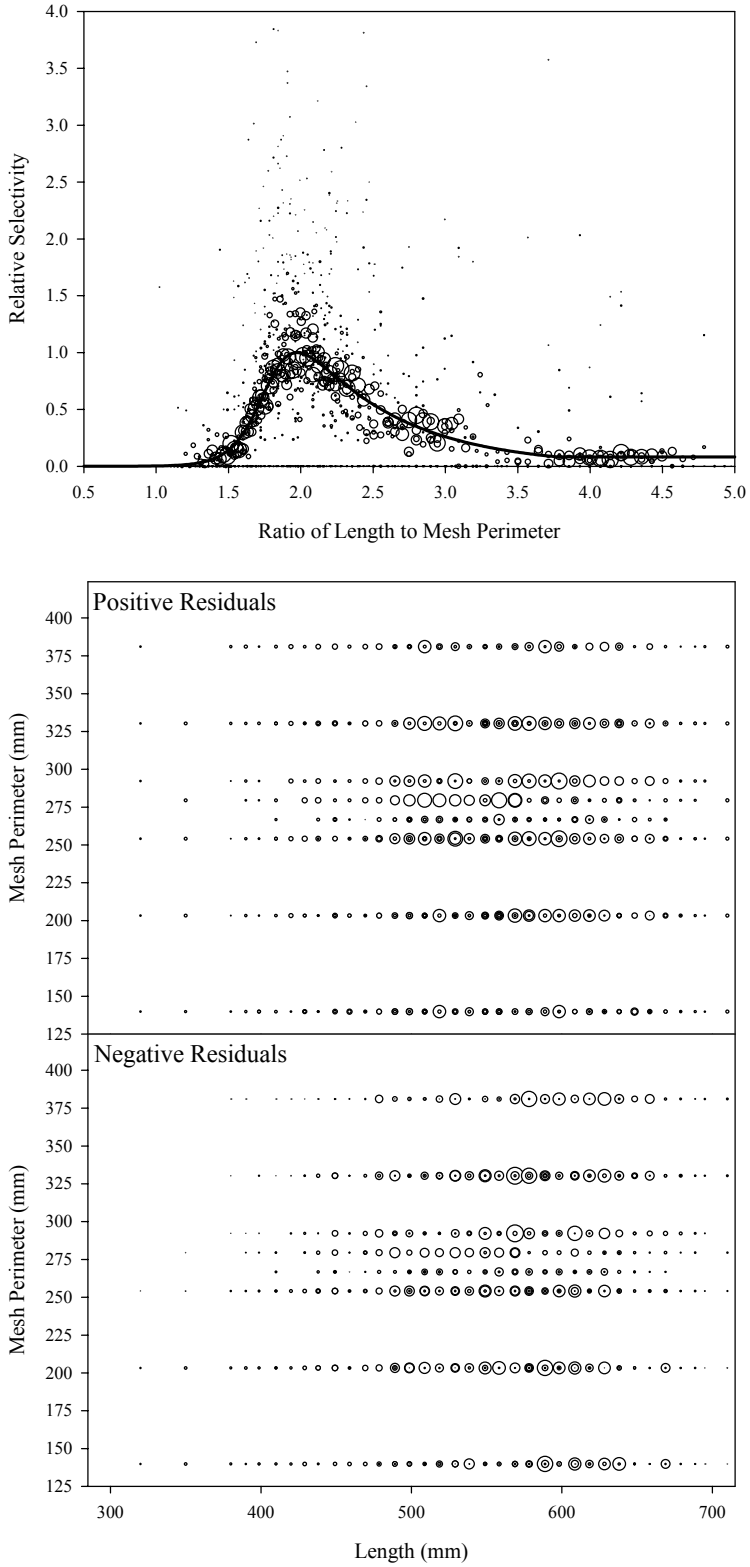

Figure B5.24. Plots of CPUE data scaled to a net selectivity model (top) and CPUE residuals (bottom); coho salmon data and Model 24.

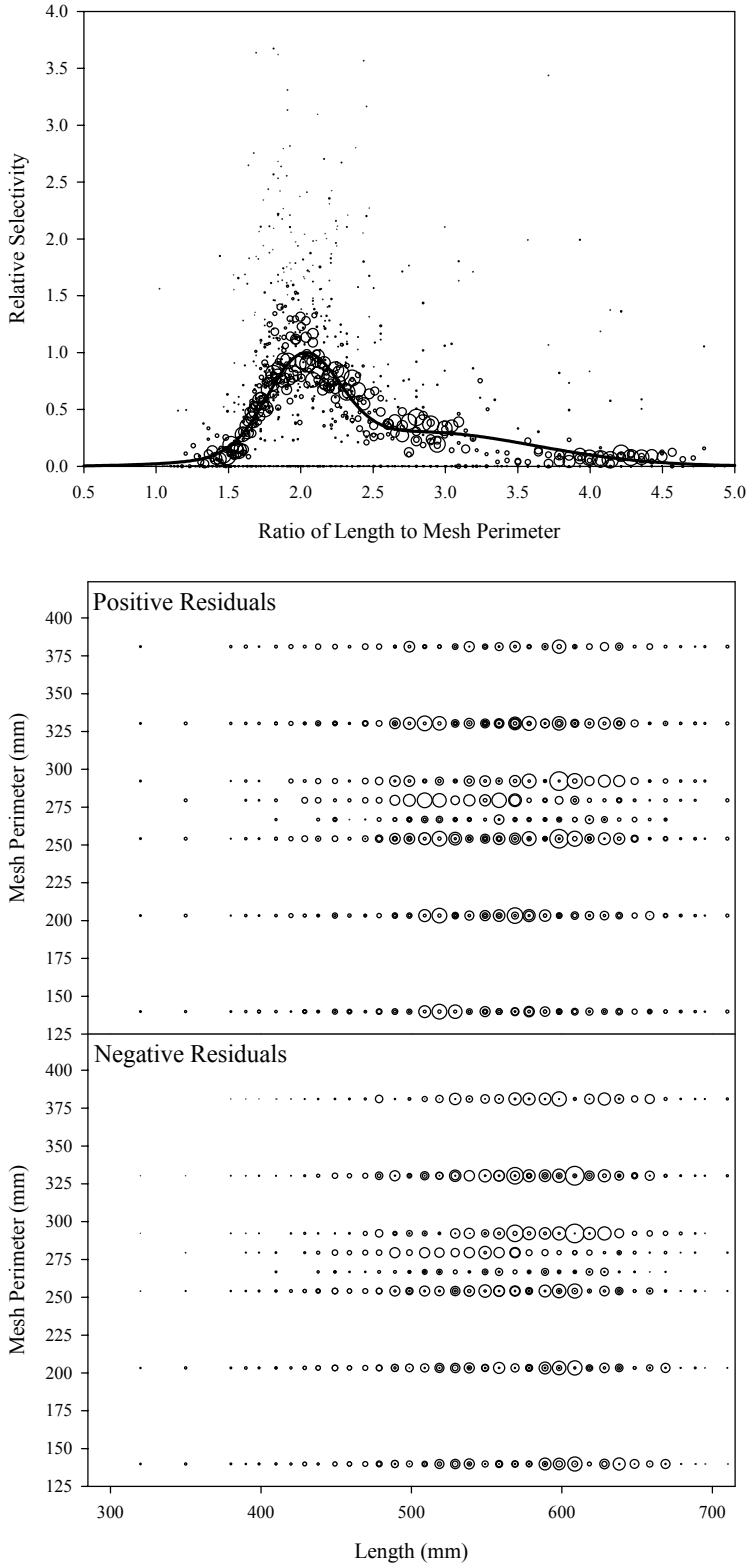

Figure B5.25. Plots of CPUE data scaled to a net selectivity model (top) and CPUE residuals (bottom); coho salmon data and Model 25.

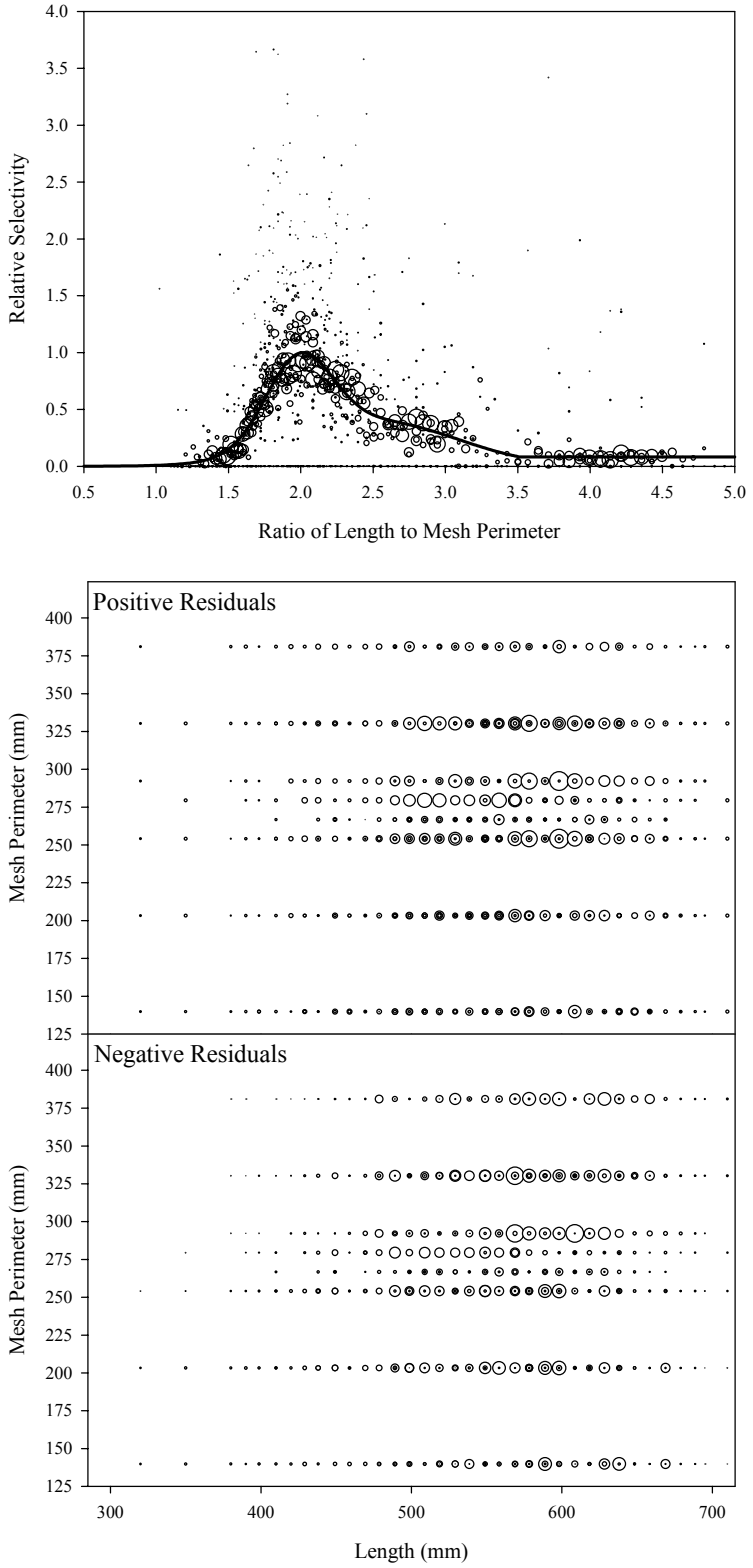

Figure B5.26. Plots of CPUE data scaled to a net selectivity model (top) and CPUE residuals (bottom); coho salmon data and Model 26.

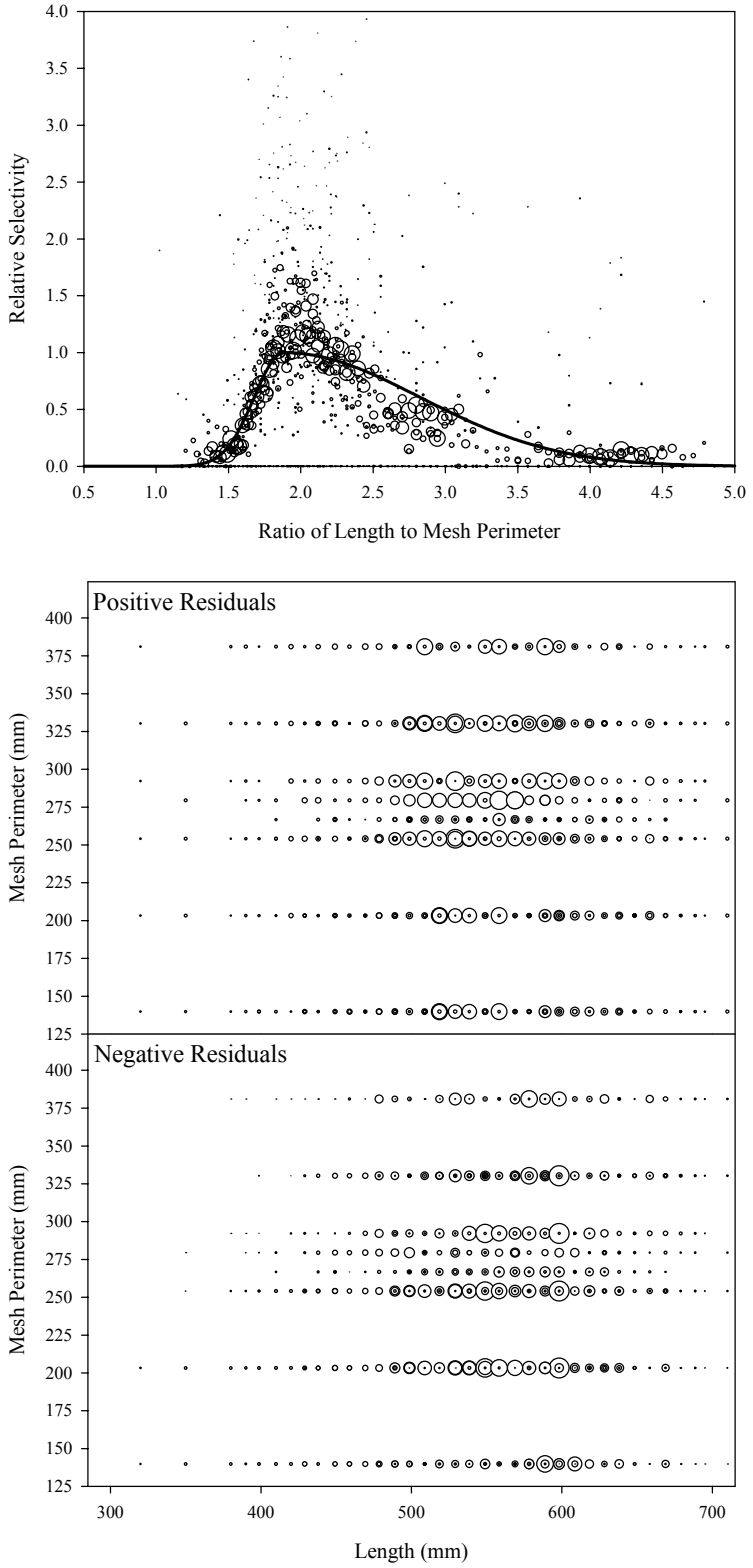

Figure B5.27. Plots of CPUE data scaled to a net selectivity model (top) and CPUE residuals (bottom); coho salmon data and Model 27.

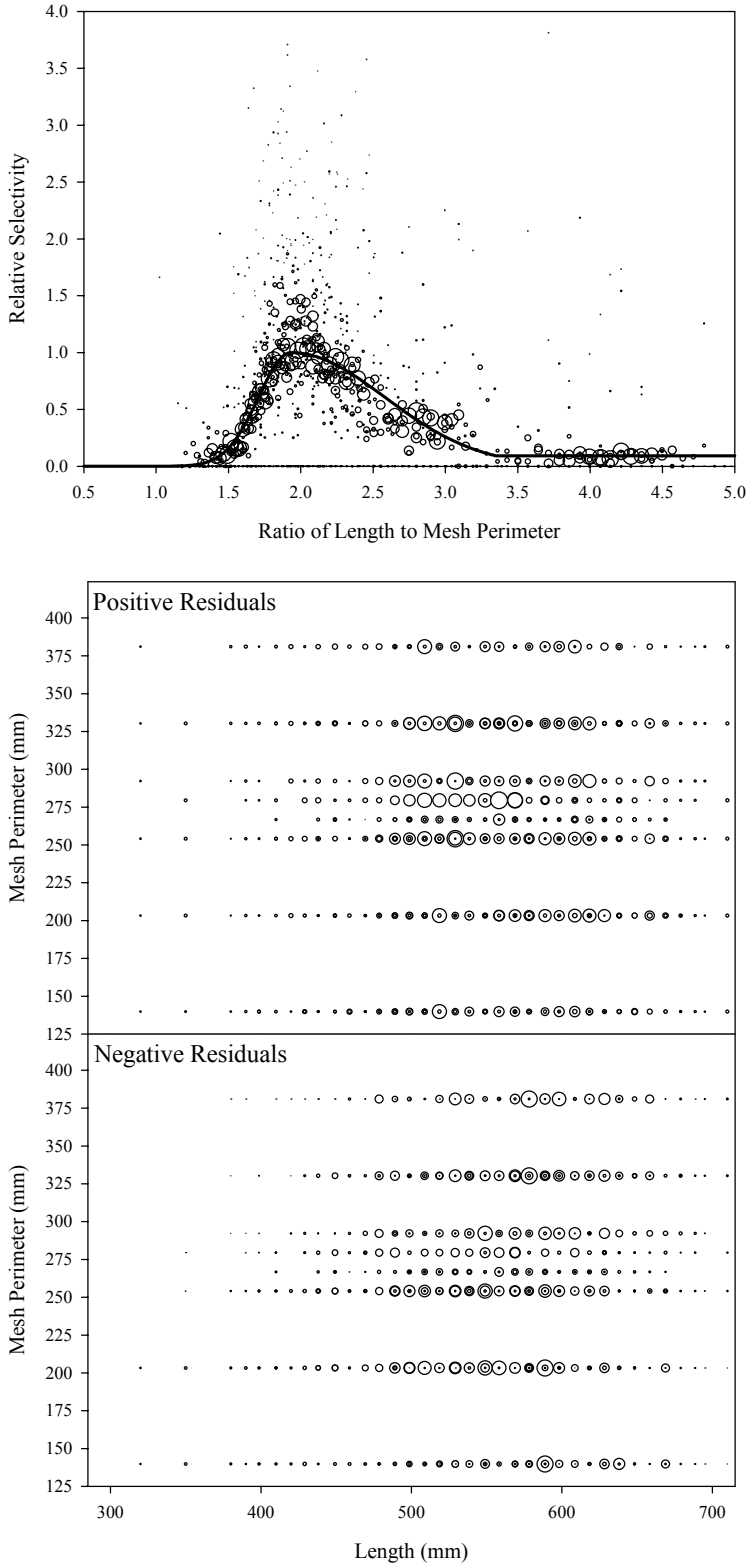

Figure B5.28. Plots of CPUE data scaled to a net selectivity model (top) and CPUE residuals (bottom); coho salmon data and Model 28.

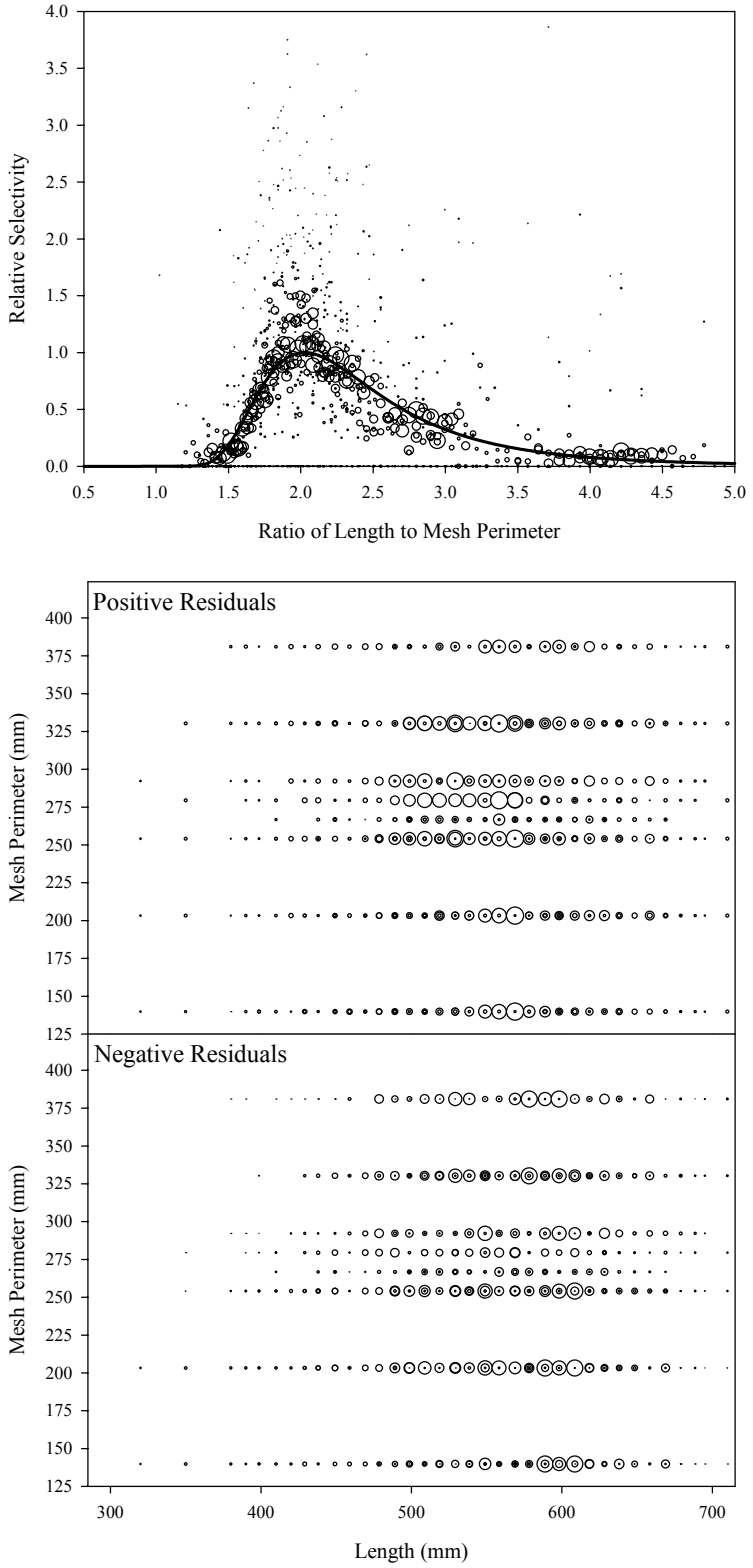

Figure B5.29. Plots of CPUE data scaled to a net selectivity model (top) and CPUE residuals (bottom); coho salmon data and Model 29.

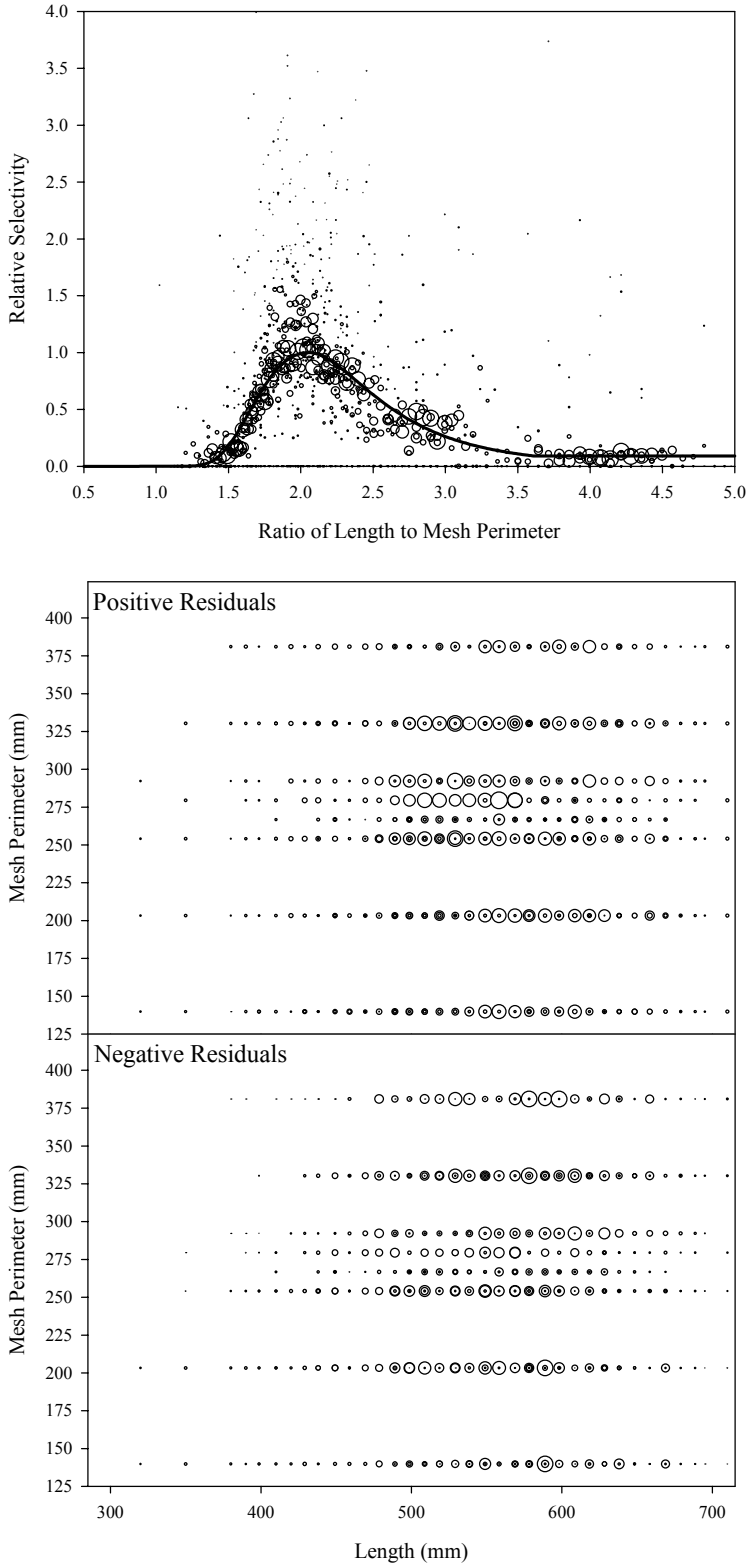

Figure B5.30. Plots of CPUE data scaled to a net selectivity model (top) and CPUE residuals (bottom); coho salmon data and Model 30.

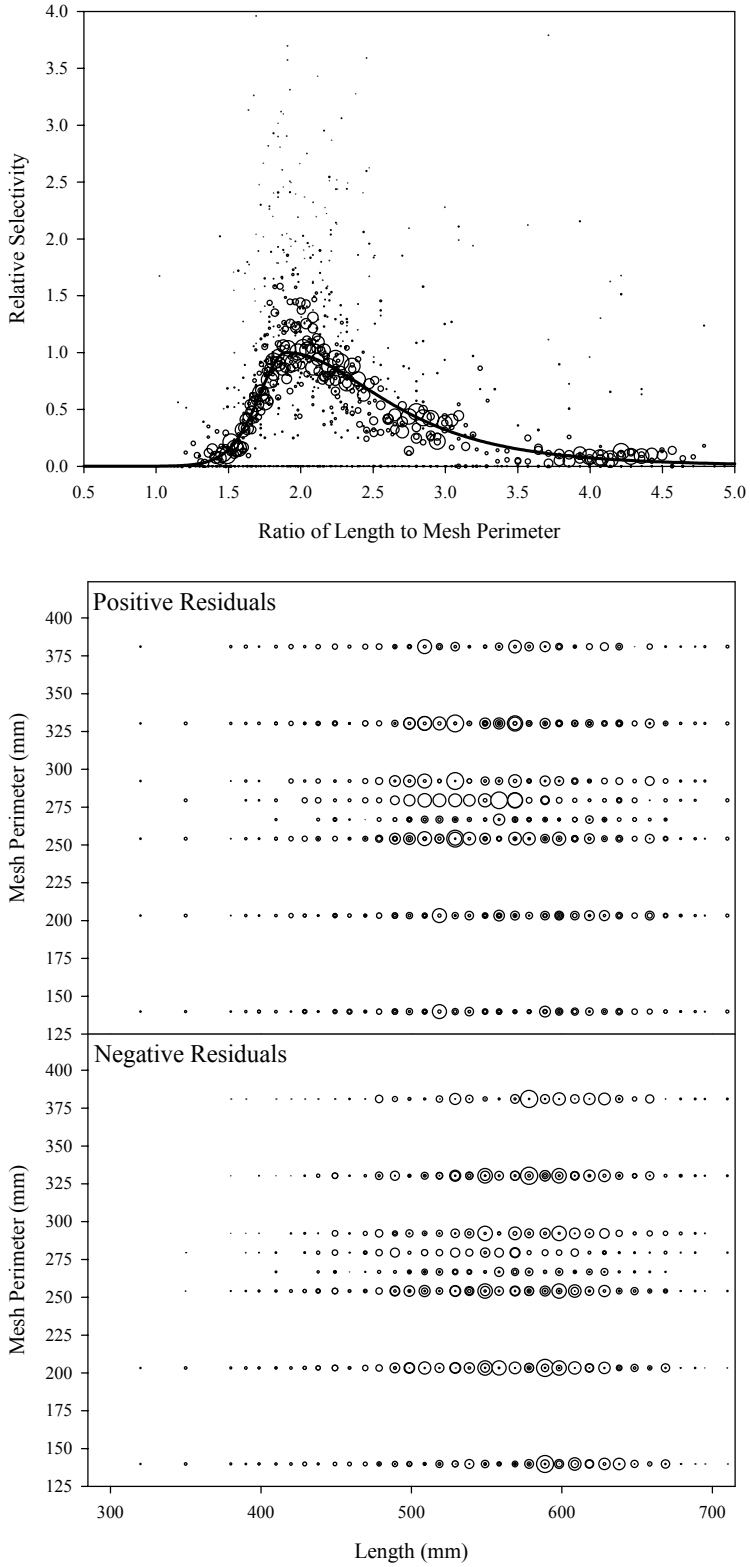

Figure B5.31. Plots of CPUE data scaled to a net selectivity model (top) and CPUE residuals (bottom); coho salmon data and Model 31.

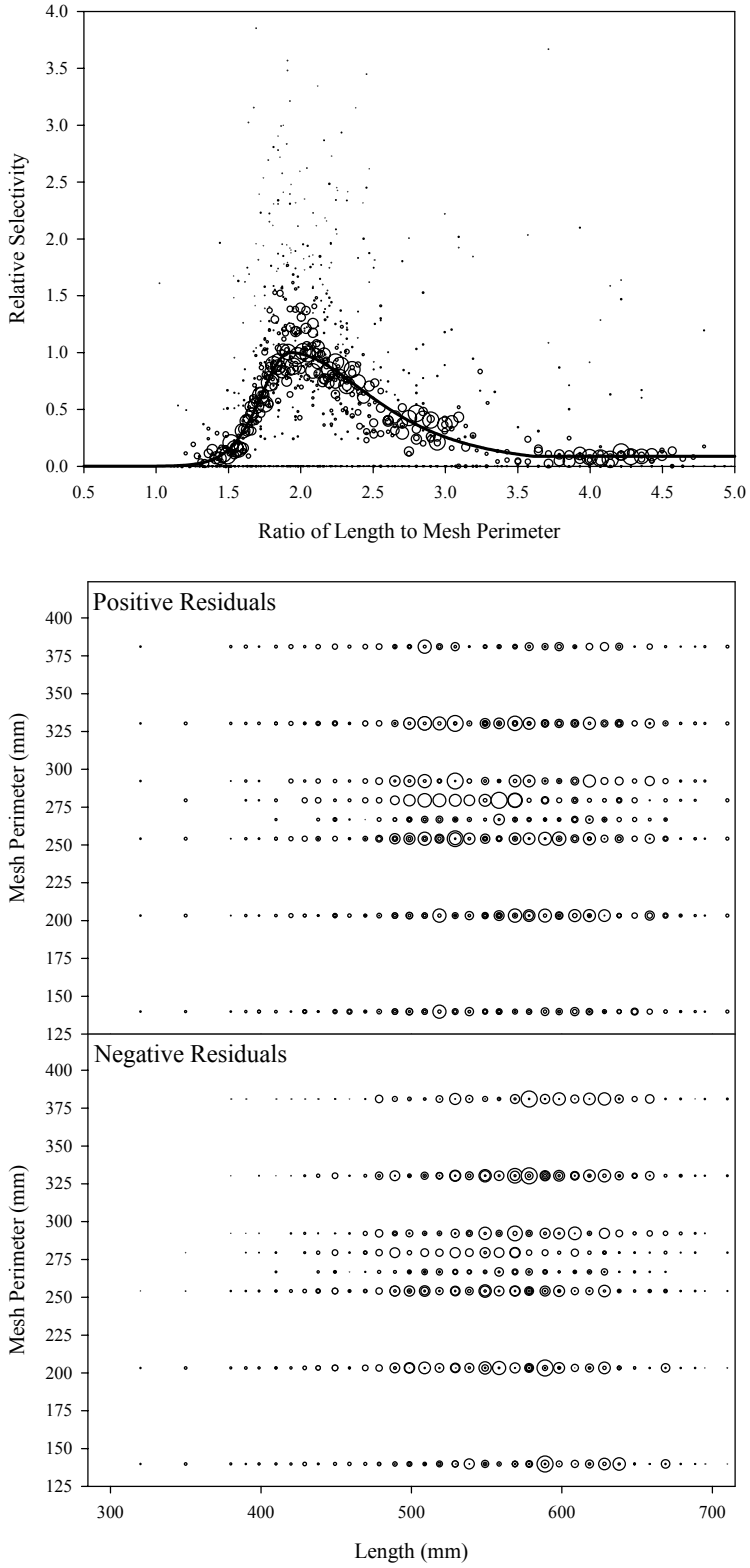

Figure B5.32. Plots of CPUE data scaled to a net selectivity model (top) and CPUE residuals (bottom); coho salmon data and Model 32.

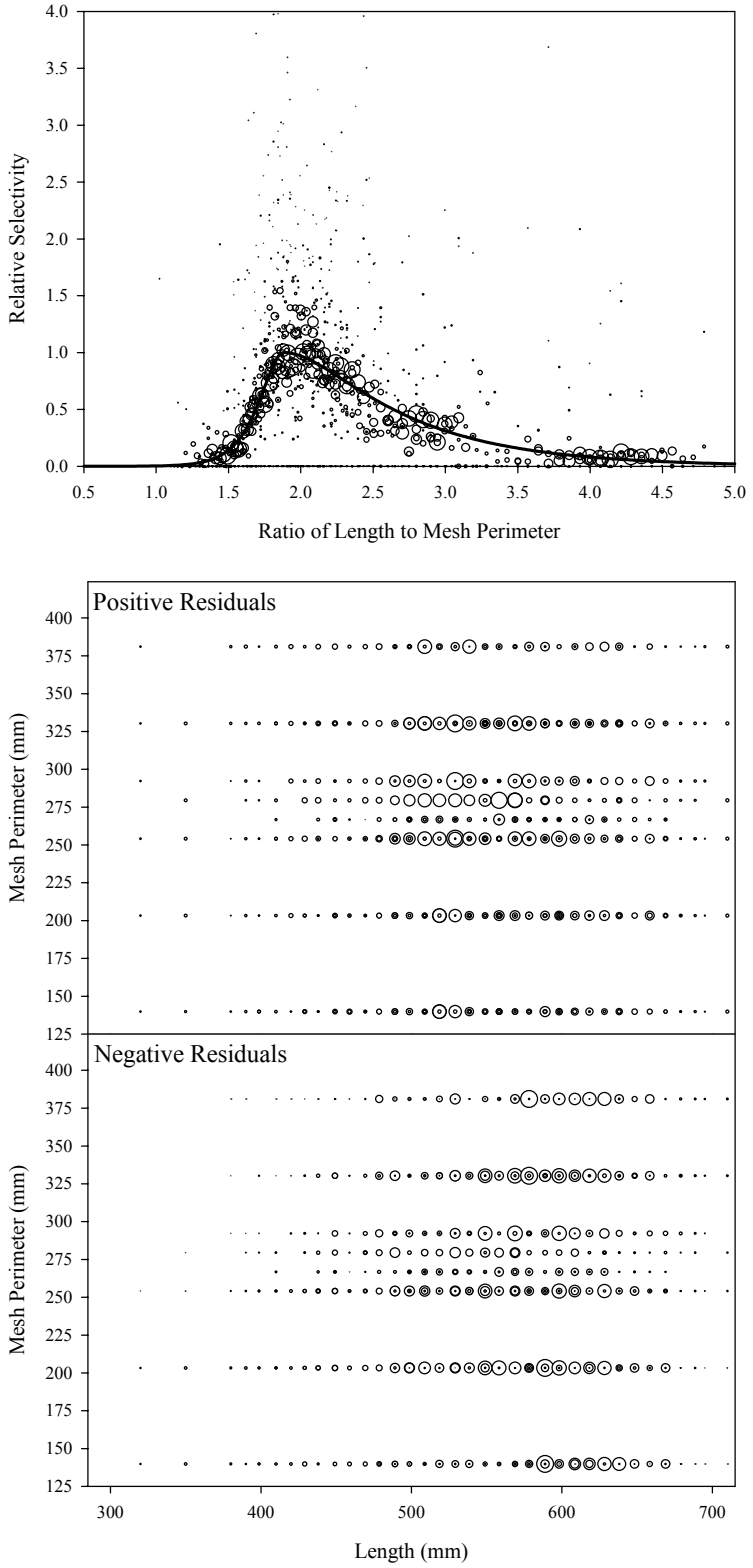

Figure B5.33. Plots of CPUE data scaled to a net selectivity model (top) and CPUE residuals (bottom); coho salmon data and Model 33.

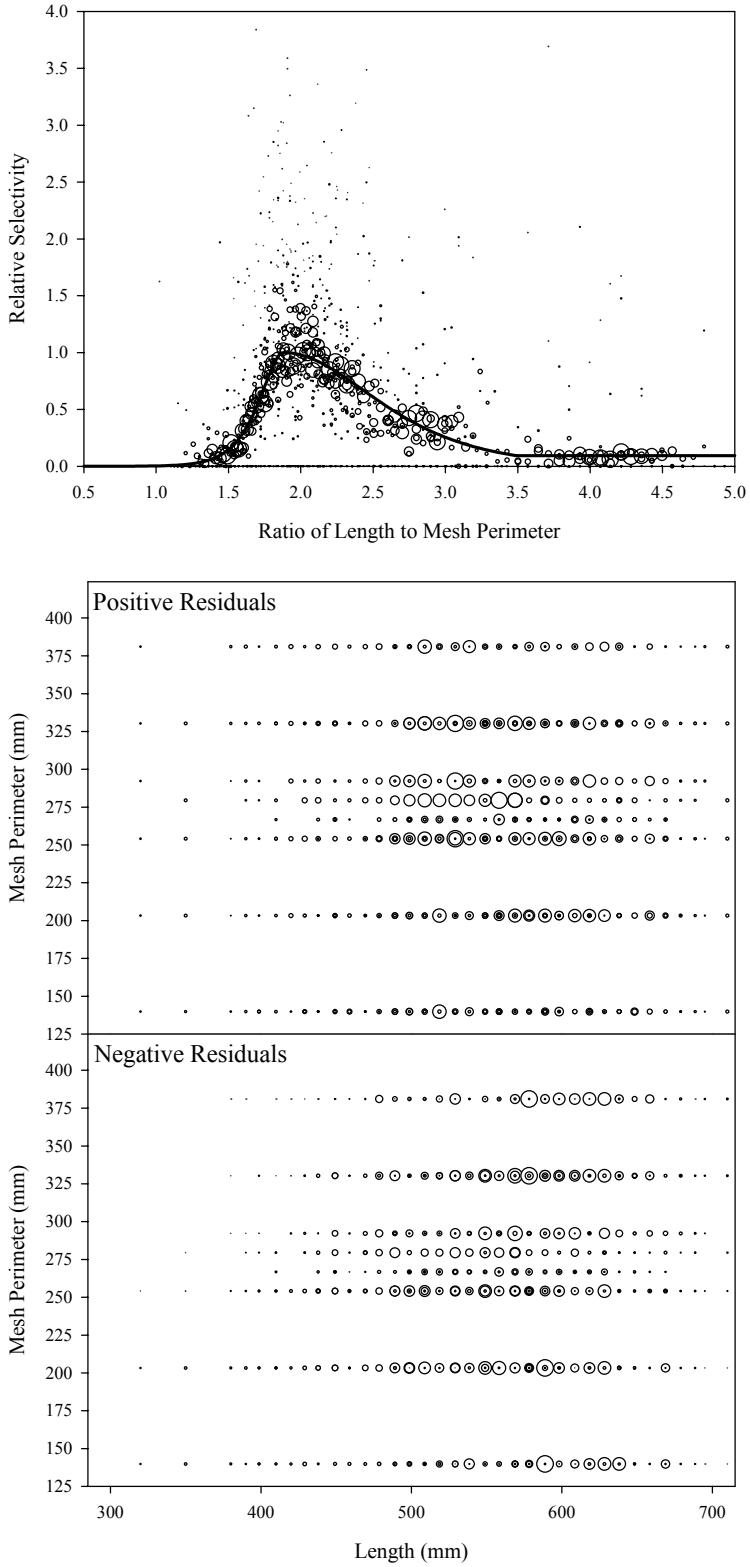

Figure B5.34. Plots of CPUE data scaled to a net selectivity model (top) and CPUE residuals (bottom); coho salmon data and Model 34.

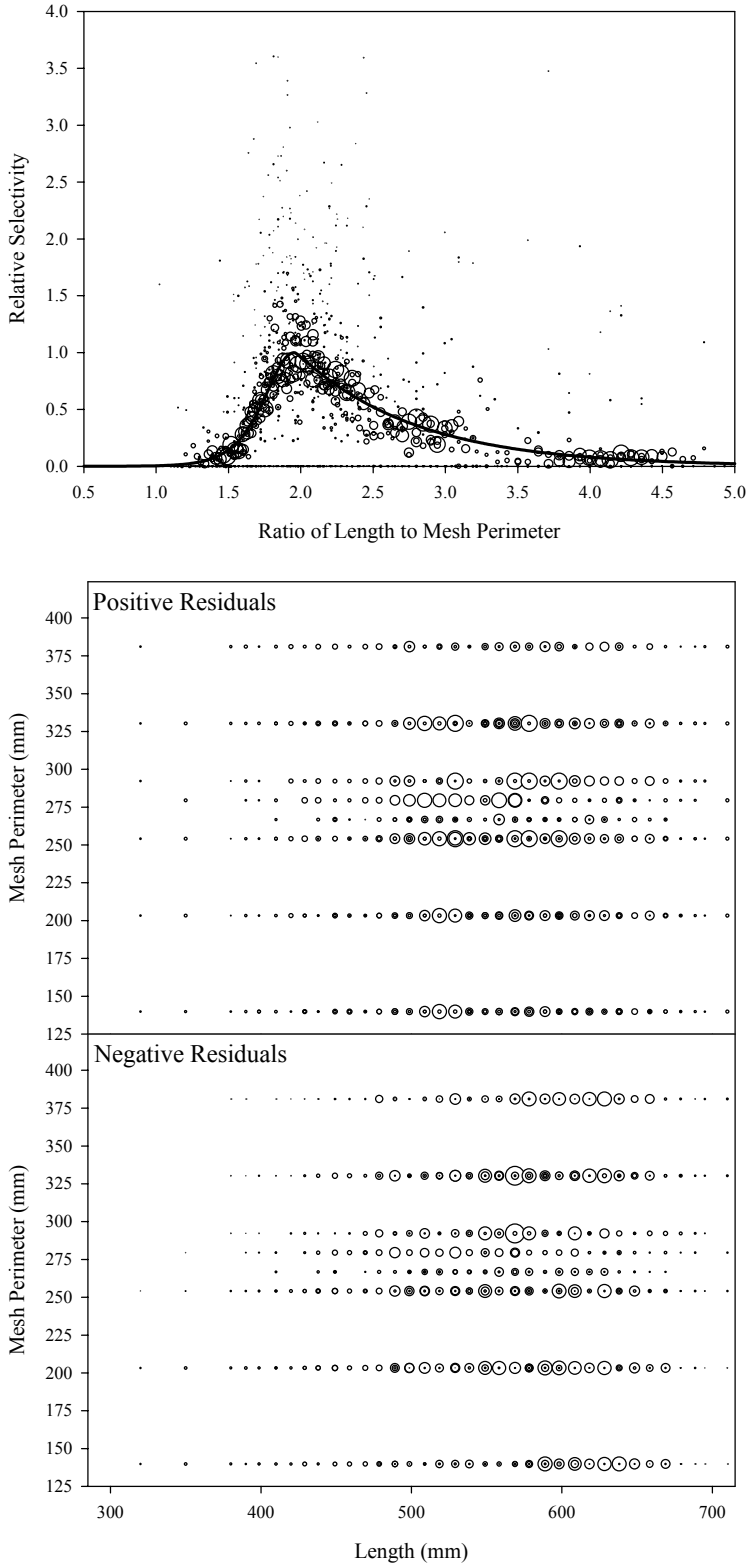

Figure B5.35. Plots of CPUE data scaled to a net selectivity model (top) and CPUE residuals (bottom); coho salmon data and Model 35.

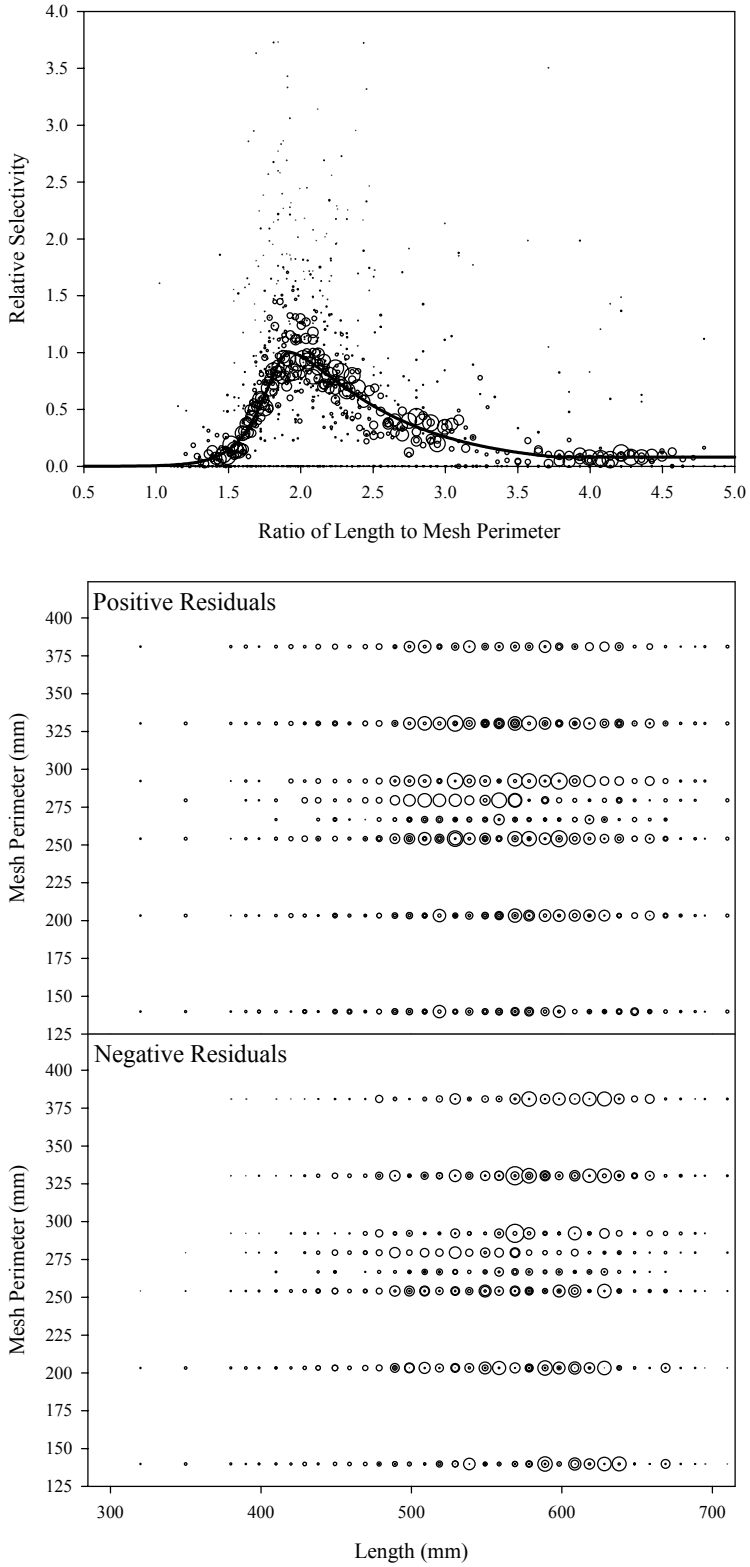

Figure B5.36. Plots of CPUE data scaled to a net selectivity model (top) and CPUE residuals (bottom); coho salmon data and Model 36.

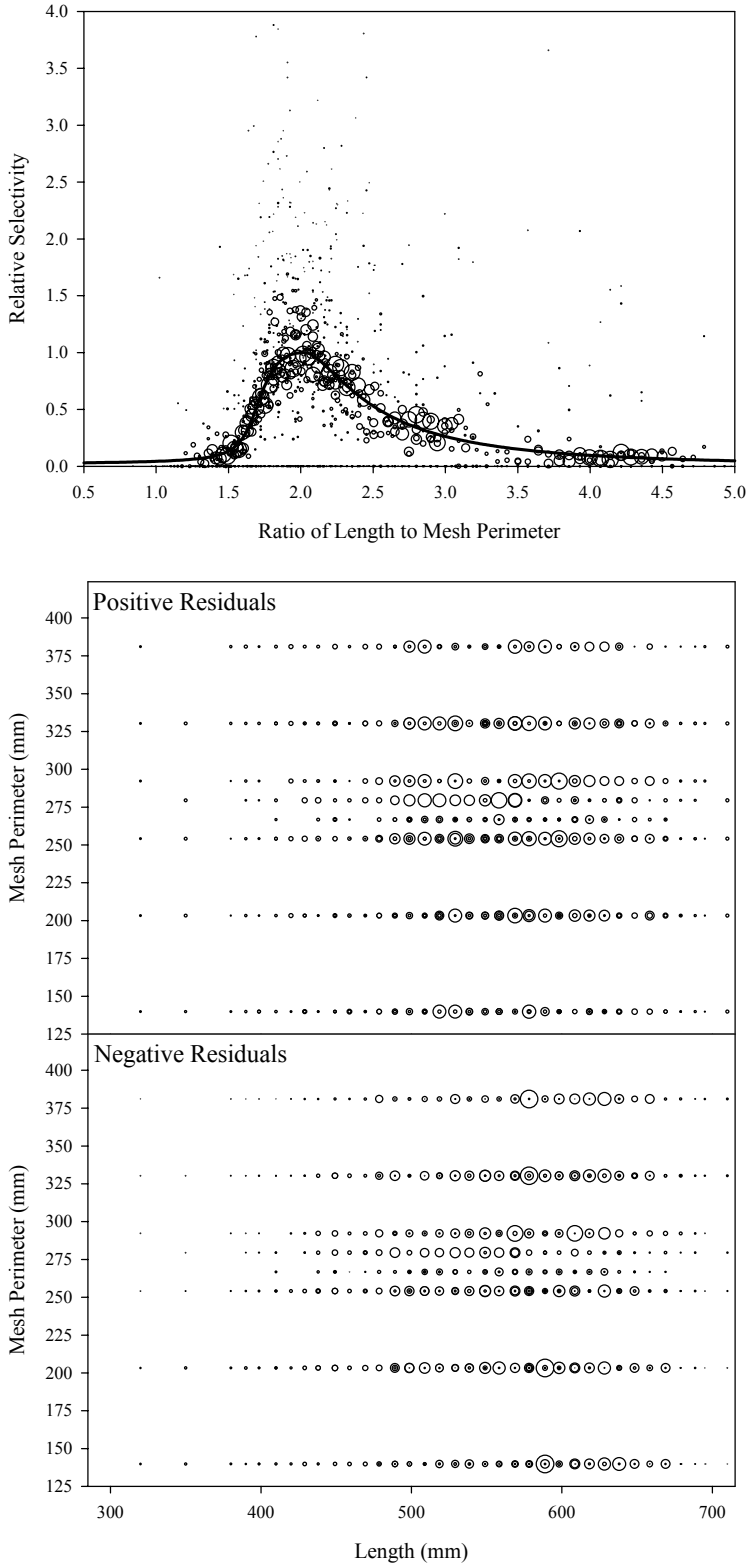

Figure B5.37. Plots of CPUE data scaled to a net selectivity model (top) and CPUE residuals (bottom); coho salmon data and Model 37.

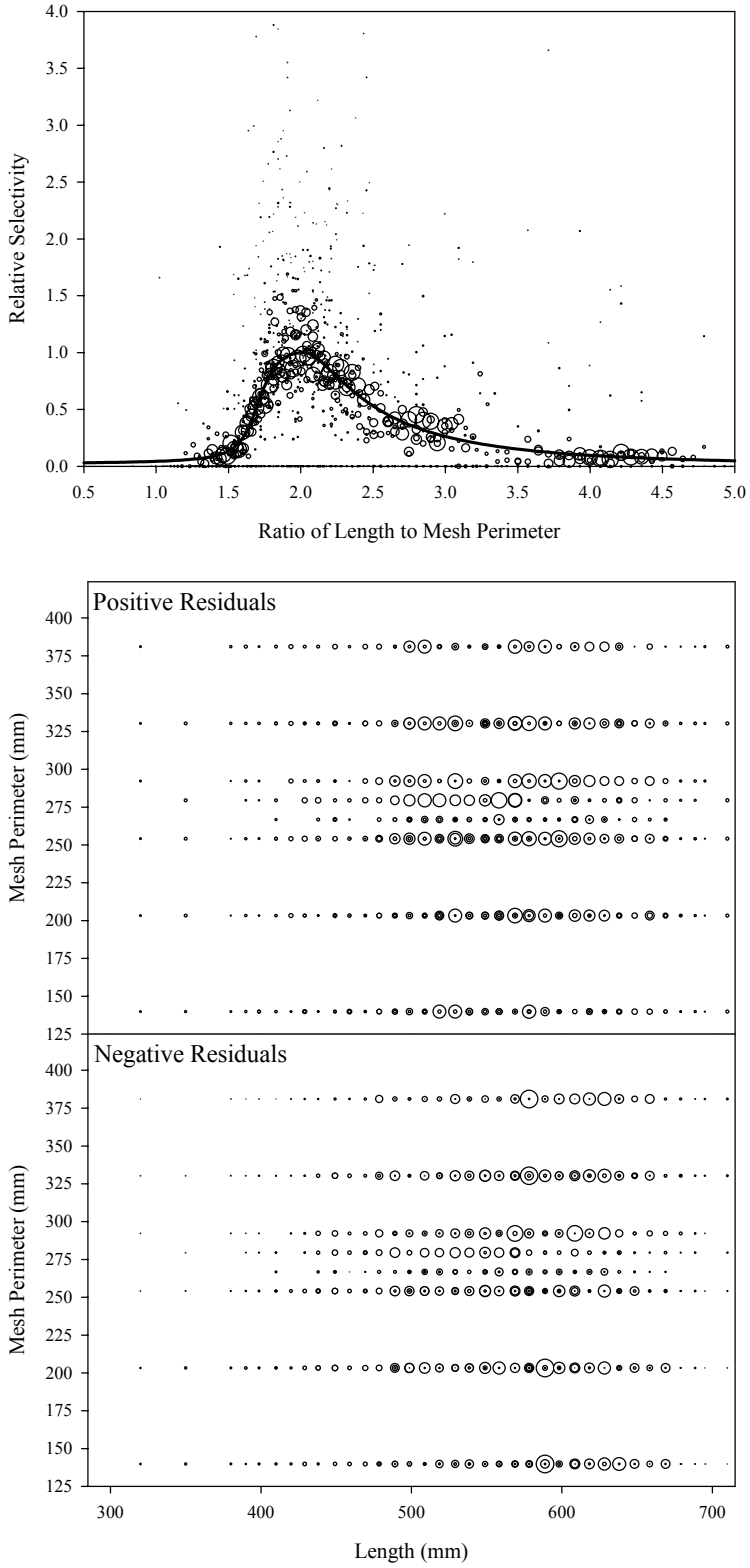

Figure B5.38. Plots of CPUE data scaled to a net selectivity model (top) and CPUE residuals (bottom); coho salmon data and Model 38.

Appendix B6
Broad Whitefish Diagnostic Plots
Figure B6.1 to Figure B6.38

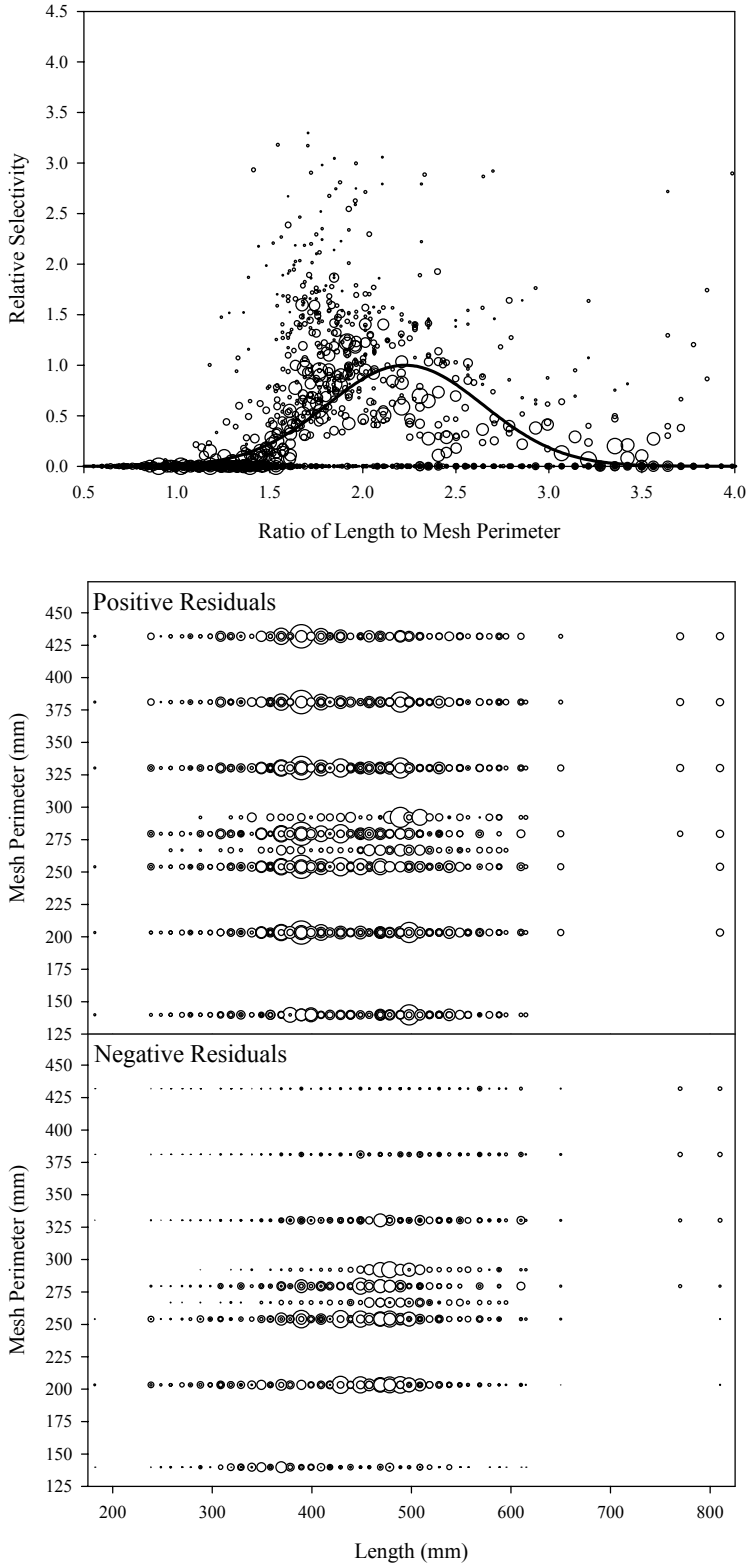

Figure B6.1. Plots of CPUE data scaled to a net selectivity model (top) and CPUE residuals (bottom); broad whitefish data and Model 1.

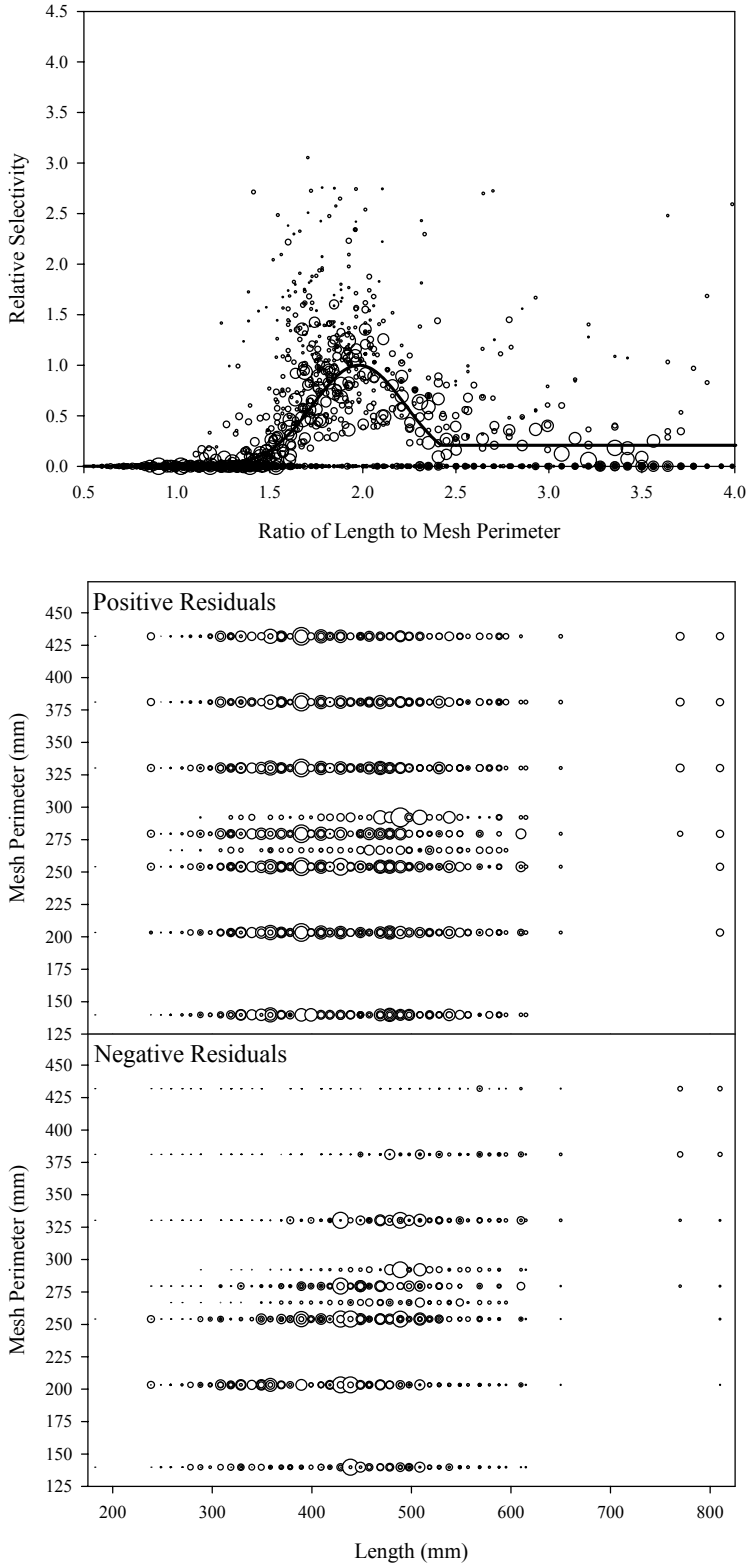

Figure B6.2. Plots of CPUE data scaled to a net selectivity model (top) and CPUE residuals (bottom); broad whitefish data and Model 2.

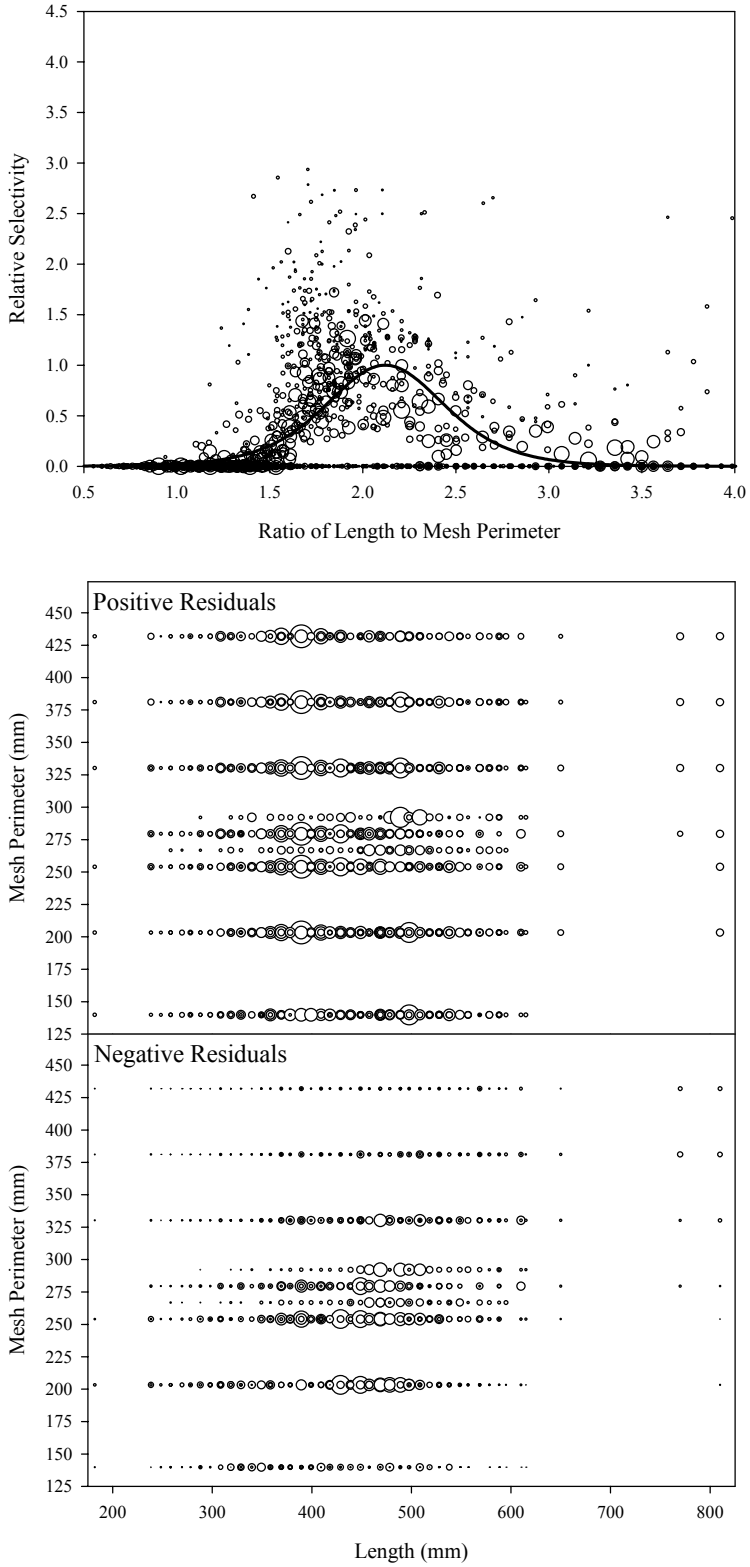

Figure B6.3. Plots of CPUE data scaled to a net selectivity model (top) and CPUE residuals (bottom); broad whitefish data and Model 3.

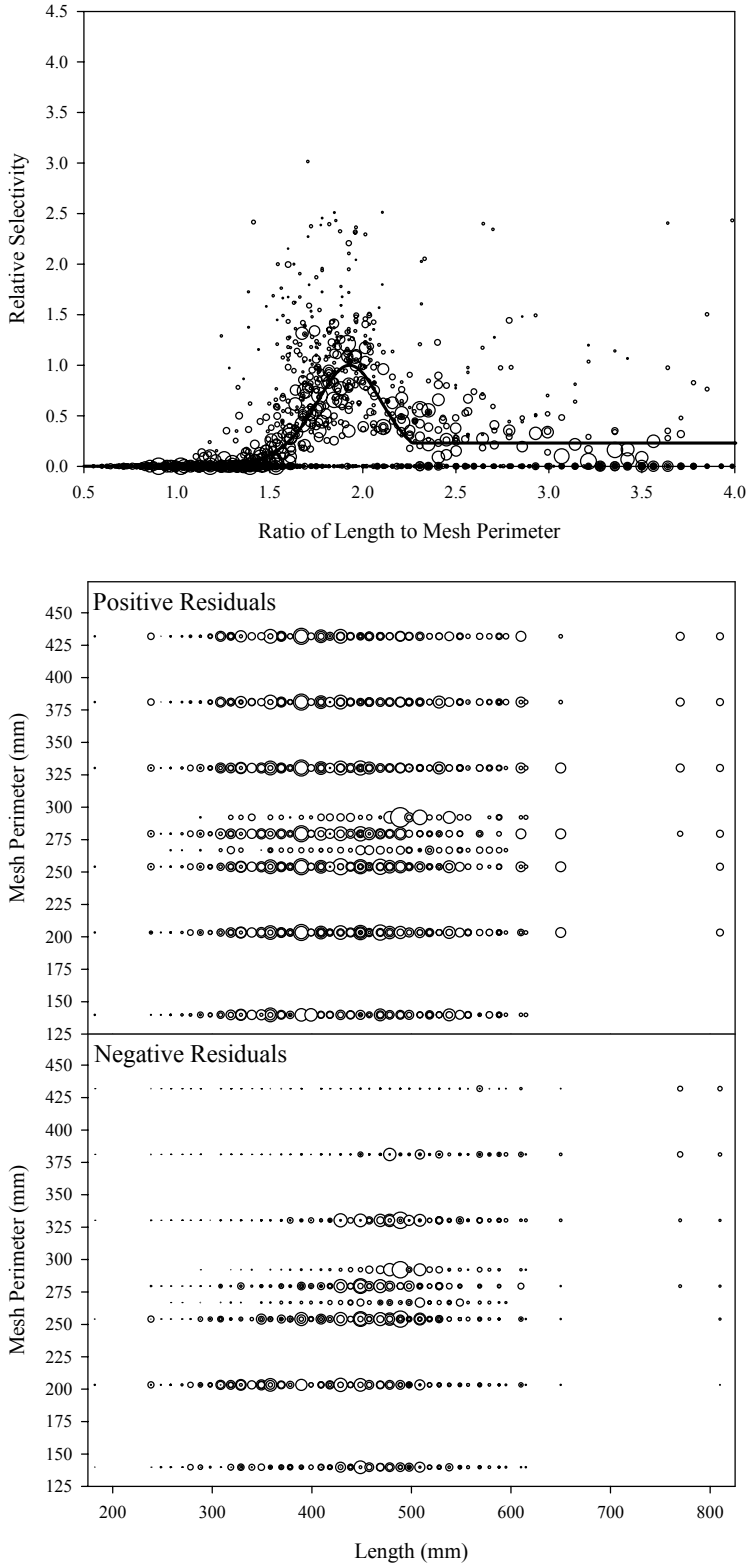

Figure B6.4. Plots of CPUE data scaled to a net selectivity model (top) and CPUE residuals (bottom); broad whitefish data and Model 4.

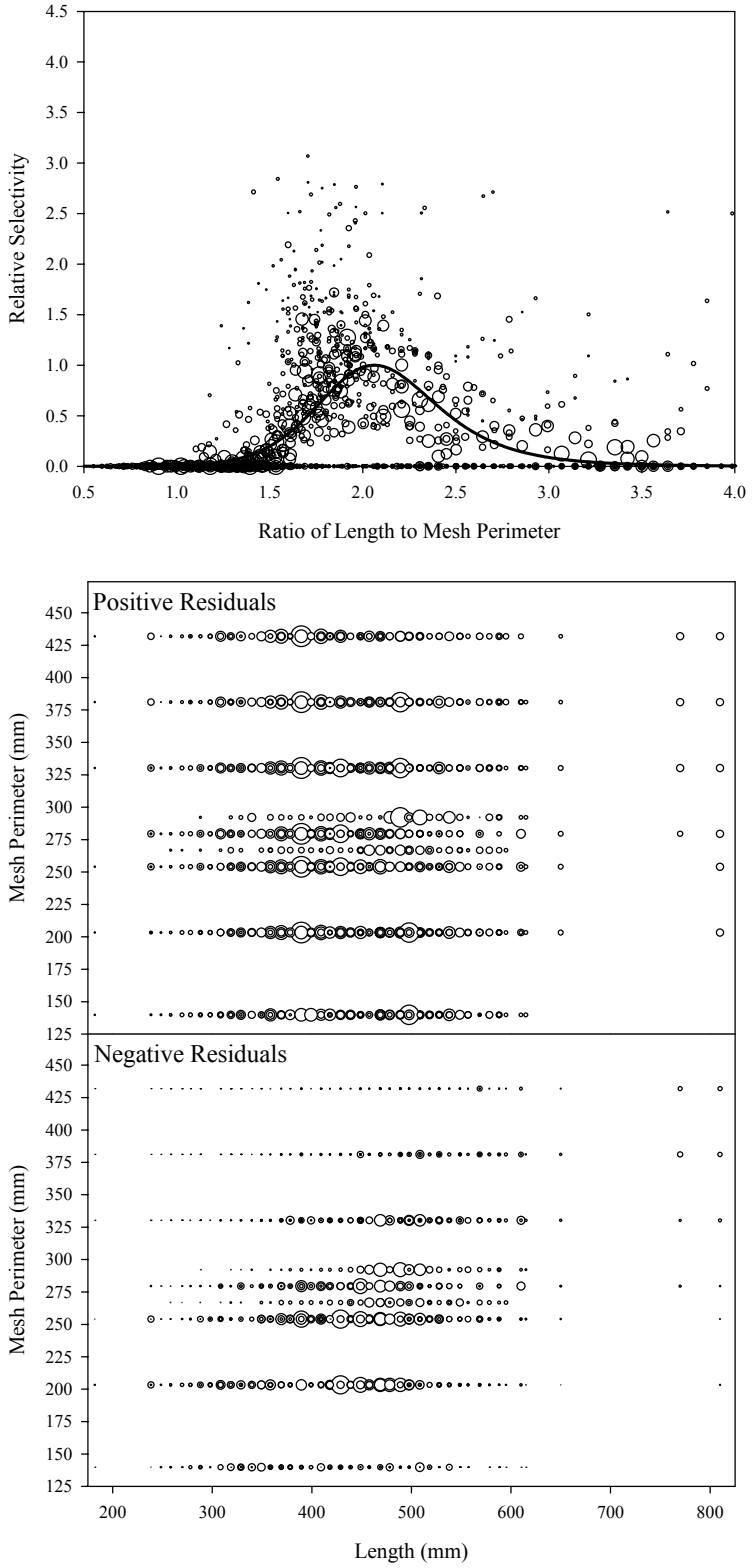

Figure B6.5. Plots of CPUE data scaled to a net selectivity model (top) and CPUE residuals (bottom); broad whitefish data and Model 5.

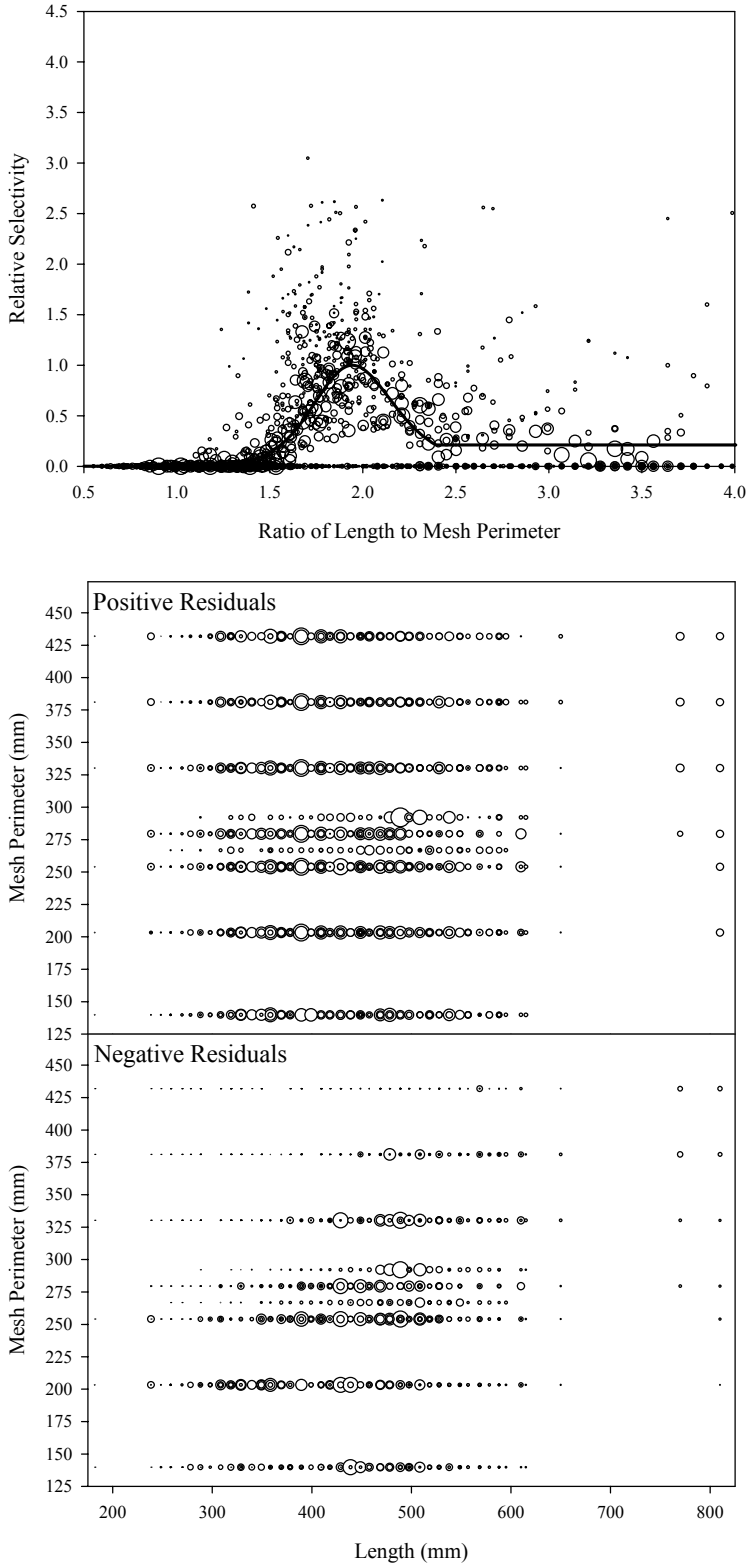

Figure B6.6. Plots of CPUE data scaled to a net selectivity model (top) and CPUE residuals (bottom); broad whitefish data and Model 6.

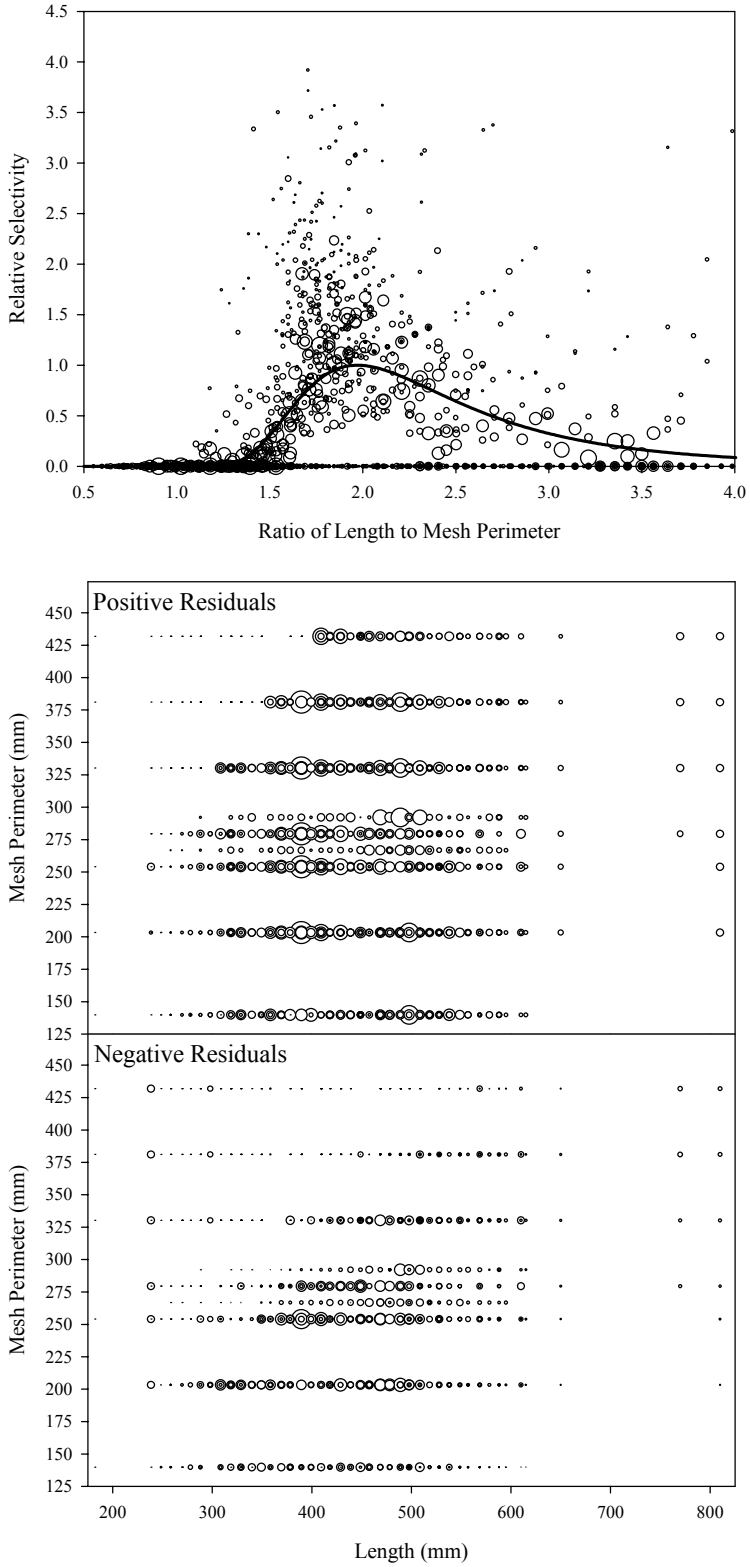

Figure B6.7. Plots of CPUE data scaled to a net selectivity model (top) and CPUE residuals (bottom); broad whitefish data and Model 7.

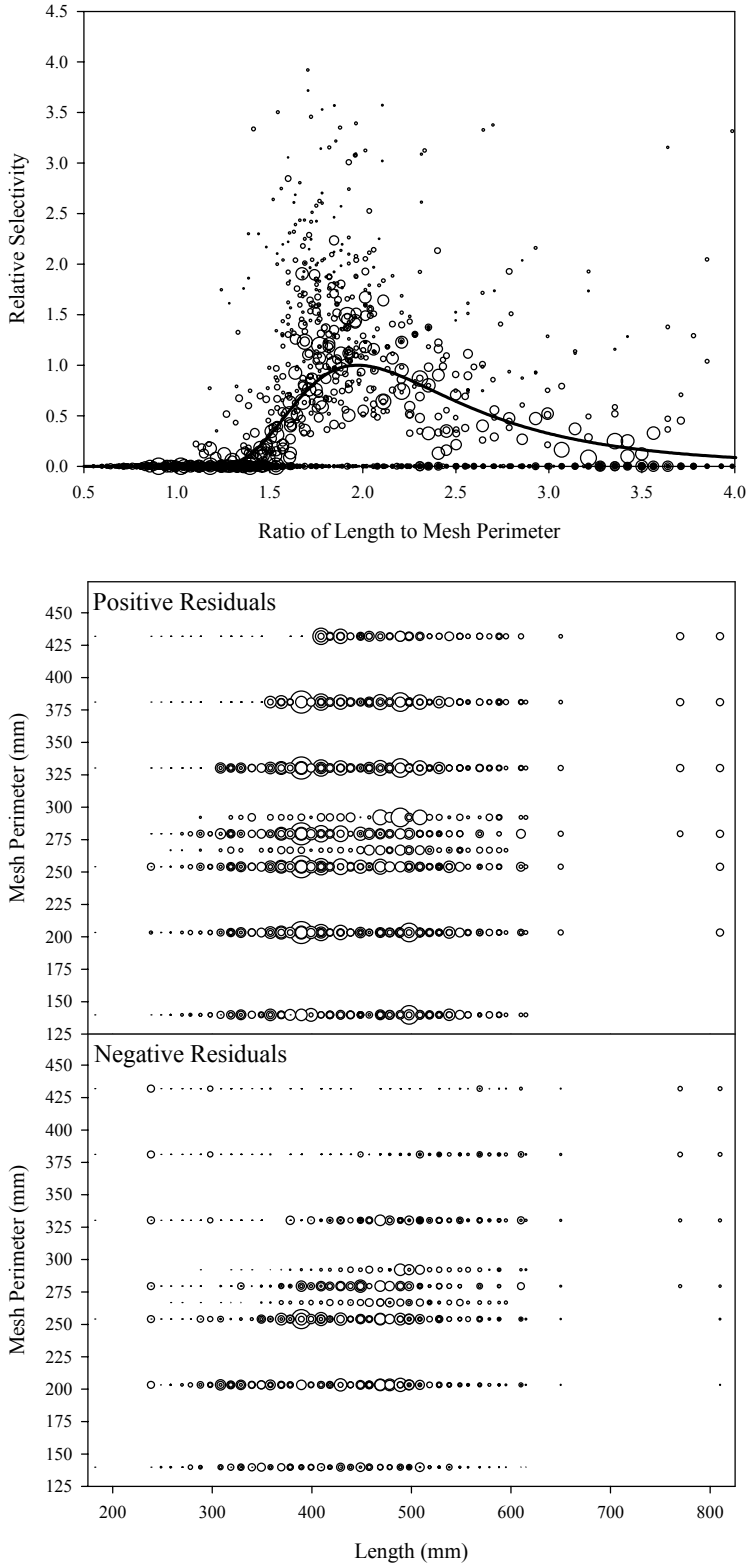

Figure B6.8. Plots of CPUE data scaled to a net selectivity model (top) and CPUE residuals (bottom); broad whitefish data and Model 8.

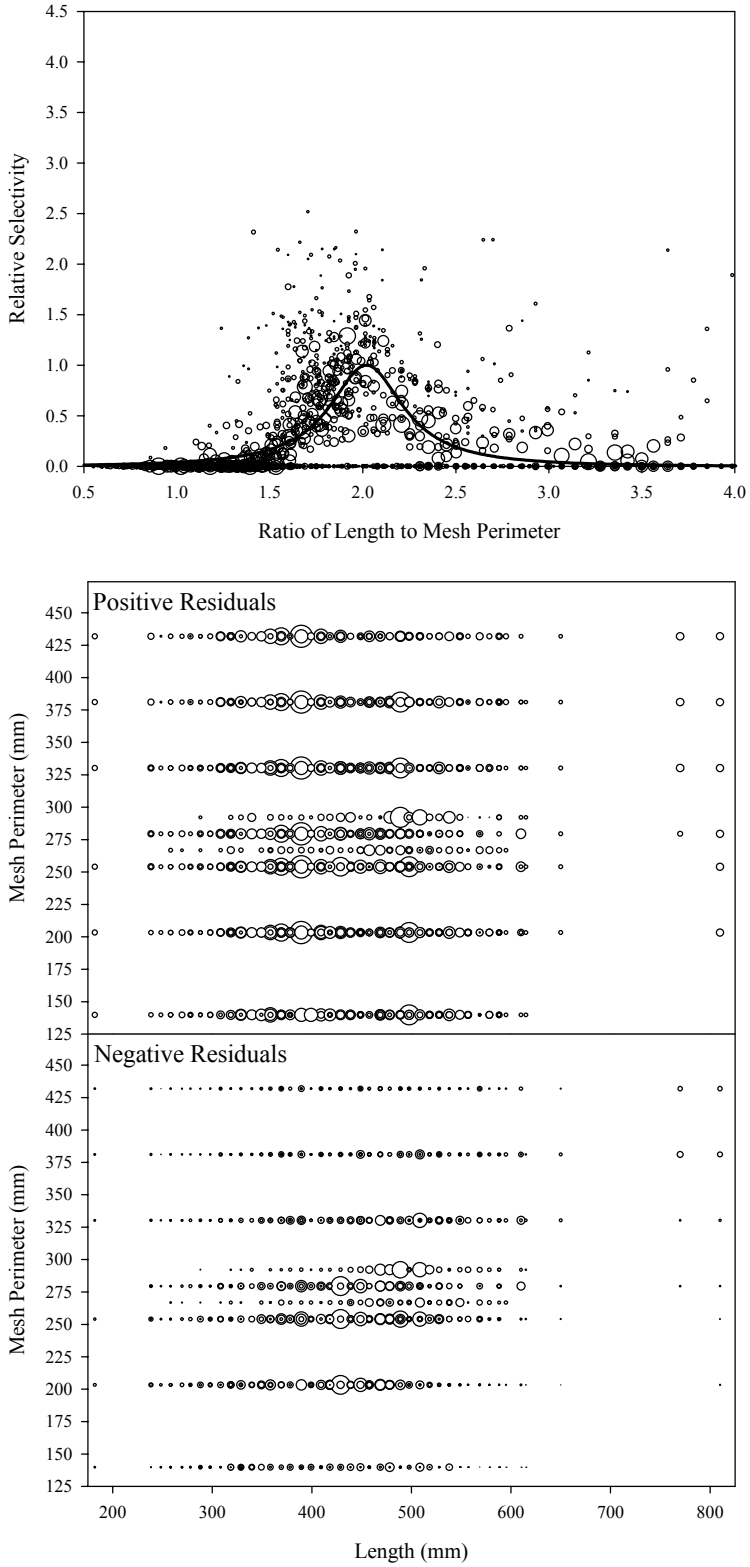

Figure B6.9. Plots of CPUE data scaled to a net selectivity model (top) and CPUE residuals (bottom); broad whitefish data and Model 9.

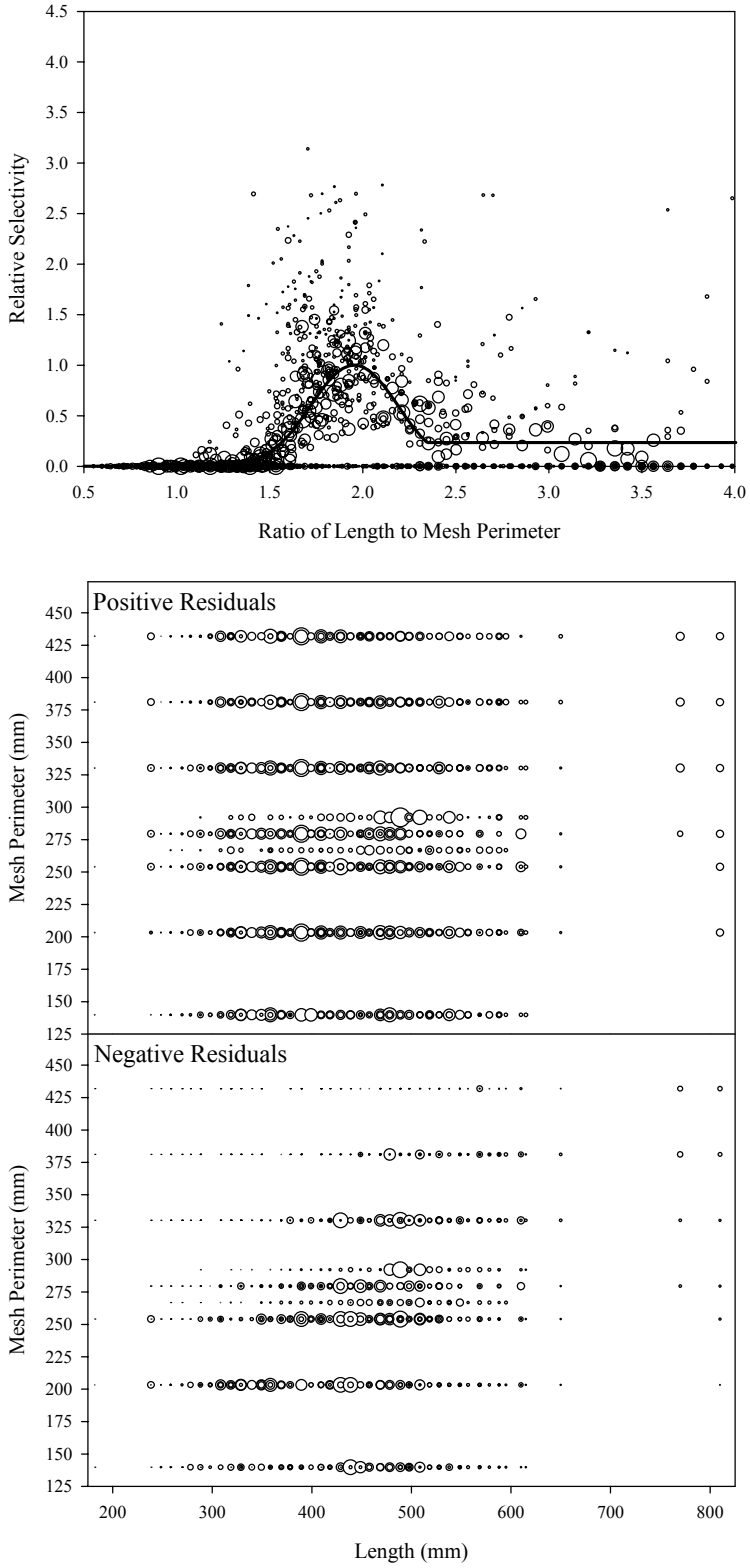

Figure B6.10. Plots of CPUE data scaled to a net selectivity model (top) and CPUE residuals (bottom); broad whitefish data and Model 10.

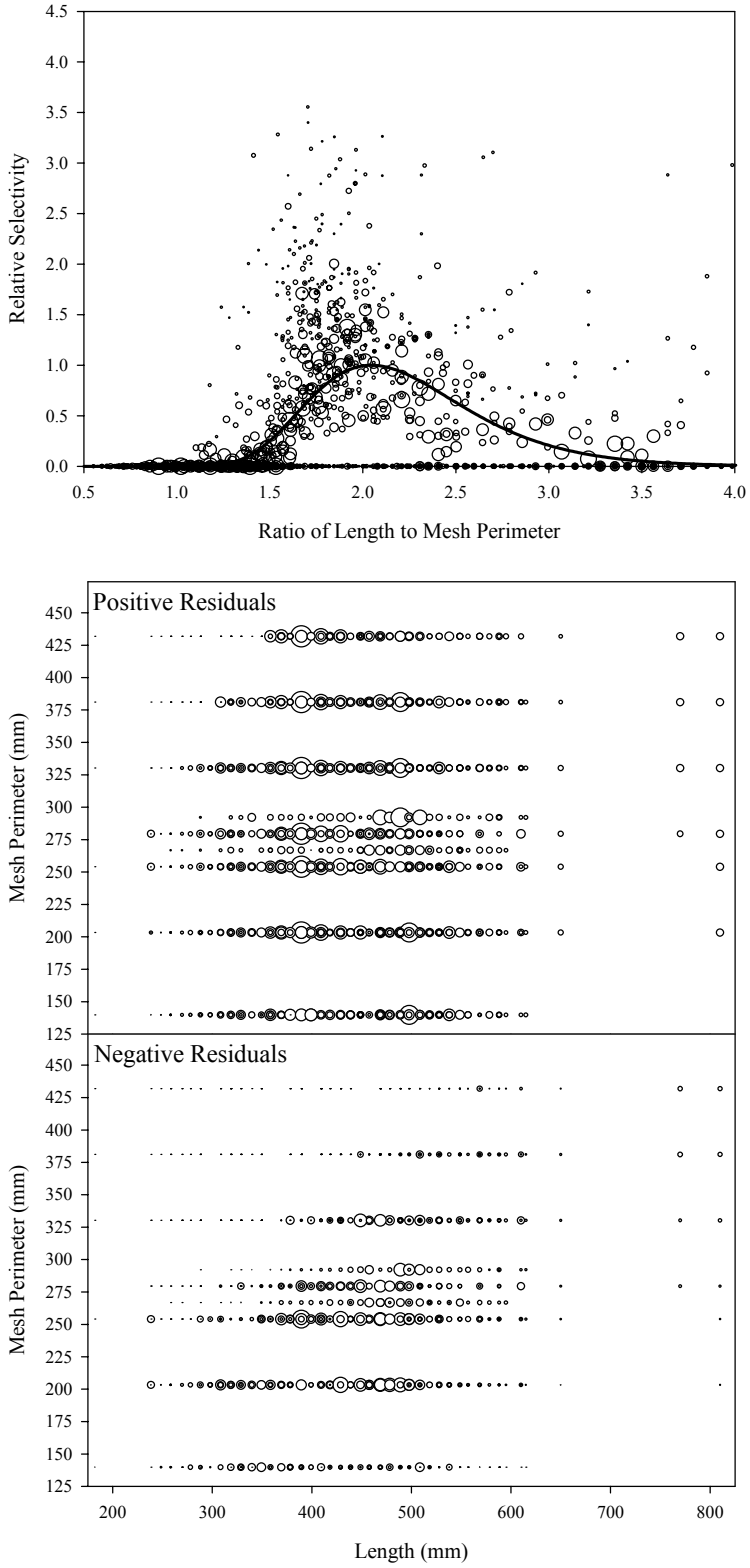

Figure B6.11. Plots of CPUE data scaled to a net selectivity model (top) and CPUE residuals (bottom); broad whitefish data and Model 11.

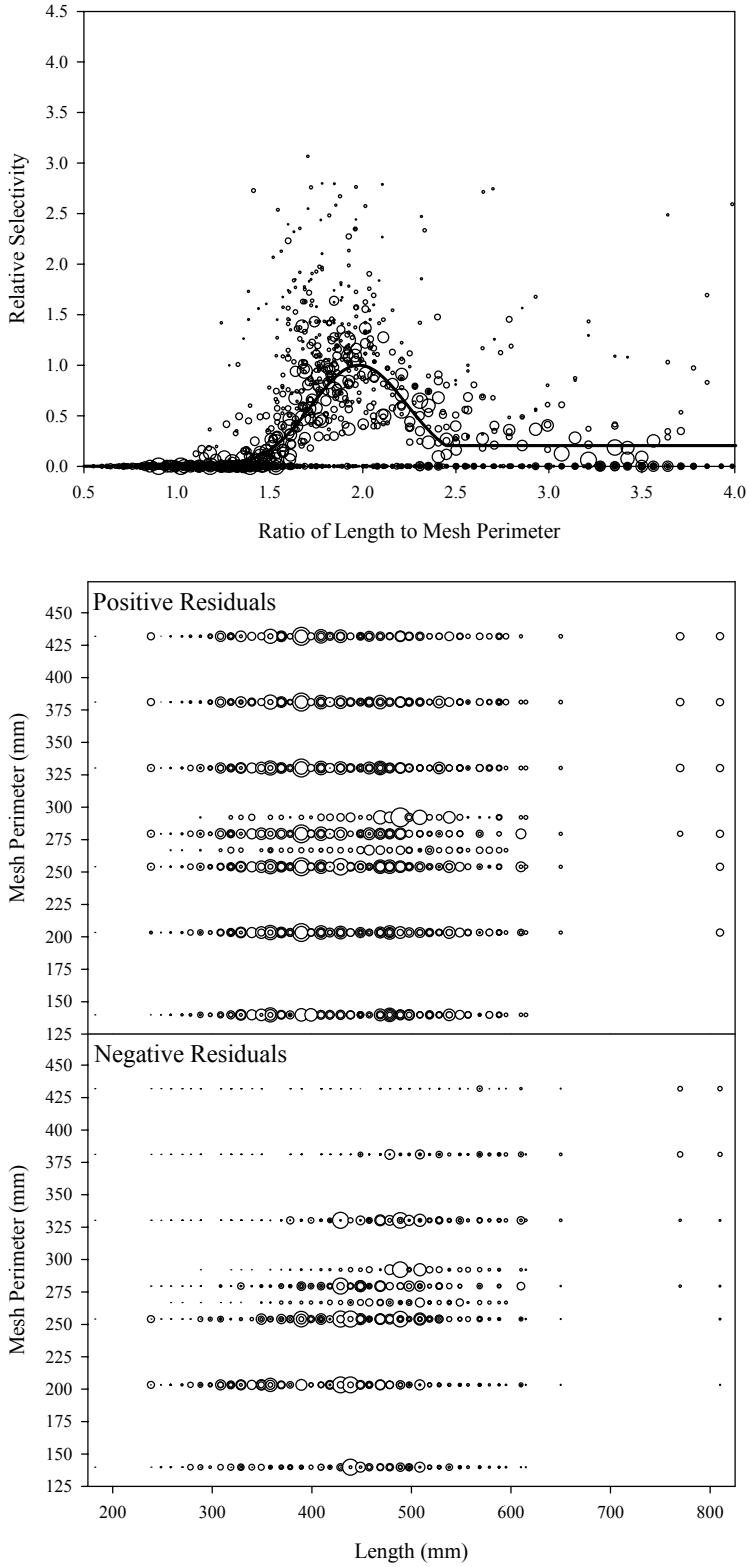

Figure B6.12. Plots of CPUE data scaled to a net selectivity model (top) and CPUE residuals (bottom); broad whitefish data and Model 12.

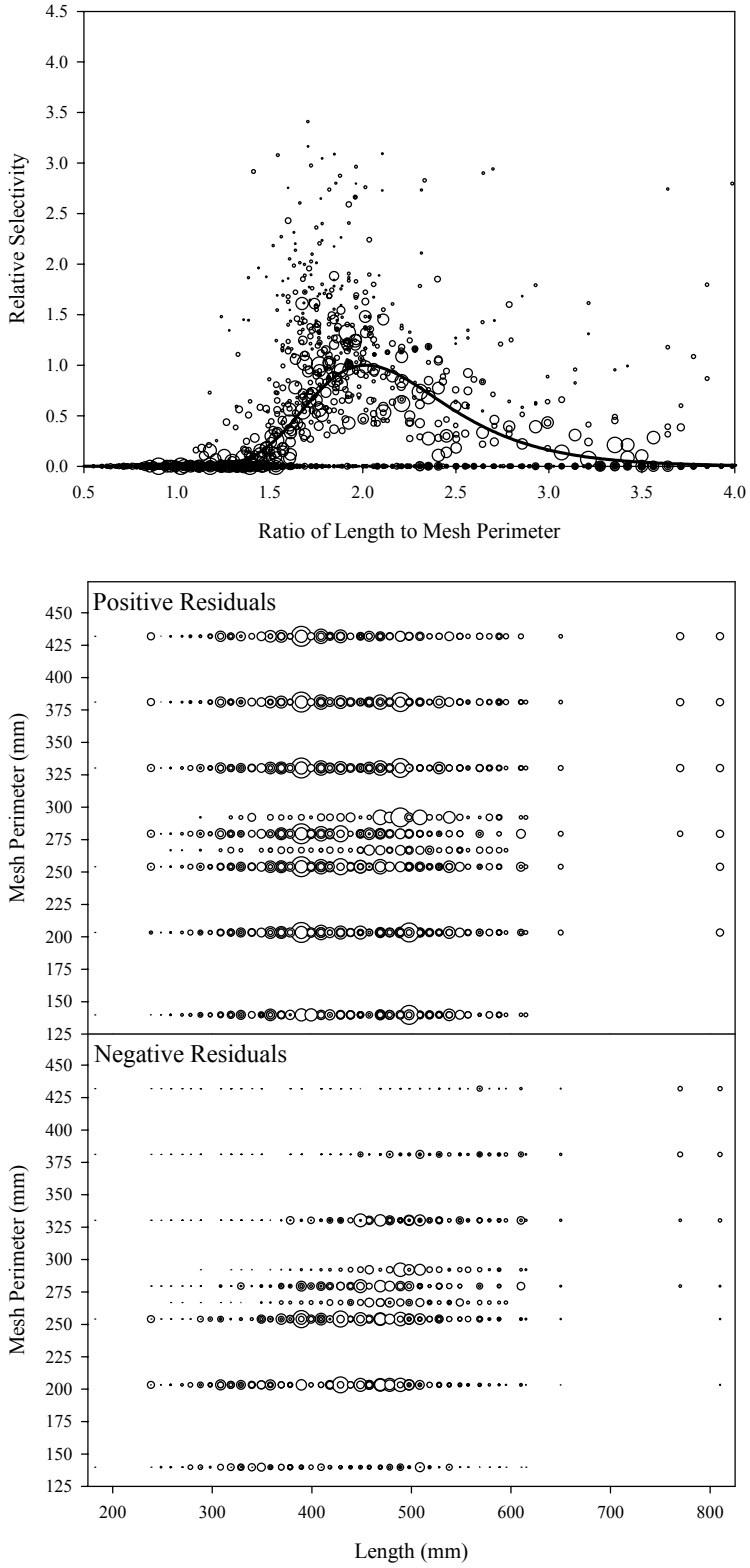

Figure B6.13. Plots of CPUE data scaled to a net selectivity model (top) and CPUE residuals (bottom); broad whitefish data and Model 13.

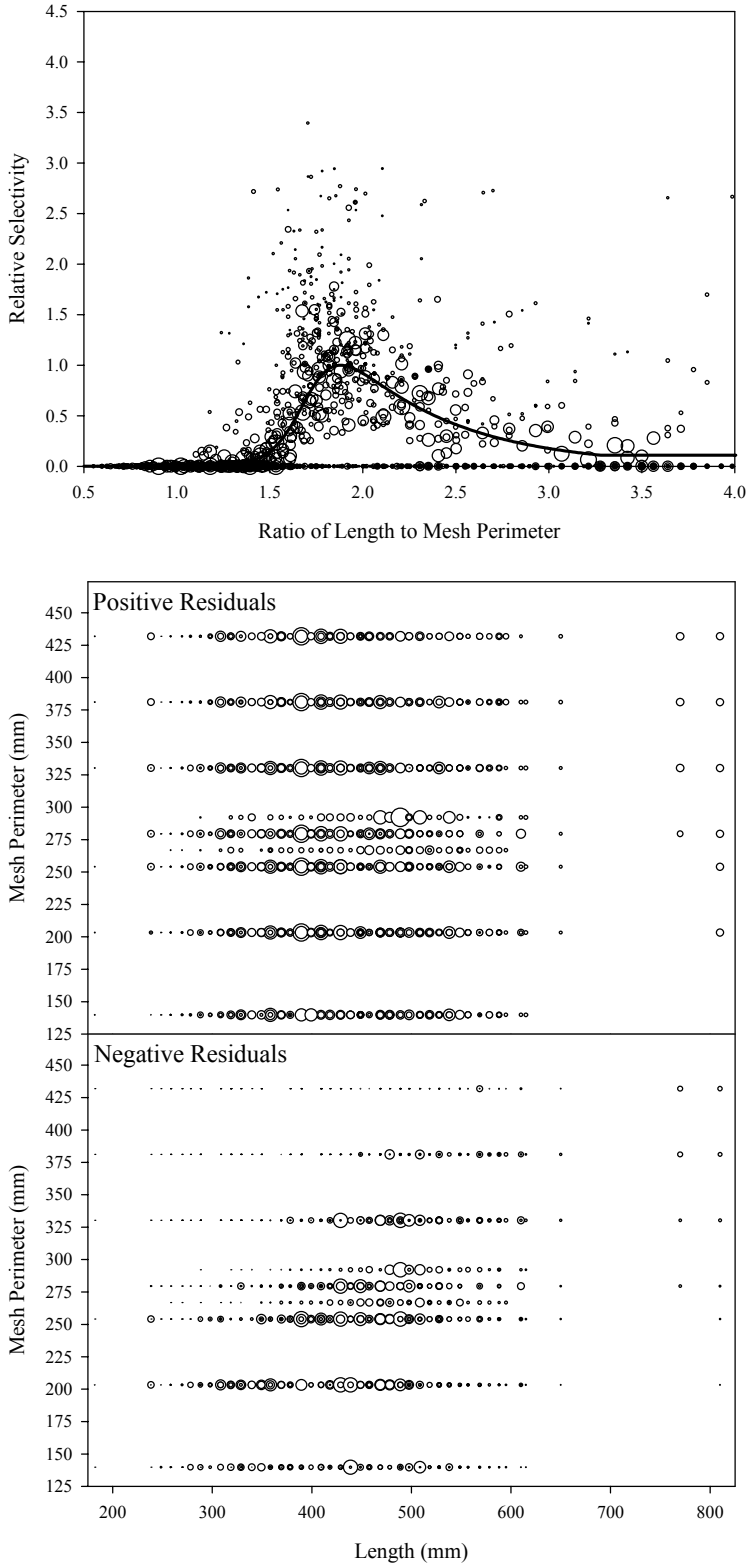

Figure B6.14. Plots of CPUE data scaled to a net selectivity model (top) and CPUE residuals (bottom); broad whitefish data and Model 14.

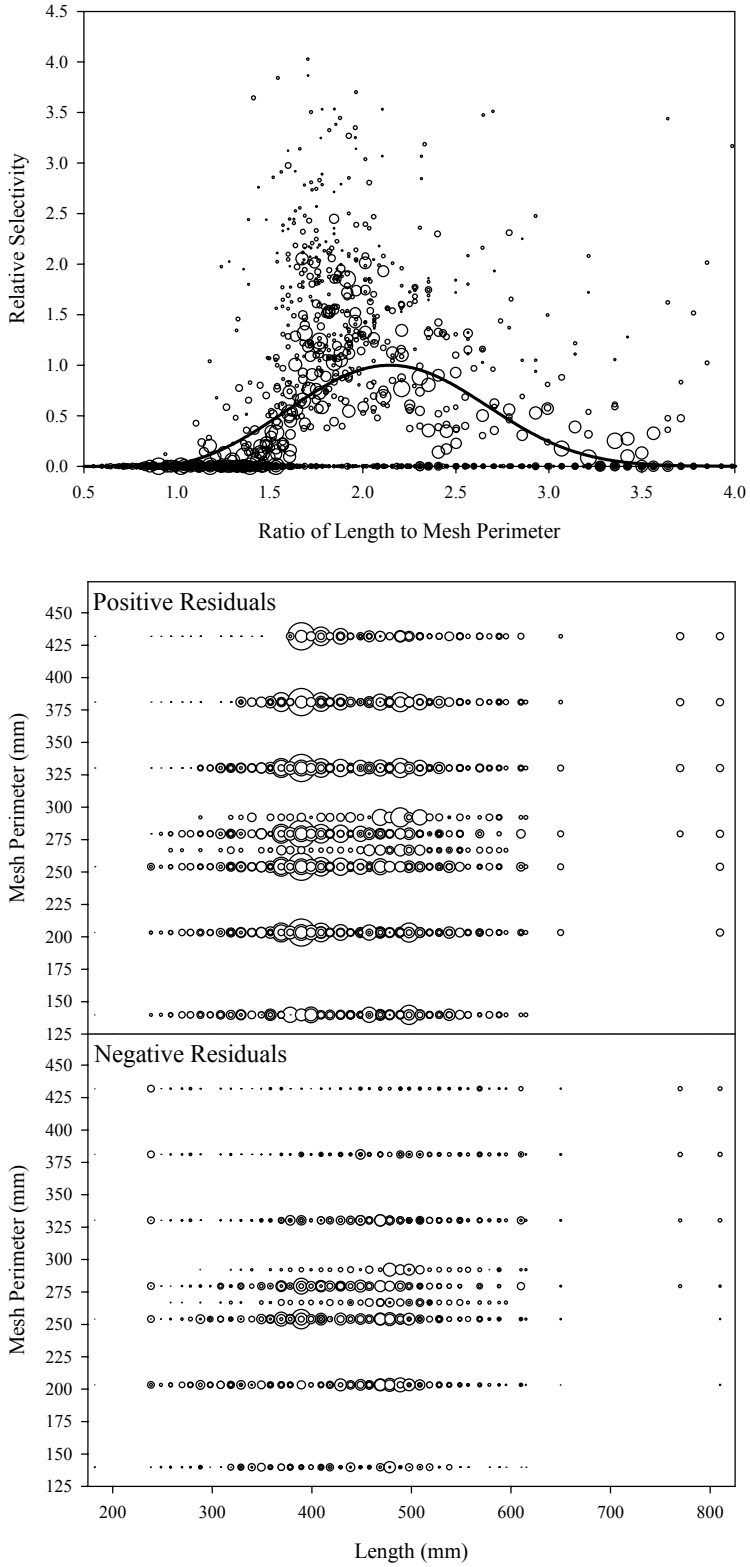

Figure B6.15. Plots of CPUE data scaled to a net selectivity model (top) and CPUE residuals (bottom); broad whitefish data and Model 15.

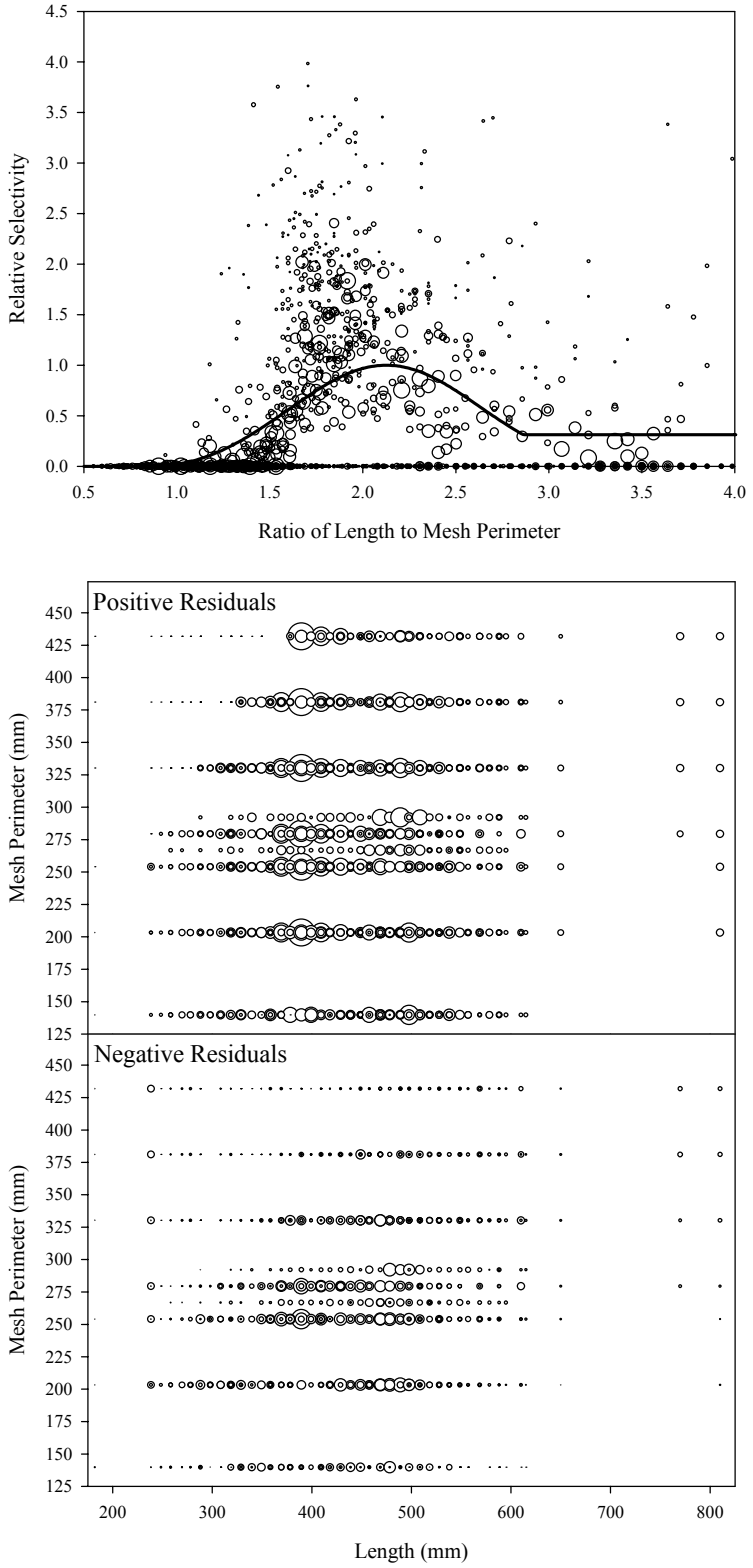

Figure B6.16. Plots of CPUE data scaled to a net selectivity model (top) and CPUE residuals (bottom); broad whitefish data and Model 16.

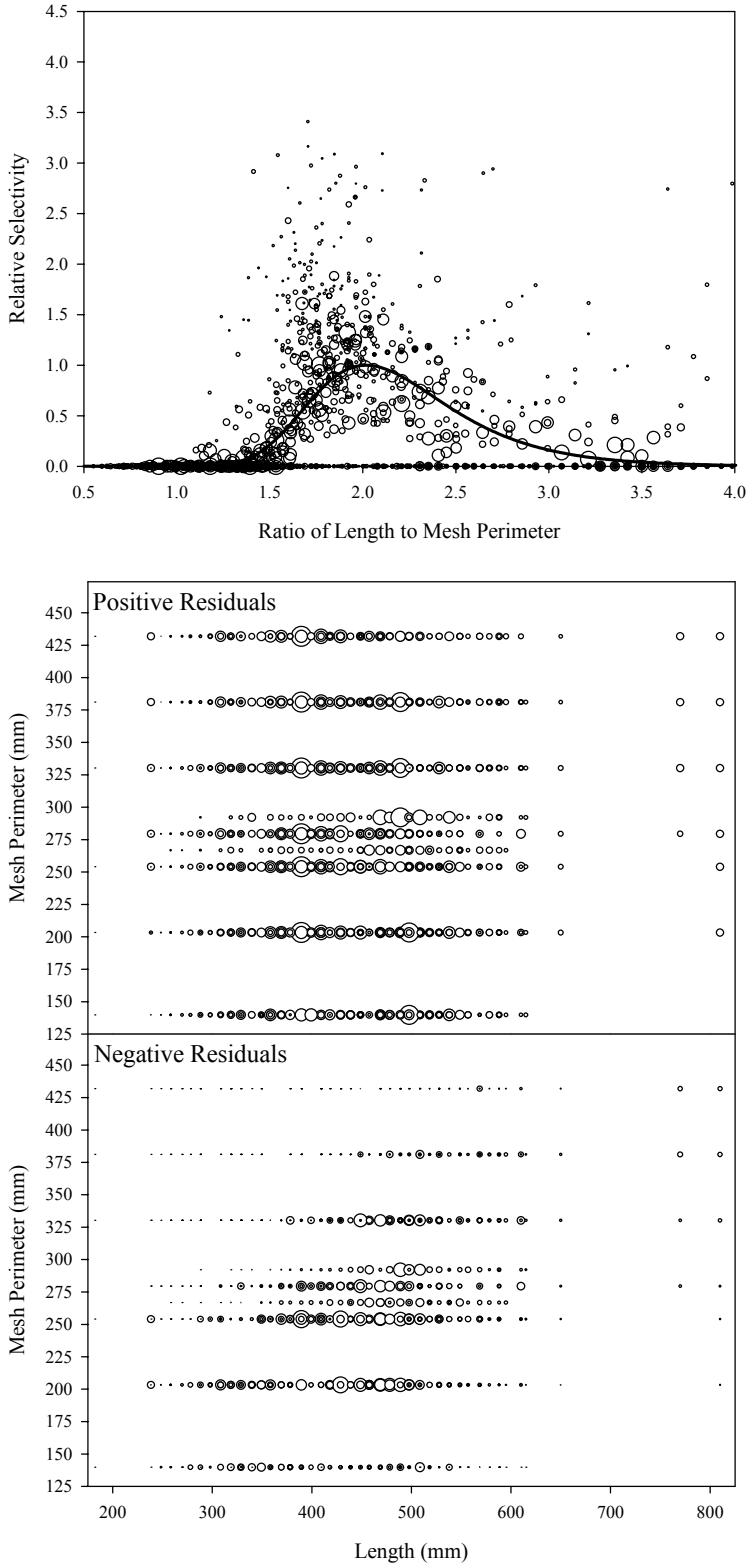

Figure B6.17. Plots of CPUE data scaled to a net selectivity model (top) and CPUE residuals (bottom); broad whitefish data and Model 17.

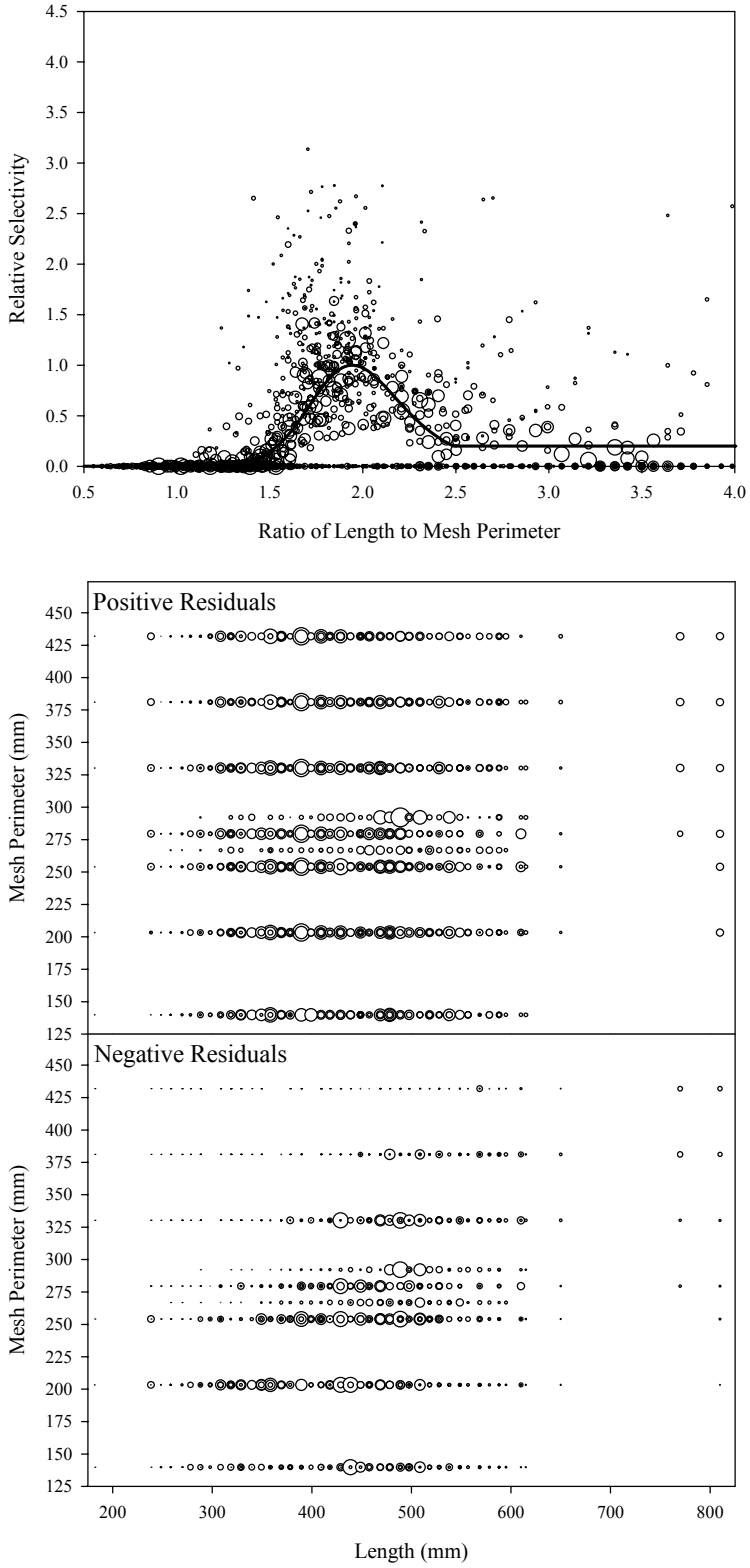

Figure B6.18. Plots of CPUE data scaled to a net selectivity model (top) and CPUE residuals (bottom); broad whitefish data and Model 18.

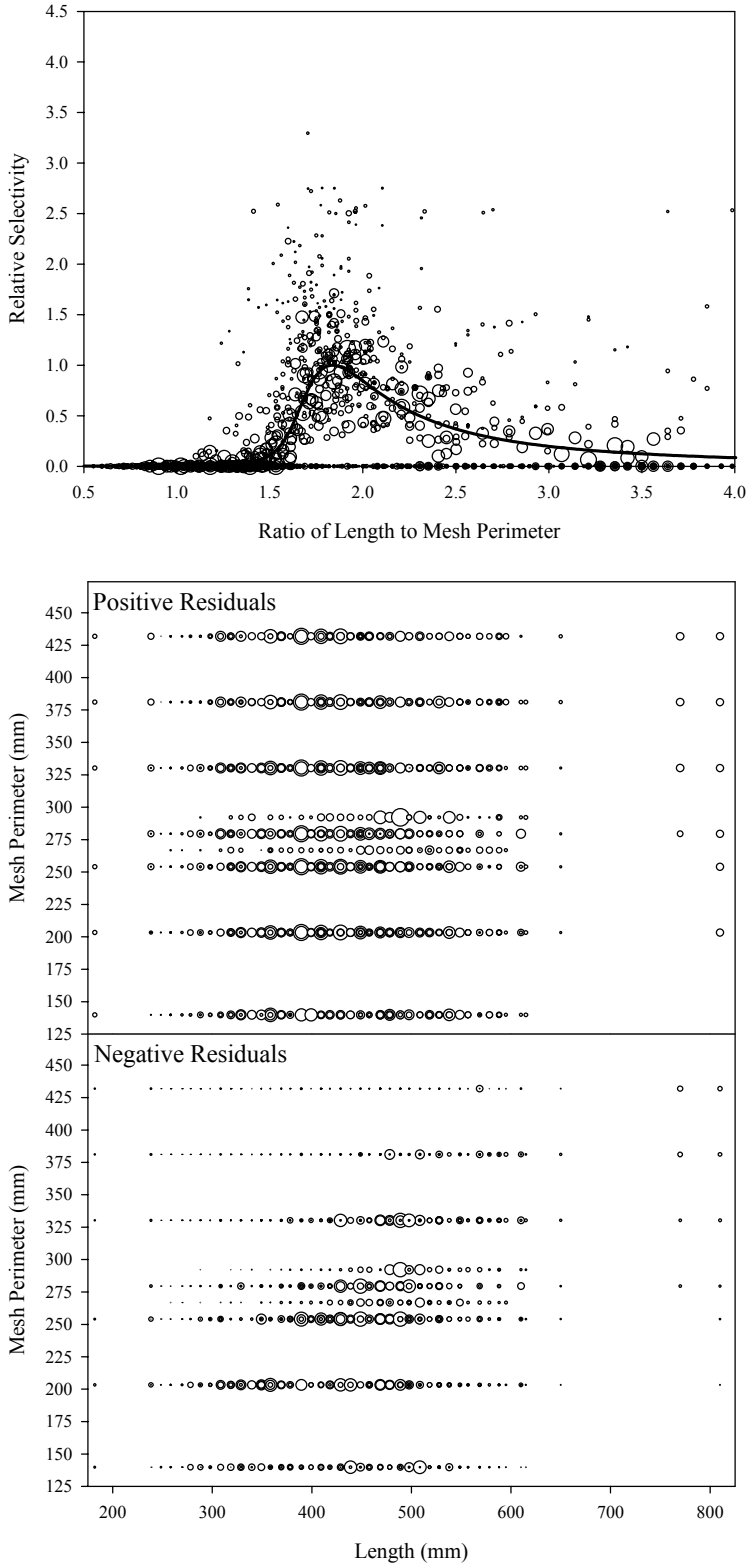

Figure B6.19. Plots of CPUE data scaled to a net selectivity model (top) and CPUE residuals (bottom); broad whitefish data and Model 19.

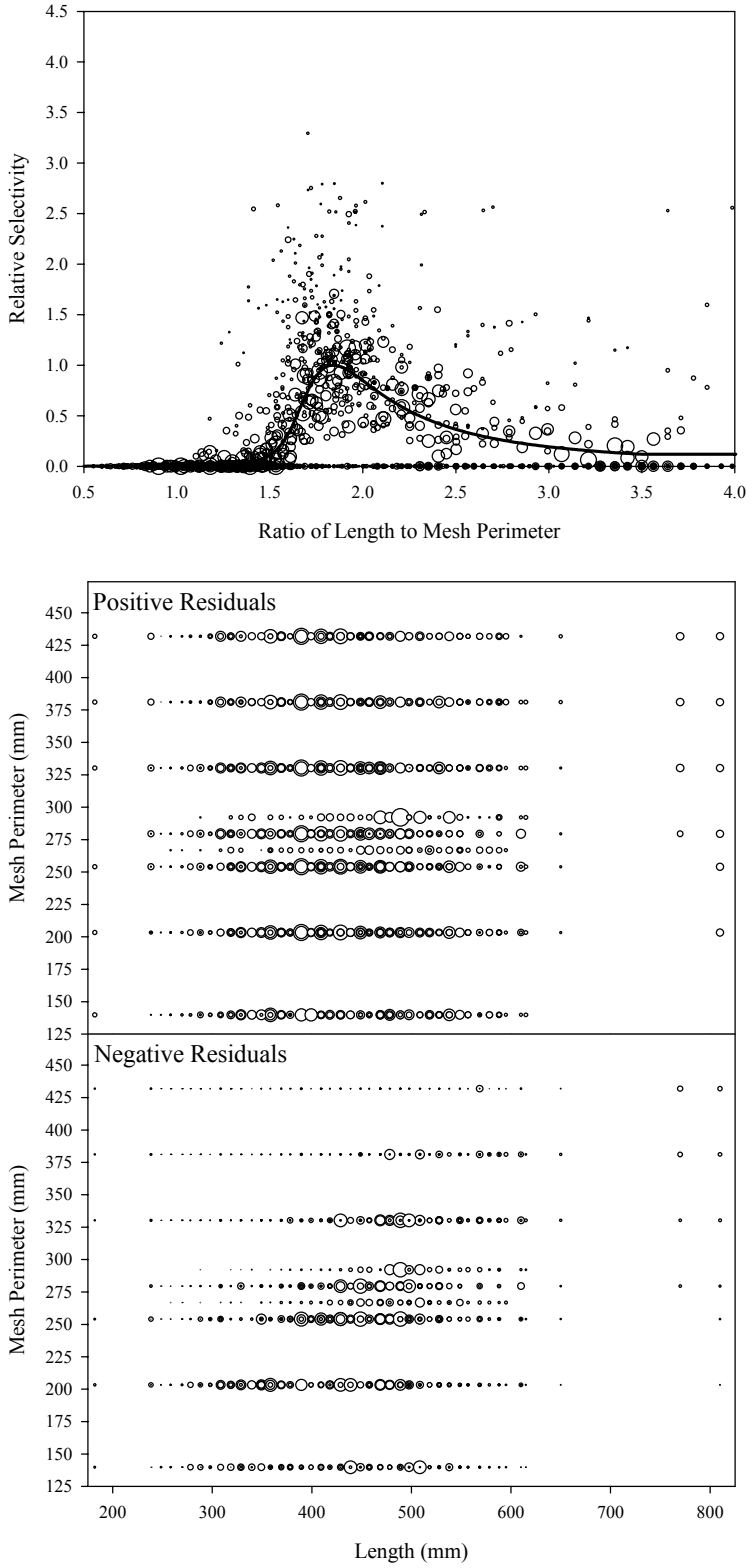

Figure B6.20. Plots of CPUE data scaled to a net selectivity model (top) and CPUE residuals (bottom); broad whitefish data and Model 20.

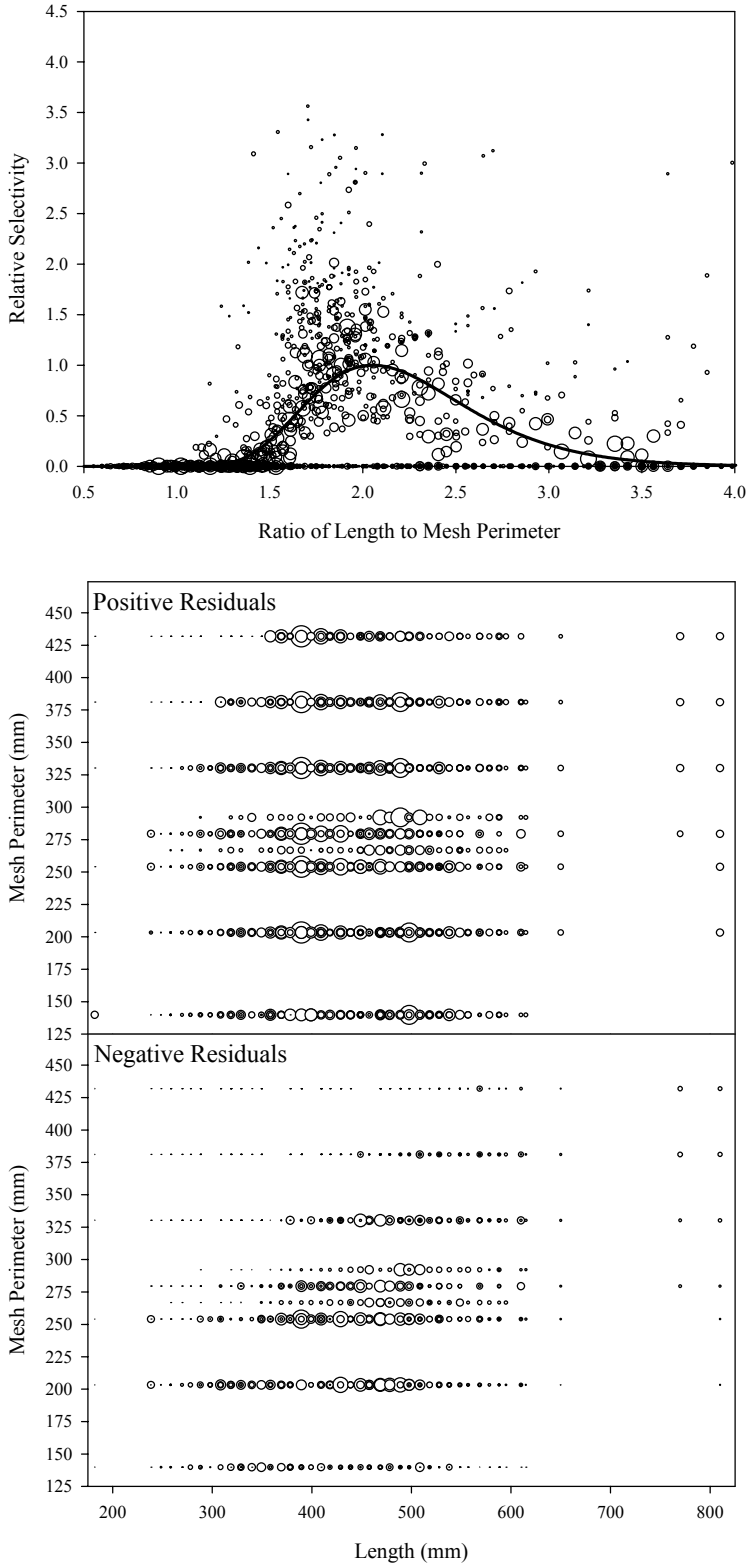

Figure B6.21. Plots of CPUE data scaled to a net selectivity model (top) and CPUE residuals (bottom); broad whitefish data and Model 21.

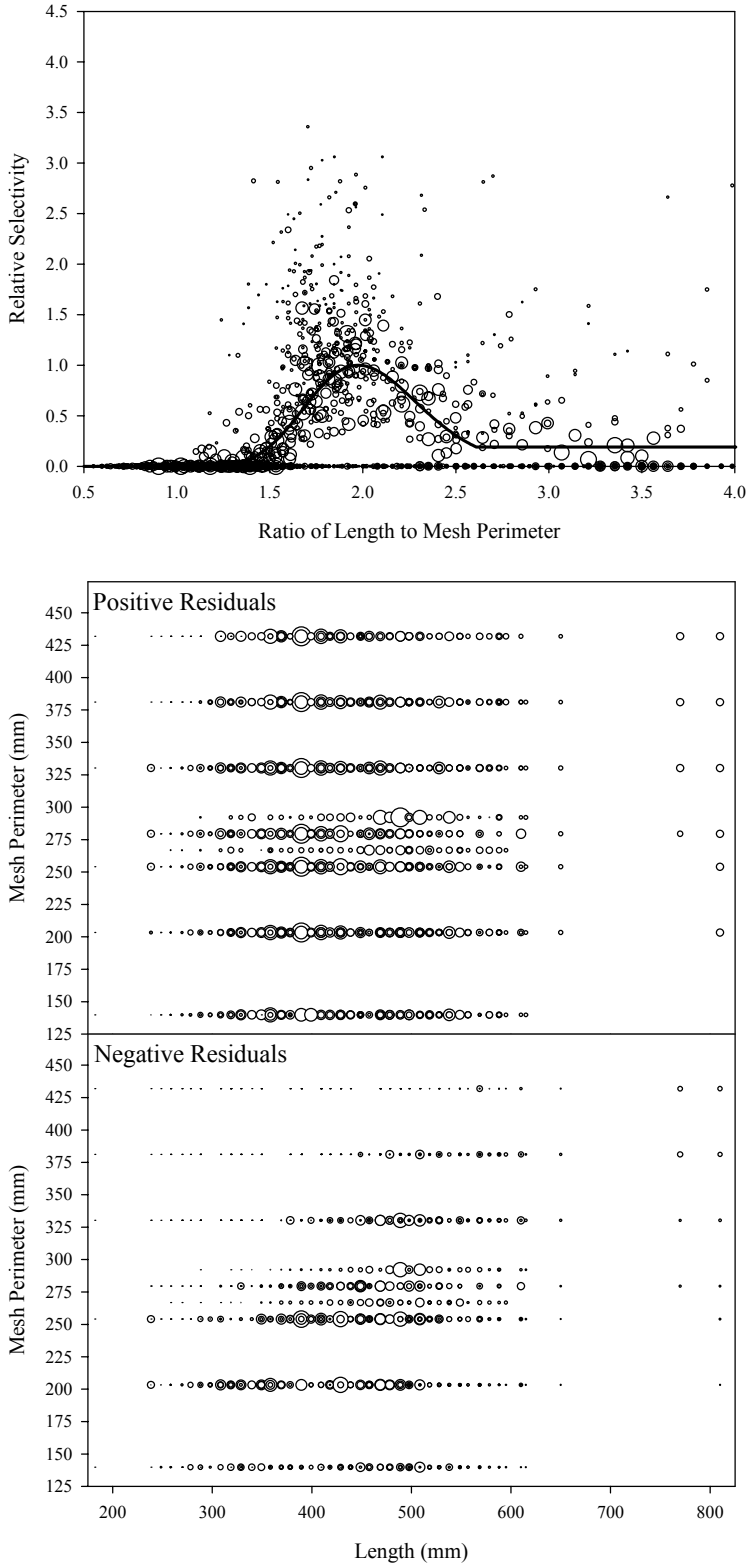

Figure B6.22. Plots of CPUE data scaled to a net selectivity model (top) and CPUE residuals (bottom); broad whitefish data and Model 22.

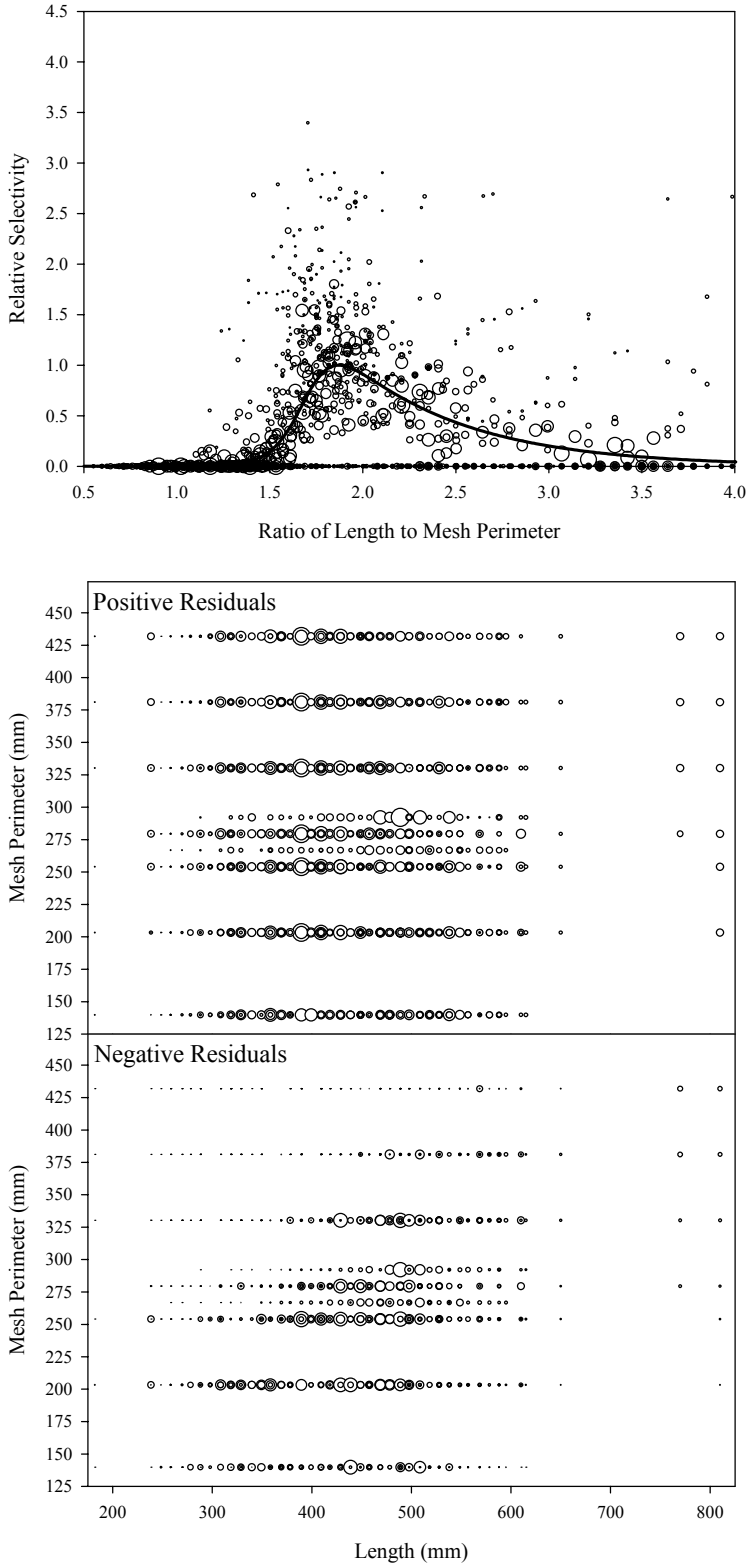

Figure B6.23. Plots of CPUE data scaled to a net selectivity model (top) and CPUE residuals (bottom); broad whitefish data and Model 23.

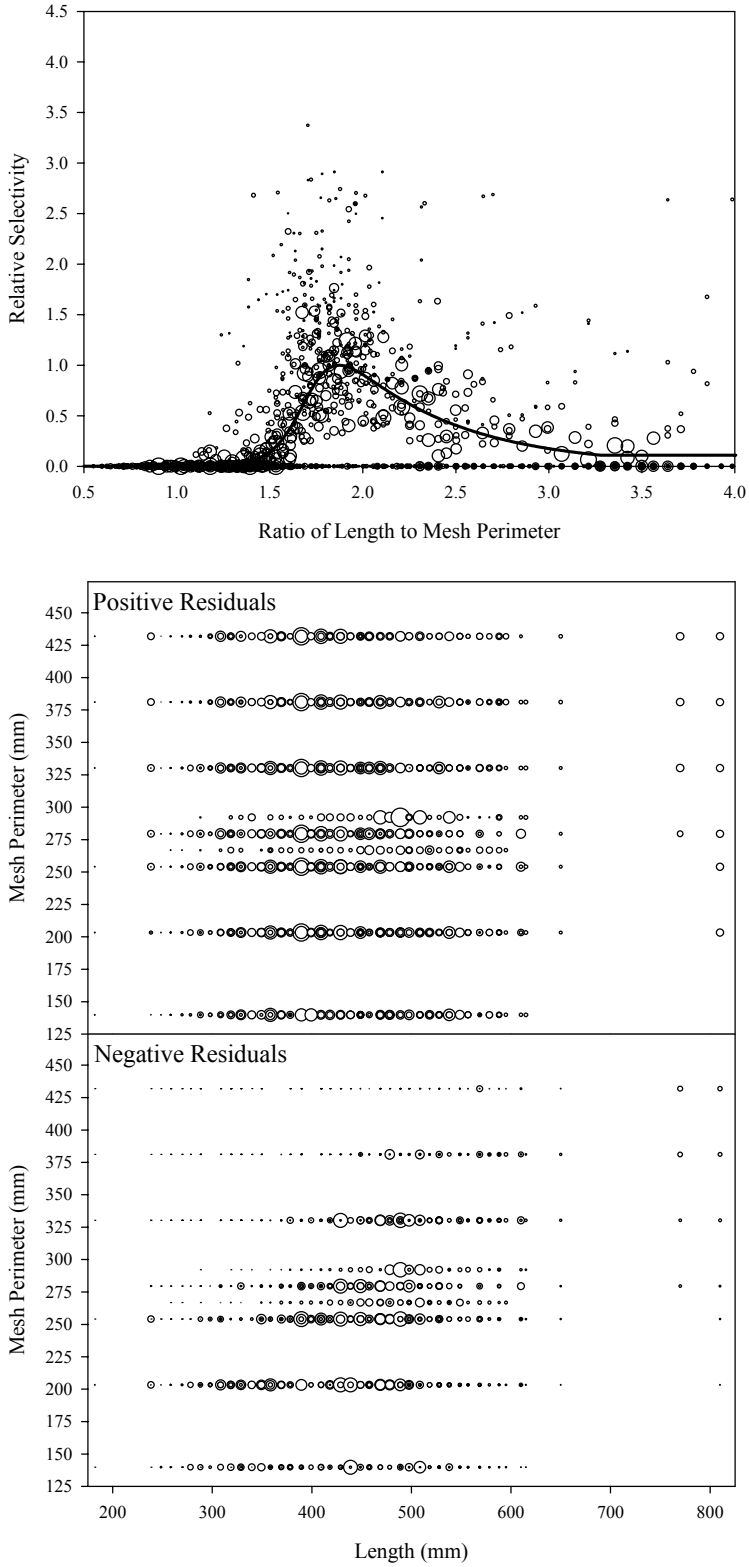

Figure B6.24. Plots of CPUE data scaled to a net selectivity model (top) and CPUE residuals (bottom); broad whitefish data and Model 24.

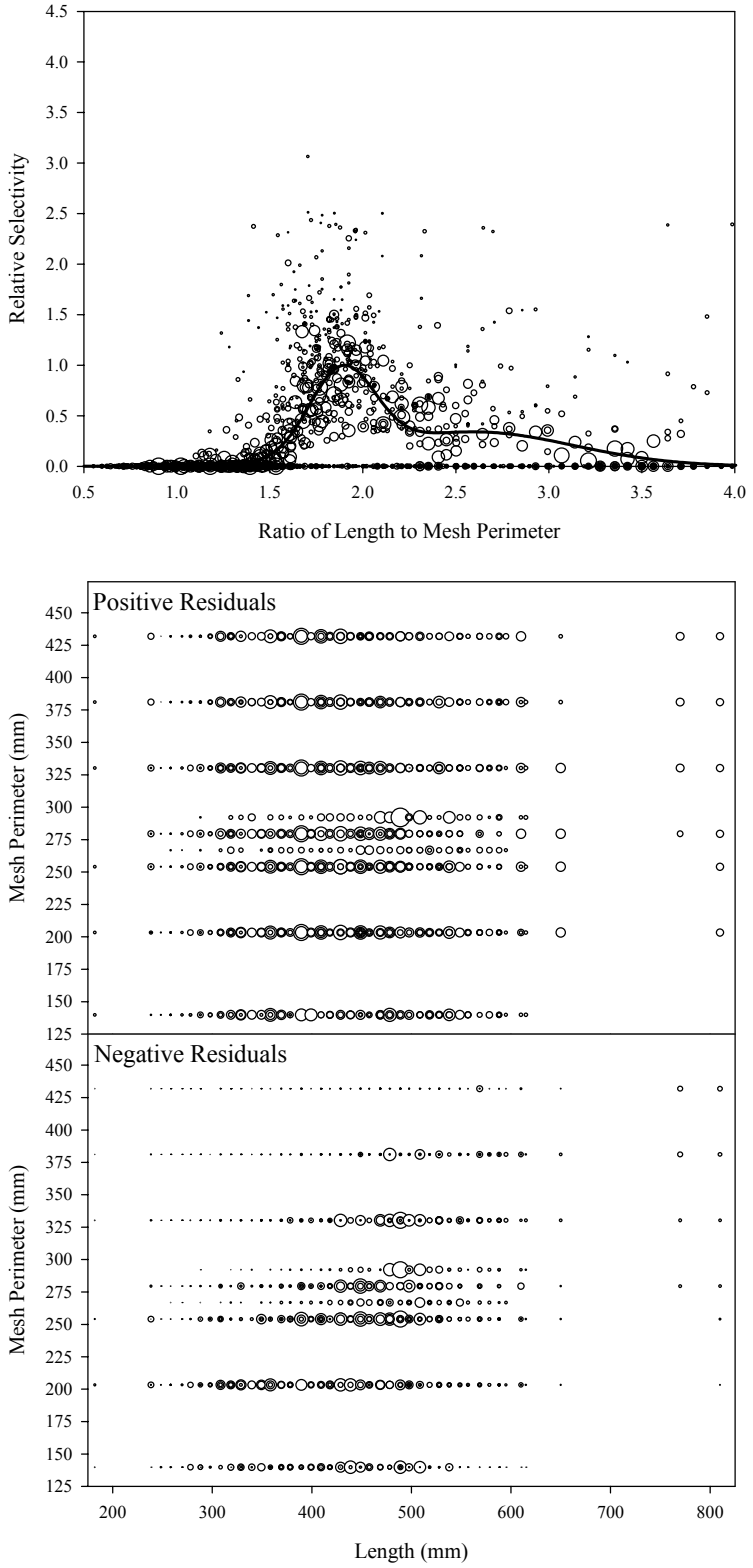

Figure B6.25. Plots of CPUE data scaled to a net selectivity model (top) and CPUE residuals (bottom); broad whitefish data and Model 25.

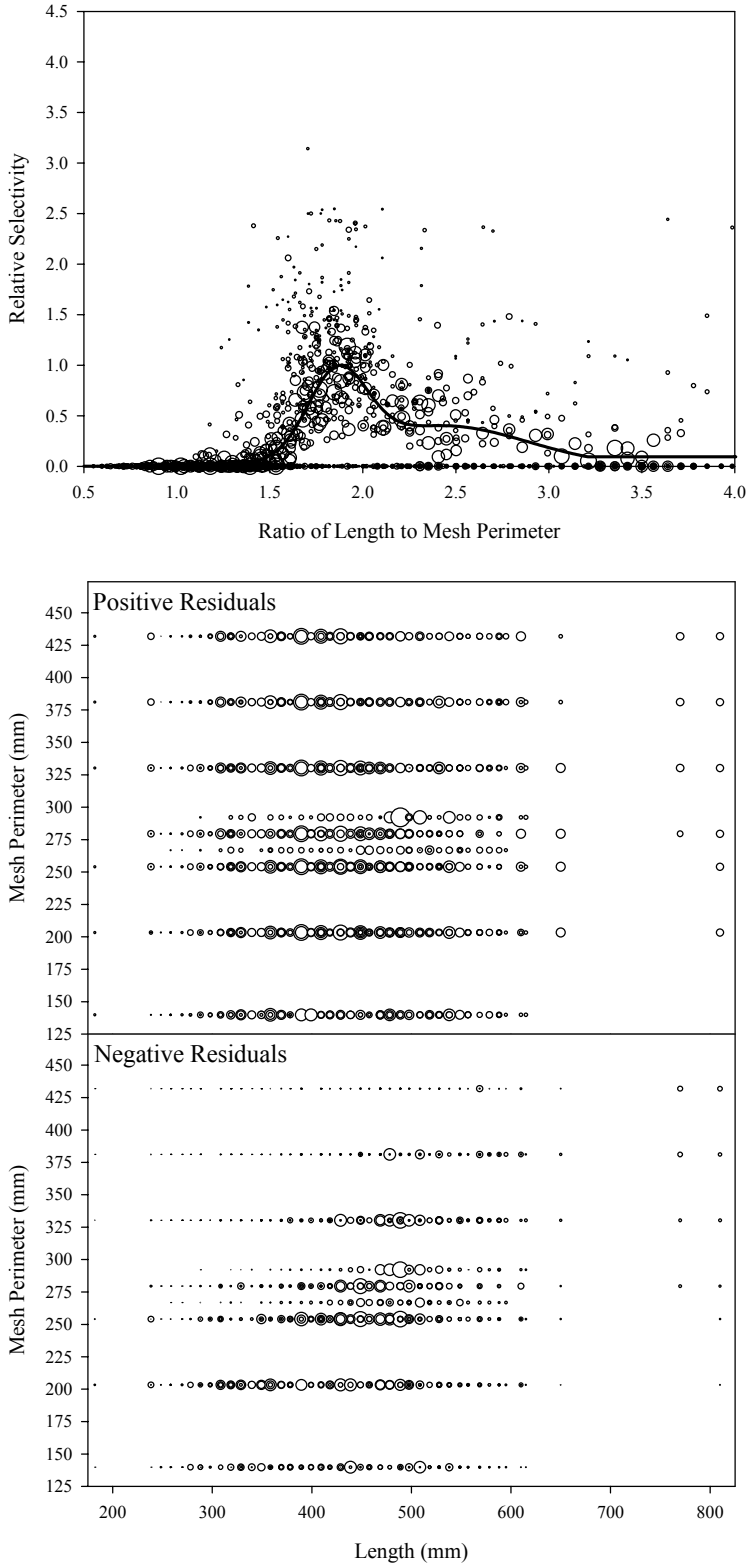

Figure B6.26. Plots of CPUE data scaled to a net selectivity model (top) and CPUE residuals (bottom); broad whitefish data and Model 26.

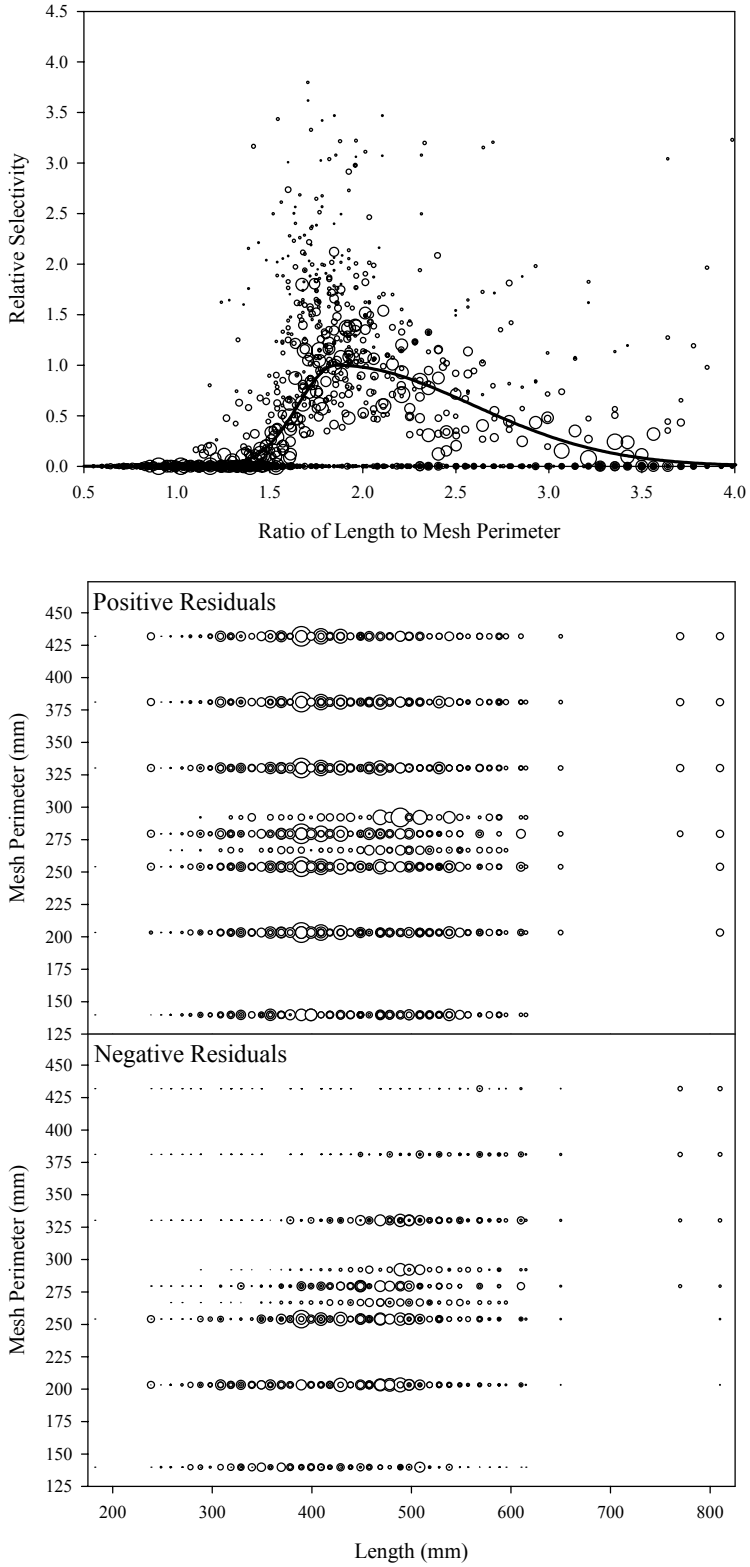

Figure B6.27. Plots of CPUE data scaled to a net selectivity model (top) and CPUE residuals (bottom); broad whitefish data and Model 27.

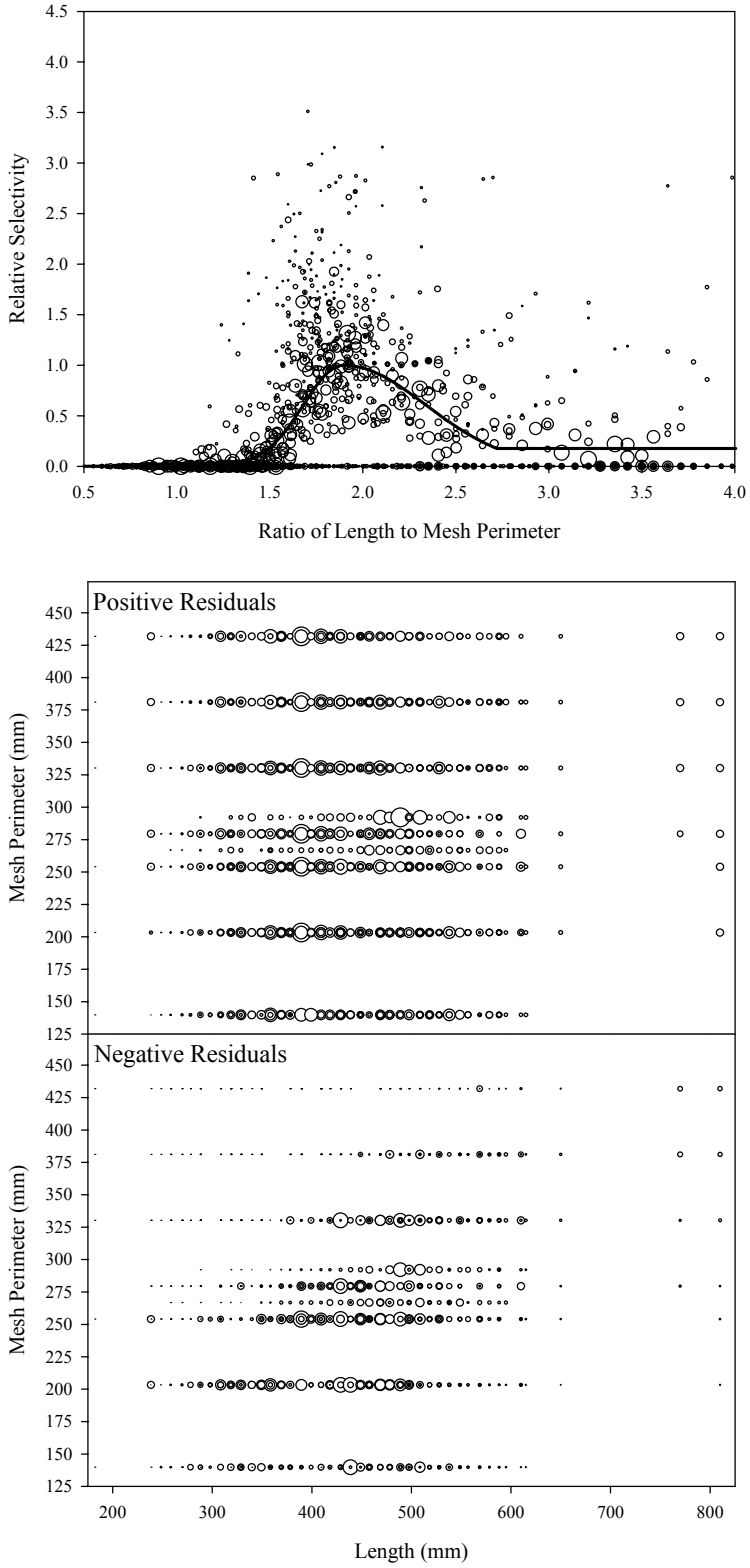

Figure B6.28. Plots of CPUE data scaled to a net selectivity model (top) and CPUE residuals (bottom); broad whitefish data and Model 28.

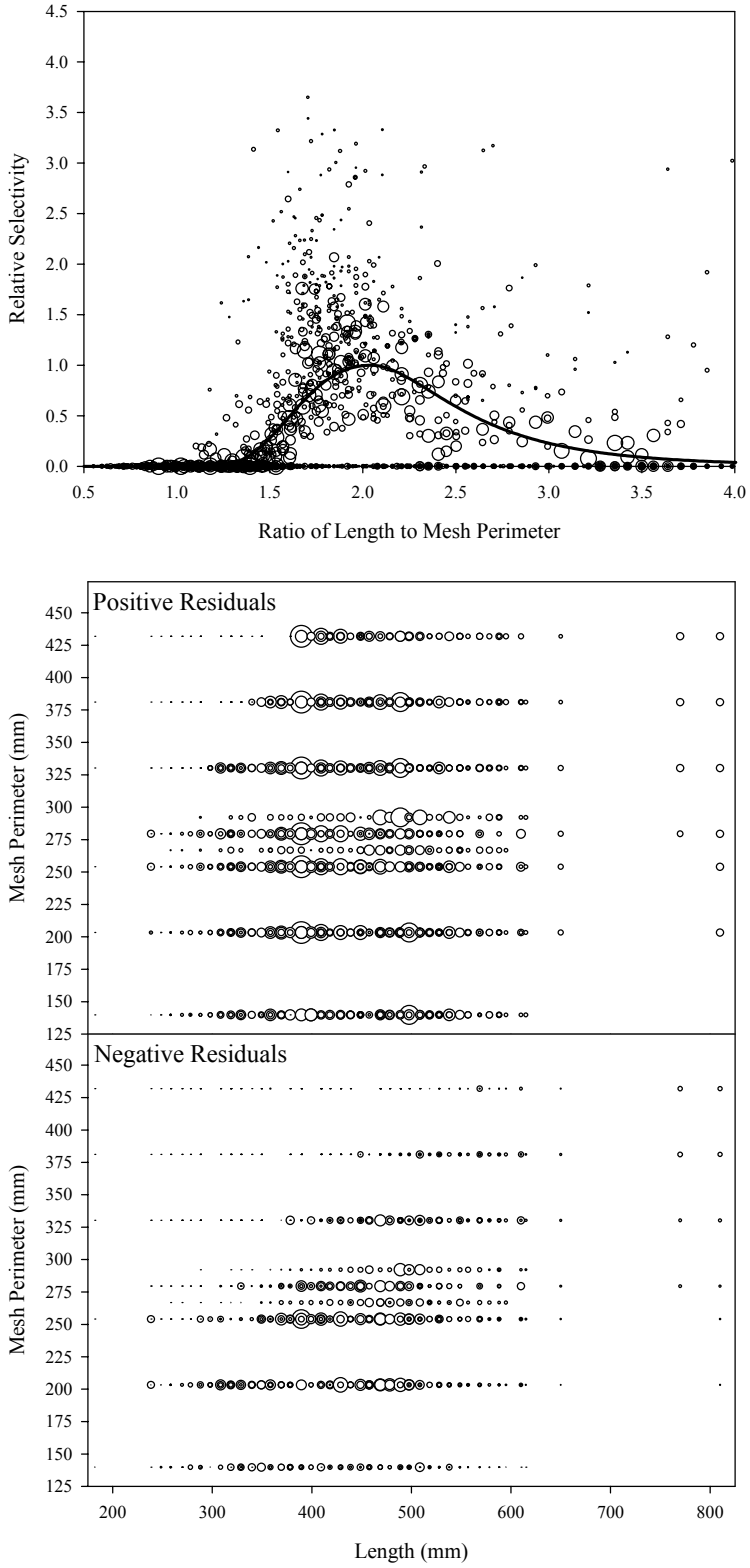

Figure B6.29. Plots of CPUE data scaled to a net selectivity model (top) and CPUE residuals (bottom); broad whitefish data and Model 29.

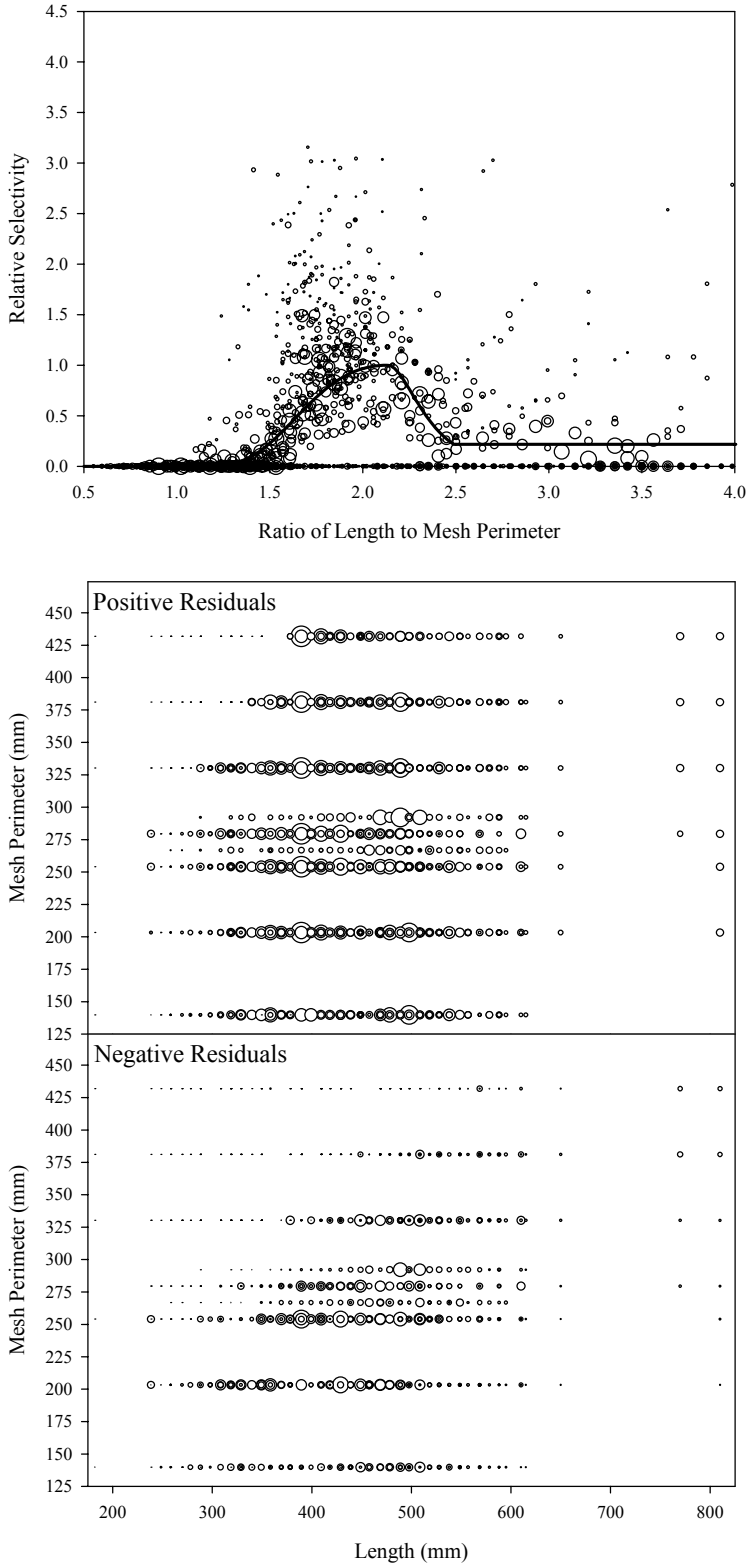

Figure B6.30. Plots of CPUE data scaled to a net selectivity model (top) and CPUE residuals (bottom); broad whitefish data and Model 30.

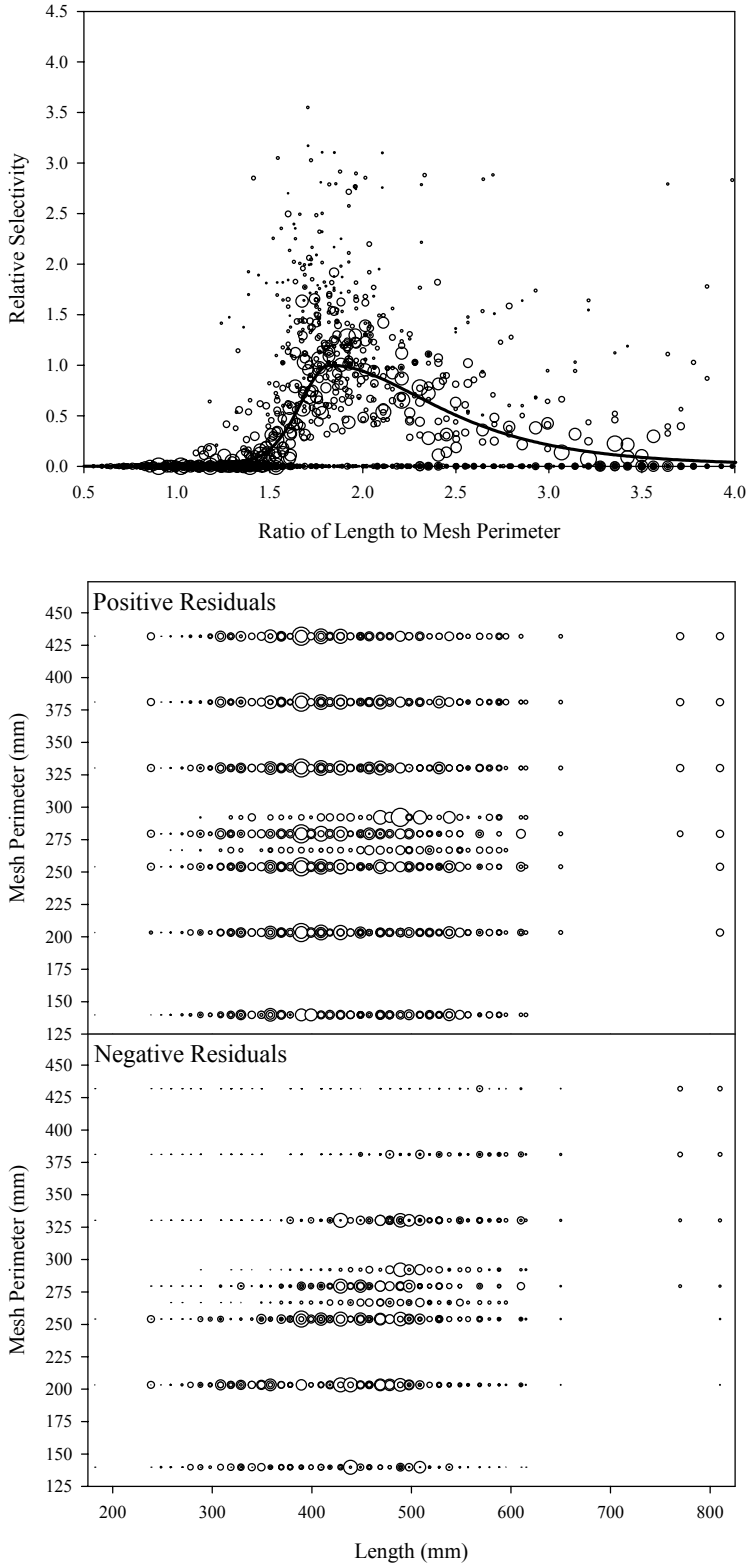

Figure B6.31. Plots of CPUE data scaled to a net selectivity model (top) and CPUE residuals (bottom); broad whitefish data and Model 31.

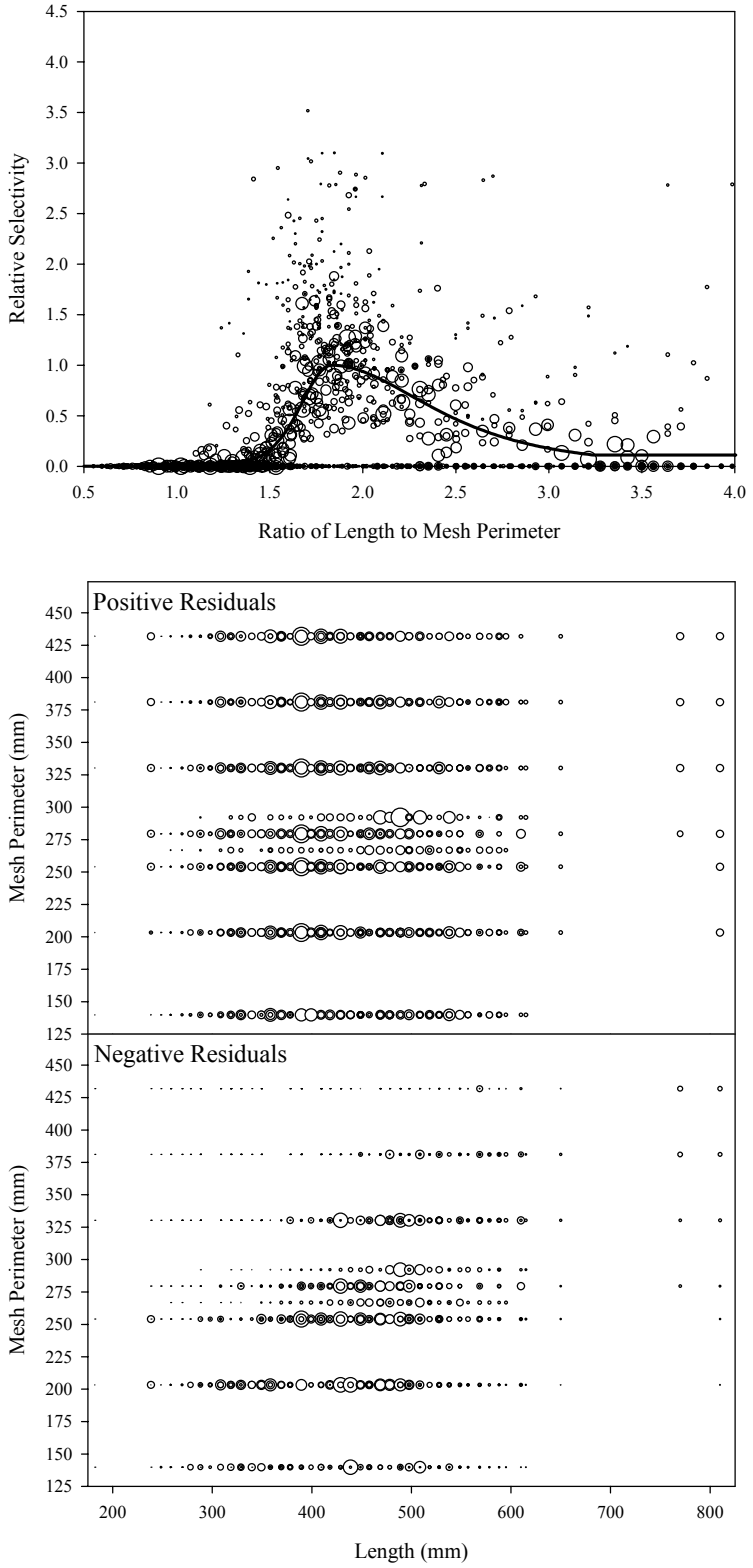

Figure B6.32. Plots of CPUE data scaled to a net selectivity model (top) and CPUE residuals (bottom); broad whitefish data and Model 32.

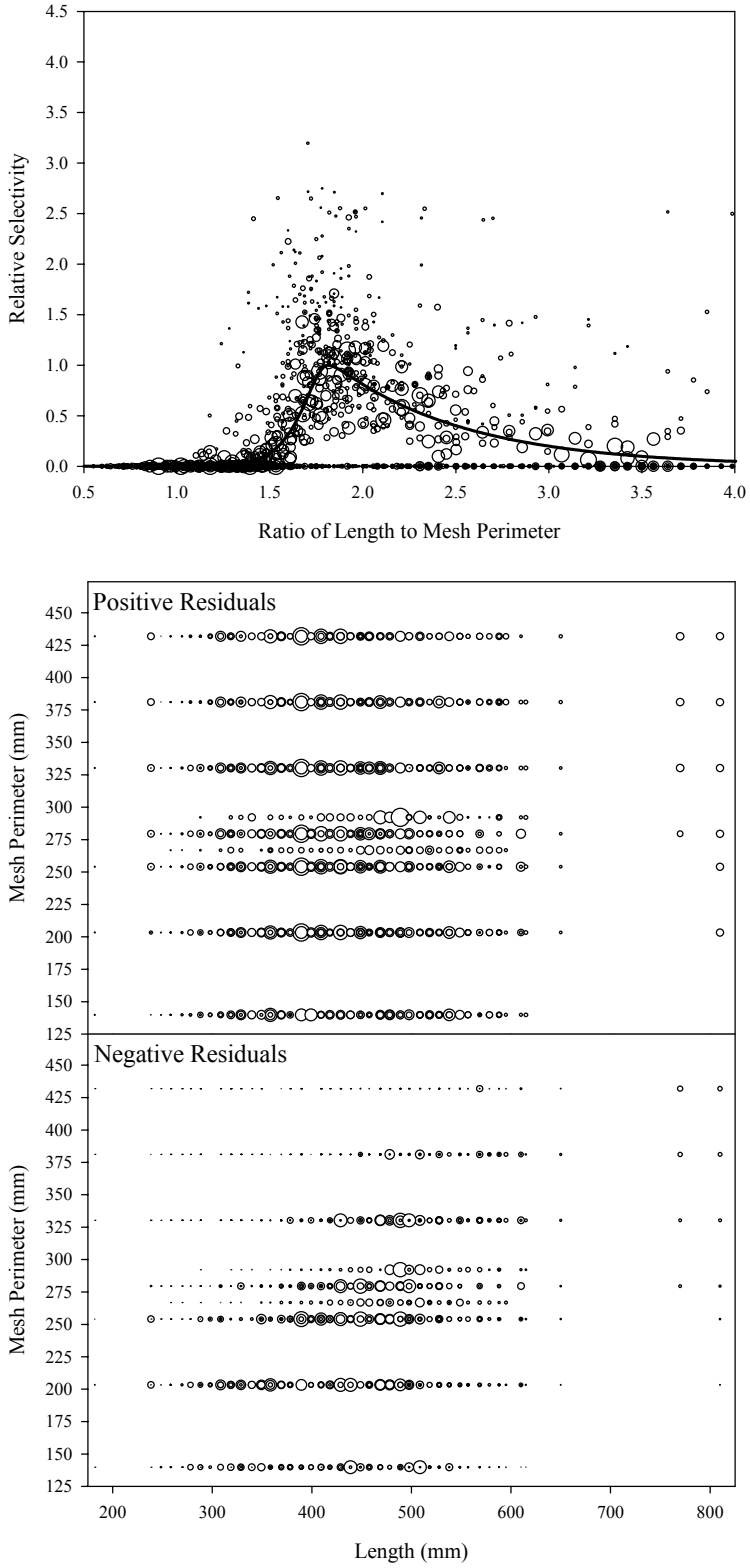

Figure B6.33. Plots of CPUE data scaled to a net selectivity model (top) and CPUE residuals (bottom); broad whitefish data and Model 33.

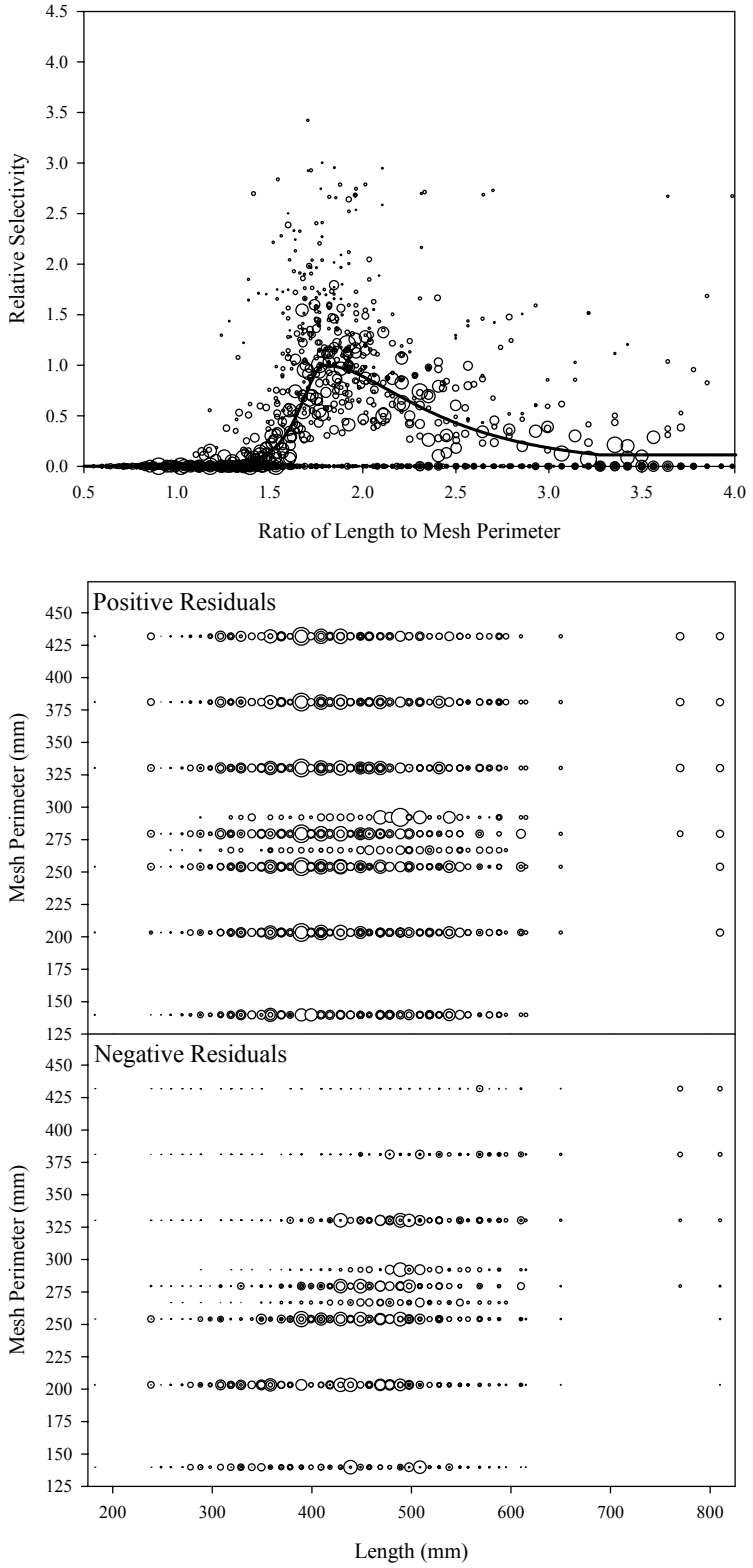

Figure B6.34. Plots of CPUE data scaled to a net selectivity model (top) and CPUE residuals (bottom); broad whitefish data and Model 34.

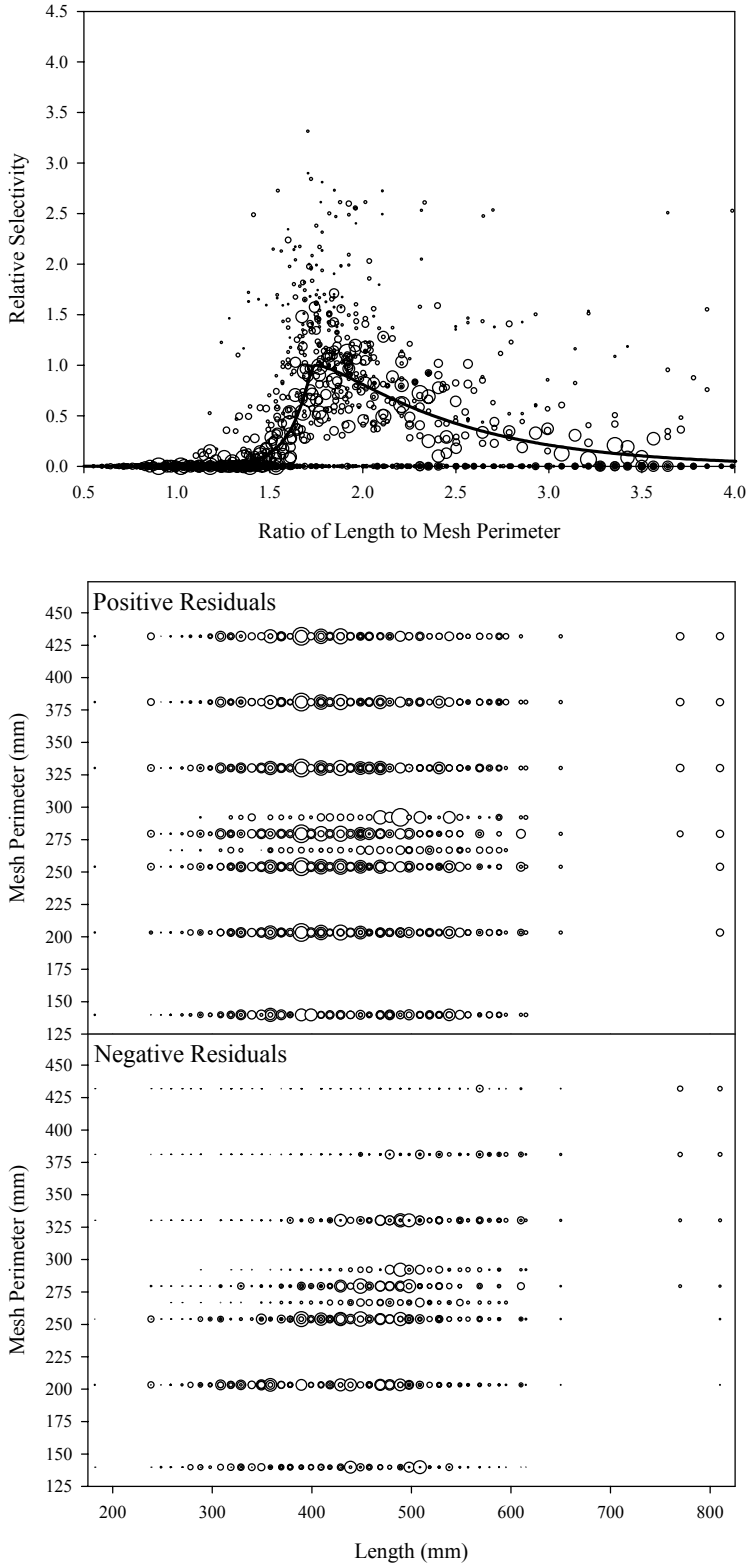

Figure B6.35. Plots of CPUE data scaled to a net selectivity model (top) and CPUE residuals (bottom); broad whitefish data and Model 35.

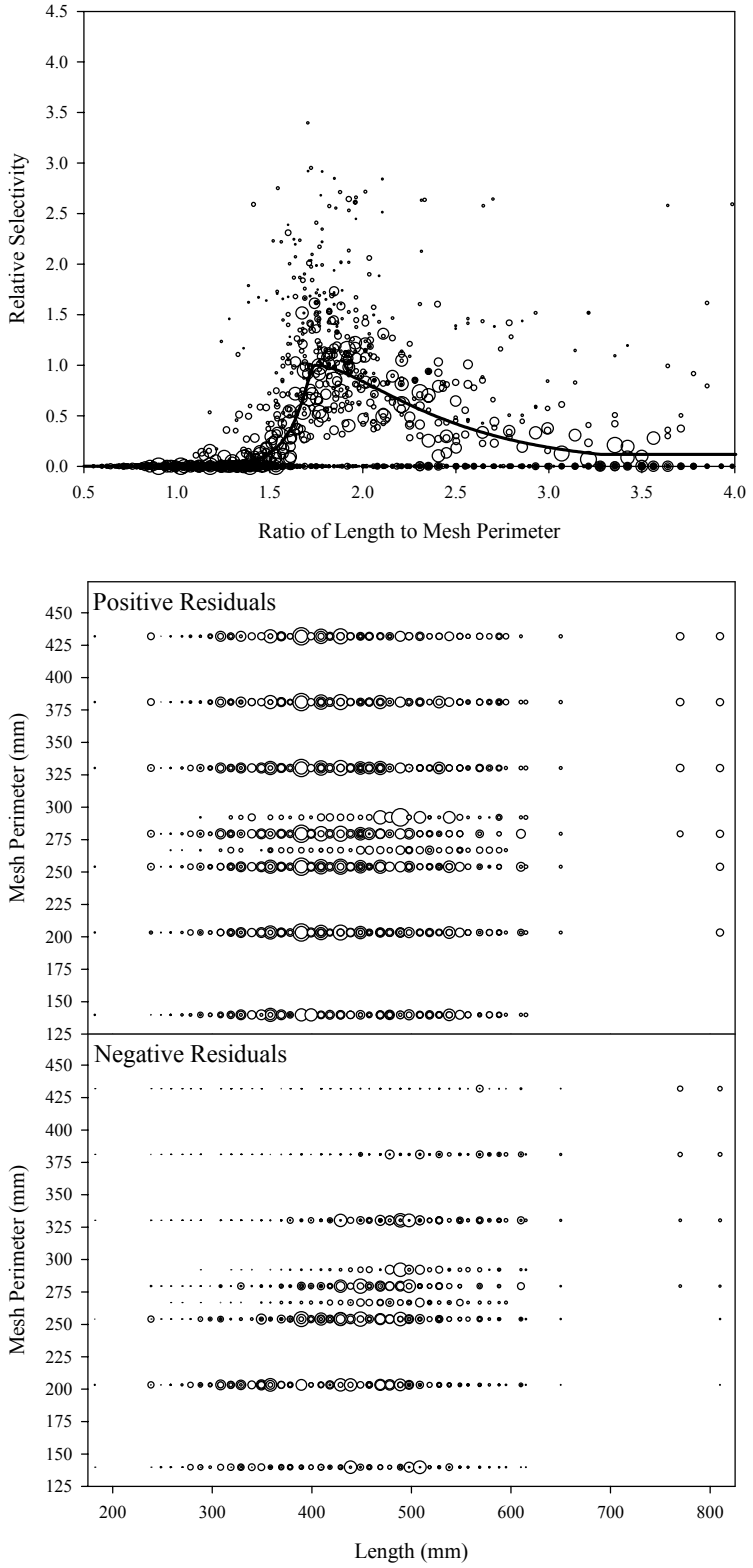

Figure B6.36. Plots of CPUE data scaled to a net selectivity model (top) and CPUE residuals (bottom); broad whitefish data and Model 36.

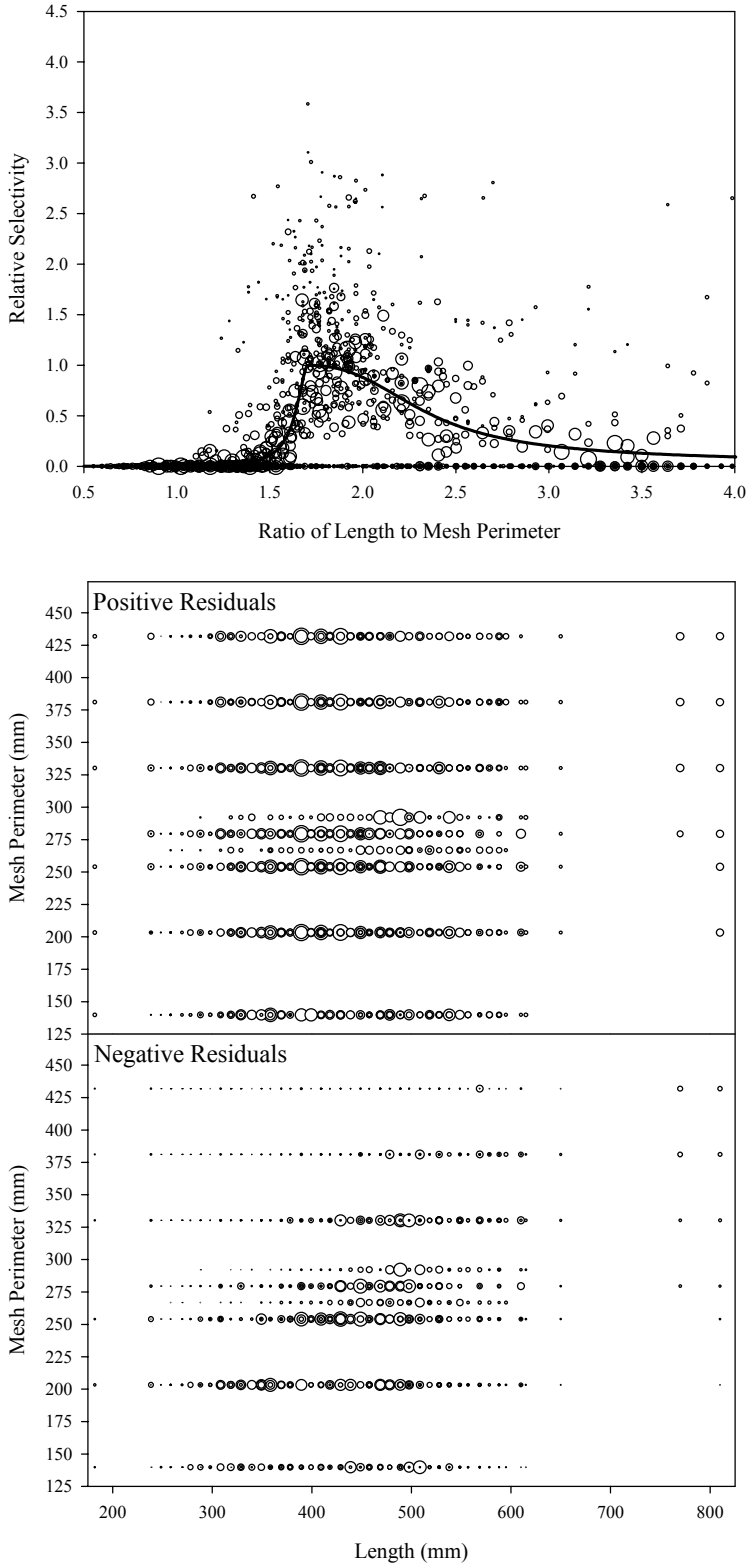

Figure B6.37. Plots of CPUE data scaled to a net selectivity model (top) and CPUE residuals (bottom); broad whitefish data and Model 37.

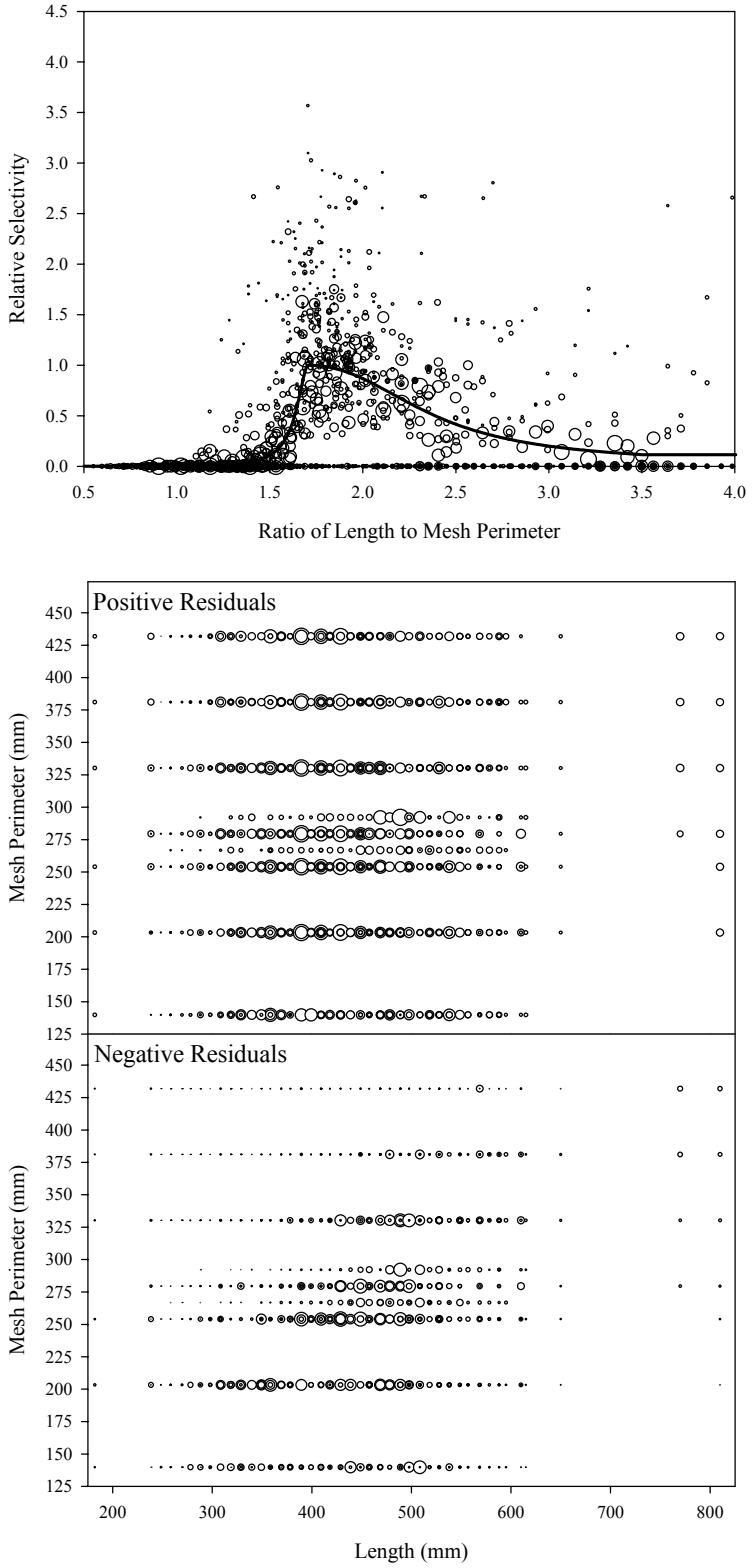

Figure B6.38. Plots of CPUE data scaled to a net selectivity model (top) and CPUE residuals (bottom); broad whitefish data and Model 38.

Appendix B7
Humpback Whitefish Diagnostic Plots
Figure B7.1 to Figure B7.38

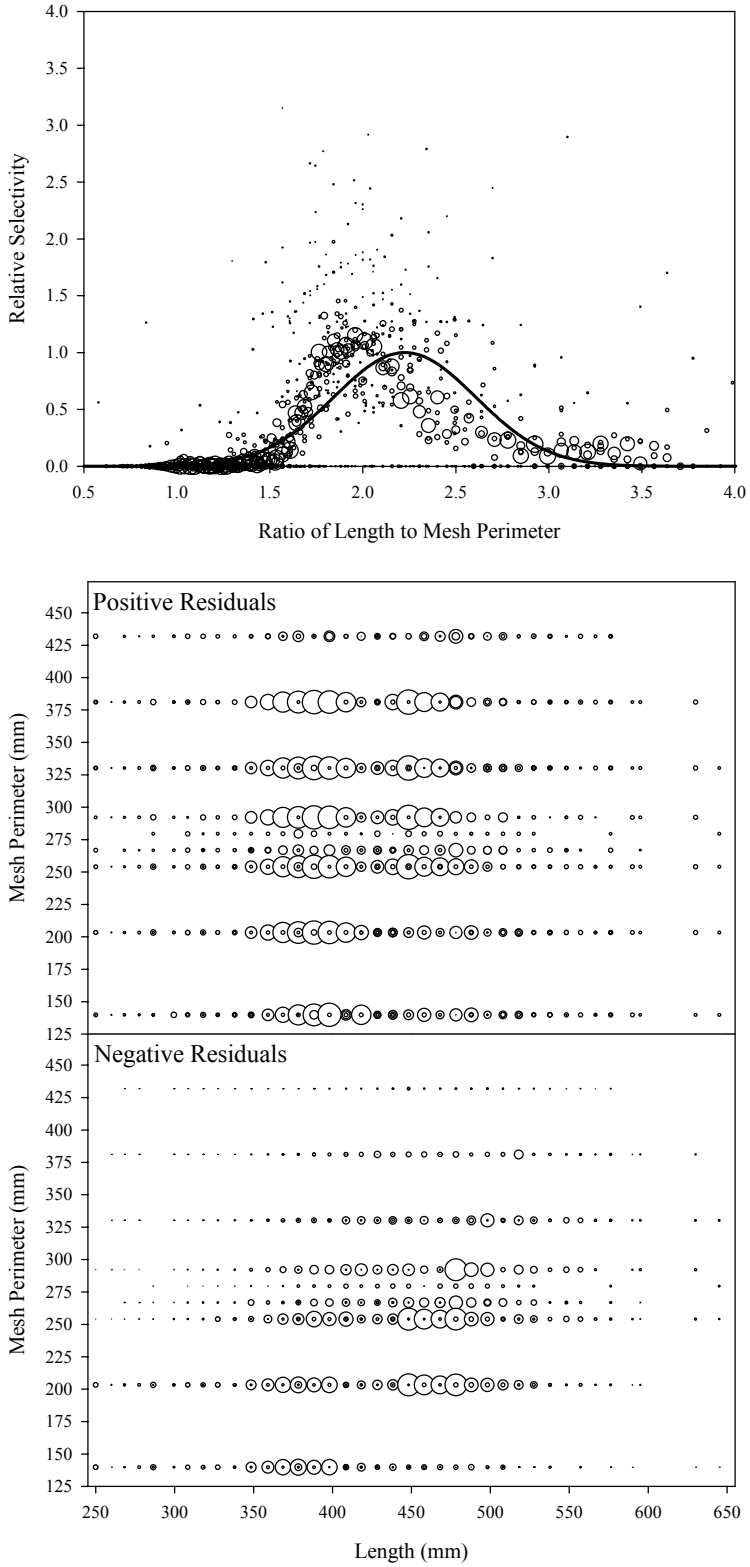

Figure B7.1. Plots of CPUE data scaled to a net selectivity model (top) and CPUE residuals (bottom); humpback whitefish data and Model 1.

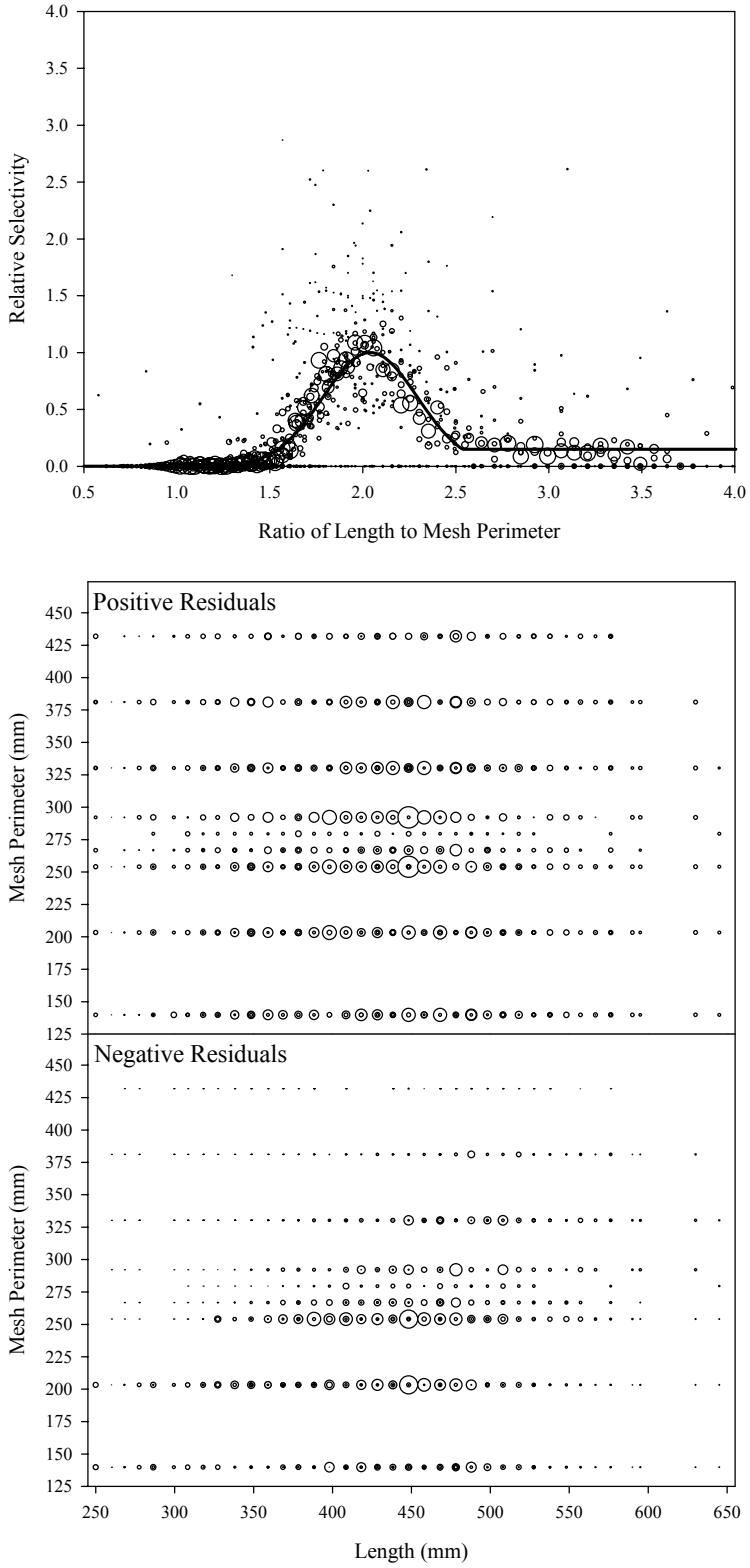

Figure B7.2. Plots of CPUE data scaled to a net selectivity model (top) and CPUE residuals (bottom); humpback whitefish data and Model 2.

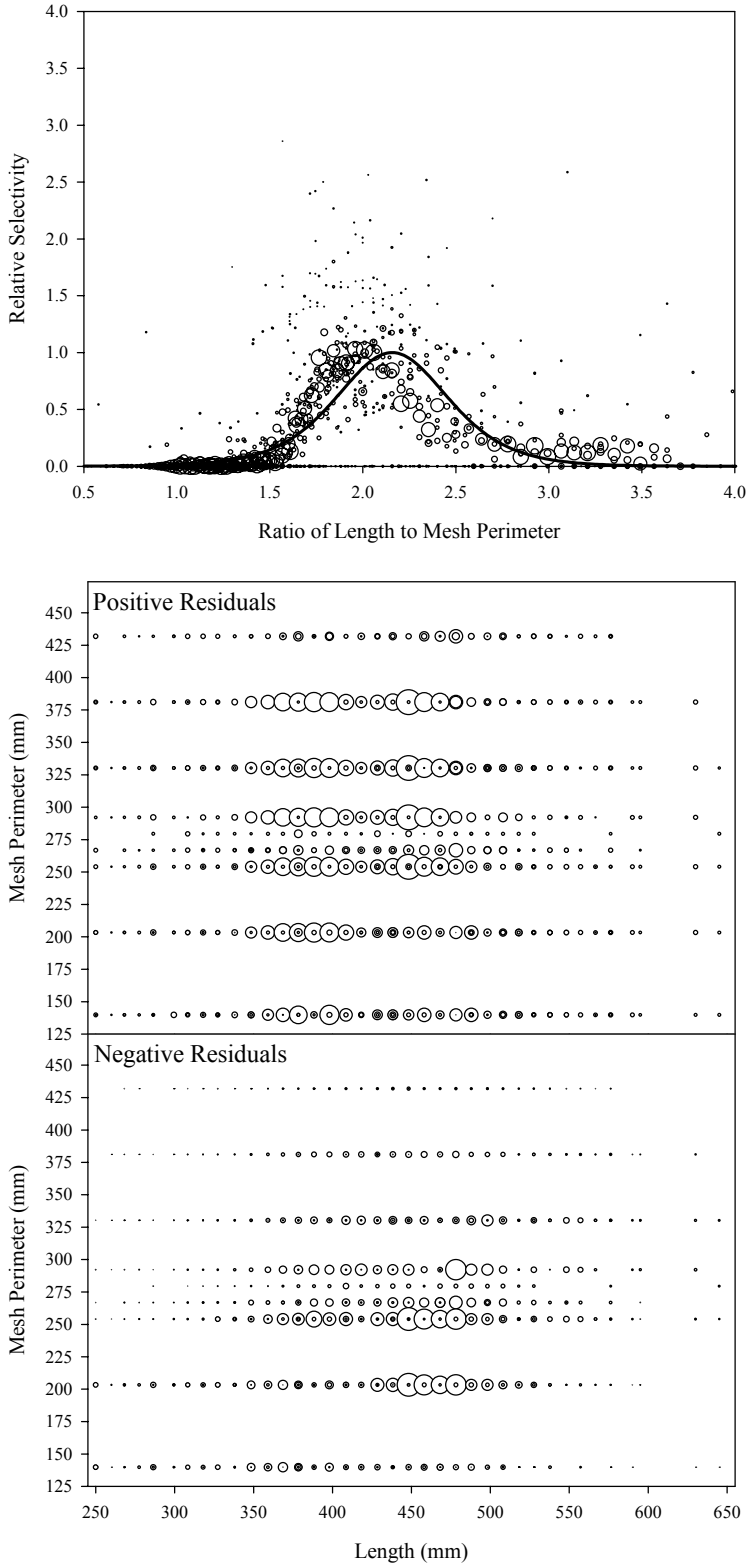

Figure B7.3. Plots of CPUE data scaled to a net selectivity model (top) and CPUE residuals (bottom); humpback whitefish data and Model 3.

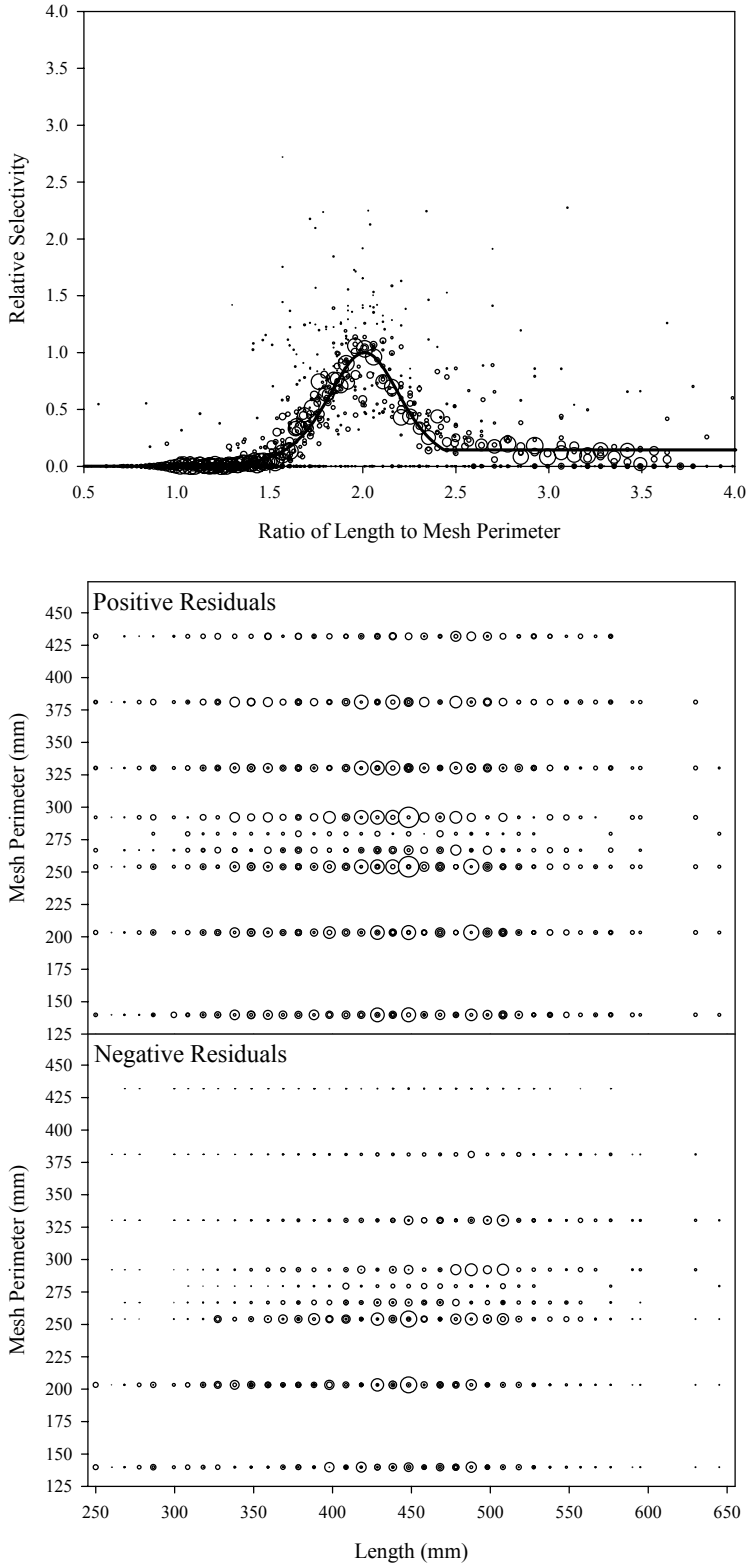

Figure B7.4. Plots of CPUE data scaled to a net selectivity model (top) and CPUE residuals (bottom); humpback whitefish data and Model 4.

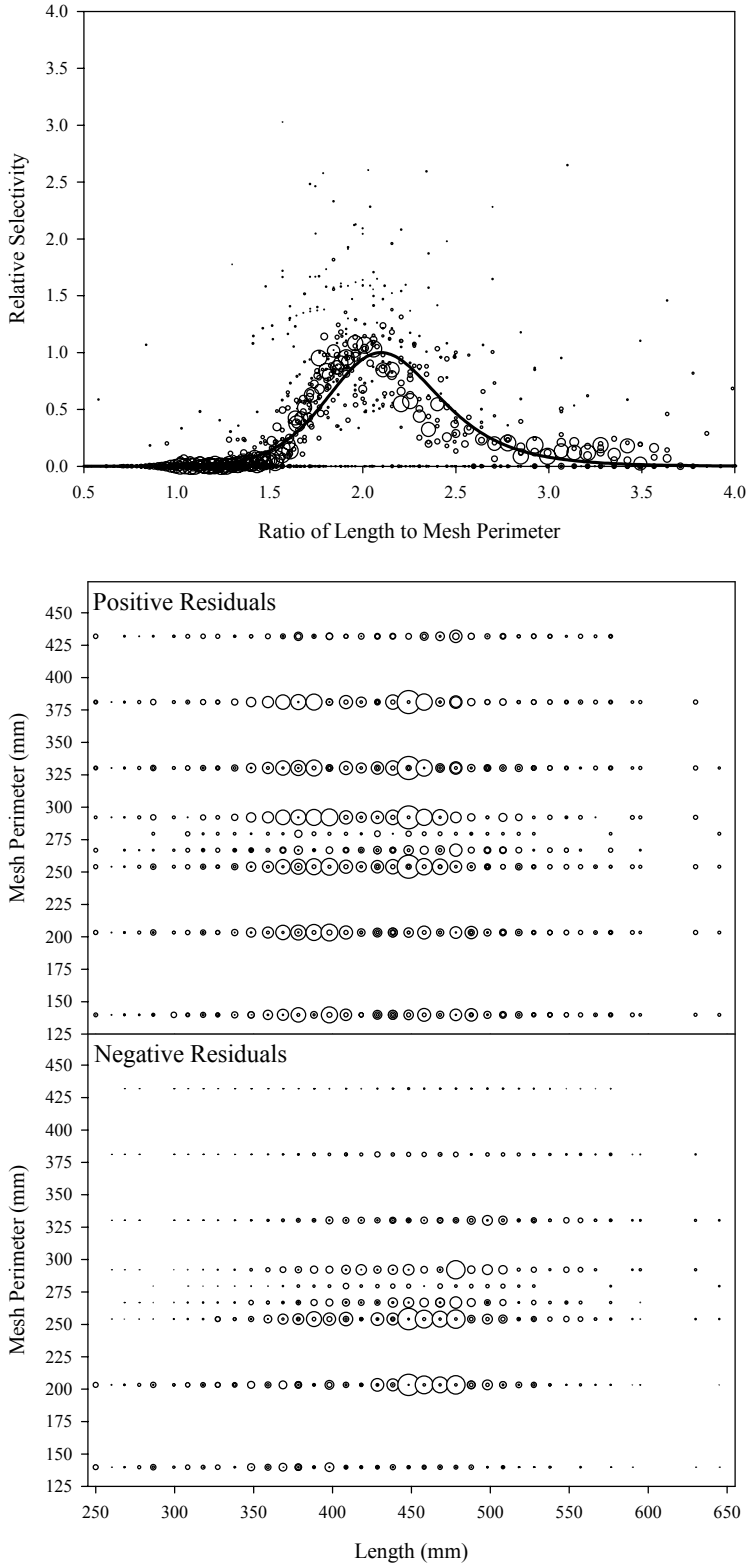

Figure B7.5. Plots of CPUE data scaled to a net selectivity model (top) and CPUE residuals (bottom); humpback whitefish data and Model 5.

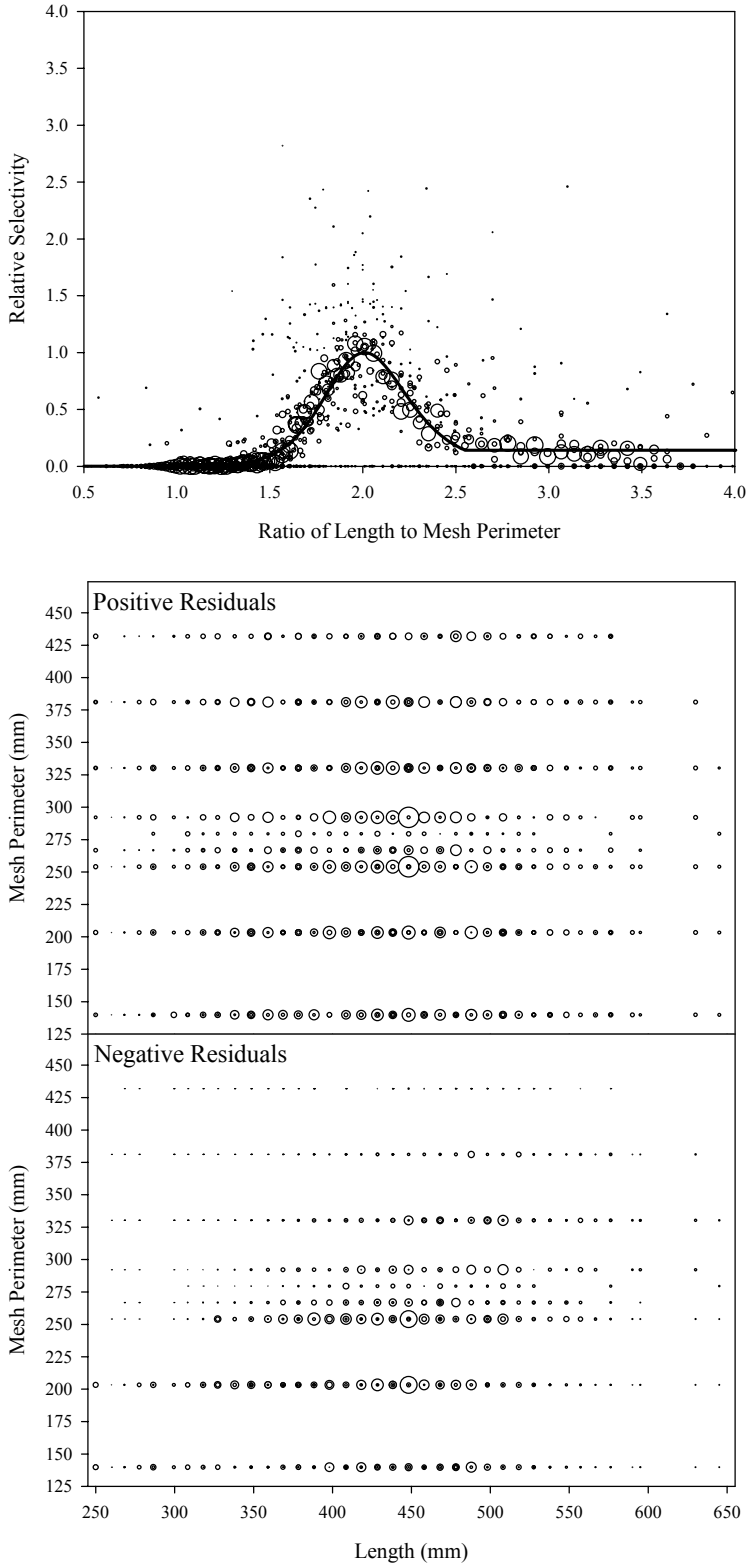

Figure B7.6. Plots of CPUE data scaled to a net selectivity model (top) and CPUE residuals (bottom); humpback whitefish data and Model 6.

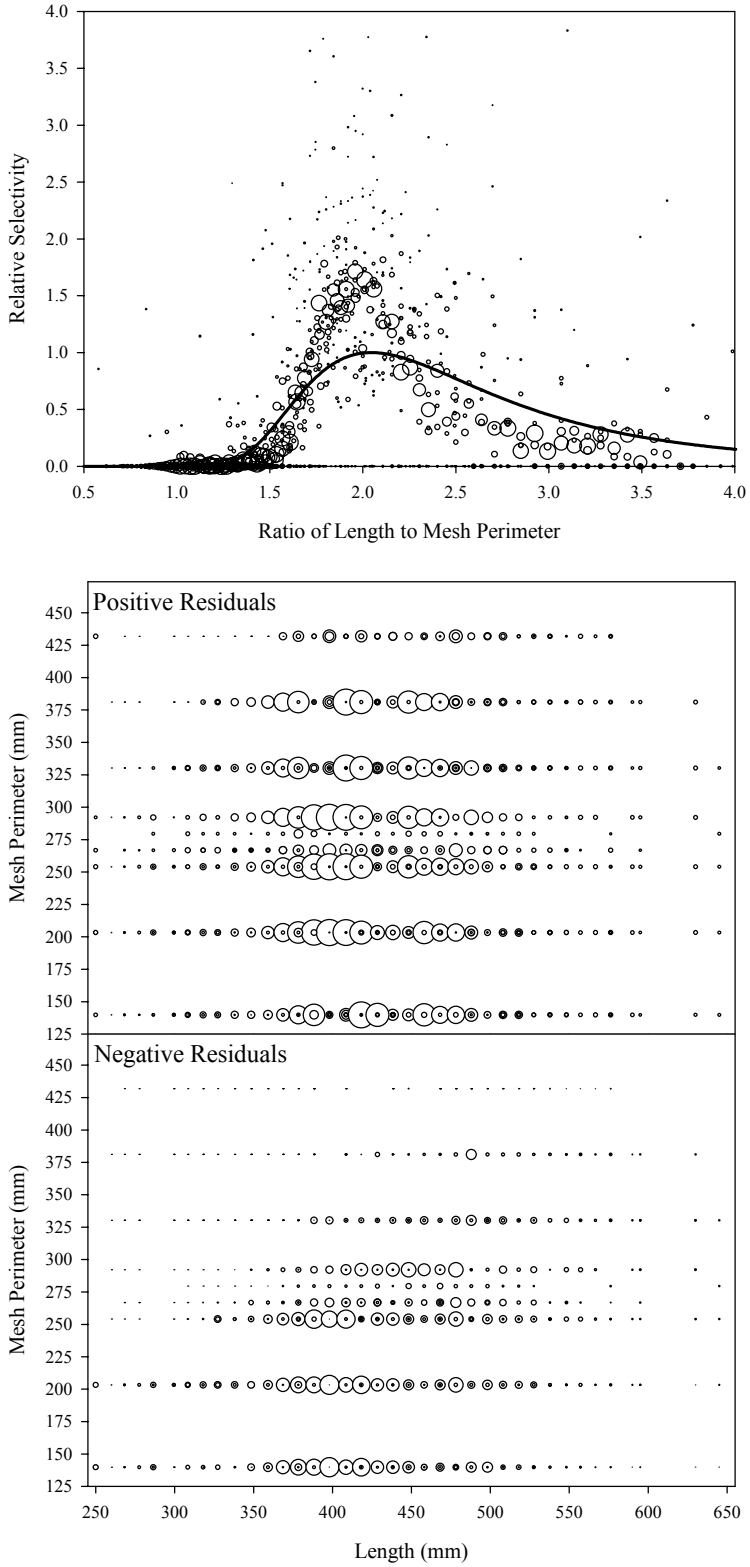

Figure B7.7. Plots of CPUE data scaled to a net selectivity model (top) and CPUE residuals (bottom); humpback whitefish data and Model 7.

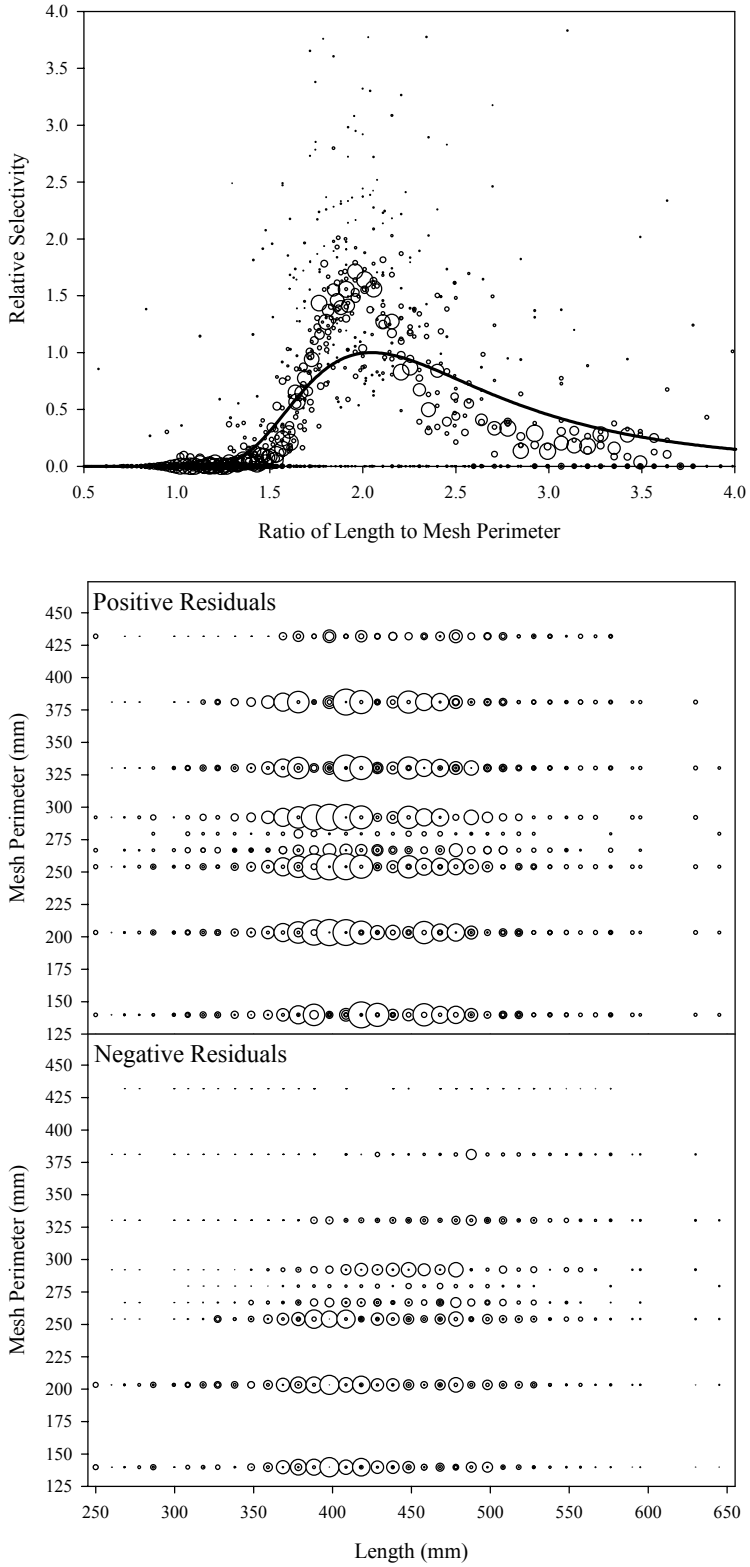

Figure B7.8. Plots of CPUE data scaled to a net selectivity model (top) and CPUE residuals (bottom); humpback whitefish data and Model 8.

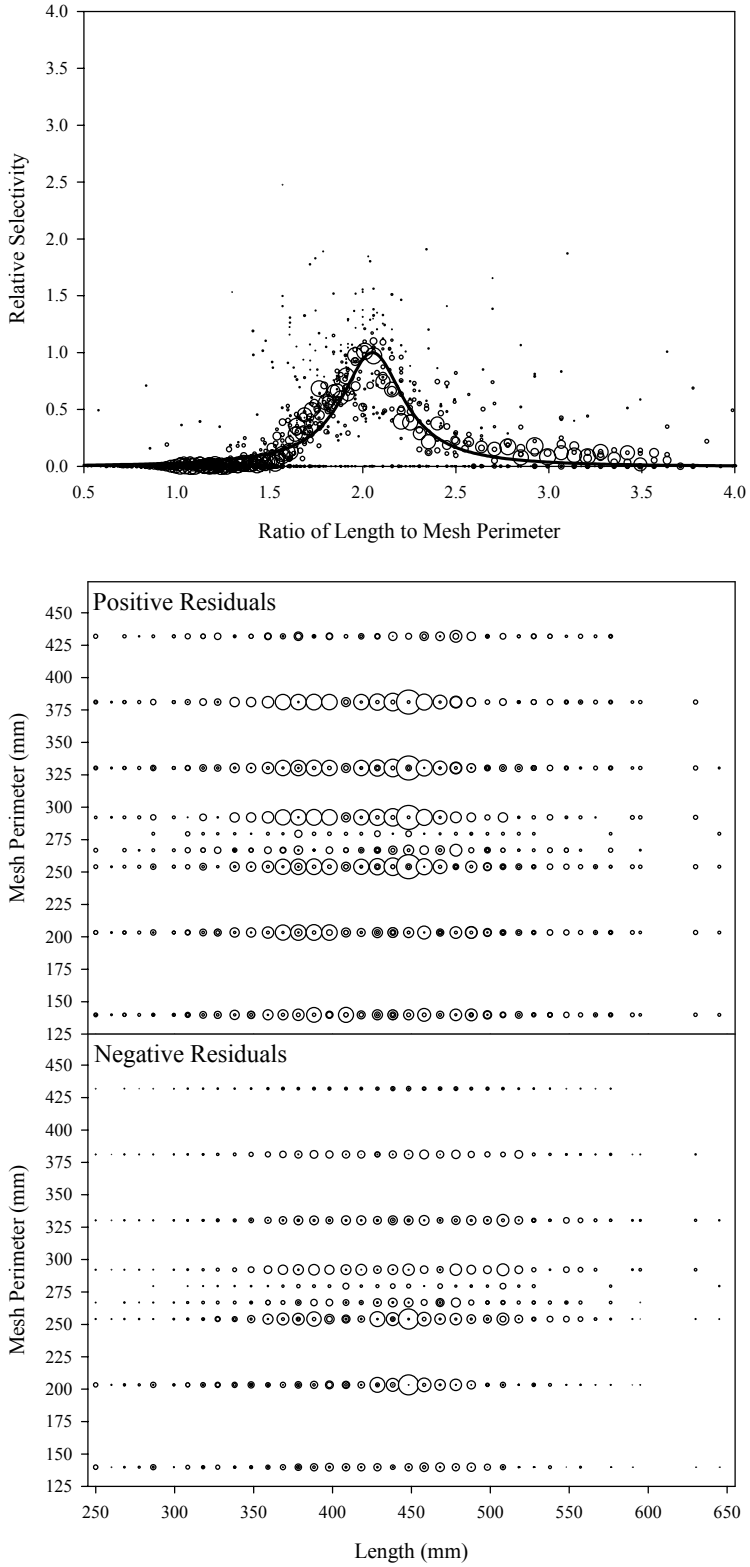

Figure B7.9. Plots of CPUE data scaled to a net selectivity model (top) and CPUE residuals (bottom); humpback whitefish data and Model 9.

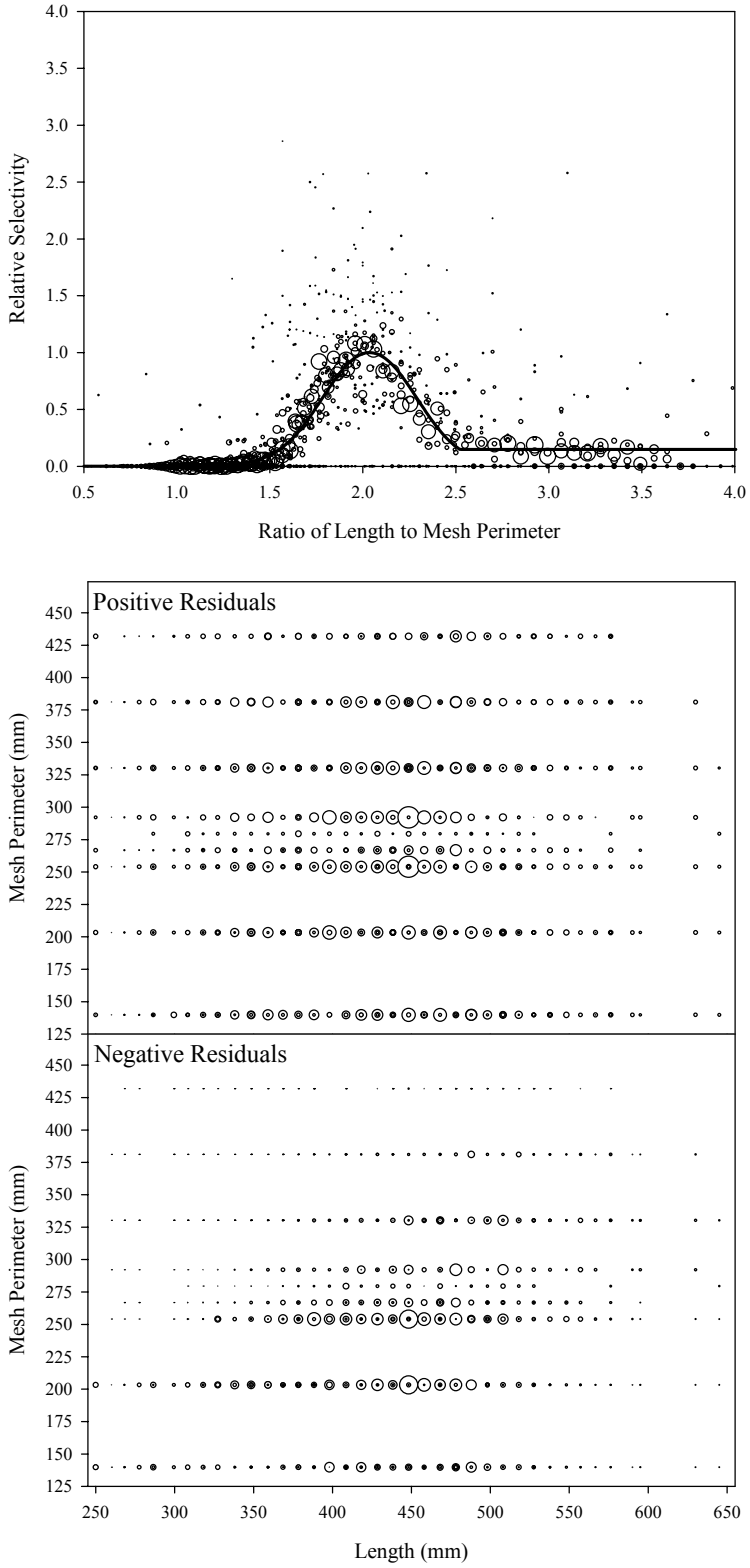

Figure B7.10. Plots of CPUE data scaled to a net selectivity model (top) and CPUE residuals (bottom); humpback whitefish data and Model 10.

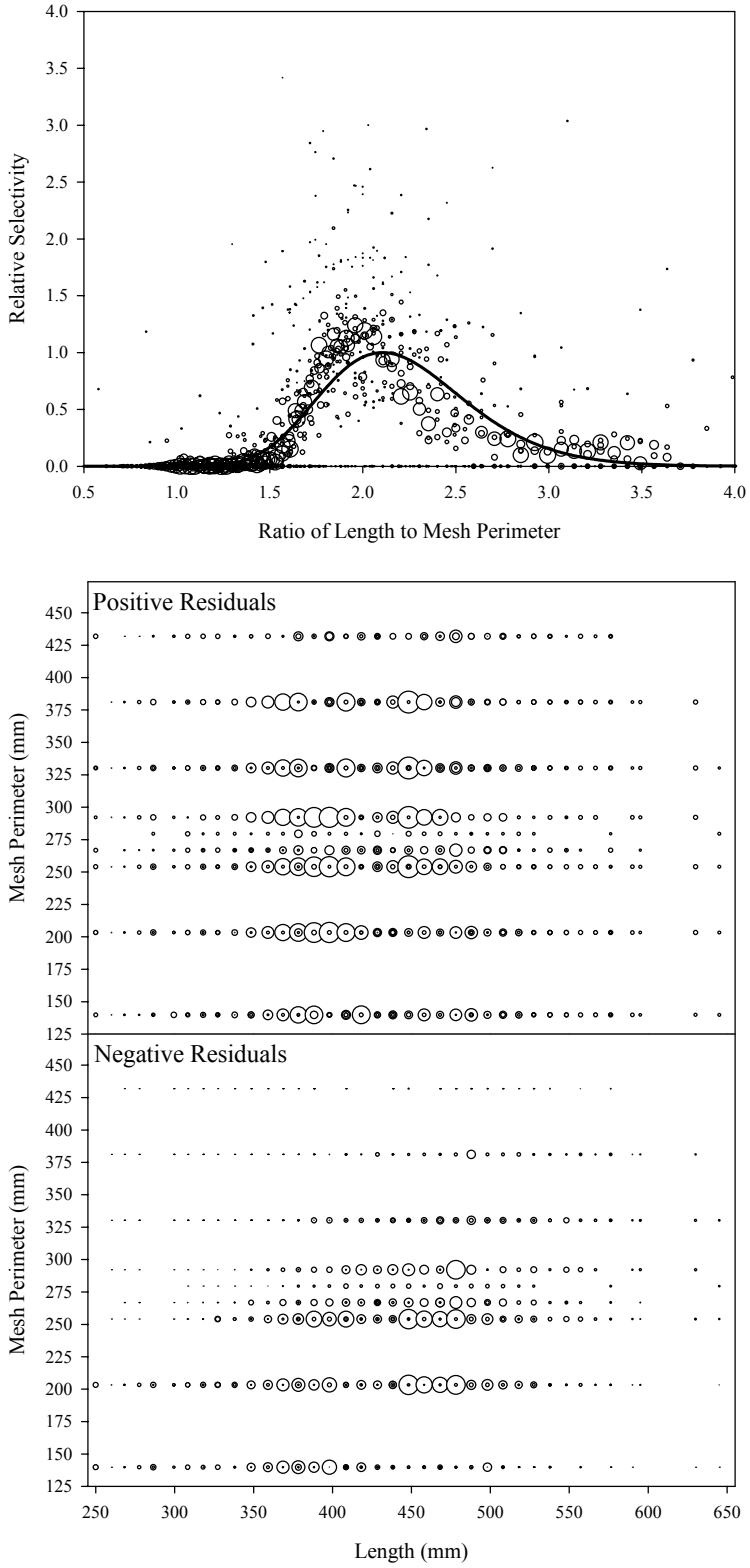

Figure B7.11. Plots of CPUE data scaled to a net selectivity model (top) and CPUE residuals (bottom); humpback whitefish data and Model 11.

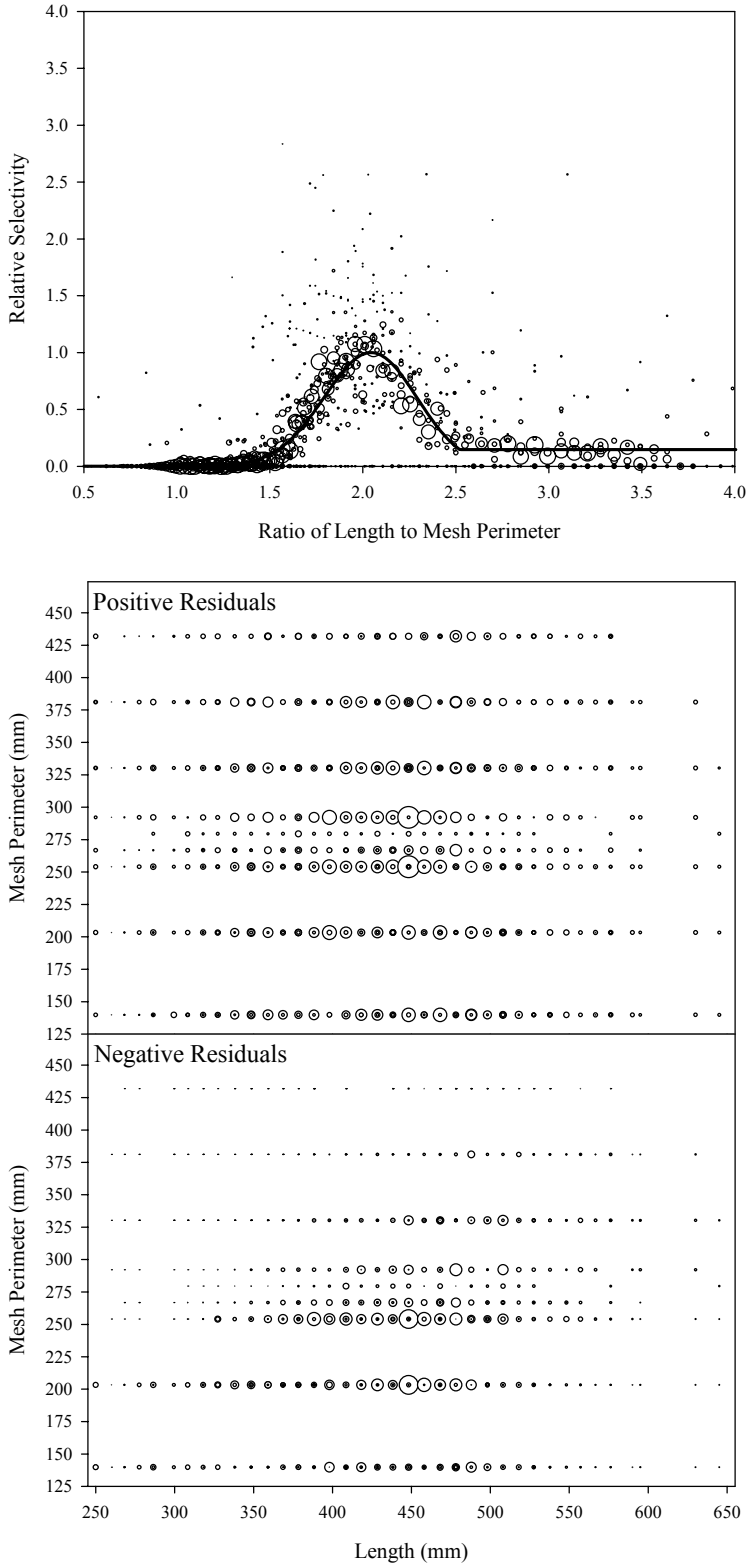

Figure B7.12. Plots of CPUE data scaled to a net selectivity model (top) and CPUE residuals (bottom); humpback whitefish data and Model 12.

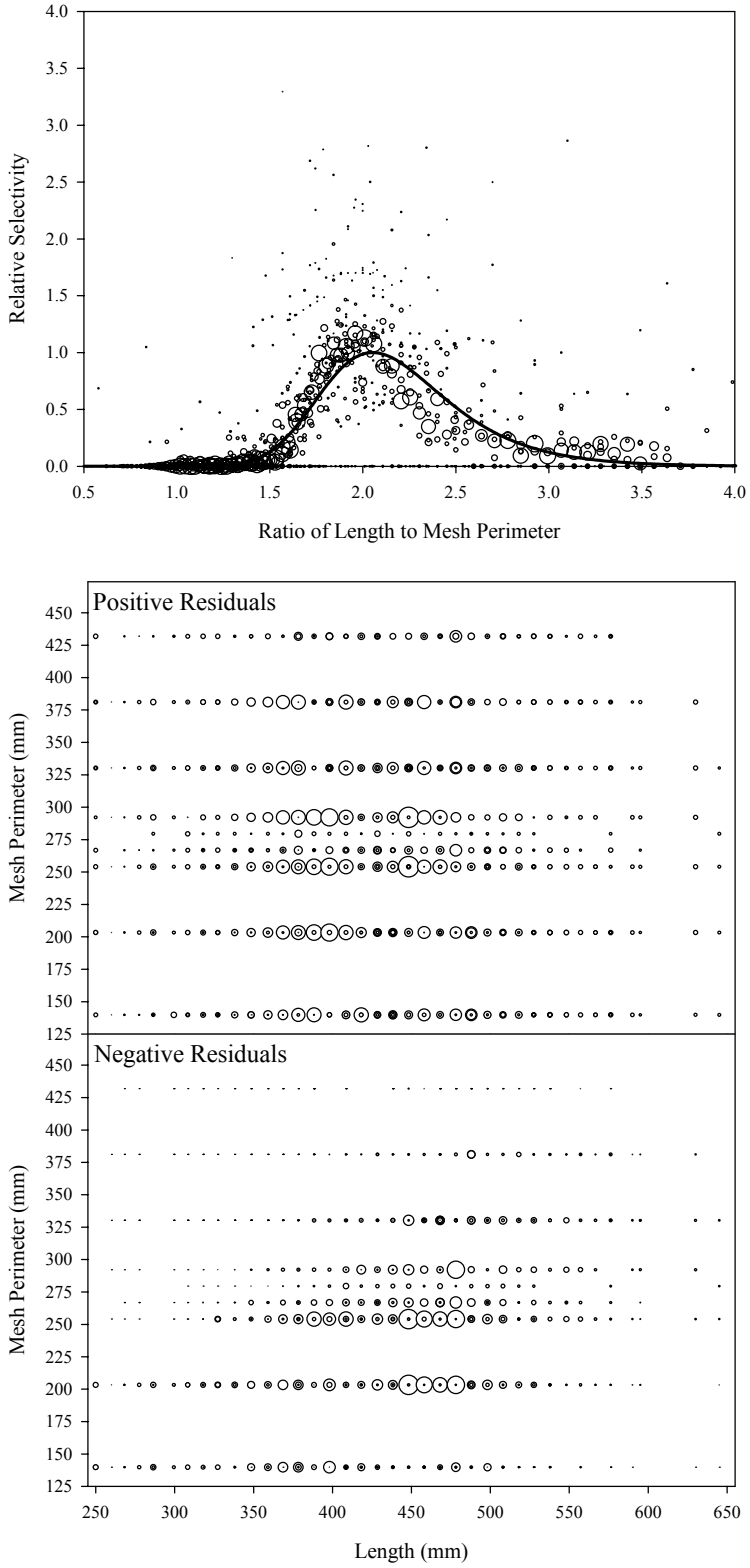

Figure B7.13. Plots of CPUE data scaled to a net selectivity model (top) and CPUE residuals (bottom); humpback whitefish data and Model 13.

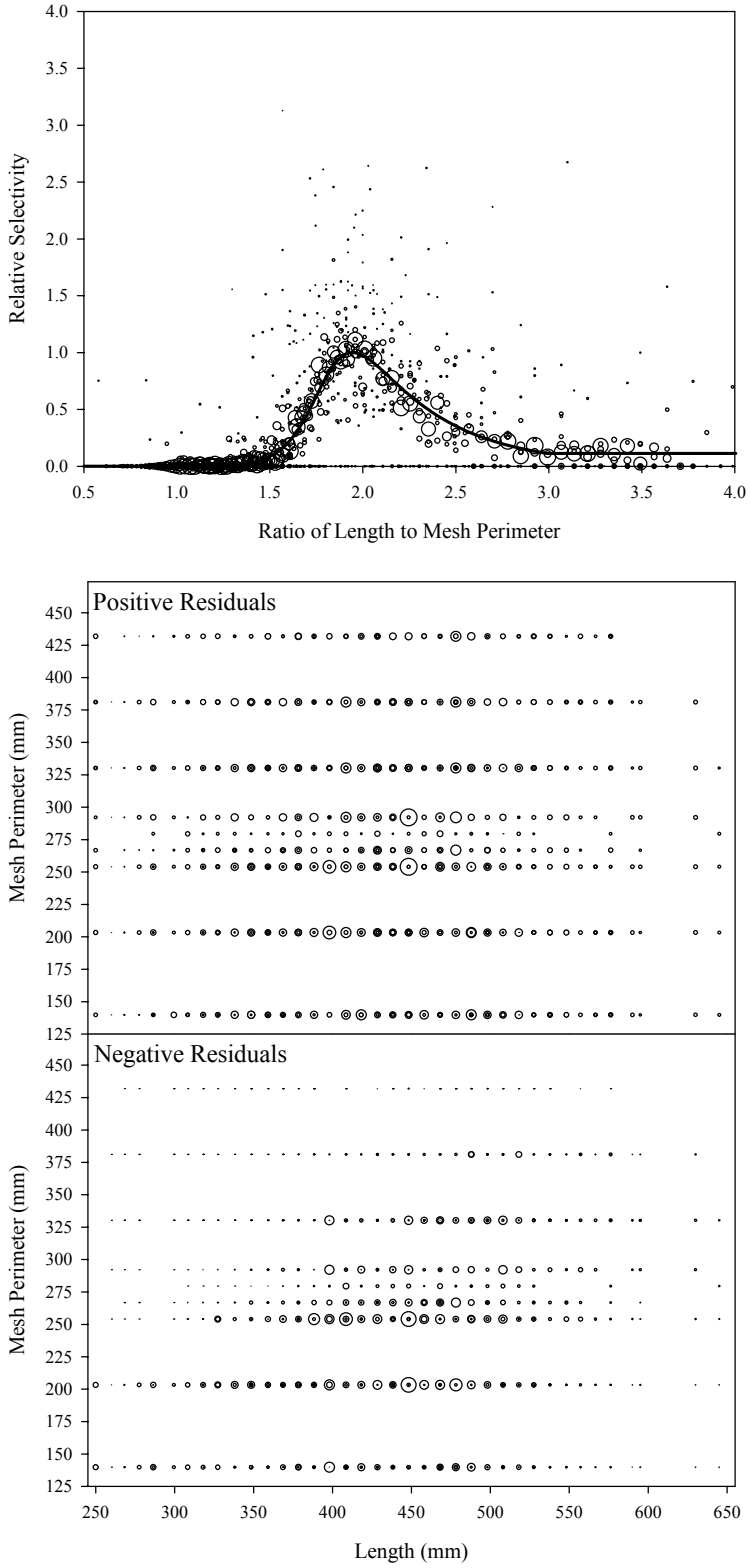

Figure B7.14. Plots of CPUE data scaled to a net selectivity model (top) and CPUE residuals (bottom); humpback whitefish data and Model 14.

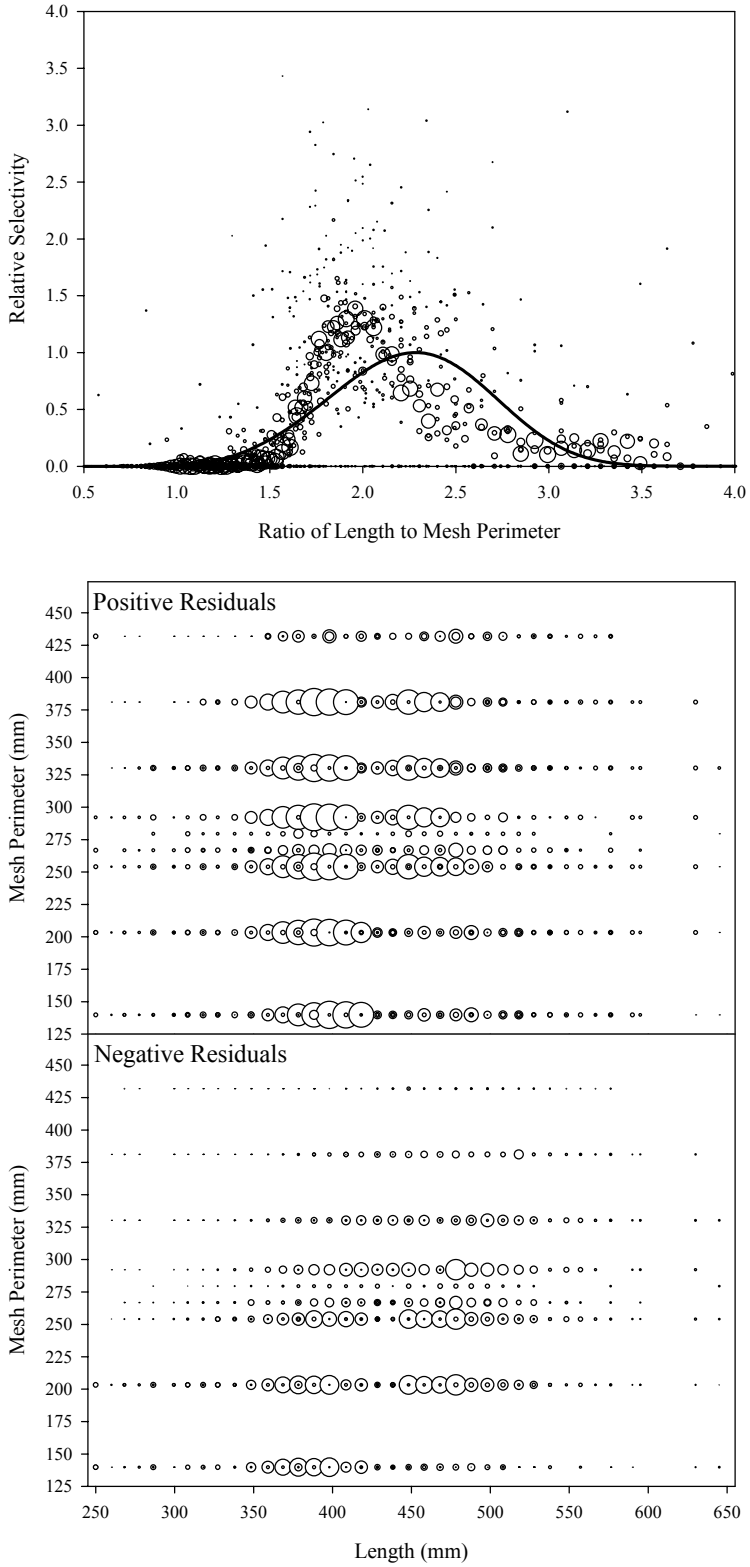

Figure B7.15. Plots of CPUE data scaled to a net selectivity model (top) and CPUE residuals (bottom); humpback whitefish data and Model 15.

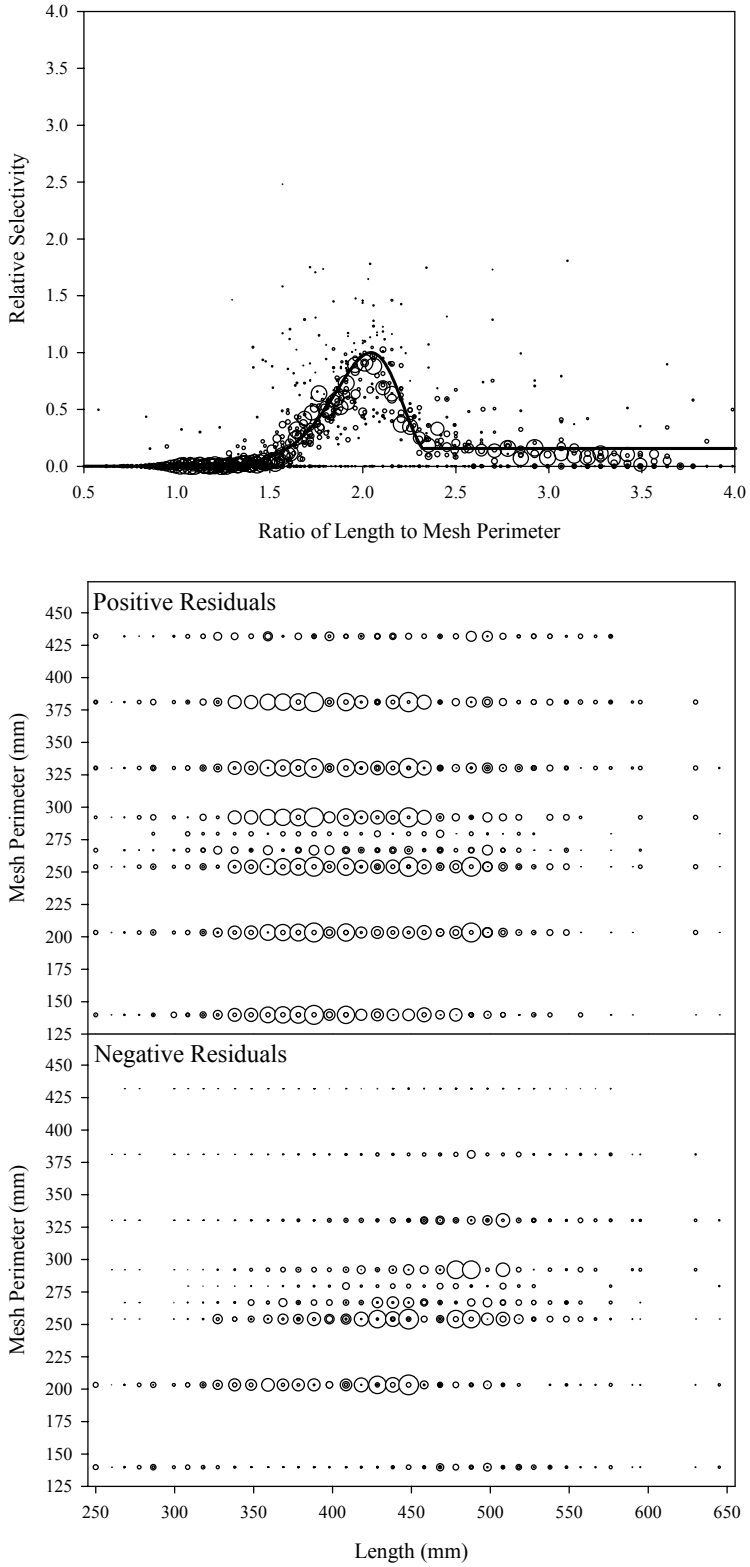

Figure B7.16. Plots of CPUE data scaled to a net selectivity model (top) and CPUE residuals (bottom); humpback whitefish data and Model 16.

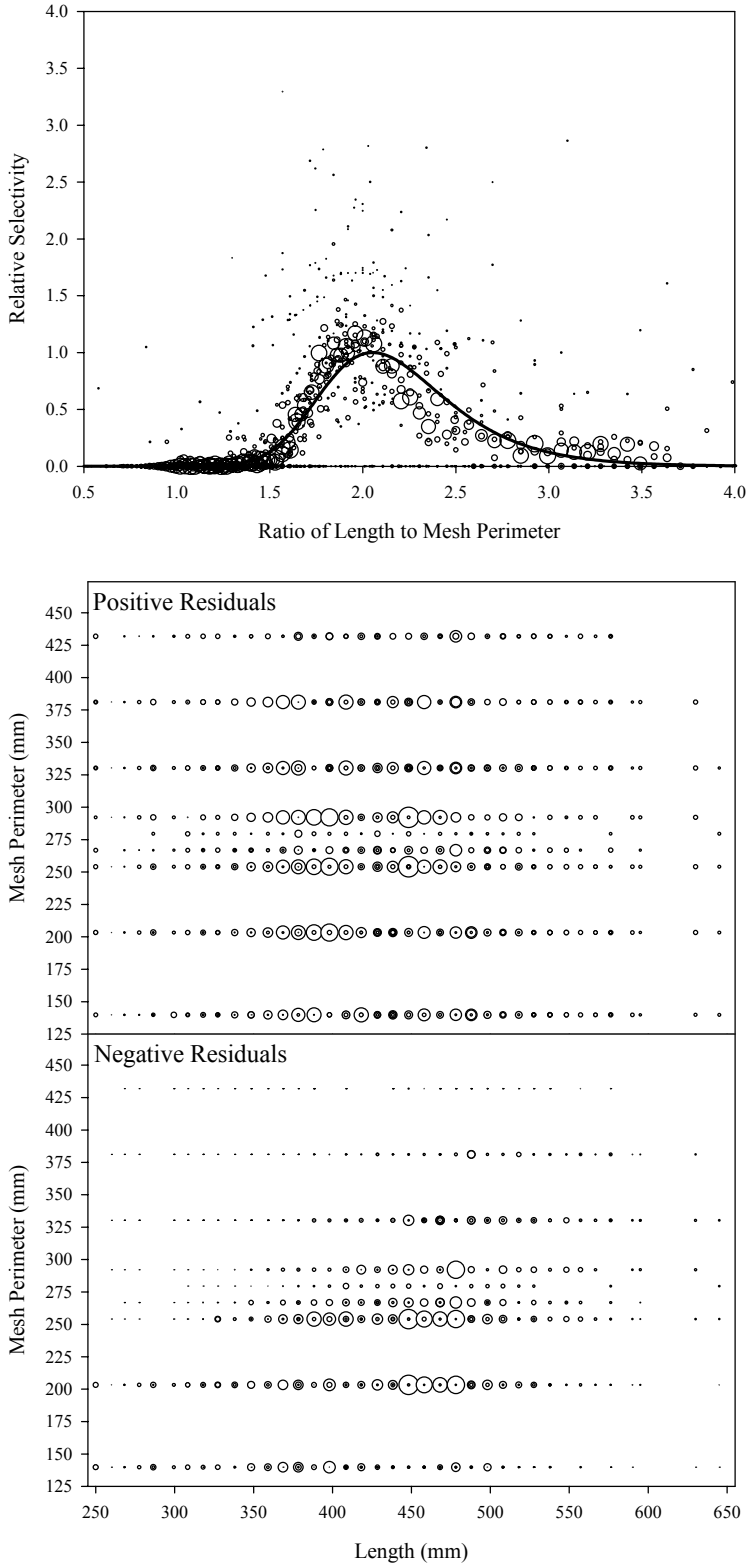

Figure B7.17. Plots of CPUE data scaled to a net selectivity model (top) and CPUE residuals (bottom); humpback whitefish data and Model 17.

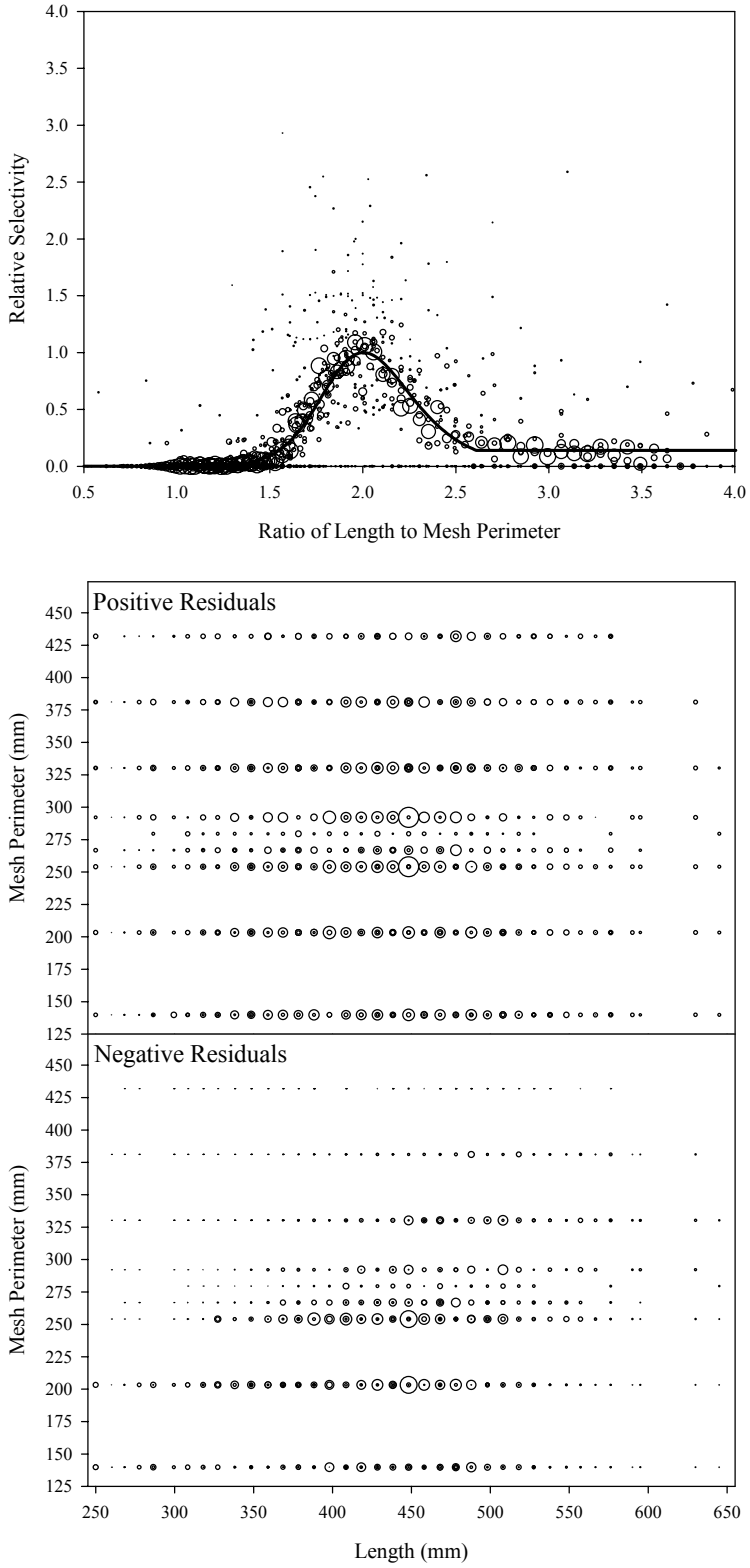

Figure B7.18. Plots of CPUE data scaled to a net selectivity model (top) and CPUE residuals (bottom); humpback whitefish data and Model 18.

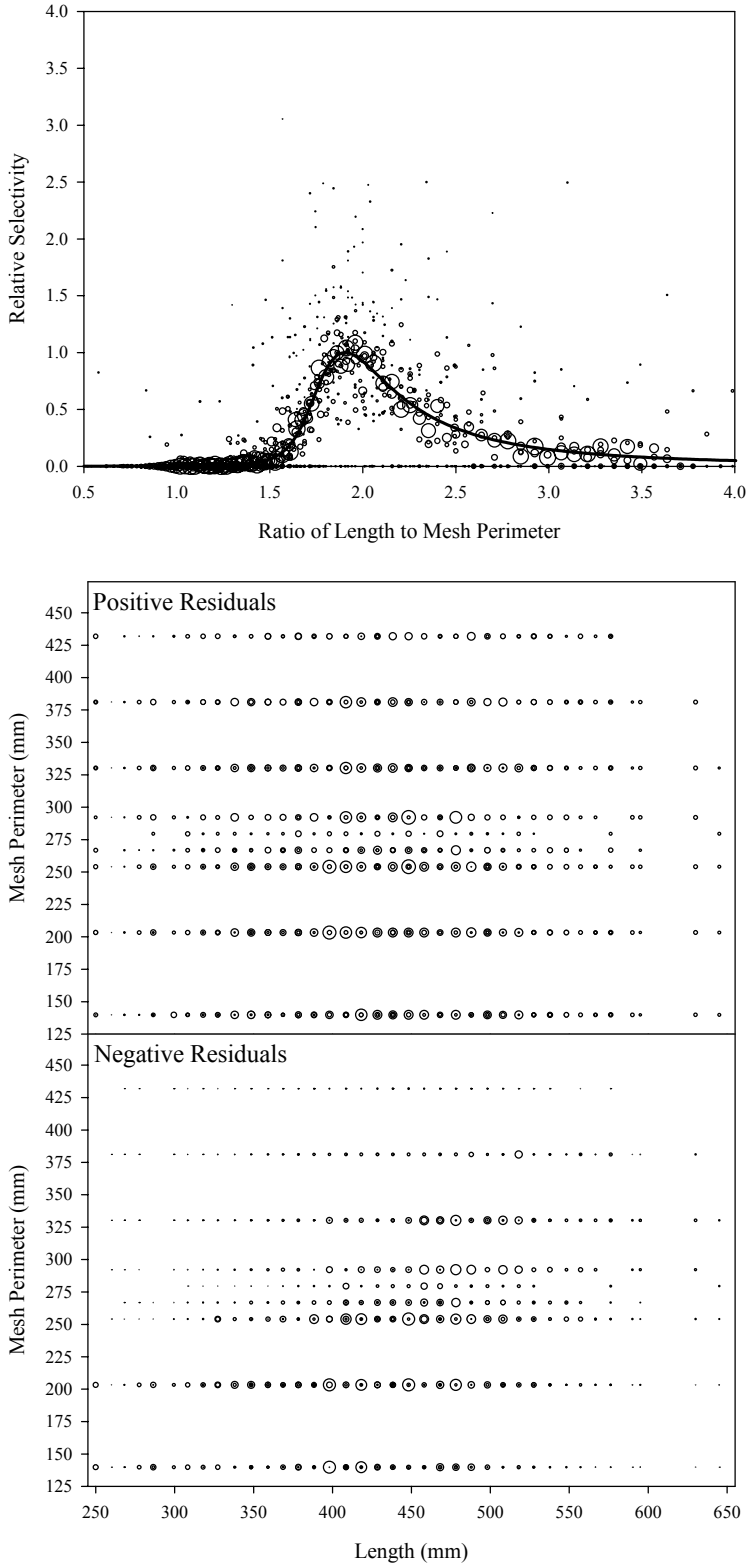

Figure B7.19. Plots of CPUE data scaled to a net selectivity model (top) and CPUE residuals (bottom); humpback whitefish data and Model 19.

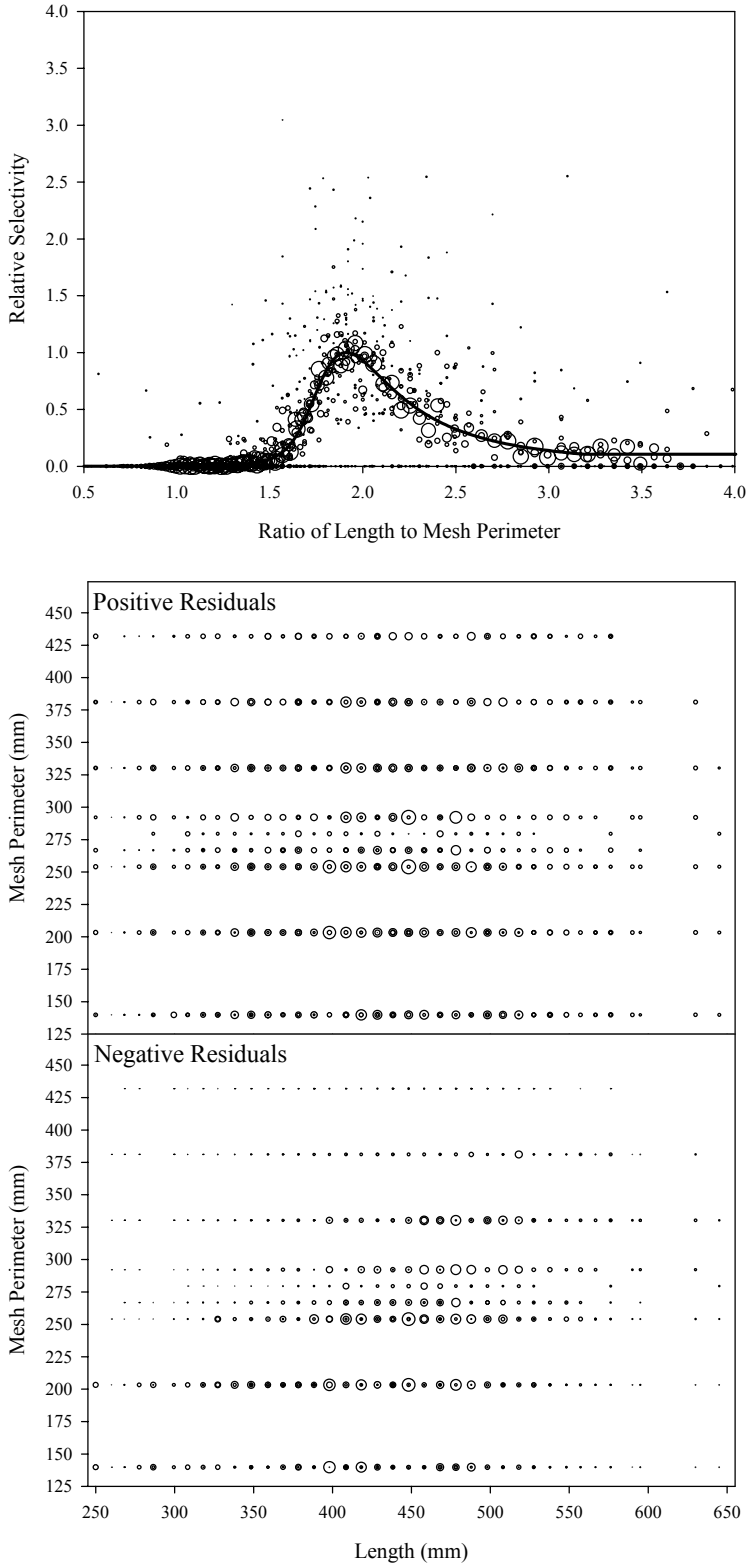

Figure B7.20. Plots of CPUE data scaled to a net selectivity model (top) and CPUE residuals (bottom); humpback whitefish data and Model 20.

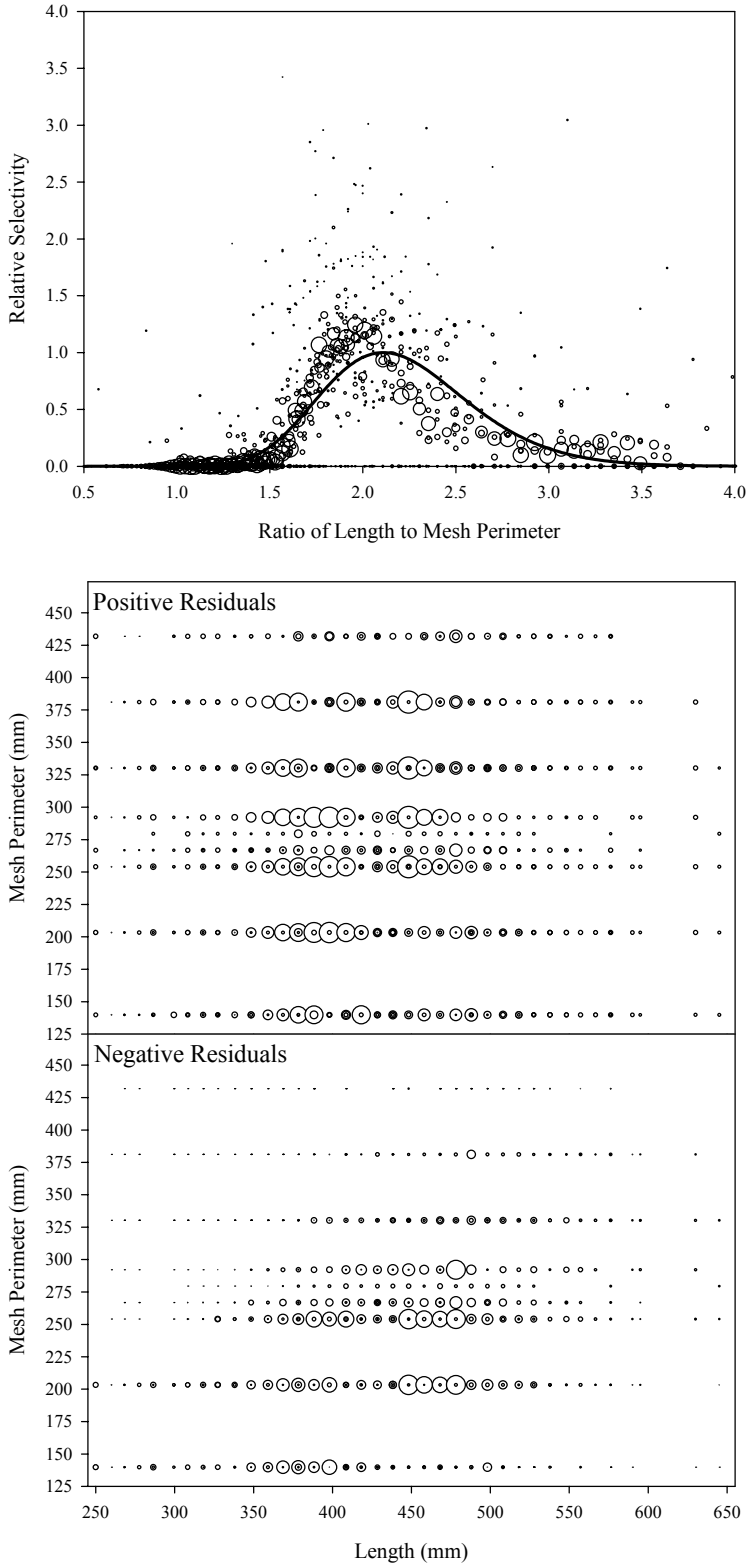

Figure B7.21. Plots of CPUE data scaled to a net selectivity model (top) and CPUE residuals (bottom); humpback whitefish data and Model 21.

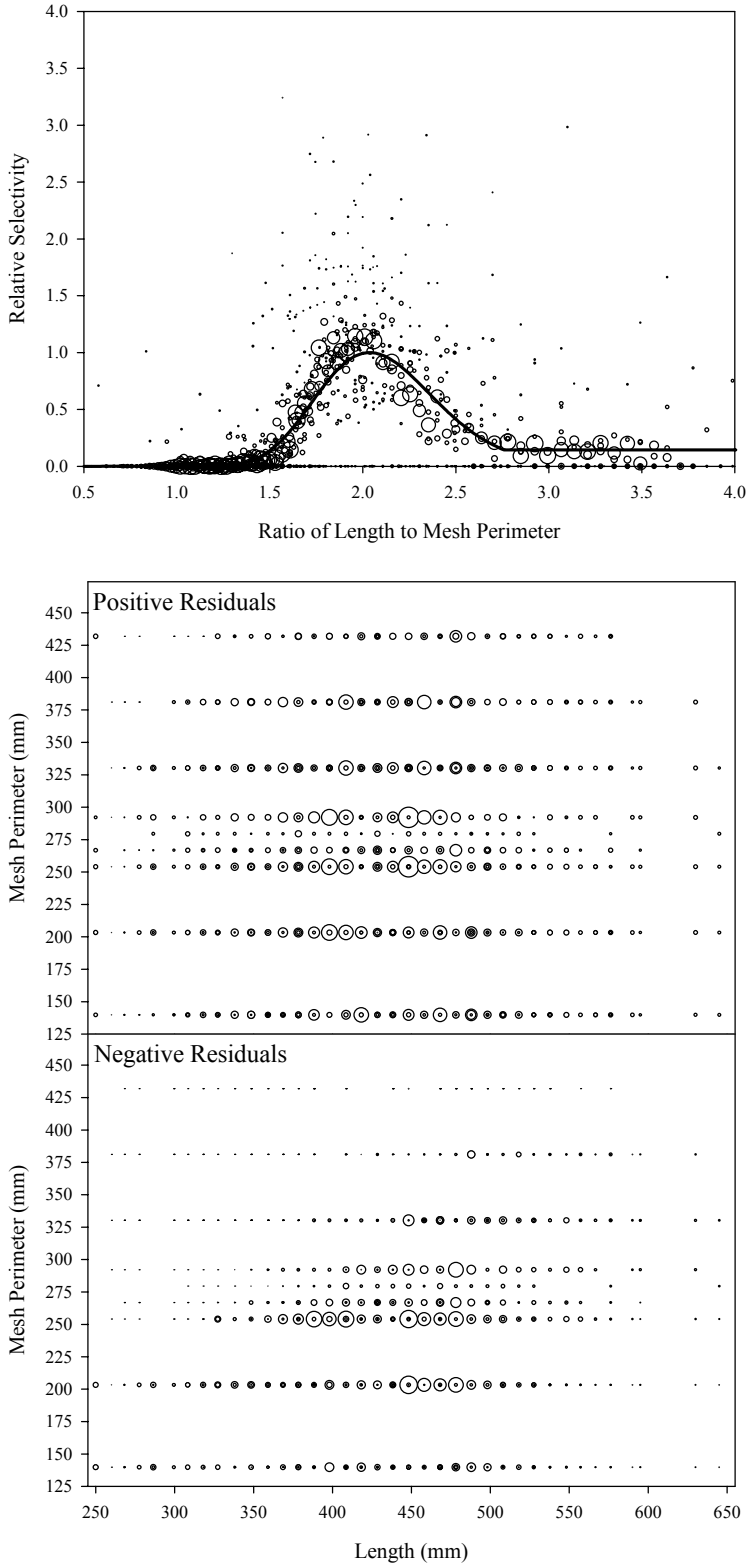

Figure B7.22. Plots of CPUE data scaled to a net selectivity model (top) and CPUE residuals (bottom); humpback whitefish data and Model 22.

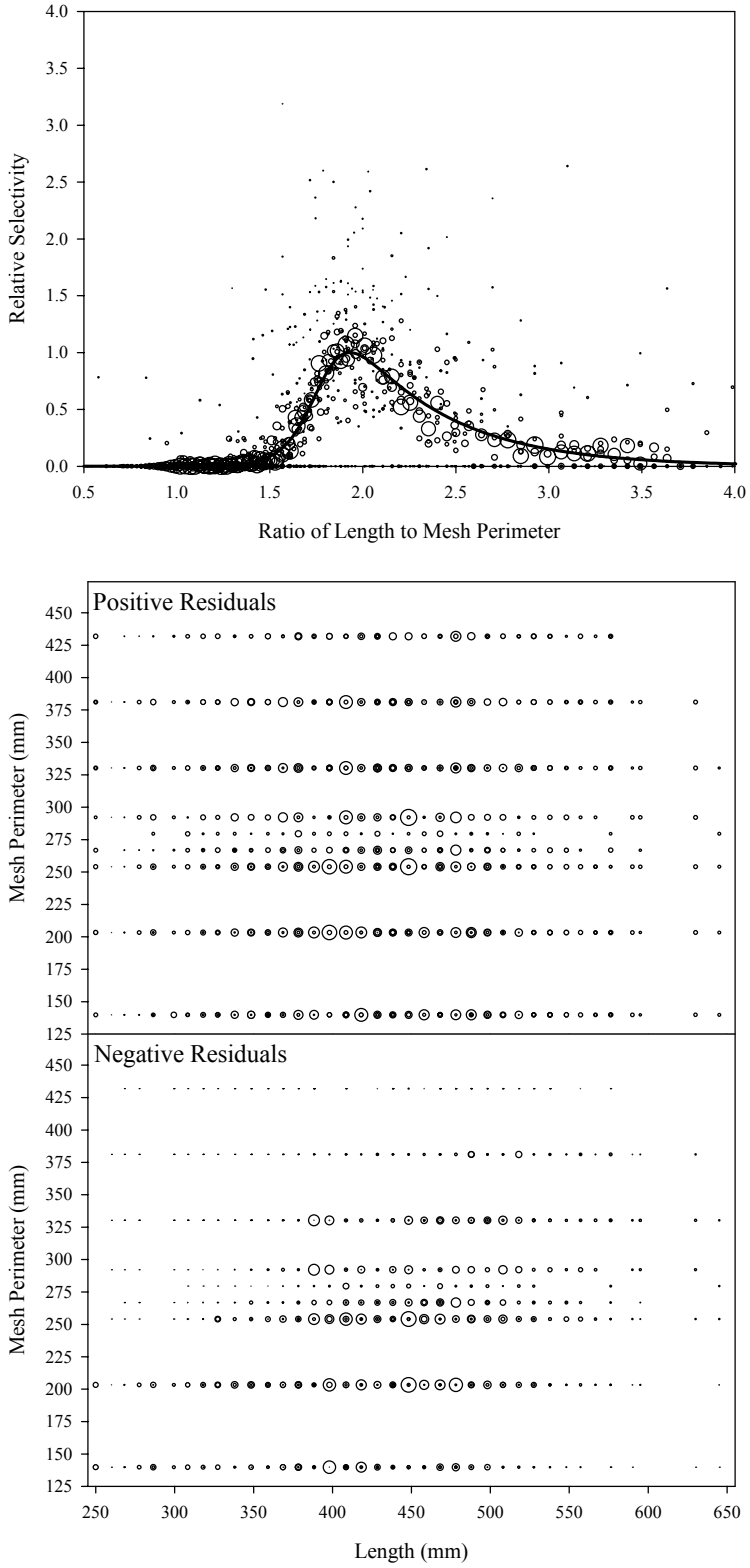

Figure B7.23. Plots of CPUE data scaled to a net selectivity model (top) and CPUE residuals (bottom); humpback whitefish data and Model 23.

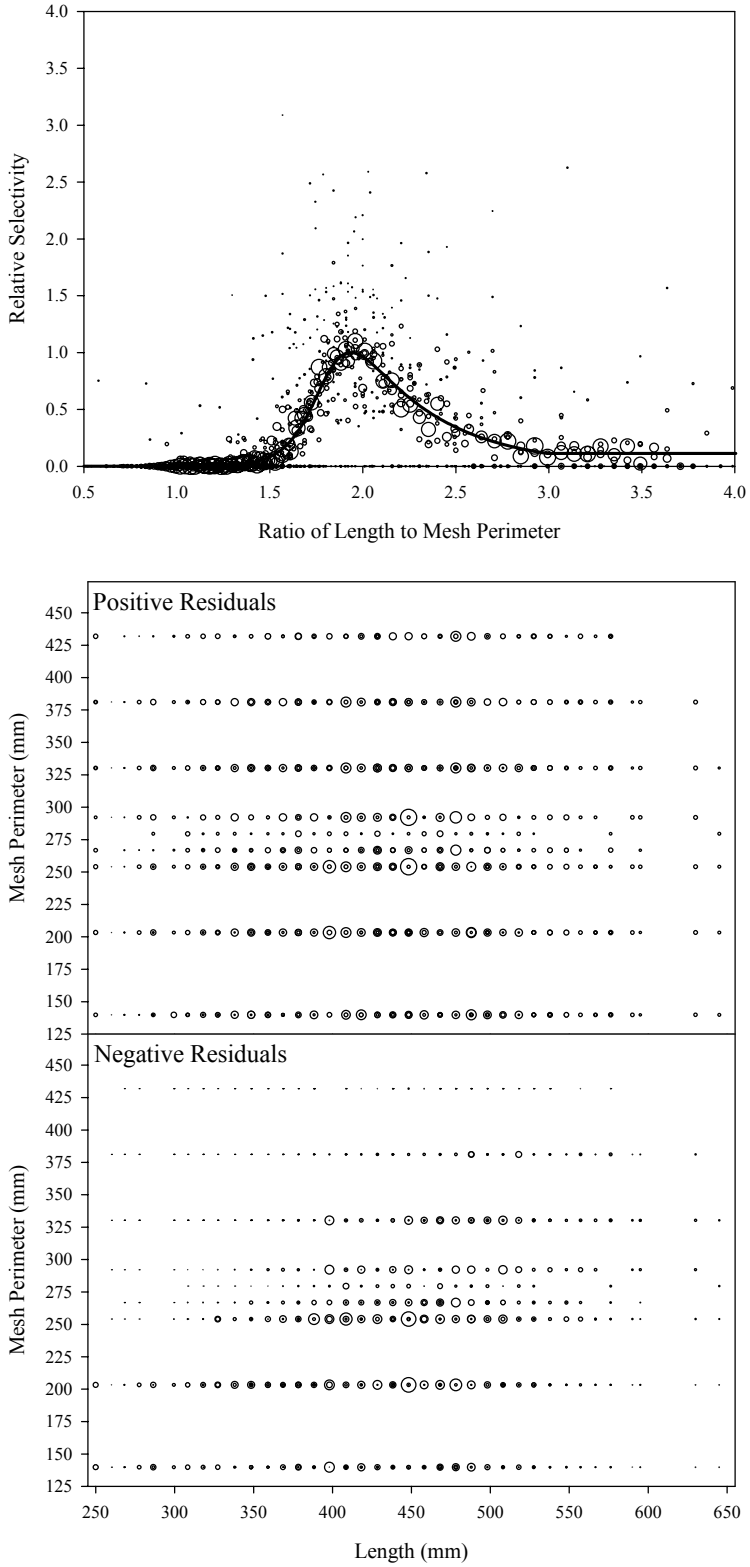

Figure B7.24. Plots of CPUE data scaled to a net selectivity model (top) and CPUE residuals (bottom); humpback whitefish data and Model 24.

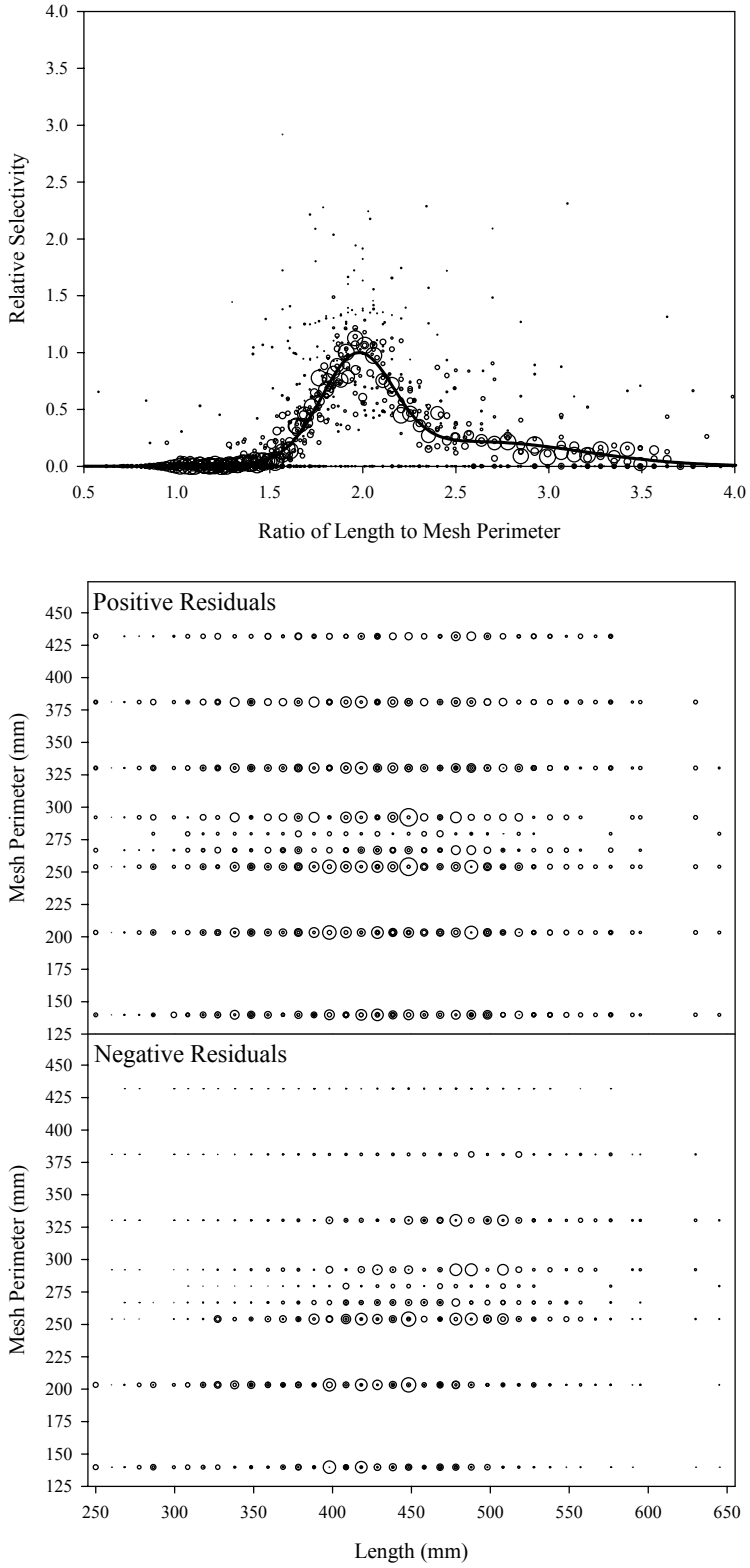

Figure B7.25. Plots of CPUE data scaled to a net selectivity model (top) and CPUE residuals (bottom); humpback whitefish data and Model 25.

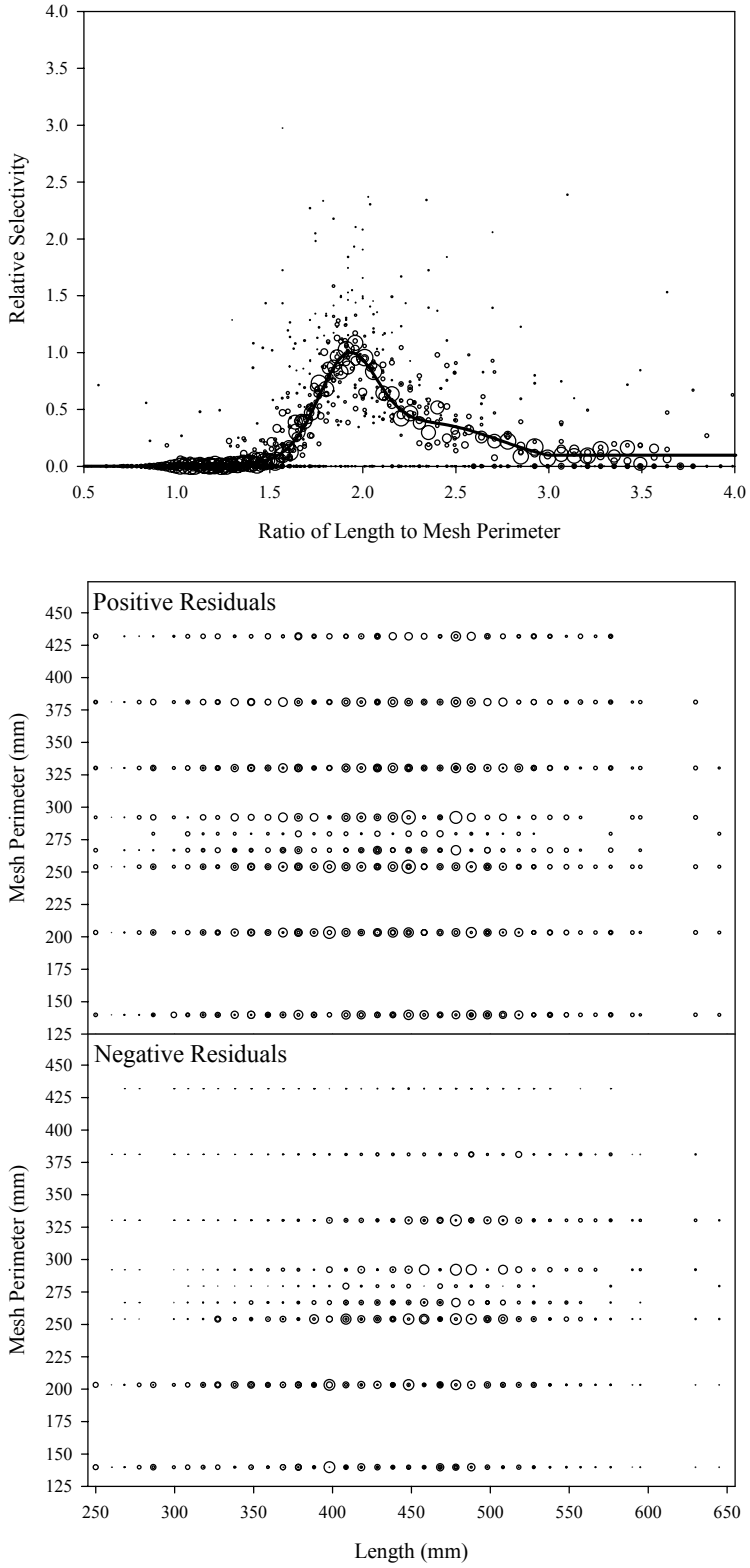

Figure B7.26. Plots of CPUE data scaled to a net selectivity model (top) and CPUE residuals (bottom); humpback whitefish data and Model 26.

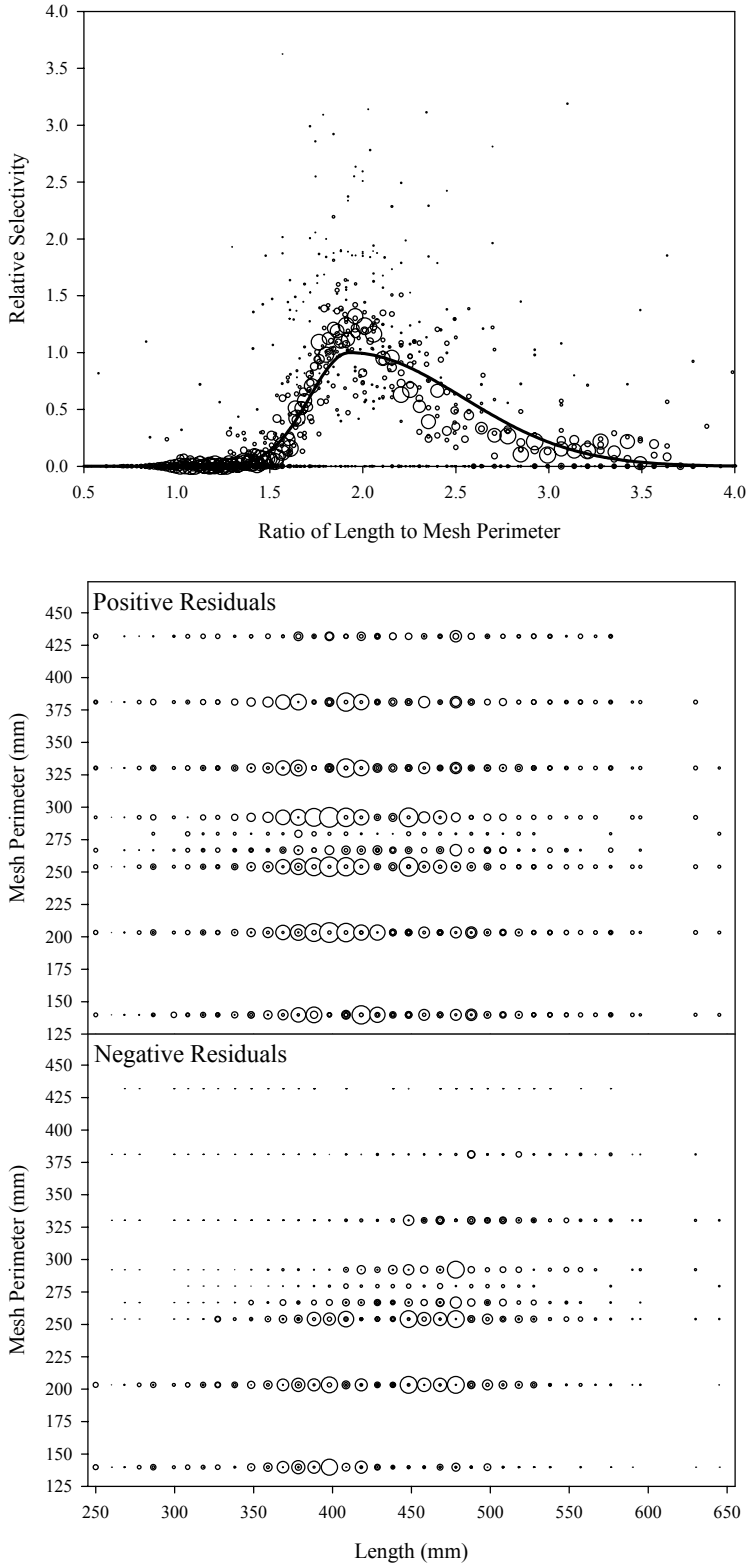

Figure B7.27. Plots of CPUE data scaled to a net selectivity model (top) and CPUE residuals (bottom); humpback whitefish data and Model 27.

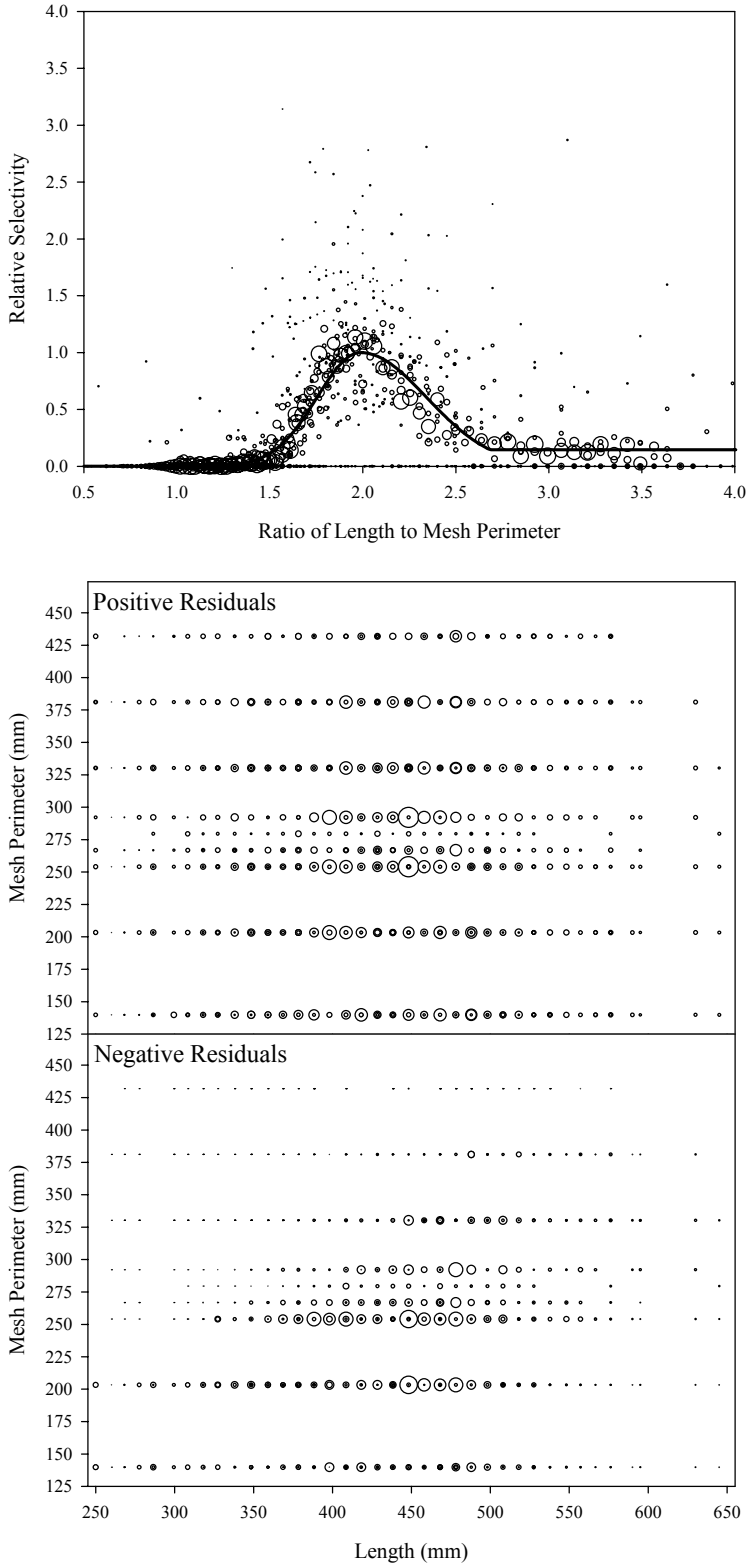

Figure B7.28. Plots of CPUE data scaled to a net selectivity model (top) and CPUE residuals (bottom); humpback whitefish data and Model 28.

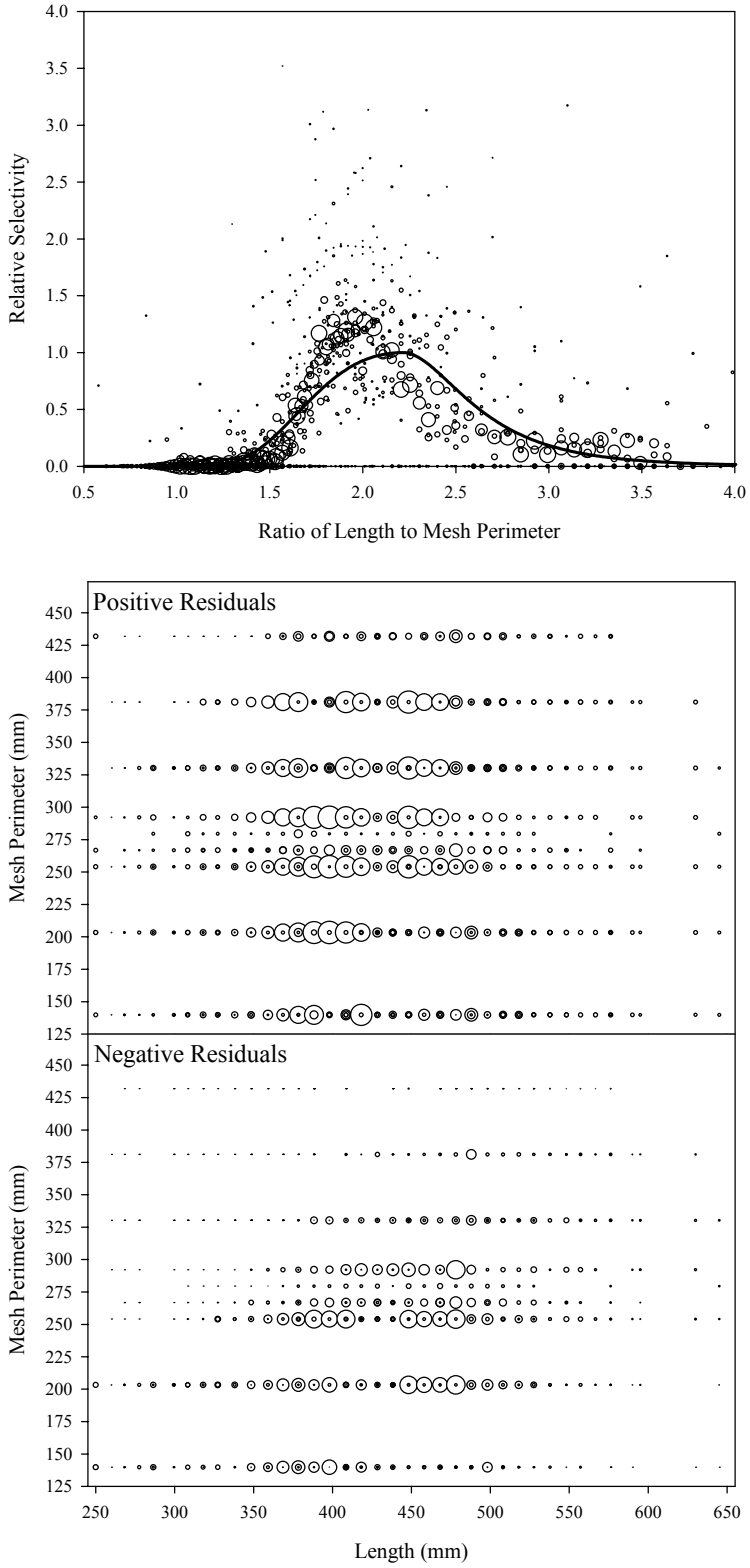

Figure B7.29. Plots of CPUE data scaled to a net selectivity model (top) and CPUE residuals (bottom); humpback whitefish data and Model 29.

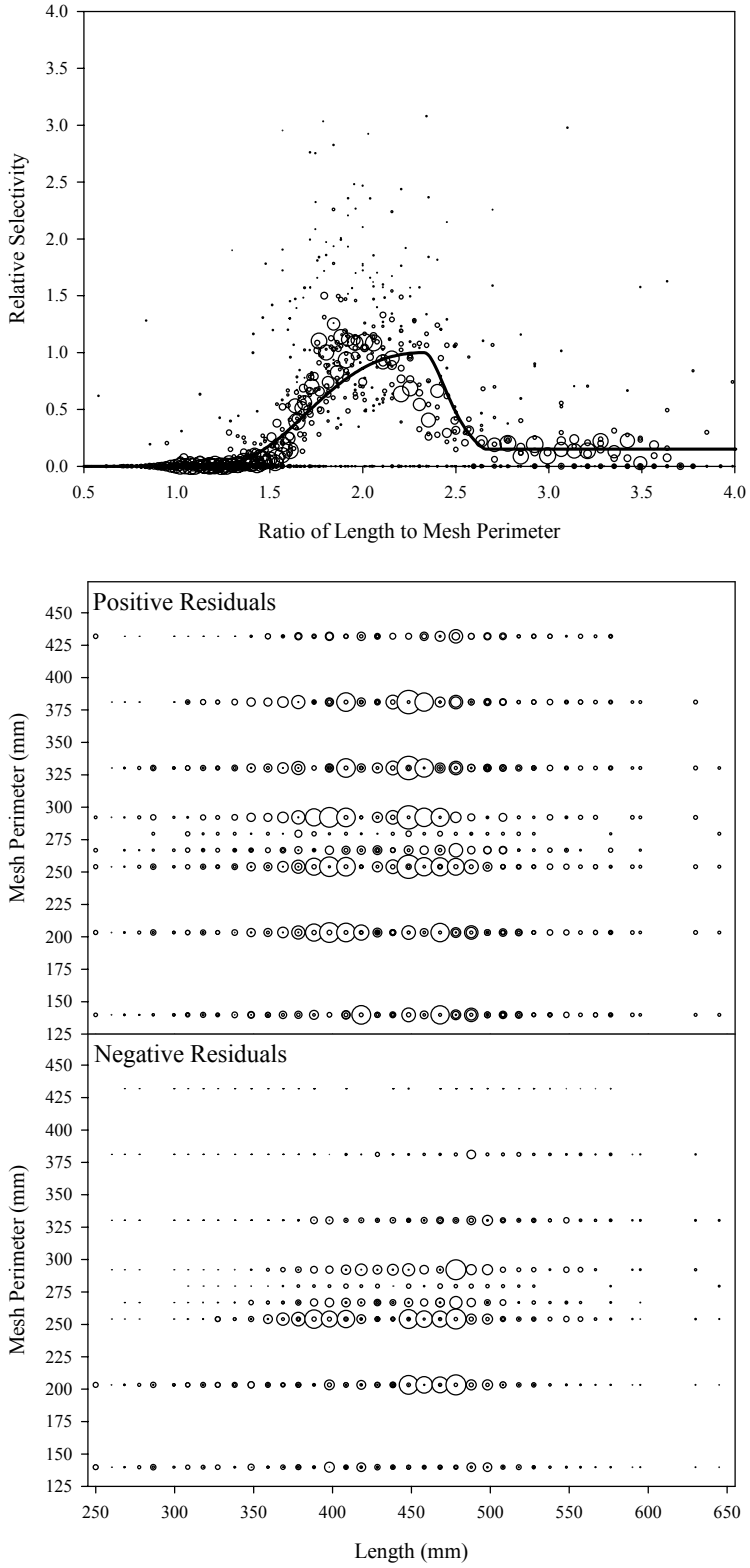

Figure B7.30. Plots of CPUE data scaled to a net selectivity model (top) and CPUE residuals (bottom); humpback whitefish data and Model 30.

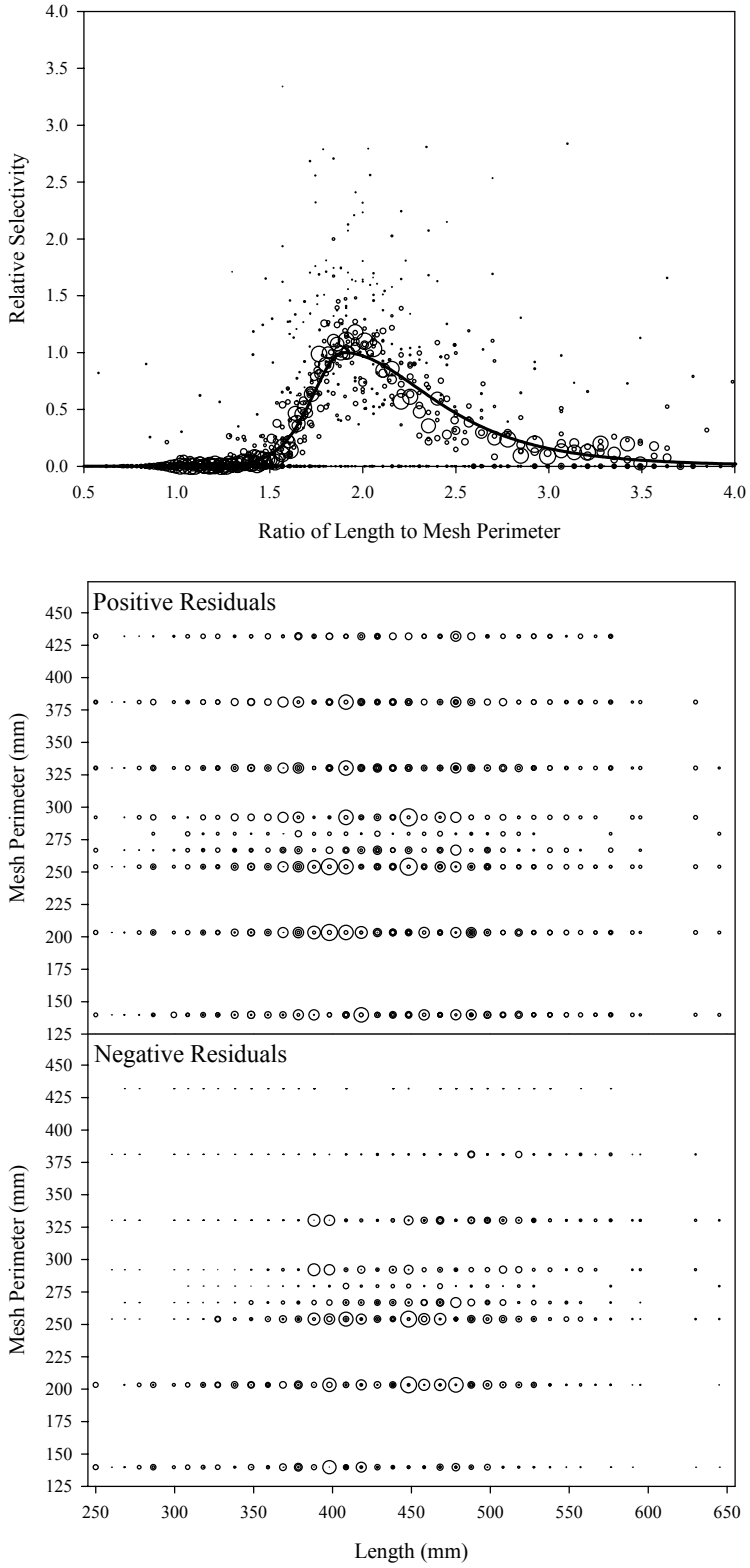

Figure B7.31. Plots of CPUE data scaled to a net selectivity model (top) and CPUE residuals (bottom); humpback whitefish data and Model 31.

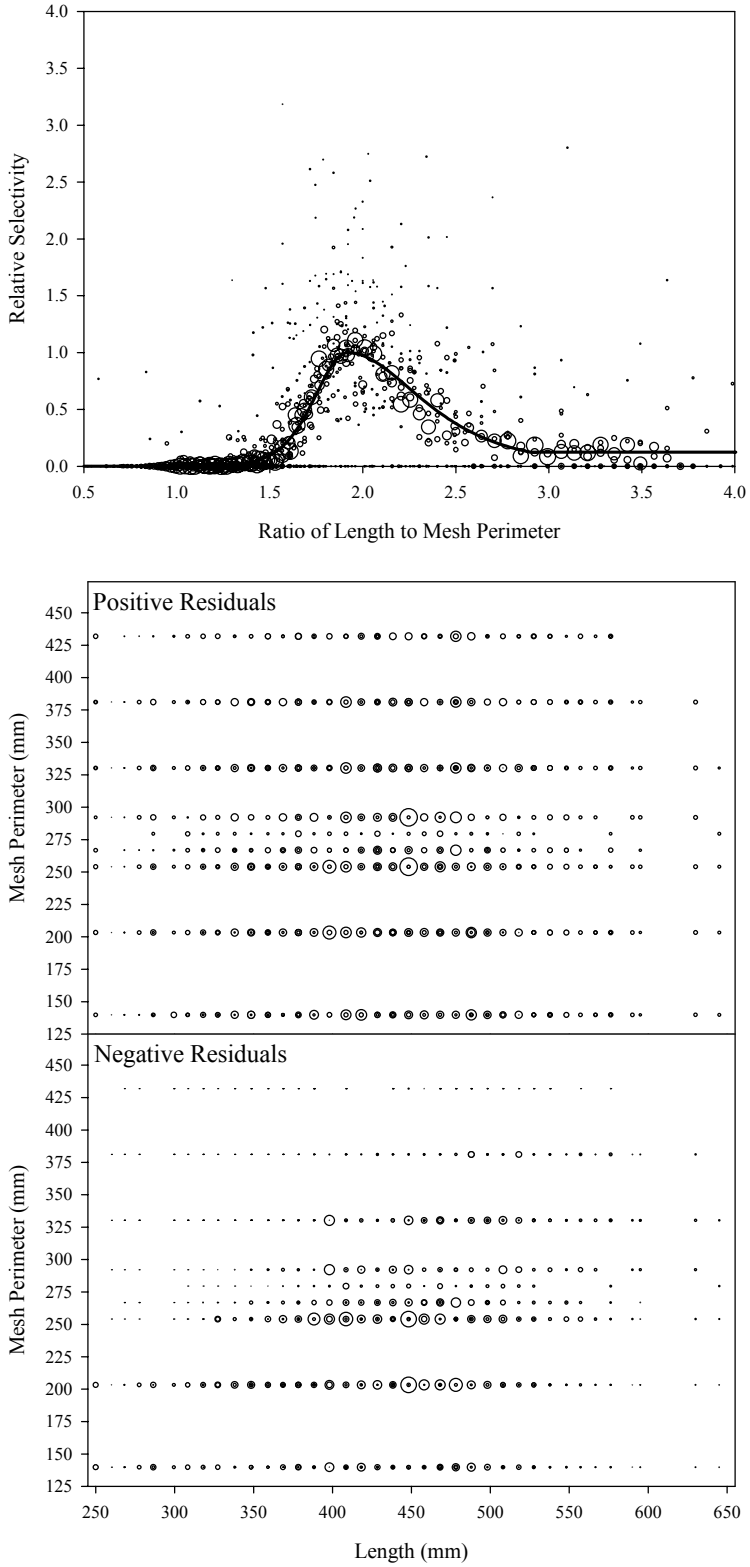

Figure B7.32. Plots of CPUE data scaled to a net selectivity model (top) and CPUE residuals (bottom); humpback whitefish data and Model 32.

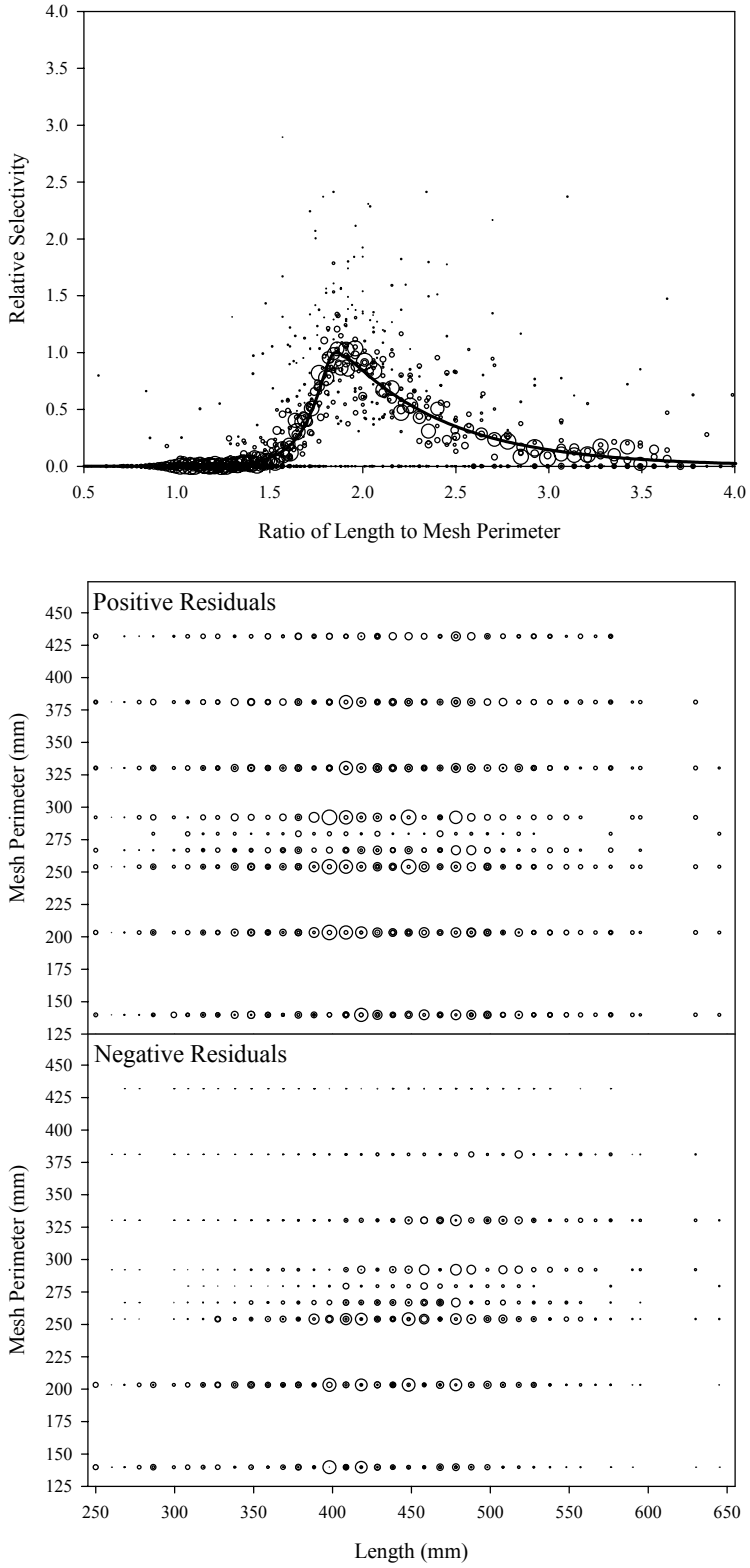

Figure B7.33. Plots of CPUE data scaled to a net selectivity model (top) and CPUE residuals (bottom); humpback whitefish data and Model 33.

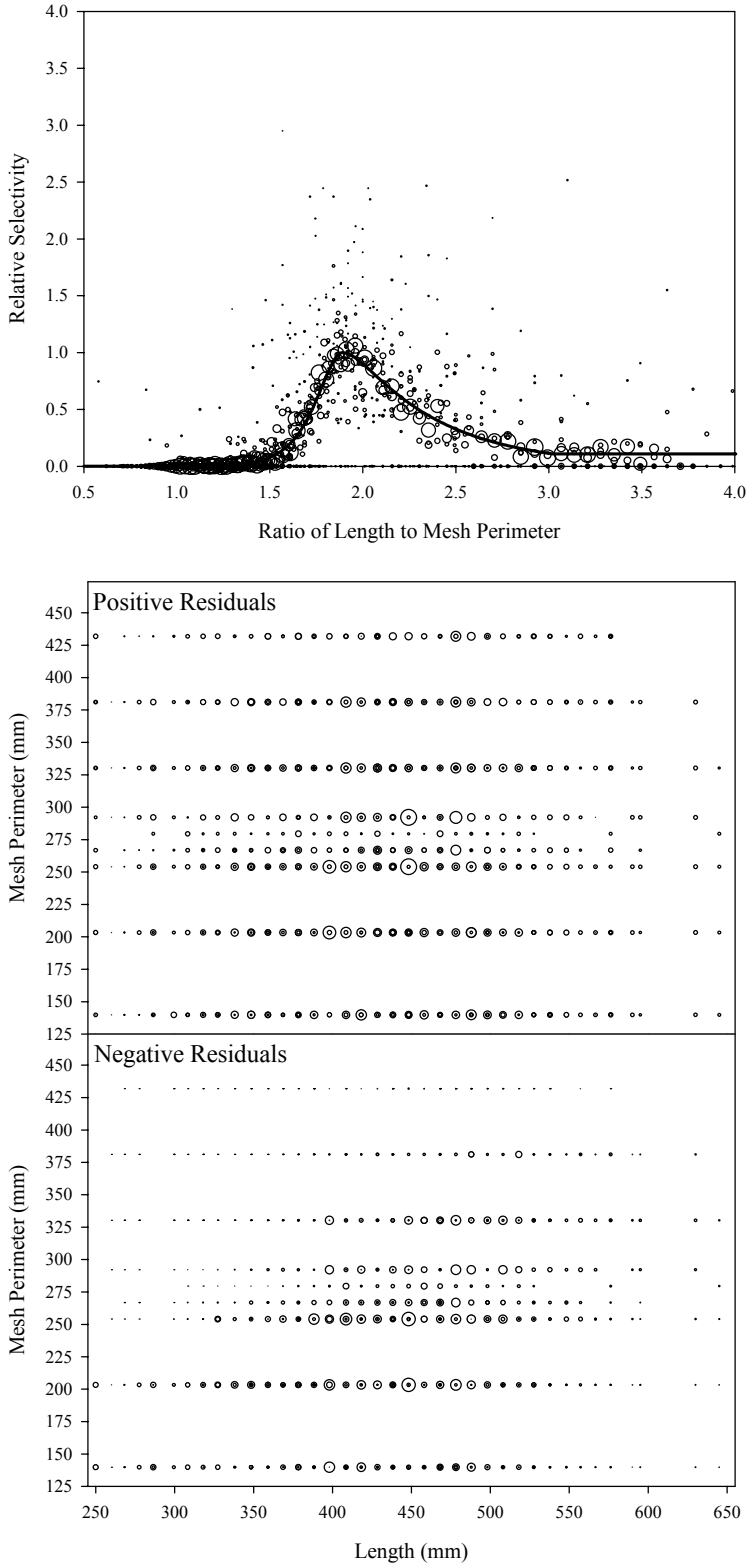

Figure B7.34. Plots of CPUE data scaled to a net selectivity model (top) and CPUE residuals (bottom); humpback whitefish data and Model 34.

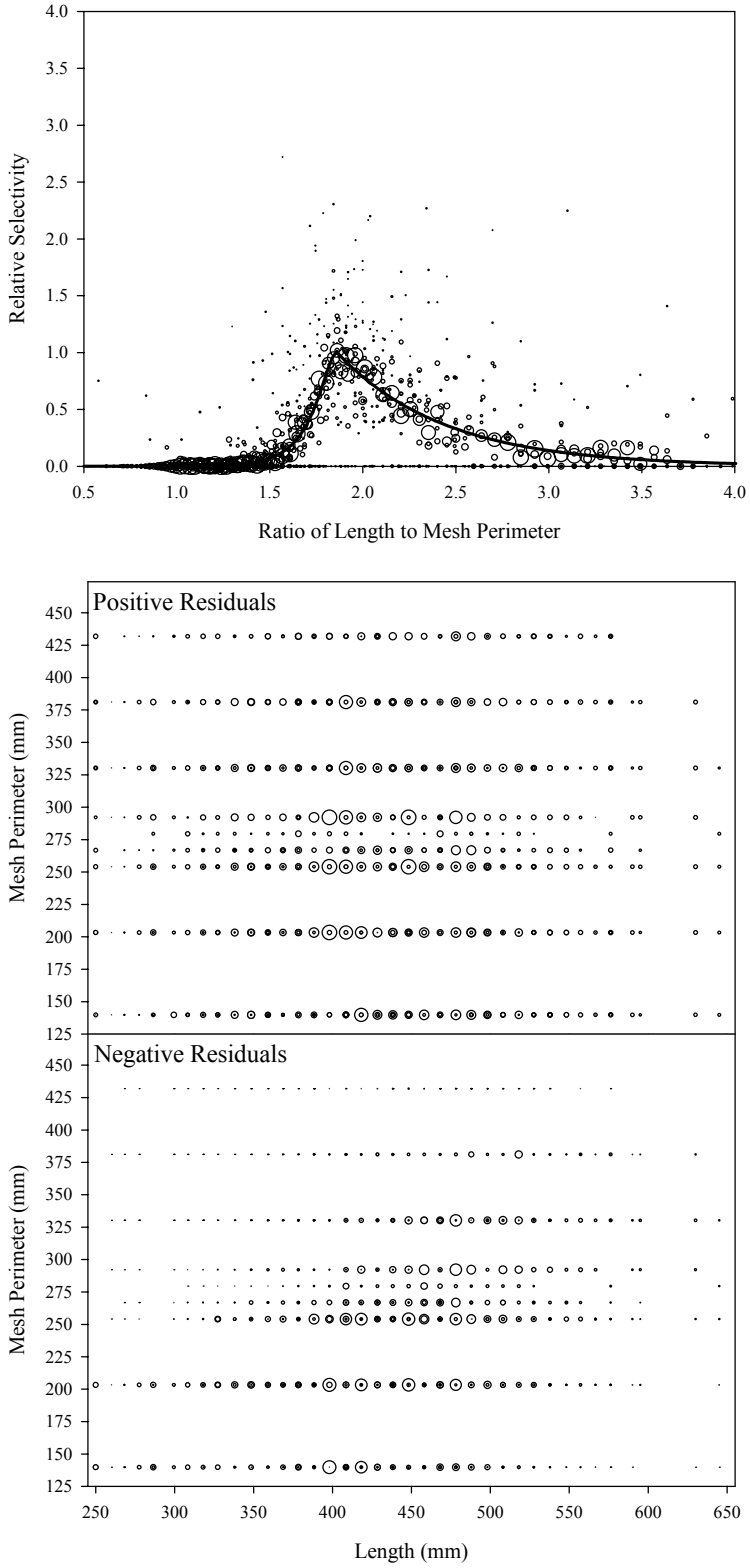

Figure B7.35. Plots of CPUE data scaled to a net selectivity model (top) and CPUE residuals (bottom); humpback whitefish data and Model 35.

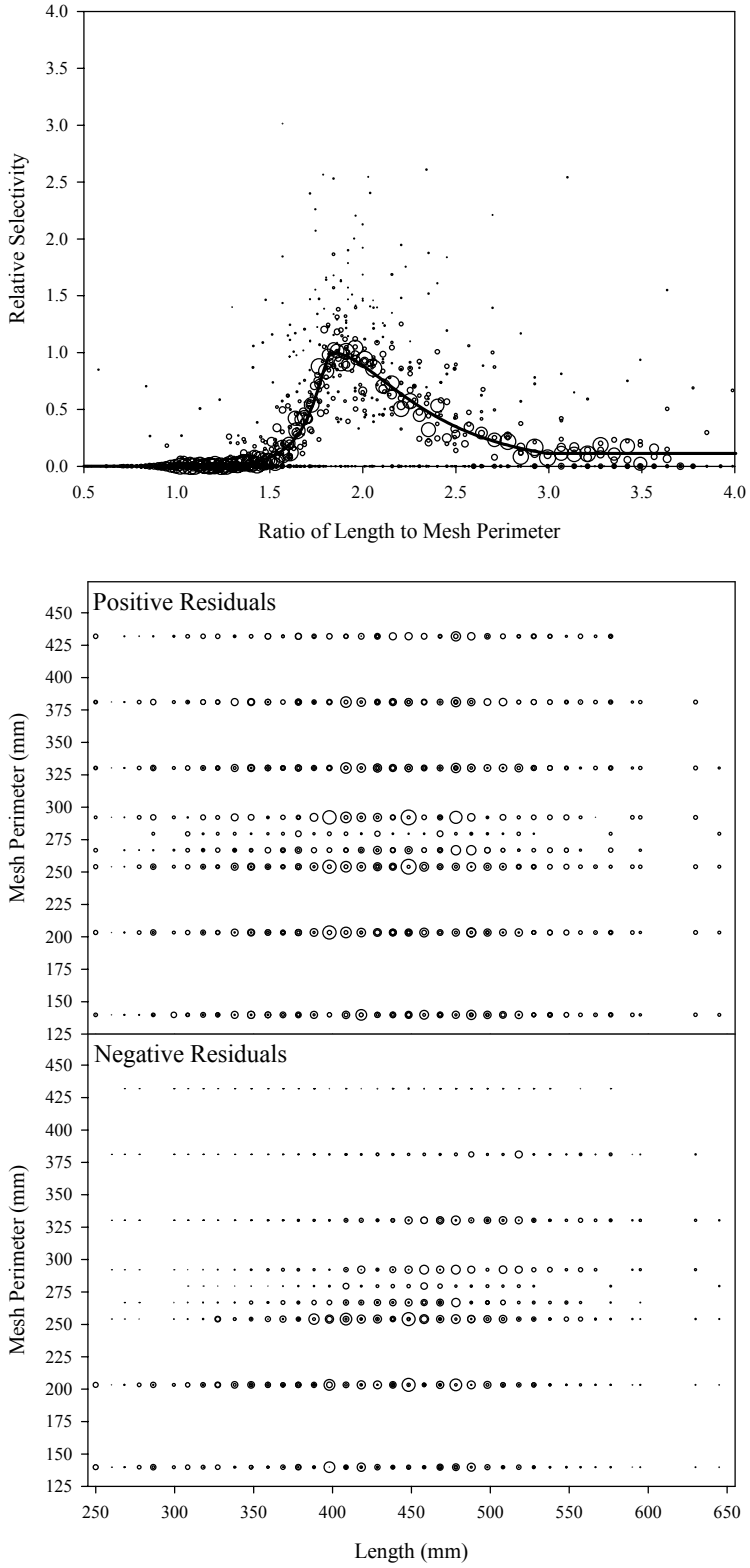

Figure B7.36. Plots of CPUE data scaled to a net selectivity model (top) and CPUE residuals (bottom); humpback whitefish data and Model 36.

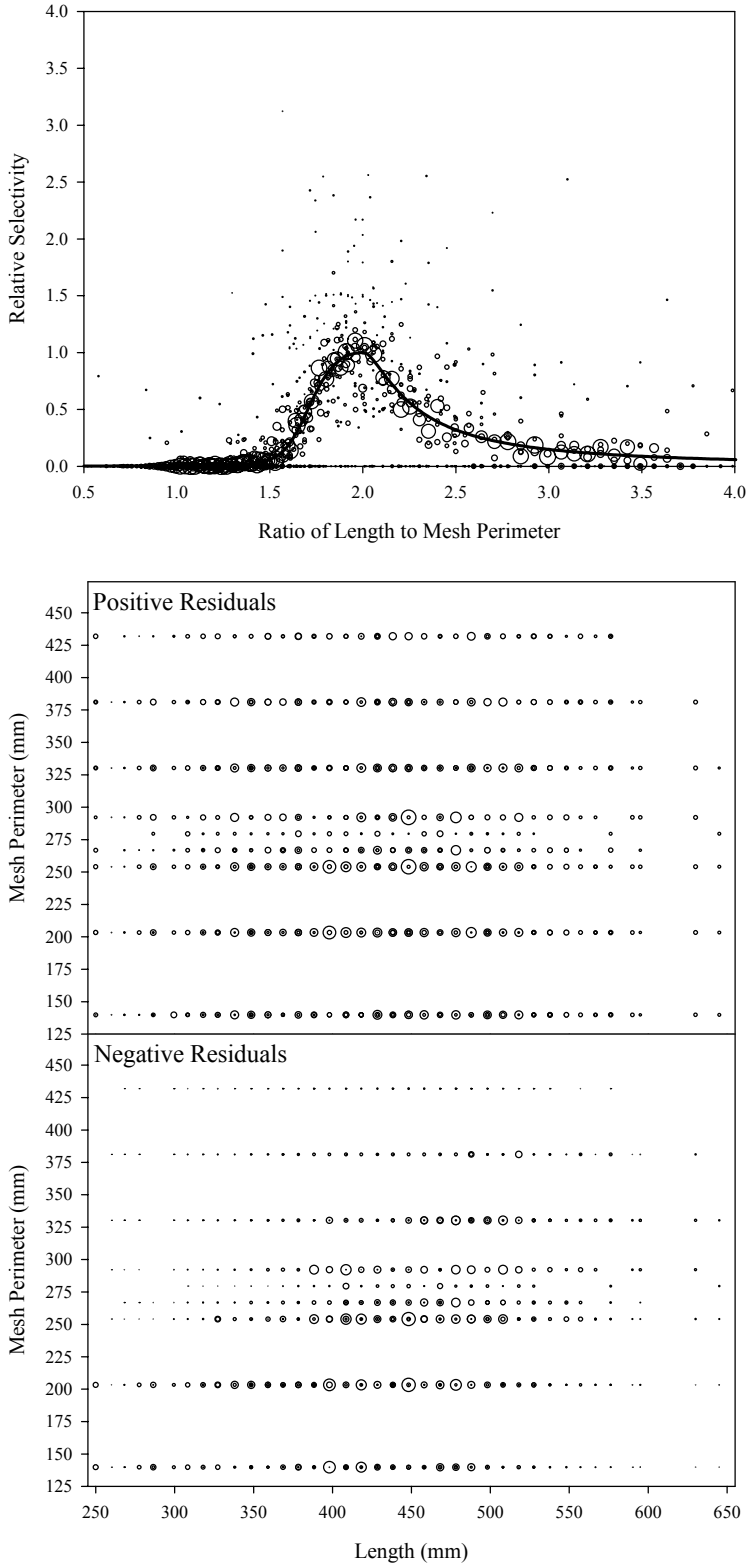

Figure B7.37. Plots of CPUE data scaled to a net selectivity model (top) and CPUE residuals (bottom); humpback whitefish data and Model 37.

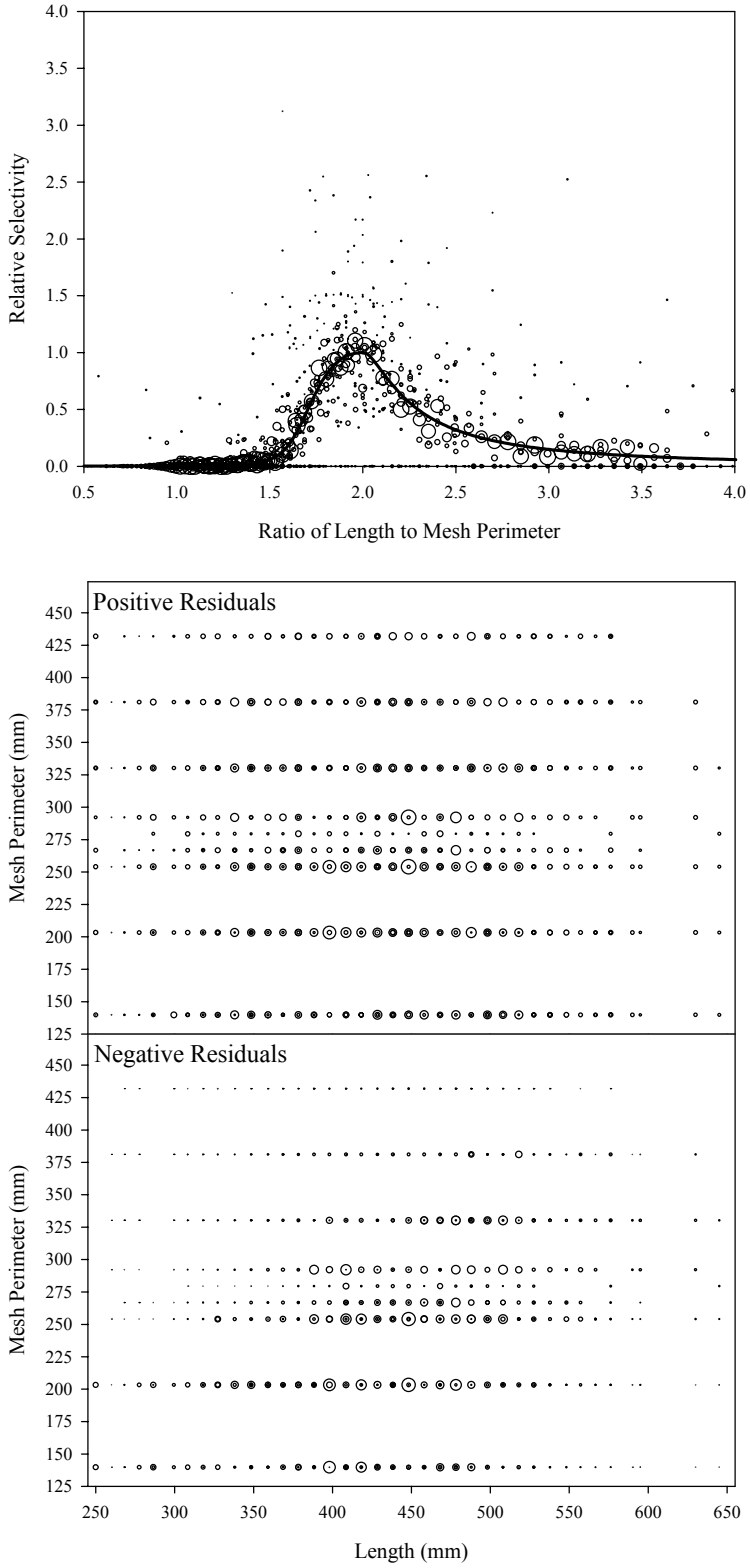

Figure B7.38. Plots of CPUE data scaled to a net selectivity model (top) and CPUE residuals (bottom); humpback whitefish data and Model 38.

Appendix B8
Cisco Diagnostic Plots
Figure B8.1 to Figure B8.34

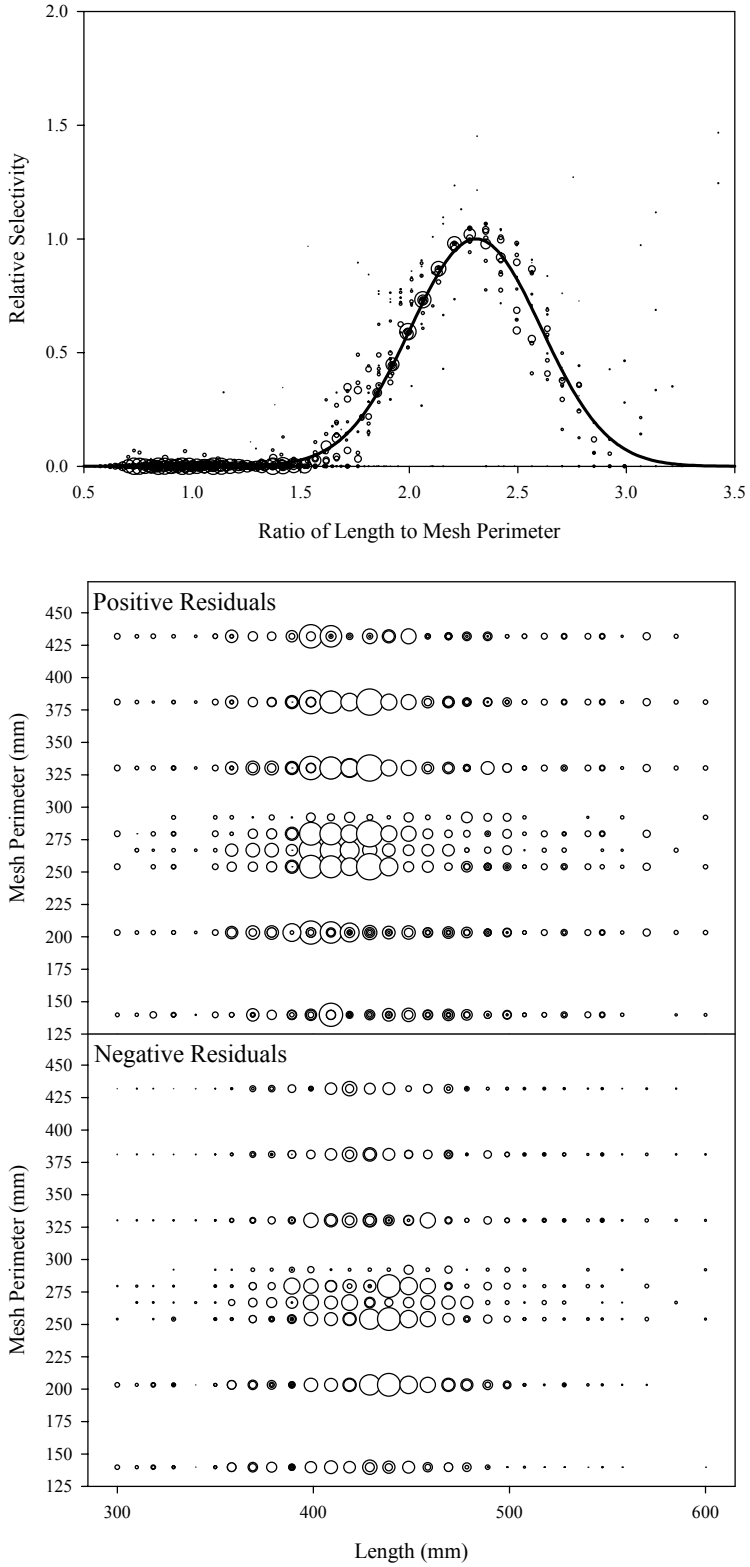

Figure B8.1. Plots of CPUE data scaled to a net selectivity model (top) and CPUE residuals (bottom); cisco data and Model 1.

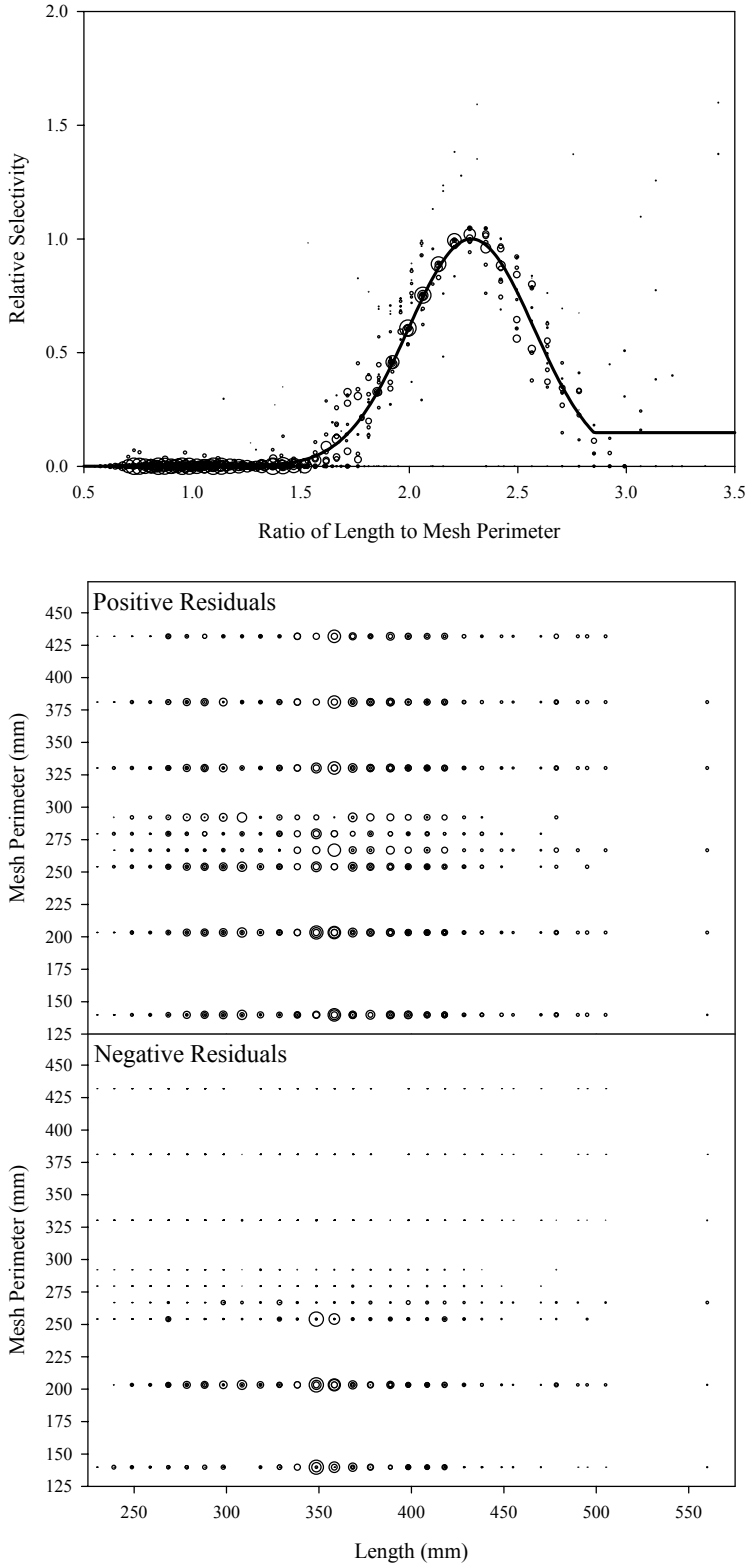

Figure B8.2. Plots of CPUE data scaled to a net selectivity model (top) and CPUE residuals (bottom); cisco data and Model 2.

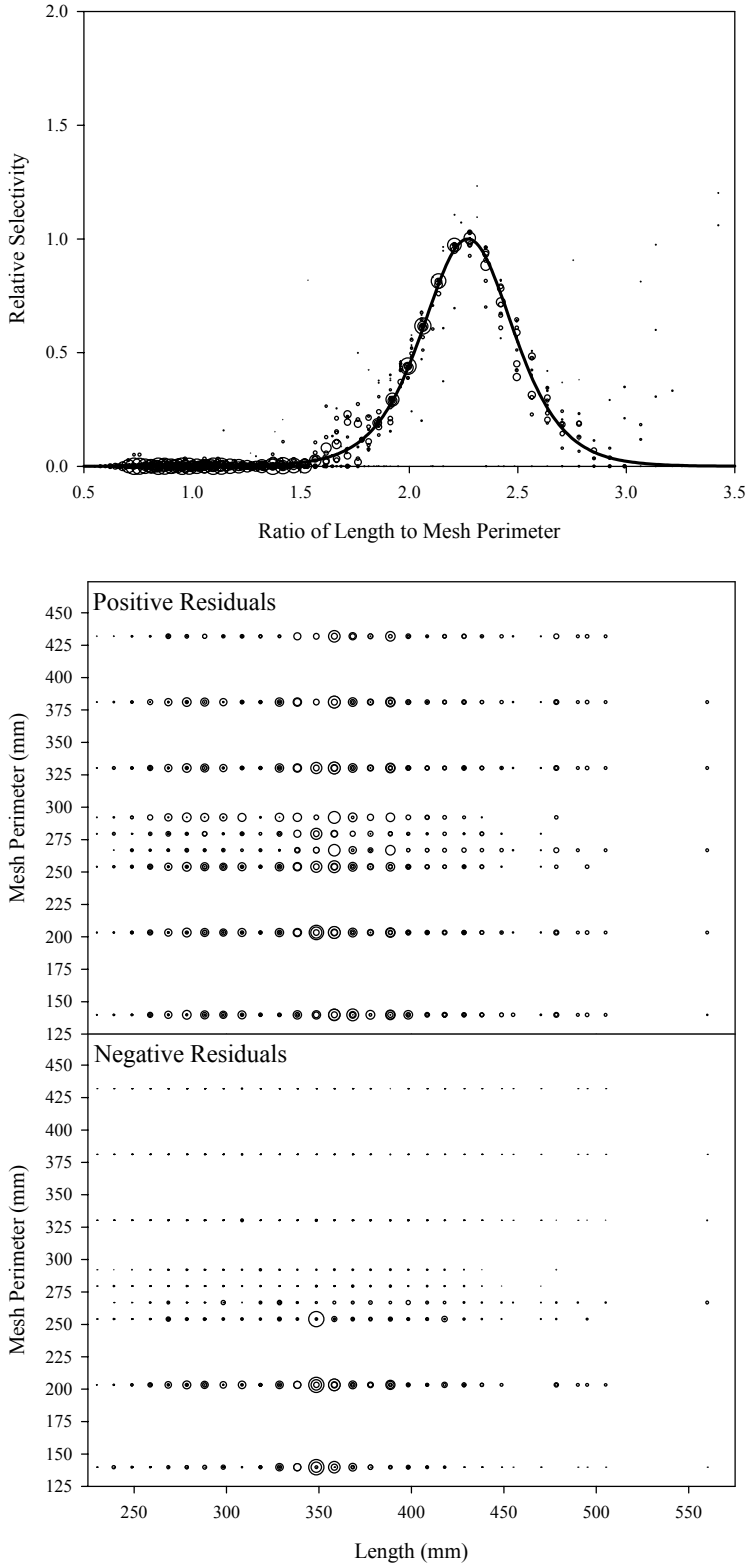

Figure B8.3. Plots of CPUE data scaled to a net selectivity model (top) and CPUE residuals (bottom); cisco data and Model 3.

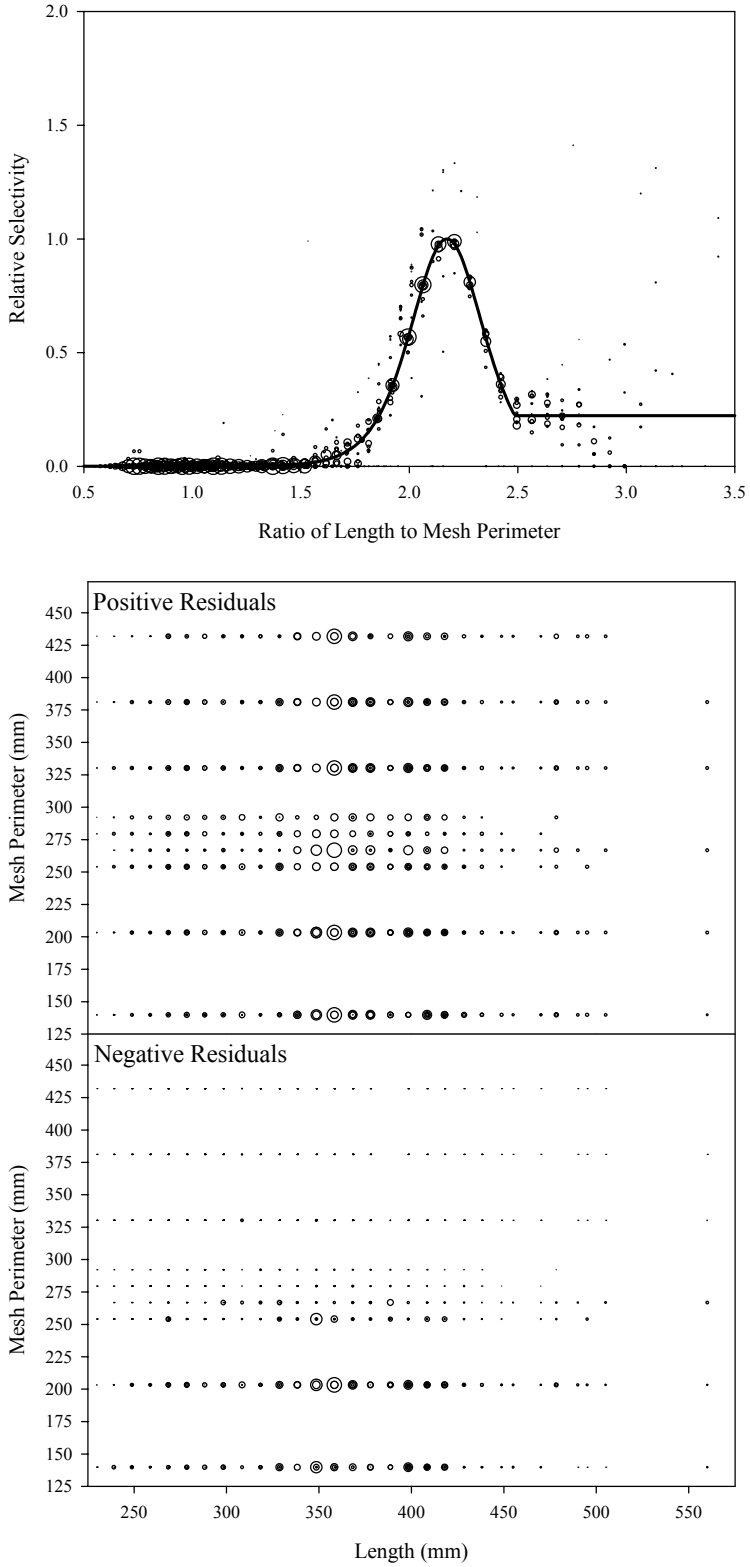

Figure B8.4. Plots of CPUE data scaled to a net selectivity model (top) and CPUE residuals (bottom); cisco data and Model 4.

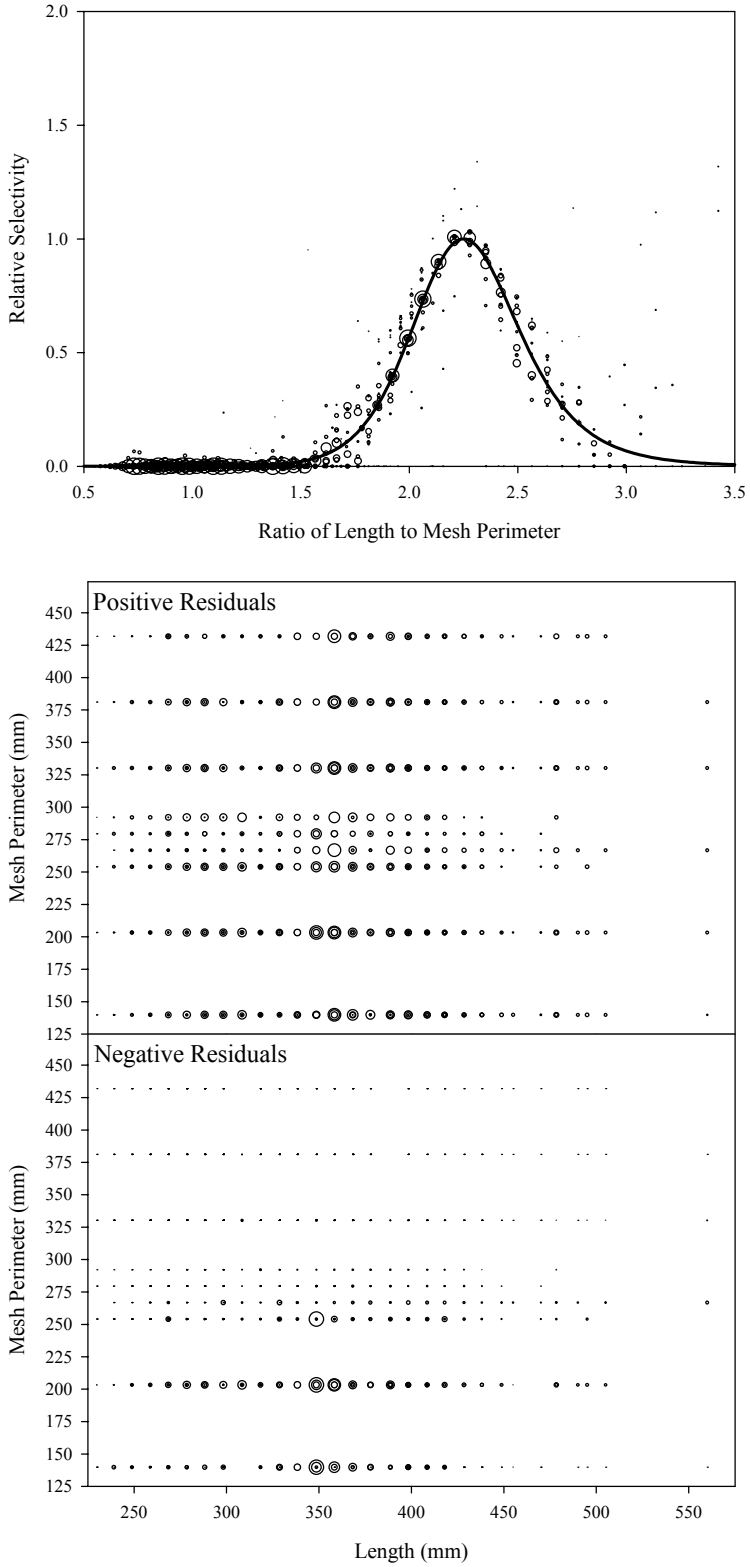

Figure B8.5. Plots of CPUE data scaled to a net selectivity model (top) and CPUE residuals (bottom); cisco data and Model 5.

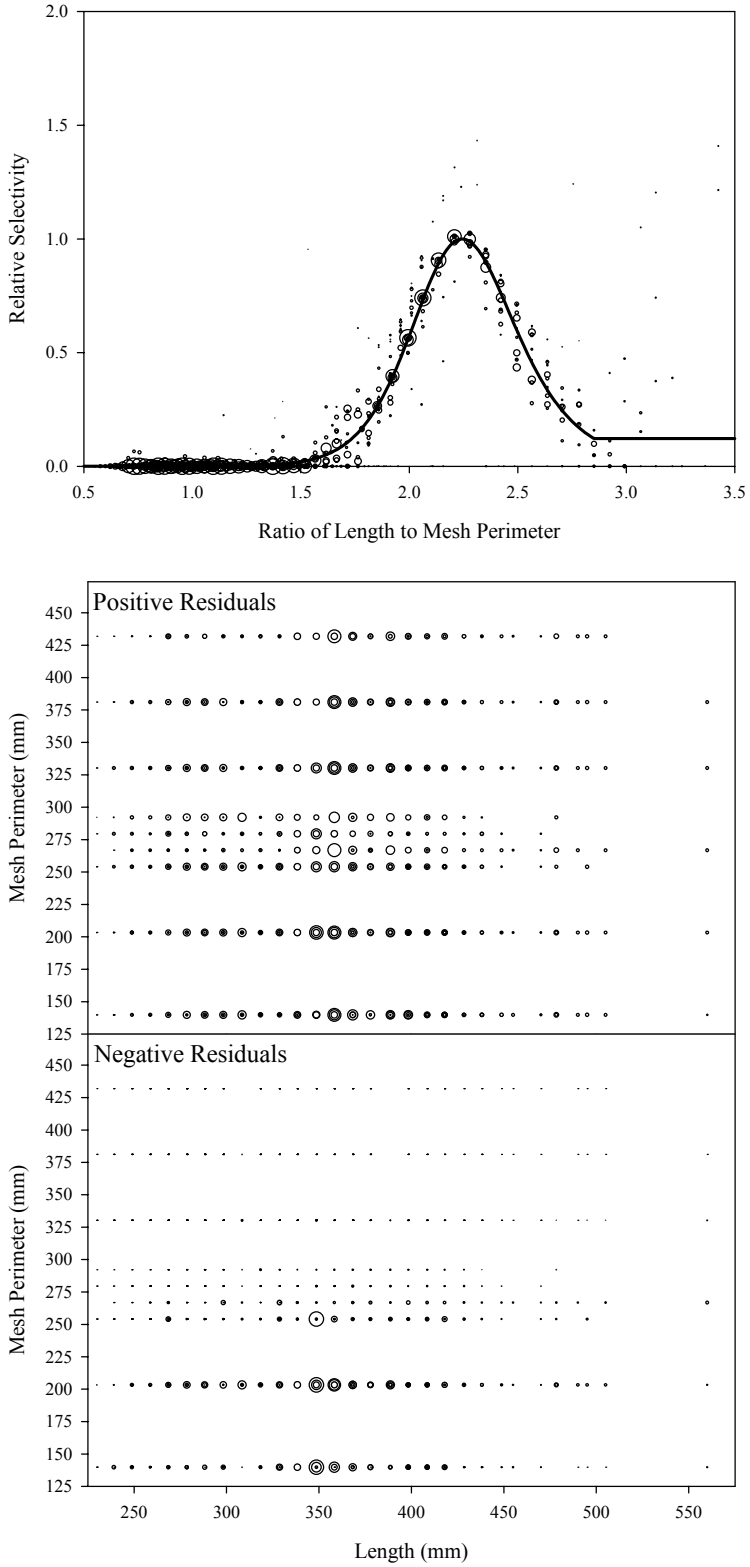

Figure B8.6. Plots of CPUE data scaled to a net selectivity model (top) and CPUE residuals (bottom); cisco data and Model 6.

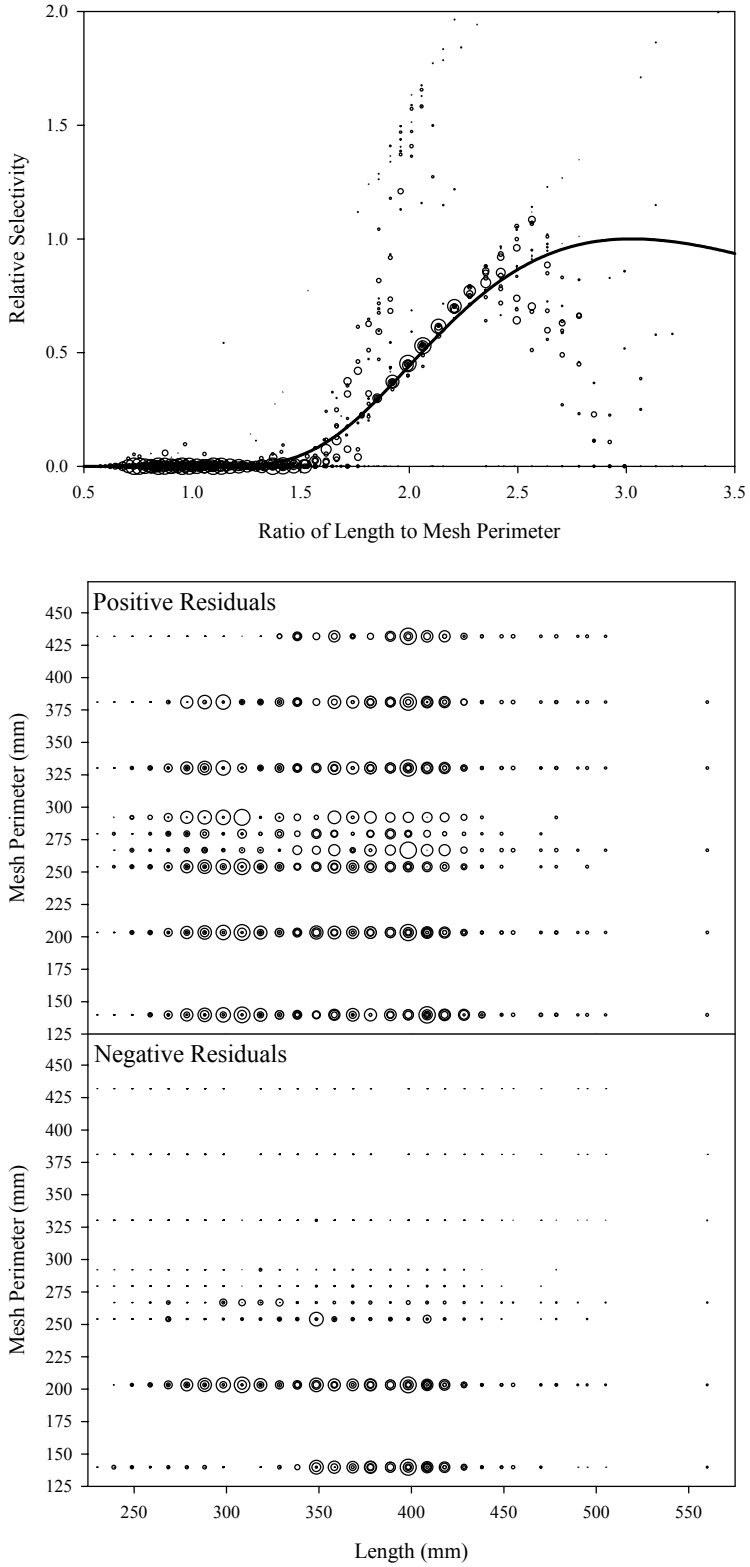

Figure B8.7. Plots of CPUE data scaled to a net selectivity model (top) and CPUE residuals (bottom); cisco data and Model 7.

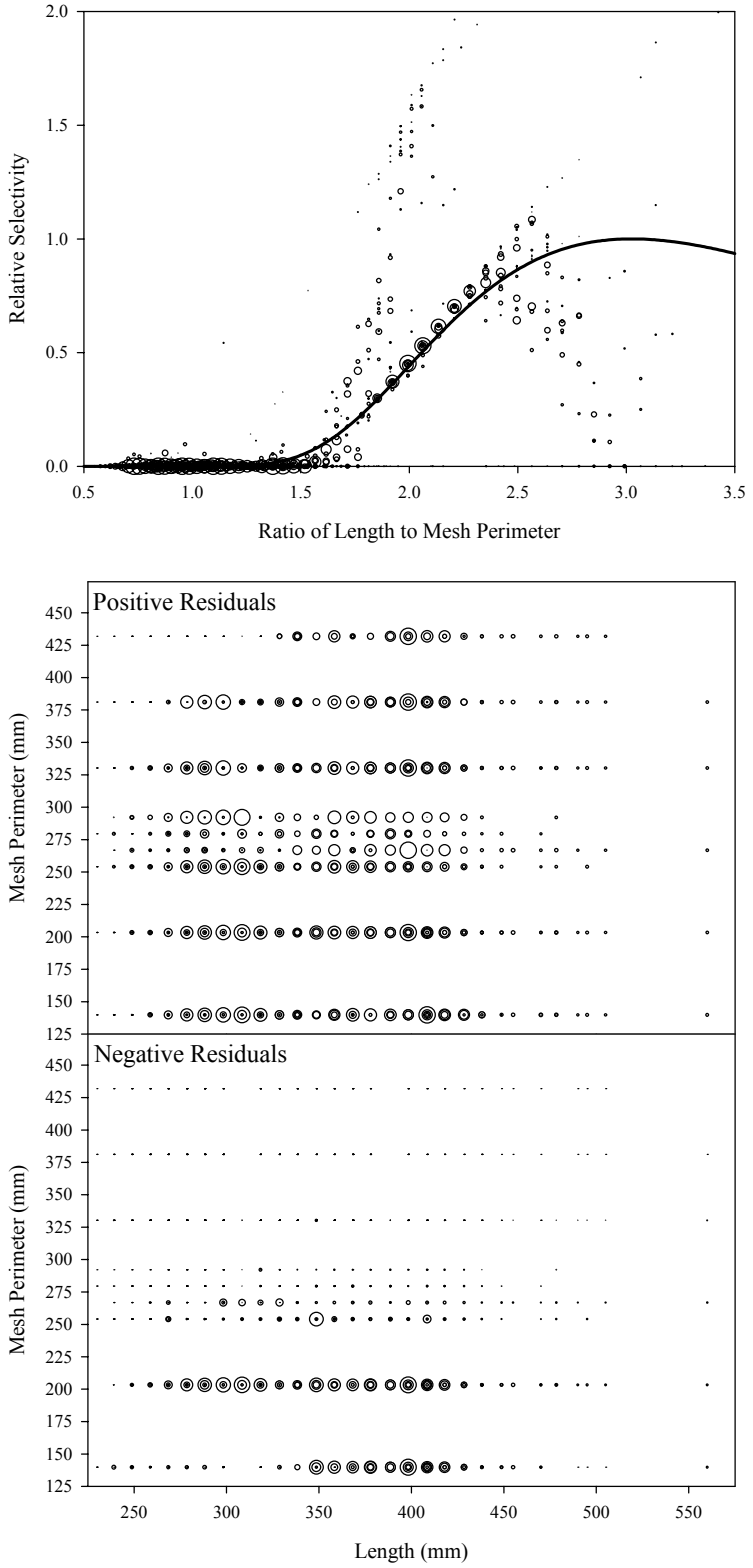

Figure B8.8. Plots of CPUE data scaled to a net selectivity model (top) and CPUE residuals (bottom); cisco data and Model 8.

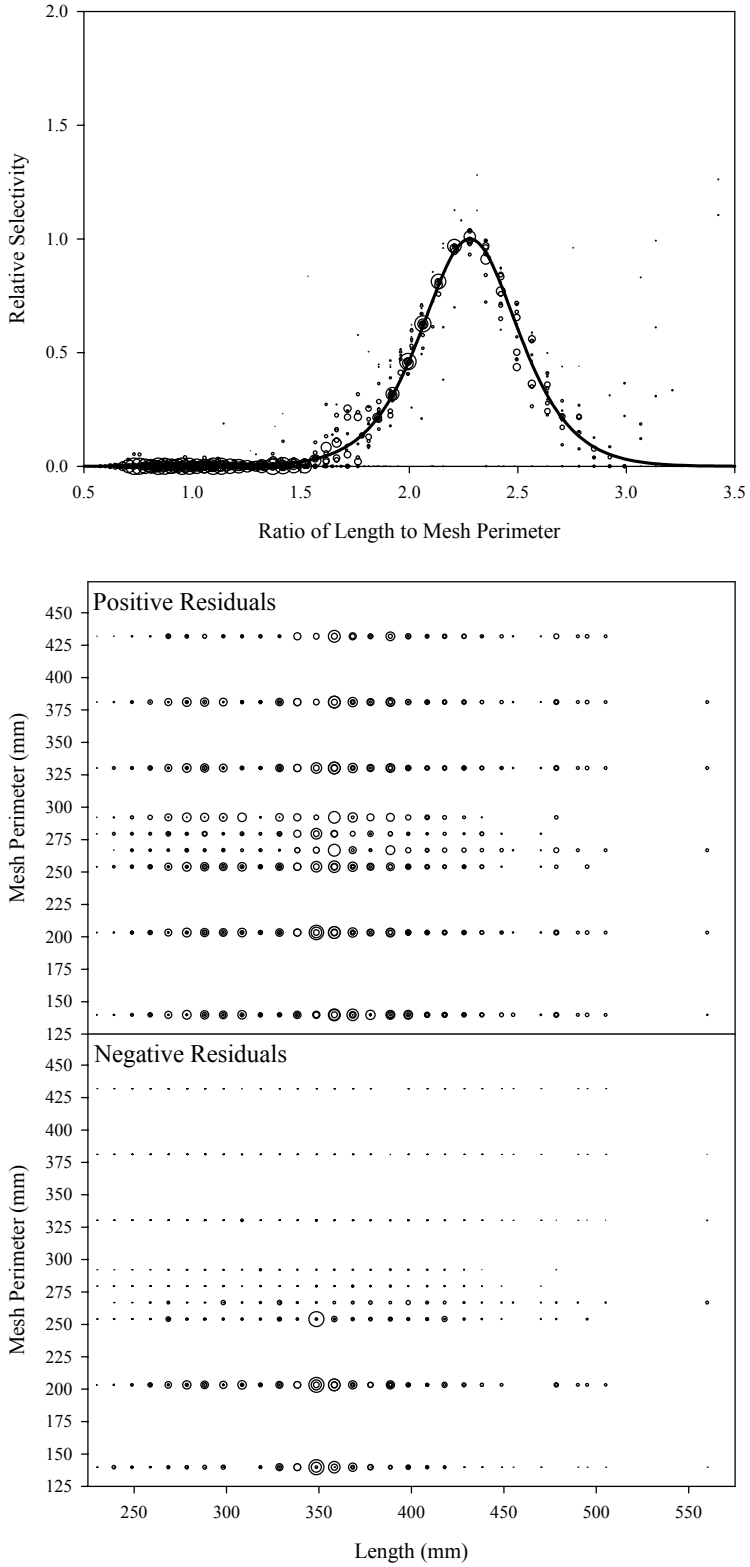

Figure B8.9. Plots of CPUE data scaled to a net selectivity model (top) and CPUE residuals (bottom); cisco data and Model 9.

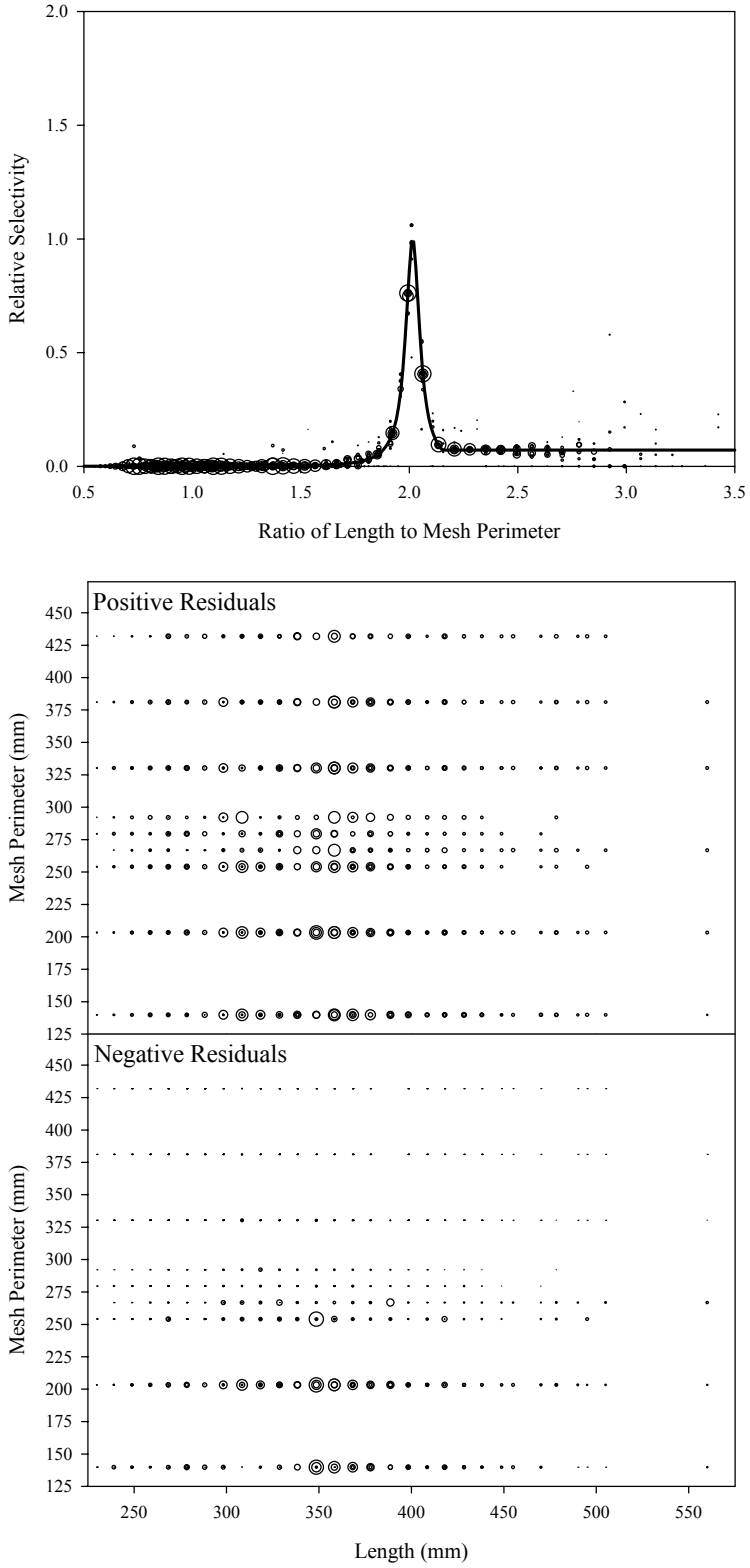

Figure B8.10. Plots of CPUE data scaled to a net selectivity model (top) and CPUE residuals (bottom); cisco data and Model 10.

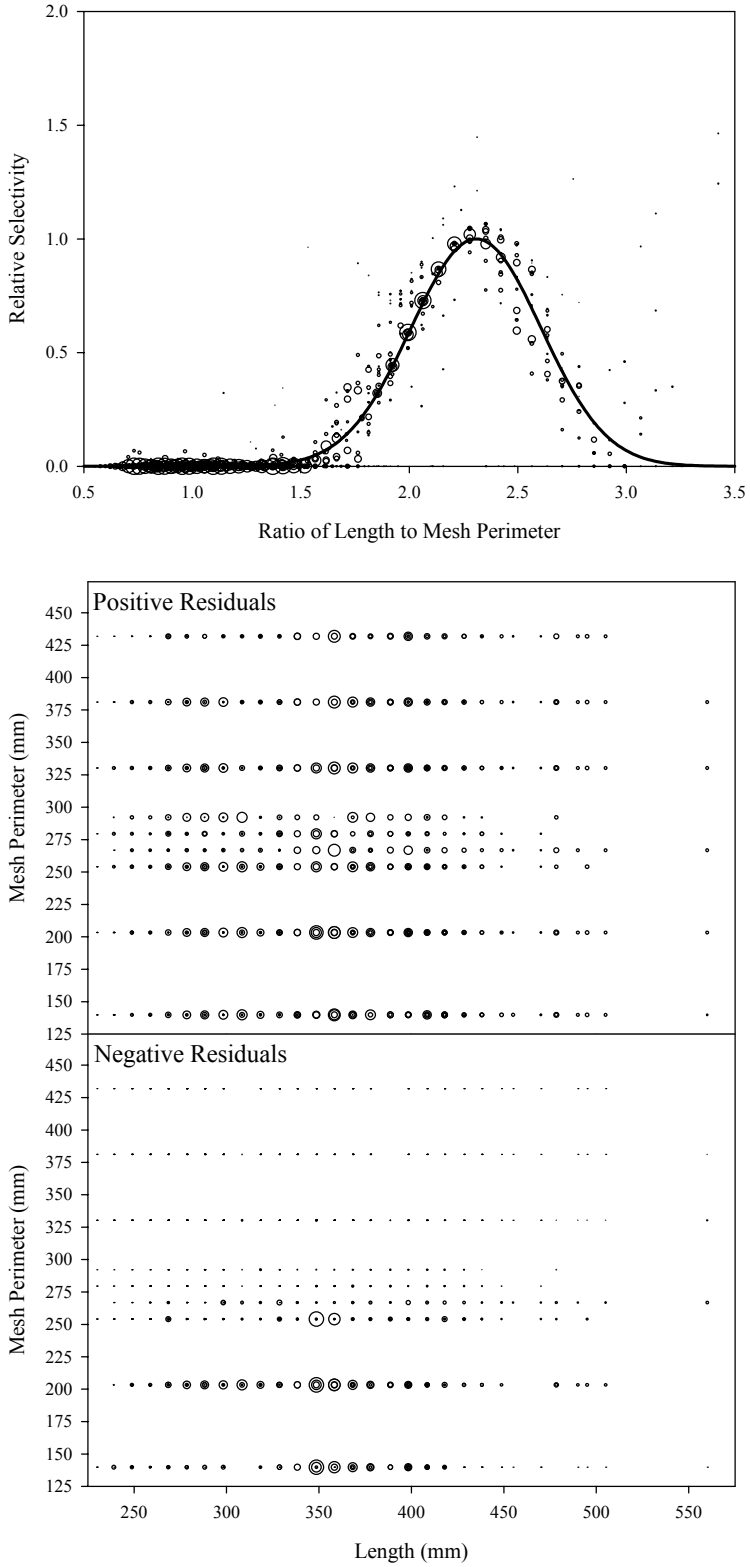

Figure B8.11. Plots of CPUE data scaled to a net selectivity model (top) and CPUE residuals (bottom); cisco data and Model 11.

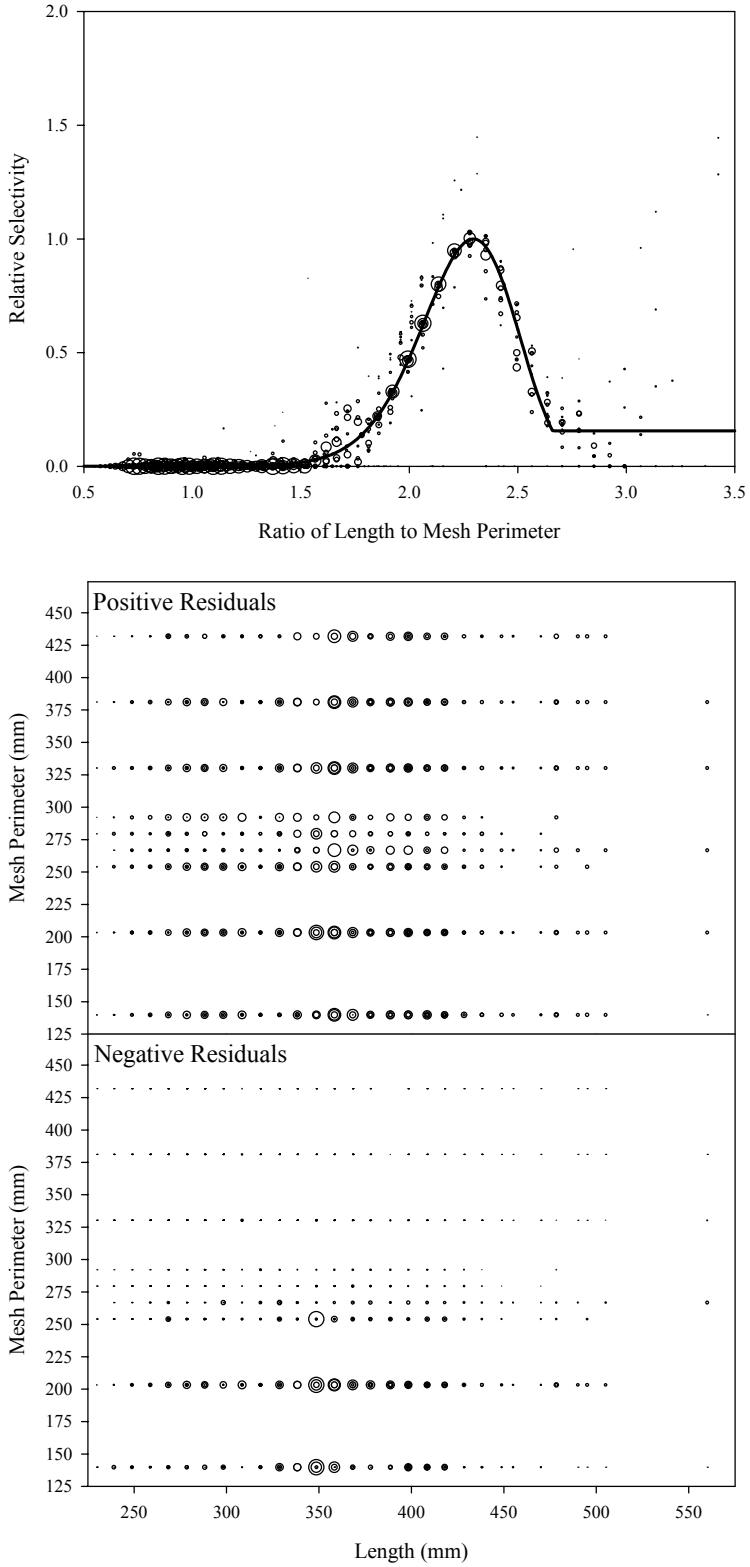

Figure B8.12. Plots of CPUE data scaled to a net selectivity model (top) and CPUE residuals (bottom); cisco data and Model 12.

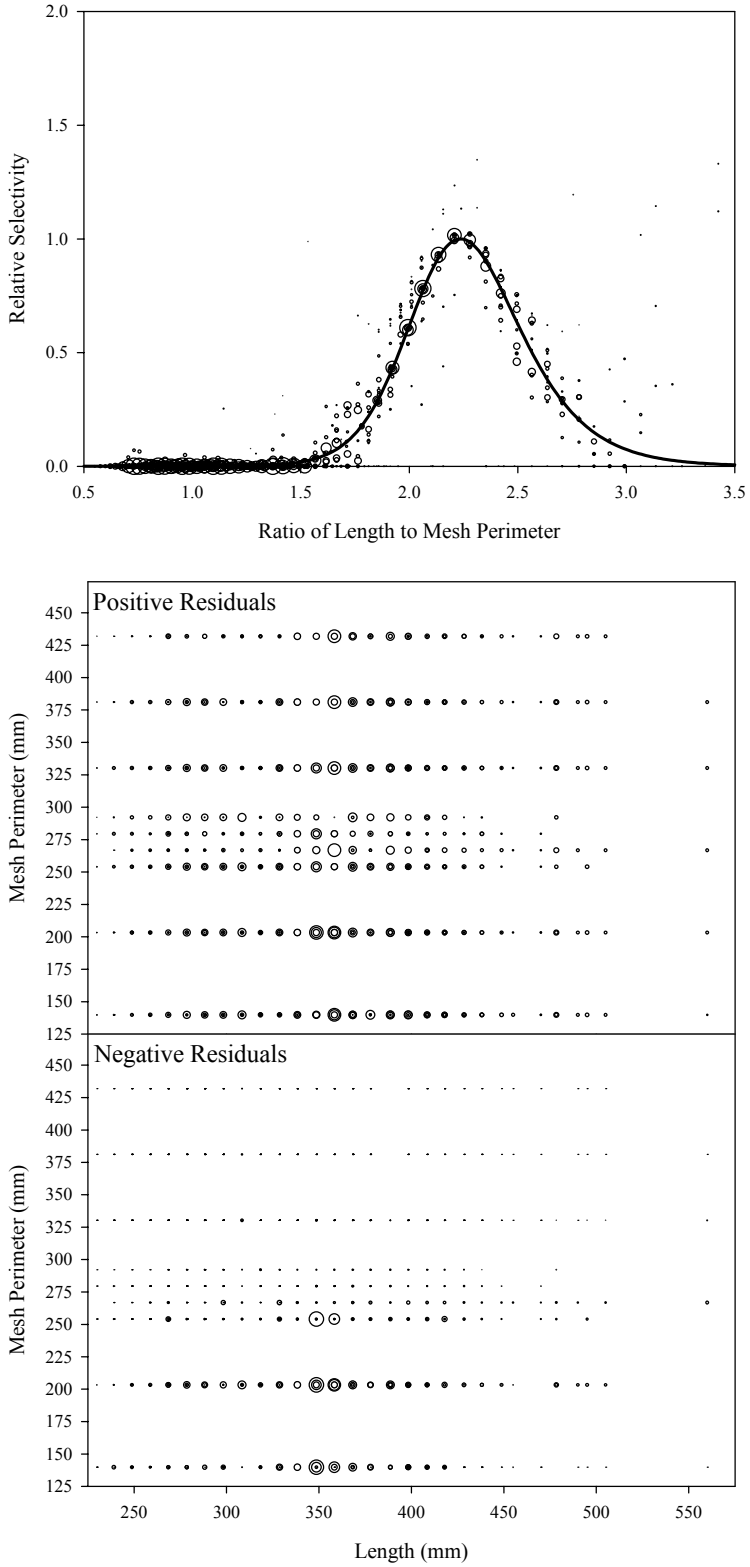

Figure B8.13. Plots of CPUE data scaled to a net selectivity model (top) and CPUE residuals (bottom); cisco data and Model 13.

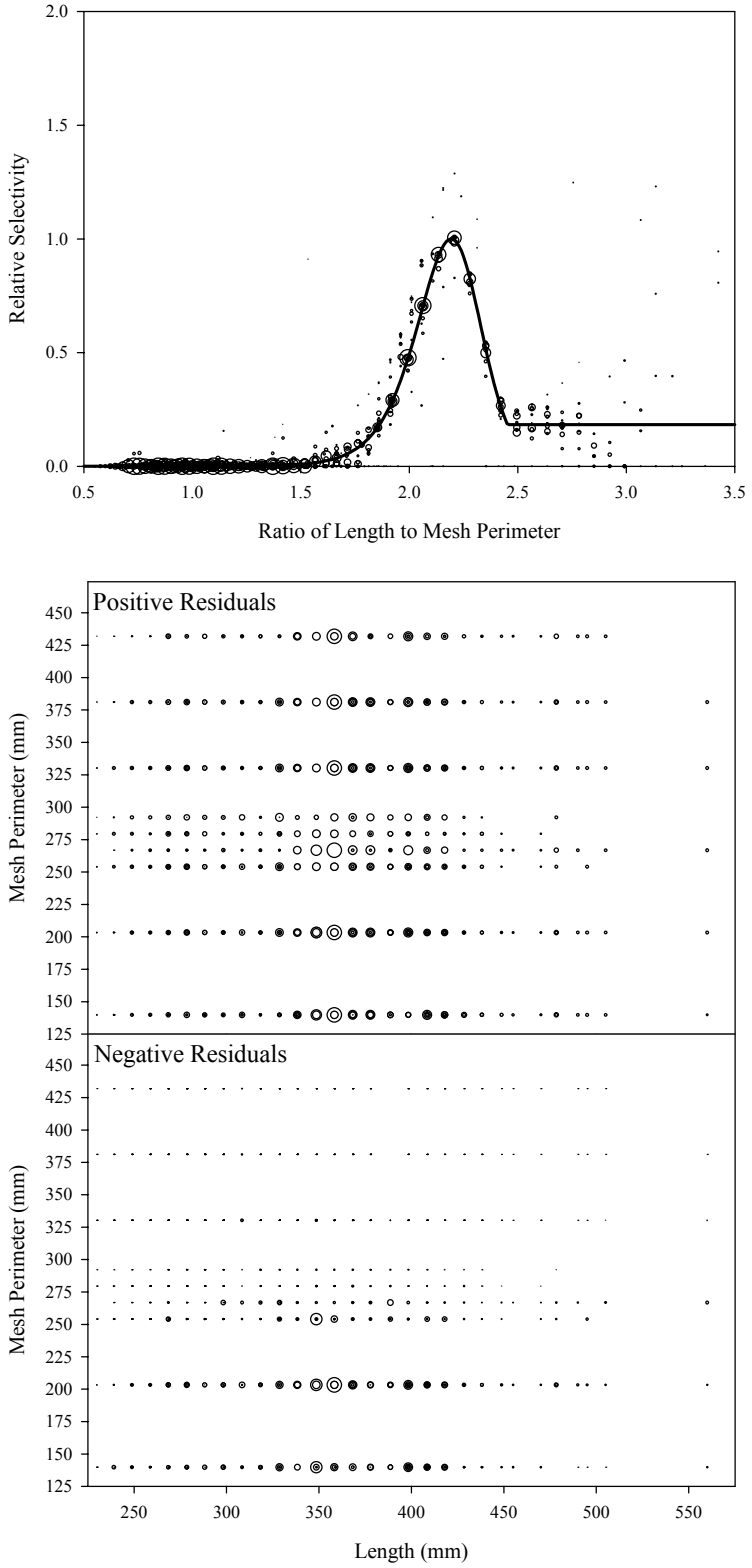

Figure B8.14. Plots of CPUE data scaled to a net selectivity model (top) and CPUE residuals (bottom); cisco data and Model 14.

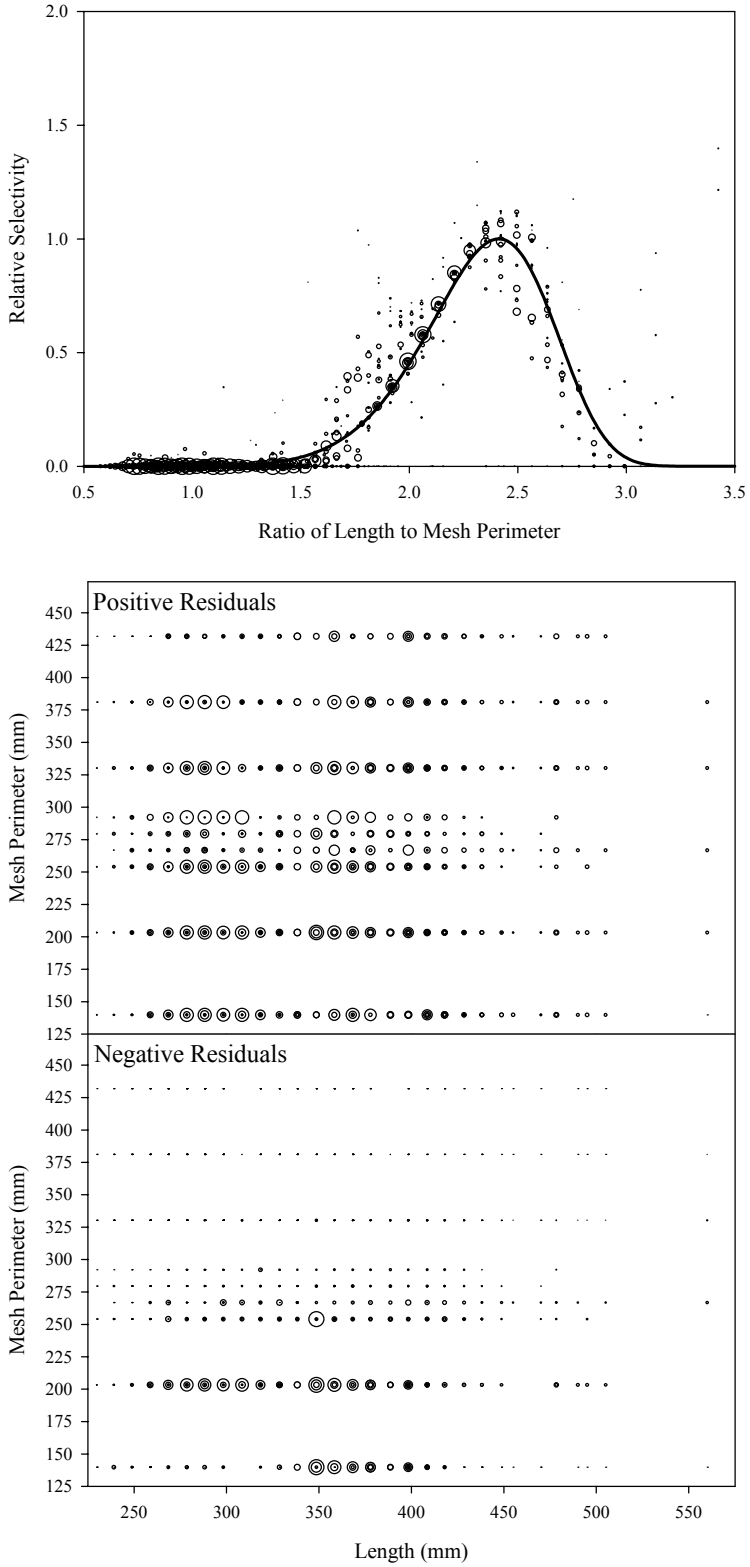

Figure B8.15. Plots of CPUE data scaled to a net selectivity model (top) and CPUE residuals (bottom); cisco data and Model 15.

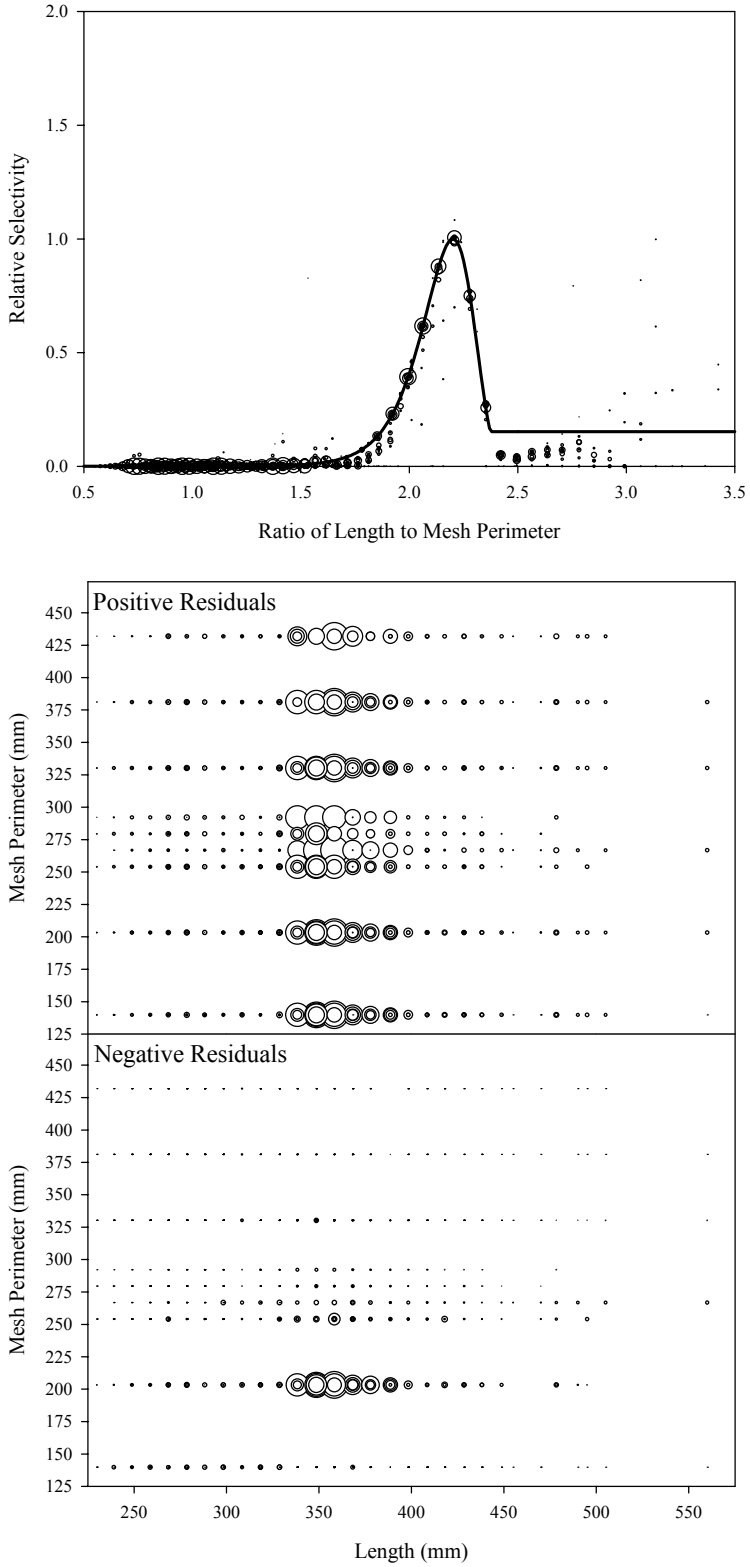

Figure B8.16. Plots of CPUE data scaled to a net selectivity model (top) and CPUE residuals (bottom); cisco data and Model 16.

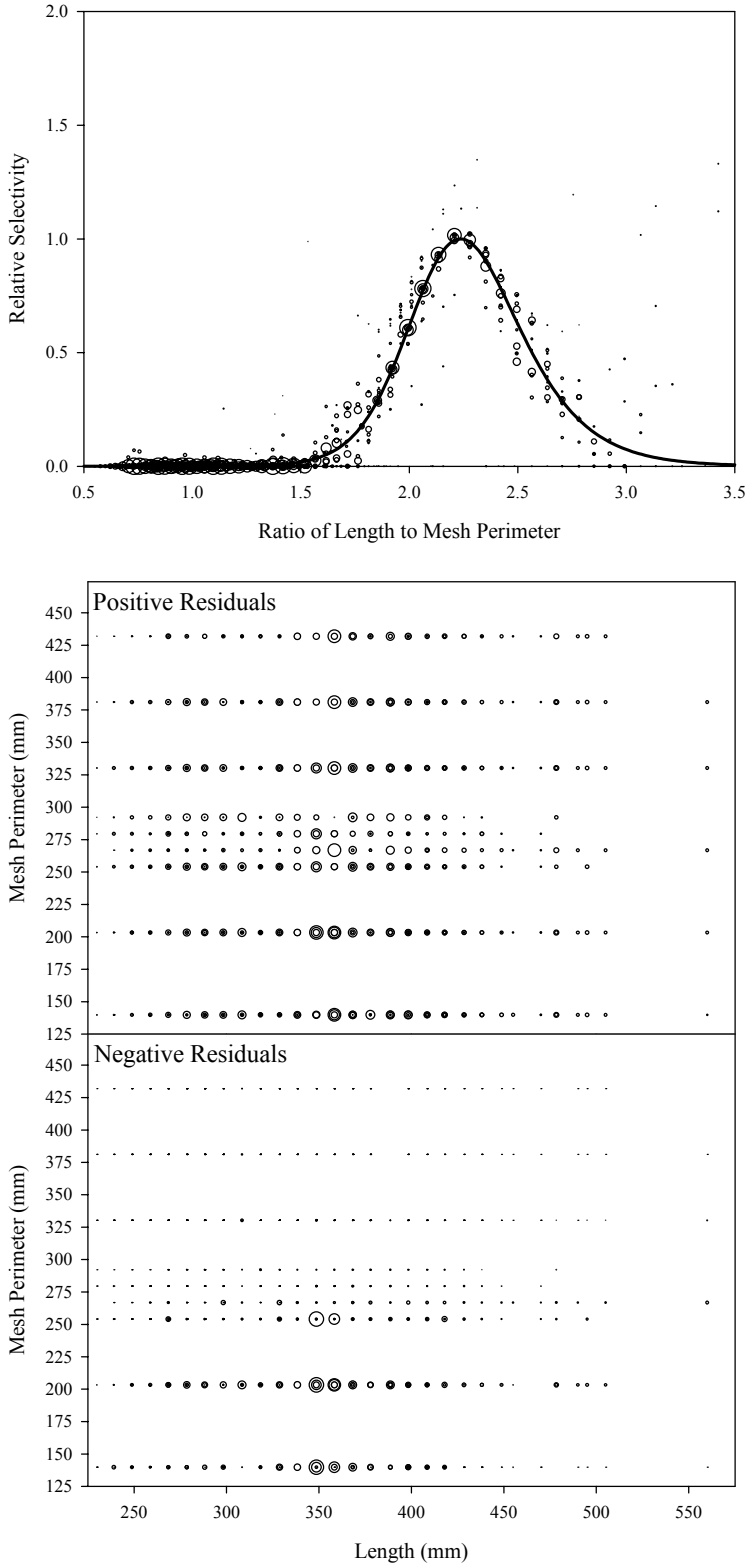

Figure B8.17. Plots of CPUE data scaled to a net selectivity model (top) and CPUE residuals (bottom); cisco data and Model 17.

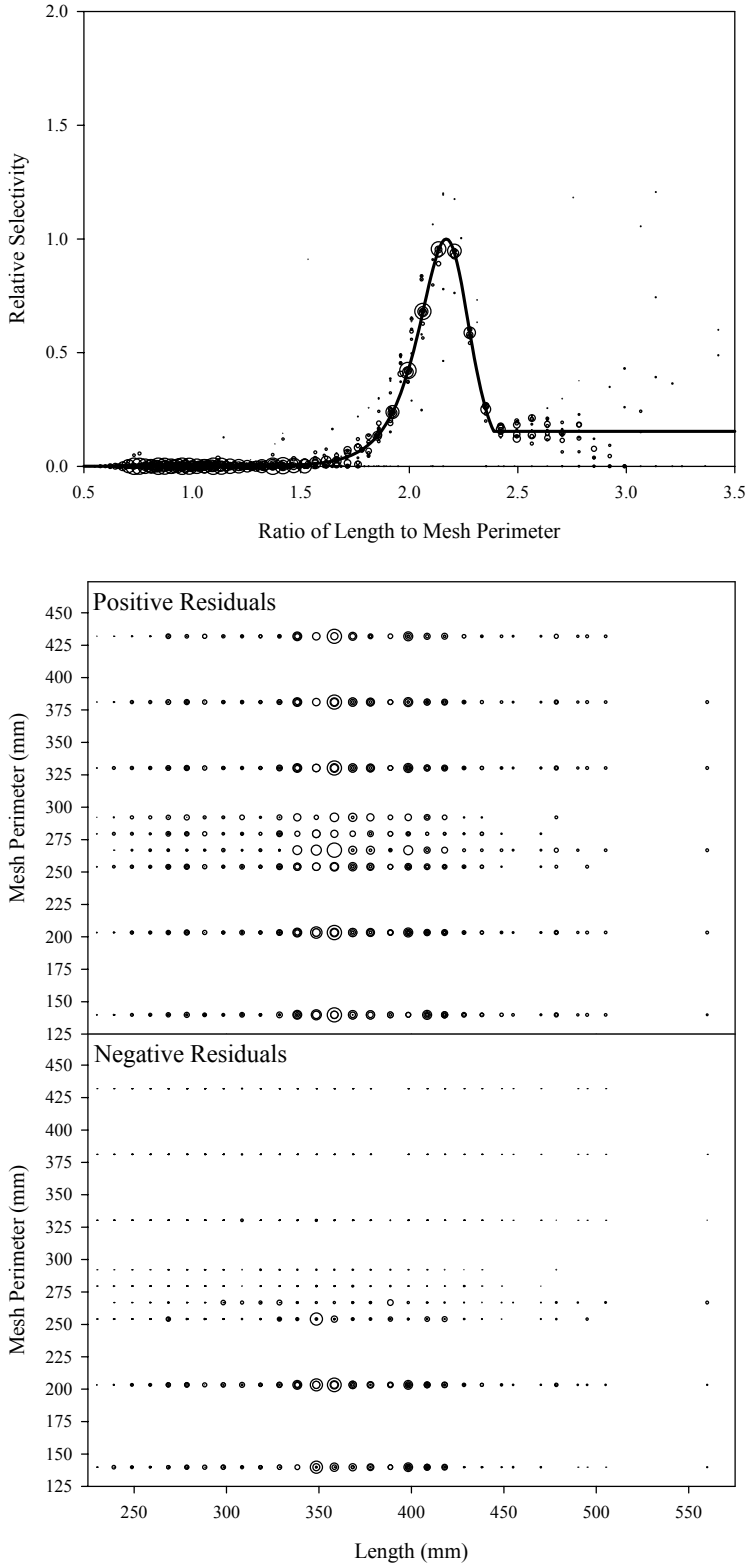

Figure B8.18. Plots of CPUE data scaled to a net selectivity model (top) and CPUE residuals (bottom); cisco data and Model 18.

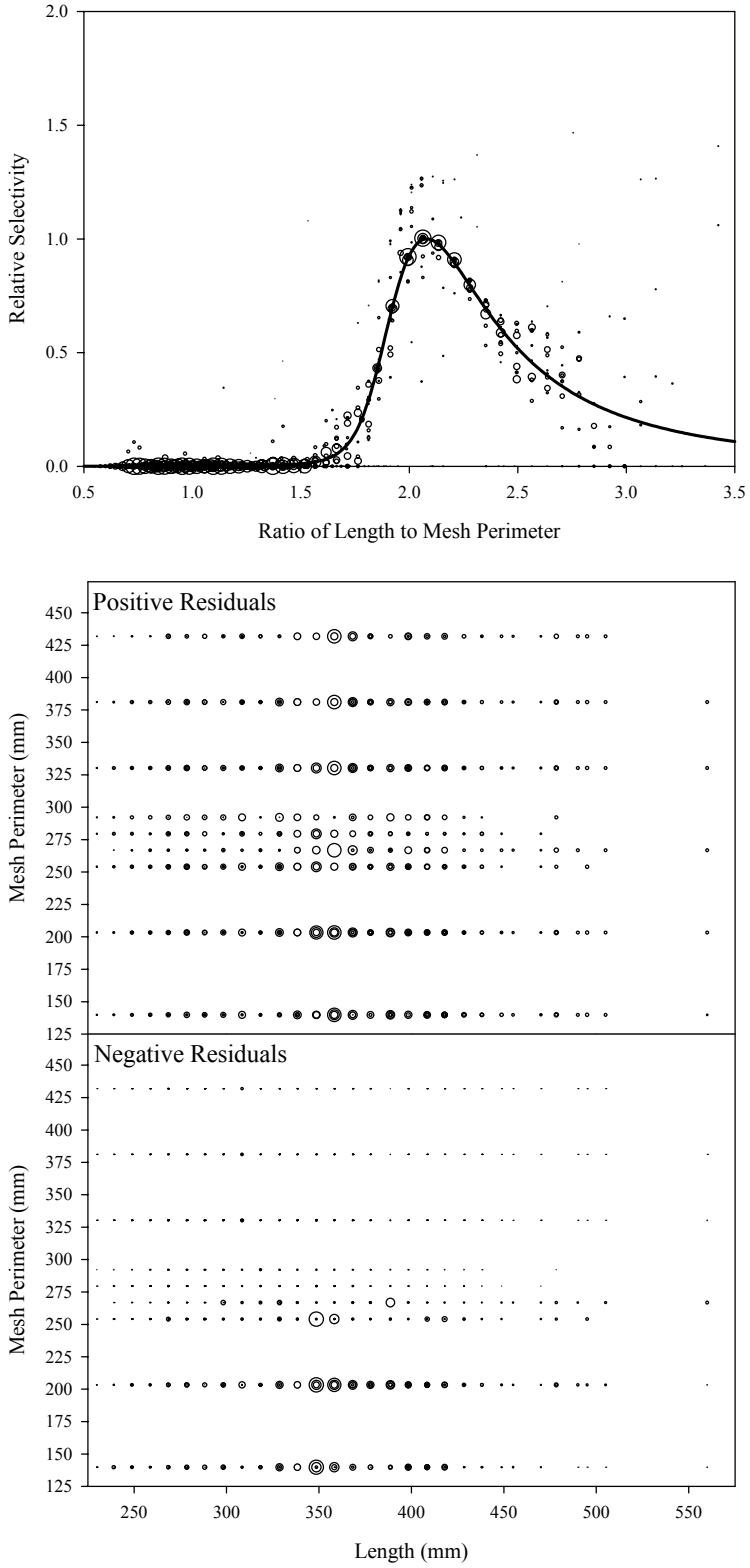

Figure B8.19. Plots of CPUE data scaled to a net selectivity model (top) and CPUE residuals (bottom); cisco data and Model 19.

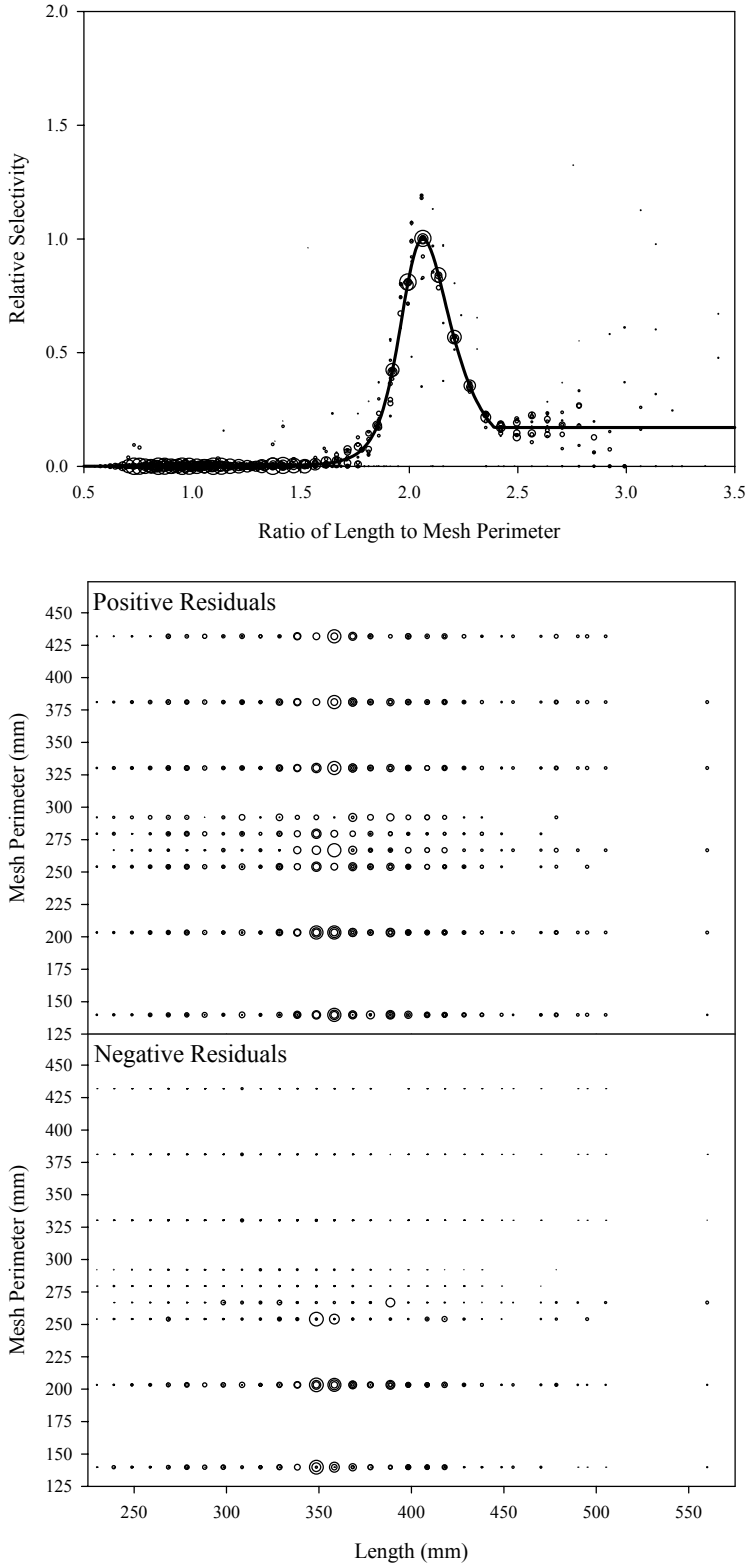

Figure B8.20. Plots of CPUE data scaled to a net selectivity model (top) and CPUE residuals (bottom); cisco data and Model 20.

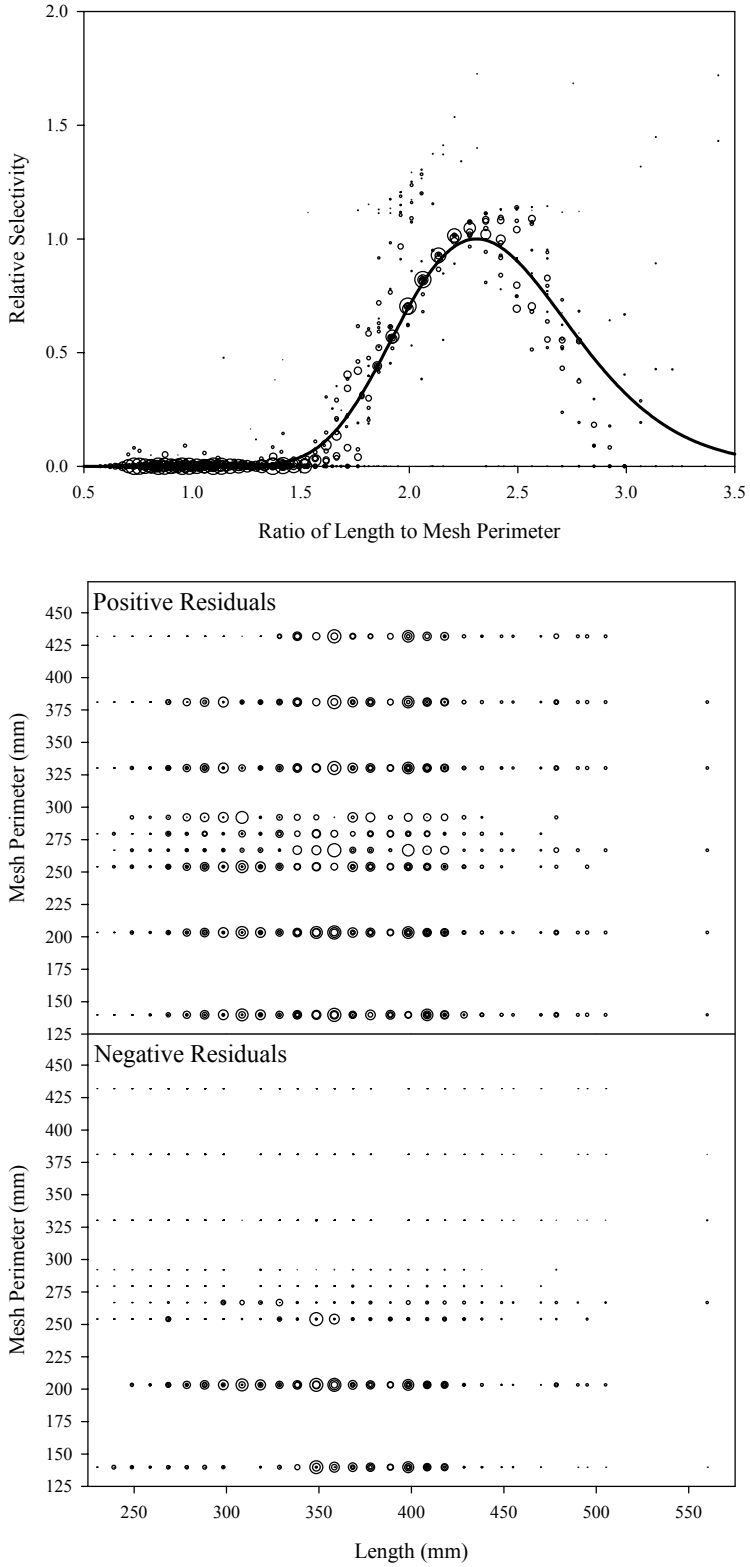

Figure B8.21. Plots of CPUE data scaled to a net selectivity model (top) and CPUE residuals (bottom); cisco data and Model 21.

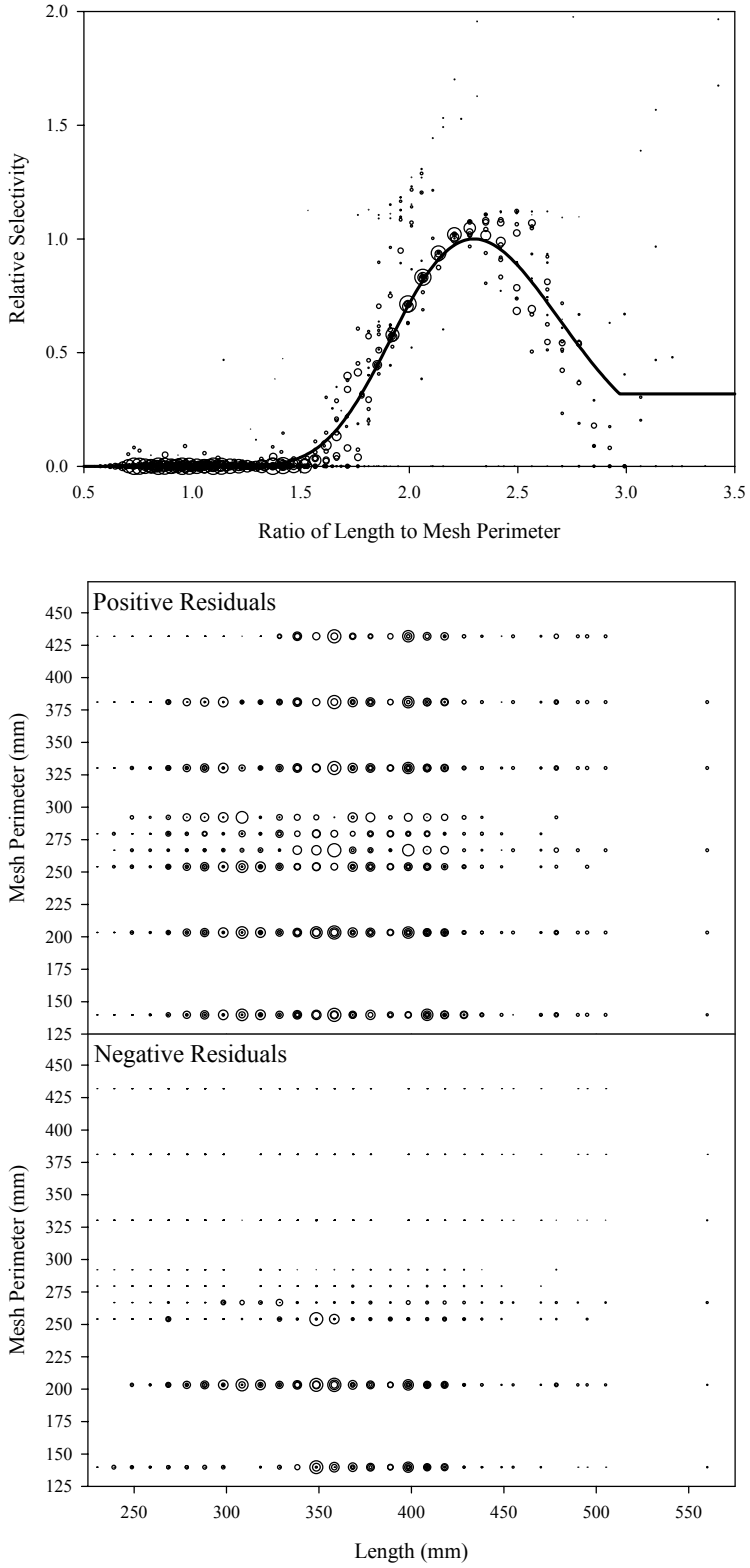

Figure B8.22. Plots of CPUE data scaled to a net selectivity model (top) and CPUE residuals (bottom); cisco data and Model 22.

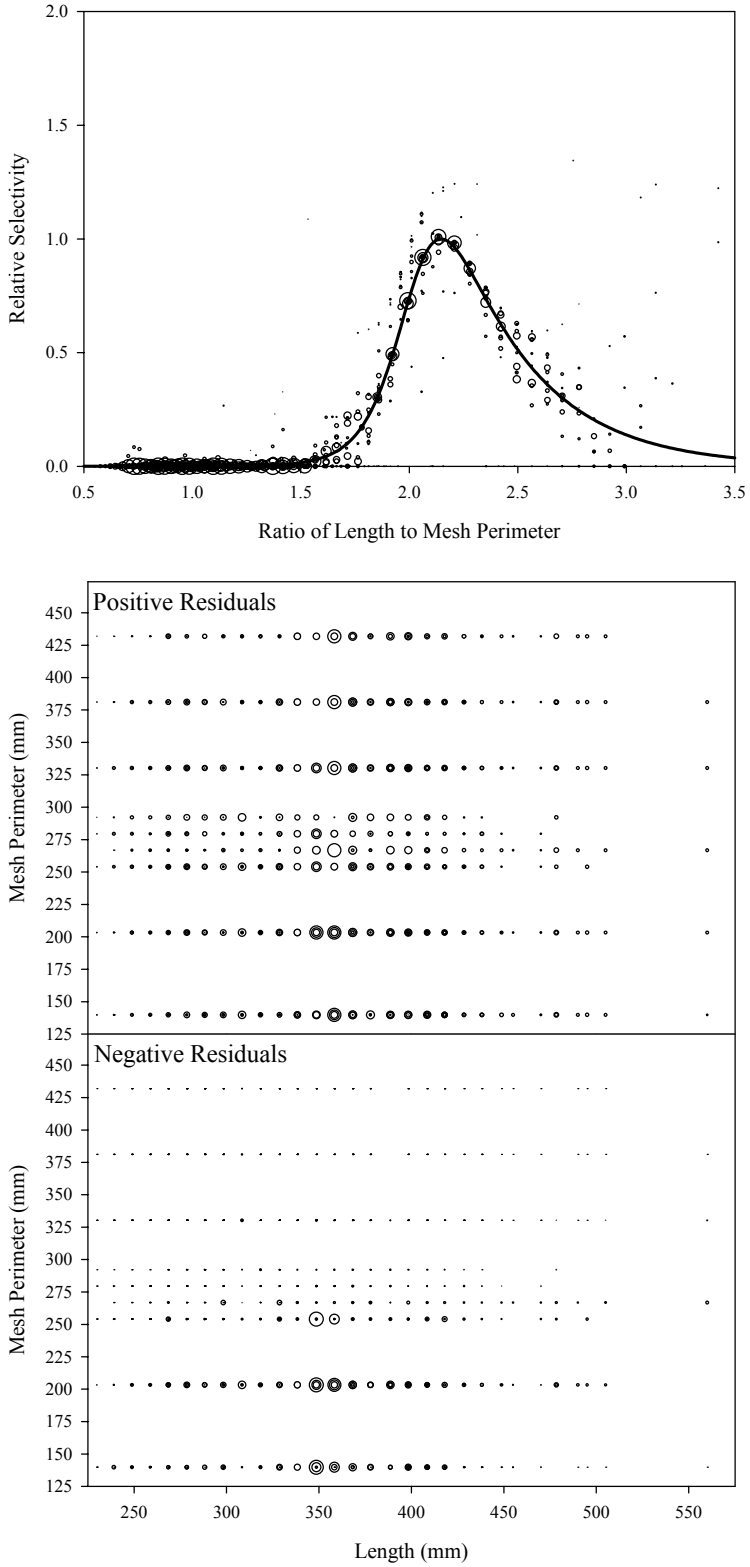

Figure B8.23. Plots of CPUE data scaled to a net selectivity model (top) and CPUE residuals (bottom); cisco data and Model 23.

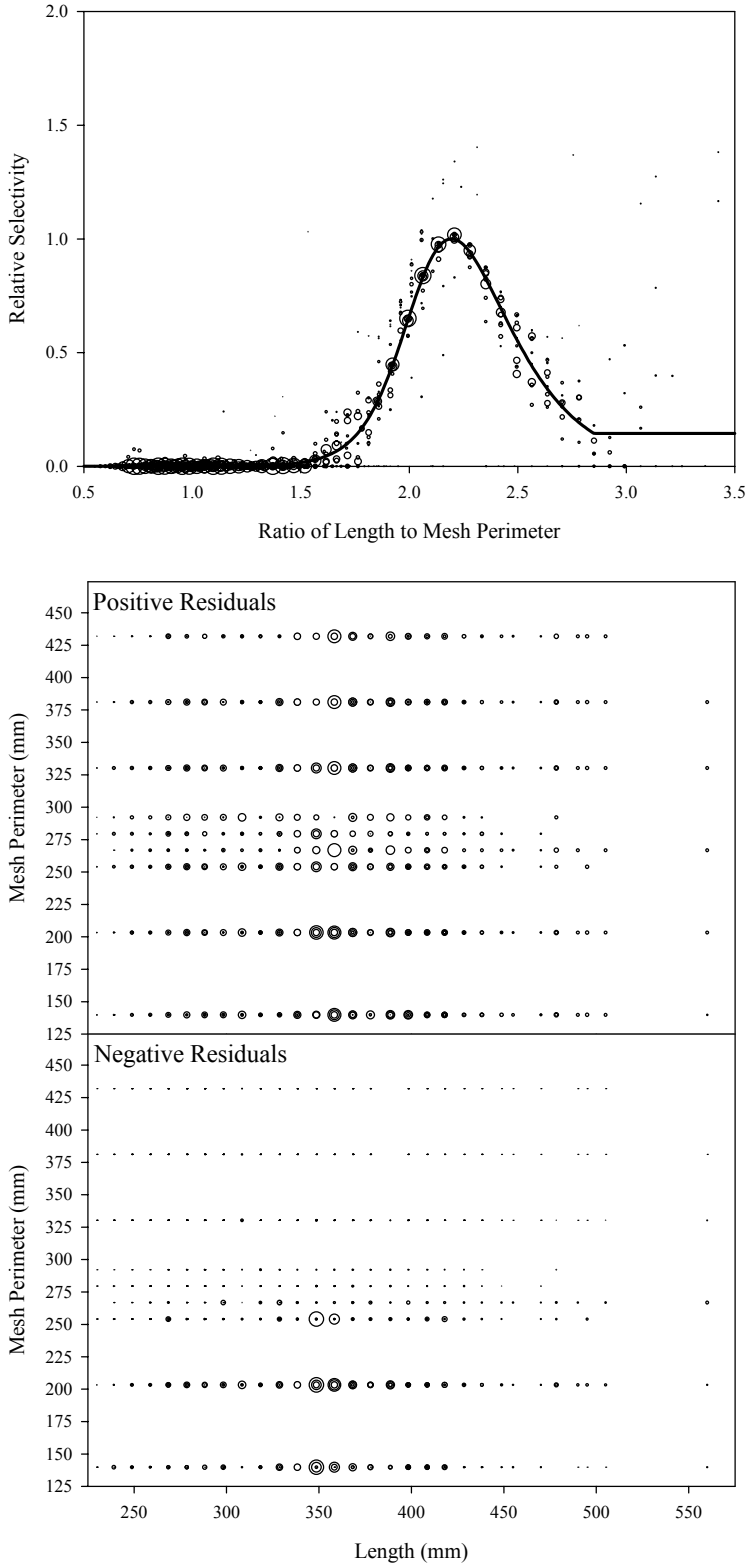

Figure B8.24. Plots of CPUE data scaled to a net selectivity model (top) and CPUE residuals (bottom); cisco data and Model 24.

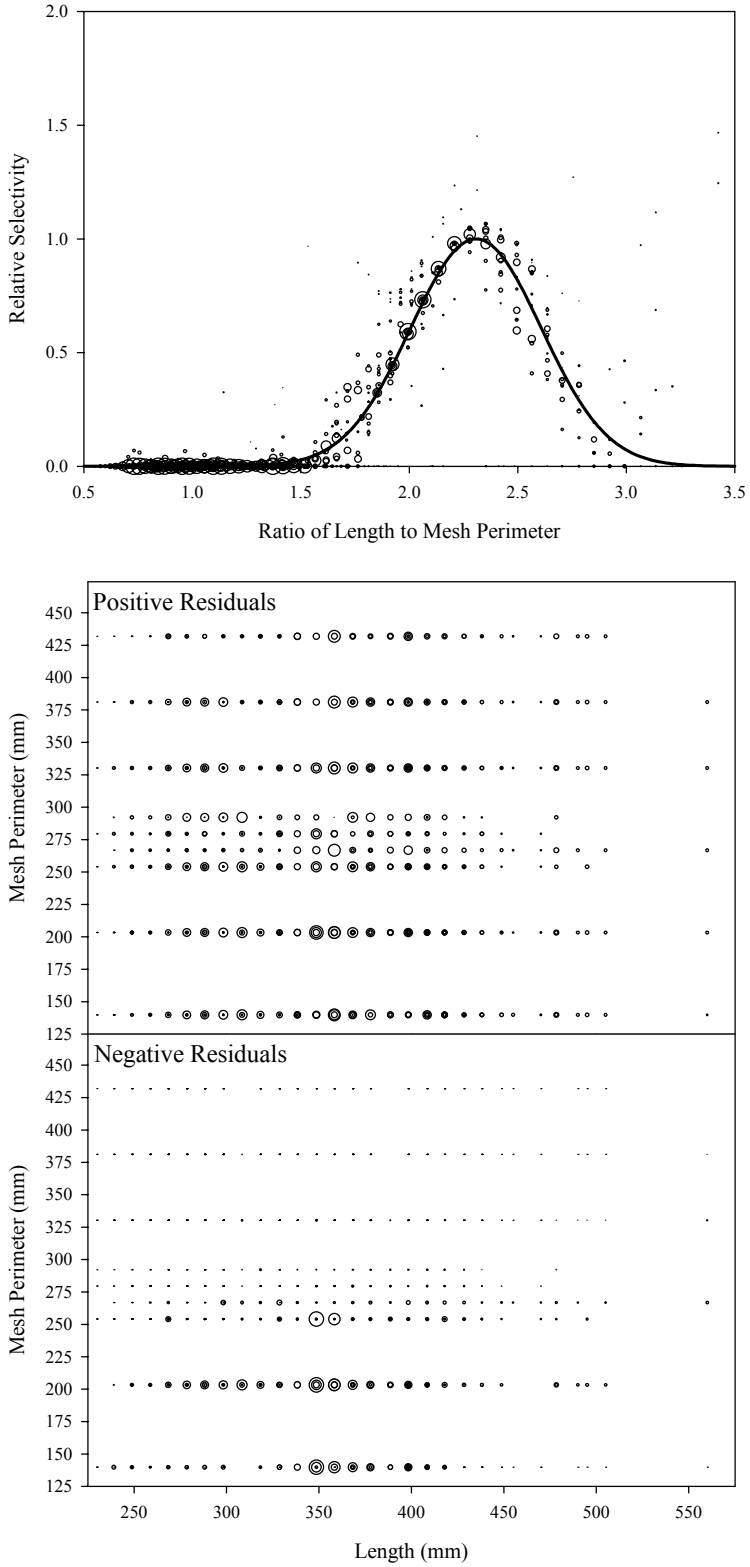

Figure B8.25. Plots of CPUE data scaled to a net selectivity model (top) and CPUE residuals (bottom); cisco data and Model 25.

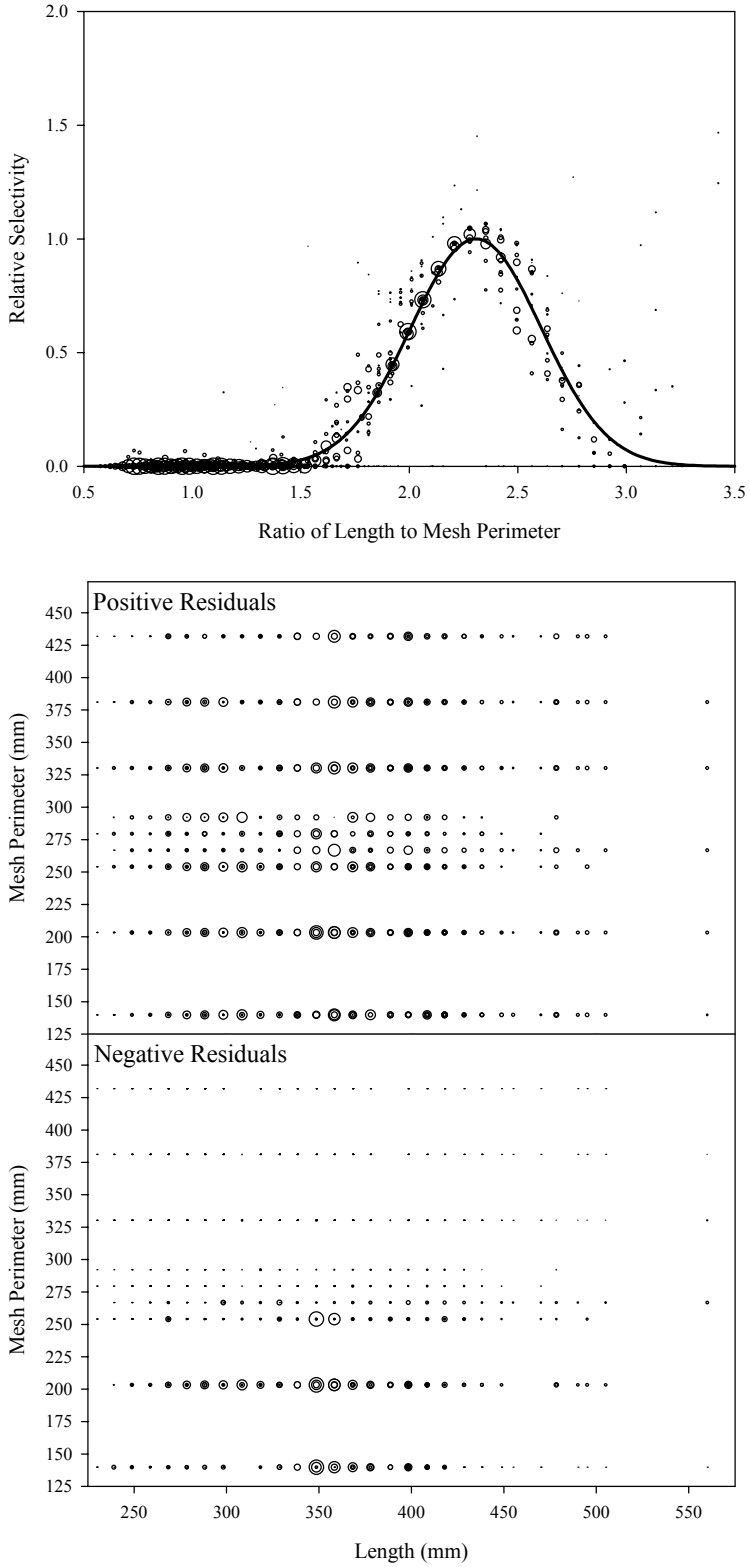

Figure B8.26. Plots of CPUE data scaled to a net selectivity model (top) and CPUE residuals (bottom); cisco data and Model 26.

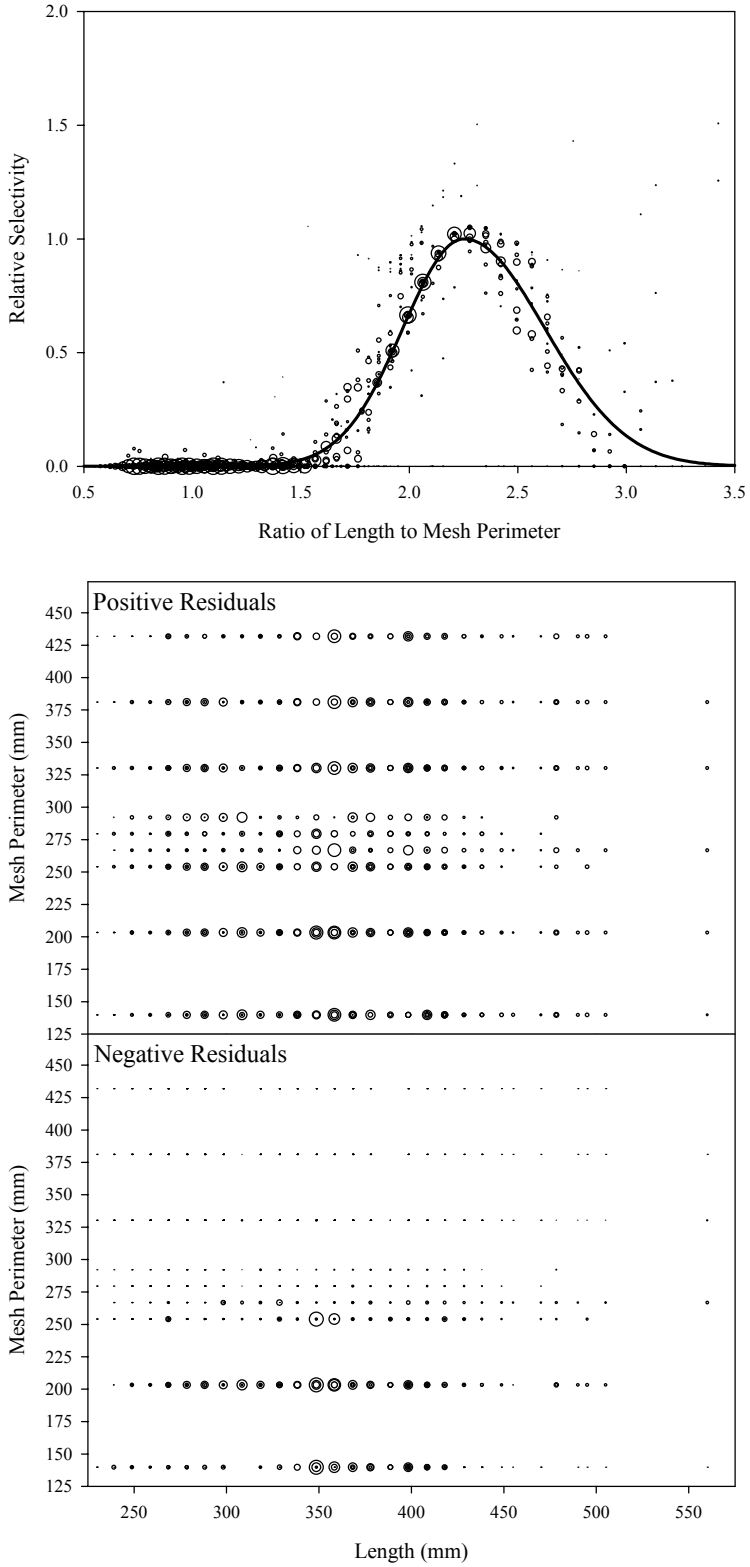

Figure B8.27. Plots of CPUE data scaled to a net selectivity model (top) and CPUE residuals (bottom); cisco data and Model 27.

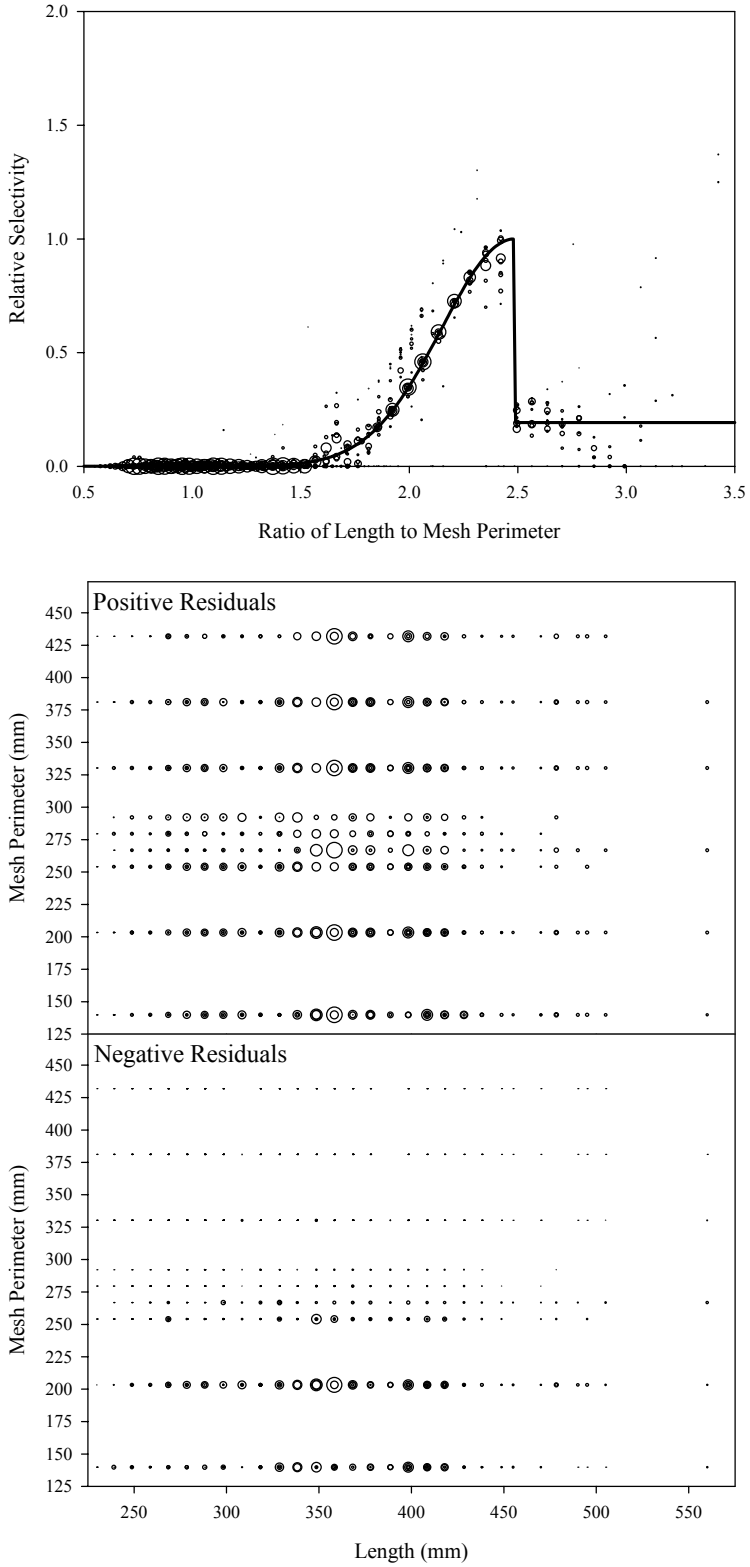

Figure B8.28. Plots of CPUE data scaled to a net selectivity model (top) and CPUE residuals (bottom); cisco data and Model 28.

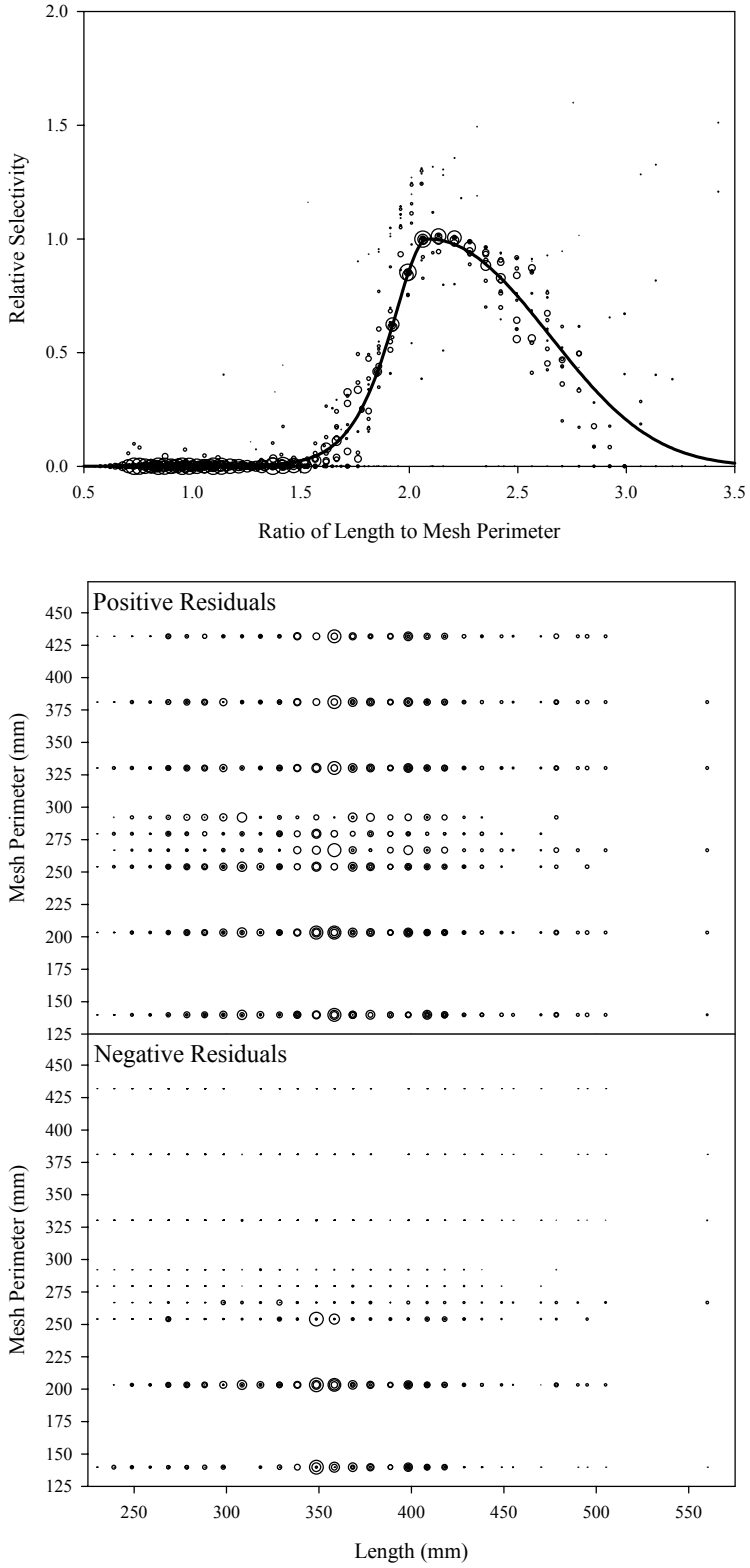

Figure B8.29. Plots of CPUE data scaled to a net selectivity model (top) and CPUE residuals (bottom); cisco data and Model 29.

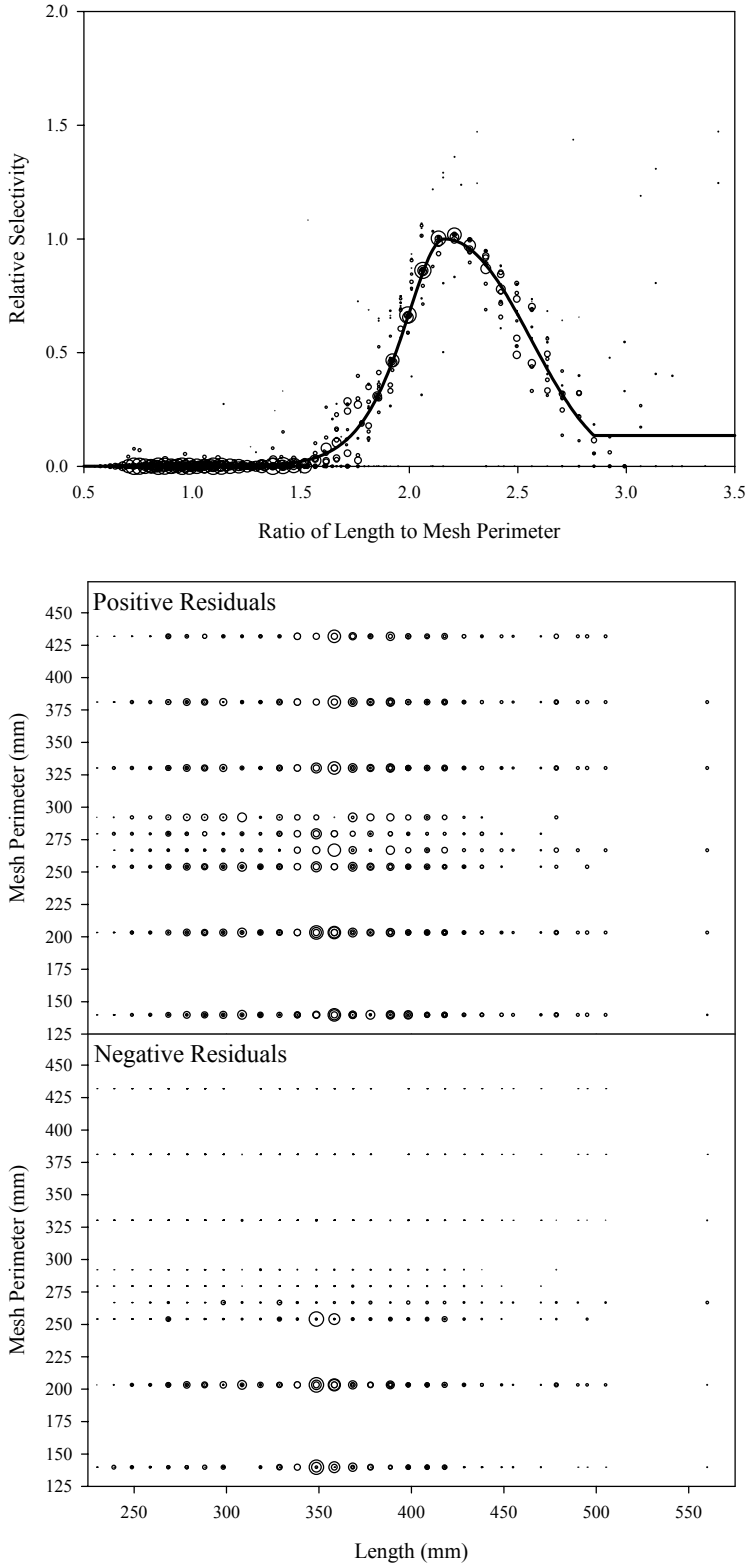

Figure B8.30. Plots of CPUE data scaled to a net selectivity model (top) and CPUE residuals (bottom); cisco data and Model 30.

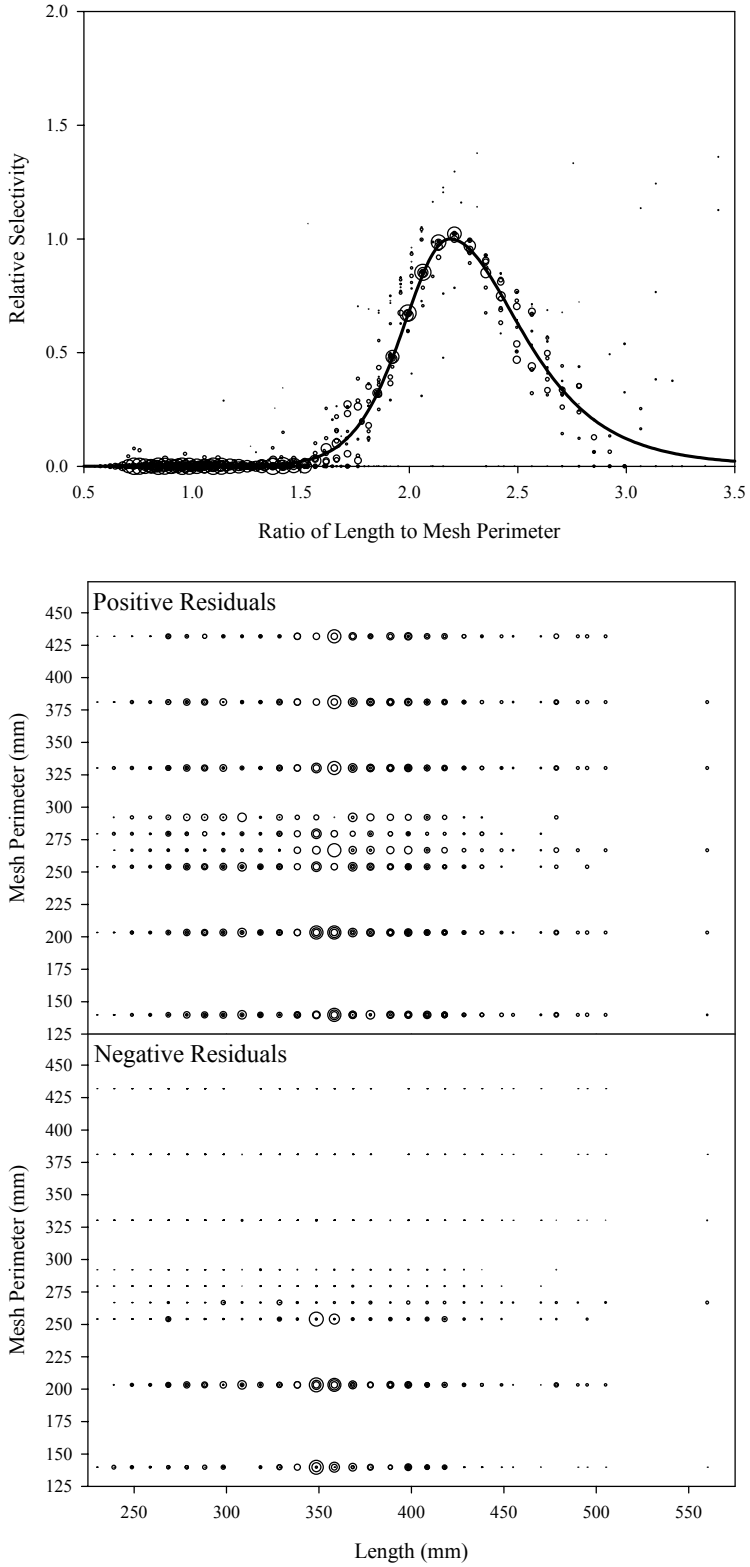

Figure B8.31. Plots of CPUE data scaled to a net selectivity model (top) and CPUE residuals (bottom); cisco data and Model 31.

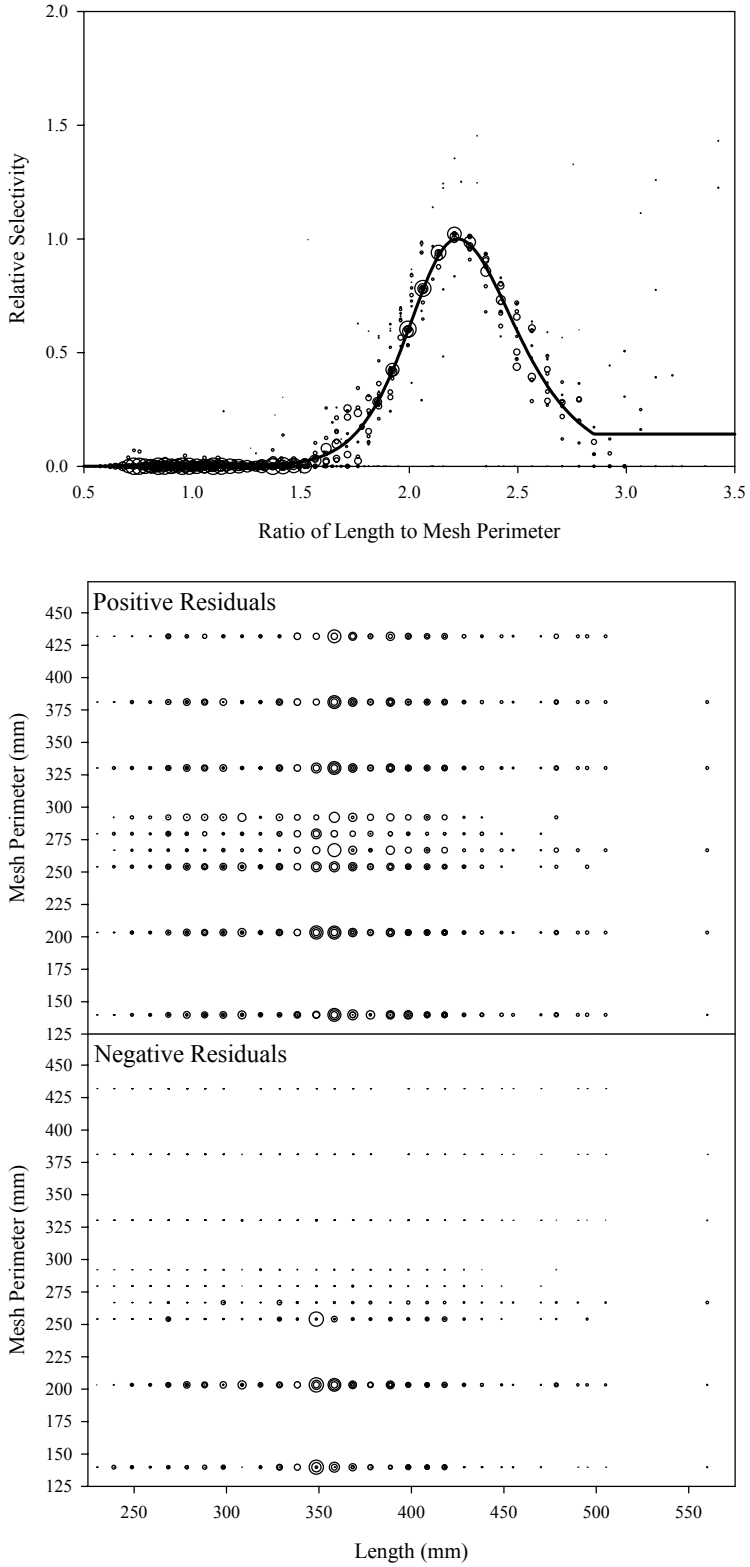

Figure B8.32. Plots of CPUE data scaled to a net selectivity model (top) and CPUE residuals (bottom); cisco data and Model 32.

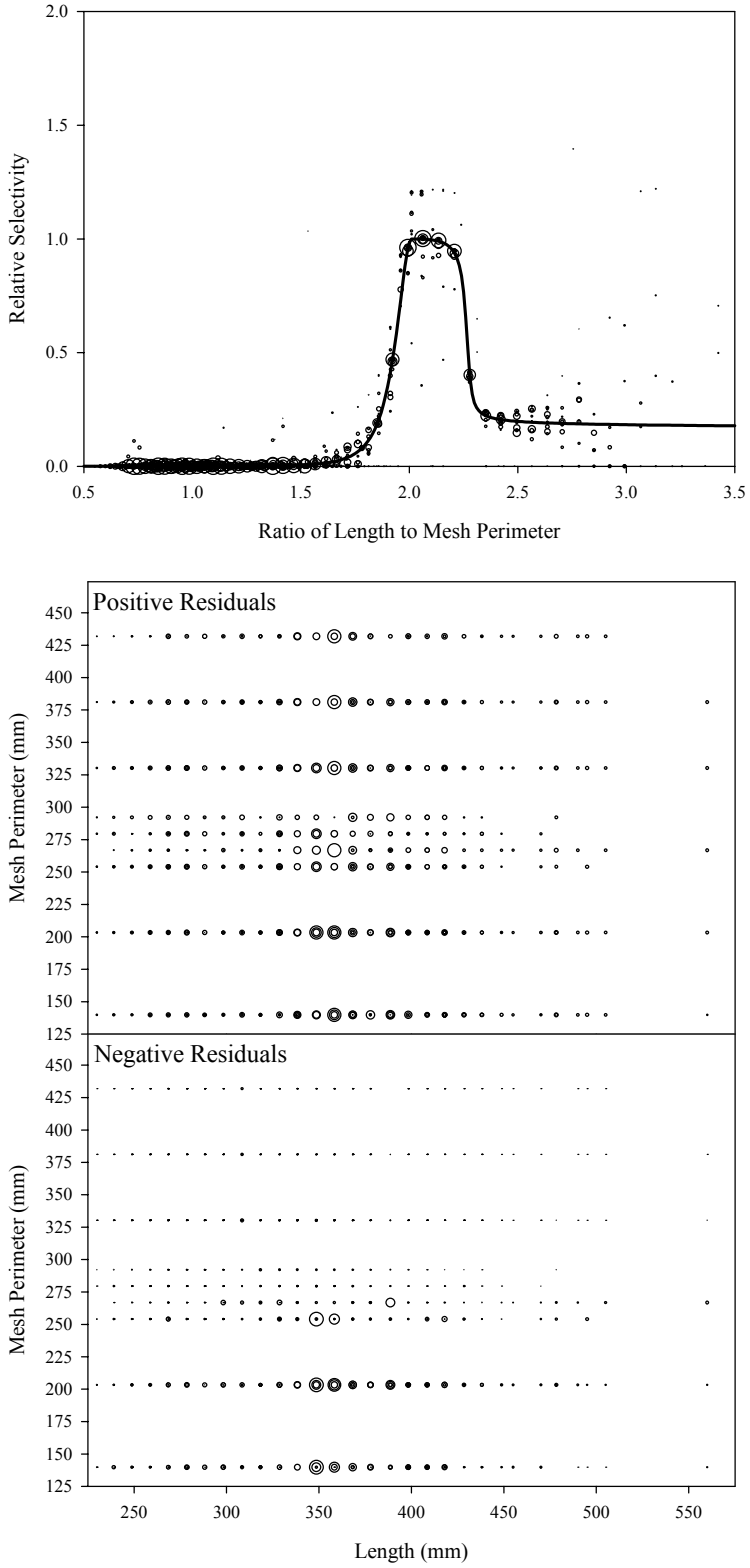

Figure B8.33. Plots of CPUE data scaled to a net selectivity model (top) and CPUE residuals (bottom); cisco data and Model 37.

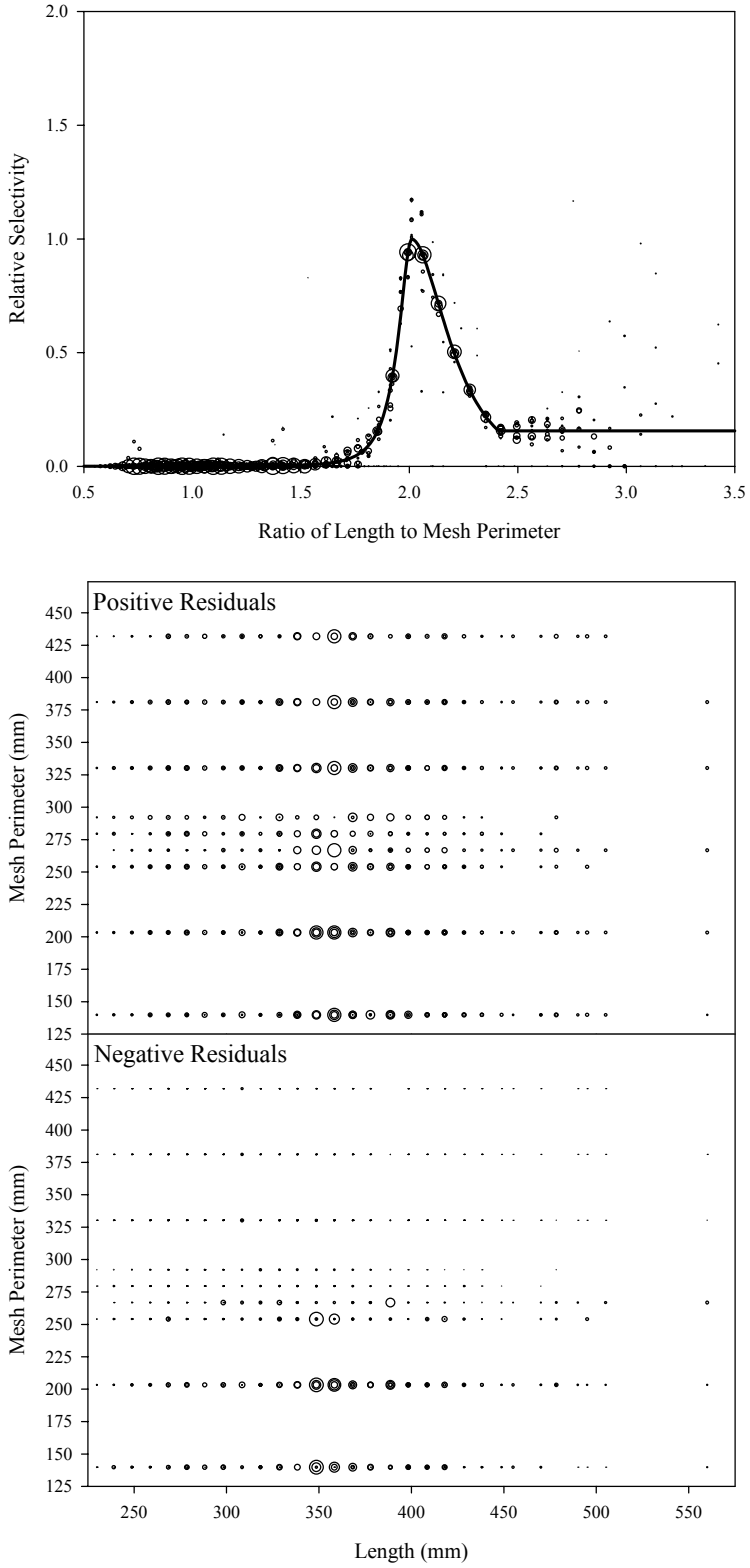

Figure B8.34. Plots of CPUE data scaled to a net selectivity model (top) and CPUE residuals (bottom); cisco data and Model 38.

Appendix B9
Other Species Group Diagnostic Plots
Figure B9.1 to Figure B9.36

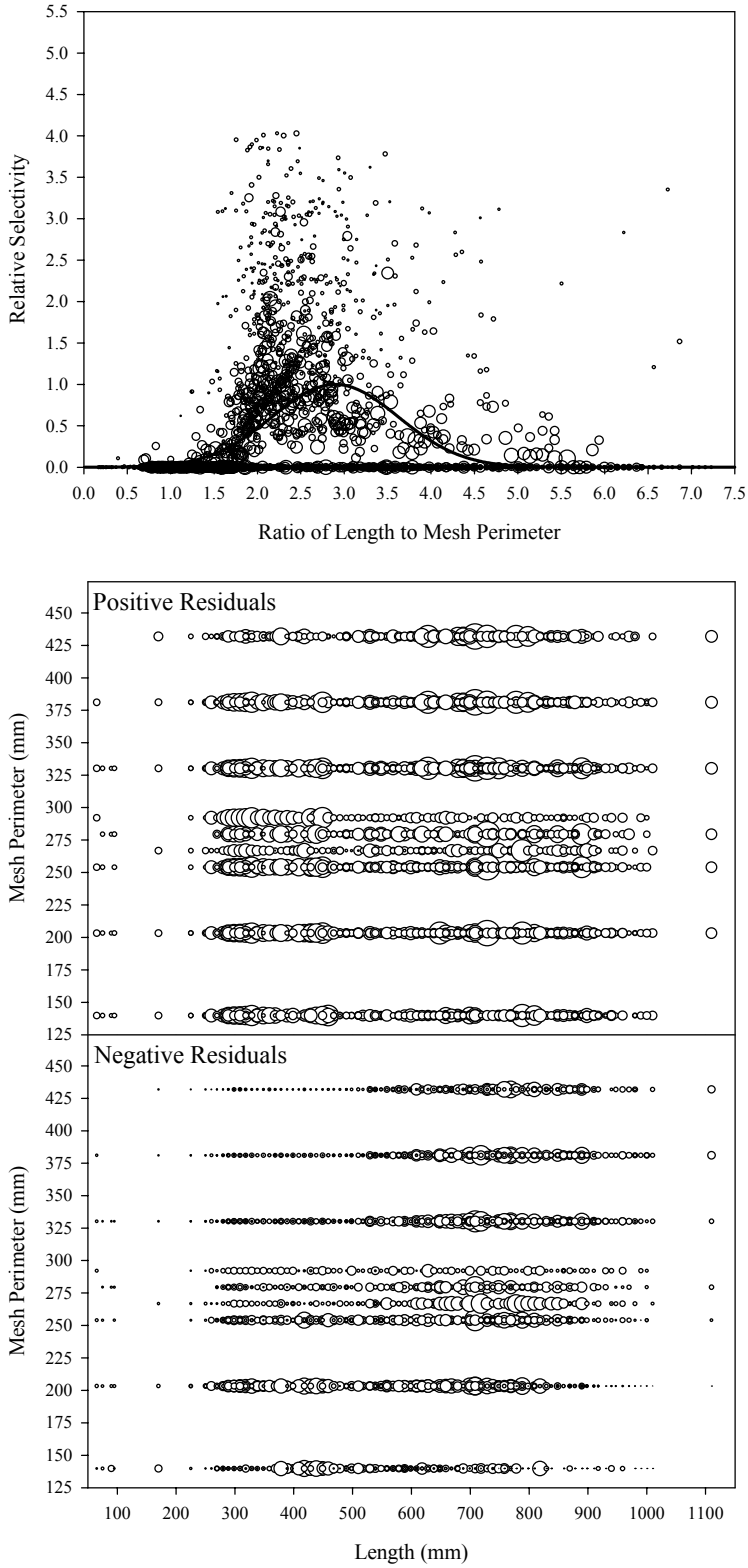

Figure B9.1. Plots of CPUE data scaled to a net selectivity model (top) and CPUE residuals (bottom); Other species group data and Model 1.

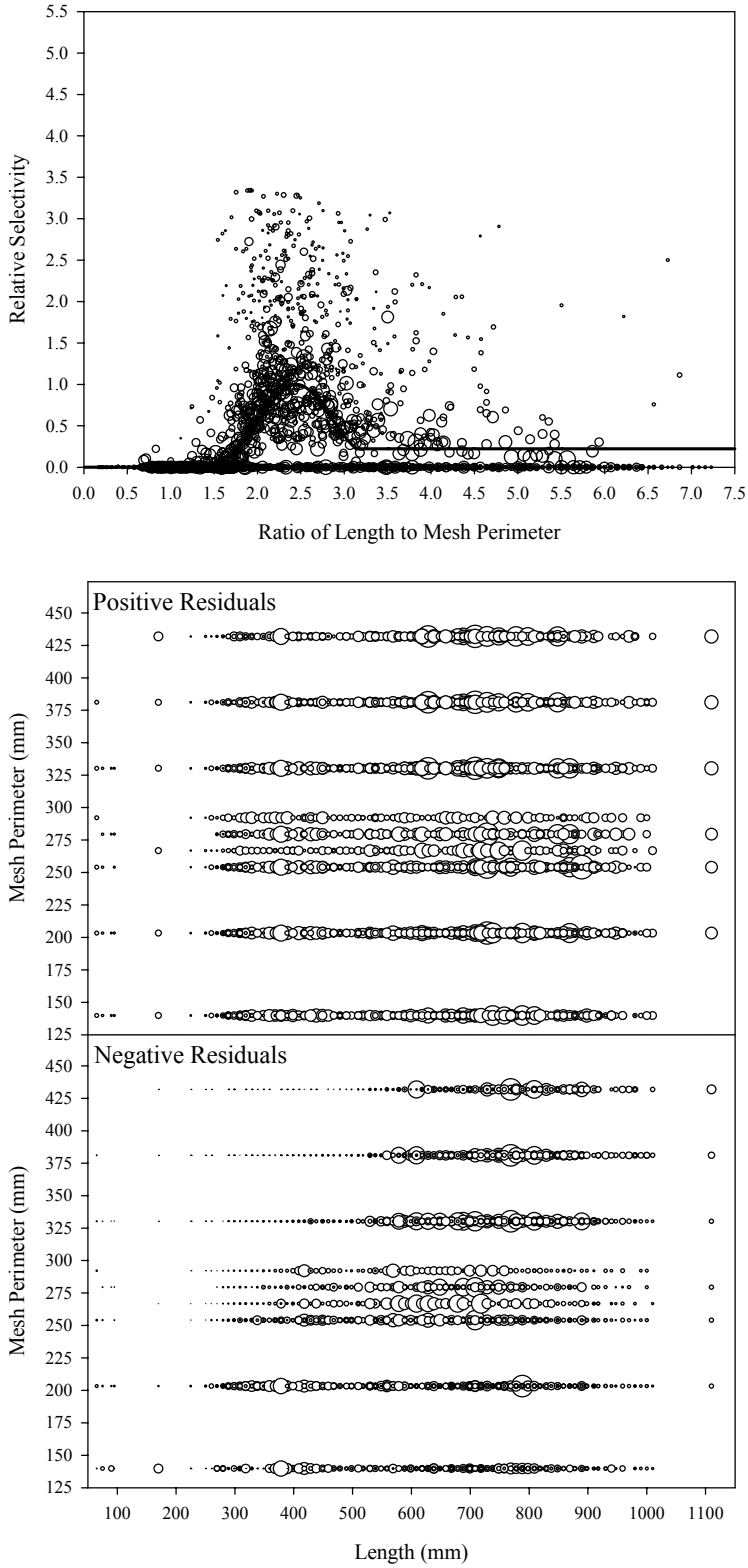

Figure B9.2. Plots of CPUE data scaled to a net selectivity model (top) and CPUE residuals (bottom); Other species group data and Model 2.

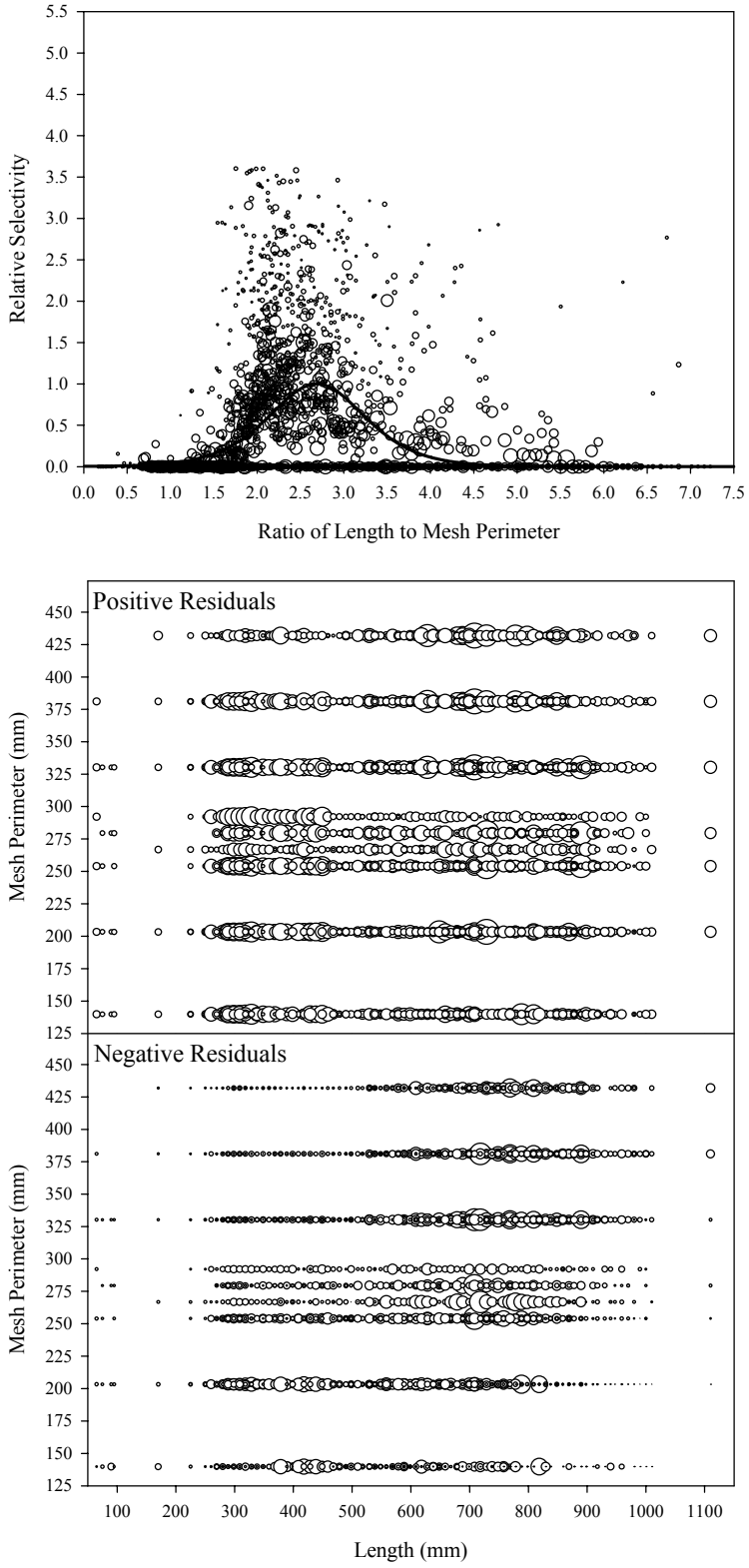

Figure B9.3. Plots of CPUE data scaled to a net selectivity model (top) and CPUE residuals (bottom); Other species group data and Model 3.

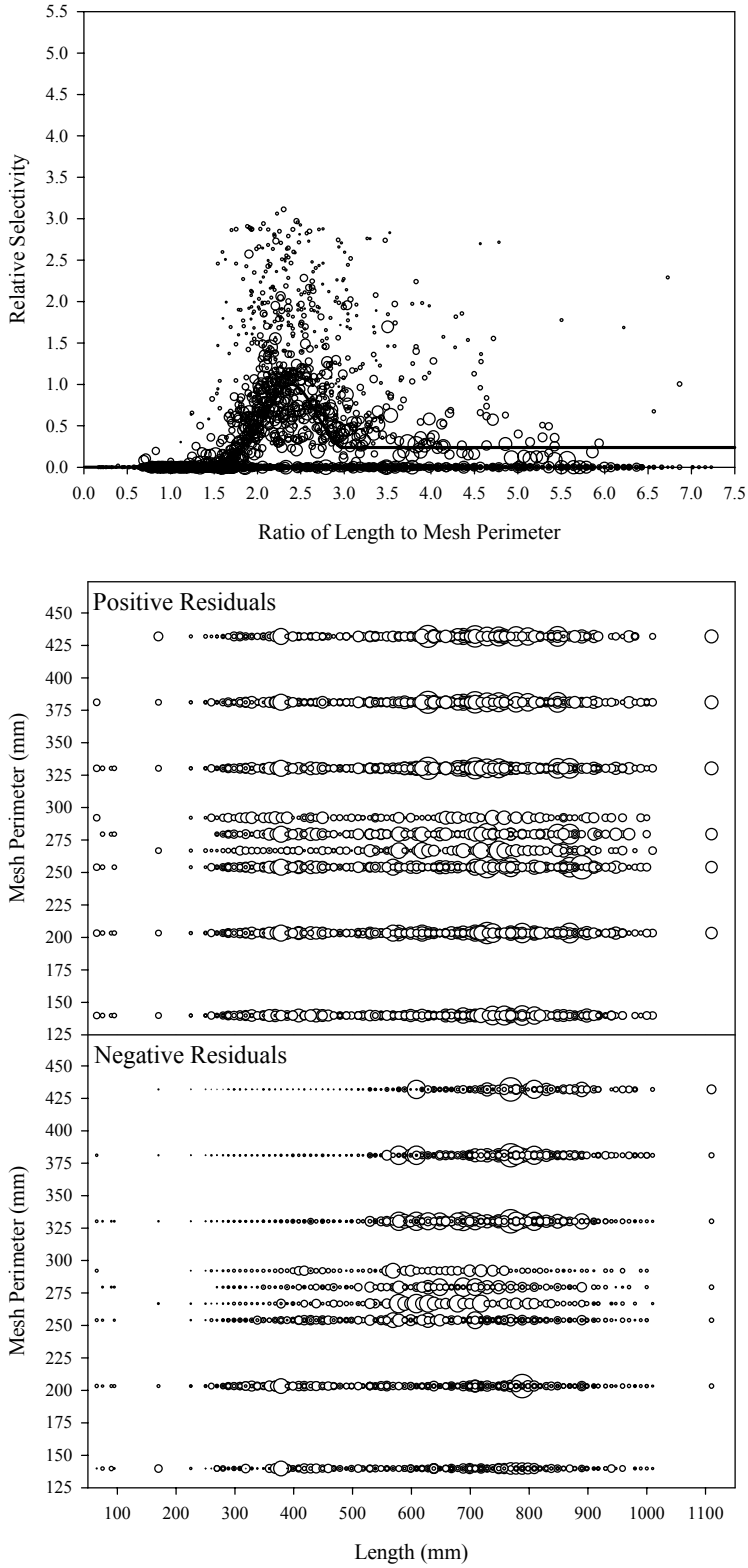

Figure B9.4. Plots of CPUE data scaled to a net selectivity model (top) and CPUE residuals (bottom); Other species group data and Model 4.

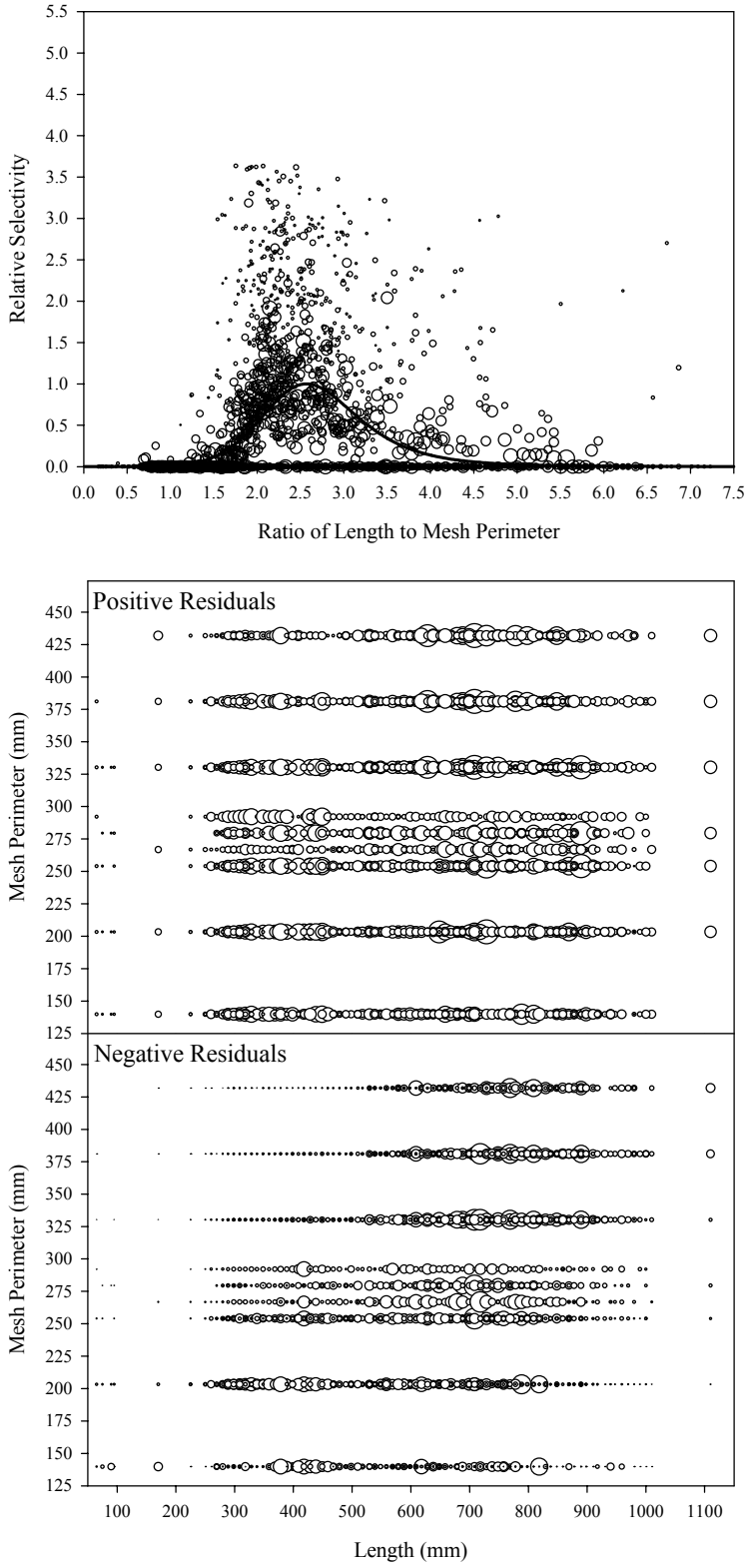

Figure B9.5. Plots of CPUE data scaled to a net selectivity model (top) and CPUE residuals (bottom); Other species group data and Model 5.

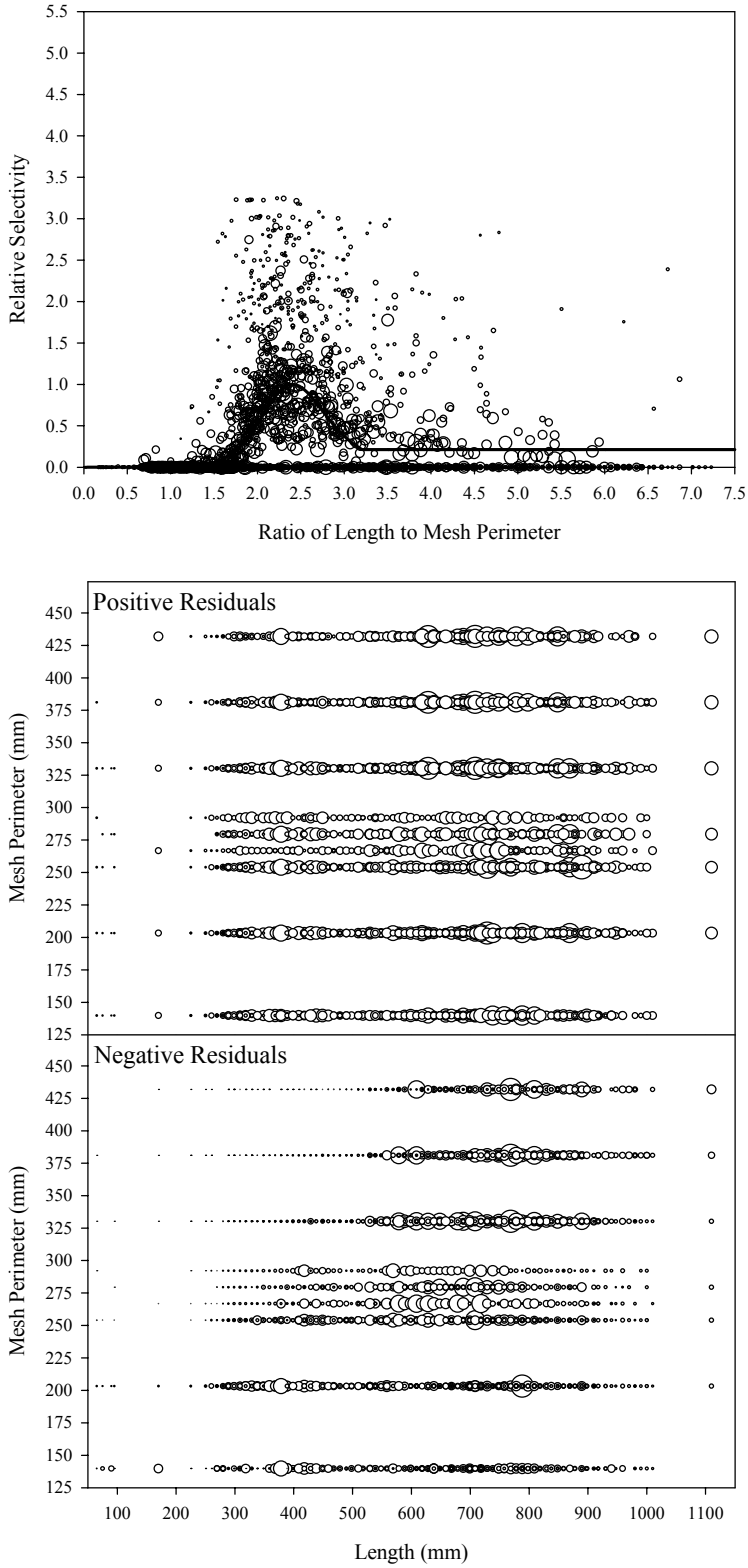

Figure B9.6. Plots of CPUE data scaled to a net selectivity model (top) and CPUE residuals (bottom); Other species group data and Model 6.

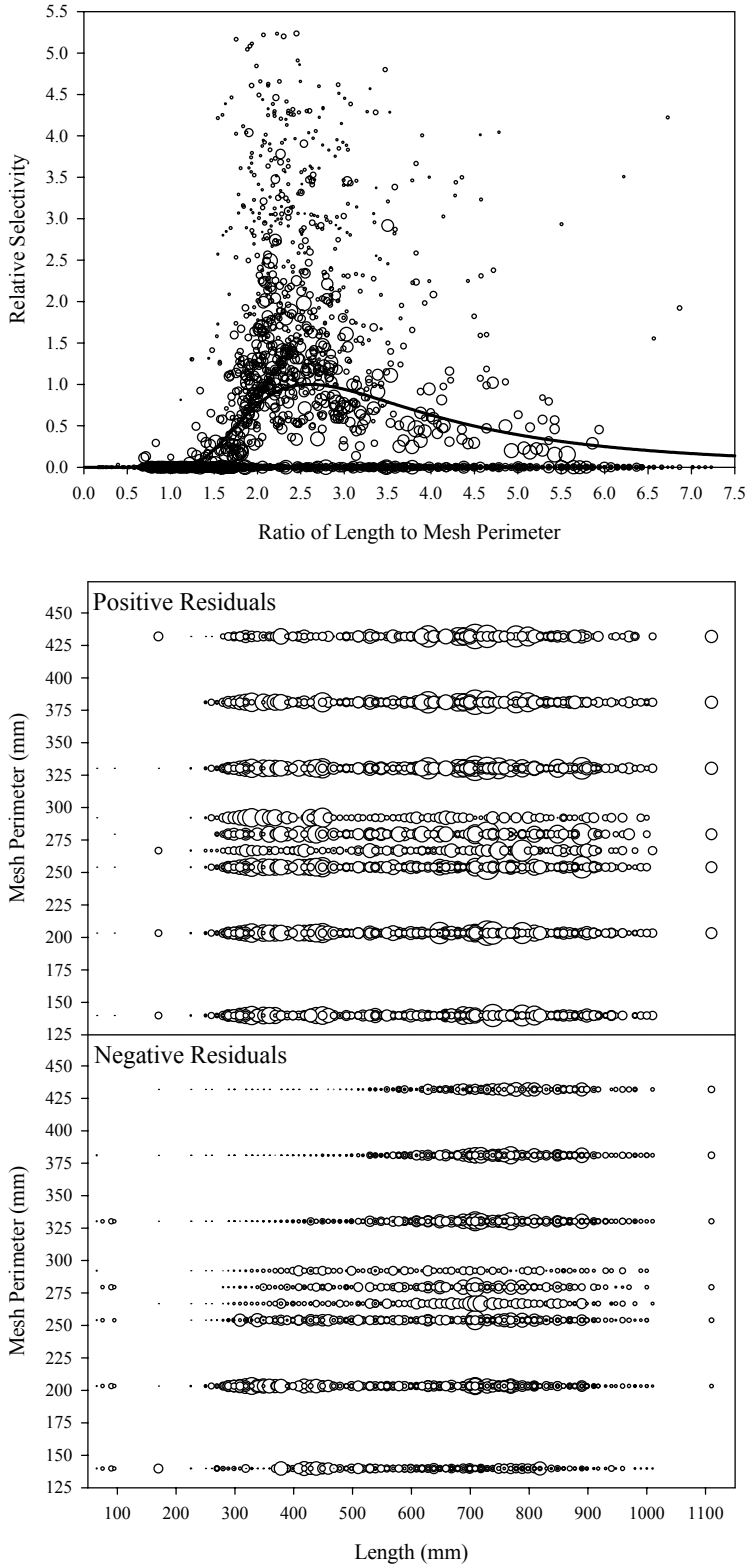

Figure B9.7. Plots of CPUE data scaled to a net selectivity model (top) and CPUE residuals (bottom); Other species group data and Model 7.

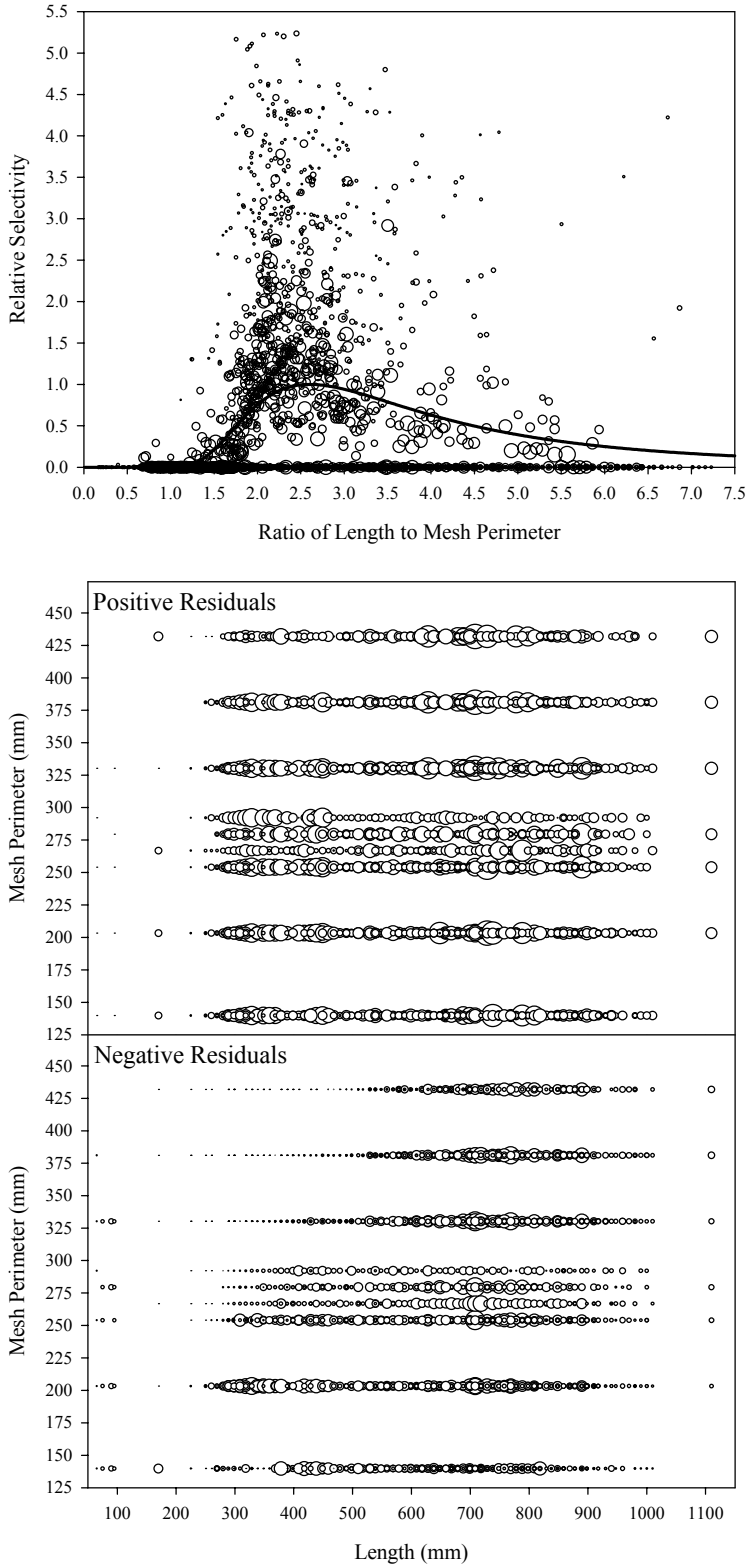

Figure B9.8. Plots of CPUE data scaled to a net selectivity model (top) and CPUE residuals (bottom); Other species group data and Model 8.

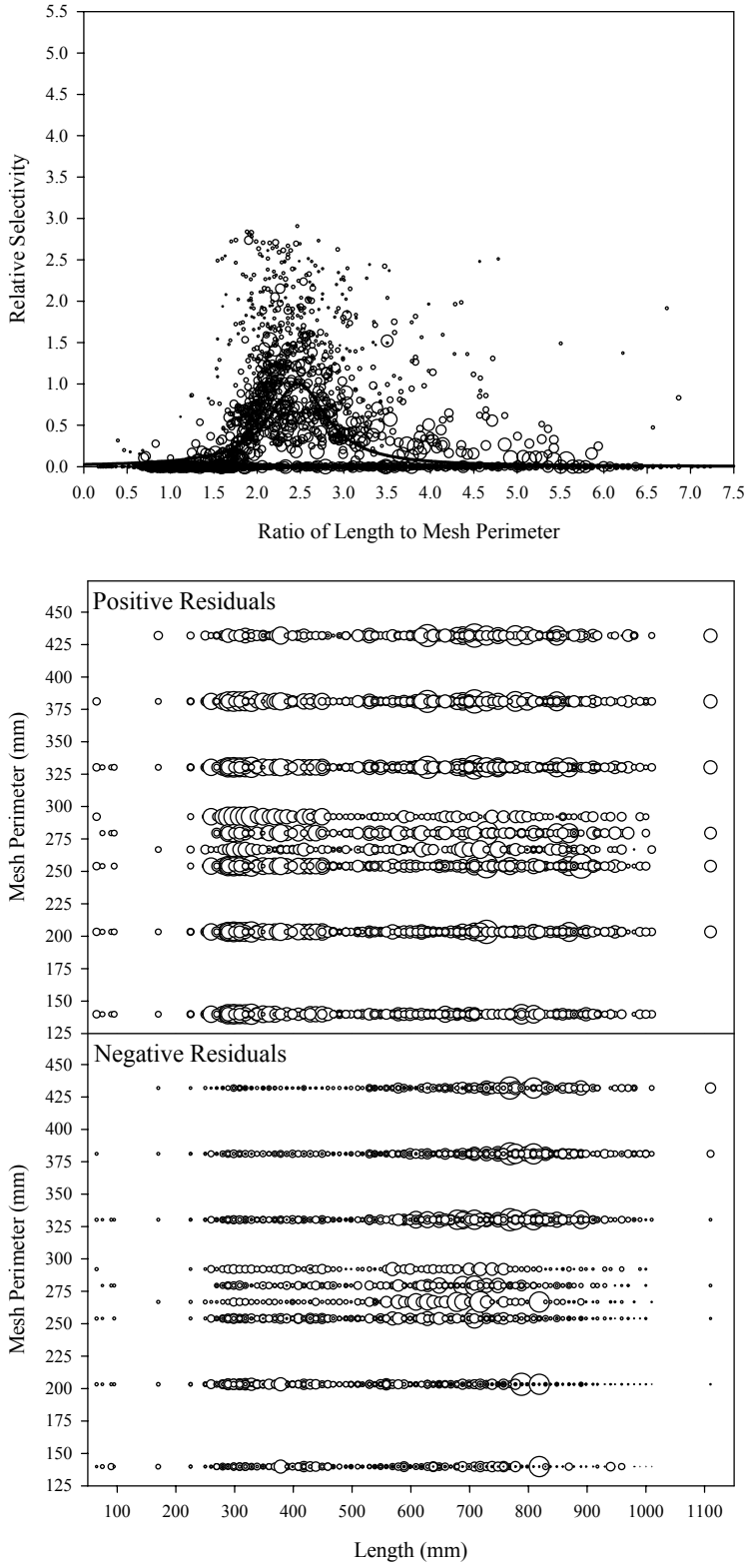

Figure B9.9. Plots of CPUE data scaled to a net selectivity model (top) and CPUE residuals (bottom); Other species group data and Model 9.

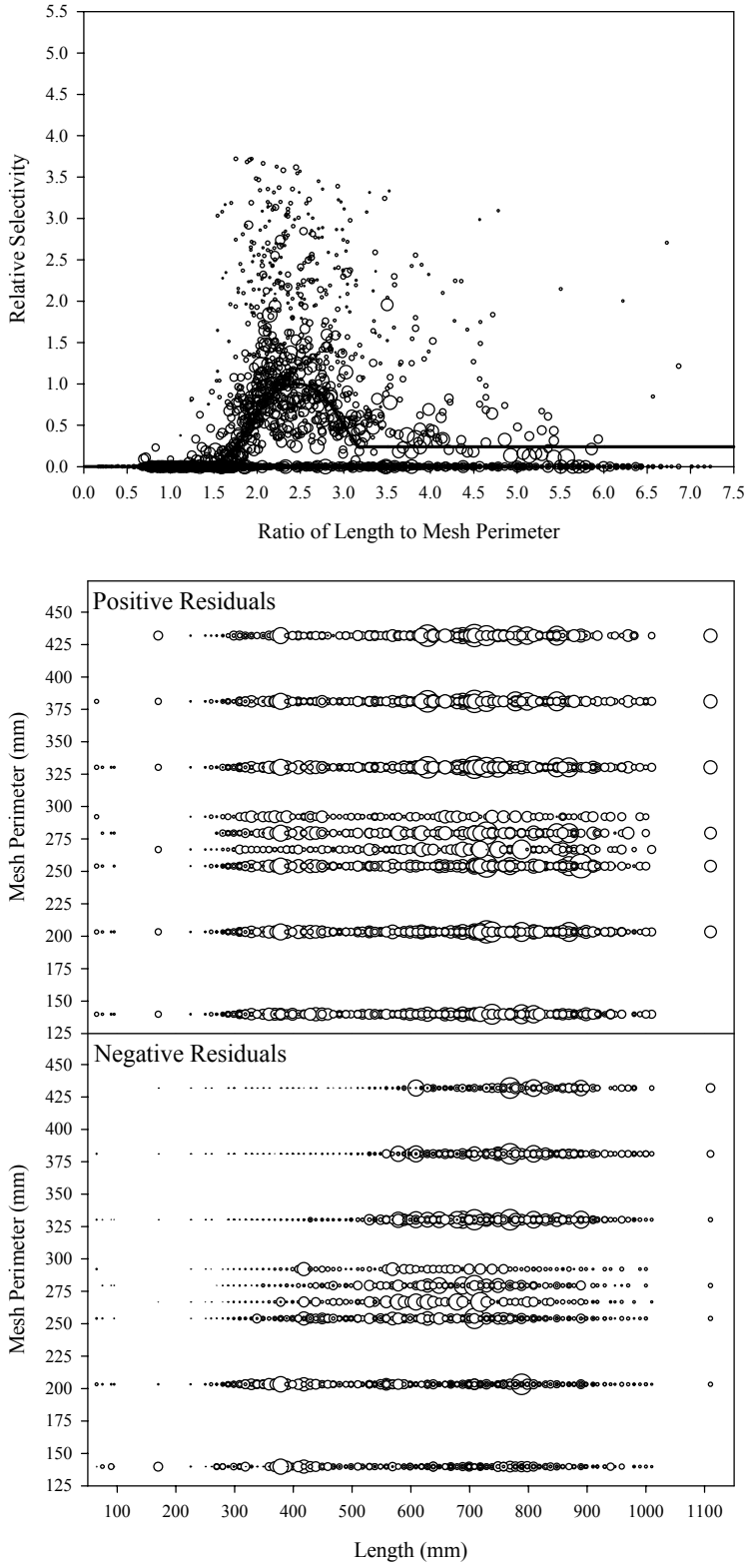

Figure B9.10. Plots of CPUE data scaled to a net selectivity model (top) and CPUE residuals (bottom); Other species group data and Model 10.

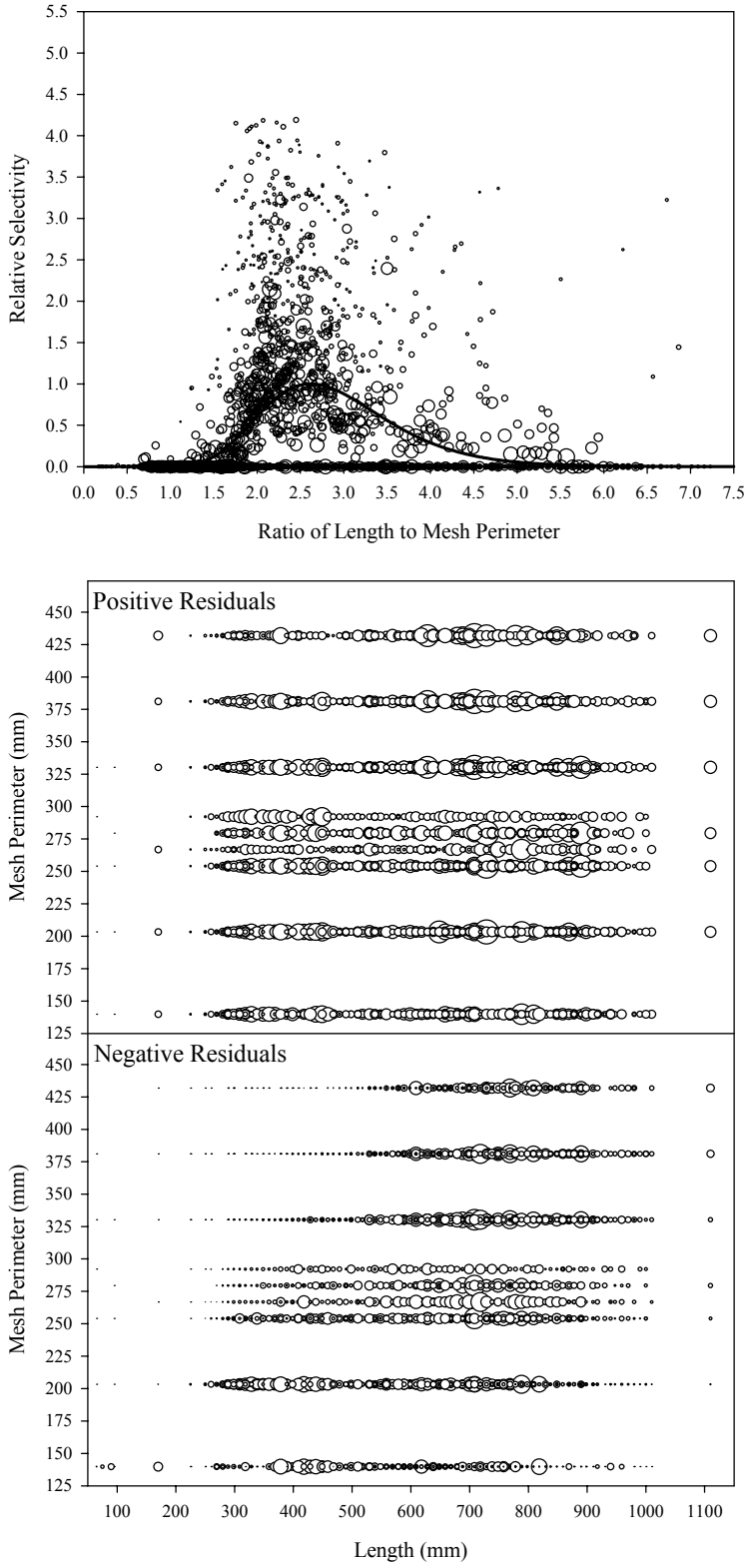

Figure B9.11. Plots of CPUE data scaled to a net selectivity model (top) and CPUE residuals (bottom); Other species group data and Model 11.

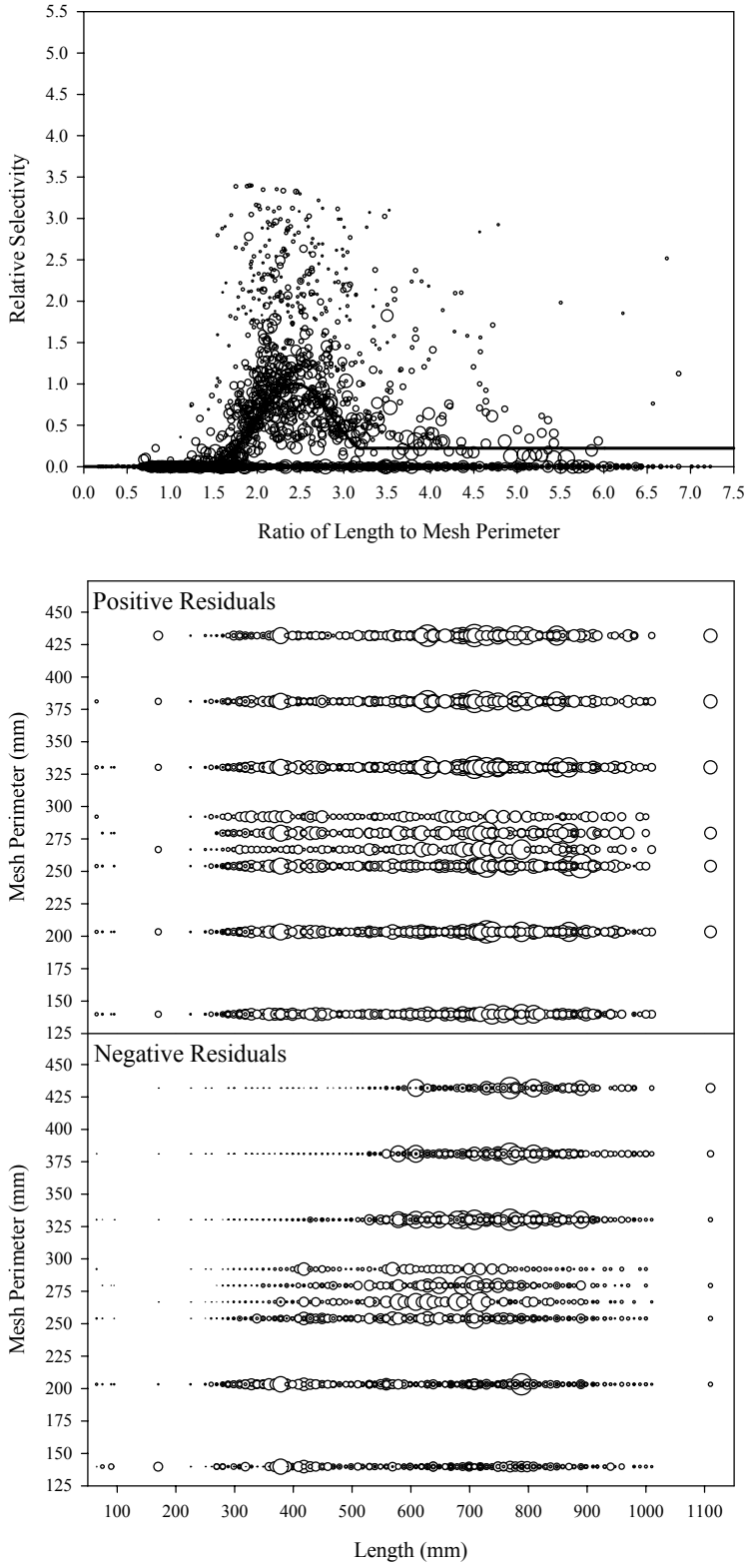

Figure B9.12. Plots of CPUE data scaled to a net selectivity model (top) and CPUE residuals (bottom); Other species group data and Model 12.

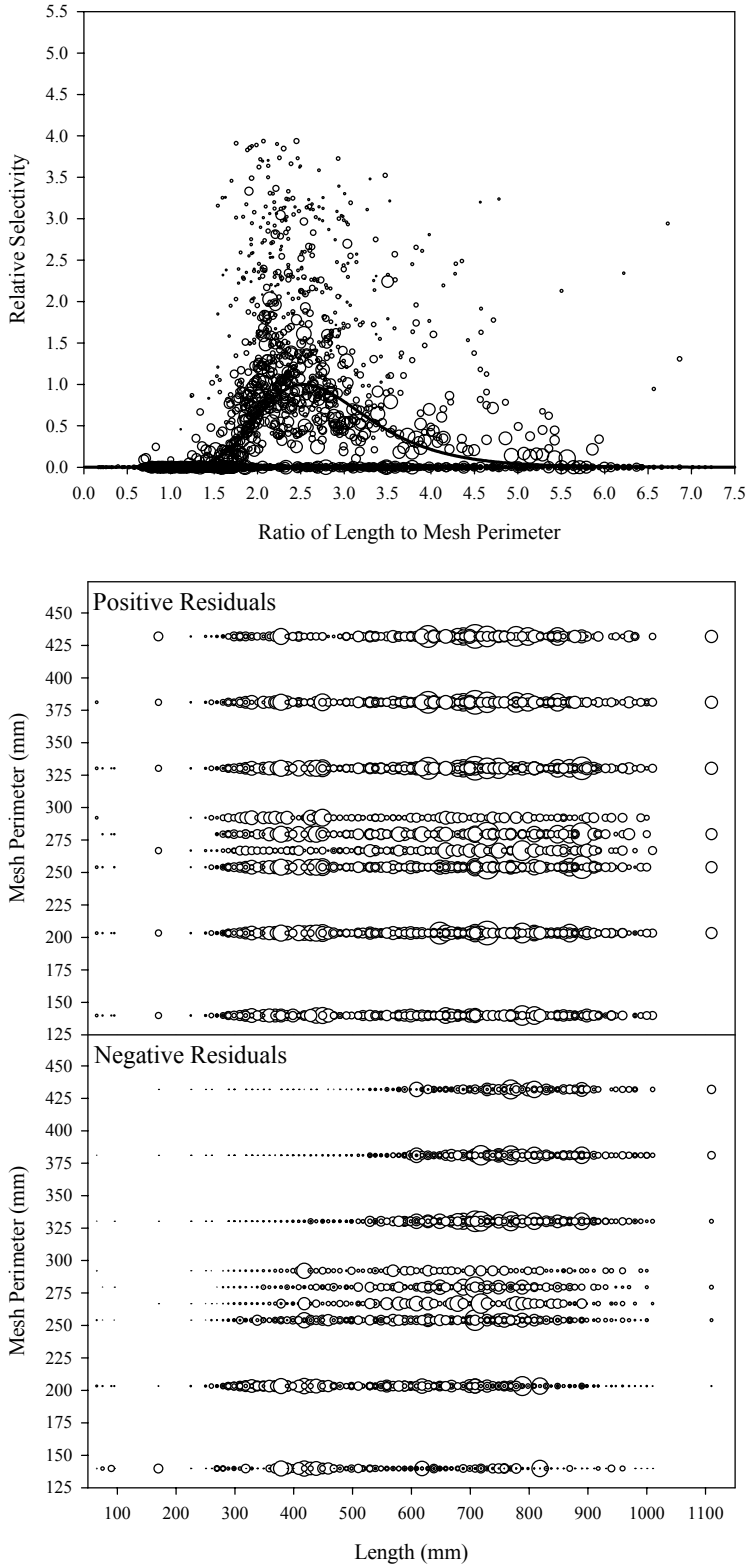

Figure B9.13. Plots of CPUE data scaled to a net selectivity model (top) and CPUE residuals (bottom); Other species group data and Model 13.

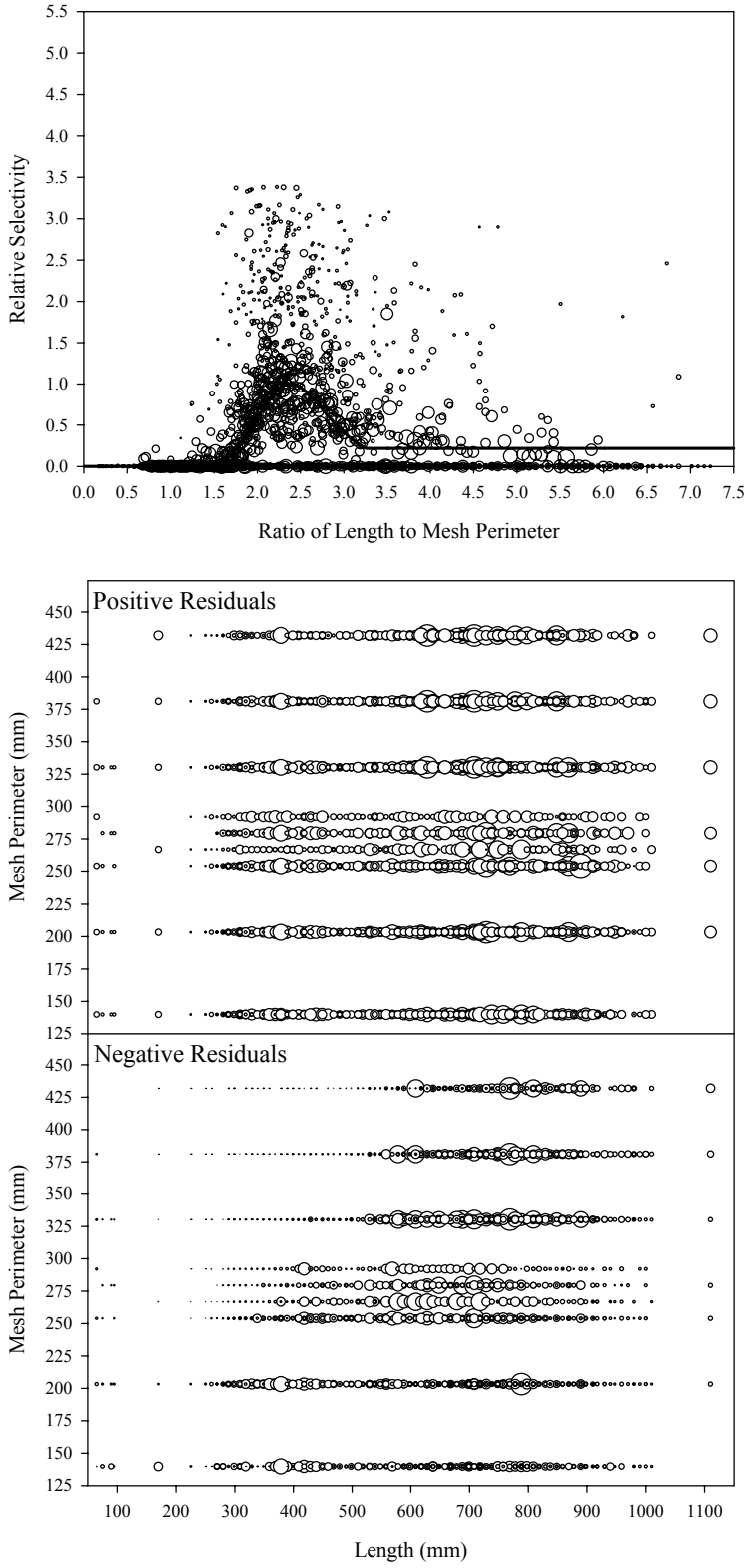

Figure B9.14. Plots of CPUE data scaled to a net selectivity model (top) and CPUE residuals (bottom); Other species group data and Model 14.

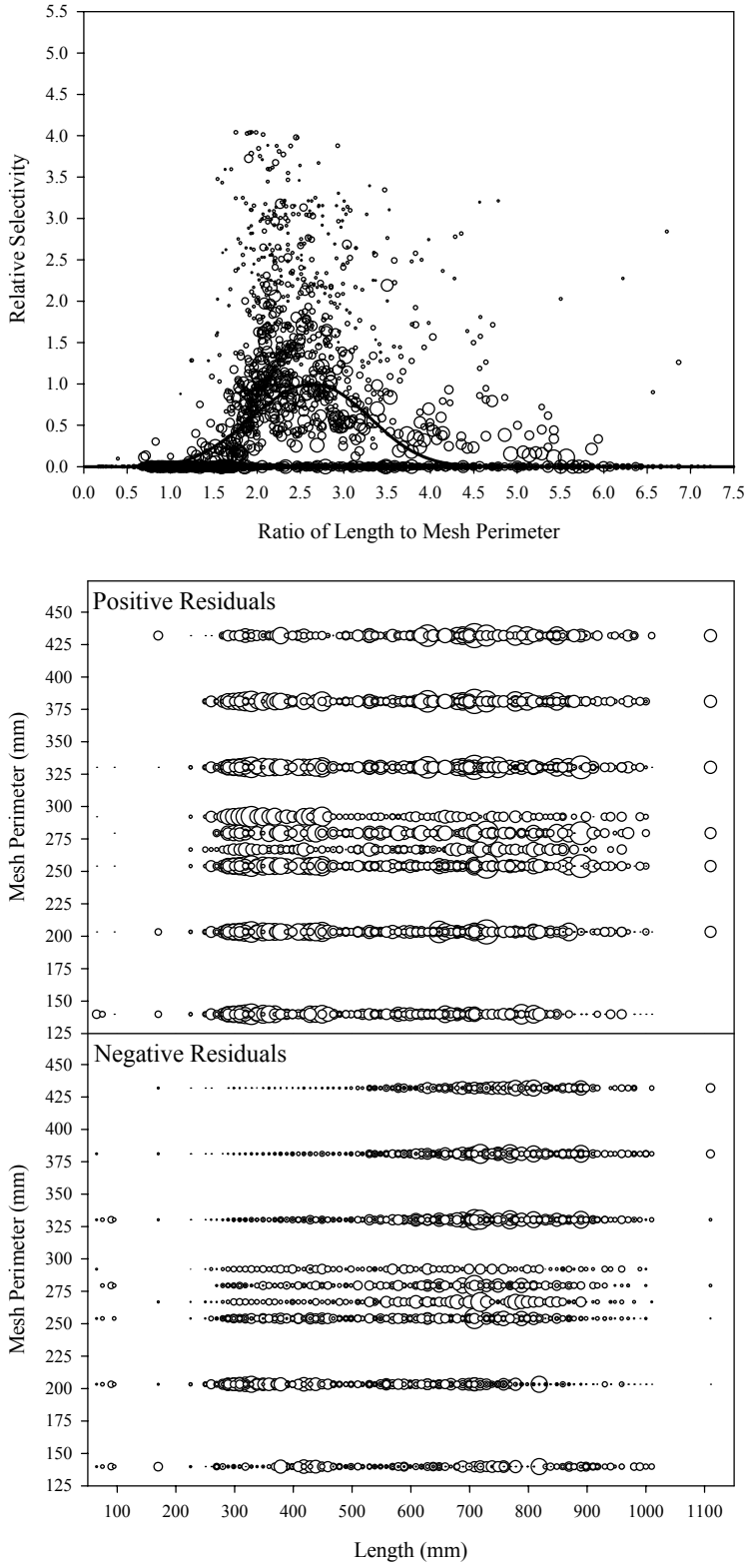

Figure B9.15. Plots of CPUE data scaled to a net selectivity model (top) and CPUE residuals (bottom); Other species group data and Model 15.

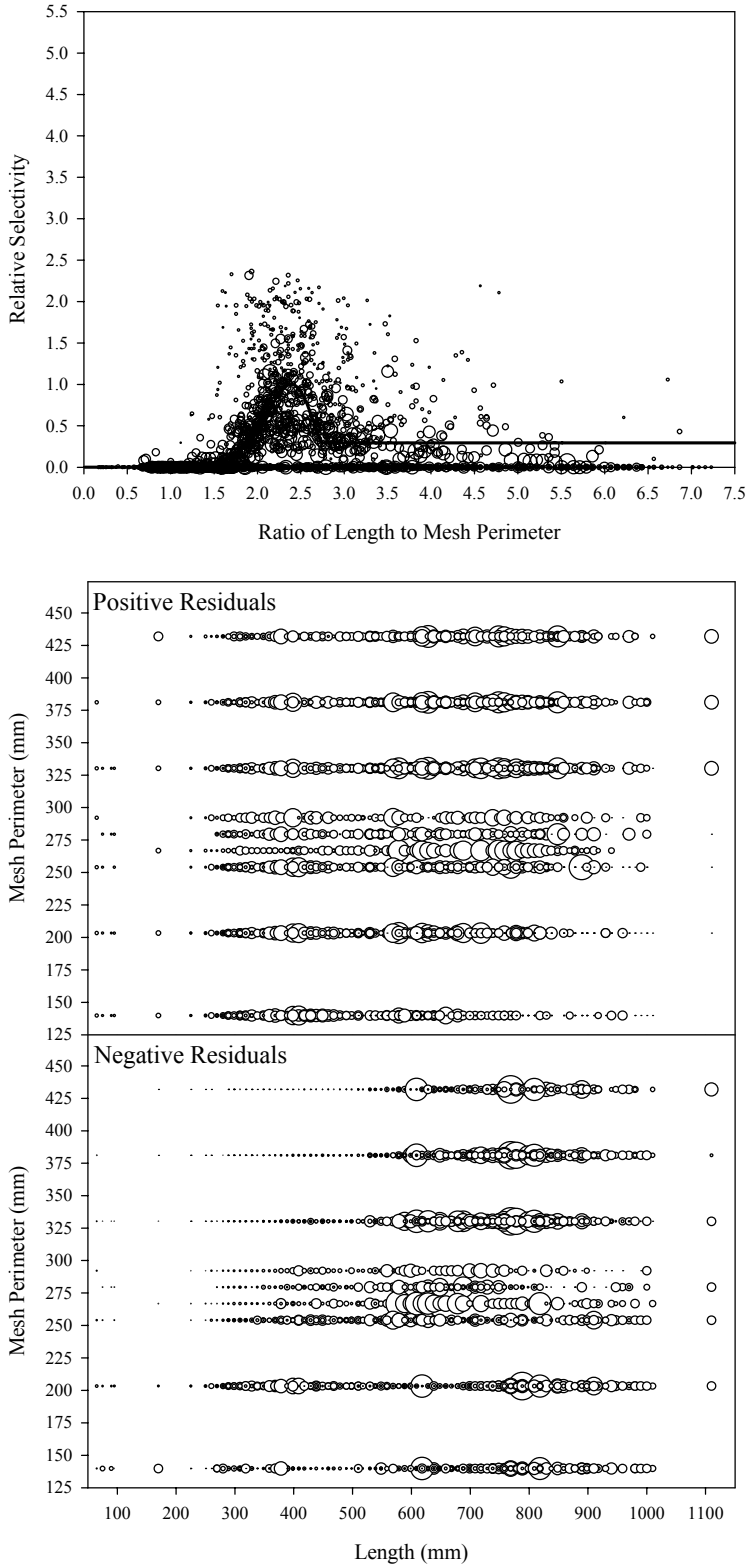

Figure B9.16. Plots of CPUE data scaled to a net selectivity model (top) and CPUE residuals (bottom); Other species group data and Model 16.

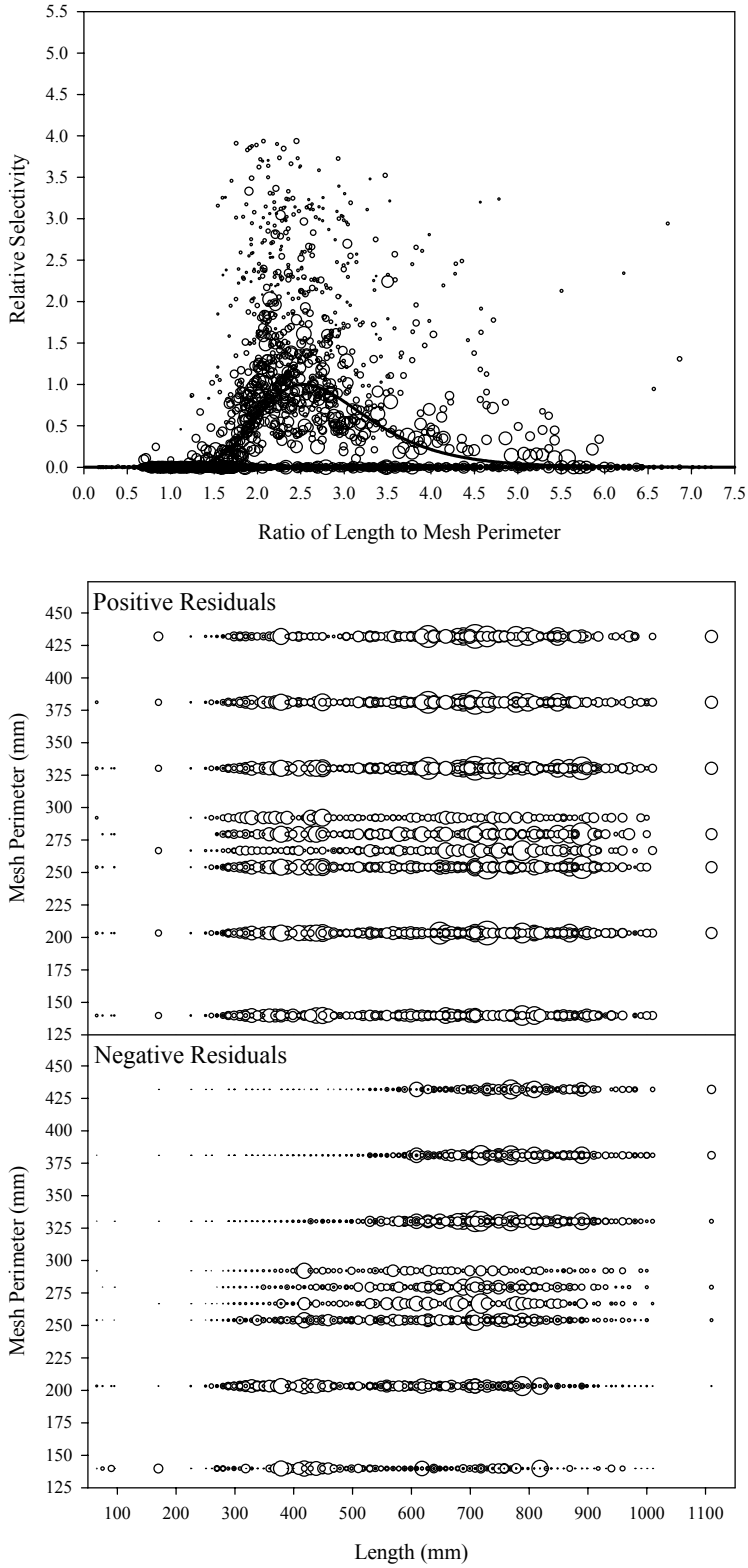

Figure B9.17. Plots of CPUE data scaled to a net selectivity model (top) and CPUE residuals (bottom); Other species group data and Model 17.

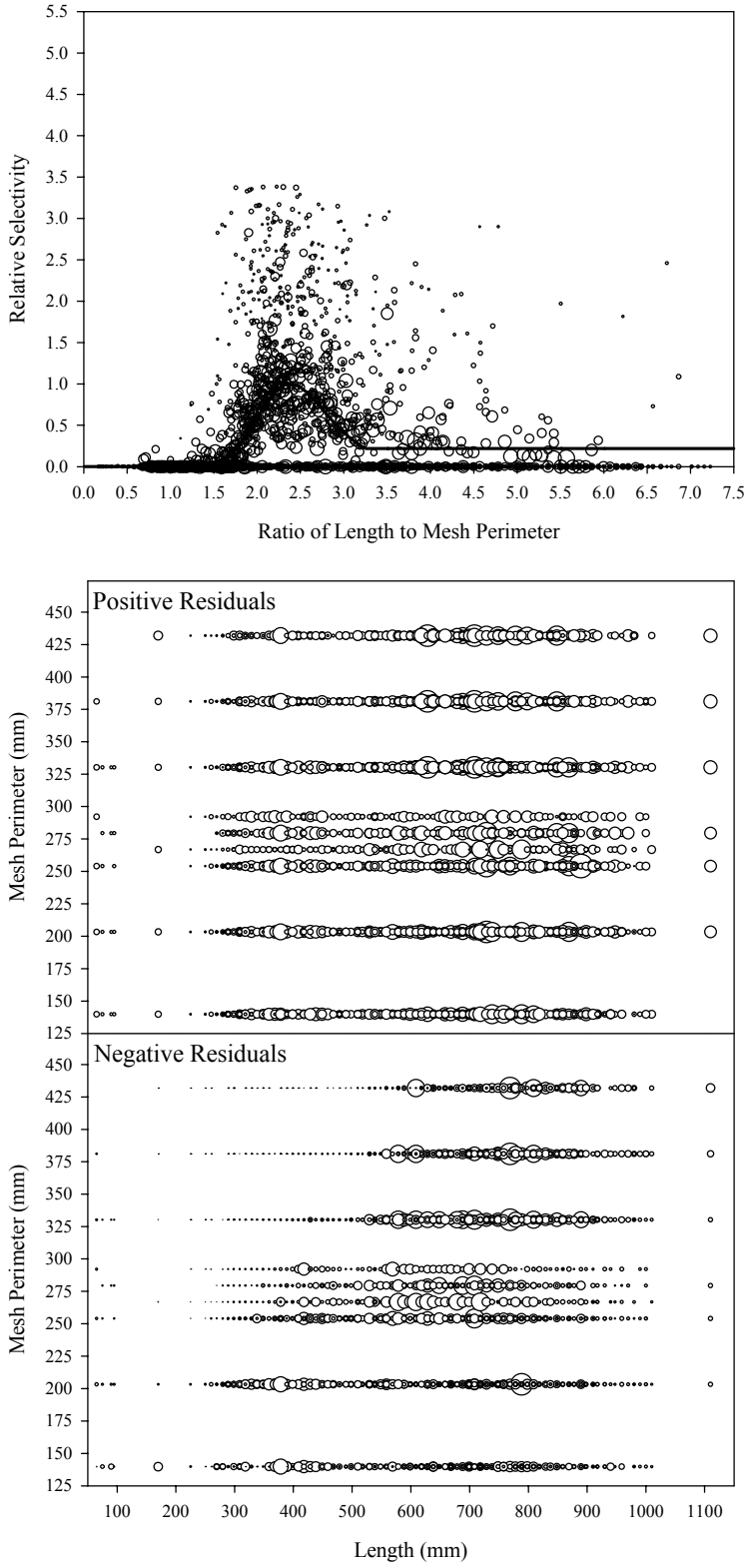

Figure B9.18. Plots of CPUE data scaled to a net selectivity model (top) and CPUE residuals (bottom); Other species group data and Model 18.

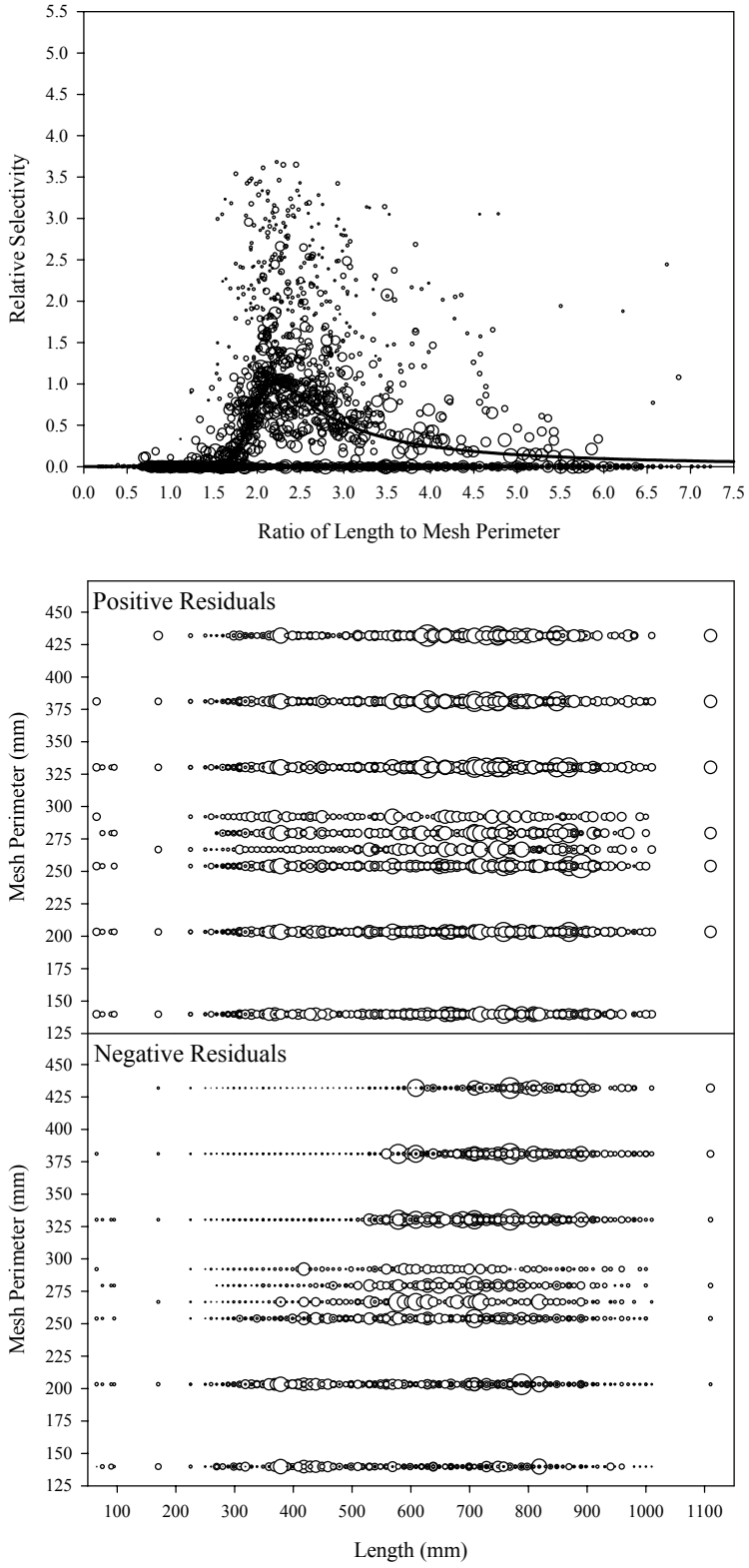

Figure B9.19. Plots of CPUE data scaled to a net selectivity model (top) and CPUE residuals (bottom); Other species group data and Model 19.

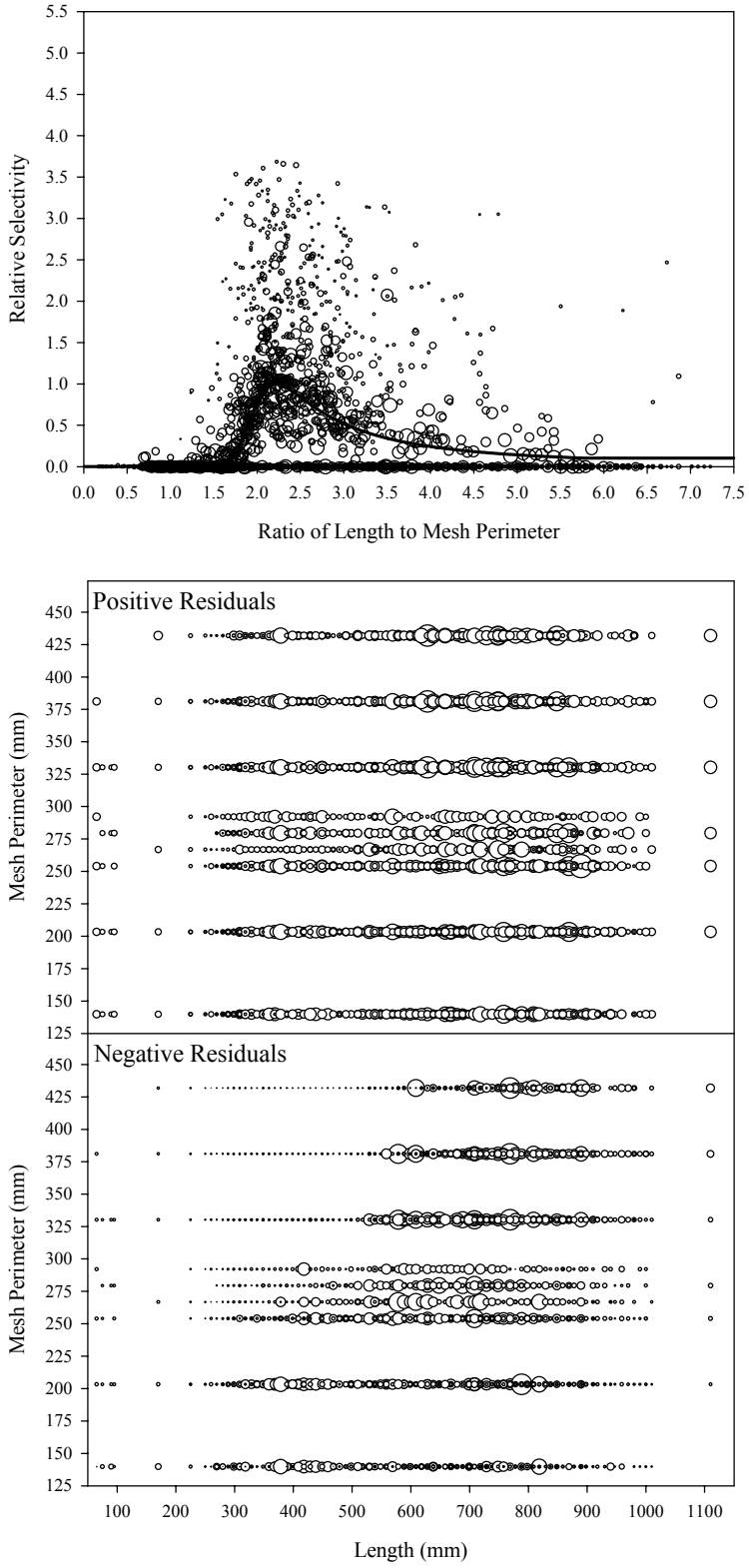

Figure B9.20. Plots of CPUE data scaled to a net selectivity model (top) and CPUE residuals (bottom); Other species group data and Model 20.

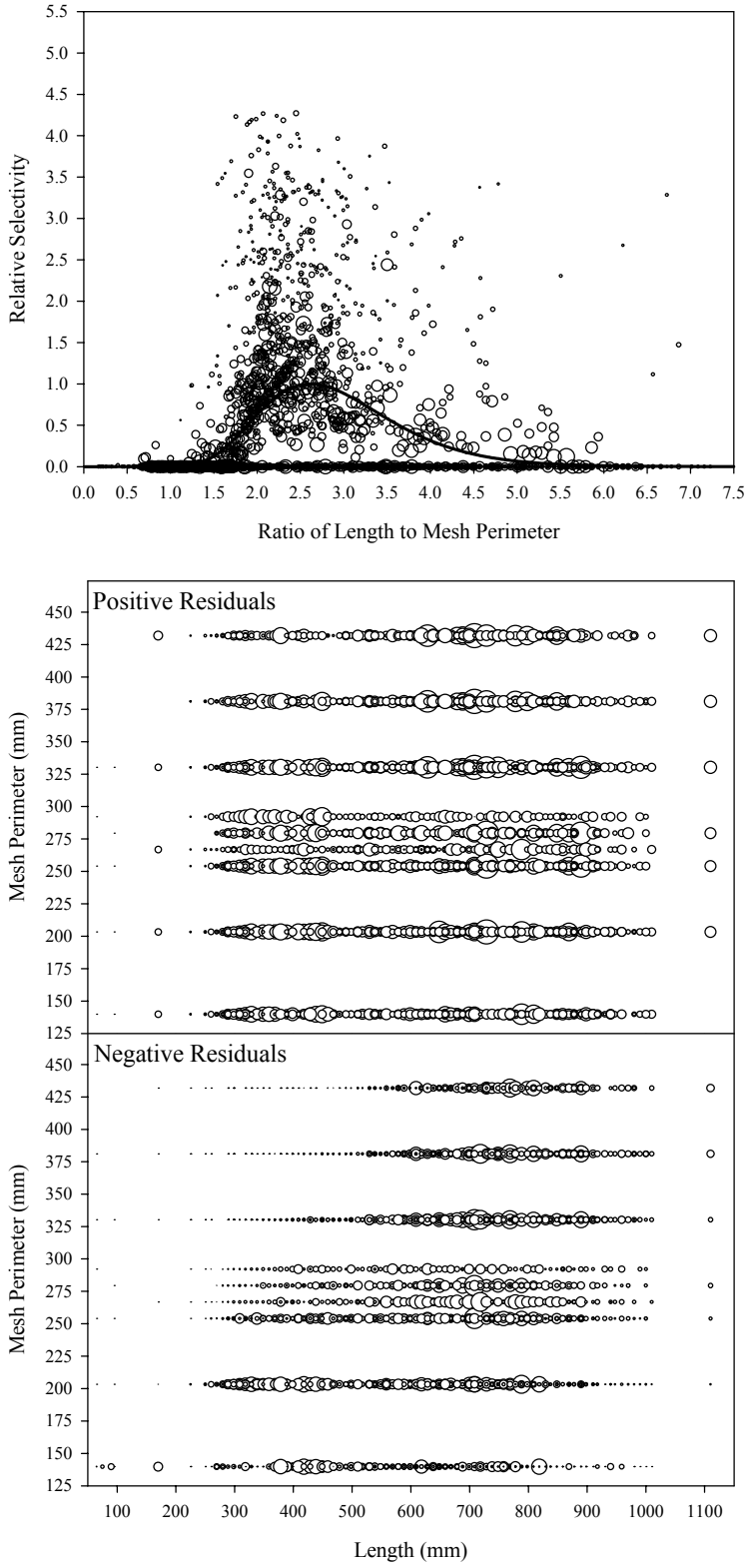

Figure B9.21. Plots of CPUE data scaled to a net selectivity model (top) and CPUE residuals (bottom); Other species group data and Model 21.

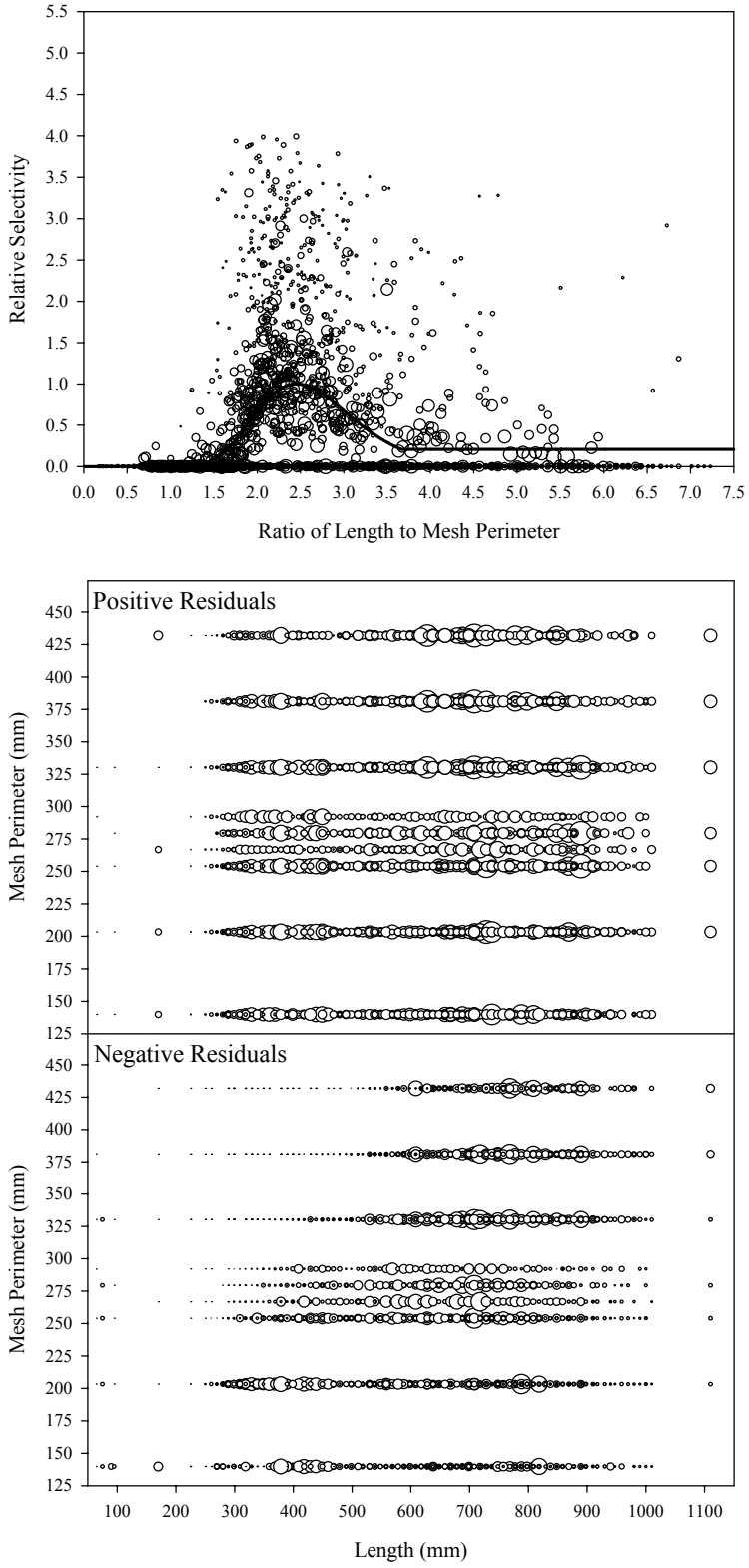

Figure B9.22. Plots of CPUE data scaled to a net selectivity model (top) and CPUE residuals (bottom); Other species group data and Model 22.

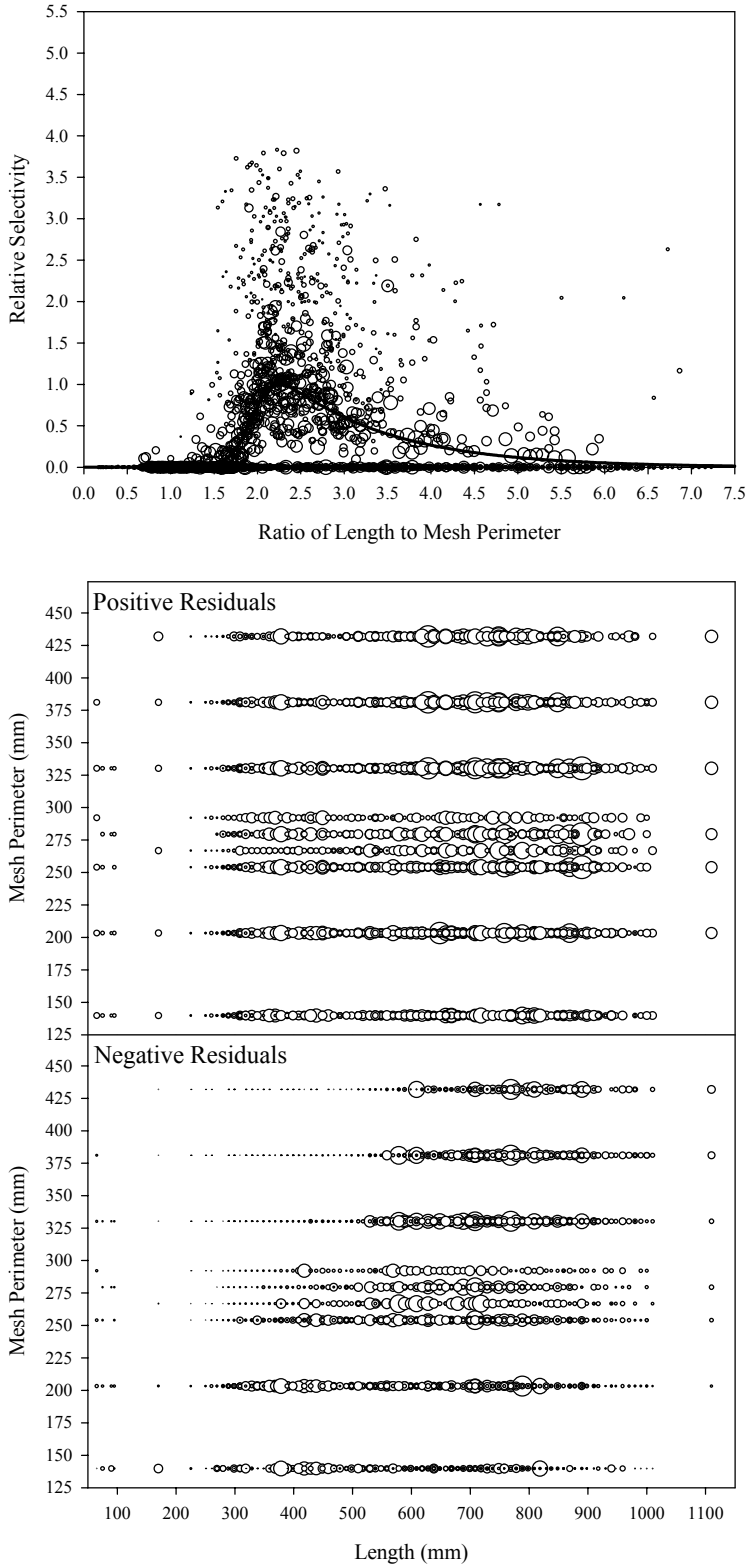

Figure B9.23. Plots of CPUE data scaled to a net selectivity model (top) and CPUE residuals (bottom); Other species group data and Model 23.

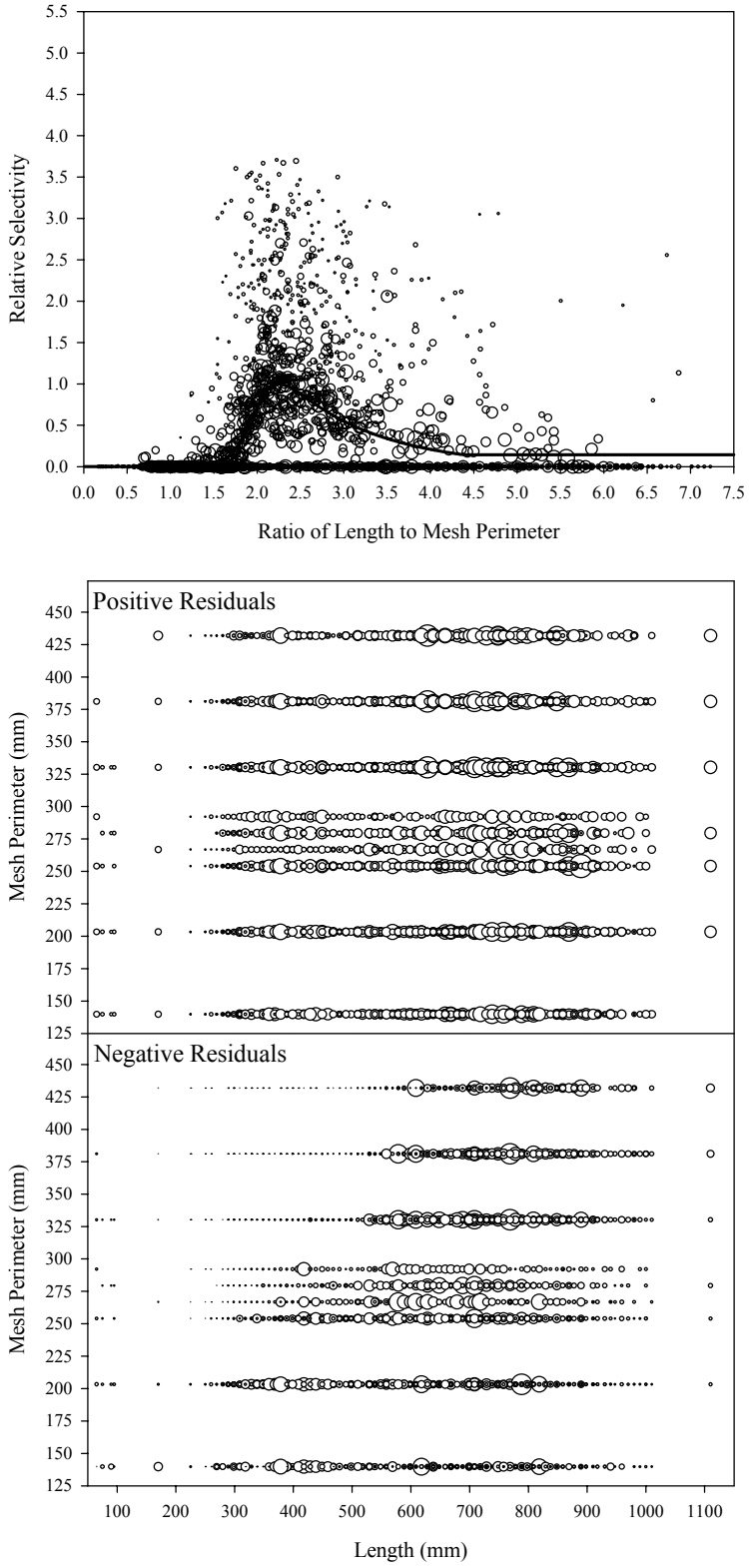

Figure B9.24. Plots of CPUE data scaled to a net selectivity model (top) and CPUE residuals (bottom); Other species group data and Model 24.

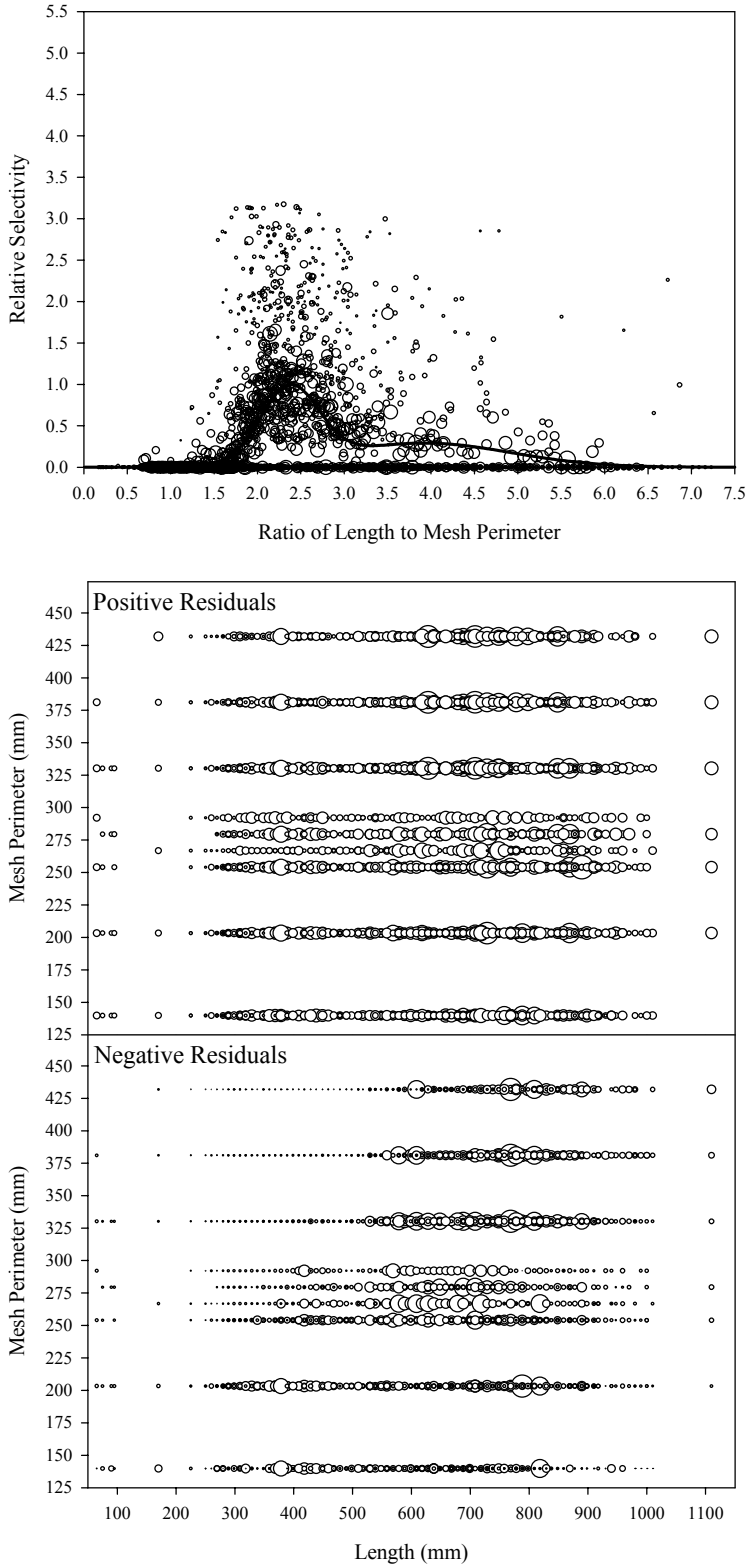

Figure B9.25. Plots of CPUE data scaled to a net selectivity model (top) and CPUE residuals (bottom); Other species group data and Model 25.

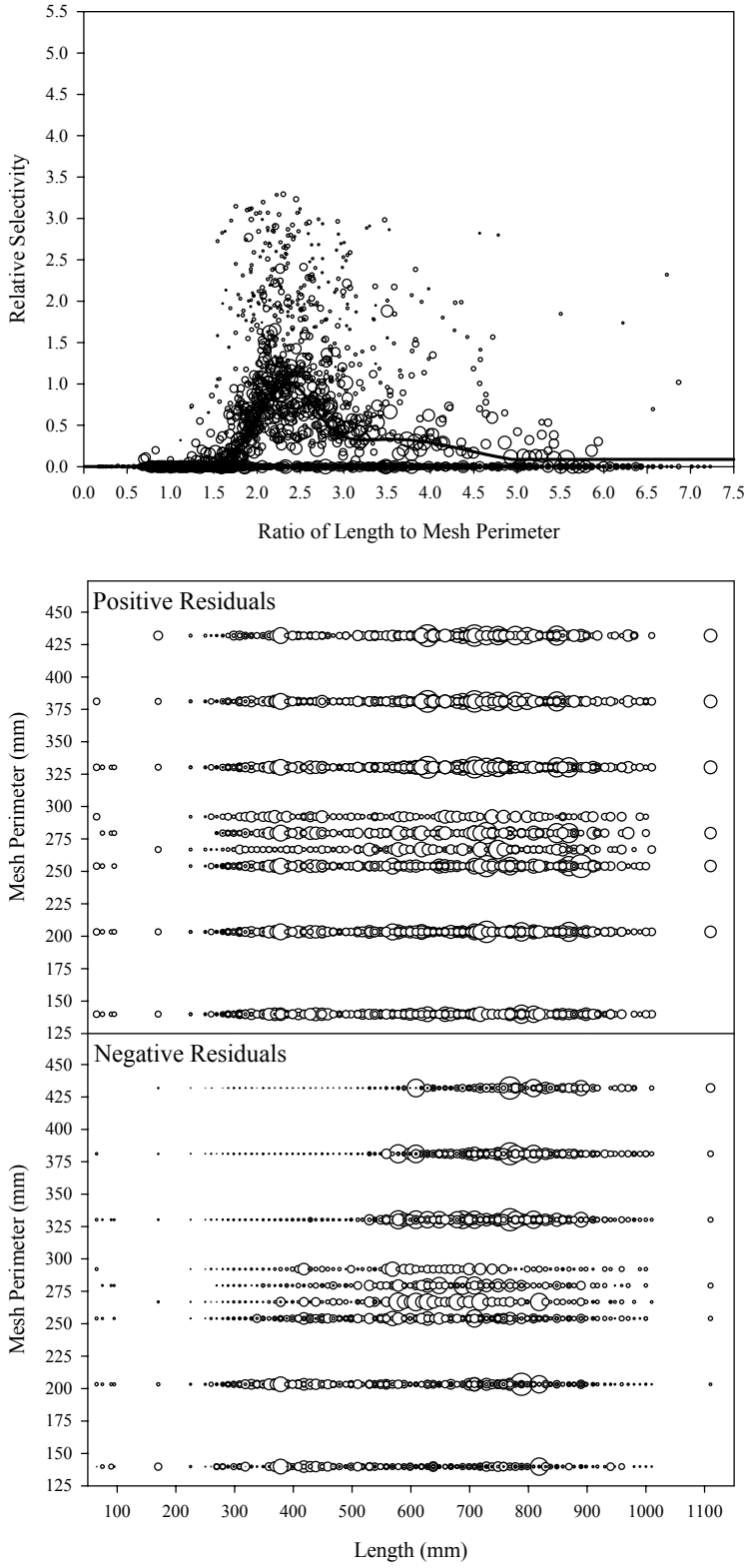

Figure B9.26. Plots of CPUE data scaled to a net selectivity model (top) and CPUE residuals (bottom); Other species group data and Model 26.

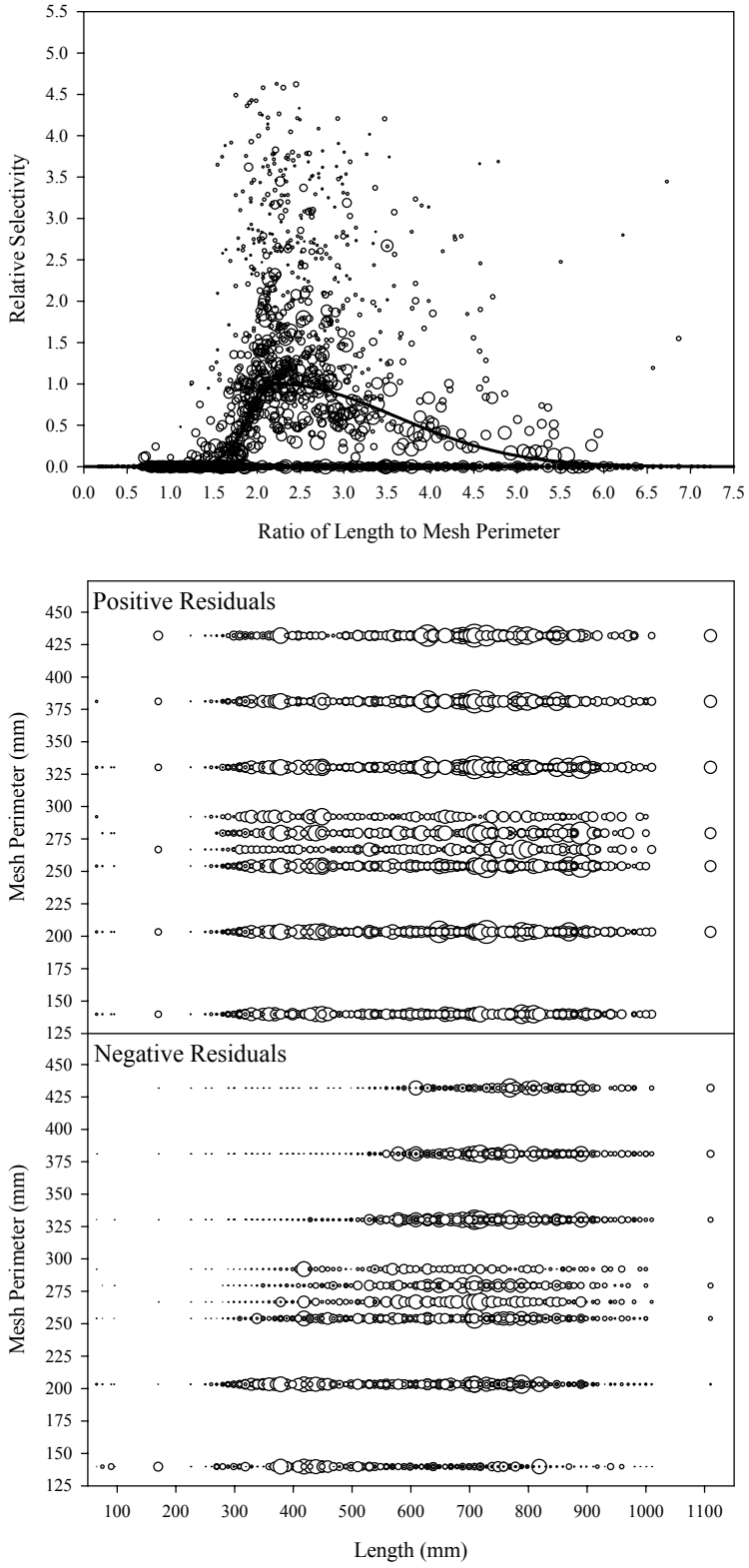

Figure B9.27. Plots of CPUE data scaled to a net selectivity model (top) and CPUE residuals (bottom); Other species group data and Model 27.

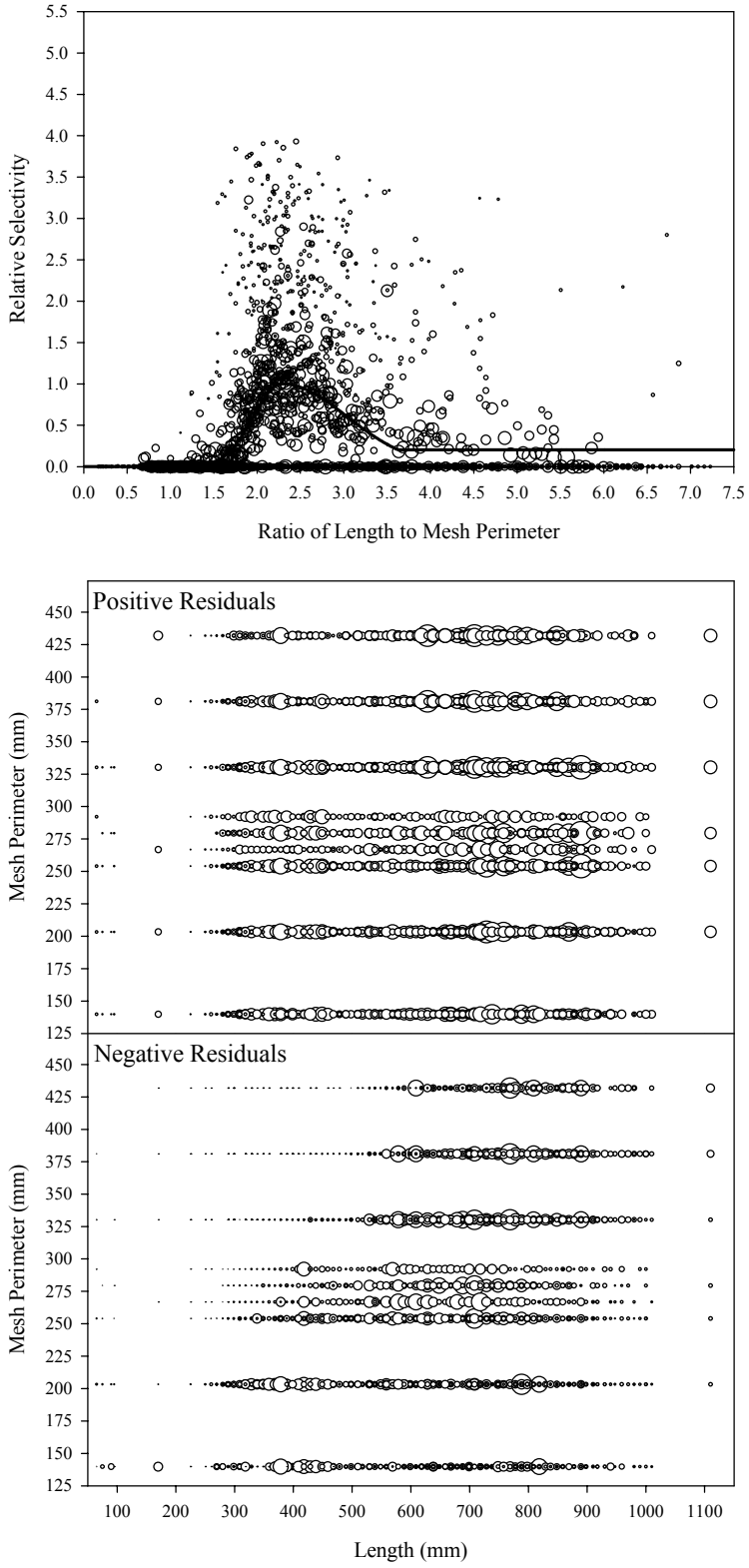

Figure B9.28. Plots of CPUE data scaled to a net selectivity model (top) and CPUE residuals (bottom); Other species group data and Model 28.

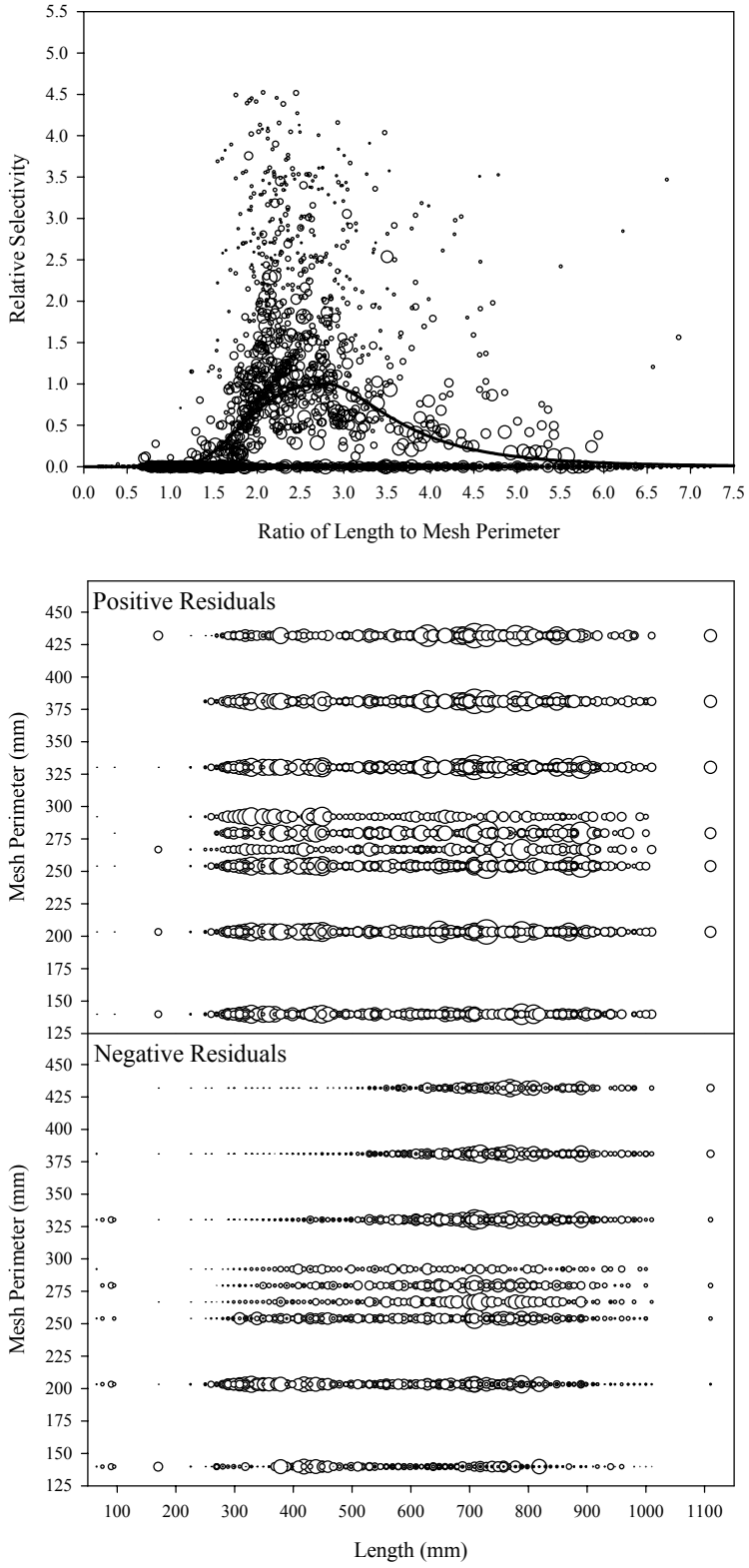

Figure B9.29. Plots of CPUE data scaled to a net selectivity model (top) and CPUE residuals (bottom); Other species group data and Model 29.

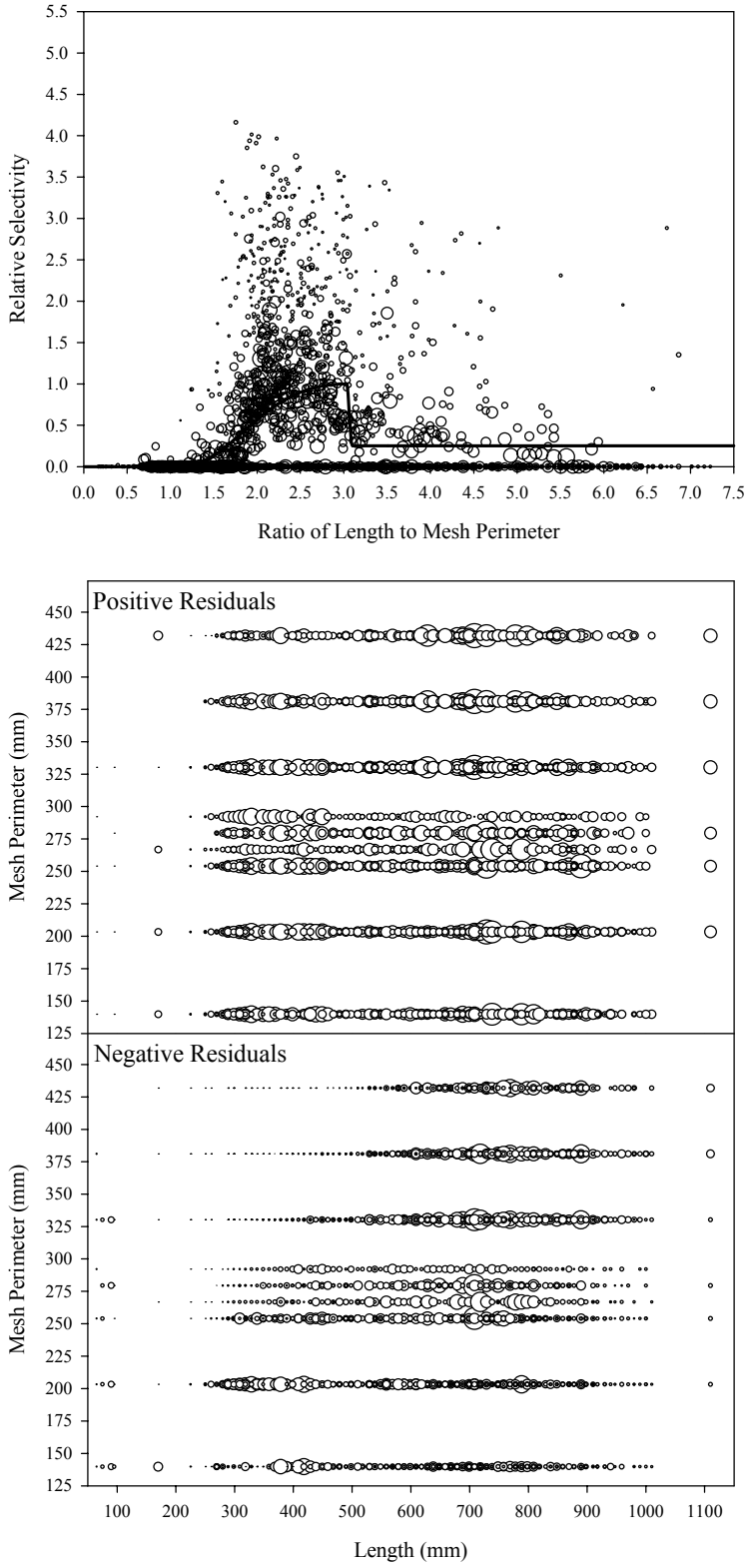

Figure B9.30. Plots of CPUE data scaled to a net selectivity model (top) and CPUE residuals (bottom); Other species group data and Model 30.

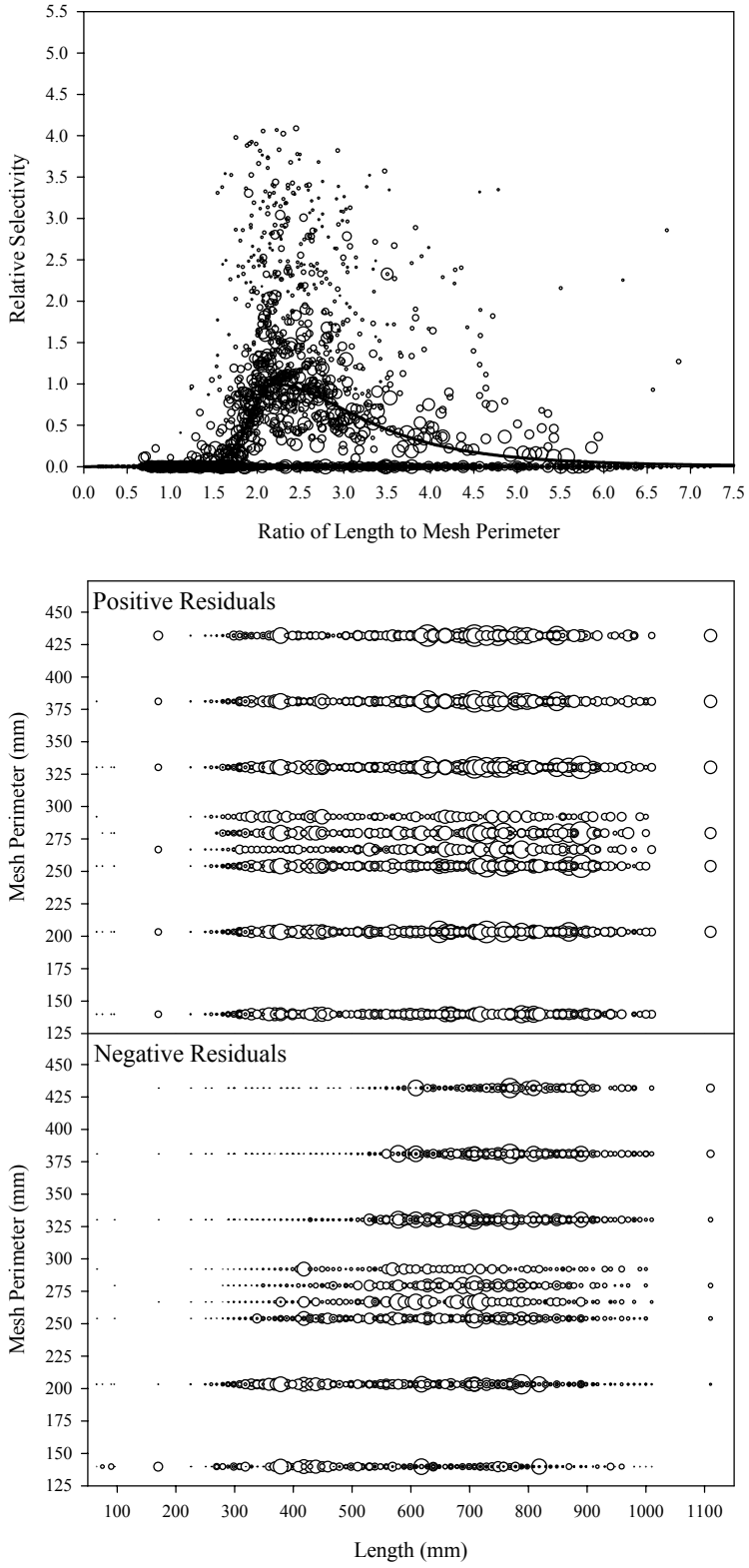

Figure B9.31. Plots of CPUE data scaled to a net selectivity model (top) and CPUE residuals (bottom); Other species group data and Model 31.

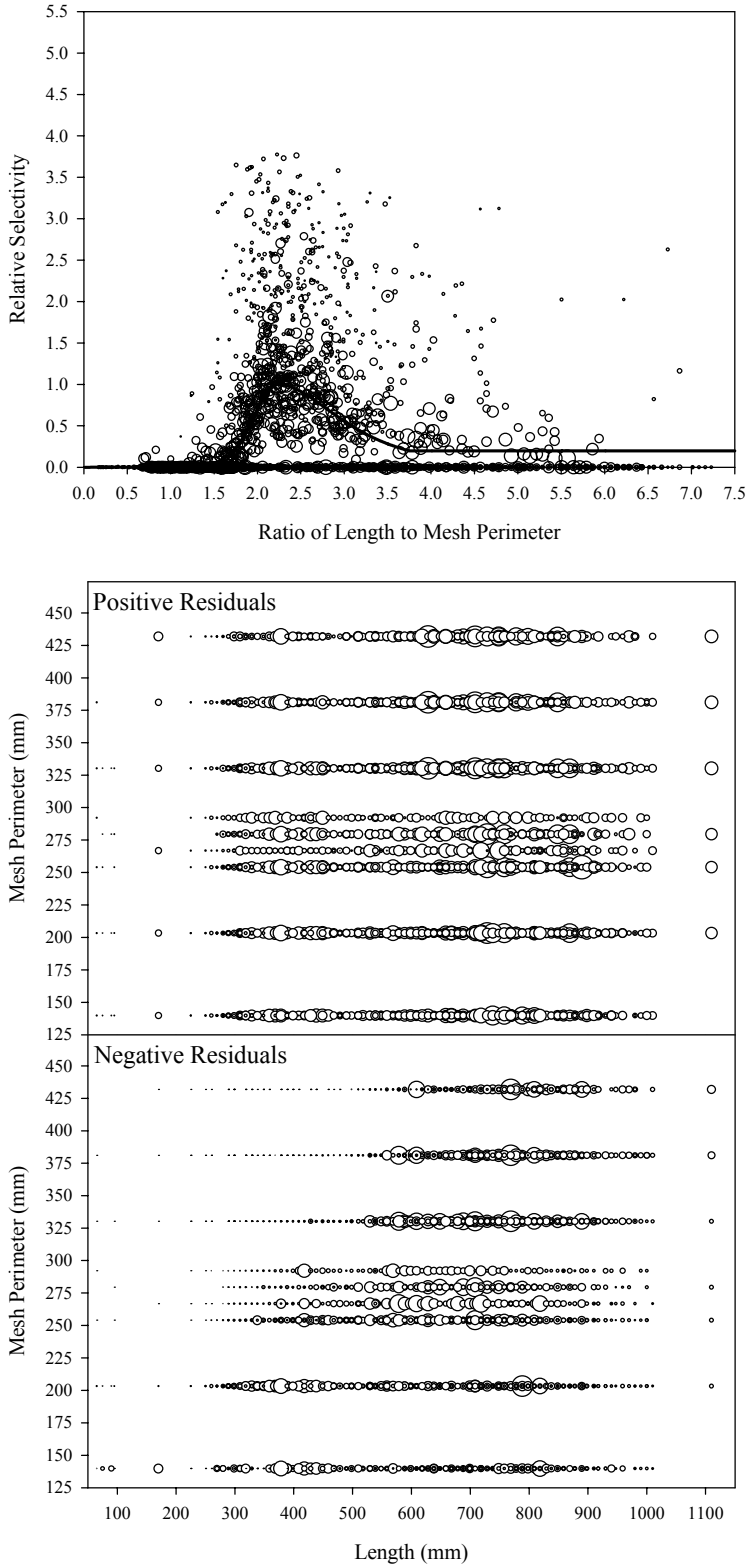

Figure B9.32. Plots of CPUE data scaled to a net selectivity model (top) and CPUE residuals (bottom); Other species group data and Model 32.

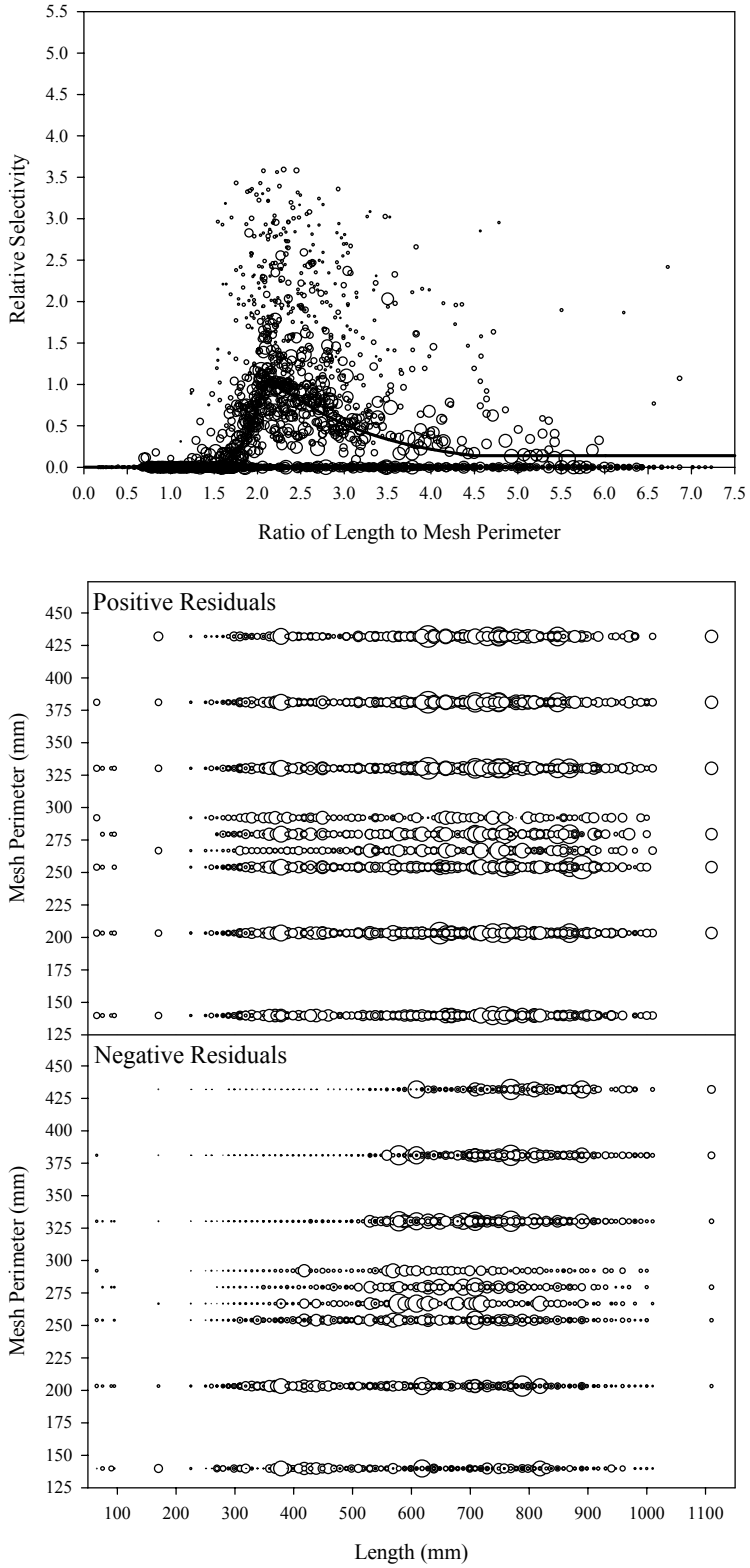

Figure B9.33. Plots of CPUE data scaled to a net selectivity model (top) and CPUE residuals (bottom); Other species group data and Model 34.

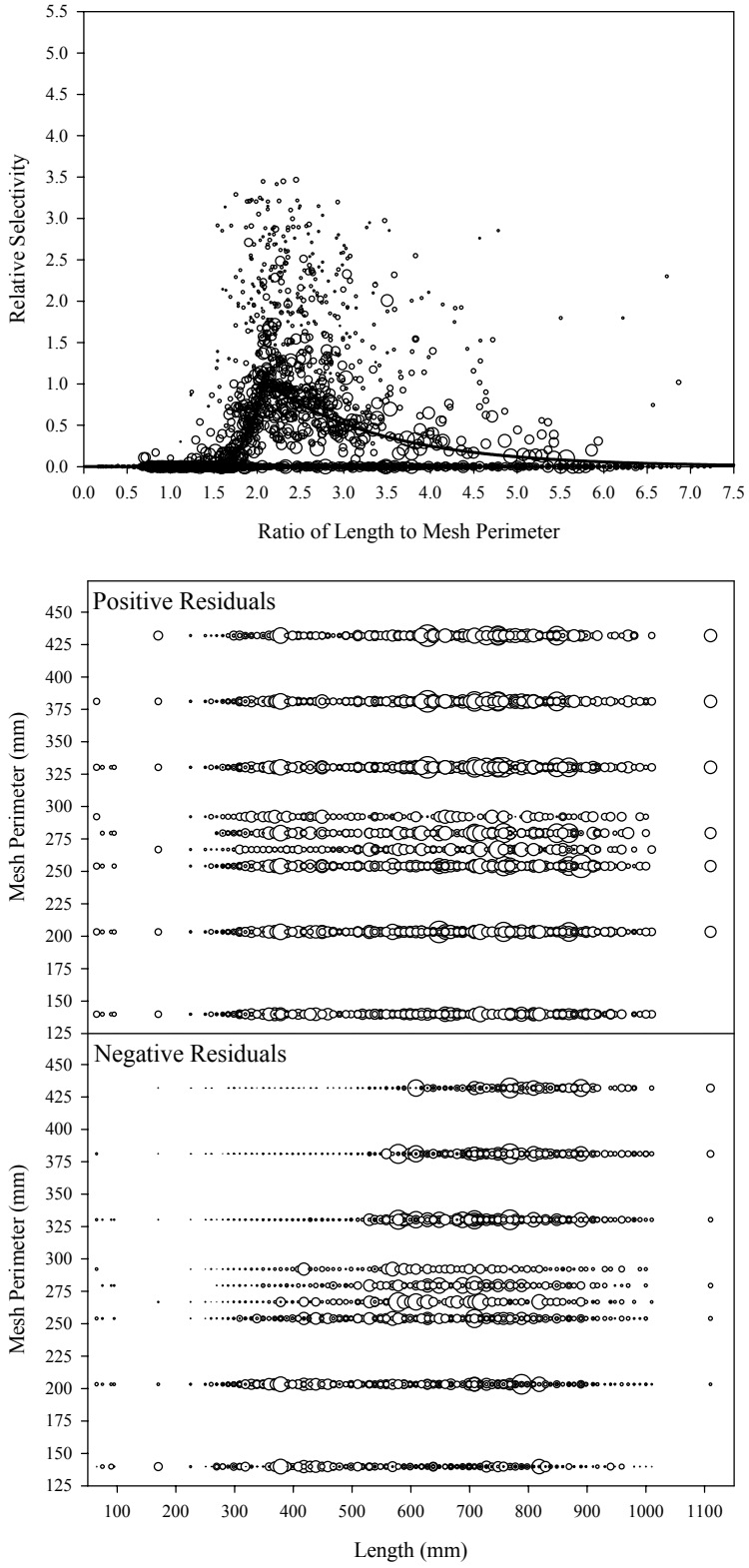

Figure B9.34. Plots of CPUE data scaled to a net selectivity model (top) and CPUE residuals (bottom); Other species group data and Model 35.

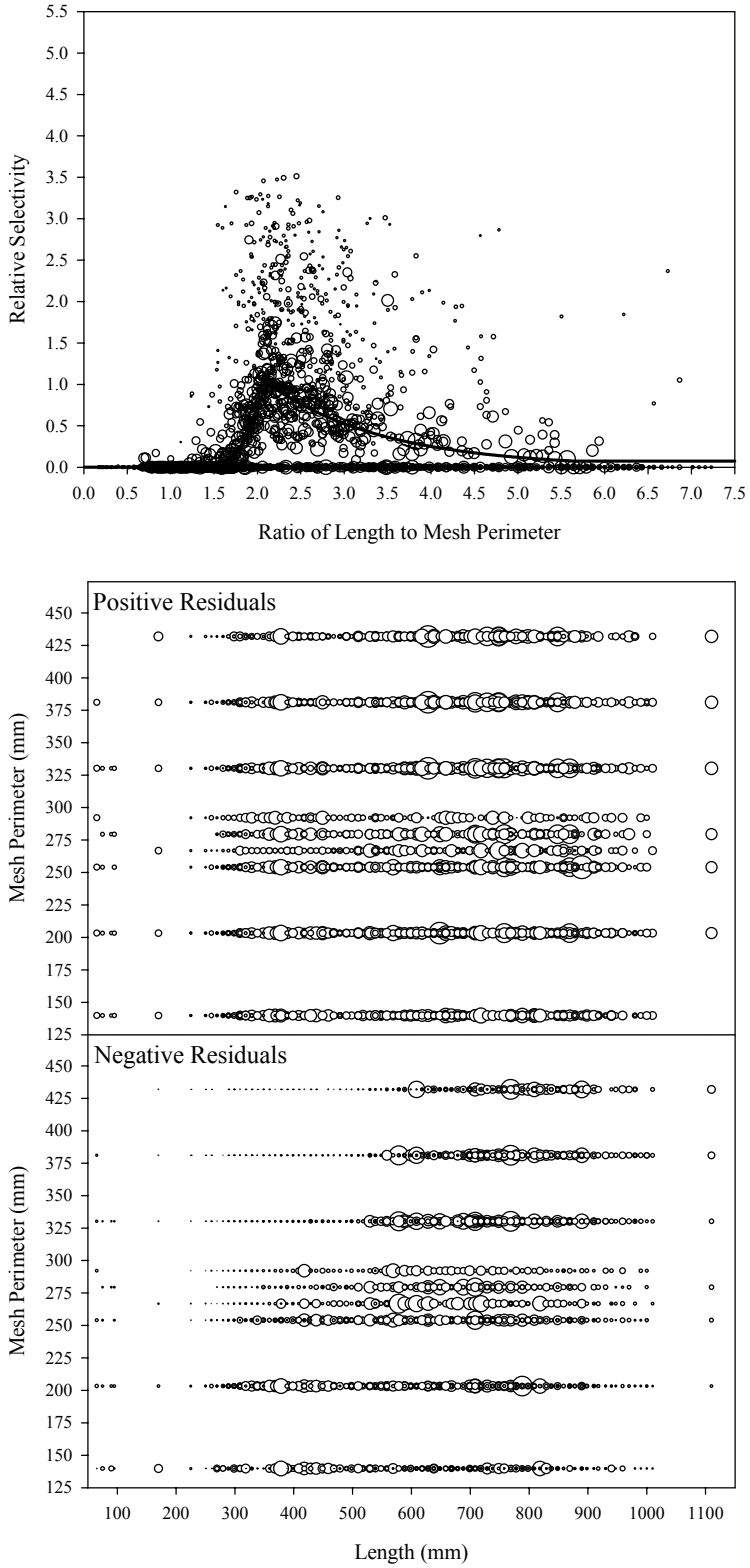

Figure B9.35. Plots of CPUE data scaled to a net selectivity model (top) and CPUE residuals (bottom); Other species group data and Model 36.

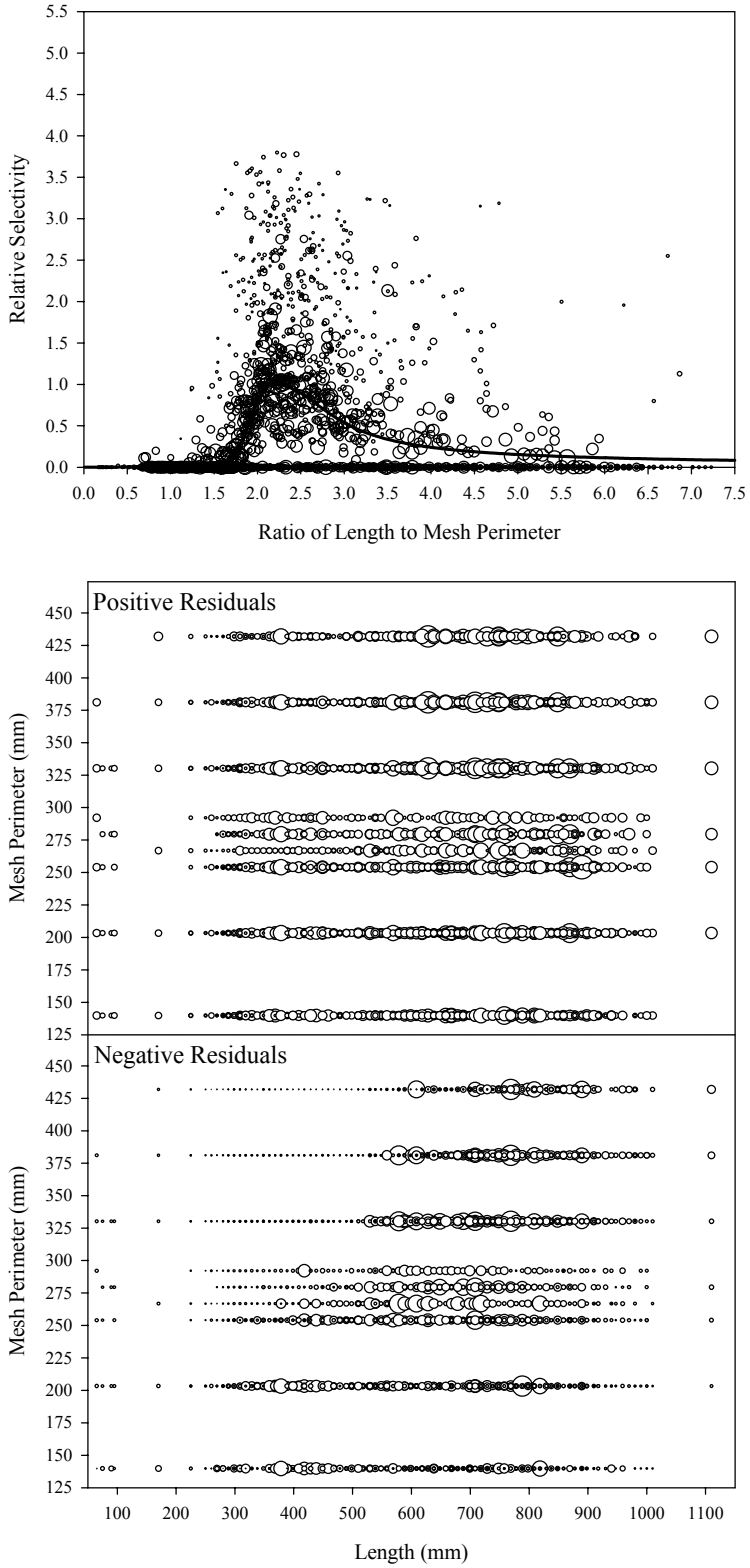

Figure B9.36. Plots of CPUE data scaled to a net selectivity model (top) and CPUE residuals (bottom); Other species group data and Model 37.

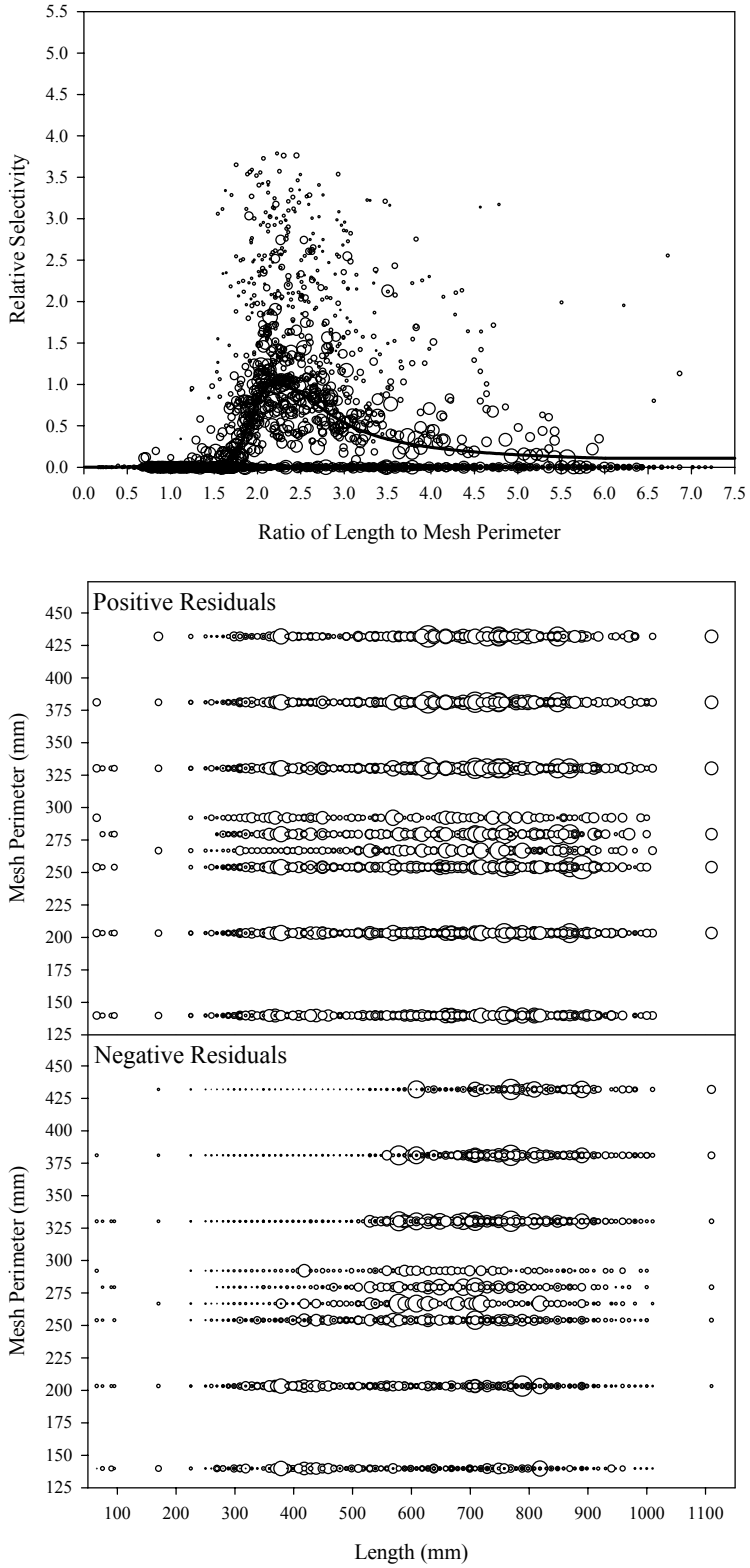

Figure B9.37. Plots of CPUE data scaled to a net selectivity model (top) and CPUE residuals (bottom); Other species group data and Model 38.